

January 25, 2008

U.S. Nuclear Regulatory Commission
11555 Rockville Pike
Rockville, MD 20852-2738

Attn: Document Control Desk

Subject: Submittal of a Request for an Amendment of Certificate of Compliance (CoC)
No. 9225 for the NAC-LWT Cask to Incorporate PWR Mixed-Oxide (MOX) Fuel
Rods as Authorized Contents

Docket No. 71-9225

Reference: 1. Model No. NAC-LWT Package, U.S. Nuclear Regulatory Commission (NRC)
Certificate of Compliance (CoC) No. 9225, Revision 45
2. Safety Analysis Report (SAR) for the NAC Legal Weight Truck Cask,
Revision 38, NAC International, November 2007

NAC International (NAC) herewith submits a request for approval of an Amendment to
Reference 1 to incorporate the following changes:

- The addition of up to 16 PWR mixed oxide (MOX), a mixture of plutonium and uranium oxides, fuel rods contained in a screened or free flow PWR/BWR Rod Transport Canister with a 5 × 5 rod insert as an approved content condition. In addition to the MOX fuel rod content condition, a mixed loading of up to 16 PWR MOX and UO₂ fuel rods is also requested as approved contents. For both content conditions, the empty rod locations of the 5 × 5 insert may be loaded with inert burnable poison rods (BPRs).
- The new PWR MOX fuel content conditions will be transported in NAC-LWT packages provided with a leaktight containment boundary, including metallic containment seals on the closure lid and the Alternate B port covers installed in the vent and drain ports, as recommended in NUREG-1617, Supplement 1.
- NAC License Drawing Nos. 315-40-01 and 315-40-104 have been revised to incorporate the new MOX fuel rod transport cask arrangement requirements, including provision of a leaktight containment boundary.

These proposed changes to the approved content conditions were reviewed and discussed with the NRC Spent Fuel Storage and Transportation staff during the October 17, 2007 meeting in Rockville, MD. The issues identified by the NRC staff regarding the proposed MOX fuel rod content condition have been addressed in the amendment request.

U.S. Nuclear Regulatory Commission
January 25, 2008
Page 2

This submittal includes eight copies of this transmittal letter and Revision LWT-08A changed pages to the Reference 2 SAR. The changed pages incorporate the requested amendment and the applicable evaluations performed to justify the addition of the proposed contents to the authorized contents of the CoC. Attachment 1 contains a brief summary of the changes to the SAR for the amendment. Consistent with NAC administrative practice, this proposed SAR revision is numbered to uniquely identify the applicable changed pages. Revision bars mark the SAR text changes on the Revision LWT-08A pages. In addition to the changes marked with revision bars, minor editorial changes have been made throughout the document. The editorial changes do not affect the technical content of the Reference 2 SAR. This submittal also includes two revised license drawings. Attachment 2 to this transmittal letter lists all drawing changes in detail. The included List of Effective Pages identifies the current revision level of all pages in the Reference 2 SAR.

In order to better facilitate the review process, NAC is providing the Revision LWT-08A changed pages as complete sections of the NAC-LWT SAR. Consequently, a considerable number of Revision LWT-08A pages with no revision bars are included. Upon final acceptance of this application, the LWT-08A changed pages will be reformatted and incorporated into the next revision of the NAC-LWT SAR.

In this amendment request, the proposed changes to the authorized contents are described in Chapter 1. The structural, thermal, containment, shielding and criticality evaluations documenting the adequacy of the NAC-LWT packaging to transport the requested content conditions are presented in SAR Chapters 2, 3, 4, 5 and 6, respectively. Chapter 7 has been revised to address the operational and loading requirements for the PWR MOX fuel rod contents. The revised requirements for the leaktight containment for the transport of PWR MOX fuel rod contents are presented in Chapter 8.

The approval of the PWR MOX fuel rod contents will permit the transport of irradiated PWR MOX and PWR UO₂ fuel rods to facilities for the completion of post-irradiation examinations (PIE) to evaluate the performance of MOX fuel rods in commercial PWR reactor facilities. It is the intent of the PWR MOX fuel supplier (MOX Services) to complete the transport of the irradiated MOX rods as soon as possible after discharge from the reactor. Per the enclosed amendment request, the PWR MOX fuel rods will be acceptable for loading and transport 90 days after reactor discharge, which would allow the initial group of PWR MOX fuel rods to be transported as soon as October 2008. In order to meet the earliest transport date, NAC requests approval of the amendment by September 1, 2008. This will allow mobilization of equipment and preparation of site-specific loading procedures to support an October 2008 loading date.

U.S. Nuclear Regulatory Commission
January 25, 2008
Page 3

If you have any comments or questions, please contact me on my direct line at 678-328-1274.

Sincerely,



Anthony L. Patko
Director, Licensing
Engineering

Attachment 1 – List of Changes, NAC-LWT SAR, Revision LWT-08A
Attachment 2 – List of Drawing Changes, NAC-LWT SAR, Revision LWT-08A

Enclosures

Attachment 1

List of Changes, NAC-LWT SAR, Revision LWT-08A,
for the Incorporation and Analysis of PWR MOX Fuel Rod Contents

Attachment 1

List of Changes, NAC-LWT SAR, Revision LWT-08A, for the Incorporation and Analysis of PWR MOX Fuel Rod Contents

Chapter 1

1. Chapter 1 List of Drawings – revised the following drawings:

315-40-01 Rev 7 Legal Weight Truck Transport Cask Assembly

315-40-104 Rev 3 Legal Weight Truck Transport Cask Assy,
PWR/BWR Rod Transport Canister

The changes to Drawing 315-40-01 were editorial. Drawing 315-40-104 was revised to introduce the option of transporting PWR MOX and PWR UO₂ fuel rods in a PWR/BWR Rod Transport Canister with a 5×5 insert.

2. Section 1, General Information, page 1-1 – Added PWR MOX fuel rods or a combination of PWR MOX and UO₂ PWR fuel rods, along with burnable poison rods, to the list of contents for a Type B(U)F-96 package. Page 1-2 – Added PWR MOX rods to the list of approved contents with 0 CSI.
3. Table 1.1-1, Terminology and Notation – Added PWR MOX fuel rods or a combination of PWR MOX and UO₂ PWR fuel rods, along with burnable poison rods, to the list of contents. Also added definition of MOX Fuel Rods.
4. Section 1.1, Introduction – Added PWR MOX fuel rods or a combination of PWR MOX and UO₂ PWR fuel rods, along with burnable poison rods, to the list of contents. Also added a paragraph describing the loading/transport requirements for the PWR MOX fuel rods or a combination of PWR MOX and UO₂ PWR fuel rods.
5. Section 1.2.1.5, Coolants – Changed “inert gas” to “helium.”
6. Section 1.2.2, Operational Features – 2nd paragraph, 4th sentence – Added “the closure lid” for clarity; revised section throughout to reflect the addition of PWR MOX fuel rod contents.
7. Section 1.2.3, Contents of Packaging – Added PWR MOX fuel rods or a combination of PWR MOX and UO₂ PWR fuel rods, along with burnable poison rods, to the list of contents. Also added the maximum decay heat for 16 PWR MOX/UO₂ fuel rods to item #4 and added item #19 to address the loading/transport requirements for the PWR MOX fuel rods or a combination of PWR MOX and UO₂ PWR fuel rods.
8. Section 1.2.3.11, PWR MOX Fuel Rods – Added a new section to describe the new contents.
9. Table 1.2-4, Fuel Characteristics – Added a column titled “PWR MOX Fuel Rods” and footnotes 6, 7 & 8.

Attachment 1 -- List of Changes, NAC-LWT SAR, Revision LWT-08A, for the Incorporation and Analysis of PWR MOX Fuel Rod Contents (cont'd)

Chapter 2

1. Section 2.6.12.2, PWR Basket Construction – Revised 2nd paragraph to add PWR MOX and UO₂ PWR fuel rods and to clarify existing information.

Chapter 3

1. Section 3.1, Discussion – Added PWR MOX fuel rods or a combination of PWR MOX and UO₂ PWR fuel rods in 2nd paragraph. Added new 3rd paragraph describing the loading requirements for the PWR MOX fuel rods or a combination of PWR MOX and UO₂ PWR fuel rods. In the 4th paragraph, added the maximum heat load for the maximum number of 16 PWR MOX fuel rods and changed “carry” to “transport.”
2. Section 3.4.1.15, High Burnup PWR MOX Rods in a PWR/BWR Rod Transport Canister – Added new section describing the thermal evaluation for this configuration.
3. Section 3.4.4.7, Maximum Internal Pressure for 16 PWR/UO₂ Fuel Rods in a Rod Holder – Added new section addressing maximum internal pressure for this configuration.
4. Section 3.5.3.13, Evaluation of 16 PWR MOX High Burnup Rods – Added new section evaluating package temperature for 16 PWR MOX high burnup rods.
5. Section 3.5.4.6, Maximum Internal Pressure for 16 PWR MOX/UO₂ Fuel Rods in a Rod Holder – Added new section addressing maximum internal pressure for this configuration.

Chapter 4

1. Section 4.1, Containment Boundary – Added information to clarify the differences between the alternate port cover and the Alternate B port cover.
2. Section 4.1.2.1, Seals – Changed “per” to “in accordance with.”
3. Section 4.1.2.1.1, Fabrication Leakage Rate Test – Revised throughout to address the two leakage rates defined for the NAC-LWT containment boundary.
4. Section 4.1.2.1.2, Fabrication Pressure Test, 2nd paragraph – Changed “an NAC-LWT cask” to “a specific NAC-LWT cask.” Also added new last sentence for clarification.
5. Section 4.1.2.1.3, Preshipment Leakage Rate Test – Revised throughout for clarification.
6. Section 4.1.3, Closure – Revised throughout for clarification.
7. Section 4.2, Containment Requirements for Normal Conditions of Transport – Revised throughout for clarification.

Attachment 1 -- List of Changes, NAC-LWT SAR, Revision LWT-08A, for the Incorporation and Analysis of PWR MOX Fuel Rod Contents (cont'd)

8. Page 4.2-6, Maximum Allowable Leak Rates – Added new last paragraph to address leaktight containment boundary configuration requirements.
9. Section 4.2.3, Containment Criteria – Revised to distinguish between the leak test requirements for the containment boundary for contents not requiring a leaktight containment and contents requiring a leaktight containment.
10. Section 4.3, Containment Requirements for Hypothetical Accident Conditions – Revised to clarify the containment boundary for the transport of contents requiring a leaktight containment.
11. Section 4.3.2.3, Containment Criteria – Added PWR MOX fuel rods.

Chapter 5

1. Section 5, Shielding Evaluation (page 5-3) – Added new paragraph to address up to 16 high burnup undamaged PWR MOX or UO₂ fuel rods loaded into a 5×5 rod holder.
2. Section 5.1.1, NAC-LWT Contents – Revised 7th bullet & added new bullet #8, “up to 16 PWR MOX or UO₂ rods in any combination (up to 62,500 MWd/MTHM).” Also added “25” to the 1st sentence of the 2nd paragraph.
3. Page 5.1.1-2, 2nd paragraph – Added “16 PWR MOX rods” & “The MOX rods require 90 days of cooling.” Deleted “The 25 design basis PWR rods burned to 60,000 MWd/MTU require 150 days of cooling.”
4. Page 5.1.1-3 – added new paragraph to describe the source terms for PWR MOX and UO₂ fuel rods.
5. Table 5.1.1-1, Type, Form, Quantity and Potential Sources of Design Basis Fuel – Added new information for PWR MOX or UO₂ fuel rods.
6. Table 5.1.1-2, Design Basis Fuel for Shielding Evaluation – Added new column for PWR MOX/UO₂ Rods, along with footnote 11.
7. Table 5.1.1-3, Nuclear and Thermal Source Parameters – Added last line to table, “16 PWR MOX Rods.”
8. Added Section 5.3.18, PWR MOX Rod Fuel Configuration, and subsections 5.3.18.1, 5.3.18.2 & 5.3.18.3 to present the results of a shielding and decay heat analysis for up to 16 high burnup PWR MOX fuel rods. Also added Figures 5.3.18-1 through 5.3.18-8 & Tables 5.3.18-1 through 5.3.18-15.

Chapter 6

1. Section 6, Criticality Evaluation, 1st paragraph – Added “up to 16 PWR UO₂ or MOX rods in a rod holder”; 2nd paragraph – added “(UO₂ or MOX).”
2. Pages 6.1-4 & 6.1-5 – Added new last paragraph to address analyses performed on the NAC-LWT with up to 16 PWR (UO₂ or MOX) fuel rods.

Attachment 1 -- List of Changes, NAC-LWT SAR, Revision LWT-08A, for the Incorporation and Analysis of PWR MOX Fuel Rod Contents (cont'd)

3. Added Section 6.7, Payload Specific Details, and subsections 6.7.1 & 6.7.2 to describe the NAC-LWT payload specific evaluation detail. Also added Figures 6.7.1-1 through 6.7.1-8, Tables 6.7.1-1 through 6.7.1-11, Figures 6.7.2-1 through 6.7.2-19 & Tables 6.7.2-1 through 6.7.2-6.
4. Added Section 6.6.15, PWR MOX Fuel Rods to the Chapter 6 Appendix, along with Figures 6.6.15-1 & 6.6.15-2, to provide sample output files from the evaluation of MOX fuel rods in the NAC-LWT cask.

Chapter 7

1. Section 7, Operating Procedures – Added additional information to the 4th paragraph to address leaktight containment configuration requirements.
2. Section 7.1, Procedures for Loading Packages – Added “(e.g., PWR MOX fuel rods).”
3. Section 7.1.11, Procedure for Dry Loading of TPBAR Waste Container – deleted step 9 as the weather seal is no longer applicable and renumbered subsequent steps.
4. Added Section 7.1.12, Procedure for Wet Loading PWR MOX Fuel Rods in a Transport Canister Into the NAC-LWT Cask, to provide a detailed wet loading procedure for these contents.
5. Section 7.2, Procedures for Unloading Package – Added clarification regarding generic procedures and site-specific procedures.
6. Section 7.2.1 – Changed the title to read “Procedures for Wet Unloading of LWR Fuel and PWR, PWR MOX and BWR Fuel Rods in Transport Canisters” for clarification.
7. Page 7.2-2, Item 20 – Revised for clarification.
8. Section 7.2.5, Procedure for Dry Unloading of TPBAR Contents, page 7.2-11 – deleted step 9 as the weather seal is no longer applicable and renumbered subsequent steps.
9. Section 7.2.6, Procedure for Dry Unloading of PWR/BWR/MOX Fuel Rod Contents – Added new section to incorporate the generic procedures for the dry unloading of PWR MOX fuel rod contents.

Chapter 8

1. Section 8.1.3.1, Closure Lid Leakage Rate Test – Revised Items 9a & 9b to differentiate between contents with and without a leaktight containment boundary.
2. Section 8.1.3.2.1, Fabrication and Periodic Leakage Rate Tests, Item 8 – Deleted “is that the measured leakage rate” for clarification.

Attachment 1 -- List of Changes, NAC-LWT SAR, Revision LWT-08A, for the Incorporation and Analysis of PWR MOX Fuel Rod Contents (cont'd)

3. Section 8.1.3.3.1, Fabrication and Periodic Leakage Rate Tests, 1st paragraph, 2nd sentence – Revised to clarify TPBAR transport contents requirements. Item 8 – added “i.e., leaktight per ANSI N14.5-1997.”
4. Section 8.1.3.3.2, Maintenance and Preshipment Leakage Rate Tests – Added “for contents requiring leaktight containment per ANSI N14.5-1997, such as TPBARs and MOX fuel rods.”
5. Section 8.2, Maintenance Program – Changed old 4th paragraph into two revised paragraphs addressing the leaktight containment boundary.

Chapter 9

1. Section 9, References – Added two new references on page 9-4.

Attachment 2

List of Drawing Changes, NAC-LWT SAR, Revision LWT-08A,
for the Incorporation and Analysis of PWR MOX Fuel Rod Contents

Attachment 2

List of Drawing Changes, NAC-LWT SAR, Revision LWT-08A, for the Incorporation and Analysis of PWR MOX Fuel Rod Contents

Drawing 315-40-01, Legal Weight Truck Transport Cask Assembly, Revision 7

- Revised Item 11:
 - Changed the name of the item to “Tamper Indicating Device (TID)”; was :”Metal Cup Seal”
 - Changed Material to N/A; was Stl.
 - Changed Description to N/A; was Ø3/4
- Revised Item 10:
 - Changed Description to N/A; was Ø0.032
- Updated title block

Drawing 315-40-104, Legal Weight Truck Transport Cask Assembly, PWR/BWR Rod Transport Canister, Revision 3

- Added Assembly 97, “PWR/BWR ROD TRANSPORT CANISTER-MOX AND MOX/UO₂ FUEL ROD CONFIGURATION,” on sheet 2 and revises B.O.M. on sheet 1 to add Assembly 97, which includes items 1, 2, 3, 4, 6, 7, 8, 9, 11, 12, 13, 14, 15, and 17 as follows:
 - B.O.M. #1, Qty 1, Impact Limiter, 315-40-05-99
 - B.O.M. #2, Qty 1, Impact Limiter, 315-40-06-99
 - B.O.M. #3, Qty 1, Cask Assembly, 315-40-02-99
 - B.O.M. #4, Qty A/R, Free Flow Can, 315-40-98-99
 - B.O.M. #6, Qty 1, PWR Insert, 315-40-105-99
 - B.O.M. #7, Qty 8, Ball Lock-Pin, 315-40-01-8
 - B.O.M. #8 Qty A/R, Wire, 315-40-01-10
 - B.O.M. #9, Qty 1, Tamper Indicating Device, 315-40-01-11
 - B.O.M. #11, Qty A/R, Pin Spacer, 315-40-103-1
 - B.O.M. #12, Qty A/R, Screened Can, 315-40-98-97
 - B.O.M. #13, Qty 1, Rod Transport Canister Spacer, 315-40-126-99
 - B.O.M. #14, Qty 4, Hex Head Bolt, St.Stl., Coml.
 - B.O.M. #15, Qty 4, Lock Washer, St.Stl., Coml.
 - B.O.M. #17, Qty 1, Basket Assembly - PWR, 315-40-10-97

Attachment 2 -- List of Drawing Changes, NAC-LWT SAR, Revision LWT-08A, for the Incorporation and Analysis of PWR MOX Fuel Rod Contents (cont'd)

Drawing 315-40-104, Legal Weight Truck Transport Cask Assembly, PWR/BWR Rod Transport Canister, Revision 3 (continued)

- Added delta note 3 as follows: “CASK ASSEMBLY TO BE A LEAKTIGHT ARRANGEMENT FOR MOX FUEL RODS. ALTERNATE B PORT COVERS AND HELIUM VERIFICATION OF LID AND PORT COVER SEALS TO LEAKTIGHT CRITERIA REQUIRED.”
- Added delta note 4 as follows: “SCREENED CAN (ITEM 12) OR FREE FLOW CAN (ITEM 4) USED FOR LOADING OF MOX FUEL RODS SHALL ONLY USE THE 5 × 5 INSERT (315-40-102-99).
- Sheet 1 – Changed name of Item 9 to “TAMPER INDICATING DEVICE (TID)” instead of “METAL CUP SEAL.”
- Sheet 1 – Changed name of Item 13 to “ROD TRANSPORT CANISTER SPACER” instead of “CAN & INSERT SPACER.”
- Sheet 1 – Changed name of Assembly 99 to “PWR/BWR ROD TRANSPORT CANISTER” instead of “PWR TRANSPORT CANISTER.”
- Changed name in the Title Block to “LEGAL WEIGHT TRUCK TRANSPORT CASK ASSY, PWR/BWR ROD TRANSPORT CANISTER” instead of “LEGAL WEIGHT TRANSPORT CASK ASSY, PWR TRANSPORT CANISTER.”
- Updated title block.

January 2008

Revision LWT-08A

NAC-LWT

Legal Weight Truck Cask System

SAFETY ANALYSIS REPORT

Volume 1 of 2

Docket No. 71-9225



Atlanta Corporate Headquarters: 3930 East Jones Bridge Road, Norcross, Georgia 30092 USA
Phone 770-447-1144, Fax 770-447-1797, www.nacintl.com

List of Effective Pages

LIST OF EFFECTIVE PAGES

Chapter 1

1-i thru 1-iv Revision LWT-08A
1-1 thru 1-5 Revision LWT-08A
1.1-1 thru 1.1-3 Revision LWT-08A
1.2-1 thru 1.2-49 Revision LWT-08A
1.3-1 Revision 38
1.4-1 Revision 38
1.5-1 Revision 38

76 drawings in the
Chapter 1 List of Drawings

Chapter 1 Appendices 1-A
through 1-G

Chapter 2

2-i thru 2-xxiv Revision LWT-08A
2-1 Revision 38
2.1.1-1 thru 2.1.1-2 Revision 38
2.1.2-1 thru 2.1.2-3 Revision 38
2.1.3-1 thru 2.1.3-8 Revision 38
2.2.1-1 thru 2.2.1-3 Revision 38
2.3-1 Revision 38
2.3.1-1 thru 2.3.1-13 Revision 38
2.4-1 Revision 38
2.4.1-1 Revision 38
2.4.2-1 Revision 38
2.4.3-1 Revision 38
2.4.4-1 Revision 38
2.4.5-1 Revision 38
2.4.6-1 Revision 38
2.5.1-1 thru 2.5.1-11 Revision 38
2.5.2-1 thru 2.5.2-17 Revision 38
2.6.1-1 thru 2.6.1-7 Revision 38
2.6.2-1 thru 2.6.2-7 Revision 38
2.6.3-1 Revision 38

2.6.4-1 Revision 38
2.6.5-1 thru 2.6.5-2 Revision 38
2.6.6-1 Revision 38
2.6.7-1 thru 2.6.7-136 Revision 38
2.6.8-1 Revision 38
2.6.9-1 Revision 38
2.6.10-1 thru 2.6.10-15 Revision 38
2.6.11-1 thru 2.6.11-12 Revision 38
2.6.12-1 thru 2.6.12-91 ... Revision LWT-08A
2.7-1 Revision 38
2.7.1-1 thru 2.7.1-117 Revision 38
2.7.2-1 thru 2.7.2-23 Revision 38
2.7.3-1 thru 2.7.3-5 Revision 38
2.7.4-1 Revision 38
2.7.5-1 thru 2.7.5-5 Revision 38
2.7.6-1 thru 2.7.6-4 Revision 38
2.7.7-1 thru 2.7.7-70 Revision 38
2.8-1 Revision 38
2.9-1 thru 2.9-13 Revision 38
2.10.1-1 thru 2.10.1-3 Revision 38
2.10.2-1 thru 2.10.2-49 Revision 38
2.10.3-1 thru 2.10.3-18 Revision 38
2.10.4-1 thru 2.10.4-11 Revision 38
2.10.5-1 Revision 38
2.10.6-1 thru 2.10.6-19 Revision 38
2.10.7-1 thru 2.10.7-66 Revision 38
2.10.8-1 thru 2.10.8-67 Revision 38
2.10.9-1 thru 2.10.9-9 Revision 38
2.10.10-1 thru 2.10.10-97 Revision 38
2.10.11-1 thru 2.10.11-10 Revision 38
2.10.12-1 thru 2.10.12-31 Revision 38
2.10.13-1 thru 2.10.13-17 Revision 38
2.10.14-1 thru 2.10.14-38 Revision 38
2.10.15-1 thru 2.10.15-10 Revision 38

LIST OF EFFECTIVE PAGES (Continued)

Chapter 3

3-i thru 3-v Revision LWT-08A
3.1-1 thru 3.1-2 Revision LWT-08A
3.2-1 thru 3.2-11 Revision 38
3.3-1 Revision 38
3.4-1 thru 3.4-84 Revision LWT-08A
3.5-1 thru 3.5-35 Revision LWT-08A
3.6-1 thru 3.6-12 Revision 38

5.3.13-1 thru 5.3.13-17 Revision 38
5.3.14-1 thru 5.3.14-21 Revision 38
5.3.15-1 thru 5.3.15-9 Revision 38
5.3.16-1 thru 5.3.16-5 Revision 38
5.3.17-1 thru 5.3.17-9 Revision 38
5.3.18-1 thru 5.3.18-29... Revision LWT-08A
5.4.1-1 thru 5.4.1-6 Revision 38

Chapter 4

4-i thru 4-iv Revision LWT-08A
4.1-1 thru 4.1-3 Revision LWT-08A
4.2-1 thru 4.2-12 Revision LWT-08A
4.3-1 thru 4.3-7 Revision LWT-08A
4.4-1 thru 4.4-2 Revision 38
4.5-1 thru 4.5-85 Revision 38

Chapter 6

6-i thru 6-xiii Revision LWT-08A
6-1 Revision LWT-08A
6.1-1 thru 6.1-5 Revision LWT-08A
6.2-1 Revision 38
6.2.1-1 thru 6.2.1-3 Revision 38
6.2.2-1 thru 6.2.2-3 Revision 38
6.2.3-1 thru 6.2.3-7 Revision 38
6.2.4-1 Revision 38
6.2.5-1 thru 6.2.5-5 Revision 38
6.2.6-1 thru 6.2.6-3 Revision 38
6.2.7-1 thru 6.2.7-2 Revision 38
6.2.8-1 thru 6.2.8-3 Revision 38
6.2.9-1 thru 6.2.9-4 Revision 38
6.2.10-1 thru 6.2.10-3 Revision 38
6.2.11-1 thru 6.2.11-3 Revision 38
6.2.12-1 thru 6.2.12-4 Revision 38
6.3.1-1 thru 6.3.1-6 Revision 38
6.3.2-1 thru 6.3.2-4 Revision 38
6.3.3-1 thru 6.3.3-9 Revision 38
6.3.4-1 thru 6.3.4-9 Revision 38
6.3.5-1 thru 6.3.5-12 Revision 38
6.3.6-1 thru 6.3.6-9 Revision 38
6.3.7-1 thru 6.3.7-4 Revision 38
6.3.8-1 thru 6.3.8-7 Revision 38

Chapter 5

5-i thru 5-xi Revision LWT-08A
5-1 thru 5-3 Revision LWT-08A
5.1.1-1 thru 5.1.1-17 ... Revision LWT-08A
5.2.1-1 thru 5.2.1-7 Revision 38
5.3.1-1 thru 5.3.1-2 Revision 38
5.3.2-1 Revision 38
5.3.3-1 thru 5.3.3-8 Revision 38
5.3.4-1 thru 5.3.4-19 Revision 38
5.3.5-1 thru 5.3.5-4 Revision 38
5.3.6-1 thru 5.3.6-18 Revision 38
5.3.7-1 thru 5.3.7-11 Revision 38
5.3.8-1 thru 5.3.8-25 Revision 38
5.3.9-1 thru 5.3.9-26 Revision 38
5.3.10-1 thru 5.3.10-14 Revision 38
5.3.11-1 thru 5.3.11-48 Revision 38
5.3.12-1 thru 5.3.12-26 Revision 38

LIST OF EFFECTIVE PAGES (Continued)

6.3.9-1 thru 6.3.9-7Revision 38
6.4.1-1 thru 6.4.1-10Revision 38
6.4.2-1 thru 6.4.2-10Revision 38
6.4.3-1 thru 6.4.3-34Revision 38
6.4.4-1 thru 6.4.4-24Revision 38
6.4.5-1 thru 6.4.5-32Revision 38
6.4.6-1 thru 6.4.6-17Revision 38
6.4.7-1 thru 6.4.7-14Revision 38
6.4.8-1 thru 6.4.8-14Revision 38
6.4.9-1 thru 6.4.9-10Revision 38
6.4.10-1 thru 6.4.10-18Revision 38
6.5.1-1 thru 6.5.1-13Revision 38
6.5.2-1 thru 6.5.2-4Revision 38
6.5.3-1 thru 6.5.3-2Revision 38
6.7.1.1 thru 6.7.1-18.....Revision LWT-08A
6.7.2.1 thru 6.7.2-47.....Revision LWT-08A

Appendix 6.6

6.6-i thru 6.6-iiiRevision LWT-08A
6.6-1Revision 38
6.6.1-1 thru 6.6.1-111Revision 38
6.6.2-1 thru 6.6.2-56Revision 38
6.6.3-1 thru 6.6.3-73Revision 38
6.6.4.-1 thru 6.6.4-77Revision 38
6.6.5-1 thru 6.6.5-101Revision 38
6.6.6-1 thru 6.6.6-76Revision 38
6.6.7-1 thru 6.6.7-84Revision 38
6.6.8-1 thru 6.6.8-183Revision 38
6.6.9-1 thru 6.6.9-52Revision 38
6.6.10-1 thru 6.6.10-33Revision 38
6.6.11-1 thru 6.6.11-47Revision 38
6.6.12-1 thru 6.6.12-20Revision 38
6.6.13-1 thru 6.6.13-22Revision 38
6.6.14-1 thru 6.6.14-7Revision 38

6.6.15-1 thru 6.6.15-43 ..Revision LWT-08A

Chapter 7

7-i thru 7-iiRevision LWT-08A
7.1-1 thru 7.1-56.....Revision LWT-08A
7.2-1 thru 7.2-14.....Revision LWT-08A
7.3-1 thru 7.3-2..... Revision 38

Chapter 8

8-iRevision LWT-08A
8.1-1 thru 8.1-11Revision LWT-08A
8.2-1 thru 8.2-4.....Revision LWT-08A
8.3-1 thru 8.3-4..... Revision 38

Chapter 9

9-iRevision LWT-08A
9-1 thru 9-10.....Revision LWT-08A

Chapter 1

Table of Contents

1 GENERAL INFORMATION 1-1

1.1 Introduction..... 1.1-1

1.2 Package Description..... 1.2-1

1.2.1 Packaging..... 1.2-1

1.2.2 Operational Features 1.2-4

1.2.3 Contents of Packaging 1.2-5

1.3 Quality Assurance 1.3-1

1.4 License Drawings..... 1.4-1

1.5 Unclassified DOE Reference Documents and Drawings..... 1.5-1

Chapter 1 Appendices

Appendix 1-A – TTQP-1-015, “Description of the Tritium-Producing Burnable Absorber Rod for the Commercial Light Water Reactor,” Revision 14

Appendix 1-B – TTQP-1-091, “Unclassified TPBAR Releases, Including Tritium,” Revision 11

Appendix 1-C – TTQP-1-111, “Unclassified Bounding Source Term, Radionuclide Concentrations, Decay Heat, and Dose Rates for the Production TPBAR,” Revision 5

Appendix 1-D – DOE Drawing H-3-307845, “Production TPBAR Reactor Interface Dimensions Watts Bar,” Revision 10, Sheet 1 of 2

Appendix 1-E – DOE Drawing H-3-308875, “Production TPBAR Reactor Interface Dimensions Sequoyah,” Revision 5, Sheet 1 of 2

Appendix 1-F – DOE Drawing H-3-310568, “Mark 8 Multi-Pencil TPBAR – Watts Bar Reactor Interface,” Revision 0, Sheet 1 of 2

Appendix 1-G – PNNL Letter, TTP-06-056, Subject: Exposure of Shipping Cask to Tritium, February 21, 2006

List of Figures

Figure 1.2.3-1	Aluminum Clad TRIGA Fuel Element	1.2-18
Figure 1.2.3-2	Aluminum Clad Instrumented Fuel Element.....	1.2-19
Figure 1.2.3-3	Stainless Steel Clad TRIGA Fuel Element.....	1.2-20
Figure 1.2.3-4	Stainless Steel Clad Instrumented Fuel Element	1.2-21
Figure 1.2.3-5	Standard Fuel Follower Control Rod Element.....	1.2-22
Figure 1.2.3-6	TRIGA Fuel Cluster and Rod Details	1.2-23
Figure 1.2.3-7	HTGR Fuel Handling Unit.....	1.2-24
Figure 1.2.3-8	RERTR Fuel Handling Unit.....	1.2-25
Figure 1.2.3-9	Typical TPBAR Assembly.....	1.2-26
Figure 1.2.3-10	TPBAR Consolidation Canister Sketch.....	1.2-27
Figure 1.2.3-11	Failed PWR/BWR Fuel Rod Capsule.....	1.2-28
Figure 1.2.3-12	NAC-LWT with TPBAR Consolidation Canister Payload	1.2-29
Figure 1.2.3-13	PULSTAR Fuel Assembly.....	1.2-30
Figure 1.2.3-14	Spiral Fuel Assembly Cross-Section Sketch	1.2-31
Figure 1.2.3-15	MOATA Plate Bundle Sketches	1.2-32
Figure 1.2.3-16	TPBAR Waste Container and Extension Weldment Sketch	1.2-33
Figure 1.2.3-17	NAC-LWT with TPBAR Waste Container Payload	1.2-34

List of Tables

Table 1.1-1	Terminology and Notation.....	1-3
Table 1.2-1	Characteristics of Design Basis TRIGA Fuel Elements Acceptable for Loading in the Poisoned TRIGA Basket.....	1.2-35
Table 1.2-2	Characteristics of Design Basis TRIGA Fuel Elements Acceptable for Loading in the Nonpoisoned TRIGA Basket	1.2-36
Table 1.2-3	Characteristics of Design Basis TRIGA Fuel Cluster Rods	1.2-37
Table 1.2-4	Fuel Characteristics	1.2-38
Table 1.2-5	PWR Fuel Characteristics.....	1.2-41
Table 1.2-6	BWR Fuel Characteristics	1.2-42
Table 1.2-7	Characteristics of General Atomics Irradiated Fuel Material (GA FM).....	1.2-43
Table 1.2-8	Typical Production TPBAR Characteristics	1.2-44
Table 1.2-9	PULSTAR Fuel Characteristics.....	1.2-45
Table 1.2-10	Spiral Fuel Assembly Characteristics.....	1.2-46
Table 1.2-11	MOATA Plate Bundle Characteristics.....	1.2-47
Table 1.2-12	Typical TPBAR Segment Characteristics in Waste Container	1.2-48
Table 1.2-13	Solid, Irradiated Hardware Characteristics.....	1.2-49

List of Drawings

315-40-01		Rev 7	Legal Weight Truck Transport Cask Assembly
315-40-02	Sheets 1 – 2	Rev 20	NAC-LWT Cask Body Assembly
315-40-03	Sheets 1 – 6	Rev 6*	NAC-LWT Transport Cask Body
315-40-03	Sheets 1 – 7	Rev 22	NAC-LWT Transport Cask Body
315-40-04		Rev 10	NAC-LWT Transport Cask Lid Assembly
315-40-05		Rev 9	NAC-LWT Transport Cask Upper Impact Limiter
315-40-06		Rev 9	NAC-LWT Transport Cask Lower Impact Limiter
315-40-08	Sheets 1 – 5	Rev 17	NAC-LWT Transport Cask Parts Detail
315-40-09		Rev 2	NAC-LWT PWR Basket Spacer
315-40-10	Sheets 1 – 2	Rev 7	NAC-LWT Cask PWR Basket
315-40-11		Rev 2	NAC-LWT BWR Fuel Basket Assembly
315-40-12		Rev 3	NAC-LWT Metal Fuel Basket Assembly
315-40-045		Rev 4	Weldment, 7 Element Basket, 42 MTR Fuel Base Module
315-40-046		Rev 4	Weldment, 7 Element Basket, 42 MTR Fuel Intermediate Module
315-40-047		Rev 4	Weldment, 7 Element Basket, 42 MTR Fuel Top Module
315-40-048		Rev 3	Legal Weight Truck Transport Cask Assembly, 42 MTR Element
315-40-049		Rev 4	Weldment, 7 Element Basket, 28 MTR Fuel Base Module
315-40-050		Rev 4	Weldment, 7 Element Basket, 28 MTR Fuel Intermediate Module
315-40-051		Rev 4	Weldment, 7 Element Basket, 28 MTR Fuel Top Module
315-40-052		Rev 3	Legal Weight Truck Transport Cask Assembly, 28 MTR Element
315-40-070		Rev 3	Weldment, 7 Cell Basket, TRIGA Fuel Base Module
315-40-071		Rev 3	Weldment, 7 Cell Basket, TRIGA Fuel Intermediate Module
315-40-072		Rev 3	Weldment, 7 Cell Basket, TRIGA Fuel Top Module
315-40-074		Rev 3	Lid Assembly, Screened Failed Fuel Can, TRIGA Fuel
315-40-075		Rev 2	Assembly, Screened Failed Fuel Can, TRIGA Fuel
315-40-076		Rev 2	Body, Screened Failed Fuel Can, TRIGA Fuel
315-40-079		Rev 4	Legal Weight Truck Transport Cask Assy, TRIGA Fuel
315-040-080		Rev 2	Weldment, 7 Cell Poison Basket, TRIGA Fuel Base Module
315-040-081		Rev 2	Weldment, 7 Cell Poison Basket, TRIGA Fuel Intermediate Module
315-040-082		Rev 2	Weldment, 7 Cell Poison Basket, TRIGA Fuel Top Module
315-040-083		Rev 0	Spacer, LWT Cask Assembly, TRIGA Fuel
315-40-084		Rev 4	Legal Weight Truck Transport Cask Assy, 140 TRIGA Elements
315-40-085		Rev 0	Axial Fuel and Cell Block Spacers, MTR and TRIGA Fuel Baskets, NAC-LWT Cask
315-40-086		Rev 1	Assembly, Sealed Failed Fuel Can, TRIGA Fuel
315-40-087		Rev 5	Canister Lid Assembly, Sealed Failed Fuel Can, TRIGA Fuel
315-40-088		Rev 2	Canister Body Assembly, Sealed Failed Fuel Can, TRIGA Fuel
315-40-090		Rev 2	Weldment, 7 Element Basket, 35 MTR Fuel Base Module
315-40-091		Rev 2	Weldment, 7 Element Basket, 35 MTR Fuel Intermediate Module
315-40-092		Rev 2	Weldment, 7 Element Basket, 35 MTR Fuel Top Module
315-40-094		Rev 4	Legal Weight Truck Transport Cask Assembly, 35 MTR Element
315-40-096		Rev 3	Fuel Rod Insert, TRIGA Fuel
315-40-098	Sheets 1 - 2	Rev 3	Can Assembly, LWT Pin Shipment
315-40-099	Sheets 1 - 3	Rev 3	Can Weldment, PWR/BWR Transport Canister

* Packaging Unit Nos. 1, 2, 3, 4 and 5 are constructed in accordance with this revision of drawing.

List of Drawings (continued)

315-40-100	Sheets 1 - 3	Rev 3	Lids, PWR/BWR Transport Canister
315-40-101		Rev 0	4 X 4 Insert, PWR/BWR Transport Canister
315-40-102		Rev 1	5 X 5 Insert, PWR/BWR Transport Canister
315-40-103		Rev 0	Pin Spacer, PWR/BWR Transport Canister
315-40-104	Sheets 1 - 2	Rev 3	Legal Weight Truck Transport Cask Assy, PWR/BWR Transport Canister
315-40-105	Sheets 1 - 2	Rev 3	PWR Insert PWR/BWR Transport Canister
315-40-106	Sheets 1 - 3	Rev 1	MTR Plate Canister, LWT Cask
315-40-108	Sheets 1 - 3	Rev 1	Weldment, 7 Cell Basket, Top Module, DIDO Fuel
315-40-109	Sheets 1 - 3	Rev 1	Weldment, 7 Cell Basket, Intermediate Module, DIDO Fuel
315-40-110	Sheets 1 - 3	Rev 1	Weldment, 7 Cell Basket, Base Module, DIDO Fuel
315-40-111		Rev 1	Legal Weight Truck, Transport Cask Assy, DIDO Fuel
315-40-113		Rev 0	Spacers, Top Module, DIDO Fuel
315-40-120	Sheets 1 - 3	Rev 2	Top Module, General Atomics IFM, LWT Cask
315-40-123	Sheets 1 - 2	Rev 1	Spacer, General Atomics IFM, LWT Cask
315-40-124		Rev 1	Transport Cask Assembly, General Atomics IFM, LWT Cask
315-40-125	Sheets 1 - 3	Rev 3	Transport Cask Assembly, Framatome/EPRI, LWT Cask
315-40-126	Sheets 1 - 2	Rev 2	Weldments, Framatome/EPRI, LWT Cask
315-40-127	Sheets 1 - 2	Rev 2	Spacer Assembly, TPBAR Shipment, LWT Cask
315-40-128	Sheets 1 - 2	Rev 2	Legal Weight Truck, Transport Cask Assy, TPBAR Shipment
032230		Rev A	RERTR Secondary Enclosure, General Atomics
032231		Rev A	HTGR Secondary Enclosure, General Atomics
032236		Rev B	RERTR Primary Enclosure, General Atomics
032237		Rev B	HTGR Primary Enclosure, General Atomics
315-40-129		Rev 1	Canister Body Assembly, Failed Fuel Can, PULSTAR
315-40-130		Rev 1	Assembly, Failed Fuel Can, PULSTAR
315-40-133	Sheets 1 - 2	Rev 1	Transport Cask Assembly, PULSTAR Shipment, LWT Cask
315-40-134		Rev 1	Body Weldment, Screened Fuel Can, PULSTAR Fuel
315-40-135		Rev 1	Assembly, Screened Fuel Can, PULSTAR Fuel
315-40-139		Rev 0	Legal Weight Truck Transport Cask Assy, ANSTO Fuel
315-40-140	Sheets 1 - 2	Rev 0	Weldment, 7 Cell Basket, Top Module, ANSTO Fuel
315-40-141	Sheets 1 - 2	Rev 0	Weldment, 7 Cell Basket, Intermediate Module, ANSTO Fuel
315-40-142	Sheets 1 - 2	Rev 0	Weldment, 7 Cell Basket, Base Module, ANSTO Fuel
315-40-145		Rev 0	Irradiated Hardware Lid Spacer Assembly, LWT Cask

1 GENERAL INFORMATION

This chapter of the NAC International, Legal Weight Truck spent fuel shipping cask (NAC-LWT) Safety Analysis Report (SAR) presents a general introduction to, and description of, the NAC-LWT cask. Terminology used throughout this report is presented in Table 1.1-1.

Shipment of the NAC-LWT cask by truck, ISO container, and/or by railcar, as a Type B(U)F-96 package, as defined in 10 CFR 71.4, is authorized for the following contents:

- PWR and BWR fuel assemblies¹;
- MTR fuel assemblies and plates;
- DIDO fuel assemblies, metallic fuel rods;
- 25 high burnup PWR and BWR fuel rods (including up to 14 fuel rods classified as damaged);
- 16 PWR MOX fuel rods (or mixed load of up to 16 PWR MOX and UO₂ PWR fuel rods) and up to 9 burnable poison rods (BPRs);
- TRIGA fuel elements and TRIGA fuel cluster rods;
- General Atomics (GA) High-Temperature Gas-Cooled Reactor (HTGR) and Reduced-Enrichment Research and Test Reactor (RERTR) Irradiated Fuel Materials (IFM);
- up to 700 PULSTAR fuel elements;
- spiral fuel assemblies; and
- MOATA plate bundles.

The authorized contents previously listed include both irradiated and unirradiated forms of the materials.

Irradiated hardware is also authorized to be shipped in the NAC-LWT cask by truck, ISO container, and/or by railcar, as a Type B(U)F-96 package, as defined in 10 CFR 71.4. Irradiated hardware is defined as solid, irradiated and contaminated fuel assembly structural or reactor internal component hardware, which may include fissile material, provided the quantity of fissile material does not exceed a Type A quantity and does not exceed the exemptions of 10 CFR 71.15, paragraphs (a), (b) and (c).

Shipment of the NAC-LWT cask by truck, ISO container, and/or by railcar, as a Type B(M)-96 package, as defined in 10 CFR 71.4, is also authorized for the following contents:

- up to 300 Tritium Producing Burnable Absorber Rods (TPBARs), of which two can be prefailed; and
- up to 55 TPBARs segmented during PIE, including segmentation debris.

In accordance with 10 CFR 71.59, the NAC-LWT cask is assigned a Criticality Safety Index (CSI) for criticality control of the approved contents as follows:

¹ NAC-LWT casks containing PWR and BWR fuel assemblies are to be transported on an open trailer with a personnel barrier.

- 100 for PWR fuel assemblies;
- 33.4 for package with any number of canned PULSTAR fuel;
- 12.5 for DIDO fuel assemblies and TRIGA payloads in a nonpoisoned basket and no canisters, or a canister loaded with up to two equivalent TRIGA elements;
- 5 for BWR fuel assemblies; and
- 0 for metallic fuels, spiral fuel assemblies, MOATA plate bundles, PWR and BWR rods, PWR MOX rods, MTR fuel assemblies, TRIGA fuel elements and fuel cluster rods, GA IFM elements, and intact PULSTAR fuel elements.

TPBARs do not contain fissile material and criticality assessments are not required. Solid, irradiated and contaminated hardware contents could include fissile material not exceeding a Type A quantity and the exemptions of 10 CFR 71.15, paragraphs (a), (b) and (c). A CSI of 0 is assigned for these contents for documentation purposes.

The estimated Transport Index (TI) for shielding for the prior listed contents is shown in Table 5.1.1-1. The actual TI for individual shipments will be determined in accordance with 10 CFR 71.4 by the licensee.

Table 1.1-1 Terminology and Notation

Cask Model	NAC-LWT
Package	The Packaging with its radioactive contents (payload), as presented for transportation (10 CFR 71.4). Within this report, the Package is denoted as the NAC-LWT cask or simply as the cask.
Packaging	The assembly of components necessary to ensure compliance with packaging requirements (10 CFR 71.4). Within this report, the Packaging is denoted as the NAC-LWT cask.
NAC-LWT Cask	This packaging consists of a spent-fuel shipping cask body and closure lid with energy absorbing impact limiters.
Contents (Payload)	<ul style="list-style-type: none">• 1 PWR assembly• up to 2 BWR assemblies• up to 25 PWR or BWR rods (including high burnup fuel rods and up to 14 fuel rods classified as damaged)• up to 16 PWR MOX fuel rods (or mixed contents of up to 16 PWR MOX and UO₂ PWR fuel rods) and up to 9 BPRs• up to 42 MTR fuel elements (including plates)• up to 42 DIDO fuel assemblies• up to 15 sound (cladding intact) metallic fuel rods• up to 9 damaged metallic fuel rods or 3 severely damaged metallic fuel rods in filters• up to 140 intact or damaged TRIGA fuel elements/debris• up to 560 intact or damaged TRIGA fuel cluster rods• 2 GA IFM packages• up to 300 TPBARs (including up to 2 prefailed TPBARs)• up to 55 TPBARs segmented into individual segments and segmentation debris• up to 700 intact or damaged PULSTAR fuel elements in either assembly or element form, including fuel debris• up to 42 intact spiral fuel assemblies (also referred to as Mark III spiral fuel). Spiral fuel assemblies may be cropped.• up to 42 intact MOATA plate bundles• any combination of individual ANSTO basket modules containing either spiral fuel assemblies or MOATA plate bundles up to a total of 42 assemblies/bundles• irradiated hardware
Impact Limiters	Aluminum honeycomb energy absorbers located at the ends of the cask.

Table 1.1-1 Terminology and Notation (cont'd)

Intact LWR Fuel (Assembly or Rod)	Spent nuclear fuel that is not Damaged LWR Fuel, as defined herein. To be classified as intact, fuel must meet the criteria for both intact cladding and structural integrity. An intact fuel assembly can be handled using normal handling methods, and any missing fuel rods have been replaced by solid filler rods that displace a volume equal to, or greater than, that of the original fuel rod.
Damaged LWR Fuel (Assembly or Rod)	<p>Spent nuclear fuel that includes any of the following conditions that result in either compromise of cladding confinement integrity or recognition of fuel assembly geometry.</p> <ol style="list-style-type: none">1. The fuel contains known or suspected cladding defects greater than a pinhole leak or a hairline crack that have the potential for release of significant amounts of fuel particles.2. The fuel assembly:<ol style="list-style-type: none">i. is damaged in such a manner as to impair its structural integrity;ii. has missing or displaced structural components such as grid spacers;iii. is missing fuel pins that have not been replaced by filler rods that displace a volume equal to, or greater than, that of the original fuel rod;iv. cannot be handled using normal handling methods.3. The fuel is no longer in the form of an intact fuel assembly and consists of, or contains, debris such as loose pellets, rod segments, etc.
Damaged Fuel (TRIGA)	TRIGA fuel (elements and cluster rods) having cladding failures greater than hairline cracks or pinhole leaks.
Fuel Debris (TRIGA)	TRIGA damaged fuel that does not maintain its structural integrity, including fuel particles, fuel debris, and broken fuel rods.
TPBAR	Tritium Producing Burnable Absorber Rod
Irradiated Fuel Material (IFM)	High-Temperature Gas-Cooled Reactor (HTGR/IFM) and Reduced-Enrichment Research and Test Reactor (RERTR/IFM) type TRIGA fuel entities produced by General Atomics.

Table 1.1-1 Terminology and Notation (cont'd)

PULSTAR Fuel Element	PULSTAR fuel rod. May be contained in either assembly, rod holder or can form for shipment. PULSTAR fuel elements may be intact or damaged.
Damaged PULSTAR Fuel Element	PULSTAR fuel rods having cladding failures greater than hairline cracks or pinhole leaks. The damaged fuel definition for PULSTAR fuel elements includes fuel debris. Damaged PULSTAR fuel elements may also be referred to as failed and must be transported in either of two types of PULSTAR cans.
Irradiated Hardware	Solid, irradiated and contaminated fuel assembly structural or reactor internal component hardware, which may include fissile material, provided the quantity of fissile material does not exceed a Type A quantity and does not exceed the exemptions of 10 CFR 71.15, paragraphs (a), (b) and (c). Authorized quantity of irradiated hardware and components is limited to 4,000 lbs (including spacers, dunnage and containers) and a gamma source term as defined in Table 1.2-13.
MOX Fuel Rods	The term as used in this SAR is defined as irradiated or unirradiated mixed uranium-plutonium oxide (MOX) fuel rods. The MOX fuel rods can be made with plutonium having various compositions of plutonium isotopes. The evaluated mixes of the various grades of plutonium are defined in the shielding (Chapter 5) and criticality (Chapter 6) evaluations.

1.1 Introduction

The NAC-LWT spent-fuel shipping cask has been developed by NAC International (NAC) as a safe means of transporting radioactive materials authorized as approved contents. The cask design is optimized for legal weight over the road transport, with a gross weight of less than 80,000 pounds. The cask provides maximum safety during the loading, transport, and unloading operations required for spent-fuel shipment. The NAC-LWT cask assembly is composed of a package that provides a containment vessel that prevents the release of radioactive material. The actual containment boundary provided by the package consists of a 4.0-inch thick bottom plate, a 0.75-inch thick, 13.375-inch inner diameter shell, an upper ring forging, and an 11.3-inch thick closure lid. The cask lid closure is accomplished using twelve, 1-inch diameter bolts. The cask has an outer shell, 1.20 inches thick, to protect the containment shell and also to enclose the 5.75-inch thick lead gamma shield. Neutron shielding is provided by a 5.0-inch thick neutron shield tank with a 0.24-inch (6mm) thick outer wall, containing a water/ethylene glycol mixture and 1.0 minimum weight percent (wt %) boron (58 wt % ethylene glycol; 39 wt % demineralized water; 3 wt % potassium tetraborate [K₂B₄O₇]). The neutron shield tank system includes an expansion tank to permit the expansion and contraction of the shield tank liquid without compromising the shielding or overstressing the shield tank structure. Aluminum honeycomb impact limiters are attached to each end of the cask to absorb kinetic energy developed during a cask drop, and limit the consequences of normal operations and hypothetical accident events.

The NAC-LWT is a legal weight truck cask designed to transport the following contents:

- 1 PWR assembly;
- up to 2 BWR assemblies;
- up to 15 sound metallic fuel rods;
- up to 42 MTR fuel elements;
- up to 42 DIDO fuel assemblies;
- up to 25 high burnup PWR fuel rods (including up to 14 rods classified as damaged);
- up to 25 high burnup BWR fuel rods (including up to 14 rods classified as damaged);
- up to 16 PWR MOX fuel rods (or a combination of 16 PWR MOX and UO₂ PWR rods) and up to 9 BPRs;
- up to 9 damaged metallic fuel rods;
- up to 3 severely damaged metallic fuel rods in filters;
- up to 140 TRIGA intact or damaged fuel elements/fuel debris (“TRIGA” is a Trademark of General Atomics);
- up to 560 TRIGA fuel cluster rods;
- 2 GA IFM packages;
- up to 300 TPBARs (of which two can be prefailed);

- up to 55 TPBARs segmented during post-irradiation examination (PIE), including segmentation debris; ,
- up to 700 PULSTAR fuel elements (intact or damaged);
- up to 42 spiral fuel assemblies;
- up to 42 MOATA plate bundles; or
- up to 4,000 lbs of solid, irradiated and contaminated hardware, which may include fissile material less than a Type A quantity and meeting the exemptions of 10 CFR 71.15, paragraphs (a), (b) and (c). Total allowed mass includes the weight of spacers, shoring and dunnage.

PWR or BWR fuel rods may be placed in a fuel rod insert (also referred to as a rod holder) or in a fuel assembly lattice. The lattice may be irradiated or unirradiated. Up to 14 of the fuel rods may be classified as damaged. Damaged fuel rods must be placed in a rod holder. Damaged fuel rods or rod sections may be encapsulated to facilitate handling prior to placement in the rod holder.

PWR MOX fuel rods (or a combination of PWR MOX and UO₂ PWR fuel rods) are required to be loaded in a screened or free flow PWR/BWR Rod Transport Canister with a 5 × 5 insert and transported in a leaktight configuration NAC-LWT.

PULSTAR fuel elements may be configured as intact fuel assemblies, may be placed into a fuel rod insert, i.e., a 4×4 rod holder (intact elements only), or may be loaded into one of two can designs, designated as the PULSTAR screened fuel can or the PULSTAR failed fuel can. Damaged PULSTAR fuel elements and nonfuel components of PULSTAR fuel assemblies must be loaded into cans. PULSTAR fuel cans may only be loaded into the top or base module of the 28 MTR basket assembly. Intact PULSTAR fuel assemblies and intact PULSTAR fuel elements in a TRIGA fuel rod insert may be loaded in any basket module.

Irradiated hardware may be loaded directly into the NAC-LWT cavity or preloaded into a canister or cage. Stainless steel dunnage may be used to limit the movement of the irradiated hardware within the cask cavity. The maximum gamma source term of the irradiated hardware shall be limited to that defined for the authorized PWR content condition as described in Chapter 5.

The NAC-LWT cask provides a testable containment for the contents during both normal operations and hypothetical accident conditions, satisfying the requirements of 10 CFR 71.51. Any number of NAC-LWT casks may be shipped at one time, each on its own vehicle.

NAC-LWT casks may be shipped in a closed International Shipping Organization (ISO) container when containing all fuel contents other than PWR and BWR fuel assemblies. NAC-LWT

casks containing PWR and BWR fuel assemblies are to be transported on an open trailer with a personnel barrier.

The terminology of MTR, DIDO and TRIGA fuel elements will be used independent of whether the element contains low, medium or high enriched uranium (i.e., LEU, MEU or HEU), except when required for analysis or loading purposes.

1.2 Package Description

This section presents a basic description of the NAC-LWT cask and the contents that may be transported. Drawings of the cask are presented within Section 1.4.

1.2.1 Packaging

1.2.1.1 Gross Weight

Gross shipping weight of the NAC-LWT spent-fuel shipping cask is approximately 52,000 pounds for the package. When mounted on the transport vehicle, the cask and vehicle weight is less than the 80,000-pound maximum for legal weight transport. A summary of overall component weights, detailed in Table 2.2.1-1, is listed below:

<u>Component</u>	<u>Weight (pounds)</u>
Cask Body	43,412
Closure Lid and Bolts	941
Payload and Basket	4,000 maximum
Impact Limiters	<u>2,855</u>
Total	51,208
SAR Analysis Weight	52,000

1.2.1.2 Materials of Construction, Dimensions, and Fabrication

The NAC-LWT cask body consists of Type 304 stainless steel forgings and closure lid with Type XM-19 stainless steel shells. Type XM-19 is a high strength stainless steel and is used in the inner and outer structural shells, which are more highly stressed than other cask components that use the more common Type 304 stainless steel. A lead gamma shield and a borated ethylene glycol/water solution neutron shield are utilized for radiation shielding. The cask provides the containment boundary for the payload and also acts as an environmental barrier. The cask is protected at each end by energy absorbing impact limiters, which consist of crushable aluminum honeycomb material with a thin aluminum shell. The impact limiters also provide thermal insulation, which protects the lid seals during the hypothetical fire transient event, although this thermal protection is conservatively neglected in this report. The cask is passively cooled because of its relatively low maximum heat loading of 2.5 kilowatts (kW). The overall arrangement of the NAC-LWT cask and design details are presented in the drawings within Section 1.4. The cask body, closure lid, and impact limiters are more fully described in the following sections.

1.2.1.2.1 Cask Body

The cask body is fabricated from Type 304 and Type XM-19 stainless steel. A poured lead gamma shield forms an annulus 5.75 inches thick and 174.9 inches long. The lead is enclosed between a 0.75-inch thick, 13.375-inch inner diameter Type XM-19 stainless steel inner shell and a 1.20-inch thick, 28.78-inch outer diameter Type XM-19 stainless steel outer shell. The Type 304 stainless steel bottom end forging of the cask is 4.0 inches thick, and the bottom also contains a 3.0-inch thick, 20.75-inch diameter lead disk enclosed by a 3.5-inch thick Type 304 stainless steel end cover.

As discussed in Chapter 8, installation of the lead into the cask is done in a carefully controlled manner. Temperatures of the inner and outer shells are continuously monitored and controlled during the lead pour and cooldown process. In addition, the welds connecting the inner and outer shells to the bottom end forging are not made until after the cooldown process is complete and the entire cask has reached a uniform temperature. Dimensional checks for straightness and ovality are also made before and after lead pour.

The upper ring forging is a Type 304 stainless steel ring 14.25 inches thick. This forging is machined to accept the closure lid and contains the penetrations to the cask cavity for the vent and fill/drain valves. Four lifting trunnions are welded to the forging to permit cask lifting and handling with a nonredundant or redundant lifting yoke.

Neutron shielding is provided by an ethylene glycol/water jacket that surrounds the 1.20-inch thick Type XM-19 stainless steel outer shell and is designed to axially blanket the active fuel length of the more common light water reactor fuels. The neutron shield region is 5.00 inches thick and 164.0 inches long. The external surface of the shield tank is a 0.24-inch thick Type 304 stainless steel shell with 0.50-inch thick end plates. An expansion tank for the neutron shield is provided to allow for thermal expansion and contraction of the liquid and is connected to the shield tank by a siphon tube. The liquid contains a solution of ethylene glycol/water and 1.0 wt % boron, which is added to reduce the secondary gamma radiation component.

The inner shell, end forgings, and the closure lid establish a cask cavity that is 177.9 inches long and 13.375 inches in diameter.

The weight of the cask body is approximately 43,412 pounds. The overall length of the cask body is 199.8 inches, and the maximum outside diameter is 44.24 inches at the neutron shield expansion tank.

1.2.1.2.2 Closure Lid

The cask closure lid is a Type 304 stainless steel forging 11.3 inches thick. The lid is machined to recess into the upper ring forging when it is installed on the cask. The closure lid and upper end forging are machined to provide a series of steps to prevent radiation streaming through the gap between the components. The closure lid attaches to the cask using 12 bolts with a 1-inch diameter. The containment boundary seal is achieved by a metallic O-ring captured in a groove machined on the underside of the closure lid (a second O-ring is provided to allow seal testing of the containment boundary O-ring). The O-rings mate against a machined sealing surface of the cask upper ring forging.

1.2.1.2.3 Impact Limiters

The impact limiters are fabricated from aluminum. The aluminum “honeycomb” has a crush strength of 3,500 psi. The honeycomb is a multidirectional crushable material that does not actually resemble a hexagonal honeycomb structure. The impact limiter is attached to the cask body at four locations. The outside diameter of the top end impact limiter is 65.25 inches and the bottom end impact limiter has a 60.25-inch diameter. The top and bottom impact limiters are 27.8 and 28.3 inches long, respectively, and both overlap the ends of the cask body by 12.0 inches.

1.2.1.3 Valves and Testing

The closure lid and the alternate and Alternate B drain and vent port covers each have a seal test port. The seal test port accesses the volume between the two O-ring seals on the cover or lid permitting leakage testing to verify proper sealing. The vent and drain valves are not considered part of the containment boundary and are used during in-plant loading operations to access the cask cavity for water filling and draining, vacuum drying, helium backfilling, etc.

1.2.1.4 Heat Dissipation

There are no special devices utilized on the NAC-LWT cask for the transfer or dissipation of heat. The package is passively cooled, which is possible because of its relatively low maximum heat load of 2.5 kW. A more detailed discussion of the package thermal characteristics is provided in Chapter 3.

1.2.1.5 Coolants

There are no coolants utilized within the package other than the normal transportation atmosphere of air or helium, depending on content conditions.

1.2.1.6 Protrusions

There are no outer protrusions on the package other than the four external lifting trunnions, the longitudinal shear ring at the upper end of the cask, and the eight impact limiter attachment lugs, four near each end of the package. All of these protrusions are located within the envelope protected by the impact limiters. The closure lid and valve port covers are recessed into the cask body and do not protrude from the cask surface. Refer to the drawings in Section 1.4 for more detail.

1.2.1.7 Lifting and Tiedown Devices

Of the four trunnions located on the exterior of the package at the upper end forging, two are intended for lifting with a nonredundant lifting yoke and the other two are used with a redundant lifting yoke. The package lifting and tiedown features are described in more detail in Section 2.5.

1.2.1.8 Shielding

A 5.75-inch annulus of lead and 2.19 inches of steel are maintained between the cask contents and the exterior radial surface of the package for the attenuation of radiation. Five inches of borated water are also provided for neutron shielding. The bottom end of the cask provides 7.5 inches of steel and 3.0 inches of lead shielding, and the closure lid provides 11.3 inches of steel shielding. Further detail is provided in Chapter 5.

1.2.2 Operational Features

The NAC-LWT cask is intended to be simple to operate. The cask is designed to be easily loaded and handled at any nuclear facility. The outer surface of the cask is electropolished and the configuration of the exposed surfaces aids in decontamination. An optional sleeving arrangement is available to limit contact between the cask and the contaminated pool water during wet loading and unloading.

The closure lid of the cask and the two valve port covers (alternate and Alternate B designs) are one-piece fixtures designed for ease of handling and to maintain personnel dose rates as low as reasonably achievable (ALARA). The closure lid has built-in alignment grooves (i.e. key ways) to facilitate installation. The alternate and Alternate B port cover designs provide clearance for valves underneath the port cover. The inner O-rings on the closure lid and the vent and drain valve port covers are components of the cask containment boundary. For the transport of TPBAR contents and other contents requiring a leaktight transport containment configuration (i.e., PWR MOX fuel rods), the cask is required to be configured with Alternate B drain and vent

port covers incorporating metallic seals. The transport arrangement drawings for TPBAR contents and PWR MOX fuel rod contents are presented in Section 1.4.

An alternative drain tube, including a drain tube alignment ring, is required to be installed and utilized when loading and transporting modular fuel baskets (i.e. not full length) and canisters.

The impact limiters and the personnel barrier are designed to be removed and installed without the aid of supplemental lifting gear or fixtures. All approved contents may be transported in an International Shipping Organization (ISO) container, except for PWR and BWR fuel assemblies.

All operational features are readily apparent from the drawings provided in Section 1.4.

Operational procedures are delineated in Chapter 7.

1.2.3 Contents of Packaging

The NAC-LWT cask is analyzed as presented in this SAR for the transport of the following contents:

- 1 PWR assembly;
- up to 2 BWR assemblies;
- up to 15 sound metallic fuel rods;
- up to 42 MTR fuel elements;
- up to 42 DIDO fuel assemblies;
- up to 25 PWR fuel rods (including up to 14 rods classified as damaged);
- up to 25 BWR fuel rods (including up to 14 rods classified as damaged);
- up to 16 PWR MOX fuel rods (or a combination of up to 16 PWR MOX and UO₂ fuel rods) plus up to 9 BPRs;
- up to 9 failed metallic fuel rods;
- up to 3 severely failed metallic fuel rods in filters;
- up to 140 TRIGA fuel elements;
- up to 560 TRIGA fuel cluster rods;
- 2 GA IFM packages;
- up to 300 TPBARs (of which two can be prefailed);
- up to 55 TPBARs segmented during PIE, including segmentation debris;
- up to 700 PULSTAR fuel elements (intact or damaged);
- up to 42 spiral fuel assemblies;
- up to 42 MOATA plate bundles;
- any combination of individual ANSTO basket modules containing either spiral fuel assemblies or MOATA plate bundles up to a total of 42 assemblies/bundles; or
- up to 4,000 lbs of solid, irradiated and contaminated hardware, which may include fissile material less than a Type A quantity and meeting the exemptions of 10 CFR 71.15,

paragraphs (a), (b) and (c). Total allowed mass includes the weight of spacers, shoring and dunnage.

Shipments in the NAC-LWT package shall not exceed the following limits:

1. The maximum contents weight shall not exceed 4,000 pounds.
2. The limits specified in Table 1.2-1 through Table 1.2-13 for the fuel and other radioactive contents shall not be exceeded.
3. Any number of casks may be shipped at one time, one cask per tractor/trailer vehicle.
4. The maximum decay heat shall not exceed the following: 2.5 kW for PWR fuel assemblies, 2.2 kW for BWR fuel assemblies, 2.3 kW for 25 high burnup PWR fuel rods, 2.1 kW for 25 high burnup BWR fuel rods, 2.3 kW for 16 PWR MOX/ UO_2 fuel rods, 1.26 kW for MTR fuel, 1.05 kW for DIDO fuel assemblies, 1.05 kW for TRIGA fuel elements or fuel cluster rods, 13.05 W for GA IFM packages, 0.693 kW for 300 TPBARs, 0.127 kW for TPBAR segments; 0.84 kW for the PULSTAR fuel contents, 0.756 kW for spiral fuel assemblies (0.126 kW per basket), 0.126 kW for MOATA plate bundles (21 W per basket), and 1.26 kW for solid, nonfissile, irradiated hardware.
5. Radiation levels shall meet the requirements delineated in 10 CFR 71.47 or 49 CFR 173.441. The neutron shield tank may be drained for shipment of metallic fuel rods.
6. Surface contamination levels shall meet the requirements of 10 CFR 71.87(i) or 49 CFR 173.443.
7. TRIGA damaged fuel and fuel debris (up to two equivalent elements) will be shipped in a sealed or screened failed fuel can.
8. TRIGA damaged fuel elements will be transported in a sealed failed fuel can (maximum of two) or in a screened can (maximum of four).
9. MTR fuel elements may consist of any combination of intact or damaged highly enriched uranium (HEU), medium enriched uranium (MEU) or low enriched uranium (LEU) fuel elements that are enveloped by the parameters listed in Table 1.2-4, as supported by information presented in Table 5.1.1-2, Table 6.4.3-21, Table 6.4.3-22, Table 6.4.3-25 and Table 6.4.3-28.
10. High burnup PWR fuel rods will be shipped in either sealed, free flow or screened cans.
11. High burnup BWR fuel rods will be shipped in either sealed, free flow or screened cans.
12. Up to 25 high burnup PWR or BWR fuel rods in a fuel assembly lattice or rod holder. Up to 14 of the fuel rods in a rod holder may be classified as damaged. Damaged fuel rods or rod sections may be placed into fuel rod capsules prior to placing them in the fuel rod holder. Typical failed fuel rod capsule configuration is shown in Figure 1.2-11.
13. Production TPBARs will be shipped in an open top consolidation canister as shown in Figure 1.2.3-10 and assembled in the cask as shown in Figure 1.2.3-12.
14. Intact PULSTAR fuel elements may be loaded into a fuel rod insert or the PULSTAR screened or failed fuel can.

15. Damaged PULSTAR fuel elements and nonfuel components of PULSTAR fuel assemblies shall be loaded into either a PULSTAR failed fuel or screened fuel can, and placed into the top or base module of the 28 MTR fuel basket. Damaged fuel, including fuel debris, may be placed in an encapsulating rod prior to loading in a PULSTAR can.
16. Any combination of spiral fuel assemblies or MOATA plate bundles, each loaded into separate ANSTO basket modules containing up to a total of 42 assemblies/bundles.
17. Segmented TPBARs will be shipped in a sealed, dry Waste Container as shown in Figure 1.2.3-16 and assembled in the cask as shown in Figure 1.2.3-17.
18. Solid, irradiated and contaminated hardware containing less than a Type A quantity of fissile material and meeting the exemptions of 10 CFR 71.15, paragraphs (a), (b) and (c), loaded directly into the cask or contained in a secondary container or basket. The irradiated hardware spacer will be installed to limit the axial movement of the hardware above the lead shielded region of the cask body. As needed, additional secondary containers, dunnage and shoring may be used to limit the movement of the contents during normal and accident conditions of transport.
19. PWR MOX fuel rods (or a combination of PWR MOX and UO₂ PWR fuel rods) are required to be loaded in a screened or free flow PWR/BWR Rod Transport Canister provided with a 5 × 5 insert and transported in a leaktight configuration NAC-LWT.

1.2.3.1 TRIGA Fuel and Basket Description

Two basic types of TRIGA fuel are to be transported in the NAC-LWT cask: TRIGA fuel elements and smaller fuel rods from TRIGA fuel cluster assemblies. TRIGA fuel elements are approximately 1-1/2 inches in diameter and are described in Section 1.2.3.1.1. TRIGA fuel cluster rods are smaller, approximately 1/2-inch in diameter, and are also described in Section 1.2.3.1.1.

Up to 140 TRIGA fuel elements in the form of: a) standard fuel elements – either aluminum clad or stainless steel clad; b) instrumented fuel elements – similar to standard fuel elements (aluminum clad or stainless steel clad), but containing thermocouple instrumentation; and c) fuel follower control rod elements (aluminum or stainless steel clad) – poison rods with a fuel follower in a single tube may be shipped in the NAC-LWT cask. Up to 560 TRIGA fuel cluster rods may also be shipped. Up to the equivalent of two damaged fuel elements and debris may be loaded and shipped in either a sealed or screened failed fuel can. The transport baskets and failed fuel cans are described in Section 1.2.3.1.2.

1.2.3.1.1 TRIGA Fuel

TRIGA Fuel Elements

The characteristics of the design basis TRIGA fuel element are presented in Table 1.2-4 and in Table 1.2-1 for the poisoned basket and in Table 1.2-2 for the nonpoisoned basket.

The fuel material in a TRIGA fuel element is a solid, homogeneous mixture of uranium-zirconium hydride alloy, i.e., a metal alloy fuel. Both the aluminum-clad and the stainless steel-clad TRIGA fuel elements are approximately 1.5-inch diameter rods by approximately 30 inches long. The fuel follower control rod elements range in length from 45 inches to 66.5 inches. Instrumented fuel elements are identical to standard fuel elements with the exception of thermocouples and wires and lead-out tubing. The lead-out tubing needs to be detached prior to shipment in order for the instrumented fuel elements to fit into the standard element height envelope. The aluminum-clad TRIGA fuel element and instrumented fuel element, the stainless steel-clad TRIGA fuel element and instrumented fuel element, and the standard fuel follower control rod element are shown in Figure 1.2.3-1 through Figure 1.2.3-5, respectively.

TRIGA Fuel Cluster Rods

The design basis TRIGA cluster rod characteristics are shown in Table 1.2-3.

The fuel material in TRIGA fuel cluster rods is a solid, homogeneous mixture of uranium-zirconium-erbium hydride alloy, i.e., a metal alloy fuel. Erbium is a burnable neutron poison that is used in the fuel to enhance the flux profile along the length of the fuel rod, and conservatively ignored in the nuclear evaluations. The rods have an external diameter of approximately 0.55 inch and are approximately 31 inches long. The rod cladding is Incoloy 800 material and is 0.015 inch thick, minimum. Instrumented rods are identical to the standard rods, with the exception of thermocouples and wires. A diagram of the TRIGA fuel cluster rods, and the individual fuel pin (cluster rod) making up the cluster, is shown in Figure 1.2.3-6.

The active fuel region of a TRIGA fuel cluster rod is a maximum of 0.53 inch in diameter, 22.5 inches in length, and has an initial uranium enrichment of up to 93.3 percent. A compression spring is utilized to fill the space in the plenum region of the rod, and top and bottom plugs are used to seal the fuel within the rod. The design-basis TRIGA fuel cluster rod characteristics are summarized in Table 1.2-3, Table 1.2-4, and Tables 5.1.1-1, 5.1.1-2, 6.2.6-1 and 6.2.6-2.

Axial fuel spacers, as shown on Drawing 315-40-085, may be used to axially position the TRIGA fuel elements. The axial spacers do not provide a safety function and are dunnage used to position the fuel elements to facilitate fuel handling. The total weight per basket module cell for the TRIGA fuel elements or cluster rods, spacer(s) and fuel cans, as applicable, shall be limited to a maximum of 80 pounds.

TRIGA Fuel Classification

The TRIGA fuel contents are divided into three categories based on fuel condition for evaluation, loading configuration and transport in the NAC-LWT:

1. Intact fuel, including fuel elements and cluster rods with no more than minor cladding failures (hairline cracks and pinhole leaks), are loaded directly into the TRIGA fuel basket modules (Section 1.2.3.1.2) with a maximum of four fuel elements per loading position. Intact cluster rods are loaded into fuel rod inserts (Drawing 315-40-096) that are inserted into the TRIGA fuel basket module cell openings. Intact fuel elements may be loaded into a screened failed fuel can if length permits.
2. Damaged fuel elements having cladding damage greater than hairline cracks and pinhole leaks, but with structural integrity, may be loaded into a screened fuel can (maximum of four elements) or into a sealed fuel can (maximum of two elements), and then loaded into a base or top basket module.
3. Fuel debris (equivalent to two fuel elements) shall be loaded into either sealed or screened failed fuel cans (Section 1.2.3.1.2). The two equivalent elements of fuel debris can be loaded in either a screened or sealed failed fuel can, which is then loaded into either a base or a top module of the TRIGA fuel basket and then stacked into the NAC-LWT.

1.2.3.1.2 TRIGA Fuel Baskets and Failed Fuel Cans

The TRIGA fuel basket assembly configurations consist of five modules – a base module, 3 intermediate modules, and a top module. The 3 intermediate modules are interchangeable, but the base and top modules are required to be in their proper positions. Two basket configurations are available, “nonpoisoned” and “poisoned,” where the poisoned basket configuration utilizes borated steel plates for additional criticality control. Each module has up to 7 cells (fuel positions) for loading TRIGA fuel elements or cluster rods. The center cell of each module of the nonpoisoned basket configuration is blocked by a welded stainless steel baffle that prevents loading of that cell. The nonpoisoned configuration is also referred to as the 24-element basket or the 120-element loading, based on the maximum of 120 intact TRIGA fuel elements that may be loaded into the baskets in this configuration. The poisoned configuration is also referred to as the 28-element basket or the 140-element loading, based on the maximum of 140 intact TRIGA fuel elements that may be loaded into the baskets in this configuration. Additionally, the nonpoisoned configuration can accommodate up to 480 intact TRIGA fuel cluster rods, while the poisoned basket can hold up to 560 intact TRIGA fuel cluster rods. Each basket module is a Type 304 stainless steel weldment consisting of longitudinal divider plates with circular support plates near each end; the top module also has a support plate at its midpoint due to its longer length. In addition, the poisoned basket modules contain four borated stainless steel plates that are seal welded to surfaces of the divider plates in the central region of the basket cross-section. The nonpoisoned basket modules are shown in Drawings 315-40-070, -071, and -072 included in Section 1.4. The poisoned basket modules are shown in Drawings 315-40-080, -081, and -082.

The nonpoisoned TRIGA fuel basket assembly in the NAC-LWT cask is shown in Drawing 315-40-079. The poisoned basket assembly in the NAC-LWT cask is shown in Drawing 315-40-084. In the poisoned basket configuration, an alternate assembly is presented that utilizes one base module and four intermediate modules, along with a spacer (Drawing 315-40-083). The spacer is utilized to fill the space differential in the cask cavity resulting from the use of an additional intermediate module, rather than a top module. This additional assembly configuration is provided for flexibility in situations where the extra length provided by the top module is not needed. The fuel basket modules are described in further detail in Section 2.6.12.8.

As described in Section 1.2.3.1.1, up to four TRIGA intact or damaged clad fuel elements may be loaded into each screened failed fuel can, or up to the equivalent of two TRIGA fuel elements as fuel debris. The screened failed fuel cans are required to be loaded into either a base or a top basket module of the TRIGA fuel basket assembly. The screened failed fuel can is a tube, approximately 3-1/4 inches square, constructed of 14 gage sheet. The bottom of the screened failed fuel can is a perforated 1/2-inch thick plate with the openings covered by a 250 mesh filter screen. The lid for the screened failed fuel can includes a bail for lifting and two spring-loaded plungers that engage slots in the side of the can for locking purposes. The screened failed fuel can is constructed of austenitic stainless steel as shown on Drawings 315-40-074, -075, and -076.

The sealed failed fuel can is designed to contain two damaged TRIGA fuel elements, up to two equivalent damaged TRIGA fuel elements as fuel debris, or six failed TRIGA fuel rod clusters and fuel debris. The sealed failed fuel canisters are required to be loaded into either a base or a top module of the TRIGA fuel basket assembly to comply with the criticality analyses.

The sealed failed fuel can is a 3.25-inch outside diameter tube with a 0.065-inch thick wall. The bottom of the sealed failed fuel can includes a check valve and drain plug to facilitate draining of the can. The top of the sealed failed fuel can is closed by a bolted lid that is sealed with a metallic O-ring and includes a diaphragm valve to facilitate draining, drying, and helium backfilling of the can. The sealed failed fuel can is constructed of austenitic stainless steels as shown on Drawings 315-40-086, -087, -088.

1.2.3.2 MTR and DIDO Fuel and Basket Description

The MTR fuel elements to be shipped are 33 to 57 inches long, including the upper and lower nonfuel-bearing hardware, which may be removed from the element prior to transport. The MTR element fuel plates consist of a U-Al, U₃O₈-Al, or U₃Si₂-Al fuel meat clad with aluminum. The fuel plates are held in a parallel arrangement with two thick aluminum slotted pieces to form a fuel element. The active fuel region is typically 22.75 inches in height, and the fuel meat is typically 0.023-inch thick. MTR elements/plates may contain cadmium wires. A maximum 100-gram cadmium source is addressed in the shielding evaluations documented in Chapter 5. Axial

fuel spacers and plates may be used in the cells of the basket modules to position MTR elements to facilitate fuel unloading and handling. The axial fuel spacers do not perform a safety function and are considered dunnage. The axial fuel spacers and plates are shown on Drawing 315-40-085.

A maximum of 42 MTR fuel elements has been analyzed for transport in the NAC-LWT cask. This configuration consists of up to seven fuel elements placed radially in each of the six axial fuel basket modules. Two alternate configurations of MTR fuel element loading provide for loads of 35 elements in five basket modules or 28 elements in four basket modules. HEU MTR fuel elements having $> 380 \text{ g } ^{235}\text{U}$, but less than $460 \text{ g } ^{235}\text{U}$, shall have a minimum of 2.0 cm (0.8 inch) of nonfuel hardware and/or spacers/plates at both ends of the fuel element. The minimum 2.0 cm nonfuel hardware and/or spacer/plate dimension assures criticality control. The axial fuel spacer and plate design is shown on Drawing 315-40-085. For the shipment of MTR fuel elements (or an equivalent number of plates in a plate canister) having ^{235}U greater than 470 g per element, or greater than 22 g per plate (up to a maximum of 640 g per element or 32 g per plate), the maximum quantity of elements per basket module is limited to four, which are to be loaded in basket positions 4, 5, 6 and 7. Cell block spacers shall be installed in basket openings 1, 2 and 3 to block these cells from being inadvertently loaded with fuel elements. The cell block spacer design is shown on Drawing 315-40-085. Therefore, for the transport of elements of greater than $470 \text{ g } ^{235}\text{U}$, if only one element exceeds the 470 g (22 g per plate) limit, a maximum of four elements shall be loaded into the seven-element basket module and cell block spacers shall be placed in basket opening positions 1, 2 and 3.

Loose MTR fuel plates may be shipped in an MTR plate canister to facilitate handling. The contents of the canister are limited to the number of plates in the original intact fuel assembly, and the fuel plate dimensions and fuel masses must be bounded by the MTR fuel element limits in Table 1.2-4. The total weight per basket module cell for the fuel element, spacer(s) and fuel plate canister, as applicable, shall be limited to a maximum of 80 pounds.

A maximum of 42 DIDO fuel assemblies has been analyzed for transport in the NAC-LWT cask. Again, up to seven fuel assemblies may be placed radially in each of six axial fuel basket modules.

DIDO fuel assemblies are similar to MTR fuel elements in that the fuel bearing hardware consists of plates of fuel meat sandwiched by cladding. However, in DIDO fuel, the plates have been formed into tubular elements that are arranged in a concentric configuration. Typical DIDO assemblies contain four of the concentric tubes.

MTR and DIDO fuel characteristics are presented in Table 1.2-4.

1.2.3.3 General Atomics Irradiated Fuel Material (GA IFM) and Basket Description

The GA IFM is made up of two separate types of fuel material—the High-Temperature Gas-Cooled Reactor (HTGR) type fuel and the Reduced-Enrichment Research and Test Reactor (RERTR) type fuel. Each type of IFM is packaged in its own unique Fuel Handling Unit (FHU). Figures 1.2-7 and 1.2-8 illustrate the HTGR and RERTR FHUs. Detailed drawings for the GA and IFM FHUs are in Section 1.4.

The HTGR IFM is comprised of fuel in four forms: fuel particles (kernels), fuel particles (coatings), fuel compacts (rods), and fuel pebbles. Fuel kernels are solid, spheridized, high-temperature sintered fully-densified, ceramic kernel substrate, composed of: UC_2 , UCO , UO_2 , $(Th,U)C_2$, or $(Th,U)O_2$. The as-manufactured enrichment of the HTGR fuel varies from ~10.0 to 93.15 wt % ^{235}U . Fuel coatings are solid, spheridized, isotropic, discrete multi-layered fuel particle coatings with chemical composition including pyrolytic-carbon (PyC) and silicon carbide (SiC). Fuel compacts are multi-coated ceramic fuel particles, bound in solid, cylindrical, injection-molded, high-temperature heat-treated compacts. The fuel compact matrix is composed of carbonized graphite shim, coke, and graphite powder. Fuel pebbles are multi-coated fuel particles, bound in solid, spherical injection-molded, high-temperature heat-treated pebbles. The fully-cured binding matrix is composed of carbonized graphite shim, coke, and graphite powder.

The RERTR IFM is comprised of 20 irradiated TRIGA fuel elements; 13 of the elements are intact and the remaining seven have been previously sectioned for examination purposes. Parameters characterizing the RERTR/TRIGA fuel elements are shown in Table 6.2.9-1. Three distinct mass loadings of uranium were used in the 20 TRIGA elements: 20, 30, and 45 wt % U; the average mass of the fueled portion of these elements is 551g with an enrichment of 19.7 wt % ^{235}U . The RERTR IFM consists of U-ZrH metal alloy fuel material and as a solid meets the requirement of 10 CFR 71.63.

Two GA IFM Fuel Handling Units (FHU) are intended for a single shipment in the NAC-LWT. The first IFM FHU contains HTGR type fuel and the second contains RERTR type fuel. Each IFM FHU consists of stainless steel weld-encapsulated primary and secondary enclosures. The FHUs are filled and sealed with air at atmospheric pressure. The two IFM FHUs are placed in the top of the NAC-LWT cavity with a bottom spacer to facilitate unloading of the IFM packages.

The GA IFM fuel characteristics are presented in Table 1.2-7.

1.2.3.4 PWR Fuel

The NAC-LWT cask is analyzed for the PWR fuel assemblies listed in Table 1.2-5. This table provides the dimensional and enrichment constraints for the PWR fuel. The burnup and decay heat limits are specified in Table 1.2-4.

1.2.3.5 BWR Fuel

The NAC-LWT cask is analyzed for the BWR fuel assemblies listed in Table 1.2-6. This table provides the dimensional constraints for the BWR fuel. The enrichment, burnup and decay heat limits are specified in Table 1.2-4.

1.2.3.6 TPBARs

The NAC-LWT cask is analyzed for the transport of two separate Tritium Producing Burnable Absorber Rod (TPBAR) content configurations. For the transport of production TPBARs from the reactor facility to the DOE processing facility, an open (i.e., unsealed) stainless steel consolidation canister is utilized to contain up to 300 TPBARs, two of which can be prefailed. The characteristics of the production TPBARs are listed in Table 1.2-8. The consolidation canister assembly is shown in Figure 1.2.3-10.

The second transport configuration is for the shipment of segmented TPBARs, following post-irradiation examination (PIE), contained in a welded stainless steel waste container containing segments and debris from up to 55 TPBARs. The characteristics of the TPBAR PIE segments are provided in Table 1.2-12. The waste container and extension weldment assembly is shown in Figure 1.2.3-16.

TPBARs are similar in size and nuclear characteristics to standard, commercial PWR, stainless steel-clad burnable absorber rods. The exterior of a typical TPBAR is a stainless steel clad tube. The internal components of the TPBAR are designed and selected to produce and retain tritium. Internal configurations differ for various TPBAR designs (see DOE reports provided in the Chapter 1 Appendices). The internal components of a typical TPBAR include a plenum spacer tube (getter tube), a spring clip or a plenum (compression) spring, pellet stack assemblies (pencils), and a bottom spacer tube. A pencil consists of a zirconium alloy liner around which lithium aluminate absorber pellets are stacked and then confined in a getter tube as shown in Figure 1.2.3-9. The unclassified design details of the various TPBAR designs are provided in the unclassified DOE documents and drawings provided in the Chapter 1 Appendices.

The transport assembly arrangements for both TPBAR content configurations are identical and include a closure lid spacer assembly, a TPBAR basket and Alternate B port covers with bolting

installed. The detailed requirements for the NAC-LWT assembly are provided in license drawing 315-40-128 in Section 1.4. The overall payload arrangement for the NAC-LWT with the consolidation canister and waste container are shown in Figure 1.2.3-12 and Figure 1.2.3-17, respectively. For the transport of fewer than 300 TPBARs in the consolidation canister, stainless steel dunnage may be used to align and protect the contents. The weight and volume of the dunnage and the reduced TPBAR contents of the consolidation canister must be less than, or equal to, the weight and volume of 300 TPBARs.

The TPBAR content conditions are analyzed and evaluated for compliance with structural, thermal, containment and shielding conditions of the NAC-LWT in the appropriate SAR chapters. TPBARs do not contain fissile material and, therefore, criticality evaluations have not been performed. The operating procedures for the wet and dry loading and dry unloading of the TPBAR contents are provided in Chapter 7. The special leakage and pressure testing requirements for NAC-LWT casks intended for the transport of TPBAR contents are provided in Chapter 8.

1.2.3.7 Cladding for PWR/BWR Fuel

The PWR and BWR fuel rod cladding is of Zirconium alloy type (Zircaloy-2, Zircaloy-4, Zirlo, M-5, etc.). Minor variations of alloy composition have no impact on performance of cladding material.

1.2.3.8 PULSTAR Fuel Element and Transport Configuration Description

PULSTAR fuel elements are transported in the NAC-LWT in the 28 MTR fuel basket assembly, which contains four modules with seven cells per module. The basket assembly is composed of a top module, a base module, and two intermediate modules (Dwgs 315-40-051, -049, and -050, respectively).

PULSTAR fuel elements may be loaded into the module cells in one of four configurations:

a) intact PULSTAR fuel assemblies b) intact PULSTAR fuel elements loaded into the 4x4 TRIGA fuel rod insert (Dwg. 315-40-096); c) intact or damaged PULSTAR fuel elements, fuel debris and nonfuel-bearing components of PULSTAR fuel assemblies in the PULSTAR screened can (Dwg. 315-40-135); or d) intact or damaged PULSTAR fuel elements, fuel debris and nonfuel-bearing components of PULSTAR fuel assemblies in the PULSTAR sealed can (Dwg. 315-40-130). The contents of either can type are restricted to a quantity of fissile material and a total volume of material equivalent to 25 PULSTAR fuel elements. The sealed cask contents are restricted to the displaced volume of 25 intact PULSTAR fuel elements. The total cask payload shall not exceed 700 PULSTAR fuel elements. Loading of modules with mixed PULSTAR

payload configurations is allowed, but PULSTAR cans, either screened or sealed, are restricted to loading in the base and top modules.

PULSTAR fuel elements are low enriched (< 7 wt%) uranium oxide rods, with zirconium alloy cladding. During reactor operation, 25 PULSTAR fuel elements are arranged in a rectangular 5×5 lattice, surrounded by a zirconium alloy box, and capped by top- and bottom-end fittings to form a PULSTAR fuel assembly. The nonfuel components of a PULSTAR fuel assembly are primarily aluminum and zirconium alloy and do not contain a significant activation source. A sketch of a PULSTAR fuel assembly is provided in Figure 1.2.3-13. Key physical, radiation protection and thermal characteristics of the PULSTAR fuel assembly/elements are listed in Table 1.2-9.

The sealed and screened PULSTAR cans are stainless steel containers that: a) minimize the dispersal of gross fuel particles that may escape from damaged fuel element cladding and/or fuel debris; b) facilitate retrieval of the contents from the transportation cask; and c) confine damaged fuel and/or debris within a known volume to facilitate criticality control, maintain dose limits, and control thermal loads within the cask. PULSTAR fuel pellets, pieces, and debris may be placed in an encapsulating rod for handling purposes prior to placement into either a sealed or screened can. The encapsulating rod is not required and has no safety significance. In addition to fuel elements, the cans may contain fuel assembly hardware up to the total content weight limit specified in Table 1.2-9. For operational/retrievability purposes, stainless steel rod inserts may be used to position the PULSTAR fuel elements within the fuel rod insert. Total content weight shall not exceed the total weight limit specified in Table 1.2-9. The fuel rod insert is composed of a 4×4 grid of 0.75-inch OD × 0.065-inch wall stainless steel tubes. The tubes provide structural support for individual intact PULSTAR fuel elements during transport in the NAC-LWT.

Spacers may be used to axially position PULSTAR fuel contents near the top of the module for ease of loading and unloading operations. The spacers are provided for ease of operations and do not provide a safety function.

1.2.3.9 ANSTO Basket and Payload Description

Two basic fuel types are to be transported in the ANSTO baskets within the NAC-LWT cask: spiral fuel assemblies and MOATA plate bundles. Spiral fuel assemblies are composed of cylindrical aluminum inner and outer shells connected by curved metallic fuel plates. Further detail on the spiral fuel assemblies is provided in Section 1.2.3.9.1. MOATA plate bundles are comprised of up to 14 MTR fuel plates. Further detail on the plate bundles is provided in Section 1.2.3.9.2. Spiral fuel assemblies and MOATA plate bundles shall be intact. Note that spiral

assemblies may be cropped by removing nonfuel-bearing hardware to fit within the basket tubes. Cropped spiral fuel assemblies are classified as intact fuel.

Up to 42 spiral fuel assemblies or 42 MOATA plate bundles may be loaded. A full cask load contains 6 baskets of up to 7 fuel assemblies or plate bundles per basket. The mixed loading of ANSTO basket modules containing either spiral fuel assemblies or MOATA plate bundles is authorized.

1.2.3.9.1 Spiral Fuel Assemblies

The design basis characteristics of spiral fuel assemblies are presented in Table 1.2-10. The fuel material in spiral fuel assembly plates is a solid, homogeneous mixture of uranium-aluminum alloy, i.e., a metal alloy fuel. The fuel meat of each plate is clad in aluminum. A set of 10 curved fuel plates is located between an inner and outer cylindrical aluminum shell. Fuel elements are cropped to fit axially within the basket envelope. Fuel material is not cut during the cropping operation. The fuel plates are located in a spiral pattern, maintaining a constant pitch between fuel plate centers. A sketch of the assembly cross-section is provided in Figure 1.2.3-14.

1.2.3.9.2 MOATA Plate Bundles

The design basis characteristics of MOATA plate bundles are presented in Table 1.2-4. The fuel material in the plate bundle is a solid, homogeneous mixture of uranium-aluminum alloy, i.e., a metal alloy fuel. Each plate is clad in aluminum. A plate bundle is comprised of up to 14 fuel plates. Two thick (0.635 cm) aluminum nonfuel side plates support the fuel plate stack from two sides, making a possible total of 16 plates per bundle. At each axial end, the plates in the stack are connected by a pin. Spacing between plates is maintained by disk spacers placed onto the top and bottom pins between each fuel plate and the aluminum side plates. A sketch of a typical MOATA plate bundle is provided in Figure 1.2.3-15.

1.2.3.10 Solid, Irradiated and Contaminated Hardware

The design basis characteristics of the solid, irradiated and contaminated hardware are provided in Table 1.2-13. As described in the content definition, the solid, irradiated and contaminated hardware may contain small quantities of fissile materials. Fissile materials in the irradiated hardware contents are acceptable if the quantity of fissile material does not exceed a Type A quantity and does not exceed the exemptions of 10 CFR 71.15, paragraphs (a), (b) and (c).

The irradiated hardware may be directly loaded into the NAC-LWT cask cavity, or may be contained in a secondary container or basket. As needed, appropriate component spacers, dunnage and shoring may be used to limit the movement of the contents during normal and accident conditions of transport.

To ensure that the movement of the irradiated hardware contents above the lead shielded length of the NAC-LWT cask body (i.e., the approximately upper 6.25 inches of the cavity length) is precluded, an Irradiated Hardware Lid Spacer as shown on Drawing No. 315-40-145 shall be installed for all irradiated hardware content configurations. The total installed height of the spacer is 6.5 inches. Therefore, the available cavity length for the irradiated hardware is approximately 171 inches. The NAC-LWT cask shall be assembled for transport as shown on NAC Drawing No. 315-40-01 with the irradiated hardware spacer installed on the lid.

A comparative shielding evaluation for a conservatively selected irradiated hardware transport configuration (i.e., a single line source with no self-shielding) or consideration of the additional shielding provided by additional spacers, dunnage, inserts or secondary containers is presented in Chapter 5. The evaluations show that the regulatory dose rate requirements per 10 CFR 71.47 for normal conditions of transport, or 10 CFR 71.51(b) under hypothetical accident conditions, are not exceeded.

1.2.3.11 PWR MOX Fuel Rods

The NAC-LWT cask is analyzed and evaluated for the transport of up to 16 PWR MOX fuel rods (or a combination of up to 16 PWR MOX and UO₂ fuel rods) loaded into a 5 × 5 insert placed in a screened or free flow PWR/BWR Rod Transport Canister and transported in a leaktight containment configuration (i.e., closure lid with metallic seal and vent and drain Alternate B port covers with metallic seals) verified by helium leakage testing to be leaktight to less than or equal to 1×10^{-7} ref cc/s (less than or equal to 2×10^{-7} cc/s, helium). The authorized characteristics of the evaluated PWR MOX fuel rods are provided in Table 1.2-4. For mixed PWR MOX and UO₂ PWR fuel rod combinations, the UO₂ PWR fuel rods may have the identical heat load, burnup and cool time characteristics as the PWR MOX fuel rods.

In addition to the 16 PWR MOX fuel rods (or a combination of PWR MOX and UO₂ PWR fuel rods), up to 9 burnable poison rods (BPRs) may be loaded in the remaining openings in the 5 × 5 insert in the PWR/BWR Rod Transport Canister.

Figure 1.2.3-1 Aluminum Clad TRIGA Fuel Element

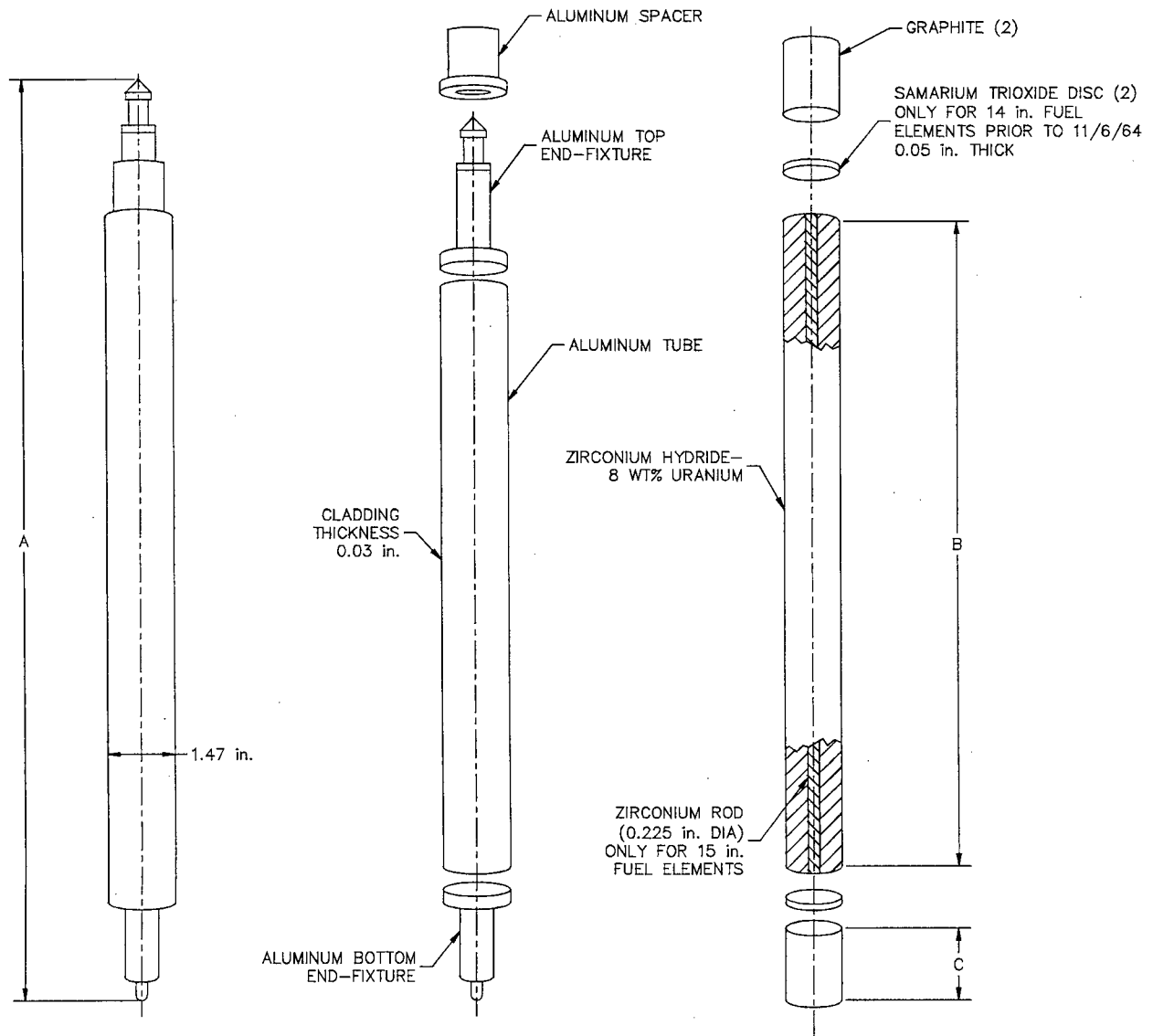


Figure 1.2.3-2 Aluminum Clad Instrumented Fuel Element

NOTE:
FOR OTHER FUEL
ELEMENT DIMENSIONS
SEE FIGURE 3-1.

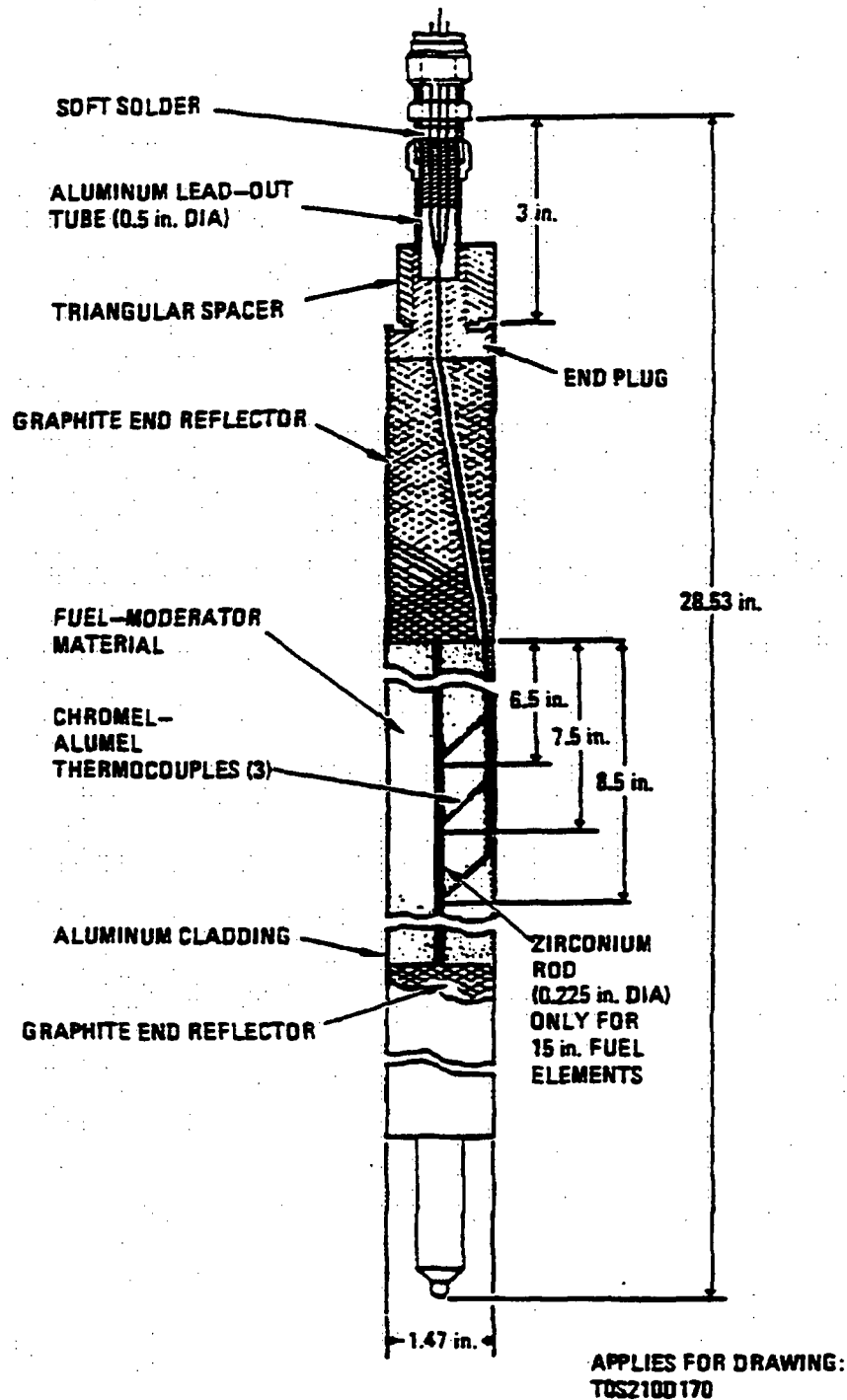
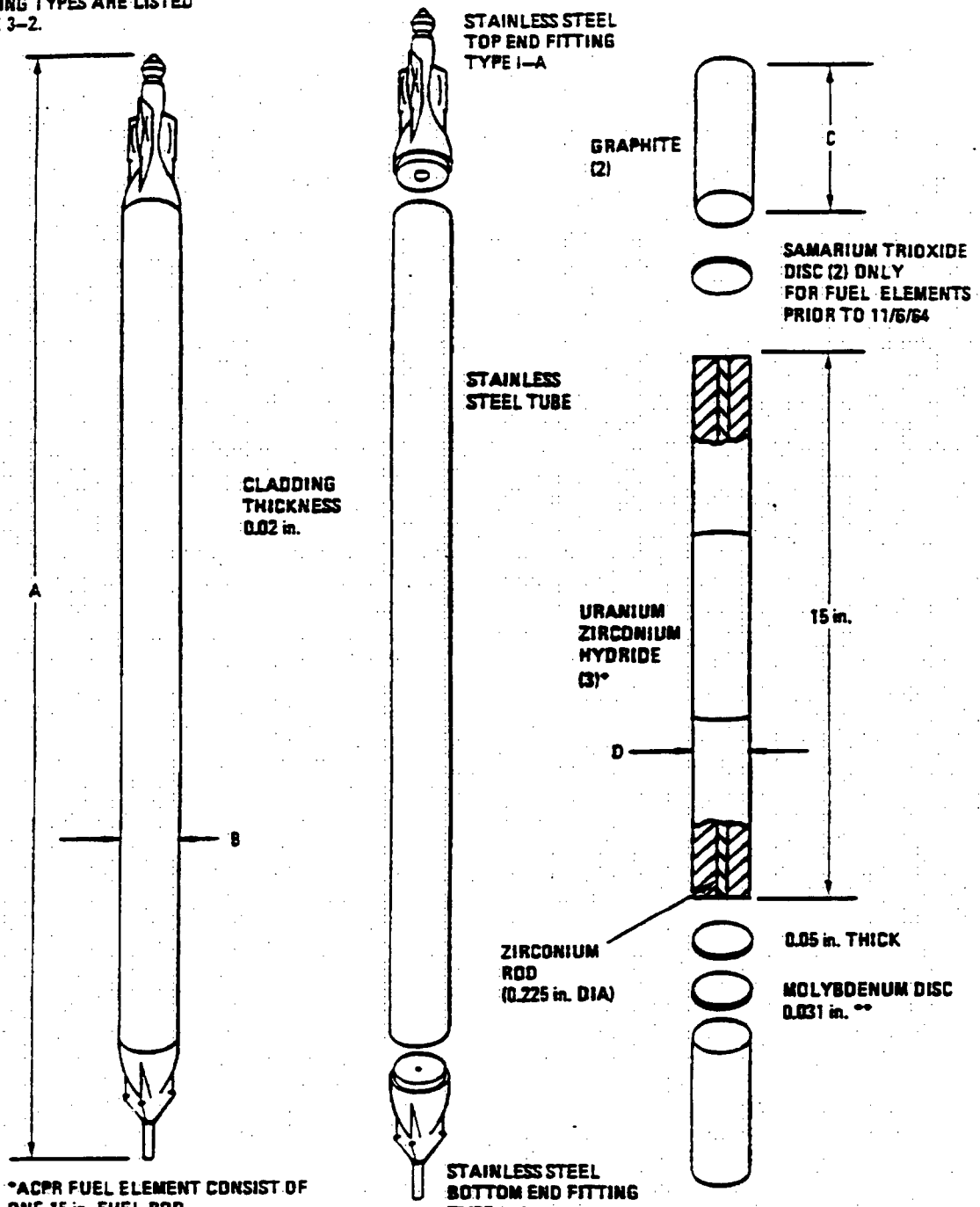


Figure 1.2.3-3 Stainless Steel Clad TRIGA Fuel Element

NOTE:
APPLICABLE DIMENSIONS "A-D"
AND FITTING TYPES ARE LISTED
ON TABLE 3-2.



*ACPR FUEL ELEMENT CONSIST OF ONE 15 in. FUEL ROD
** NOT INCLUDED IN FUEL ELEMENTS PRIOR TO 4/15/71 AND IN ACPR FUEL ELEMENTS

APPLIES FOR DRAWINGS:
T13S210D210
T0S210D210
T4S210D105
T5A210D210

Figure 1.2.3-4 Stainless Steel Clad Instrumented Fuel Element

NOTE:
FITTING TYPES ARE LISTED ON
TABLE 3-4. SEE FIGURE 3-3
FOR OTHER FUEL ELEMENT
DIMENSIONS.

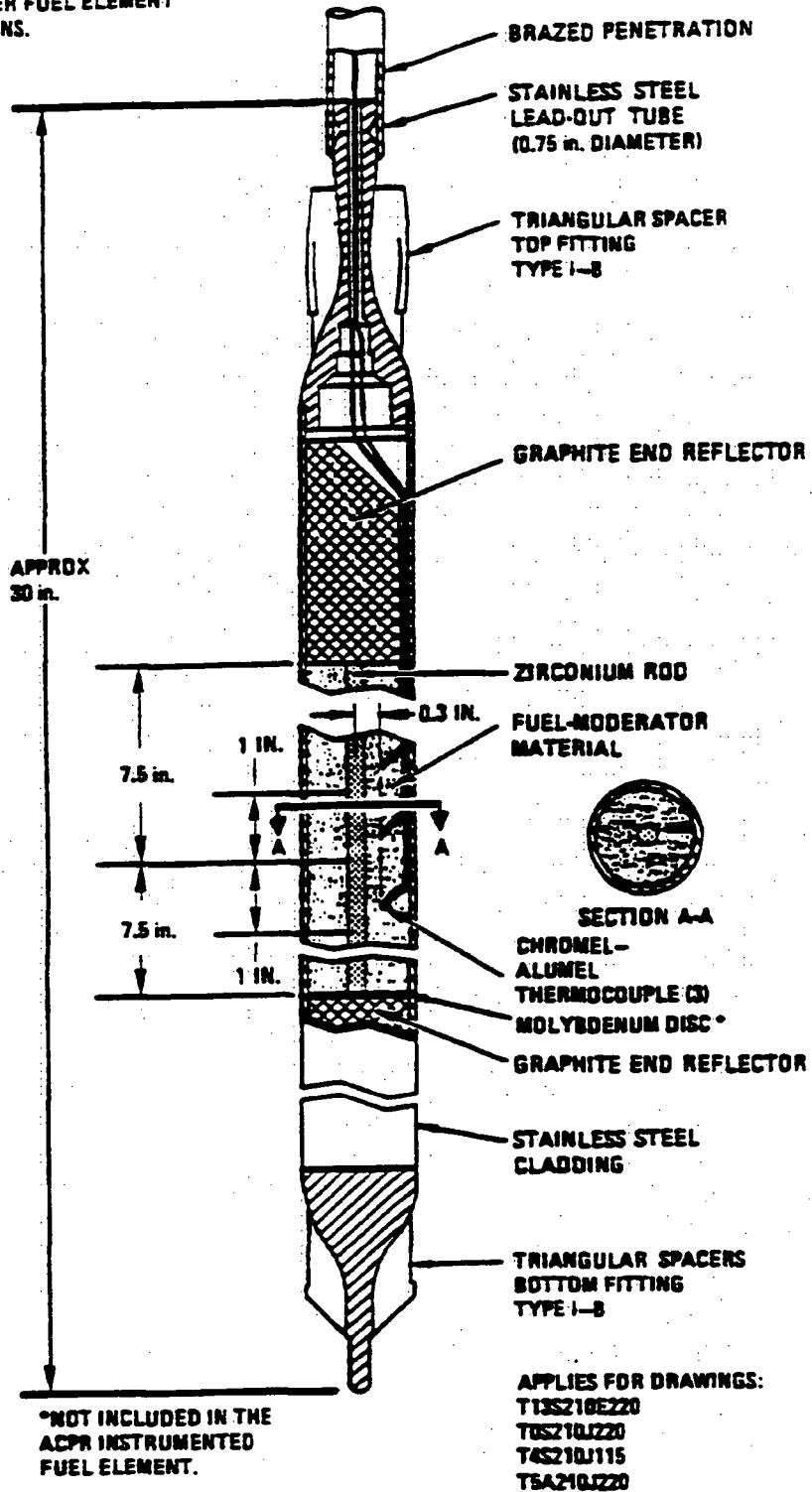


Figure 1.2.3-5 Standard Fuel Follower Control Rod Element

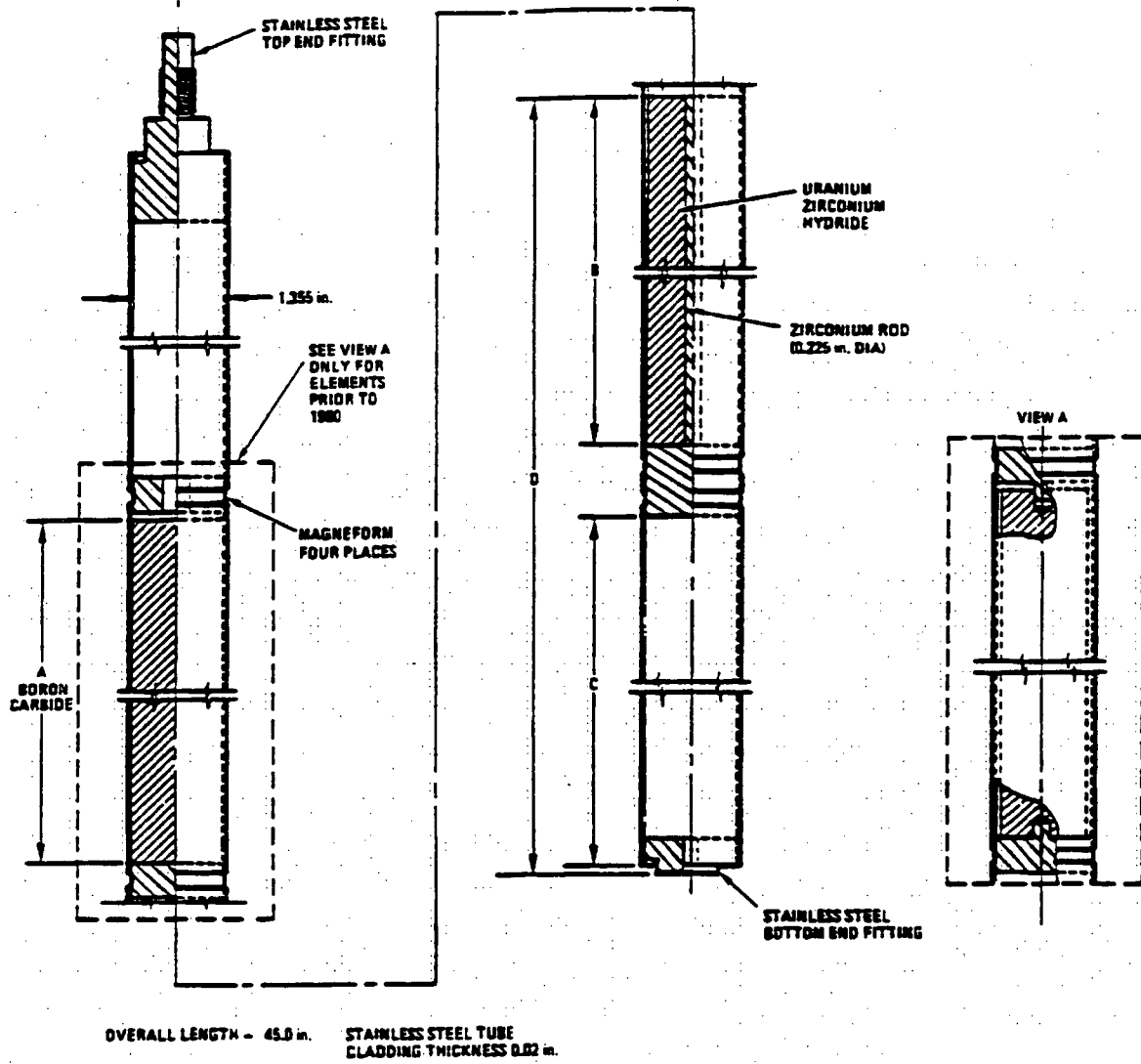


Figure 1.2.3-6 TRIGA Fuel Cluster and Rod Details

TRIGA FUEL CLUSTER

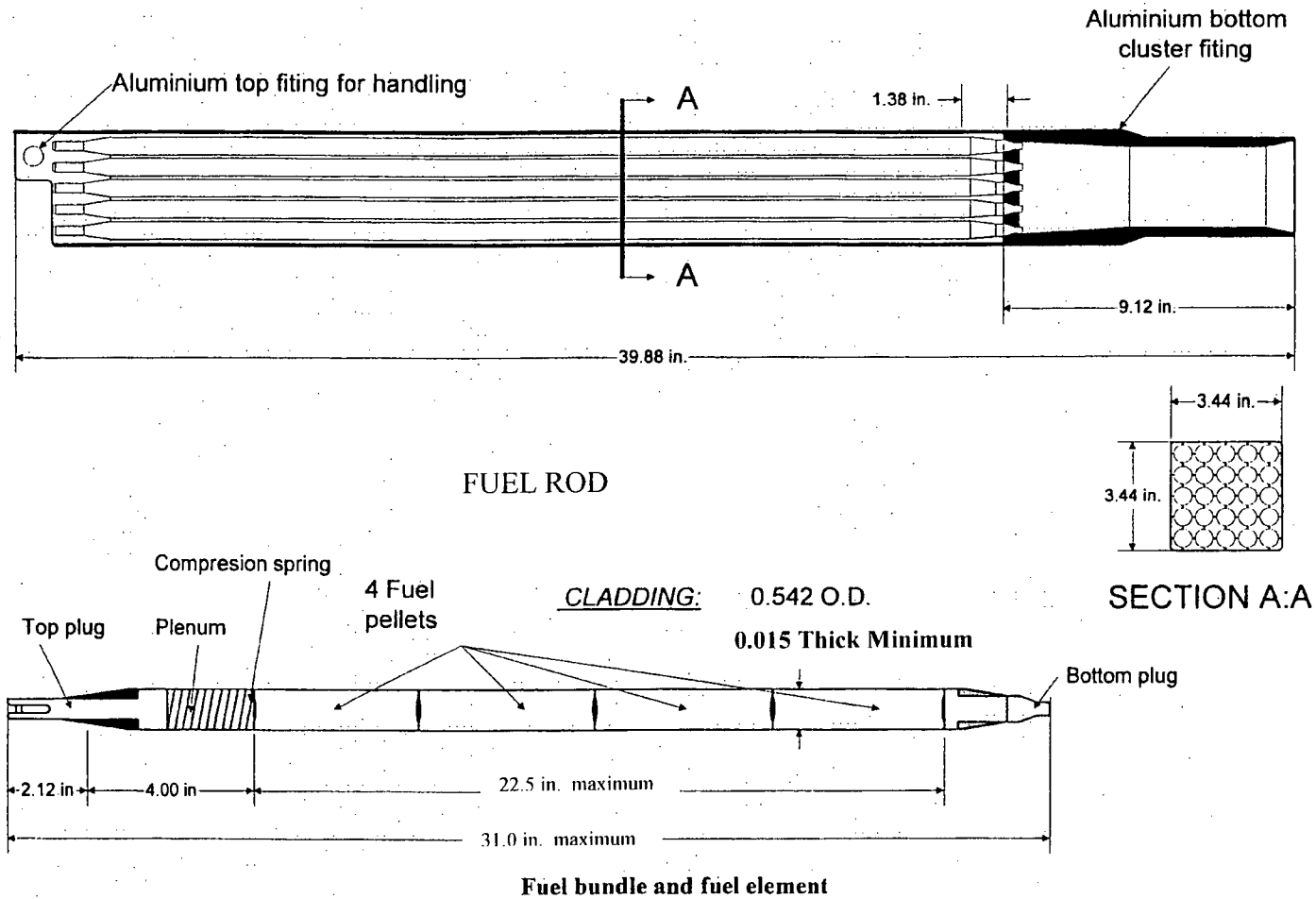
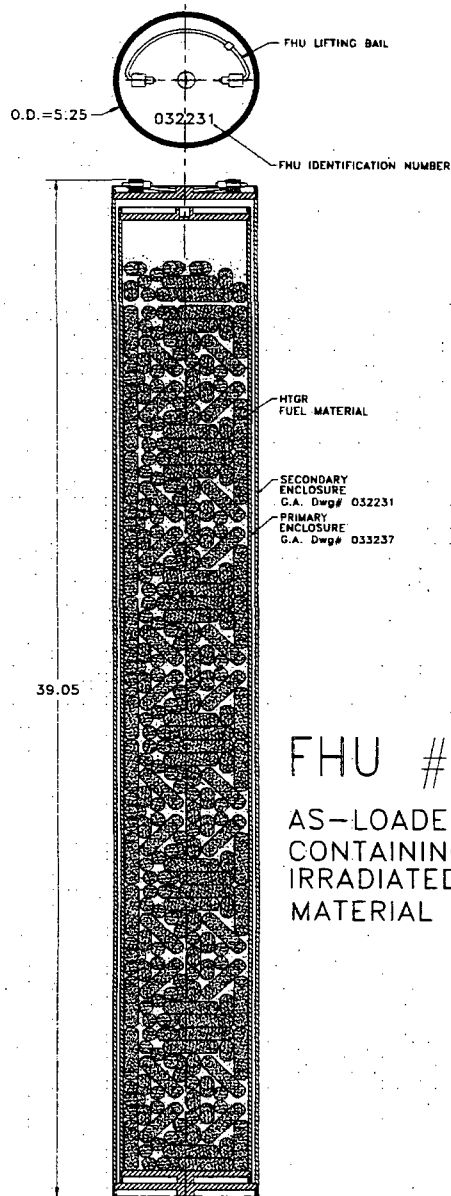


Figure 1.2.3-7 HTGR Fuel Handling Unit



FHU #032231

AS-LOADED ASSEMBLY
CONTAINING HTGR
IRRADIATED FUEL
MATERIAL

Figure 1.2.3-8 RERTR Fuel Handling Unit

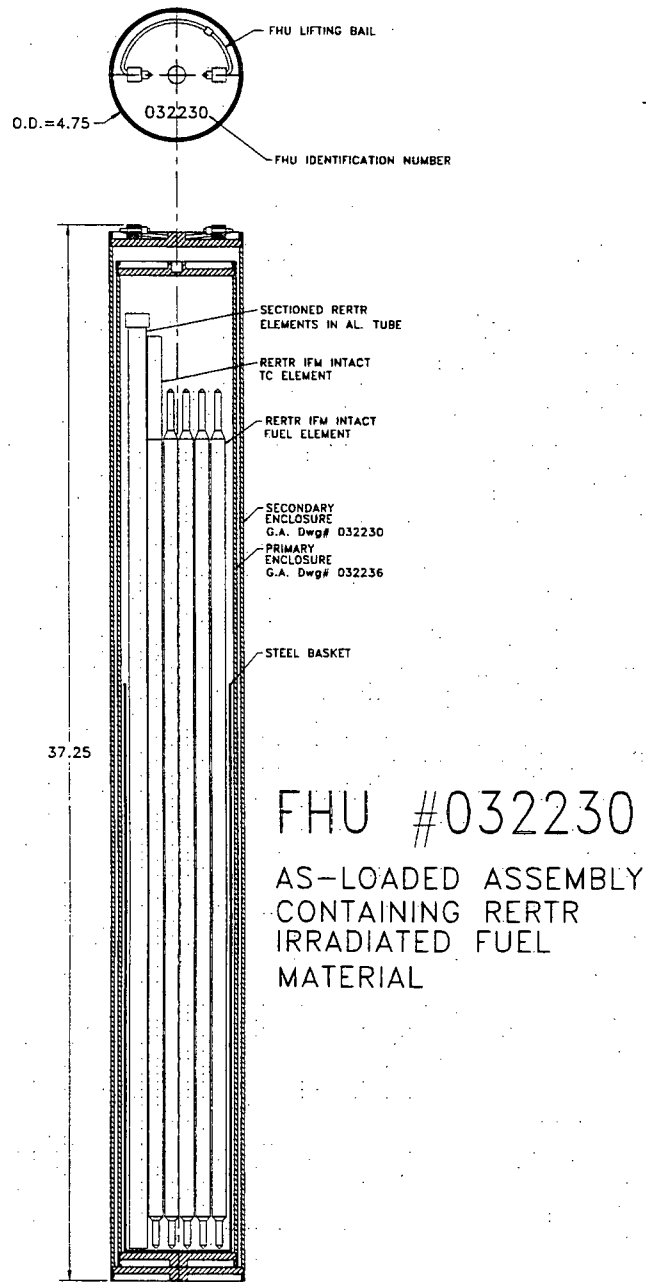


Figure 1.2.3-9 Typical TPBAR Assembly

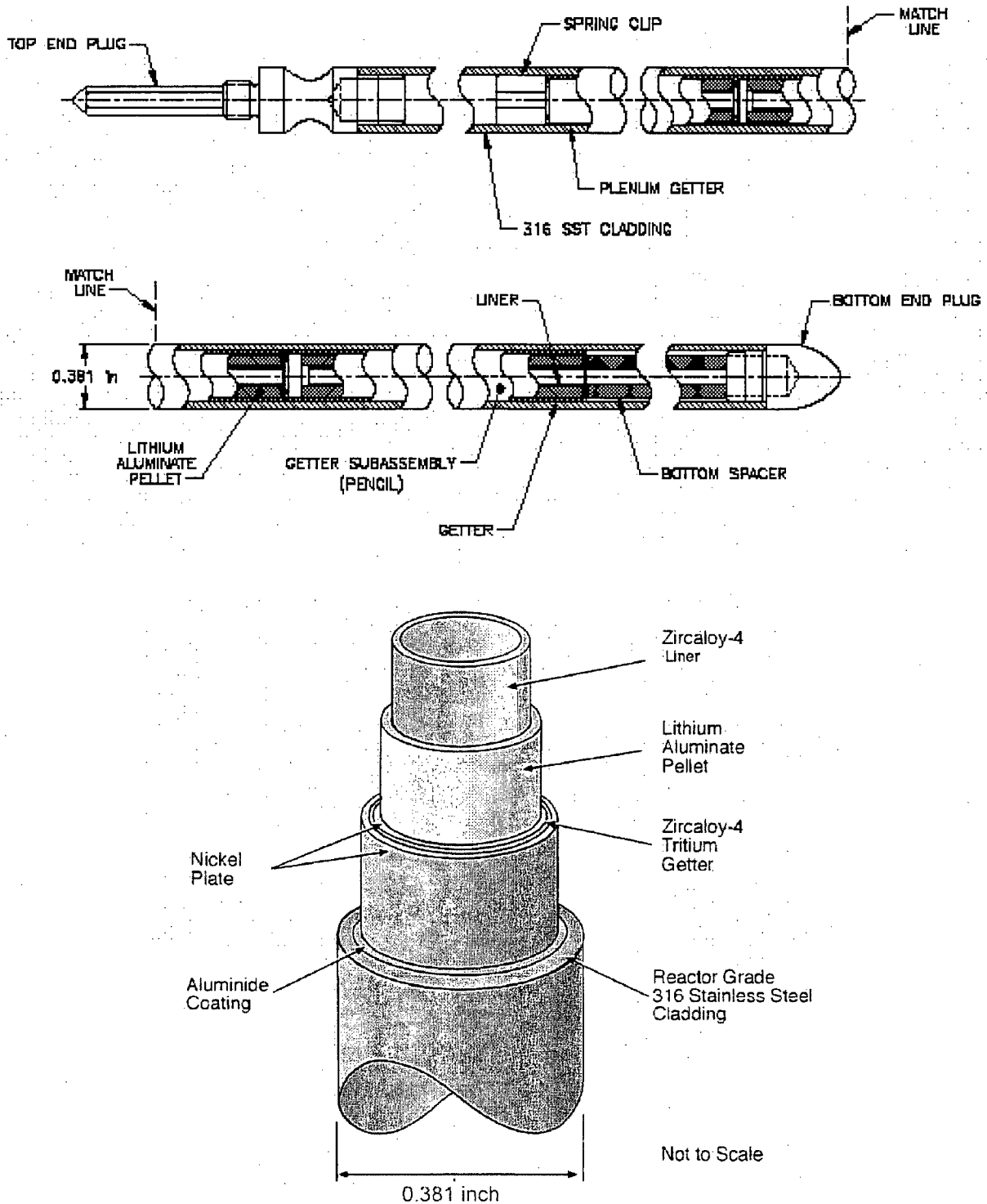
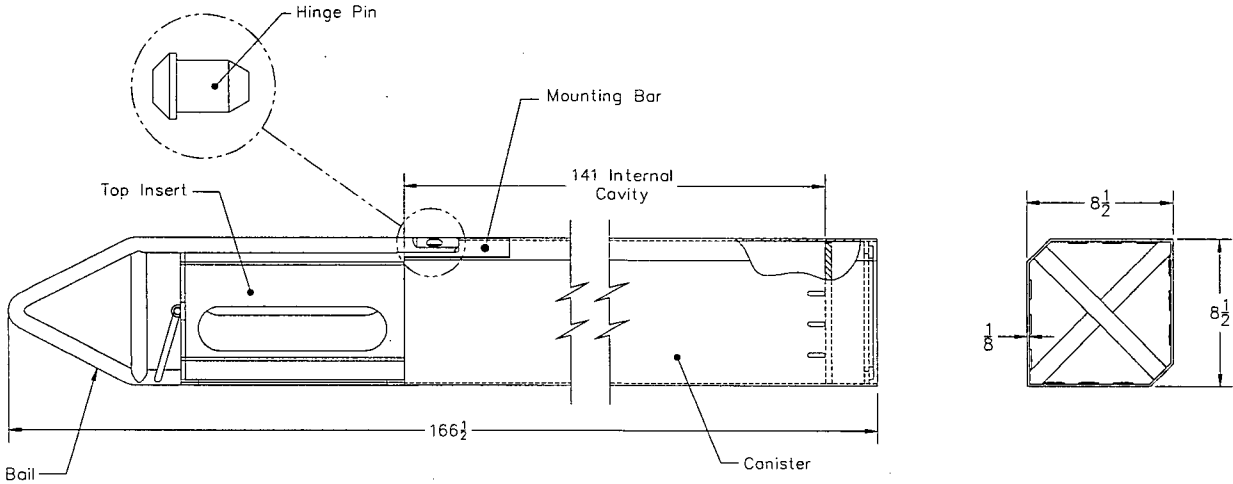


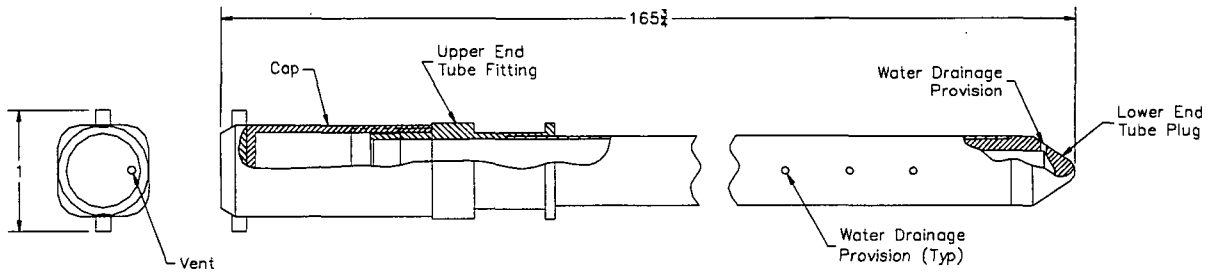
Figure 1.2.3-10 TPBAR Consolidation Canister Sketch



Conceptual Layout with Approximate Dimensions

Note: Material of construction is stainless steel.

Figure 1.2.3-11 Failed PWR/BWR Fuel Rod Capsule



Failed Fuel Rod Capsule Conceptual Layout

All Dimensions Approximate

Note: Material of construction is stainless steel.

Figure 1.2.3-12 NAC-LWT with TPBAR Consolidation Canister Payload

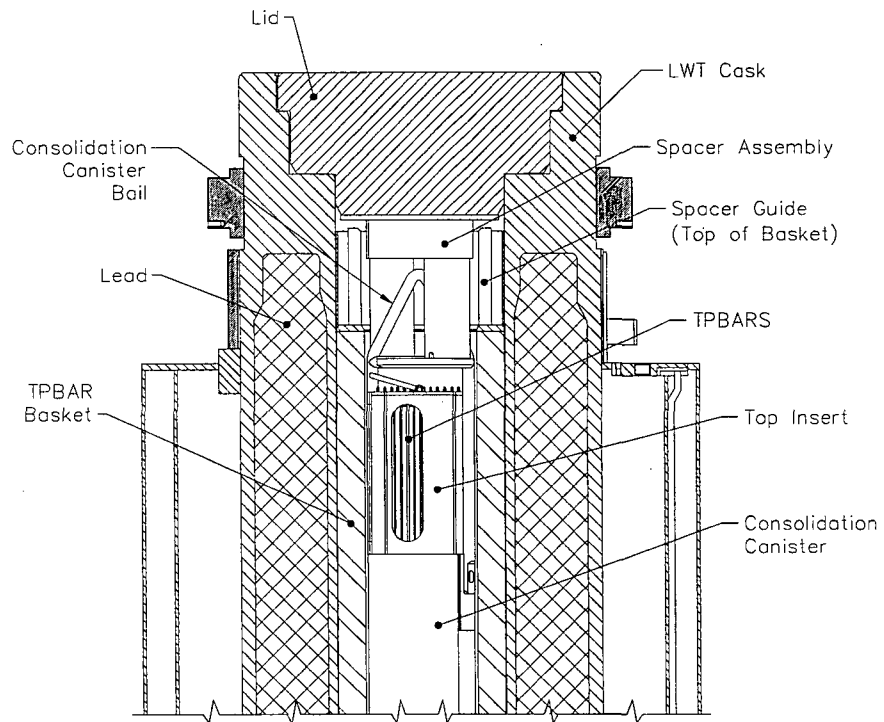


Figure 1.2.3-13 PULSTAR Fuel Assembly

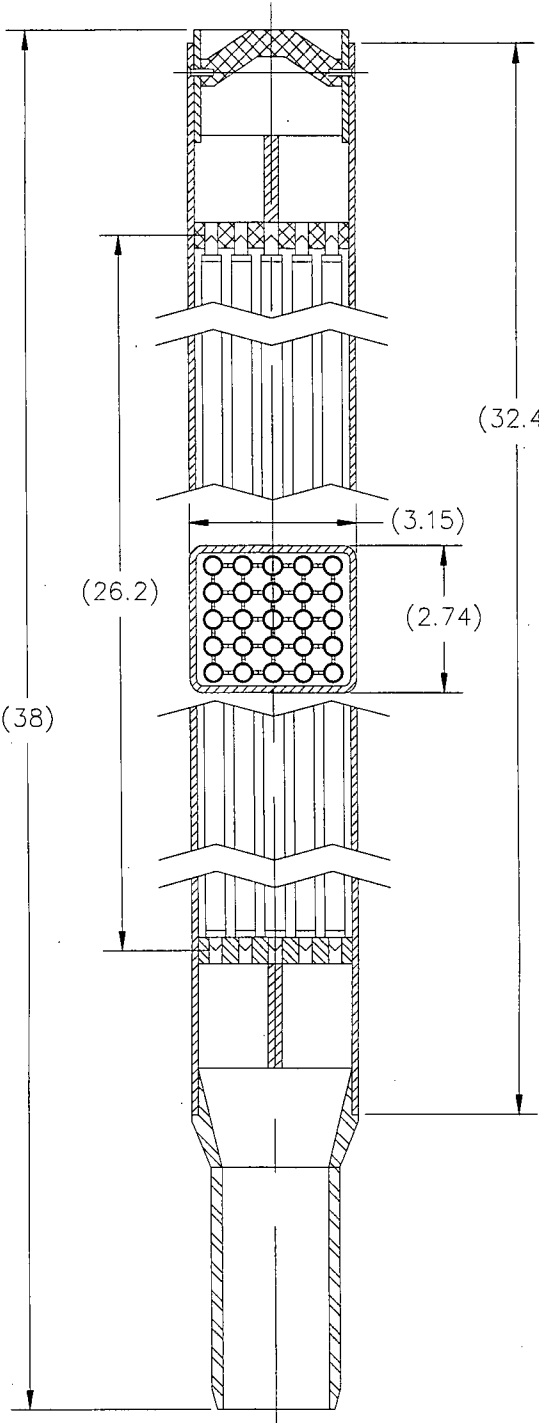
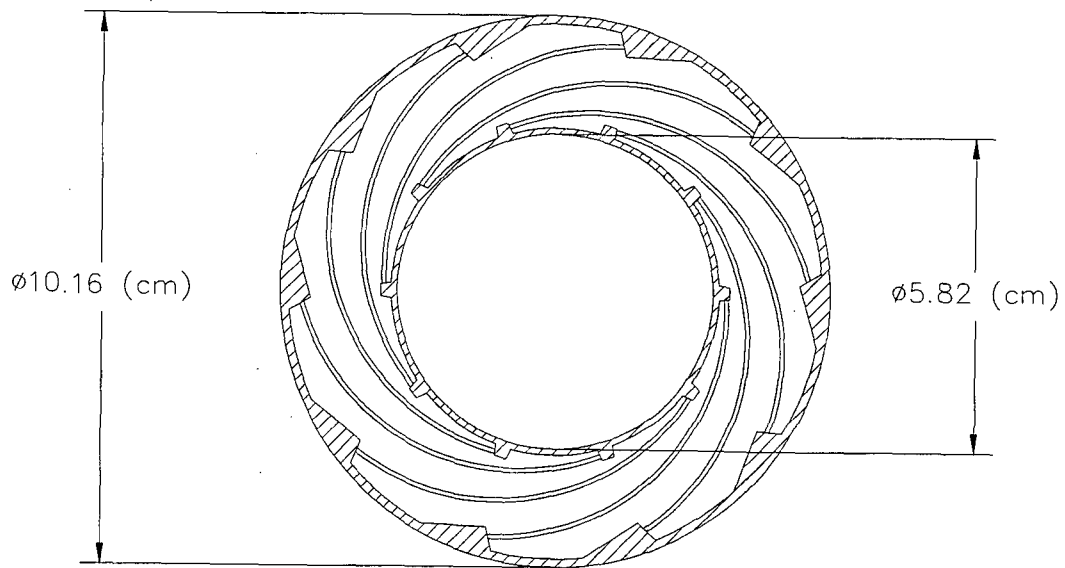
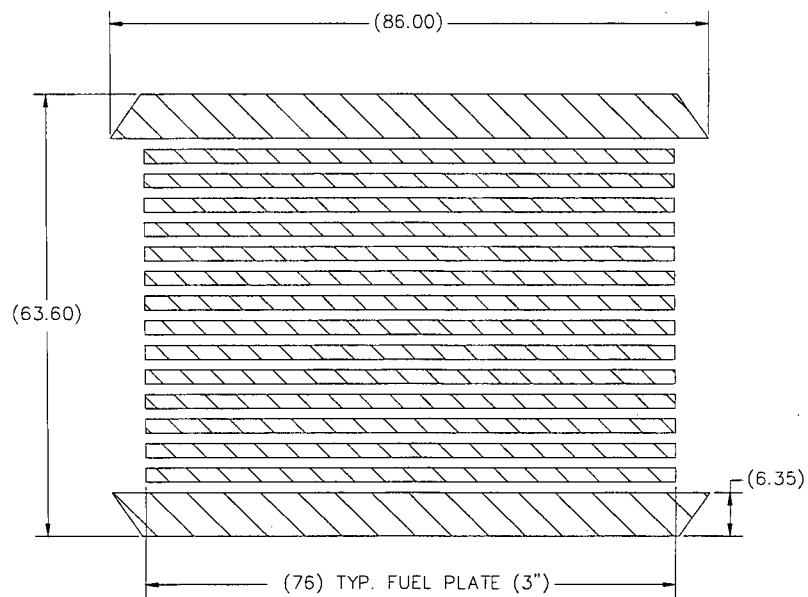
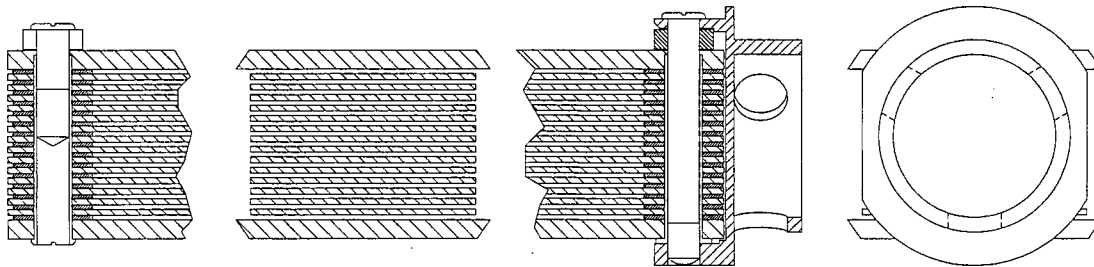


Figure 1.2.3-14 Spiral Fuel Assembly Cross-Section Sketch



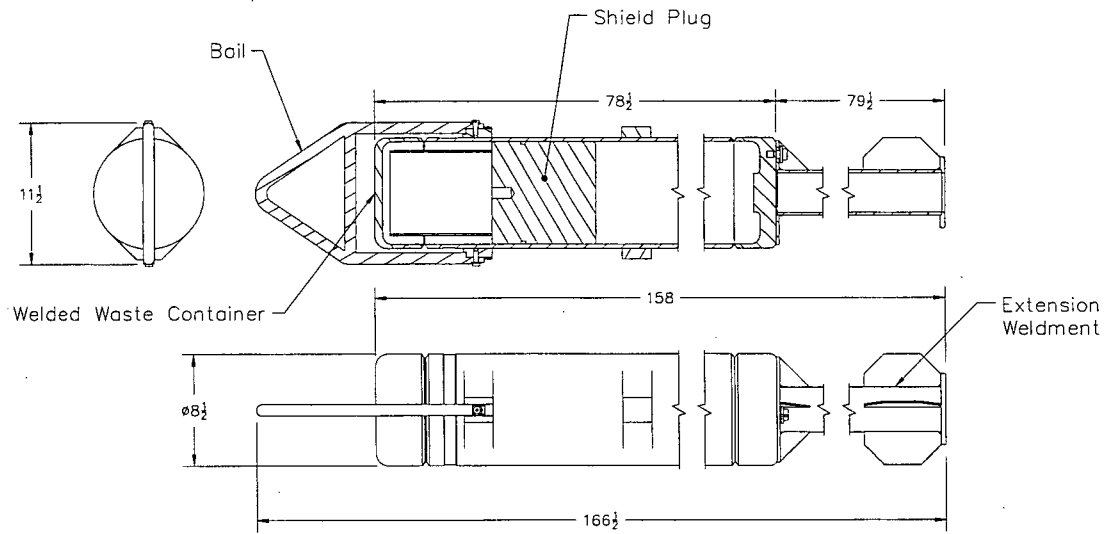
Note: Nominal dimensions

Figure 1.2.3-15 MOATA Plate Bundle Sketches



Note: 14-plate bundle configuration. Dimensions are reference values. Bundles with a reduced number of plates retain the plate pitch and compensate by wider side plates and outside spacers to retain overall bundle dimensions.

Figure 1.2.3-16 TPBAR Waste Container and Extension Weldment Sketch



Conceptual Layout with Approximate Dimensions

Note: Material of construction is stainless steel.

Figure 1.2.3-17 NAC-LWT with TPBAR Waste Container Payload

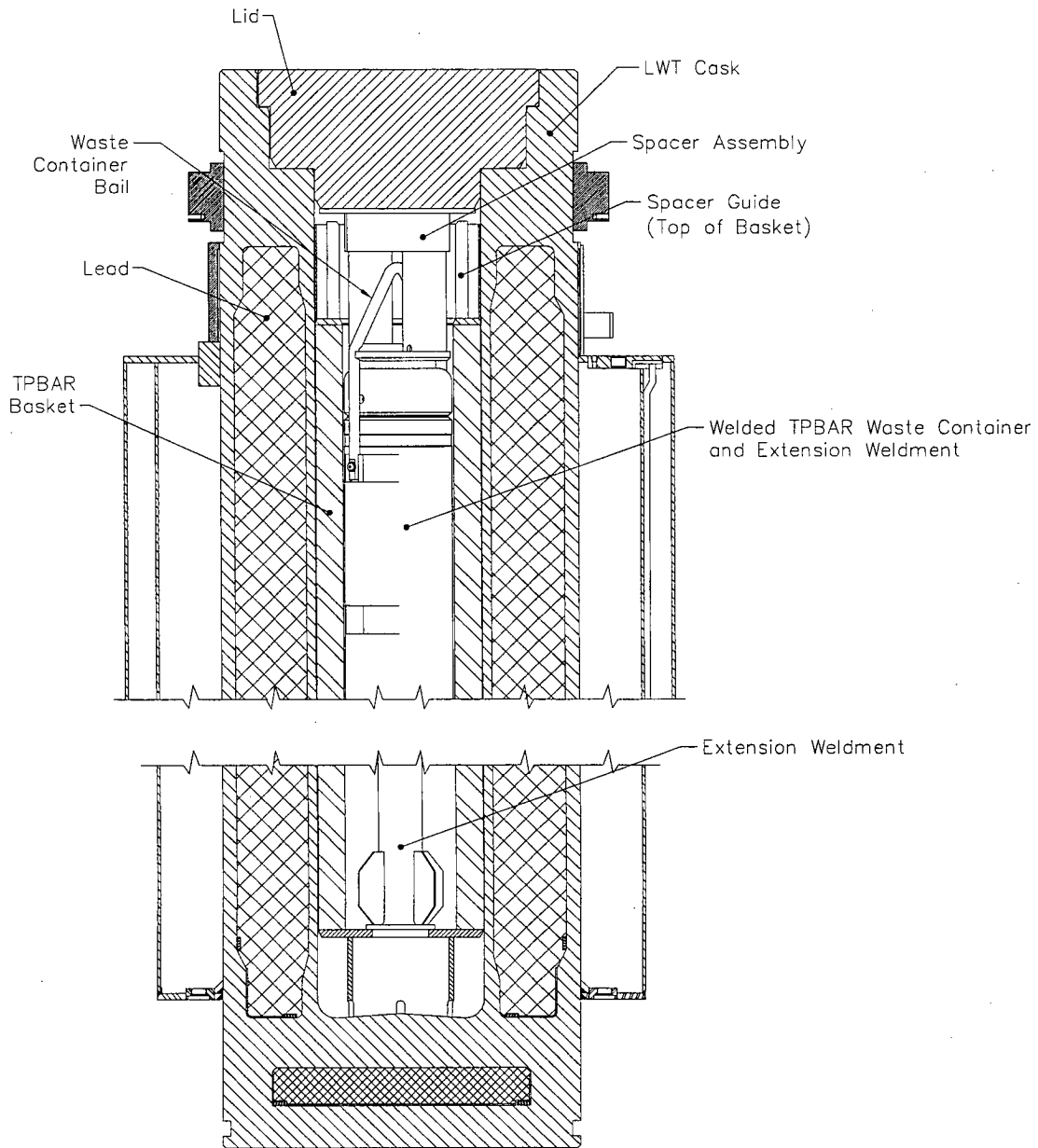


Table 1.2-1 Characteristics of Design Basis TRIGA Fuel Elements Acceptable for Loading in the Poisoned TRIGA Basket

	TRIGA HEU (Notes 1, 2, 6 & 7)	TRIGA LEU (Notes 1, 2, 6 & 7)	TRIGA LEU (Notes 1, 2, 6 & 7)
Fuel Form	Clad U-ZrH rod	Clad U-ZrH rod	Clad U-ZrH rod
Maximum Element Weight, lbs	13.2	13.2	13.2
Maximum Element Length, in	47.74	47.74	47.74
Element Cladding	Stainless Steel	Stainless Steel	Aluminum
Clad Thickness, in	0.02	0.02	0.03
Active Fuel Length, in	15	15	14-15 (Note 4)
Element Diameter, in	1.478 max.	1.478 max.	1.47 max.
Fuel Diameter, in	1.435 max.	1.435 max.	1.41 max.
Maximum Initial U Content/Element, kilograms	0.196	0.845	0.205
Maximum Initial ²³⁵ U Mass, grams	137	169	41
Maximum Initial ²³⁵ U Enrichment, weight percent	70	20	20
Zirconium Mass, grams (Note 5)	2060	1886-2300	2300
Hydrogen to Zirconium Ratio, max. (Note 5)	1.6	1.7	1.0
Maximum Average Burnup, MWd/MTU	460,000 (80% ²³⁵ U)	151,100 (80% ²³⁵ U)	151,100 (80% ²³⁵ U)
Minimum Cooling Time	90 days (Note 3)	90 days (Note 3)	90 days (Note 3)

Notes:

1. Mixed TRIGA LEU and HEU contents authorized.
2. TRIGA Standard, instrumented and fuel follower control rod type elements authorized.
3. Maximum decay heat of any element is 7.5 watts.
4. Aluminum clad fuel with 14-inch active fuel is solid and has no central hole with a zirconium rod.
5. Zirconium mass and H/Zr ratio apply to the fuel material (U-Zr-H_x) and do not include the center zirconium rod.
6. Listed TRIGA fuel elements have a 0.225-inch diameter zirconium rod in the center.
7. Dimensions listed are as-fabricated (unirradiated) nominal values.

Table 1.2-2 Characteristics of Design Basis TRIGA Fuel Elements Acceptable for Loading in the Nonpoisoned TRIGA Basket

	TRIGA HEU (Notes 1, 2, 6)	TRIGA LEU (Notes 1, 2, 6)	TRIGA LEU (Notes 1, 2, 6)
Fuel Form	Clad U-ZrH rod (Note 4)	Clad U-ZrH rod (Note 4)	Clad U-ZrH rod (Note 4)
Maximum Element Weight, lbs	13.2	13.2	13.2
Maximum Element Length, in	47.74	47.74	47.74
Element Cladding	Stainless Steel	Stainless Steel	Aluminum
Minimum Clad Thickness, in	0.01	0.01	0.01
Active Fuel Length, in	(Note 5)	(Note 5)	(Note 5)
Maximum Element Diameter, in	1.5 max.	1.5 max.	1.5 max.
Fuel Diameter, in	(Note 5)	(Note 5)	(Note 5)
Maximum Initial U Content/Element, kilograms	0.196	0.845	0.205
Maximum Initial ²³⁵ U Mass, grams	137	169	41
Maximum Initial ²³⁵ U Enrichment, weight percent	70	20	20
Zirconium Mass, grams	(Note 5)	(Note 5)	(Note 5)
Hydrogen to Zirconium Ratio, max.	(Note 5)	(Note 5)	(Note 5)
Maximum Average Burnup, MWd/MTU	460,000 (80% ²³⁵ U)	151,100 (80% ²³⁵ U)	151,100 (80% ²³⁵ U)
Minimum Cooling Time	90 days (Note 3)	90 days (Note 3)	90 days (Note 3)

Notes:

1. Mixed TRIGA LEU and HEU contents authorized.
2. TRIGA Standard, instrumented and fuel follower control rod type elements authorized.
3. Maximum decay heat of any element is 7.5 watts.
4. Element may contain zirconium rod in the center.
5. See criticality analyses in Chapter 6, Section 6.4.5.6, for the evaluations determining critical fuel characteristics.
6. Dimensions listed are as-fabricated (unirradiated) nominal values.

Table 1.2-3 Characteristics of Design Basis TRIGA Fuel Cluster Rods

Element Type	TRIGA Fuel Cluster Rod
Rod Diameter (in.)	0.542
Max. Rod Length (in.)	31.0
Max. Active Length (in.)	22.5
Clad Material	Incoloy 800
Min. Clad Thickness (in.)	0.015
Fuel Material	U-ZrH
Max. Pellet Diameter (in.)	0.53
Maximum Rod Weight (kg)	0.65
U in U-ZrH (wt %)	10.2
²³⁵ U in U (wt %)	93.3
²³⁵ U Mass (g)	45.4
H to Zr Ratio	1.6
Zr Mass (g)	421

Table 1.2-4 Fuel Characteristics

Parameter	PWR Fuel Assembly	BWR Fuel Assembly	PWR Rods	High Burnup PWR Rods	PWR MOX Fuel Rods ⁶	High Burnup BWR Rods 7 x 7	High Burnup BWR Rods ¹ 8 x 8 ²
Maximum Number of Assemblies, Elements or Rods	1	2	25 rods	25 rods	16 rods	25 rods	25 rods
Maximum Overall Weight, lbs	1650	750	N/A	N/A	N/A	N/A	N/A
Maximum Overall Length, in	178.25	176.1	162	162	162	176.1	176.1
Maximum Active Fuel Length, in	150	150	150	150	153.5	150	150
Fuel Rod Cladding	Zirc	Zirc	Zirc	Zirc	Zirc	Zirc	Zirc
Maximum Uranium, kg U	475	198	58.2	65.6	41.6 ⁷	198	198
Maximum Initial ²³⁵ U, wt %	See below ³	4.0	5.0	5.0	7.0 max/2.0 min, fissile Pu ⁸	5.0	5.0
Maximum Burnup, MWd/MTU	35,000	30,000	60,000 ⁴	80,000	62,500	60,000 - 80,000	80,000
Maximum Unit Decay Heat, kW	2.5	1.1	0.564	0.92	0.143	0.84	0.84
Maximum Cask Decay Heat, kW	2.5	2.2	1.41	2.3	2.3	2.1	2.1
Minimum Cool Time, yr	2	2	150 days	150 days	90 days	210 - 270 days ⁵	150 days

¹ High burnup rods are loaded in a fuel assembly lattice or rod holder. Up to 14 rods, loaded in a rod holder, may be classified as damaged. The lattice may be irradiated.

² Includes rods from all larger BWR assembly arrays (e.g., 9 x 9, 10 x 10).

³ See Table 1.2-5 for maximum PWR fuel enrichment by fuel type.

⁴ Up to 2 of the 25 PWR rods may have a maximum burnup of 65,000 MWd/MTU.

⁵ Minimum cool time for high burnup BWR 7 x 7 rods is determined by extent of burnup. See Section 5.3.8 and Table 5.3.8-23.

⁶ Up to 16 PWR MOX fuel rods or a combination of up to 16 MOX PWR and UO₂ PWR fuel rods can be loaded.

⁷ Maximum fuel mass is 2.6 kg HM/rod.

⁸ Maximum 5.0 wt % ²³⁵U for UO₂ rods.

Table 1.2-4 Fuel Characteristics (Continued)

Parameter	Metallic Fuel 15 rods (sound)	Metallic Fuel 9 rods (failed)	Metallic Fuel 3 rods (severely failed in filters)	MTR HEU 42 ¹	MTR MEU 42	MTR LEU 42 ²	TRIGA LEU Element 140	TRIGA HEU Element 140	TRIGA Cluster Rod 560
Maximum Overall Weight, lbs	1805	1805	1805	30 (max) ³	30 (max) ³	30 (max) ³	13.2 (max) ³	8.82 (nom.) 13.2 (max) ³	1.5 ³
Maximum Overall Length, in	120.5	120.5	120.5	25.4 ⁴	26.1 ⁴	26.1 ⁴	47.74 ⁵	47.74 ⁵	31.0
Maximum Active Fuel Length, in	120.0	120.0	120.0	24.8	25.6	25.6	15	15	22.5
Fuel Rod Cladding	Al	Al	Al	Al	Al	Al	Al or SS	Al or SS	Incoloy 800
Maximum Uranium, kg U	54.5	54.5	54.5	0.422 0.511	0.950	2.474 3.368 ²	0.824	0.196	0.0486
Maximum Initial ²³⁵ U, wt %	Natural	Natural	Natural	94	94 ⁶	25	20	70	93.3
Maximum Burnup, MWd/MTU	1,600	1,600	1,600	Variable up to 660,000 ⁷	Variable up to 293,300	Variable up to 139,300	151,100 (80% ²³⁵ U)	460,000 (80% ²³⁵ U)	600,000 (80% ²³⁵ U)
Maximum Unit Decay Heat, kW	0.036	0.036	0.036	Variable ⁸	0.030 ⁸	0.030 ⁸	0.0075	0.0075	0.001875
Maximum Cask Decay Heat, kW	0.54	0.54	0.54	1.26	1.26	1.26	1.05	1.05	1.05
Minimum Cool Time, yr	1	1	1	Variable ⁸	Variable ⁸	Variable ⁸	Variable ⁹	Variable ⁹	Variable ⁹

- 1 For NISTR fuel, 42 assemblies may be cut in half, producing 84 fuel-bearing pieces. Each fuel-bearing piece may contain up to 0.211 kgU.
- 2 MTR fuel elements having ²³⁵U content >470 g (>22 g per plate) are limited to a total of 4 elements in a 7-element basket. Basket openings 1, 2 and 3 shall be blocked by cell block spacers to ensure that MTR elements are not loaded in these openings. Therefore, depending on the number of such 4-element baskets, the maximum number of elements per cask will be reduced accordingly.
- 3 Maximum weight of fuel element(s), spacer(s) and fuel can, as applicable, per basket module cell shall be 80 pounds.
- 4 For MTR fuel elements, which are cut to remove nonfuel-bearing hardware prior to transport, a nominal 0.28 inch of nonfuel or spacer hardware will remain above and below the active fuel region to allow for fuel handling operations. The HFBR element, with an element length of 57.24 inches, must be cut prior to shipment. For HEU MTR elements having >380 g ²³⁵U but less than 460 g ²³⁵U, a minimum of 2.0 cm (0.8 inch) of nonfuel hardware and/or spacers/plates shall be provided at the ends of the element.
- 5 Permissible fuel element length is limited to basket cavity length, which is a minimum 47.74 inches for the basket top module, 30.94 inches for the intermediate modules, and 32.64 inches for the bottom module.
- 6 Typical MEU enrichment is 45 wt% ²³⁵U. Criticality analysis supports up to 94 wt% under the MEU fuel definition.
- 7 Maximum burnup is 660,000 MWd/MTU for 380g ²³⁵U and 577,500 MWd/MTU for 460g ²³⁵U
- 8 Minimum cool times for MTR fuel, down to 30 days, shall be determined using the procedure presented in Section 7.1.5.
- 9 Minimum cool times for TRIGA fuel elements and fuel cluster rods, down to 90 days, are determined so that the maximum decay heat of any element to be shipped is 7.5 watts and any fuel cluster rod is 1.875 watts.

Table 1.2-4 Fuel Characteristics (Continued)

Parameter	DIDO HEU	DIDO MEU	DIDO LEU
Number of Fuel Cylinders per Assembly	4	4	4
Maximum Overall Weight (lb) ¹	15	15	15
Minimum Plate Thickness, in	0.051	0.051	0.051
Minimum Clad Thickness (Al), in	0.00984	0.00984	0.00984
Maximum ²³⁵ U per Element, g	190	190	190
Maximum Initial ²³⁵ U, wt %	94	94	94
Minimum Initial ²³⁵ U, wt %	90	40	19
Maximum Uranium, kg U	0.2111	0.4750	1.0000
Minimum Active Fuel Height, in	23.13	23.13	23.13
Minimum Element Height ² , in	24.21	24.21	24.21
Maximum Burnup, MWd/MTU	577,460	256,650	121,910
Maximum Unit Decay Heat ³ , kW	0.025	0.025	0.025
Maximum Cask Decay Heat, kW	1.05	1.05	1.05
Minimum Cool Time ⁴ , yr	Variable	Variable	Variable

¹ Maximum weight of fuel element(s), spacer(s) and fuel can, as applicable, per basket module cell shall be 80 pounds.

² Element height provides for spacing of fissile material. An optional spacer may be used to maintain spacing if the element is cut shorter than 24.21 inches.

³ Maximum unit decay heat of 0.025 kW allowed only in conjunction with spacers for top basket (see Section 7.1.4), otherwise the limit is 0.018 kW.

⁴ Minimum cool times for DIDO fuel assemblies, down to 180 days, shall be determined using the procedure presented in Section 7.1.4.

Table 1.2-5 PWR Fuel Characteristics

Fuel Type	No. of Fuel Rods	Max. Assembly Length (in.)	Max. Assembly Weight (lb)	Max. Enrich. (wt %)	Max. MTU	Pitch (in.)	Rod Dia. (in.)	Clad Thick. (in.)	Pellet Dia.(in.)	Max. Active Length (in.)
B&W 15 x 15	208	165.63	1515	3.5	0.4750	0.5680	0.430	0.0265	0.3686	144.0
B&W 17 x 17	264	165.72	1505	3.5	0.4658	0.5020	0.379	0.0240	0.3232	143.0
CE 14 x 14	176	157.00	1270	3.7	0.4037	0.5800	0.440	0.0280	0.3765	137.0
CE 16 x 16	236	178.25	1430	3.7	0.4417	0.5060	0.382	0.0250	0.3250	150.0
WE 14 x 14 Std	179	159.71	1302	3.7	0.4144	0.5560	0.422	0.0225	0.3674	145.2
WE 14 x 14 OFA	179	159.71	1177	3.7	0.3612	0.5560	0.400	0.0243	0.3444	144.0
WE 15 x 15	204	159.71	1472	3.5	0.4646	0.5630	0.422	0.0242	0.3659	144.0
WE 17 x 17 Std	264	159.77	1482	3.5	0.4671	0.4960	0.374	0.0225	0.3225	144.0
WE 17 x 17 OFA	264	160.10	1373	3.5	0.4282	0.4960	0.360	0.0225	0.3088	144.0
Ex/ANF 14 x 14 WE	179	160.13	1271	3.7	0.3741	0.5560	0.424	0.0300	0.3505	144.0
Ex/ANF 14 x 14 CE	176	157.24	1292	3.7	0.3814	0.5800	0.440	0.0310	0.3700	134.0
Ex/ANF 15 x 15 WE	204	159.70	1433	3.7	0.4410	0.5630	0.424	0.0300	0.3565	144.0
Ex/ANF 17 x 17 WE	264	159.71	1348	3.5	0.4123	0.4960	0.360	0.0250	0.3030	144.0

Table 1.2-6 BWR Fuel Characteristics

Fuel Type	No. of Fuel Rods	No. of Water Rods	Max. Assembly Length (in.)	Max. Assembly Weight (lb)	Max. MTU	Pitch (in.)	Rod Dia. (in.)	Clad Thick. (in.)	Pellet Dia. (in.)	Max. Active Length (in.)
GE 7 x 7	49	0	175.9	678.9	0.1923	0.738	0.563	0.037	0.477	146
GE 8 x 8-1	63	1	175.9	681.0	0.1880	0.640	0.493	0.034	0.416	146
GE 8 x 8-2	62	2	175.9	681.0	0.1847	0.640	0.483	0.032	0.410	150 ¹
GE 8 x 8-4	60	4	176.1	665.0	0.1787	0.640	0.484	0.032	0.410	150 ^{1,2}
GE 9 x 9	74	2 ³	176.1	646.0	0.1854	0.566	0.441	0.028	0.376	150 ^{1,4}
	79	2	176.1	646.0	0.1979	0.566	0.441	0.028	0.376	150 ^{1,4}
Ex/ANF 7 x 7	49	0	171.3	619.1	0.1960	0.738	0.570	0.036	0.490	144
Ex/ANF 8 x 8-1	63	1	171.3	562.3	0.1764	0.641	0.484	0.036	0.4045	145.2
Ex/ANF 8 x 8-2	62	2	176.1	587.8	0.1793	0.641	0.484	0.036	0.4045	150
Ex/ANF 9 x 9	79	2	176.1	575.3	0.1779	0.572	0.424	0.03	0.3565	150
	74	2 ³	176.1	575.3	0.1666	0.572	0.424	0.03	0.3565	150

¹ 6" natural uranium blankets on top and bottom.

² May have 1 large water hole - 3.2 cm ID, 0.1 cm thickness.

³ 2 large water holes occupying 7 fuel rod locations - 2.5 cm ID, 0.07 cm thickness.

⁴ Shortened active fuel length in some rods.

Table 1.2-7 Characteristics of General Atomics Irradiated Fuel Material (GA IFM)

Parameter	RERTR	HTGR
Maximum Number of Assemblies, Elements or Rods	13 intact; 7 sectioned	N/A
Maximum Loaded Enclosure Weight, lbs	76.0	71.5
Maximum Fuel Weight, lbs	23.73	23.52
Maximum Overall Length, in	29.92	N/A
Maximum Active Fuel Length, in	22.05	N/A
Fuel Material	U-ZrH	UC ₂ , UCO, UO ₂ , (Th,U)C ₂ , (Th,U)O ₂
Fuel Rod Cladding	Incoloy 800	N/A
Maximum Uranium, kg U	3.86	0.21
Maximum Initial ²³⁵ U, wt %	19.7	93.15
Maximum Burnup, MWd/MTU	N/A	N/A
Maximum Unit Decay Heat, W	11.0	2.05
Maximum Cask Decay Heat, W	13.05	13.05
Earliest Shipment Date	1/1/96	1/1/96
Maximum Activity, Ci	2920	483

Table 1.2-8 Typical Production TPBAR Characteristics¹

Parameter Description	Value
Maximum Number of TPBARs per Consolidation Canister	300
Number of Consolidation Canisters per Cask	1
TPBAR Clad Material	316 L Stainless Steel
Rod Length ² , in	153.04
Rod Diameter ² , in	0.381
Maximum Rod Heat Load, W	2.31
Maximum Cask Heat Load, kW	0.693
Maximum Tritium Content per Rod, gram	1.2
Maximum Activity per Cask ³ , Ci	3.84×10^6
Loaded TPBAR Consolidation Canister Maximum Weight, pounds ⁴	1,000
Maximum Event Failed Tritium Release (Ci/rod)	<55
Minimum Cooling Time, days	30

¹ Refer to Section 1.5, Chapter 1 Appendices, Unclassified DOE Reference Documents and Drawings.

² Beginning of life, nominal, unirradiated dimensions.

³ Primary dose contribution: 1.1×10^4 Ci ⁶⁰Co/cask.

⁴ The bounding weight employed in the structural analysis.

Table 1.2-9 PULSTAR Fuel Characteristics

Description	Value
Maximum Pellet Diameter (inch)	0.423
Minimum Element (Rod) Cladding Thickness (inch)	0.0185
Minimum Element (Rod) Diameter (inch)	0.470
Maximum Active Fuel Height (inch)	24.1
Element (Rod) Length (inch)	26.2
Rod Pitch (inch)	0.525 × 0.607
Assembly Length (inch)	38
Box Outside Width (inch)	2.745 × 3.155
Box Thickness (inch)	0.06
Maximum Assembly or Loaded Can Weight (lb) ¹	80
Maximum PULSTAR Can Content Weight (lb) ²	39.6
Maximum Enrichment (wt % ²³⁵ U)	6.5
Maximum ²³⁵ U Content per Element (g)	33
No. of Elements (Rods) per Assembly	25
No. of Elements (Rods) per Can ²	25
Maximum Depletion (% ²³⁵ U)	45
Minimum Cool Time (yrs)	1.5
Maximum Heat Load per Assembly (W)	30
Maximum Heat Load per Element (W)	1.2

¹ Listed weight is the maximum weight evaluated for the structural calculation to bound all payload configurations, including loaded cans, and spacers. Nominal PULSTAR assembly weight is 45 pounds.

² The contents of a PULSTAR can are restricted to the equivalent of the fuel material in 25 PULSTAR fuel elements and of the displaced volume of 25 intact PULSTAR fuel elements. Fuel material may be in damaged form including fuel debris. The listed weight represents the can content limit established by the structural analyses.

Table 1.2-10 Spiral Fuel Assembly Characteristics

Parameter	Value
Number of elements per assembly	10
Fuel element type	Curved plate
Nominal dimensions of element (cm)	0.147 × 7.33 × 63.5 (individual plate)
Chemical form of fuel meat	U-Al _x -alloy
Cladding material	Aluminum
Nominal over-all dimensions (cm)	63.818 (height) × 10.16 diameter ¹
Max total weight of ²³⁵ U (g)	160 (total per assembly)
Maximum enrichment (wt % ²³⁵ U)	85
Side plate material	Aluminum (inner and outer tubes)
Nominal side plate – dimensions (cm)	Inner 6.045 OD, 5.82 ID × 63.818 Outer 10.16 OD, 9.85 ID × 63.818 ²
Max. assembly weight (lb)	18 ³
Assembly maximum heat load (W)	15.7 ⁴
Burnup/cool time limit	Variable ⁵

¹ Cropped to fit within ANSTO fuel basket module nominal height of 28.3 inches.

² Criticality evaluations reduced inner and outer shell thickness to 0.01 cm to provide additional moderator within the assembly.

³ Typical assembly weight is 7.9 pounds. Bounding structural analysis weight is listed.

⁴ Thermal and shielding evaluation employed 18 W per element. Based on cool time constraint, 15.7 W represents maximum heat load.

⁵ Spiral fuel is constrained to DIDO MEU cool time limits as a function of burnup. Minimum cool times for the spiral assembly, down to 270 days, shall be determined using the procedure presented in Section 7.1.4 for 18 W DIDO MEU fuel.

Table 1.2-11 MOATA Plate Bundle Characteristics

Parameter	Value
Maximum number of elements per assembly	14
Nominal dimensions of element (cm)	66 cm long, 7.6 cm wide and 0.203 cm thick
Nominal dimensions of fuel meat (cm)	58.4 cm long, 6.99 cm wide and 0.1016 cm thick (bounding active fuel width evaluated to a maximum of 7.32 cm)
Chemical form of fuel meat	U-Al _x -alloy
Cladding material	Aluminum
Nominal clad thickness (cm)	0.05 cm (evaluated to 0.01 cm minimum)
Plate spacer thickness (cm)	0.147 min, 0.152 max (evaluated to 0.18 maximum)
Maximum weight of ²³⁵ U (g) per plate	22.3
Maximum enrichment (wt % ²³⁵ U)	92
Nominal side plate thickness (cm)	0.635 (bounding evaluation replaced by cavity moderator)
Max. assembly weight (lb)	18 ¹
Maximum heat load per assembly (W) ²	3 (total for 14 fuel plates)
Maximum burnup	30,000 MWd/MTU or 4.1 % depletion ²³⁵ U
Minimum cool time (years)	10

¹ Typical assembly weight is 13.6 pounds. Bounding structural analysis weight is listed.

² Actual heat load at limiting burnup and cool time < 1 Watt. Thermal evaluations at 3 Watt per bundle.

Table 1.2-12 Typical TPBAR Segment Characteristics in Waste Container

Parameter/Description	Value
Maximum Number of TPBAR Segments and Debris per Waste Container, equivalent number of TPBARs	55
Number of Waste Containers per Cask	1
Waste Container Material	316L Stainless Steel
Maximum Tritium Content per TPBAR equivalent, gram	1.2
Maximum Activity per Cask, Ci	6.66×10^5
Maximum Heat Load per Waste Container, watts	127
Maximum Loaded Waste Container Weight, pounds	700 ¹
Minimum Cooling Time, years	90

¹ Design basis weight of a loaded waste container is 700 pounds. Applying a maximum payload of 55 TPBARs, with storage canister, yields a maximum weight of 662 pounds. Use of shrouds to contain segments and/or TPBAR debris reduces overall waste container weight due to a reduction in TPBAR payload capacity resulting from the reduced container free volume.

Table 1.2-13 Solid, Irradiated Hardware Characteristics¹

Parameter	Value
Maximum Content Weight	4,000 pounds ²
Maximum Content Length	171.5 inches ³
Hardware Material	Solid, irradiated and contaminated fuel assembly structural or reactor internal component hardware ⁴
Maximum Cask Heat Load	1.0 KW
Maximum Activity per Cask, Ci	6.0 x 10E+6
Maximum Source Term, gamma/sec	6.0 x 10E+15
Maximum Source Term, MeV/sec	1.0 x 10E+15

¹ Maximum content weight includes any spacers, containers or dunnage loaded in the cavity with the irradiated hardware.

² Length of cavity is limited to 171.5 inches by the installation and use of an irradiated hardware spacer bolted to the underside of the closure lid.

³ Appropriate secondary containers will be used to prevent any contact and cross-contamination between the carbon steel contents and the stainless steel internals of the cask cavity.

⁴ The irradiated hardware contents may contain fissile material, provided the quantity of fissile material does not exceed a Type A quantity and does not exceed the mass limits of 10 CFR 71.53.

Figure Withheld Under 10 CFR 2.390


			
LEGAL WEIGHT TRUCK TRANSPORT CASK ASSEMBLY SAFETY ANALYSIS REPORT			
PROJECT	315-40	DRAWING	01
SCALE	WEIGHT	SH 1 OF 1	REV 7
11:23PM 10-31-2001			

Figure Withheld Under 10 CFR 2.390




			
LEGAL WEIGHT TRUCK TRANSPORT CASK ASSY, PWR/BWR ROD 3 TRANSPORT CANISTER			
PROJECT	315-40	DRAWING	104
SCALE	WEIGHT	SH 1 OF 2	REV 3 10-31-2007

Figure Withheld Under 10 CFR 2.390

		
LEGAL WEIGHT TRUCK TRANSPORT CASK ASSY PWR/BWR ROD  TRANSPORT CANISTER		
PROJECT	315-40	REV
		3
	DRAWING	104
	SH 2	OF 2
		10-21-2007

Chapter 2

Table of Contents

2	STRUCTURAL EVALUATION	2-1
2.1	Structural Design	2.1.1-1
2.1.1	Discussion.....	2.1.1-1
2.1.2	Basic Design Criteria	2.1.2-1
2.1.2.1	Containment Structures.....	2.1.2-1
2.1.2.2	Noncontainment Structures.....	2.1.2-1
2.1.3	Miscellaneous Structural Failure Modes	2.1.3-1
2.1.3.1	Brittle Fracture	2.1.3-1
2.1.3.2	Fatigue – Normal Operating Cycles	2.1.3-1
2.1.3.3	Extreme Total Stress Intensity Range.....	2.1.3-5
2.1.3.4	Buckling.....	2.1.3-5
2.2	Weights and Centers of Gravity.....	2.2.1-1
2.2.1	Major Component Statistics.....	2.2.1-1
2.3	Properties of Materials	2.3-1
2.3.1	Mechanical Properties of Materials	2.3.1-1
2.3.1.1	Cask Body Materials.....	2.3.1-1
2.3.1.2	Port Cover Materials	2.3.1-1
2.3.1.3	Fuel Basket Materials	2.3.1-1
2.3.1.4	Bolting Material	2.3.1-2
2.3.1.5	Shielding Material (Gamma Radiation).....	2.3.1-2
2.4	General Standards for All Packages	2.4-1
2.4.1	Minimum Package Size	2.4.1-1
2.4.2	Tamperproof Feature	2.4.2-1
2.4.3	Positive Closure	2.4.3-1
2.4.4	Chemical and Galvanic Reactions	2.4.4-1
2.4.5	Cask Design	2.4.5-1
2.4.6	Continuous Venting	2.4.6-1
2.5	Lifting and Tiedown Standards.....	2.5.1-1
2.5.1	Lifting Devices.....	2.5.1-1
2.5.1.1	Lifting Trunnion.....	2.5.1-1
2.5.1.2	Lid Lifting Bolts	2.5.1-7
2.5.1.3	Can Assembly (315-40-98).....	2.5.1-8
2.5.2	Tiedown Devices	2.5.2-1
2.5.2.1	Discussion and Loads	2.5.2-1
2.5.2.2	Rear Support	2.5.2-5
2.5.2.3	Front Support	2.5.2-11
2.6	Normal Conditions of Transport.....	2.6.1-1
2.6.1	Hot Case	2.6.1-1
2.6.1.1	Discussion.....	2.6.1-1
2.6.1.2	Analysis Description.....	2.6.1-1
2.6.1.3	Detailed Analysis.....	2.6.1-2
2.6.1.4	Conclusion	2.6.1-3
2.6.2	Cold Case.....	2.6.2-1

Table of Contents (continued)

2.6.2.1	Discussion	2.6.2-1
2.6.2.2	Analysis Description	2.6.2-1
2.6.2.3	Detailed Analysis	2.6.2-2
2.6.2.4	Conclusion	2.6.2-3
2.6.3	Reduced External Pressure	2.6.3-1
2.6.4	Increased External Pressure	2.6.4-1
2.6.5	Vibration	2.6.5-1
2.6.6	Water Spray	2.6.6-1
2.6.7	Free Drop (1 Foot)	2.6.7-1
2.6.7.1	End Drop (1 Foot)	2.6.7-1
2.6.7.2	Side Drop (1 Foot)	2.6.7-2
2.6.7.3	Corner Drop (1 Foot)	2.6.7-3
2.6.7.4	Impact Limiters	2.6.7-4
2.6.7.5	Closure Lid	2.6.7-20
2.6.7.6	Bolts – Closure Lid (Normal Conditions of Transport)	2.6.7-22
2.6.7.7	Neutron Shield Tank	2.6.7-24
2.6.7.8	Expansion Tank	2.6.7-39
2.6.7.9	Upper Ring/Outer Shell Intersection Analysis	2.6.7-42
2.6.7.10	Rod Shipment Can Assembly (Rod Holder) Analysis	2.6.7-47
2.6.8	Corner Drop	2.6.8-1
2.6.9	Compression	2.6.9-1
2.6.10	Penetration	2.6.10-1
2.6.10.1	Impact Limiter – Penetration	2.6.10-1
2.6.10.2	Expansion Tank – Penetration	2.6.10-1
2.6.10.3	Neutron Shield Tank – Penetration	2.6.10-5
2.6.10.4	Port Cover – Penetration	2.6.10-6
2.6.10.5	Alternate Port Cover – Penetration	2.6.10-8
2.6.11	Fabrication Conditions	2.6.11-1
2.6.11.1	Lead Pour	2.6.11-1
2.6.11.2	Cooldown	2.6.11-3
2.6.11.3	Lead Creep	2.6.11-12
2.6.12	Fuel Basket Analysis	2.6.12-1
2.6.12.1	Discussion	2.6.12-1
2.6.12.2	PWR Basket Construction	2.6.12-1
2.6.12.3	PWR Basket Analysis	2.6.12-2
2.6.12.4	BWR Basket Construction	2.6.12-4
2.6.12.5	Metallic Fuel Basket Construction	2.6.12-5
2.6.12.6	MTR Fuel Basket Construction	2.6.12-7
2.6.12.7	TRIGA Fuel Basket One-Foot Drop Evaluation	2.6.12-25
2.6.12.8	DIDO Fuel Basket Construction	2.6.12-52
2.6.12.9	General Atomics IFM Basket Construction	2.6.12-61
2.6.12.10	TPBAR Basket Analysis	2.6.12-70
2.6.12.11	ANSTO Basket Analysis	2.6.12-84

Table of Contents (continued)

	2.6.12.12 Conclusion	2.6.12-91
2.7	Hypothetical Accident Conditions.....	2.7-1
	2.7.1 Free Drop (30 Feet).....	2.7.1-1
	2.7.1.1 End Drop.....	2.7.1-2
	2.7.1.2 Side Drop	2.7.1-5
	2.7.1.3 Oblique Drops.....	2.7.1-10
	2.7.1.4 Shielding for Lead Slump Accident.....	2.7.1-18
	2.7.1.5 Bolts - Closure Lid (Hypothetical Accident - Free Drop)	2.7.1-19
	2.7.1.6 Crush.....	2.7.1-20
	2.7.1.7 Rod Shipment Can Assembly Analysis	2.7.1-21
	2.7.2 Puncture	2.7.2-1
	2.7.2.1 Puncture - Cask Side Midpoint.....	2.7.2-1
	2.7.2.2 Puncture - Center of Cask Closure Lid.....	2.7.2-3
	2.7.2.3 Puncture - Center of Cask Bottom.....	2.7.2-6
	2.7.2.4 Puncture - Port Cover.....	2.7.2-9
	2.7.2.5 Puncture Accident - Shielding Consequences	2.7.2-17
	2.7.2.6 Puncture - Conclusion.....	2.7.2-17
	2.7.3 Fire	2.7.3-1
	2.7.3.1 Discussion.....	2.7.3-1
	2.7.3.2 Thermal Stress Evaluation	2.7.3-1
	2.7.3.3 Bolts - Closure Lid (Hypothetical Accident - Fire).....	2.7.3-3
	2.7.3.4 Inner Shell Evaluation.....	2.7.3-4
	2.7.3.5 Conclusion	2.7.3-5
	2.7.4 Immersion - Fissile Material.....	2.7.4-1
	2.7.5 Immersion – Irradiated Nuclear Fuel Packages	2.7.5-1
	2.7.5.1 Method of Analysis.....	2.7.5-1
	2.7.5.2 Closure Lid Stresses.....	2.7.5-1
	2.7.5.3 Outer Bottom Head Forging Stresses	2.7.5-2
	2.7.5.4 Cask Cylindrical Shell Stresses	2.7.5-3
	2.7.5.5 Containment Seal Evaluation.....	2.7.5-5
	2.7.6 Damage Summary.....	2.7.6-1
	2.7.7 Fuel Basket Accident Analysis	2.7.7-1
	2.7.7.1 Discussion.....	2.7.7-1
	2.7.7.2 PWR Basket Construction	2.7.7-1
	2.7.7.3 PWR Basket Analysis	2.7.7-1
	2.7.7.4 BWR Basket Construction.....	2.7.7-3
	2.7.7.5 Metallic Fuel Basket Analysis	2.7.7-6
	2.7.7.6 MTR Fuel Basket Construction	2.7.7-8
	2.7.7.7 Conclusion	2.7.7-18
	2.7.7.8 PWR Spacer.....	2.7.7-18
	2.7.7.9 TRIGA Fuel Basket Thirty-Foot Drop Evaluation	2.7.7-23
	2.7.7.10 DIDO Fuel Basket Construction.....	2.7.7-46
	2.7.7.11 General Atomics IFM Basket Construction.....	2.7.7-51

Table of Contents (continued)

	2.7.7.12	TPBAR Basket Analysis.....	2.7.7-54
	2.7.7.13	ANSTO Basket Analysis	2.7.7-66
2.8		Special Form	2.8-1
2.9		Spent Fuel Contents	2.9-1
	2.9.1	PWR and BWR Fuel Rods.....	2.9-1
	2.9.2	TRIGA Fuel Elements	2.9-1
	2.9.2.1	End Drop.....	2.9-2
	2.9.2.2	Side Drop	2.9-3
	2.9.3	PULSTAR Intact Fuel Elements.....	2.9-5
	2.9.4	ANSTO Fuels.....	2.9-6
	2.9.4.1	MARK III Spiral Fuel Assemblies	2.9-6
	2.9.4.2	MOATA Plate Bundles.....	2.9-10
2.10		Appendices.....	2.10.1-1
	2.10.1	Computer Program Descriptions.....	2.10.1-1
	2.10.1.1	ANSYS	2.10.1-1
	2.10.1.2	RBCUBED - A Program to Calculate Impact Limiter Dynamics	2.10.1-2
	2.10.2	Finite Element Model Description.....	2.10.2-1
	2.10.2.1	Boundary and Loading Conditions Used in the 30-Foot Drop Finite Element Analysis.....	2.10.2-2
	2.10.3	Finite Element Evaluations	2.10.3-1
	2.10.3.1	Isothermal Plot - Hot Case.....	2.10.3-1
	2.10.3.2	Isothermal Plot - Cold Case	2.10.3-1
	2.10.3.3	Determination of Component Critical Stresses.....	2.10.3-1
	2.10.4	Oblique Drop Slapdown	2.10.4-1
	2.10.4.1	Discussion.....	2.10.4-1
	2.10.4.2	Analysis.....	2.10.4-1
	2.10.4.3	Energy Calculation.....	2.10.4-3
	2.10.4.4	Rotational Velocity Change	2.10.4-4
	2.10.5	Lead Slump - End Drop	2.10.5-1
	2.10.6	Inner Shell Buckling Design Criteria and Evaluation.....	2.10.6-1
	2.10.6.1	Code Case N-284	2.10.6-1
	2.10.6.2	Theoretical Elastic Buckling Stresses.....	2.10.6-1
	2.10.6.3	Capacity Reduction Factors	2.10.6-2
	2.10.6.4	Plasticity Reduction Factors	2.10.6-3
	2.10.6.5	Upper Bound Magnitudes for Compressive Stresses and In-Plane Shear Stresses	2.10.6-3
	2.10.6.6	Interaction Equations	2.10.6-4
	2.10.6.7	Detailed Buckling Evaluation - Sample Calculation	2.10.6-4
	2.10.6.8	Conclusion	2.10.6-7
	2.10.7	Detailed Finite Element Stress Summary	2.10.7-1
	2.10.7.1	Finite Element Stress Tables - Normal Operation Hot Condition.....	2.10.7-1

Table of Contents (continued)

2.10.7.2	Finite Element Stress Tables - Normal Operation Cold Condition.....	2.10.7-1
2.10.7.3	Finite Element Stress Tables – 1-Foot End Drop	2.10.7-1
2.10.7.4	Finite Element Stress Tables – 1-Foot Side Drop.....	2.10.7-1
2.10.7.5	Finite Element Stress Tables – 1-Foot Corner Drop.....	2.10.7-1
2.10.7.6	Finite Element Stress Tables – 30-Foot End Drop	2.10.7-1
2.10.7.7	Finite Element Stress Tables – 30-Foot Side Drop.....	2.10.7-1
2.10.7.8	Finite Element Stress Tables – 30-Foot Oblique Drop.....	2.10.7-2
2.10.8	Quarter-Scale Model Drop Test Program for the NAC-LWT Cask.....	2.10.8-1
2.10.8.1	Introduction.....	2.10.8-1
2.10.8.2	Purpose.....	2.10.8-1
2.10.8.3	Summary	2.10.8-1
2.10.8.4	Description of Quarter-Scale LWT Cask Model	2.10.8-4
2.10.8.5	Description of Test Procedures and Instrumentation.....	2.10.8-5
2.10.8.6	Detailed Test Results	2.10.8-7
2.10.8.7	Metrology Results.....	2.10.8-14
2.10.8.8	Discussion of Test Results	2.10.8-15
2.10.8.9	Post-Test Revisions.....	2.10.8-17
2.10.9	Bolts – Closure Lid (Stress Evaluations).....	2.10.9-1
2.10.9.1	Analysis Approach.....	2.10.9-1
2.10.9.2	Closure Bolt Analyses – Analytics and Assumptions.....	2.10.9-2
2.10.10	Finite Element Stress Results for the 30-Foot Drop Accident Conditions.....	2.10.10-1
2.10.10.1	Discussion.....	2.10.10-1
2.10.10.2	Procedures.....	2.10.10-1
2.10.10.3	Analysis and Results.....	2.10.10-3
2.10.10.4	Conclusion	2.10.10-6
2.10.11	Hand Calculation for the 30-Foot Drop Accident Conditions.....	2.10.11-1
2.10.11.1	Top End Drop	2.10.11-1
2.10.11.2	Side Drop	2.10.11-2
2.10.12	Impact Limiter Force-Deflection Curves and Data	2.10.12-1
2.10.12.1	Potential Energy and Cask Drop Motion.....	2.10.12-1
2.10.12.2	Potential to Kinetic Energy Conversion	2.10.12-3
2.10.12.3	Deceleration Forces and Energy Absorption Calculation	2.10.12-4
2.10.12.4	RBCUBED Calculated Force-Deflection Graphs.....	2.10.12-7
2.10.12.5	Quarter-Scale Model Quasi-Static Force-Deflection Tests.....	2.10.12-7
2.10.13	Structural Evaluation of Failed Fuel Cans and Liners (Baskets).....	2.10.13-1
2.10.13.1	Discussion.....	2.10.13-1
2.10.13.2	Method of Analysis.....	2.10.13-1
2.10.13.3	Input Geometry & Data	2.10.13-2
2.10.13.4	Mechanical Properties of Materials	2.10.13-3

Table of Contents (continued)

2.10.13.5	Thermal Evaluation.....	2.10.13-3
2.10.13.6	Structural Evaluation	2.10.13-3
2.10.13.7	Results and Conclusion.....	2.10.13-11
2.10.13.8	Failed Fuel Shipment Component Drawings.....	2.10.13-12
2.10.14	Structural Evaluation of the NAC-LWT Cask Body with TPBAR Contents	2.10.14-1
2.10.14.1	Normal Conditions of Transport for Cask Body with TPBAR Contents	2.10.14-1
2.10.14.2	Hypothetical Accident Conditions for Cask Body with TPBAR Contents	2.10.14-3
2.10.14.3	Inner Shell Buckling	2.10.14-4
2.10.14.4	NAC-LWT Cask Closure Lid and Bolts.....	2.10.14-5
2.10.14.5	Conclusion	2.10.14-6
2.10.15	NAC-LWT Alternate B Port Cover.....	2.10.15-1
2.10.15.1	Alternate B Port Cover Bolt Analysis.....	2.10.15-1

List of Figures

Figure 2.1.3-1	Design Fatigue Curve for High Strength Steel Bolting	2.1.3-7
Figure 2.3.1-1	Static Stress-Strain Curve for Chemical Copper Lead	2.3.1-3
Figure 2.3.1-2	Dynamic Deformation Stress-Strain Curve for Chemical Copper Lead.....	2.3.1-4
Figure 2.5.1-1	Trunnion Cross-Section and Forging Shear Area.....	2.5.1-10
Figure 2.5.2-1	Front Support and Tiedown Geometry	2.5.2-13
Figure 2.5.2-2	Pressure Distribution of Horizontal Bearing Between Cask and Support Saddle	2.5.2-14
Figure 2.5.2-3	Free Body Diagram of Cask Subjected to Lateral Load	2.5.2-15
Figure 2.5.2-4	Rotation Trunnion Pocket.....	2.5.2-16
Figure 2.6.1-1	NAC-LWT Cask Critical Sections (Hot Case)	2.6.1-4
Figure 2.6.2-1	NAC-LWT Cask Critical Sections (Cold Case)	2.6.2-4
Figure 2.6.7-1	1-Foot Bottom End Drop with 130°F Ambient Temperature and Maximum Decay Heat Load.....	2.6.7-60
Figure 2.6.7-2	1-Foot Bottom End Drop with -40°F Ambient Temperature and Maximum Decay Heat Load.....	2.6.7-61
Figure 2.6.7-3	1-Foot Bottom End Drop with -40°F Ambient Temperature and No Decay Heat Load.....	2.6.7-62
Figure 2.6.7-4	1-Foot Top End Drop with 130°F Ambient Temperature and Maximum Decay Heat Load.....	2.6.7-63
Figure 2.6.7-5	1-Foot Top End Drop with -40°F Ambient Temperature and Maximum Decay Heat Load.....	2.6.7-64
Figure 2.6.7-6	NAC-LWT Cask Critical Sections (1-Foot Side Drop with 100°F Ambient Temperature).....	2.6.7-65
Figure 2.6.7-7	1-Foot Top Corner Drop with 130°F Ambient Temperature and Maximum Decay Heat Load - Drop Orientation = 15.74 Degrees.....	2.6.7-66
Figure 2.6.7-8	1-Foot Bottom Corner Drop with 130°F Ambient Temperature and Maximum Decay Heat Load - Drop Orientation = 15.74 Degrees.....	2.6.7-67
Figure 2.6.7-9	1-Foot Top Corner Drop with -40°F Ambient Temperature and No Decay Heat Load - Drop Orientation = 15.74 Degrees	2.6.7-68
Figure 2.6.7-10	NAC-LWT Cask with Impact Limiters	2.6.7-69
Figure 2.6.7-11	Cross-Section of Top Impact Limiter	2.6.7-70
Figure 2.6.7-12	Load versus Deflection Curve (Typical Aluminum Honeycomb).....	2.6.7-71
Figure 2.6.7-13	Quarter-Scale Model Limiter End Drop Cross-Section.....	2.6.7-72
Figure 2.6.7-14	End Drop Impact Limiter Cross-Section	2.6.7-73
Figure 2.6.7-15	Impact Limiter Lug Detail	2.6.7-74
Figure 2.6.7-16	Cask Lug Detail	2.6.7-75
Figure 2.6.7-17	RBCUBED Output Summary – Center of Gravity Over Top Corner ...	2.6.7-76
Figure 2.6.7-18	Free Body Diagram - Top Impact Limiter - Center of Gravity Over Corner	2.6.7-77
Figure 2.6.7-19	Free Body Diagram - Top Impact Limiter - Cask Wedging Forces	2.6.7-78
Figure 2.6.7-20	Cask Lid Configuration.....	2.6.7-79
Figure 2.6.7-21	Closure Lid Free Body Diagram.....	2.6.7-80

List of Figures (continued)

Figure 2.6.7-22	NAC-LWT Cask Cross-Section.....	2.6.7-81
Figure 2.6.7-23	Component Parts of Shield Tank Structure	2.6.7-82
Figure 2.6.7-24	Shield Tank Cross-Section.....	2.6.7-83
Figure 2.6.7-25	Shield Tank Quarter-Section Geometry.....	2.6.7-84
Figure 2.6.7-26	Partial Bottom/Top End Plate Plan and Cross-Section.....	2.6.7-85
Figure 2.6.7-27	Shield Tank End Plate.....	2.6.7-86
Figure 2.6.7-28	Gusset Profile.....	2.6.7-87
Figure 2.6.7-29	End Plate Welds.....	2.6.7-88
Figure 2.6.7-30	Component Parts of the Expansion Tank Structure	2.6.7-89
Figure 2.6.7-31	Expansion Tank Top and Bottom End Plate.....	2.6.7-90
Figure 2.6.7-32	Expansion Tank Stiffener Load Geometry	2.6.7-91
Figure 2.6.7-33	Cask Upper Ring at Trunnion - ANSYS Model	2.6.7-92
Figure 2.6.7-34	Cask Upper Ring at Trunnion - Model Loads and Boundary Conditions.....	2.6.7-93
Figure 2.6.7-35	NAC-LWT Cask Upper Ring at Trunnion - Critical Sections.....	2.6.7-94
Figure 2.6.10-1	Impact of Penetration Cylinder on Neutron Shield Tank and Expansion Tank – Points of Impact.....	2.6.10-12
Figure 2.6.10-2	Impact of Penetration Cylinder on Neutron Shield Tank and Expansion Tank – Details for Analysis	2.6.10-13
Figure 2.6.10-3	Impact of Penetration Cylinder on Port Cover	2.6.10-14
Figure 2.6.10-4	One-Sixth Model of the Alternate Port Cover – 60° Symmetry.....	2.6.10-15
Figure 2.6.12-1	Cask Side Drop Fuel Tube Loading – MTR Fuel Basket.....	2.6.12-23
Figure 2.6.12-2	Baseplate Supports for Cask End Drop Loads - MTR Fuel Basket.....	2.6.12-24
Figure 2.6.12-3	DIDO Fuel Basket Module Structural Model – Top View.....	2.6.12-56
Figure 2.6.12-4	DIDO Fuel Basket Module Structural Model – Bottom View	2.6.12-57
Figure 2.6.12-5	DIDO Fuel Basket Module Maximum Stress Locations for the Side Drop Orientation	2.6.12-58
Figure 2.6.12-6	DIDO Fuel Basket Module Maximum Stress Locations for the End Drop Orientation	2.6.12-59
Figure 2.6.12-7	Cross-Section of TPBAR Basket.....	2.6.12-82
Figure 2.6.12-8	TPBAR Spacer Schematic Triangular Top Plate and Tube.....	2.6.12-83
Figure 2.7.1-1	30-Foot Bottom End Drop with 130°F Ambient Temperature and Maximum Decay Heat Load.....	2.7.1-30
Figure 2.7.1-2	30-Foot Bottom End Drop with -40°F Ambient Temperature and Maximum Decay Heat Load.....	2.7.1-31
Figure 2.7.1-3	30-Foot Bottom End Drop with -40°F Ambient Temperature and No Decay Heat Load.....	2.7.1-32
Figure 2.7.1-4	30-Foot Top End Drop with 130°F Ambient Temperature and Maximum Decay Heat Load.....	2.7.1-33
Figure 2.7.1-5	30-Foot Top End Drop with -40°F Ambient Temperature and Maximum Decay Heat Load.....	2.7.1-34
Figure 2.7.1-6	Circumferential Load Distribution for Cask Side Drop Impact.....	2.7.1-35

List of Figures (continued)

Figure 2.7.1-7	Six Term Fourier Series Representation of Circumferential Load Distribution for Cask Side Drop Impact.....	2.7.1-36
Figure 2.7.1-8	NAC-LWT Cask Critical Sections (30-Foot Side Drop with 100°F Ambient Temperature).....	2.7.1-37
Figure 2.7.1-9	Circumferential Load Distribution for Cask Oblique Drop Impact.....	2.7.1-38
Figure 2.7.1-10	30-Foot Top Corner Drop with 130°F Ambient Temperature - Drop Orientation = 15.74 Degrees.....	2.7.1-39
Figure 2.7.1-11	30-Foot Top Oblique Drop with 130°F Ambient Temperature - Drop Orientation = 30 Degrees.....	2.7.1-40
Figure 2.7.1-12	30-Foot Top Oblique Drop with 130°F Ambient Temperature - Drop Orientation = 45 Degrees.....	2.7.1-41
Figure 2.7.1-13	30-Foot Oblique Drop with 130°F Ambient Temperature - Drop Orientation = 60 Degrees.....	2.7.1-42
Figure 2.7.1-14	30-Foot Top Corner Drop with -40°F Ambient Temperature - Drop Orientation = 15.74 Degrees.....	2.7.1-43
Figure 2.7.1-15	30-Foot Top Oblique Drop with -40°F Ambient Temperature - Drop Orientation = 30 Degrees.....	2.7.1-44
Figure 2.7.1-16	30-Foot Top Oblique Drop with -40°F Ambient Temperature - Drop Orientation = 45 Degrees.....	2.7.1-45
Figure 2.7.1-17	30-Foot Top Oblique Drop with -40°F Ambient Temperature - Drop Orientation = 60 Degrees.....	2.7.1-46
Figure 2.7.1-18	30-Foot Bottom Oblique Drop with 130°F Ambient Temperature - Drop Orientation = 15.74 Degrees.....	2.7.1-47
Figure 2.7.1-19	30-Foot Bottom Oblique Drop with 130°F Ambient Temperature - Drop Orientation = 30 Degrees.....	2.7.1-48
Figure 2.7.1-20	30-Foot Bottom Oblique Drop with 130°F Ambient Temperature - Drop Orientation = 45 Degrees.....	2.7.1-49
Figure 2.7.1-21	30-Foot Bottom Oblique Drop with 130°F Ambient Temperature - Drop Orientation = 60 Degrees.....	2.7.1-50
Figure 2.7.1-22	Sectional Stress Plot - 30-Foot Bottom Oblique Drop with 130°F Ambient Temperature - Drop Orientation = 60 Degrees.....	2.7.1-51
Figure 2.7.1-23	Sectional Stress Plot (P_m) - 30-Foot Bottom Oblique Drop with 130°F Ambient Temperature - Drop Orientation = 60 Degrees.....	2.7.1-52
Figure 2.7.1-24	Sectional Stress Plot ($P_m + P_b$) - 30-Foot Bottom Oblique Drop with 130°F Ambient Temperature - Drop Orientation = 60 Degrees.....	2.7.1-53
Figure 2.7.1-25	Bottom Closure Plate - Section Cut Identification.....	2.7.1-54
Figure 2.7.1-26	Sectional Stress Plot - 30-Foot Bottom Oblique Drop with 130°F Ambient Temperature - Drop Orientation = 45 Degrees.....	2.7.1-55
Figure 2.7.1-27	Sectional Stress Plot - 30-Foot Bottom Oblique Drop with 130°F Ambient Temperature - Drop Orientation = 30 Degrees.....	2.7.1-56
Figure 2.7.2-1	NAC-LWT Cask Midpoint Section.....	2.7.2-18
Figure 2.7.2-2	Cask Lid Configuration.....	2.7.2-19
Figure 2.7.2-3	NAC-LWT Cask Bottom Design Configuration.....	2.7.2-20

List of Figures (continued)

Figure 2.7.2-4	Port Cover Geometry	2.7.2-21
Figure 2.7.2-5	Puncture of Cask at Valve Cover Region	2.7.2-22
Figure 2.7.2-6	Alternate Port Cover Thermal Analysis Geometry	2.7.2-23
Figure 2.7.7-1	PWR Spacer Geometry	2.7.7-22
Figure 2.10.2-1	ANSYS Finite Element Model – NAC-LWT Cask.....	2.10.2-5
Figure 2.10.2-2	Cask Bottom of Model.....	2.10.2-6
Figure 2.10.2-3	Inner, Lead and Outer Shells – Lower Region of Model.....	2.10.2-7
Figure 2.10.2-4	Inner, Lead and Outer Shells – Lower Middle Region of Model	2.10.2-8
Figure 2.10.2-5	Inner, Lead and Outer Shells – Upper Middle Region of Model.....	2.10.2-9
Figure 2.10.2-6	Inner, Lead and Outer Shells – Upper Region of Model	2.10.2-10
Figure 2.10.2-7	Upper Ring Forging on Model.....	2.10.2-11
Figure 2.10.2-8	Closure Lid on Model	2.10.2-12
Figure 2.10.2-9	ANSYS Finite Element Model – Component Identification	2.10.2-13
Figure 2.10.3-1	NAC-LWT Cask Isotherms (Hot Case).....	2.10.3-3
Figure 2.10.3-2	NAC-LWT Cask Isotherms (Cold Case)	2.10.3-4
Figure 2.10.3-3	Stress Contour Plot – Hot Case.....	2.10.3-5
Figure 2.10.4-1	Cask Slapdown Geometry.....	2.10.4-6
Figure 2.10.4-2	Force Deflection Curve of Drop Tested Limiter – 0-Degree Impact.....	2.10.4-7
Figure 2.10.4-3	Force Deflection Curve of Drop Tested Limiter – 14-Degree Impact...	2.10.4-8
Figure 2.10.4-4	Force Deflection Curve of Drop Tested Limiter – 90-Degree Impact...	2.10.4-9
Figure 2.10.4-5	Oblique Drop	2.10.4-10
Figure 2.10.7-1	Representative Section Cut Diagram	2.10.7-3
Figure 2.10.8-1	Drawing of Quarter-Scale Model.....	2.10.8-19
Figure 2.10.8-2	Drawing of Model Body	2.10.8-20
Figure 2.10.8-3	Drawing of Model Lid	2.10.8-23
Figure 2.10.8-4	Drawing of Model Upper Impact Limiter.....	2.10.8-24
Figure 2.10.8-5	Drawing of Model Lower Impact Limiter	2.10.8-25
Figure 2.10.8-6	Drawing of Model Simulated Cask Contents	2.10.8-26
Figure 2.10.8-7	Quarter-Scale Model.....	2.10.8-27
Figure 2.10.8-8	Model Rigged for 30-Foot End Drop.....	2.10.8-28
Figure 2.10.8-9	Model Positioned for 30-Foot End Drop	2.10.8-29
Figure 2.10.8-10	Model Position Following 30-Foot End Drop	2.10.8-30
Figure 2.10.8-11	Top End Impact Limiter Following 30-Foot End Drop.....	2.10.8-31
Figure 2.10.8-12	Exterior of Top Impact Limiter Following 30-Foot End Drop.....	2.10.8-32
Figure 2.10.8-13	Model Rigged for 30-Foot Corner Drop.....	2.10.8-33
Figure 2.10.8-14	Model Positioned for 30-Foot Corner Drop.....	2.10.8-34
Figure 2.10.8-15	Model Following 30-Foot Corner Drop.....	2.10.8-35
Figure 2.10.8-16	Top Impact Limiter Following 30-Foot Corner Drop.....	2.10.8-36
Figure 2.10.8-17	Model Position Following 30-Foot Side Drop – View 1	2.10.8-37
Figure 2.10.8-18	Model Position Following 30-Foot Side Drop – View 2.....	2.10.8-38
Figure 2.10.8-19	Top Impact Limiter Following 30-Foot Side Drop.....	2.10.8-39
Figure 2.10.8-20	Bottom Impact Limiter Following 30-Foot Side Drop – View 1	2.10.8-40
Figure 2.10.8-21	Bottom Impact Limiter Following 30-Foot Side Drop – View 2	2.10.8-41

List of Figures (continued)

Figure 2.10.8-22	Model Rigged for 30-Foot Oblique Drop	2.10.8-42
Figure 2.10.8-23	Model Positioned for 30-Foot Oblique Drop.....	2.10.8-43
Figure 2.10.8-24	Model Position Following 30-Foot Oblique Drop.....	2.10.8-44
Figure 2.10.8-25	Bottom Impact Limiter Following 30-Foot Oblique Drop	2.10.8-45
Figure 2.10.8-26	Top Impact Limiter Following 30-Foot Oblique Drop.....	2.10.8-46
Figure 2.10.8-27	Model Rigged for Midpoint 40-Inch Pin Drop.....	2.10.8-47
Figure 2.10.8-28	Model Positioned for 40-Inch Pin Drop.....	2.10.8-48
Figure 2.10.8-29	Instant Before Midpoint 40-Inch Pin Drop.....	2.10.8-49
Figure 2.10.8-30	Model Position Following Midpoint 40-Inch Pin Drop.....	2.10.8-50
Figure 2.10.8-31	Impact Location – Midpoint 40-Inch Pin Drop	2.10.8-51
Figure 2.10.8-32	Angular Orientation of Instrumentation.....	2.10.8-52
Figure 2.10.8-33	Strain Gauge Time History for Channel 3 – End Drop	2.10.8-53
Figure 2.10.8-34	Strain Gauge Time History for Channel 4 – End Drop	2.10.8-54
Figure 2.10.8-35	Strain Gauge Time History for Channel 5 – End Drop	2.10.8-55
Figure 2.10.8-36	Strain Gauge Time History for Channel 3 – Side Drop.....	2.10.8-56
Figure 2.10.8-37	Strain Gauge Time History for Channel 4 – Side Drop.....	2.10.8-57
Figure 2.10.8-38	Strain Gauge Time History for Channel 5 – Side Drop.....	2.10.8-58
Figure 2.10.8-39	Location of Block Sets.....	2.10.8-59
Figure 2.10.10-1	Stress Point Locations.....	2.10.10-7
Figure 2.10.11-1	Mathematical Model of NAC-LWT Cask (30-foot Top End Impact)...	2.10.11-8
Figure 2.10.12-1	Side Drop ($\theta = 90^\circ$).....	2.10.12-9
Figure 2.10.12-2	End Drop ($0^\circ \leq \theta < 15^\circ$)	2.10.12-10
Figure 2.10.12-3	Oblique Drop ($15^\circ \leq \theta < 90^\circ$).....	2.10.12-11
Figure 2.10.12-4	Force-Deflection Graph (0-Degree, Top End Drop).....	2.10.12-12
Figure 2.10.12-5	Force-Deflection Graph (0-Degree, Bottom End Drop).....	2.10.12-13
Figure 2.10.12-6	Force-Deflection Graph (15.74-Degree, Top Corner Drop).....	2.10.12-14
Figure 2.10.12-7	Force-Deflection Graph (14.5-Degree, Bottom Corner Drop)	2.10.12-15
Figure 2.10.12-8	Force-Deflection Graph (30-Degree, Top Oblique Drop)	2.10.12-16
Figure 2.10.12-9	Force-Deflection Graph (30-Degree, Bottom Oblique Drop).....	2.10.12-17
Figure 2.10.12-10	Force-Deflection Graph (45-Degree, Top Oblique Drop)	2.10.12-18
Figure 2.10.12-11	Force-Deflection Graph (45-Degree, Bottom Oblique Drop).....	2.10.12-19
Figure 2.10.12-12	Force-Deflection Graph (60-Degree, Top Oblique Drop)	2.10.12-20
Figure 2.10.12-13	Force-Deflection Graph (60-Degree, Bottom Oblique Drop).....	2.10.12-21
Figure 2.10.12-14	Force-Deflection Graph (75-Degree, Top Oblique Drop)	2.10.12-22
Figure 2.10.12-15	Force-Deflection Graph (75-Degree, Bottom Oblique Drop).....	2.10.12-23
Figure 2.10.12-16	Force-Deflection Graph (90-Degree, Top Side Drop).....	2.10.12-24
Figure 2.10.12-17	Force-Deflection Graph (90-Degree, Bottom Side Drop)	2.10.12-25
Figure 2.10.12-18	Force-Deflection Curve (0-Degree Impact, Drop Tested Limiter)....	2.10.12-26
Figure 2.10.12-19	Force-Deflection Curve (14-Degree Impact, Drop Tested Limiter)..	2.10.12-27
Figure 2.10.12-20	Force-Deflection Curve (90-Degree Impact, Drop Tested Limiter)..	2.10.12-28
Figure 2.10.12-21	End Drop Impact Limiter Cross Section.....	2.10.12-29
Figure 2.10.13-1	LWT Cask, Metal Fuel Basket Assembly Safety Analysis Report, NAC Drawing No. 315-40-12.....	2.10.13-13

List of Figures (continued)

Figure 2.10.13-2	Liner-Failed Fuel Can, 2.75 I.D., LWT Cask, Safety Analysis Report, NAC Drawing No. 315-040-43	2.10.13-14
Figure 2.10.13-3	Failed Fuel Rod Can – 4.00 I.D., Fuel Rod Containerization, NAC Drawing No. 340-108-D1	2.10.13-15
Figure 2.10.13-4	Failed Fuel Rod Can – 2.75 I.D., Fuel Rod Containerization, NAC Drawing No. 340-108-D2	2.10.13-16
Figure 2.10.13-5	Failed Fuel Filter, NAC Drawing No. 491-042	2.10.13-17
Figure 2.10.14-1	ANSYS Finite Element Model of the Cask Body	2.10.14-7
Figure 2.10.14-2	Detailed View of the Cask Body Finite Element Model Top	2.10.14-8
Figure 2.10.14-3	Detailed View of the Cask Body Finite Element Model Bottom	2.10.14-9
Figure 2.10.14-4	Location of Sections of the NAC-LWT Cask Body Model.....	2.10.14-10
Figure 2.10.15-1	Alternate B Port Cover Finite Element Model	2.10.15-10

List of Tables

Table 2.1.2-1	Allowable Stress Limits for Containment Structures	2.1.2-2
Table 2.1.2-2	Allowable Stress Limits for Noncontainment Structures	2.1.2-3
Table 2.1.3-1	Extreme Total Stress Intensities.....	2.1.3-8
Table 2.2.1-1	Weights of the NAC-LWT Cask Major Components.....	2.2.1-2
Table 2.2.1-2	Weights and Center of Gravity Locations for the NAC-LWT Cask Shipping Configurations	2.2.1-3
Table 2.3.1-1	Mechanical Properties of Type 304 Stainless Steel.....	2.3.1-5
Table 2.3.1-2	Mechanical Properties of Type XM-19 Stainless Steel	2.3.1-6
Table 2.3.1-3	Mechanical Properties of SA-705, Grade 630, Precipitation- Hardened Stainless Steel.....	2.3.1-7
Table 2.3.1-4	Mechanical Properties (6061-T6 and T651 per ASTM B-209).....	2.3.1-8
Table 2.3.1-5	Mechanical Properties of SA-193, Grade B6 High Alloy, Steel Bolting Material	2.3.1-9
Table 2.3.1-6	Mechanical Properties of SA-453, Grade 660 High Alloy, Steel Bolting Material	2.3.1-10
Table 2.3.1-7	Static Mechanical Properties of Chemical Copper Lead	2.3.1-11
Table 2.3.1-8	Dynamic Mechanical Properties of Chemical Copper Lead.....	2.3.1-12
Table 2.3.1-9	Mechanical Properties of SB-637, Grade N07718, Nickel Alloy Steel Bolting Material	2.3.1-13
Table 2.5.1-1	Maximum Capacity of the Lifting Components	2.5.1-11
Table 2.5.2-1	Reactions Caused By Tiedown Devices	2.5.2-17
Table 2.6.1-1	Critical Stress Summary (Hot Case) - P_m	2.6.1-5
Table 2.6.1-2	Critical Stress Summary (Hot Case) - $P_m + P_b$	2.6.1-6
Table 2.6.1-3	Critical Stress Summary (Hot Case) - Total Range	2.6.1-7
Table 2.6.2-1	Critical Stress Summary (Cold Case) - P_m	2.6.2-5
Table 2.6.2-2	Critical Stress Summary (Cold Case) - $P_m + P_b$	2.6.2-6
Table 2.6.2-3	Critical Stress Summary (Cold Case) - Total Range	2.6.2-7
Table 2.6.7-1	Critical Stress Summary (1-Foot Bottom End Drop) – Loading Condition 1 – P_m	2.6.7-95
Table 2.6.7-2	Critical Stress Summary (1-Foot Bottom End Drop) – Loading Condition 1 - $P_m + P_b$	2.6.7-96
Table 2.6.7-3	Critical Stress Summary (1-Foot Bottom End Drop) – Loading Condition 1 - Total Range.....	2.6.7-97
Table 2.6.7-4	Critical Stress Summary (1-Foot Bottom End Drop) – Loading Condition 2 – P_m	2.6.7-98
Table 2.6.7-5	Critical Stress Summary (1-Foot Bottom End Drop) – Loading Condition 2 - $P_m + P_b$	2.6.7-99
Table 2.6.7-6	Critical Stress Summary (1-Foot Bottom End Drop) – Loading Condition 2 - Total Range.....	2.6.7-100
Table 2.6.7-7	Critical Stress Summary (1-Foot Bottom End Drop) – Loading Condition 3 – P_m	2.6.7-101
Table 2.6.7-8	Critical Stress Summary (1-Foot Bottom End Drop) – Loading Condition 3 - $P_m + P_b$	2.6.7-102

List of Tables (continued)

Table 2.6.7-9	Critical Stress Summary (1-Foot Bottom End Drop) – Loading Condition 3 - Total Range.....	2.6.7-103
Table 2.6.7-10	Critical Stress Summary (1-Foot Top End Drop) – Loading Condition 1 - P_m	2.6.7-104
Table 2.6.7-11	Critical Stress Summary (1-Foot Top End Drop) – Loading Condition 1 - $P_m + P_b$	2.6.7-105
Table 2.6.7-12	Critical Stress Summary (1-Foot Top End Drop) – Loading Condition 1 - Total Range.....	2.6.7-106
Table 2.6.7-13	Critical Stress Summary (1-Foot Top End Drop) – Loading Condition 2 - P_m	2.6.7-107
Table 2.6.7-14	Critical Stress Summary (1-Foot Top End Drop) – Loading Condition 2 - $P_m + P_b$	2.6.7-108
Table 2.6.7-15	Critical Stress Summary (1-Foot Top End Drop) – Loading Condition 2 - Total Range.....	2.6.7-109
Table 2.6.7-16	Critical Stress Summary (1-Foot Side Drop) – Loading Condition 1 - P_m	2.6.7-110
Table 2.6.7-17	Critical Stress Summary (1-Foot Side Drop) – Loading Condition 1 - $P_m + P_b$	2.6.7-111
Table 2.6.7-18	Critical Stress Summary (1-Foot Side Drop) – Loading Condition 1 - S_n	2.6.7-112
Table 2.6.7-19	Critical Stress Summary (1-Foot Side Drop) – Loading Condition 1 - Total Range.....	2.6.7-113
Table 2.6.7-20	Critical Stress Summary (1-Foot Top Corner Drop) – Loading Condition 1 - P_m – Drop Orientation = 15.74 Degrees.....	2.6.7-114
Table 2.6.7-21	Critical Stress Summary (1-Foot Top Corner Drop) – Loading Condition 1 - $P_m + P_b$ – Drop Orientation = 15.74 Degrees.....	2.6.7-115
Table 2.6.7-22	Critical Stress Summary (1-Foot Top Corner Drop) – Loading Condition 1 - S_n – Drop Orientation = 15.74 Degrees.....	2.6.7-116
Table 2.6.7-23	Critical Stress Summary (1-Foot Top Corner Drop) – Loading Condition 1 - Total Range – Drop Orientation = 15.74 Degrees.....	2.6.7-117
Table 2.6.7-24	Critical Stress Summary (1-Foot Bottom Corner Drop) – Loading Condition 1 - P_m – Drop Orientation = 15.74 Degrees.....	2.6.7-118
Table 2.6.7-25	Critical Stress Summary (1-Foot Bottom Corner Drop) – Loading Condition 1 - $P_m + P_b$ – Drop Orientation = 15.74 Degrees.....	2.6.7-119
Table 2.6.7-26	Critical Stress Summary (1-Foot Bottom Corner Drop) – Loading Condition 1 - S_n – Drop Orientation = 15.74 Degrees.....	2.6.7-120
Table 2.6.7-27	Critical Stress Summary (1-Foot Bottom Corner Drop) – Loading Condition 1 - Total Range – Drop Orientation = 15.74 Degrees.....	2.6.7-121
Table 2.6.7-28	Critical Stress Summary (1-Foot Top Corner Drop) – Loading Condition 3 - P_m – Drop Orientation = 15.74 Degrees.....	2.6.7-122
Table 2.6.7-29	Critical Stress Summary (1-Foot Top Corner Drop) – Loading Condition 3 - $P_m + P_b$ – Drop Orientation = 15.74 Degrees.....	2.6.7-123

List of Tables (continued)

Table 2.6.7-30	Critical Stress Summary (1-Foot Top Corner Drop) – Loading Condition 3 - S_n – Drop Orientation = 15.74 Degrees.....	2.6.7-124
Table 2.6.7-31	Critical Stress Summary (1-Foot Top Corner Drop) – Loading Condition 3 - Total Range – Drop Orientation = 15.74 Degrees.....	2.6.7-125
Table 2.6.7-32	Summary of Results - Impact Limiter Analysis for 1-Foot Free Drop	2.6.7-126
Table 2.6.7-33	Summary of Results - Impact Limiter Analysis for 30-Foot Free Drop Subsequent to a 1-Foot Fall	2.6.7-128
Table 2.6.7-34	Summary of Cask Drop Equivalent G Load Factors	2.6.7-130
Table 2.6.7-35	NAC-LWT Cask Hot Bolt Analysis – Normal Conditions	2.6.7-131
Table 2.6.7-36	NAC-LWT Cask Cold Bolt Analysis – Normal Conditions.....	2.6.7-132
Table 2.6.7-37	Summary of Neutron Shield Tank Analysis.....	2.6.7-133
Table 2.6.7-38	Normal Transport Shield Tank Temperatures	2.6.7-134
Table 2.6.7-39	Normal Transport Shield Tank Pressures	2.6.7-135
Table 2.6.7-40	Summary of Expansion Tank Analysis.....	2.6.7-135
Table 2.6.7-41	Upper Ring – Cross-Section Principal Stresses	2.6.7-136
Table 2.6.12-1	Maximum Primary Membrane Stress for the 1-Foot Drop (DIDO Basket)	2.6.12-60
Table 2.6.12-2	Maximum Primary Membrane Plus Bending Stress for the 1-Foot Drop (DIDO Basket).....	2.6.12-60
Table 2.7.1-1	Critical Stress Summary (30-Foot Bottom End Drop) – Loading Condition 1 – P_m	2.7.1-57
Table 2.7.1-2	Critical Stress Summary (30-Foot Bottom End Drop) – Loading Condition 1 - $P_m + P_b$	2.7.1-58
Table 2.7.1-3	Critical Stress Summary (30-Foot Bottom End Drop) – Loading Condition 1 - Total Range.....	2.7.1-59
Table 2.7.1-4	Critical Stress Summary (30-Foot Bottom End Drop) – Loading Condition 2 – P_m	2.7.1-60
Table 2.7.1-5	Critical Stress Summary (30-Foot Bottom End Drop) – Loading Condition 2 - $P_m + P_b$	2.7.1-61
Table 2.7.1-6	Critical Stress Summary (30-Foot Bottom End Drop) – Loading Condition 2 - Total Range.....	2.7.1-62
Table 2.7.1-7	Critical Stress Summary (30-Foot Bottom End Drop) – Loading Condition 3 – P_m	2.7.1-63
Table 2.7.1-8	Critical Stress Summary (30-Foot Bottom End Drop) – Loading Condition 3 - $P_m + P_b$	2.7.1-64
Table 2.7.1-9	Critical Stress Summary (30-Foot Bottom End Drop) – Loading Condition 3 - Total Range.....	2.7.1-65
Table 2.7.1-10	Critical Stress Summary (30-Foot Top End Drop) – Loading Condition 1 – P_m	2.7.1-66
Table 2.7.1-11	Critical Stress Summary (30-Foot Top End Drop) – Loading Condition 1 - $P_m + P_b$	2.7.1-67

List of Tables (continued)

Table 2.7.1-12	Critical Stress Summary (30-Foot Top End Drop) – Loading Condition 1 - Total Range.....	2.7.1-68
Table 2.7.1-13	Critical Stress Summary (30-Foot Top End Drop) – Loading Condition 2 – P_m	2.7.1-69
Table 2.7.1-14	Critical Stress Summary (30-Foot Top End Drop) – Loading Condition 2 - $P_m + P_b$	2.7.1-70
Table 2.7.1-15	Critical Stress Summary (30-Foot Top End Drop) – Loading Condition 2 - Total Range.....	2.7.1-71
Table 2.7.1-16	Side Drop Load Analysis Description	2.7.1-72
Table 2.7.1-17	Critical Stress Summary (30-Foot Side Drop) – Loading Condition 1 - P_m	2.7.1-73
Table 2.7.1-18	Critical Stress Summary (30-Foot Side Drop) – Loading Condition 1 - $P_m + P_b$	2.7.1-74
Table 2.7.1-19	Critical Stress Summary (30-Foot Side Drop) – Loading Condition 1 - Total Range.....	2.7.1-75
Table 2.7.1-20	G Loads – Oblique Drop.....	2.7.1-76
Table 2.7.1-21	Impact and Contents Pressures – Oblique Drop	2.7.1-77
Table 2.7.1-22	Fourier Series Modal Coefficients – Oblique Drop.....	2.7.1-78
Table 2.7.1-23	Oblique Drop Load Analysis Description.....	2.7.1-79
Table 2.7.1-24	Critical Stress Summary (30-Foot Top Corner Drop) – Loading Condition 1 - P_m – Drop Orientation = 15.74 Degrees	2.7.1-80
Table 2.7.1-25	Critical Stress Summary (30-Foot Top Corner Drop) – Loading Condition 1 - $P_m + P_b$ – Drop Orientation = 15.74 Degrees	2.7.1-81
Table 2.7.1-26	Critical Stress Summary (30-Foot Top Corner Drop) – Loading Condition 1 – Total Range – Drop Orientation = 15.74 Degrees	2.7.1-82
Table 2.7.1-27	Critical Stress Summary (30-Foot Top Oblique Drop) – Loading Condition 1 - P_m – Drop Orientation = 30 Degrees	2.7.1-83
Table 2.7.1-28	Critical Stress Summary (30-Foot Top Oblique Drop) – Loading Condition 1 - $P_m + P_b$ – Drop Orientation = 30 Degrees	2.7.1-84
Table 2.7.1-29	Critical Stress Summary (30-Foot Top Oblique Drop) – Loading Condition 1 – Total Range – Drop Orientation = 30 Degrees	2.7.1-85
Table 2.7.1-30	Critical Stress Summary (30-Foot Top Oblique Drop) – Loading Condition 1 - P_m – Drop Orientation = 45 Degrees	2.7.1-86
Table 2.7.1-31	Critical Stress Summary (30-Foot Top Oblique Drop) – Loading Condition 1 - $P_m + P_b$ – Drop Orientation = 45 Degrees	2.7.1-87
Table 2.7.1-32	Critical Stress Summary (30-Foot Top Oblique Drop) – Loading Condition 1 – Total Range – Drop Orientation = 45 Degrees	2.7.1-88
Table 2.7.1-33	Critical Stress Summary (30-Foot Top Oblique Drop) – Loading Condition 1 - P_m – Drop Orientation = 60 Degrees	2.7.1-89
Table 2.7.1-34	Critical Stress Summary (30-Foot Top Oblique Drop) – Loading Condition 1 - $P_m + P_b$ – Drop Orientation = 60 Degrees	2.7.1-90
Table 2.7.1-35	Critical Stress Summary (30-Foot Top Oblique Drop) – Loading Condition 1 – Total Range – Drop Orientation = 60 Degrees	2.7.1-91

List of Tables (continued)

Table 2.7.1-36	Critical Stress Summary (30-Foot Top Corner Drop) – Loading Condition 3 - P_m – Drop Orientation = 15.74 Degrees 2.7.1-92
Table 2.7.1-37	Critical Stress Summary (30-Foot Top Corner Drop) – Loading Condition 3 - $P_m + P_b$ – Drop Orientation = 15.74 Degrees 2.7.1-93
Table 2.7.1-38	Critical Stress Summary (30-Foot Top Corner Drop) – Loading Condition 3 – Total Range – Drop Orientation = 15.74 Degrees 2.7.1-94
Table 2.7.1-39	Critical Stress Summary (30-Foot Top Oblique Drop) – Loading Condition 3 - P_m – Drop Orientation = 30 Degrees 2.7.1-95
Table 2.7.1-40	Critical Stress Summary (30-Foot Top Oblique Drop) – Loading Condition 3 - $P_m + P_b$ – Drop Orientation = 30 Degrees 2.7.1-96
Table 2.7.1-41	Critical Stress Summary (30-Foot Top Oblique Drop) – Loading Condition 3 – Total Range – Drop Orientation = 30 Degrees 2.7.1-97
Table 2.7.1-42	Critical Stress Summary (30-Foot Top Oblique Drop) – Loading Condition 3 - P_m – Drop Orientation = 45 Degrees 2.7.1-98
Table 2.7.1-43	Critical Stress Summary (30-Foot Top Oblique Drop) – Loading Condition 3 - $P_m + P_b$ – Drop Orientation = 45 Degrees 2.7.1-99
Table 2.7.1-44	Critical Stress Summary (30-Foot Top Oblique Drop) – Loading Condition 3 – Total Range – Drop Orientation = 45 Degrees 2.7.1-100
Table 2.7.1-45	Critical Stress Summary (30-Foot Top Oblique Drop) – Loading Condition 3 - P_m – Drop Orientation = 60 Degrees 2.7.1-101
Table 2.7.1-46	Critical Stress Summary (30-Foot Top Oblique Drop) – Loading Condition 3 - $P_m + P_b$ – Drop Orientation = 60 Degrees 2.7.1-102
Table 2.7.1-47	Critical Stress Summary (30-Foot Top Oblique Drop) – Loading Condition 3 – Total Range – Drop Orientation = 60 Degrees 2.7.1-103
Table 2.7.1-48	Critical Stress Summary (30-Foot Bottom Oblique Drop) – Loading Condition 1 - P_m – Drop Orientation = 15.74 Degrees 2.7.1-104
Table 2.7.1-49	Critical Stress Summary (30-Foot Bottom Oblique Drop) – Loading Condition 1 - $P_m + P_b$ – Drop Orientation = 15.74 Degrees 2.7.1-105
Table 2.7.1-50	Critical Stress Summary (30-Foot Bottom Oblique Drop) – Loading Condition 1 – Total Range – Drop Orientation = 15.74 Degrees 2.7.1-106
Table 2.7.1-51	Critical Stress Summary (30-Foot Bottom Oblique Drop) – Loading Condition 1 - P_m – Drop Orientation = 30 Degrees 2.7.1-107
Table 2.7.1-52	Critical Stress Summary (30-Foot Bottom Oblique Drop) – Loading Condition 1 - $P_m + P_b$ – Drop Orientation = 30 Degrees 2.7.1-108
Table 2.7.1-53	Critical Stress Summary (30-Foot Bottom Oblique Drop) – Loading Condition 1 – Total Range – Drop Orientation = 30 Degrees 2.7.1-109
Table 2.7.1-54	Critical Stress Summary (30-Foot Bottom Oblique Drop) – Loading Condition 1 - P_m – Drop Orientation = 45 Degrees 2.7.1-110
Table 2.7.1-55	Critical Stress Summary (30-Foot Bottom Oblique Drop) – Loading Condition 1 - $P_m + P_b$ – Drop Orientation = 45 Degrees 2.7.1-111
Table 2.7.1-56	Critical Stress Summary (30-Foot Bottom Oblique Drop) – Loading Condition 1 – Total Range – Drop Orientation = 45 Degrees 2.7.1-112

List of Tables (continued)

Table 2.7.1-57	Critical Stress Summary (30-Foot Bottom Oblique Drop) – Loading Condition 1 - P_m – Drop Orientation = 60 Degrees	2.7.1-113
Table 2.7.1-58	Critical Stress Summary (30-Foot Bottom Oblique Drop) – Loading Condition 1 - $P_m + P_b$ – Drop Orientation = 60 Degrees	2.7.1-114
Table 2.7.1-59	Critical Stress Summary (30-Foot Bottom Oblique Drop) – Loading Condition 1 – Total Range – Drop Orientation = 60 Degrees	2.7.1-115
Table 2.7.1-60	NAC-LWT Cask Hot Bolt Analysis Hypothetical Accident Conditions	2.7.1-116
Table 2.7.1-61	NAC-LWT Cask Cold Bolt Analysis Hypothetical Accident Conditions	2.7.1-117
Table 2.7.6-1	Summary of Maximum Calculated Stresses – 30-Foot Drop	2.7.6-2
Table 2.7.6-2	Summary of Maximum Calculated Stresses – 40-Inch Free Drop	2.7.6-3
Table 2.7.6-3	Summary of Maximum Calculated Stresses - Fire	2.7.6-4
Table 2.7.7-1	Maximum Primary Membrane Stress for the 30-Foot Drop.....	2.7.7-50
Table 2.7.7-2	Maximum Primary Membrane Plus Bending Stress for the 30-Foot Drop	2.7.7-50
Table 2.10.2-1	Node Definitions.....	2.10.2-14
Table 2.10.2-2	Applied Impact Pressure Loadings – 30-Foot Hypothetical Accident Conditions	2.10.2-48
Table 2.10.3-1	P_m Stress Summary – Upper Ring Critical Section	2.10.3-6
Table 2.10.3-2	$P_m + P_b$ Stress Summary – Upper Ring Critical Section.....	2.10.3-11
Table 2.10.4-1	Determination of Maximum Energy for Secondary Impact – Full- Scale Impact Limiter.....	2.10.4-11
Table 2.10.6-1	Inner Shell Geometry Parameters	2.10.6-8
Table 2.10.6-2	Material Properties of Type XM-19 Stainless Steel for Buckling Analysis Input (ASME, Section III, Appendix I)	2.10.6-9
Table 2.10.6-3	Theoretical Elastic Buckling Stress Values (Temperature Independent Form).....	2.10.6-10
Table 2.10.6-4	Theoretical Elastic Buckling Stresses for Selected Temperatures.....	2.10.6-11
Table 2.10.6-5	Capacity Reduction Factors for the Type XM-19 Stainless Steel Inner Shell.....	2.10.6-12
Table 2.10.6-6	Fabrication Tolerances for the NAC-LWT Cask Inner Shell	2.10.6-13
Table 2.10.6-7	Upper Bound Buckling Stresses	2.10.6-14
Table 2.10.6-8	Calculated Maximum Compressive Stresses in the Inner Shell	2.10.6-15
Table 2.10.6-9	Calculated Stresses with ASME Factors of Safety	2.10.6-17
Table 2.10.6-10	Results – Interaction Equations	2.10.6-18
Table 2.10.7-1	Section Cut Identification	2.10.7-4
Table 2.10.7-2	P_m Stress Summary (Hot Case).....	2.10.7-5
Table 2.10.7-3	$P_m + P_b$ Stress Summary (Hot Case).....	2.10.7-6
Table 2.10.7-4	P_m Stress Summary (Cold Case).....	2.10.7-7
Table 2.10.7-5	$P_m + P_b$ Stress Summary (Cold Case).....	2.10.7-8
Table 2.10.7-6	P_m Stress Summary (1-Foot Bottom End Drop) – Loading Condition 1.....	2.10.7-9

List of Tables (continued)

Table 2.10.7-7	$P_m + P_b$ Stress Summary (1-Foot Bottom End Drop) – Loading Condition 1.....	2.10.7-10
Table 2.10.7-8	P_m Stress Summary (1-Foot Bottom End Drop) – Loading Condition 2.....	2.10.7-11
Table 2.10.7-9	$P_m + P_b$ Stress Summary (1-Foot Bottom End Drop) – Loading Condition 2.....	2.10.7-12
Table 2.10.7-10	P_m Stress Summary (1-Foot Bottom End Drop) – Loading Condition 3.....	2.10.7-13
Table 2.10.7-11	$P_m + P_b$ Stress Summary (1-Foot Bottom End Drop) – Loading Condition 3.....	2.10.7-14
Table 2.10.7-12	P_m Stress Summary (1-Foot Top End Drop) – Loading Condition 1 ..	2.10.7-15
Table 2.10.7-13	$P_m + P_b$ Stress Summary (1-Foot Top End Drop) – Loading Condition 1.....	2.10.7-16
Table 2.10.7-14	P_m Stress Summary (1-Foot Top End Drop) – Loading Condition 2 ..	2.10.7-17
Table 2.10.7-15	$P_m + P_b$ Stress Summary (1-Foot Top End Drop) – Loading Condition 2.....	2.10.7-18
Table 2.10.7-16	P_m Stress Summary (1-Foot Side Drop) – Loading Condition 1	2.10.7-19
Table 2.10.7-17	$P_m + P_b$ Stress Summary (1-Foot Side Drop) – Loading Condition 1 ..	2.10.7-20
Table 2.10.7-18	S_n Stress Summary (1-Foot Side Drop) – Loading Condition 1	2.10.7-21
Table 2.10.7-19	P_m Stress Summary (1-Foot Top Corner Drop) – Loading Condition 1 – Drop Orientation = 15.74 Degrees.....	2.10.7-22
Table 2.10.7-20	$P_m + P_b$ Stress Summary (1-Foot Top Corner Drop) – Loading Condition 1 – Drop Orientation = 15.74 Degrees.....	2.10.7-23
Table 2.10.7-21	S_n Stress Summary (1-Foot Top Corner Drop) – Loading Condition 1 – Drop Orientation = 15.74 Degrees.....	2.10.7-24
Table 2.10.7-22	P_m Stress Summary (1-Foot Bottom Corner Drop) – Loading Condition 1 – Drop Orientation = 15.74 Degrees.....	2.10.7-25
Table 2.10.7-23	$P_m + P_b$ Stress Summary (1-Foot Bottom Corner Drop) – Loading Condition 1 – Drop Orientation = 15.74 Degrees.....	2.10.7-26
Table 2.10.7-24	S_n Stress Summary (1-Foot Bottom Corner Drop) – Loading Condition 1 – Drop Orientation = 15.74 Degrees.....	2.10.7-27
Table 2.10.7-25	P_m Stress Summary (1-Foot Top Corner Drop) – Loading Condition 3 – Drop Orientation = 15.74 Degrees.....	2.10.7-28
Table 2.10.7-26	$P_m + P_b$ Stress Summary (1-Foot Top Corner Drop) – Loading Condition 3 – Drop Orientation = 15.74 Degrees.....	2.10.7-29
Table 2.10.7-27	S_n Stress Summary (1-Foot Top Corner Drop) – Loading Condition 3 – Drop Orientation = 15.74 Degrees.....	2.10.7-30
Table 2.10.7-28	P_m Stress Summary (30-Foot Bottom End Drop) – Loading Condition 1.....	2.10.7-31
Table 2.10.7-29	$P_m + P_b$ Stress Summary (30-Foot Bottom End Drop) – Loading Condition 1.....	2.10.7-32
Table 2.10.7-30	P_m Stress Summary (30-Foot Bottom End Drop) – Loading Condition 2.....	2.10.7-33

List of Tables (continued)

Table 2.10.7-31	$P_m + P_b$ Stress Summary (30-Foot Bottom End Drop) – Loading Condition 2.....	2.10.7-34
Table 2.10.7-32	P_m Stress Summary (30-Foot Bottom End Drop) – Loading Condition 3.....	2.10.7-35
Table 2.10.7-33	$P_m + P_b$ Stress Summary (30-Foot Bottom End Drop) – Loading Condition 3.....	2.10.7-36
Table 2.10.7-34	P_m Stress Summary (30-Foot Top End Drop) – Loading Condition 1.....	2.10.7-37
Table 2.10.7-35	$P_m + P_b$ Stress Summary (30-Foot Top End Drop) – Loading Condition 1.....	2.10.7-38
Table 2.10.7-36	P_m Stress Summary (30-Foot Top End Drop) – Loading Condition 2.....	2.10.7-39
Table 2.10.7-37	$P_m + P_b$ Stress Summary (30-Foot Top End Drop) – Loading Condition 2.....	2.10.7-40
Table 2.10.7-38	P_m Stress Summary (30-Foot Side Drop) – Loading Condition 1	2.10.7-41
Table 2.10.7-39	$P_m + P_b$ Stress Summary (30-Foot Side Drop) – Loading Condition 1.....	2.10.7-42
Table 2.10.7-40	P_m Stress Summary (30-Foot Top Corner Drop) – Loading Condition 1 – Drop Orientation = 15.74 Degrees.....	2.10.7-43
Table 2.10.7-41	$P_m + P_b$ Stress Summary (30-Foot Top Corner Drop) – Loading Condition 1 – Drop Orientation = 15.74 Degrees.....	2.10.7-44
Table 2.10.7-42	P_m Stress Summary (30-Foot Top Oblique Drop) – Loading Condition 1 – Drop Orientation = 30 Degrees.....	2.10.7-45
Table 2.10.7-43	$P_m + P_b$ Stress Summary (30-Foot Top Oblique Drop) – Loading Condition 1 – Drop Orientation = 30 Degrees.....	2.10.7-46
Table 2.10.7-44	P_m Stress Summary (30-Foot Top Oblique Drop) – Loading Condition 1 – Drop Orientation = 45 Degrees.....	2.10.7-47
Table 2.10.7-45	$P_m + P_b$ Stress Summary (30-Foot Top Oblique Drop) – Loading Condition 1 – Drop Orientation = 45 Degrees.....	2.10.7-48
Table 2.10.7-46	P_m Stress Summary (30-Foot Top Oblique Drop) – Loading Condition 1 – Drop Orientation = 60 Degrees.....	2.10.7-49
Table 2.10.7-47	$P_m + P_b$ Stress Summary (30-Foot Top Oblique Drop) – Loading Condition 1 – Drop Orientation = 60 Degrees.....	2.10.7-50
Table 2.10.7-48	P_m Stress Summary (30-Foot Top Corner Drop) – Loading Condition 3 – Drop Orientation = 15.74 Degrees.....	2.10.7-51
Table 2.10.7-49	$P_m + P_b$ Stress Summary (30-Foot Top Corner Drop) – Loading Condition 3 – Drop Orientation = 15.74 Degrees.....	2.10.7-52
Table 2.10.7-50	P_m Stress Summary (30-Foot Top Oblique Drop) – Loading Condition 3 – Drop Orientation = 30 Degrees.....	2.10.7-53
Table 2.10.7-51	$P_m + P_b$ Stress Summary (30-Foot Top Oblique Drop) – Loading Condition 3 – Drop Orientation = 30 Degrees.....	2.10.7-54
Table 2.10.7-52	P_m Stress Summary (30-Foot Top Oblique Drop) – Loading Condition 3 – Drop Orientation = 45 Degrees.....	2.10.7-55

List of Tables (continued)

Table 2.10.7-53	$P_m + P_b$ Stress Summary (30-Foot Top Oblique Drop) – Loading Condition 3 – Drop Orientation = 45 Degrees.....	2.10.7-56
Table 2.10.7-54	P_m Stress Summary (30-Foot Top Oblique Drop) – Loading Condition 3 – Drop Orientation = 60 Degrees.....	2.10.7-57
Table 2.10.7-55	$P_m + P_b$ Stress Summary (30-Foot Top Oblique Drop) – Loading Condition 3 – Drop Orientation = 60 Degrees.....	2.10.7-58
Table 2.10.7-56	P_m Stress Summary (30-Foot Bottom Corner Drop) – Loading Condition 1 – Drop Orientation = 15.74 Degrees.....	2.10.7-59
Table 2.10.7-57	$P_m + P_b$ Stress Summary (30-Foot Bottom Corner Drop) – Loading Condition 1 – Drop Orientation = 15.74 Degrees.....	2.10.7-60
Table 2.10.7-58	P_m Stress Summary (30-Foot Bottom Oblique Drop) – Loading Condition 1 – Drop Orientation = 30 Degrees.....	2.10.7-61
Table 2.10.7-59	$P_m + P_b$ Stress Summary (30-Foot Bottom Oblique Drop) – Loading Condition 1 – Drop Orientation = 30 Degrees.....	2.10.7-62
Table 2.10.7-60	P_m Stress Summary (30-Foot Bottom Oblique Drop) – Loading Condition 1 – Drop Orientation = 45 Degrees.....	2.10.7-63
Table 2.10.7-61	$P_m + P_b$ Stress Summary (30-Foot Bottom Oblique Drop) – Loading Condition 1 – Drop Orientation = 45 Degrees.....	2.10.7-64
Table 2.10.7-62	P_m Stress Summary (30-Foot Bottom Oblique Drop) – Loading Condition 1 – Drop Orientation = 60 Degrees.....	2.10.7-65
Table 2.10.7-63	$P_m + P_b$ Stress Summary (30-Foot Bottom Oblique Drop) – Loading Condition 1 – Drop Orientation = 60 Degrees.....	2.10.7-66
Table 2.10.8-1	Scaling Relations	2.10.8-60
Table 2.10.8-2	Metrology Results of Inner Diameter Measurements Before Drop.....	2.10.8-62
Table 2.10.8-3	Metrology Results of Outer Diameter Measurements Before Drop	2.10.8-63
Table 2.10.8-4	Metrology Results of External Length Measurements Before Drop ...	2.10.8-64
Table 2.10.8-5	Metrology Results of Inner Diameter Measurements After Drop	2.10.8-65
Table 2.10.8-6	Metrology Results of Outer Diameter Measurements After Drop.....	2.10.8-66
Table 2.10.8-7	Metrology Results of External Length Measurements After Drop.....	2.10.8-67
Table 2.10.9-1	NAC-LWT Cask Hot Bolt Analysis Hypothetical Accident Conditions.....	2.10.9-9
Table 2.10.10-1	Stress Point Locations.....	2.10.10-8
Table 2.10.10-2	Constraint Forces for the 30-Foot Top End Drop Condition ($\phi = 0^\circ$).....	2.10.10-12
Table 2.10.10-3	Constraint Forces for the 30-Foot Top Corner Drop Condition ($\phi = 15.74^\circ$).....	2.10.10-13
Table 2.10.10-4	Constraint Forces for the 30-Foot Top Oblique Drop Condition ($\phi = 60^\circ$).....	2.10.10-13
Table 2.10.10-5	Constraint Forces for the 30-Foot Side Drop Condition ($\phi = 90^\circ$)...	2.10.10-13
Table 2.10.10-6	Stress Components – Thermal; 130°F; 1.12-Inch Outer Shell Thickness	2.10.10-14
Table 2.10.10-7	Stress Components – Internal Pressure; 50 psi; 1.12-Inch Outer Shell Thickness.....	2.10.10-18

List of Tables (continued)

Table 2.10.10-8	Stress Components – Bolt Preload; 1.12-Inch Outer Shell Thickness	2.10.10-22
Table 2.10.10-9	Stress Components – Impact and Inertial Loads; 30-Foot Top End Drop; $\phi = 0^\circ$; 1.12-Inch Outer Shell Thickness	2.10.10-26
Table 2.10.10-10	Stress Components – Impact and Inertial Loads; 30-Foot Top Corner Drop; $\phi = 15.74^\circ$; 1.12-Inch Outer Shell Thickness	2.10.10-30
Table 2.10.10-11	Impact and Inertial Loads; 30-Foot Top Oblique Drop; $\phi = 60^\circ$; 1.12-Inch Outer Shell Thickness.....	2.10.10-34
Table 2.10.10-12	Stress Components – Impact and Inertial Loads; 30-Foot Side Drop; $\phi = 90^\circ$; 1.20-Inch Outer Shell Thickness; Circumferential Location = 0°	2.10.10-38
Table 2.10.10-13	Stress Components – Thermal; 130°F; 1.20-Inch Outer Shell Thickness	2.10.10-42
Table 2.10.10-14	Stress Components – 50 psi Internal Pressure and Bolt Preload; 1.20-Inch Outer Shell Thickness.....	2.10.10-46
Table 2.10.10-15	Primary Stresses; 30-Foot Top End Drop; $\phi = 0^\circ$; 1.12-Inch Outer Shell Thickness	2.10.10-50
Table 2.10.10-16	Primary Plus Secondary Stresses; 30-Foot Top End Drop; $\phi = 0^\circ$; 1.12-Inch Outer Shell Thickness.....	2.10.10-54
Table 2.10.10-17	Primary Membrane (P_m) Stresses; 30-Foot Top End Drop; $\phi = 0^\circ$; 1.12-Inch Outer Shell Thickness.....	2.10.10-58
Table 2.10.10-18	Primary Membrane Plus Primary Bending ($P_m + P_b$) Stresses; 30-Foot Top End Drop; $\phi = 0^\circ$; 1.12-Inch Outer Shell Thickness	2.10.10-59
Table 2.10.10-19	Primary Membrane (P_m) and Primary Membrane Plus Primary Bending ($P_m + P_b$) Stress Qualification; 30-Foot Top End Drop; $\phi = 0^\circ$; 1.12-Inch Outer Shell Thickness	2.10.10-60
Table 2.10.10-20	Primary Stresses; 30-Foot Top Corner Drop; $\phi = 15.74^\circ$; 1.12-Inch Outer Shell Thickness	2.10.10-61
Table 2.10.10-21	Primary Plus Secondary Stresses; 30-Foot Top Corner Drop; $\phi = 15.74^\circ$; 1.12-Inch Outer Shell Thickness.....	2.10.10-65
Table 2.10.10-22	Primary Membrane (P_m) Stresses; 30-Foot Top Corner Drop; $\phi = 15.74^\circ$; 1.12-Inch Outer Shell Thickness.....	2.10.10-69
Table 2.10.10-23	Primary Membrane Plus Primary Bending ($P_m + P_b$) Stresses; 30-Foot Top Corner Drop; $\phi = 15.74^\circ$; 1.12-Inch Outer Shell Thickness	2.10.10-70
Table 2.10.10-24	Primary Membrane (P_m) and Primary Membrane Plus Primary Bending ($P_m + P_b$) Stresses; 30-Foot Top Corner Drop; $\phi = 15.74^\circ$; 1.12-Inch Outer Shell Thickness.....	2.10.10-71
Table 2.10.10-25	Primary Stresses; 30-Foot Top Oblique Drop; $\phi = 60^\circ$; 1.12-Inch Outer Shell Thickness	2.10.10-72
Table 2.10.10-26	Primary Plus Secondary Stresses; 30-Foot Top Oblique Drop; $\phi = 60^\circ$; 1.12-Inch Outer Shell Thickness.....	2.10.10-76

List of Tables (continued)

Table 2.10.10-27	Primary Membrane (P_m) Stresses; 30-Foot Top Oblique Drop; $\phi = 60^\circ$; 1.12-Inch Outer Shell Thickness.....	2.10.10-80
Table 2.10.10-28	Primary Membrane Plus Primary Bending ($P_m + P_b$) Stresses; 30-Foot Top Oblique Drop; $\phi = 60^\circ$; 1.12-Inch Outer Shell Thickness .	2.10.10-81
Table 2.10.10-29	Primary Membrane (P_m) and Primary Membrane Plus Primary Bending ($P_m + P_b$) Stresses; 30-Foot Top Oblique Drop; $\phi = 60^\circ$; 1.12-Inch Outer Shell Thickness.....	2.10.10-82
Table 2.10.10-30	Primary Stresses; 30-Foot Side Drop; $\phi = 90^\circ$; 1.20-Inch Outer Shell Thickness; Circumferential Location = 0°	2.10.10-83
Table 2.10.10-31	Primary Plus Secondary Stresses; 30-Foot Side Drop; $\phi = 90^\circ$; 1.20-Inch Outer Shell Thickness; Circumferential Location = 0°	2.10.10-87
Table 2.10.10-32	Primary Membrane (P_m) Stresses; 30-Foot Side Drop; $\phi = 90^\circ$; 1.20-Inch Outer Shell Thickness; Circumferential Location = 0°	2.10.10-91
Table 2.10.10-33	Primary Membrane Plus Primary Bending ($P_m + P_b$) Stresses; 30-Foot Side Drop; $\phi = 90^\circ$; 1.20-Inch Outer Shell Thickness; Circumferential Location = 0°	2.10.10-92
Table 2.10.10-34	Primary Membrane (P_m) Stresses; 30-Foot Side Drop; $\phi = 90^\circ$; 1.20-Inch Outer Shell Thickness; Circumferential Location = 90° ...	2.10.10-93
Table 2.10.10-35	Primary Membrane Plus Primary Bending ($P_m + P_b$) Stresses; 30-Foot Side Drop; $\phi = 90^\circ$; 1.20-Inch Outer Shell Thickness; Circumferential Location = 90°	2.10.10-94
Table 2.10.10-36	Primary Membrane (P_m) Stresses; 30-Foot Side Drop; $\phi = 90^\circ$; 1.20-Inch Outer Shell Thickness; Circumferential Location = 180° .	2.10.10-95
Table 2.10.10-37	Primary Membrane Plus Primary Bending ($P_m + P_b$) Stresses; 30-Foot Side Drop; $\phi = 90^\circ$; 1.20-Inch Outer Shell Thickness; Circumferential Location = 180°	2.10.10-96
Table 2.10.10-38	Primary Membrane (P_m) and Primary Membrane Plus Primary Bending ($P_m + P_b$) Stress Qualification; 30-Foot Side Drop; $\phi = 90^\circ$; 1.20-Inch Outer Shell Thickness; Circumferential Location = 0°	2.10.10-97
Table 2.10.11-1	Geometric Dimensions of the Cask	2.10.11-9
Table 2.10.11-2	Comparison of the Hand-Calculated and Finite Element Results	2.10.11-10
Table 2.10.12-1	Determination of Maximum Energy Remaining for Secondary Impact – Full-Scale Impact Limiter	2.10.12-30
Table 2.10.12-2	Determination of Extreme Force During Cask Deceleration (First Limiter) – Quarter-Scale Impact Limiter	2.10.12-31
Table 2.10.14-1	Material Designations for Sections.....	2.10.14-11
Table 2.10.14-2	1-Foot Side Drop with Internal Pressure, P_m Stresses, ksi.....	2.10.14-12
Table 2.10.14-3	Side Drop with Internal Pressure, $P_m + P_b$ Stresses, ksi.....	2.10.14-13
Table 2.10.14-4	1-Foot Side Drop with Internal Pressure, $P + Q$ Stresses, ksi.....	2.10.14-14
Table 2.10.14-5	1-Foot Top-End Drop with Normal Internal Pressure, P_m Stresses, ksi.....	2.10.14-15

List of Tables (continued)

Table 2.10.14-6	1-Foot Top-End Drop with Internal Pressure, $P_m + P_b$ Stresses, ksi..	2.10.14-16
Table 2.10.14-7	1-Foot Top-End Drop with Internal Pressure, $P + Q$ Stresses, ksi	2.10.14-17
Table 2.10.14-8	1-Foot Top-Corner Drop with Internal Pressure, P_m Stresses, ksi	2.10.14-18
Table 2.10.14-9	1-Foot Top-Corner Drop with Internal Pressure, $P_m + P_b$ Stresses, ksi.....	2.10.14-19
Table 2.10.14-10	1-Foot Top-Corner Drop with Internal Pressure, $P + Q$ Stresses, ksi	2.10.14-20
Table 2.10.14-11	1-Foot Bottom-End Drop with Internal Pressure, P_m Stresses, ksi.....	2.10.14-21
Table 2.10.14-12	1-Foot Bottom-End Drop with Internal Pressure, $P_m + P_b$ Stresses, ksi.....	2.10.14-22
Table 2.10.14-13	1-Foot Bottom-End Drop with Internal Pressure, $P + Q$ Stresses, ksi.....	2.10.14-23
Table 2.10.14-14	1-Foot Bottom-Corner Drop with Internal Pressure, P_m Stresses, ksi.....	2.10.14-24
Table 2.10.14-15	1-Foot Bottom-Corner Drop with Internal Pressure, $P_m + P_b$ Stresses, ksi	2.10.14-25
Table 2.10.14-16	1-Foot Bottom-Corner Drop with Internal Pressure, $P + Q$ Stresses, ksi.....	2.10.14-26
Table 2.10.14-17	30-Foot Side Drop with Internal Pressure, P_m Stresses, ksi.....	2.10.14-27
Table 2.10.14-18	30-Foot Side Drop with Internal Pressure, $P_m + P_b$ Stresses, ksi	2.10.14-28
Table 2.10.14-19	30-Foot Top-End Drop with Internal Pressure, P_m Stresses, ksi	2.10.14-29
Table 2.10.14-20	30-Foot Top-End Drop with Internal Pressure, $P_m + P_b$ Stresses, ksi.....	2.10.14-30
Table 2.10.14-21	30-Foot Top-Corner Drop with Internal Pressure, P_m Stresses, ksi ...	2.10.14-31
Table 2.10.14-22	30-Foot Top-Corner Drop with Internal Pressure, $P_m + P_b$ Stresses, ksi.....	2.10.14-32
Table 2.10.14-23	30-Foot Bottom-End Drop with Internal Pressure, P_m Stresses, ksi..	2.10.14-33
Table 2.10.14-24	30-Foot Bottom-End Drop with Internal Pressure, $P_m + P_b$ Stresses, ksi.....	2.10.14-34
Table 2.10.14-25	30-Foot Bottom-Corner Drop with Internal Pressure, P_m Stresses, ksi.....	2.10.14-35
Table 2.10.14-26	30-Foot Bottom-Corner Drop with Internal Pressure, $P_m + P_b$ Stresses, ksi	2.10.14-36
Table 2.10.14-27	Accident Internal Pressure with Inertia Load, P_m Stresses, ksi	2.10.14-37
Table 2.10.14-28	Accident Internal Pressure with Inertia Load, $P_m + P_b$ Stresses, ksi..	2.10.14-38

2.6.12 Fuel Basket Analysis

2.6.12.1 Discussion

To assure that the cask contents are retained in a subcritical and safe configuration, a fuel basket supports the contents both laterally and longitudinally. During normal transport, the cask may sustain a 1-foot free fall to either the side, corner or end drop orientations. Fuel basket designs examined under normal operations conditions are: the PWR basket (Section 2.6.12.2); the BWR basket (Section 2.6.12.4); the metallic fuel basket (Section 2.6.12.5); the MTR basket (Section 2.6.12.6); the TRIGA fuel basket (Section 2.6.12.7); the DIDO fuel basket (Section 2.6.12.8); the GA IFM basket (Section 2.6.12.9); and the TPBAR basket and spacer (Section 2.6.12.10). The analyses demonstrate that each of the basket designs is supported by the inner shell in bearing during a side drop, and that none of the basket designs will buckle during an end drop. The effects of a corner drop are bounded by the side and end drops.

2.6.12.2 PWR Basket Construction

The cylindrical basket body is fabricated from 6061-T6 aluminum alloy extrusions. An open, square, central core extends the length of the basket and provides lateral support for the cask contents. A 13.25-inch outside diameter, 0.125-inch thick aluminum tube that is 4.38 inches long, is bolted to the top of the basket body. This top tube protects the cask inner shell from damage during fuel loading operations and provides lifting points, which are used when the basket is removed from the cask. An aluminum spacer plate assembly is bolted to the bottom of the basket body. The spacer plate assembly supports the fuel basket and contents longitudinally, providing their movement within the cask. Additional spacer fixtures are either bolted to the cask lid or to the base of the fuel basket, if the cask contents do not fill the basket. The maximum spacer loads occur for the 30-foot drop hypothetical accident load conditions. The spacer analysis is presented in Section 2.7.7.8. A groove on the outside of the basket body is provided for the cask drain tube. The drain tube is connected to a fitting on the cask body, and is used to drain or fill the cask during cask loading or unloading operations.

For the shipment of up to 25 PWR or BWR rods, or up to 16 PWR MOX rods (or mixed MOX and UO₂ rods), a canister with insert will be utilized to position the fuel rod contents within the PWR basket. The canister for the fuel rods will be fabricated from Type 304 stainless steel (minimum thickness 0.12 inch) and will be designed to allow positive handling of the canister during loading and unloading operations. The size, shape, closure design and capacity of the canister will vary depending on the requirements of the shipping and/or receiving facilities. A spacer fabricated from stainless steel may be utilized, as required, to position the PWR/BWR rod canister longitudinally within the NAC-LWT cask cavity. A PWR insert fabricated from

6061-T651 aluminum is used to laterally position the rod canister within the PWR basket. The total weight of the fuel rods, canister and basket insert will be less than the maximum PWR fuel assembly payload weight of 1,650 pounds. Therefore, the up to 25 fuel rods content condition is bounded by the current PWR basket analyses.

2.6.12.3 PWR Basket Analysis

The minimum ambient temperature during normal transport, -40°F, combined with the maximum decay heat load produces an average inner wall temperature of 151°F. The 6061-T6 aluminum alloy expands approximately 1.5 times more per degree Fahrenheit than stainless steel.

Assuming that both the cask and basket respond linearly, the maximum as-designed gap between the basket and the cavity, when the basket is centered in the cavity, is 0.094 in. Since aluminum expands faster than stainless steel, any increase in temperature will serve to decrease the basket-cavity gap. Since the gap is small, it is assumed that there is no relative motion between the basket and cask, and that the basket is in contact bearing on the inner shell during a side drop. The basket bearing loads are transmitted to the inner shell and cask structure.

2.6.12.3.1 Bearing Stress Calculation

The bearing stress is calculated using Case 6 (Roark, page 320), which models the cylindrical basket in a circular groove. The maximum compressive stress is calculated using:

$$S_{c_{max}} = 0.798 \left[\frac{\frac{P(D_1 - D_2)}{D_1 D_2}}{\frac{1 - \nu_1^2}{E_1} + \frac{1 - \nu_2^2}{E_2}} \right]^{0.5}$$

= 1570 psi

where the material properties at 250°F are:

Stainless Steel

$$D_1 = 13.405 \text{ inches}$$

$$E_1 = 27.3 \times 10^6 \text{ psi}$$

$$\nu_1 = 0.275$$

Aluminum (6061-T6)

$$D_2 = 13.25 \text{ inches}$$

$$E_2 = 9.4 \times 10^6 \text{ psi}$$

$$\nu_2 = 0.334$$

$$\text{contents} + \text{basket weight} = 4,000 \text{ lbs}$$

$$P_{1g} = 4,000 \text{ lb}/178 \text{ in} = 22.5 \text{ lb/in}$$

$$P_{24.3g} = (22.5 \text{ lb/in})(24.3 \text{ g}) = 547 \text{ lb/in}$$

(The 24.3 g side drop load is obtained from Table Table 2.6.7-34.)

The allowable compressive stress is selected to be the yield strength (S_y)_{250°F} of Type 304 stainless steel, 23,800 psi. The margin of safety is calculated as:

$$\text{M.S.} = \frac{S_y}{S_{c_{\max}}} - 1 = \text{+Large}$$

2.6.12.3.2 Compressive Stress Calculation

The PWR basket and inner cavity length are designed to ensure that there is very limited longitudinal movement of the basket relative to the cask when the cask is carrying fuel. Additional spacers are attached to the cask or added in the PWR basket, if the fuel contents do not fill the basket cavity. The fuel contents are not attached to the PWR basket, and do not impart any longitudinal structural load on the basket body. However, the PWR basket must support itself during an end drop accident. To determine if the PWR basket is self-supporting, it is analyzed as a column, acted upon by a structural (weight) compressive load.

The PWR basket weighs 840 pounds, which, during a normal operations 1-foot fall, is decelerated at 15.8 g. The g loads are completely described for all cask drop orientations in Section 2.6.7.4. The total compressive load acting over the basket body cross section, 59.2 square inches, is $P_{\max} = 840 \times 15.8 = 13,272$ pounds. The compressive stress (S_c), conservatively considered to act on the basket body, is $13,272/59.2 = 224$ psi.

An Euler column analysis is used to determine the critical buckling stress of the PWR basket body. Assuming that the impacting end is fixed and the other is free, the critical buckling stress (Shigley, page 116) is calculated as:

$$P_{cr} = \frac{n\pi^2 EI}{L^2}$$

$$= 670,700 \text{ psi}$$

where:

$$n = 0.25, \text{ end fixity coefficient}$$

$$E_{Al_{250^\circ F}} = 9.4 \times 10^6 \text{ psi}$$

$$I_{\text{basket body}} = 870 \text{ in}^4 \text{ (Roark, Case 10, page 75)}$$

L = 178 inches, inner cavity length

$$\text{M.S.} = \frac{P_{\text{cr}}}{P_{\text{max}}} - 1 = \underline{+Large}$$

2.6.12.4 BWR Basket Construction

The BWR basket is fabricated from 6061-T6 aluminum alloy extrusions. Two open, square cores, located in the center of the basket body, extend the length of the basket, providing lateral support for the cask contents. A 13.25-inch outside diameter, 0.25-inch thick stainless steel tube that is 5.4 inches long is welded to a 0.62-inch thick plate and the top cover assembly is bolted to the basket body. The top cover protects the cask inner shell from damage during fuel loading operations and provides lifting points, which are used when the basket is removed from the cask. A stainless steel spacer plate assembly is bolted to the bottom of the basket body. The spacer plate assembly supports the fuel basket and contents longitudinally, preventing their movement within the cask. Additional spacer fixtures are either bolted to the cask lid or the base of the fuel basket if the cask contents do not fill the basket. A groove on the outside of the basket body is provided for the cask drain tube.

2.6.12.4.1 BWR Basket Analysis

The BWR basket body is fabricated from the same material as the PWR basket body. Moreover, the outer diameter and its tolerance are exactly the same for both basket designs. Therefore, the BWR basket is also considered to be in contact bearing for similar reasons to those stated in Section 2.6.12.3, and all basket bearing loads are transmitted to the cask inner shell.

2.6.12.4.2 Bearing Stress Calculation

The BWR basket and its contents weigh 2,624 pounds. The normal operations conditions 1-foot side drop g load is 24.3, resulting in a total bearing load of 63,760 pounds (2,624 lb x 24.3 g). The bearing load per unit length ($P_{24.3g}$) is 358 pounds/inch (63,760 lb/178 in). Using Case 6 (Roark, page 320) and the same material properties as described in Section 2.6.12.3.1, the $S_{c_{\text{max}}} = 1383$ psi. The allowable compressive stress is selected to be the yield strength (S_y)_{250°F} of Type 304 stainless steel, 23,800 psi. The margin of safety is calculated as:

$$\text{M.S.} = \frac{S_y}{S_{c_{\text{max}}}} - 1 = \underline{+LARGE}$$

2.6.12.4.3 Compressive Stress Calculation

For the same reasons that are stated in Section 2.6.12.3.2, the BWR basket needs only to be self-supporting. The BWR basket weighs 1124 pounds, which during a normal operations 1-foot fall, is decelerated at 15.8 g. The total compressive load acting over the basket body cross-section (72.5 in²), is $P_c = 1,124 \text{ lb} \times 15.8 \text{ g} = 17,759 \text{ pounds}$. The compressive stress (S_c) conservatively considered to act on the basket body is $17,759 \text{ lb}/72.5 \text{ in}^2 = 245 \text{ psi}$, which is negligible.

An Euler column analysis is used to determine the critical buckling stress of the BWR basket body. Assuming that the impacting end is fixed and the other end is free, the critical buckling stress (Shigley, page 116) is calculated as:

$$P_{cr} = \frac{n\pi^2 EI}{L^2}$$

$$= 1.0 \times 10^6 \text{ psi}$$

where:

$$n = 0.25, \text{ end fixity coefficient}$$

$$E_{Al_{250^\circ F}} = 9.4 \times 10^6 \text{ psi}$$

$$I_{\text{basket body}} = 1,298 \text{ in}^4 \text{ (Roark, Case 10, page 75)}$$

$$L = 178 \text{ in, inner cavity length}$$

$$M.S. = \frac{P_{cr}}{P_c} - 1 = \underline{+LARGE}$$

2.6.12.5 Metallic Fuel Basket Construction

The metallic fuel basket is fabricated from three 5.625-inch outer diameter 6061-T6 aluminum tubes, laterally restrained by five 13.0-inch diameter 0.25-inch thick, 6061-T6 aluminum bulkheads welded along the length of the tubes. Each tube provides lateral support for the cask contents. The uppermost bulkhead has three attachment points, which are lifting points used when the basket is removed from the cask. Welded to the bottom bulkhead is a 9.0-inch outer diameter, 0.25-inch thick, 6061-T6 aluminum spacer tube, 29.5 inches long, which supports the fuel basket and contents longitudinally, preventing their movement within the cask. A groove on the outside of the basket body is provided for the cask drain tube.

2.6.12.5.1 Metallic Fuel Basket Analysis

The metallic fuel basket body is fabricated from similar material to the PWR basket body. Moreover, the outer diameter of the bulkheads and its tolerance are exactly the same for both

basket designs. Therefore, the metallic fuel basket bulkheads are also considered in contact bearing for the same reasons stated in Section 2.6.12.3, and all basket bearing loads are transmitted to the inner shell and cask structure.

2.6.12.5.2 Bearing Stress Calculation

The metallic fuel basket and its contents weigh 2,208 pounds. The normal operations conditions 1-foot side drop g load is 24.3, resulting in a total bearing load of 53,654 pounds (2,208 lb × 24.3 g). It is assumed that the entire bearing load is distributed over the five 0.25-inch thick bulkheads. The bearing load per unit length ($P_{24.3g}$) is 42,924 pounds/inch (53,654 lb/1.25 in). From Case 6 (Roark, page 320) the maximum compressive stress is calculated using:

$$S_{c_{max}} = 0.798 \left[\frac{\frac{P(D_1 - D_2)}{D_1 D_2}}{\frac{1 - \nu_1^2}{E_1} + \frac{1 - \nu_2^2}{E_2}} \right]^{0.5}$$

$$= 36,530 \text{ psi}$$

where the material properties at 250°F are:

Stainless Steel

$$D_1 = 13.405 \text{ inches}$$

$$E_1 = 27.3 \times 10^6 \text{ psi}$$

$$\nu_1 = 0.275$$

Aluminum (6061-T6)

$$D_2 = 13.0 \text{ inches}$$

$$E_2 = 9.4 \times 10^6 \text{ psi}$$

$$\nu_2 = 0.334$$

The allowable compressive stress is selected to be $(1.5)(S_y)_{250^\circ\text{F}}$ of 6061-T6 aluminum, 44,685 psi. The margin of safety is calculated as:

$$M.S. = \frac{S_y}{S_{c_{max}}} - 1 = \underline{+0.22}$$

2.6.12.5.3 Compressive Stress Calculation

For the same reasons that are stated in Section 2.6.12.3.2, the metallic fuel basket needs only to be self-supporting. The metallic fuel basket weighs 128 pounds, which during a normal operating conditions 1-foot fall, is decelerated at 15.8 g. The total compressive load acting over the three fuel tubes is $P_F = 2,022$ pounds ($128 \text{ lb} \times 15.8 \text{ g}$). The total cross sectional area of the three aluminum fuel tubes is 6.48 square inches, resulting in a normal operating conditions compressive stress ($S_{c_{fuel}}$) of 312 psi ($2,022 \text{ lb}/6.48 \text{ in}^2$). The spacer tube must support the basket and its contents during a bottom end drop. The total weight that the spacer tube supports is 2,208 pounds, resulting in a normal operating conditions 1-foot bottom end drop compressive load of $P_c = 34,886$ pounds. The cross sectional area of the 9.0-inch outer diameter aluminum spacer tube is 6.87 square inches, resulting in a compressive stress ($S_{c_{spacer}}$) of 5078 psi. Assuming that the impacting end is fixed and the other end is free, the critical buckling stresses for each tube column (Shigley, page 116) is calculated:

$$\begin{aligned}
 & \text{Fuel Tubes (3)} \\
 P_{cr} &= \frac{n\pi^2 EI}{L^2} \\
 &= 33,550 \text{ psi}
 \end{aligned}$$

$$\begin{aligned}
 & \text{Spacer Tube} \\
 P_{cr} &= \frac{n\pi^2 EI}{L^2} \\
 &= 1,754,000 \text{ psi}
 \end{aligned}$$

where:

$$\begin{aligned}
 n &= 0.25, \text{ end fixity coefficient} \\
 E_{Al250^\circ F} &= 9 \times 4 \times 10^6 \text{ psi} \\
 I_{\text{basket body}} &= 46 \text{ in}^4 \\
 L &= 145.25 \text{ in, fuel tube length} \\
 MS &= \frac{P_{cr}}{P_F} - 1 = \underline{+Large}
 \end{aligned}$$

$$\begin{aligned}
 n &= 0.25, \text{ end fixity coefficient} \\
 E_{Al250^\circ F} &= 9.4 \times 10^6 \text{ psi} \\
 I_{\text{spacer tube}} &= 66 \text{ in}^4 \\
 L &= 29.5 \text{ in, spacer tube length} \\
 MS &= \frac{P_{cr}}{P_c} - 1 = \underline{+Large}
 \end{aligned}$$

2.6.12.6 MTR Fuel Basket Construction

The MTR modular basket assembly has four configurations. One configuration is for 28 uncut (intact) MTR fuel assemblies (28 MTR – 4 unit basket); the second is for 35 partially cut MTR elements that have had portions of the upper and lower end fittings removed (35 MTR – 5 unit basket). The third configuration is for 42 MTR fuel assemblies (42 MTR – 6 unit basket) with the upper and lower end fittings removed; and the fourth configuration is for up to 700 PULSTAR fuel elements loaded in the 28 MTR basket. The PULSTAR fuel may be intact fuel assemblies, intact fuel elements (rods) loaded in a fuel rod insert or in fuel cans, or damaged fuel elements, fuel debris, and nonfuel components of fuel assemblies loaded in fuel cans. Each

MTR basket configuration consists of one base module, one top module, and two, three or four intermediate modules for the 28, 35 and 42 element configurations, respectively. Each MTR basket module is designed to hold up to seven MTR or PULSTAR fuel assemblies. The modules are not interchangeable between basket configurations. The structural analysis is not affected by the specific fuel element design or enrichment as long as the fuel characteristics are in compliance with the fuel characteristics listed in Table 1.2-4.

Axial fuel and plate spacers may be used to axially position the MTR fuel assemblies in the basket modules. Cell block spacers are used to prevent the loading of fuel assemblies in basket module positions 1, 2 and 3 when LEU MTR fuel elements having $>470 \text{ g } ^{235}\text{U}$ per element ($>22 \text{ g } ^{235}\text{U}$ per plate) are loaded. The presence and/or use of spacers, fuel plate canisters or fuel cans does not affect the structural integrity of the MTR fuel baskets as the total weight of fuel element, spacer and fuel plate canister or fuel can is limited to the evaluated load of 80 pounds/cell. The axial fuel and cell block spacers perform no safety function and are considered dunnage. Plate spacers are used, if required, to ensure that the criticality evaluation required minimum nonfuel hardware is provided.

Each module, fabricated from Type 304 stainless steel, is a weldment made up of two 1/2-inch thick, 13.265-inch diameter, circular plates at each end of the longitudinal divider plates creating seven MTR fuel assembly cavities. The outside wall of the four symmetric outermost fuel compartments is fabricated from 11-gage Type 304 stainless steel sheet. The 1/2-inch thick plate at the top end of the MTR fuel basket module is welded to the exterior surfaces of the fuel tube weldment with a 1/8-inch continuous weld on the under side of the top plate and with a continuous fillet seal weld on the top side. The 1/2-inch thick baseplate is continuously welded to the 1/4-inch thick divider plates and the 5/16-inch thick web plates. The 11-gage sheet metal and the 5/16-inch intermediate webs are discontinued at 1/4 inch from the surface of the baseplate to provide for compartment drainage. The 5/16-inch plate material may be machined to a minimum thickness of 0.28 inch. In addition to the drainage path at the base of each assembly cavity, a 1-inch diameter hole is located at the center of each of the compartments in the module. Each MTR basket base module sits on a 1.5-inch long, 10-inch schedule 80S pipe welded to the 1/2-inch thick baseplate. The 10-inch schedule 80S pipe carries the total weight of the MTR basket assembly and bears directly on the bottom forging of the cask.

The MTR fuel basket base module and intermediate modules have guide pins fixed to the surface of the top support plate. The guide pins fit into holes in the base plate of the top and intermediate modules and provide controlled alignment of the basket assembly. A groove slot on the outside of each basket unit support plate is provided for the clearance of cask drain tube and for circumferential alignment of the MTR basket assembly.

The MTR Plate Canister (canister) is an all-aluminum rectangular canister that is suitable for transport in the NAC-LWT MTR 42 element basket. The canister may be transported in the 28 or

35 element basket if appropriate dunnage is used. The canister is fabricated from ASTM B209 or ASTM B221 6061 aluminum. The canister body comprises two thick walls and two thin walls that are welded together into a rectangular tube to contain up to 23 MTR fuel plates. Each end of the canister body is closed by identical aluminum lids milled from a solid piece to incorporate a lifting bail. The lids are fastened securely to the thick wall plates using aluminum socket head cap screws that are captive in the lid to facilitate closing the canister.

2.6.12.6.1 MTR Fuel Basket Analysis

The MTR basket assembly and the inner shell are both fabricated from Type 304 stainless steel material. The nominal radial gap between the MTR basket assembly and the cask inner shell is 0.055 inch. The nominal radial gap between the basket and the inner shell is 0.0531 inch at the design basis fuel normal operation steady-state temperature. As defined for other NAC-LWT fuel specific basket designs, since the gap between the basket and cask inner shell wall is small, it is assumed that there is no relative motion between the basket and the cask, and that the basket is in contact bearing on the inner shell during a side drop. The basket bearing loads are transmitted to the inner shell and cask structure.

The analysis of the MTR plate canister is presented in Section 2.6.12.6.6.

2.6.12.6.2 MTR Fuel Basket Normal Conditions 1-foot Side Drop

This section evaluates the MTR fuel basket for the normal conditions of transport 1-foot side drop.

Bearing Stress Calculation—Inner Shell (Cask 1-foot Side Drop)

The bearing stress is calculated using Roark's, Table 33, Case 2 (Roark's, 6th Edition), which models the cylindrical basket in a circular groove. The 28 MTR fuel assembly base module is the heaviest module when loaded with 25 PULSTAR fuel elements. The maximum compressive stress, for two elastic bodies with similar elastic modulus, is:

$$\sigma_c = 0.798 \sqrt{\frac{gP(D_1 - D_2)}{\frac{D_1 D_2}{2(1-\nu^2)} \frac{1}{E}}} = 16,679 \text{ psi}$$

where:

g = 1-foot side drop acceleration = 24.3

E = Elastic modulus = 28.3×10^6 psi (conservatively use E @ 70°F)

ν = Poisson's ratio for steel material = 0.275

$$\begin{aligned}
 D_1 &= \text{Cask cavity diameter} = 13.405 \text{ inches} \\
 D_2 &= \text{Basket diameter} = 13.265 \text{ inches} \\
 t &= \text{Thickness of stiffener at mid section of base module (less chamfers)} \\
 &= 0.5 - 2 \times 0.13 = 0.24 \text{ in} \\
 W &= \text{Maximum weight of MTR basket with contents (PULSTAR fuel elements)} \\
 &= 3,222 \text{ lbs} \\
 W_r &= \text{Load supported by 28-assembly basket base module middle ring} \\
 &= W/9 = 358 \text{ lbs} \\
 P &= W_r/t = 358 \text{ lb}/0.24 \text{ in} = 1,491 \text{ lb/in}
 \end{aligned}$$

The allowable compressive stress, S_y , of Type 304 stainless steel at a conservative maximum operating temperature envelope of 600°F is 18,200 psi. The margin of safety is calculated as:

$$MS = \frac{S_y}{\sigma_c} - 1 = +0.09$$

Fuel Tube Stresses (Cask 1-foot Side Drop)

The maximum stress in the fuel tubes occurs in the 0.12-inch thick, 11-gage sheet metal tubes which support the entire length of the MTR fuel elements or PULSTAR fuel elements. There are two cases to consider. In the first case, the weight of the fuel assembly is transmitted to the tube through the two aluminum plates at the sides of the fuel assembly. As shown in Figure 2.6.12-1, this load path creates a uniform line load along the length of the tube located about 0.315 inch from the corners. The tube is analyzed as a simple beam, 1-inch wide, 0.12-inch thick, and 3.44-inches long with a concentrated load at 0.315 inch from the ends. The maximum bending moment, M_i , is:

$$M_i = \frac{(8Pa + WL^2) \times g}{8} = 14.0 \text{ in-lb/in}$$

where:

$$\begin{aligned}
 W &= \text{Unit tube body weight} = 0.288 \times t = 0.0346 \text{ lb/in}^2 \\
 L &= \text{Length} = 3.44 \text{ inches} \\
 P &= \text{Bounding fuel load} = P_f / (2 \times L_f) = 1.67 \text{ lb/in} \\
 P_f &= \text{Fuel weight} = 80.0 \text{ lbs} \\
 L_f &= \text{Shortest length over which fuel load is applied} = 24 \text{ inches} \\
 a &= \text{Distance from applied load, P to support} = 0.315 \text{ in} \\
 g &= \text{1-foot side drop acceleration} = 24.3
 \end{aligned}$$

In the second case, the weight of the fuel assembly is transmitted to the tube as a uniform load. The load path is shown in Figure 2.6.12-1. The maximum bending moment for this case, M_{II} , is:

$$M_{II} = \frac{(2PL^2 + WL^3) \times g}{8L} = 36.1 \text{ in-lb/in}$$

The maximum bending stress, σ , is:

$$\sigma = \frac{6M_{II}}{t^2} = 15,042 \text{ psi}$$

where:

$$t = \text{Fuel tube thickness} = 0.12 \text{ in}$$

The stress allowable, $1.5S_m$, is 24,600 psi for Type 304 stainless steel at a conservative temperature of 600°F. The margin of safety is:

$$MS = \frac{24,600}{15,042} - 1 = +0.64$$

The 11-gage sheet metal tube is continuously welded to the adjacent divider plates with a 1/8-inch fillet weld. This weld resists shear developed in the simple beam analyzed above.

$$V = \frac{(2P + WL) \times g}{L} = 24.4 \text{ lb/in}$$

The shear stress, τ , is:

$$\tau = \frac{V}{t} = 203 \text{ psi}$$

The “throat” thickness of the weld is 0.088 in. The ratio of the plate thickness (0.12 in) to the weld “throat” thickness (0.088 in) is 1.36. The maximum stress of 203 psi calculated above is adjusted by a factor of 1.36 to obtain the maximum stress in the weld for the 1-foot side drop (24.3g). Maximum stress in the weld, S_w , is:

$$S_w = 1.36 \times \tau = 276 \text{ psi}$$

The ASME Code, Subsection NG-3352 recommends that the allowable stress be determined for a fillet weld with PT or MT surface examination by implementing a quality factor, n , of 0.4. The stress allowable, S_y , of the base metal, Type 304 stainless steel, is 18,200 psi at a conservative operating temperature envelope of 600°F. The margin of safety for the fillet weld is:

$$MS = \frac{S_y \times n}{S_w} - 1 = \underline{+Large}$$

2.6.12.6.3 MTR Fuel Basket Normal Conditions 1-foot End Drop

This section evaluates the MTR fuel basket for the normal conditions of transport 1-foot end drop.

Bearing Stress Calculation—Bottom Forging (Cask 1-foot End Drop)

When in the vertical position a 0.5-inch thick, 10-inch nominal diameter schedule 80S pipe supports the MTR basket assembly. The 1.5-inch long pipe is welded to the baseplate of the base module. The compressive stress is:

$$\sigma_c = \frac{g \times W}{A} = 3,162 \text{ psi}$$

where:

W = Maximum weight of MTR basket with contents (PULSTAR fuel elements)
= 3,222 lbs

A = Cross-sectional area of base pipe support = 16.1 in²

g = 1-foot end drop acceleration = 15.8

The allowable stress, S_y, of Type 304 stainless steel at a conservative maximum operating temperature of 600°F is 18,200 psi. The margin of safety is:

$$MS = \frac{S_y}{\sigma_c} - 1 = +4.76$$

Compressive Stress Calculation—Fuel Tubes (Cask 1-foot End Drop)

The MTR basket assembly and the inner cavity length are designed to ensure that there is minimal longitudinal movement of the basket relative to the cask. The base module of the MTR basket assembly supports itself and the weight of the other basket modules, including fuel content during a 1-foot end drop. The normal operation load compressive stress developed in the basket tube wall is:

$$\sigma_c = \frac{g \times W}{A} = 6,208 \text{ psi}$$

where:

W = Maximum weight of MTR basket with contents (PULSTAR fuel elements)
= 3,222 lbs

g = 1-foot end drop acceleration = 15.8

A = Total compartment cross-sectional area at baseplate (Figure 2.6.12-2)
= 8.20 in²

The allowable compressive stress, S_m , is 16,400 psi conservatively evaluated for Type 304 stainless steel at a conservative maximum operating temperature of 600°F. The margin of safety is:

$$MS = \frac{S_m}{\sigma_c} - 1 = +1.64$$

The Euler elastic buckling load formulation is used to determine the critical buckling load of the MTR basket base module. The base module is treated as simply supported, which results in an effective length that is twice the actual length, thus reducing the critical buckling load by a factor of 4.0. The basket base module buckling load is:

$$P_{cr} = \frac{\pi^2 EI_i}{(L_e)^2} = 1.55 \times 10^6 \text{ lb}$$

The margin of safety is:

$$MS = \frac{P_{cr}}{P_c} - 1 = \underline{+Large}$$

where:

$$P_c = \text{Compressive load} = 15.8g \times 3,222 \text{ lbs} = 50,908 \text{ lbs}$$

$$I_i = \text{Basket inertia moment} = 47.92 \text{ in}^4$$

$$E = \text{Elastic modulus (@ 600°F)} = 25.3 \times 10^6 \text{ psi}$$

$$L_e = \text{Effective length of 28 assembly basket} = 2 \times 44.0 \text{ inches} = 88 \text{ inches}$$

Baseplate Stresses (Cask 1-foot End Drop)

The support plate at the top end of the basket modules is continuously welded to the outside periphery of the fuel compartment tubes. The baseplate of a typical basket module is continuously welded to the two 11.57-inch wide, 5/16-inch (min. 0.28-inch considering machining tolerance) thick web plates, and to the two 3.44-inch wide, 1/4-inch thick divider plates as shown in Figure 2.6.12-2. The ½-inch thick baseplate supports seven MTR or seven DIDO fuel assemblies or 25 PULSTAR fuel elements and is conservatively assumed to be supported by the main longitudinal webs mentioned above during a cask end drop. Two separate load cases are examined. The maximum stress for each case is then combined to obtain the total stress on the baseplate. Figure 2.6.12-2 details the baseplate support.

The first case, Case I, examines a 3.44-inch square plate with two adjacent sides fixed and the other two sides free. The applied pressure over the entire plate is uniform (Roark's, 6th edition, Table 26, Case 11a). The bending stress is:

$$\sigma_I = \frac{-g\beta_I P b^2}{a t^2} = -8,947 \text{ psi}$$

where:

- P = Fuel weight = 80.0 lbs
- g = 1-foot end drop acceleration = 15.8
- a = Area of plate = (3.44 in)² = 11.83 in²
- t = Plate thickness = 0.5 inch
- b = Plate width = 3.44 inches
- β_I = Boundary condition stress factor = 1.769

The second case, Case II, examines a rectangular plate, 11.57 inches by 3.44 inches, fixed along the long edges, free along the short edges and uniformly loaded (Roark's, 6th edition, Table 26, Case 6a). The bending stress is:

$$\sigma_{II} = \frac{-g\beta_{II} P b^2}{a t^2} = -747 \text{ psi}$$

where:

- a = Area of plate = 11.57 × 3.44 in = 39.8 in²
- β_{II} = Boundary condition stress factor = 0.497

The total bending stress is conservatively obtained by adding the individual stresses:

$$\sigma = \sigma_I + \sigma_{II} = -9,694 \text{ psi}$$

The allowable stress, 1.5 S_m, is 24,600 psi for Type 304 stainless steel at the conservative maximum temperature envelope of 600°F. The margin of safety is:

$$MS = \frac{24,600}{9,694} - 1 = +1.54$$

2.6.12.6.4 Fuel Tube Stresses (Cask 1-foot Oblique Drop)

Table 2.6.7-34 summarizes the cask drop g-load factors for six drop orientations: the cask end drop (0 degrees), the cask corner drop (15.74 degrees), the cask oblique drops (30, 45 and, 60 degrees) and the cask side drop (90 degrees). To conservatively envelope the maximum stresses expected for all the 1-foot oblique drops, the calculated stresses of 6,208 psi in Section 2.6.12.6.3 for the end drop and 15,042 psi in Section 2.6.12.6.2 for the side drop are added as absolute values. The maximum stress in the MTR basket that envelopes the maximum stresses expected for any 1-foot oblique drop is 21,250 psi. The margin of safety, against stress allowable, 1.5 S_m, of 24,600 psi, at 600°F, is:

$$MS = \frac{24,600}{21,250} - 1 = +0.16$$

2.6.12.6.5 Fuel Cans in a MTR Basket (Damaged PULSTAR Elements)

PULSTAR Damaged Fuel Can

The PULSTAR can is a modification of the existing damaged fuel can for TRIGA fuel, which has two different design lengths. The PULSTAR fuel can has the same cross-section (can width and wall thickness) as the TRIGA fuel can and is approximately four inches longer than the shorter TRIGA fuel can design. Identical materials of fabrication are used for both TRIGA and PULSTAR fuel cans. As shown in Section 2.6.12.7.6, the TRIGA fuel can is evaluated for a maximum weight of 59.6 lb, which includes a can weight of 20 lbs and a payload of 39.6 lbs. The weights of the PULSTAR fuel can and its maximum payload are approximately 15 lbs and 35 lbs, respectively, for a maximum total weight of 50 lbs. Therefore, the stress evaluation for inertia loads for the PULSTAR can is bounded by the evaluation for the TRIGA can.

The maximum internal pressure for the PULSTAR can is 3.4 atm (gage). The calculation for the TRIGA can in the section titled "Sealed Failed Fuel Can Bolt Evaluation" used a value of 3 atm (gage). In the evaluation of the bolt stresses and loads, the calculation in this section conservatively used a linear load of 700 lb/inch, which bounds the increased internal pressure of 3.4 atm (gage) for the PULSTAR can.

For the evaluation of the failed fuel can tube, the minimum margin of safety is +0.77 (actual stress is 9,241 psi) in the section titled "Sealed Failed Fuel Can Plate Stress Due to Side Drop" for the 1-foot side drop. Considering the damaged fuel can as a thin wall cylinder with a bounding internal pressure of 60 psig, the stresses in circumferential, radial, and longitudinal directions are:

$$\sigma_{\theta} = \frac{P \times r}{t} = 1,500 \text{ psi}$$

$$\sigma_r = -P = -60 \text{ psi}$$

$$\sigma_z = \frac{P \times r}{2 \times t} = 750 \text{ psi}$$

where:

$$P = 60 \text{ psig}$$

$$r = 3.25/2 \text{ in.}, \text{ the radius of the can}$$

$$t = 0.065 \text{ in.}, \text{ the thickness of the can}$$

Combining the stresses caused by can contents (1-ft side drop) and the internal pressure, the bounding stress intensity is:

$$S_{int} = (1,500 + 9,241) - (-60) = 10,801 \text{ psi}$$

The minimum margin of safety for the one-foot side drop and internal pressure is:

$$\text{M.S.} = \frac{1.5 S_m}{S_{int}} - 1 = +1.28$$

It is concluded that the PULSTAR fuel can is structurally adequate for normal conditions of transport. No additional analysis is required.

PULSTAR Screened Fuel Can

The PULSTAR screened can is a modification of the existing screened fuel can for TRIGA fuel, which has two different design lengths. The PULSTAR screened fuel can has the same cross-section (can width and wall thickness) as the TRIGA screened fuel can and is approximately four inches longer than the shorter TRIGA screened fuel can design. Identical materials of fabrication are used for both TRIGA and PULSTAR fuel cans. As shown in Section 2.6.12.7.5, the TRIGA fuel can is evaluated for a maximum weight of 71 lbs, which includes a maximum can weight of 17 lbs and a payload of 54 lbs. The weights of the PULSTAR screened fuel can and its maximum payload are 12 lbs and 54 lbs, respectively, for a maximum total weight of 66 lbs. Therefore, the evaluation presented in Section 2.6.12.7.5 for the TRIGA screened fuel can bounds the evaluation for the PULSTAR screened fuel can and it may be concluded that the PULSTAR screened fuel can is structurally adequate for normal conditions of transport. No additional analysis is required.

PULSTAR Fuel Rod Insert and Spacer

Intact PULSTAR fuel elements can be placed into the TRIGA fuel rod insert (Dwg. 315-40-096). This insert is identical to the TRIGA fuel rod insert evaluated in Section 2.6.12.7.9. The weight of the individual PULSTAR fuel element is 1.31 lbs, which is bounded by the weight of an individual TRIGA rod of 1.44 lbs reported in Section 2.6.12.7.9. Therefore no additional evaluation for PULSTAR fuel elements contained in the TRIGA fuel rod insert is required.

For an end drop, the maximum stress is computed using the accelerations for the accident condition, but is compared to the stress allowables for the normal condition. The stress in the aluminum spacer is:

$$\sigma = \frac{Pg}{A} = 0.5 \text{ ksi}$$

where:

- P = 65 lbs Bounding load
- g = End drop g-load for the 30-foot end drop = 60.0g
- A = $\pi r^2 = 8.3 \text{ in}^2$
- r = Radius of cylinder = $3.25/2 = 1.625 \text{ inches}$
- t = Wall thickness = 0.125 in

The margin of safety is

$$MS = \frac{0.7S_u}{\sigma} - 1 = \frac{0.7 \times 30.2}{0.5} - 1 = \underline{+Large}$$

Using NUREG / CR-6322, a buckling evaluation of the spacer is performed for the accident condition which corresponds to an acceleration of 60g. The critical buckling stress for the spacer is:

$$\sigma_c = \frac{\pi^2 E}{\left(\frac{KL}{r}\right)^2} = 99.7 \text{ ksi}$$

where:

- K = Effective length factor for fixed-free end conditions = 2.0
- L = spacer length = 16.5 inches, which bounds 12-inch length
- r = Radius of gyration = $\sqrt{I/A} = 1.1 \text{ in}$
- A = Cross-sectional area of spacer = $\pi D t = 1.28 \text{ in}^2$
- I = Moment of inertia = $\frac{\pi D^3 t}{8} = 1.69 \text{ in}^4$
- D = Spacer diameter = 3.25 inches
- t = Spacer thickness = 0.125 in
- E = Modulus of elasticity of aluminum = $9.1 \times 10^6 \text{ psi}$

The margin of safety against buckling is:

$$MS = \frac{\sigma_c}{\sigma} - 1 = \frac{99.7}{0.5} - 1 = \underline{+Large}$$

2.6.12.6.6 MTR Plate Canister Analysis

The MTR Plate Canister (canister) is a handling fixture designed to assist loading MTR fuel plates into the removable modules of the NAC-LWT MTR fuel basket. The fuel basket modules

are used to load and unload fuel from the NAC-LWT cask and are the analyzed support structure for the fuel and canister. Therefore, the canister is not a required operational feature for loading or unloading fuel from the cask and serves only as a spacer (dunnage) once inserted into a basket module.

In this section, the canister is evaluated and found to be structurally adequate for all normal conditions of handling and transport. Stresses developed during the normal (one-foot drop) conditions meet all appropriate allowable criteria with positive margins. Classical hand calculations are used to determine the stresses in the canister. Calculated stresses are compared to allowable stresses for non-containment structures shown in Table 2.1.2-2, "Allowable Stress Limits for Noncontainment Structures."

Design deceleration (g) factors used in the canister analysis are shown in Table 2.6.7-34, "Summary of Cask Drop Equivalent G Load Factors." A temperature of 295°F bounds the highest calculated canister temperature and is used for both normal and accident conditions analyses. Stresses for corner and oblique drops are considered to be enveloped by the stresses produced by the end and side drops based on the cask drop acceleration component loads summarized in Table 2.6.7-34.

Maximum Canister Temperature

The maximum heat load allowed in an MTR basket cell is 120 W (409.8 Btu/hr), which is assumed to be transmitted only through one plate of the canister, resulting in a conservative estimate of the ΔT through the thickness of the canister shell. The maximum basket temperature is listed in Table 3.4-6 as 292°F.

The change in temperature through the thickness of the shell is calculated using the following formula:

$$\Delta T = Q t / kA = 409.8 \text{ Btu/hr} \times 0.24 \text{ inch} / (6.23 \text{ Btu/hr-in-F} \times 76.26 \text{ in}^2) = 0.21^\circ\text{F}$$

where:

$$k = 6.77 - 0.0025 \times (292 - 77) = 6.23 \text{ Btu/hr-in-F at } 292^\circ\text{F}$$

$$A = 25.85(3.2 - 0.125 \times 2) = 76.26 \text{ in}^2 \text{ is the cross-sectional area of the plate}$$

The peak canister shell temperature is then $292^\circ\text{F} + 0.21^\circ\text{F} = 292.21^\circ\text{F}$. A temperature of 295°F is conservatively used for the temperature of the canister.

MTR Plate Canister Weight

The canister component weights are determined by conservatively calculating the volume of each component and multiplying by the density of 6061 aluminum, 0.098 lb/in³ ("ASME Boiler and Pressure Vessel Code, Section II, Part D – Properties," 1995 with 1995 Addendum).

Can Weldment

$$W_{\text{canister}} = W_1 + W_2 + W_3 + W_4 = 6.8 \text{ lbs (use 10 lbs for analysis)}$$

where:

Item/Description	Calculation of Weight
1 Plate-A (2)	$W_1 = 25.85 \times 3.20 \times 0.24 \times 0.098 \times 2 = 3.9 \text{ lbs}$
2 Plate-B (2)	$W_2 = 25.85 \times 2.95 \times 0.125 \times 0.098 \times 2 = 1.9 \text{ lbs}$
3 Lid (2)	$W_3 = 3.30 \times 3.20 \times 0.25 \times 0.098 \times 2 = 0.5 \text{ lb}$
4 Bail (2)	$W_4 = [(0.46(4) + 2.94(2)) \times 0.125] + 1.04 \times 0.25 \times 0.098 \times 2 = 0.5 \text{ lb}$

This weight calculation conservatively neglects holes in the lids.

NAC-LWT MTR Plate Canister Stress Analysis

The canister is evaluated for stresses developed during the normal (one-foot drop) conditions. The empty canister weight is assumed to be 10 pounds and the loaded canister weight is assumed to be 30 lbs throughout the calculations.

Side Drop

The canister is contained within the NAC-LWT MTR 42-element basket assembly in the side-drop case. Because of the support provided by the basket, only the uppermost canister plate is subjected to bending. Bending of the plate is analyzed by considering a 1-inch section as a fixed-fixed beam equal in length to the width of the plate and uniformly loaded by the plate weight times the appropriate acceleration (g).

Normal Operating Condition (1-foot drop)

With the 0.125-in. thick plate uppermost:

The maximum moment (M_{max}) is:

$$M_{\text{max}} = \frac{wL^2}{12} = \frac{(0.30)(3.3^2)}{12} = 0.272 \text{ in-lb}$$

$$S_b = \frac{Mc}{I} = \frac{(0.272)(0.0625)}{1.63 \times 10^{-4}} = 104 \text{ psi for the normal operating condition}$$

where:

$$w = 0.125 \times 1.0 \times 1.0 \times 0.098 \times 24.3g = 0.30 \text{ lb/in}$$

$$I = \frac{bh^3}{12} = \frac{(1.0)(0.125^3)}{12} = 1.63 \times 10^{-4} \text{ in}^4$$

With the 0.24-in. thick plate uppermost:

The maximum moment (M_{max}) is:

$$M_{\max} = \frac{wL^2}{12} = \frac{(0.57)(3.3^2)}{12} = 0.517 \text{ in-lb}$$

$$S_b = \frac{Mc}{I} = \frac{(0.517)(0.125)}{1.15 \times 10^{-3}} = 56 \text{ psi for the normal operating condition}$$

where:

$$w = 0.24 \times 1.0 \times 1.0 \times 0.098 \times 24.3g = 0.57 \text{ lb/in}$$

$$I = \frac{bh^3}{12} = \frac{(1.0)(0.24^3)}{12} = 1.15 \times 10^{-3} \text{ in}^4$$

The minimum margin of safety (MS) for bending is:

$$MS = \frac{1.5S_m}{S_b} - 1 = \frac{(1.5)(11,500)}{104} - 1 = \text{+Large}$$

Side Plate Buckling

The 0.125-inch-thick side plates are evaluated as axially loaded compression members.

Buckling of the 0.24-inch thick plates is based on this analysis. Considering a 1-inch section of the plate, the slenderness ratio (C_c) is:

$$C_c = \sqrt{\frac{2\pi^2 E}{S_y}} = \sqrt{\frac{2\pi^2 9.6 \times 10^6}{27,900}} = 82.4$$

The radius of gyration (r) is:

$$r = \sqrt{\frac{I}{A}} = 0.036 \text{ in}^4$$

where:

$$I = \frac{bh^3}{12} = \frac{1.0(0.125)^3}{12} = 1.628 \times 10^{-4} \text{ in}^4$$

$$A = 0.125 \times 1.0 = 0.125 \text{ in}^2$$

For $K = 1$,

$$\frac{KL}{r} = \frac{1(3.3)}{0.036} = 91.67$$

For $KL/r = 91.67 > C_c = 82.4$, the allowable stress (S_a) is:

$$S_a = \frac{12\pi^2 E}{23 \left(\frac{KL}{r} \right)^2} = \frac{12\pi^2 (9.6 \times 10^6)}{23(91.67^2)} = 5,882 \text{ psi}$$

The allowable load (P_a) is:

$$P_a = S_a \times A = 5,882 \text{ psi} \times 0.125 \text{ in}^2 = 735 \text{ lbs}$$

The load (P) imposed upon the 0.125-inch-thick side plate by the 0.24-inch-thick side plate in the normal condition, one-foot side drop is:

$$P = 0.24 \times 1.0 \times 3.3 \times 0.098 \times 24.3g \cong 2 \text{ lbs}$$

This 2-pound load is conservative because the load from the thicker plate is actually shared between the two thinner plates.

The margin of safety (MS) is:

$$MS = \frac{P_a}{P} - 1 = \frac{735}{2} - 1 = \underline{+Large}$$

End Drop

For the end drop, the can weldment is loaded by its own weight. The canister contents bear against the bottom or top of the canister, depending on drop orientation.

Under normal operating conditions the canister body weldment is evaluated for a 15.8g end drop acceleration. The compressive load (P) on the tube is the combined weight of the lid and body plates times the appropriate g factor.

The compressive stress (S_c) in the canister body weldment is:

$$S_c = \frac{P}{A} = \frac{158 \text{ lb}}{2.24 \text{ in}^2} \cong 70.5 \text{ psi}$$

where:

$$A = (3.2 \times 0.24 + 2.82 \times 0.125)(2) = 2.24 \text{ in}^2$$

$$P = 10 \text{ lb} \times 15.8g = 158 \text{ lb} \text{ (Conservatively, the entire weight of the canister is used)}$$

The margin of safety (MS) is then:

$$MS = \frac{S_m}{S_c} - 1 = \frac{11,500 \text{ psi}}{70.5 \text{ psi}} - 1 = \underline{+Large}$$

Lifting Bail Compressive Stress

Under normal operating conditions, the lifting bail is evaluated for a 1-foot end drop (15.8g acceleration). The compressive load (P) on the lifting bail is the combined weight of the canister and its contents (30 lbs) times the appropriate g factor.

The compressive stress (S_c) in the canister body weldment is:

$$S_c = \frac{P}{A} = \frac{474 \text{ lb}}{0.965 \text{ in}^2} = 491 \text{ psi}$$

where:

$$A = (0.46 \times 4 + 2.94 \times 2)(0.125) = 0.965 \text{ in}^2$$

$$P = 30 \text{ lb} \times 15.8\text{g} = 474 \text{ lbs}$$

The margin of safety (MS) is then:

$$MS = \frac{S_m}{S_c} - 1 = \frac{11,500 \text{ psi}}{491 \text{ psi}} - 1 = \text{+Large}$$

Canister Body Buckling

The canister body is evaluated for buckling during the end drop by using the Euler formula to determine the critical buckling load (P_{cr}):

$$P_{cr} = \frac{K\pi^2 EI}{L^2} = \frac{0.722\pi^2 (9.6 \times 10^6) (2.98)}{(25.85)^2} = 305,073 \text{ lbs, assuming lower end fixed, upper end free}$$

where:

$$E = 9.6 \times 10^6 \text{ psi}$$

$$K = 0.722 \quad (\text{Reference Roark's Table 34, Case 3a})$$

$$I = \left(\frac{3.3 \times 3.2^3 - 2.82 \times 2.95^3}{12} \right) = 2.98^4, \text{ minimum moment of inertia}$$

$$L = \text{tube body length (25.85 in.)}$$

Because the maximum compressive load ($10 \text{ lbs} \times 60\text{g} = 600 \text{ lbs}$ under the accident condition) is much less than the critical buckling load (305,073 lbs), the canister body has adequate resistance to buckling.

As noted in the first paragraph of this section, the plate canister is only a handling fixture (not a structural component) and only serves as a spacer once inserted into the basket. Thus, retempering of the aluminum plates after welding is not required. The criticality evaluation presented in Section 6.4.3.10 includes the hypothetical separation of the canister fixture.

Figure 2.6.12-1 Cask Side Drop Fuel Tube Loading – MTR Fuel Basket

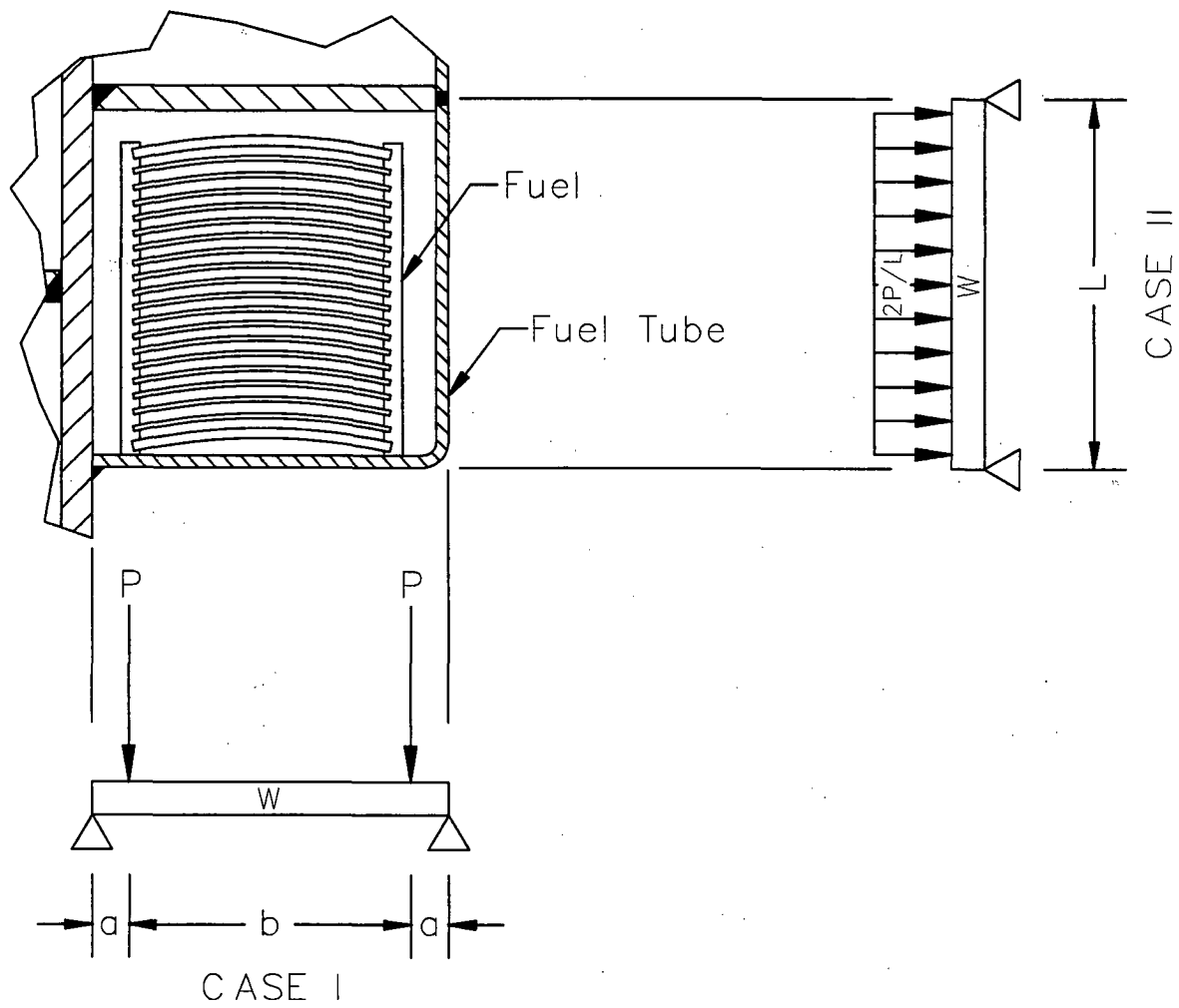
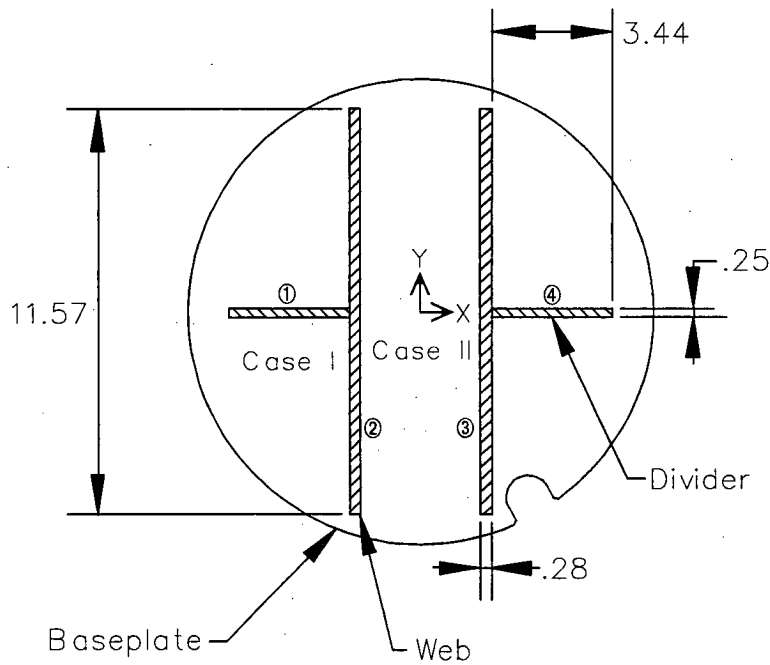
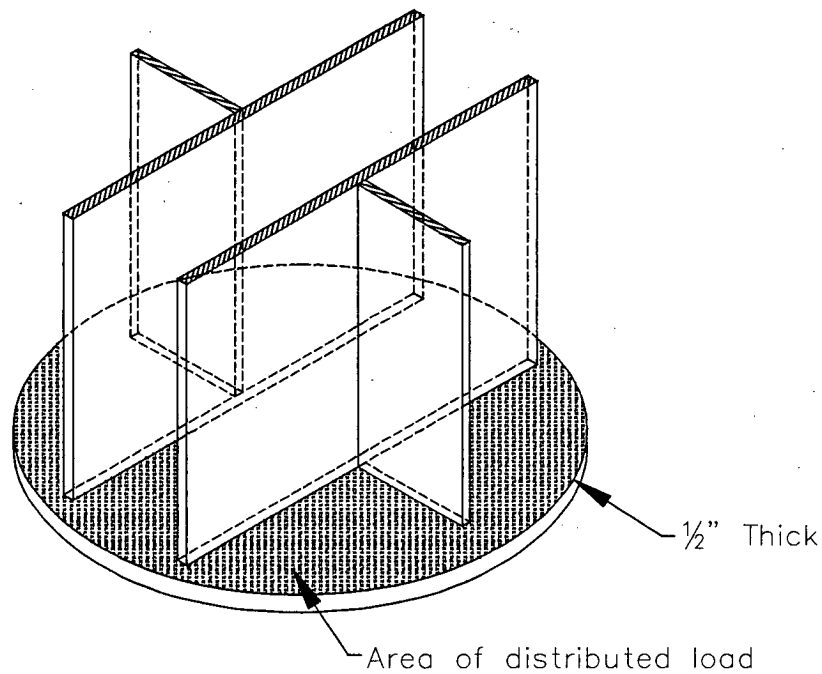


Figure 2.6.12-2 Baseplate Supports for Cask End Drop Loads - MTR Fuel Basket



Notes:
Area of shaded portion = 8.20 in²



2.6.12.7 TRIGA Fuel Basket One-Foot Drop Evaluation

This section evaluates the stresses in TRIGA fuel baskets as a result of the normal condition one-foot drop. The basket assembly consists of 5 basket modules - a base module, a top module and 3 intermediate modules. During transport all 5 modules must be installed in the cask. The 3 intermediate modules are interchangeable, but the base and top modules are not. The top module is sized to accept TRIGA Fuel Follower elements, which are longer than the typical element. Two basket configurations are available, "nonpoisoned" and "poisoned," where the poisoned basket configuration utilizes borated steel plates for additional criticality control. Each module has up to 7 cells and each open cell holds up to 4 TRIGA fuel elements or up to 16 TRIGA fuel cluster rods. The center cell of each module of the nonpoisoned basket configuration is blocked by a solid 11-gage stainless steel plate that precludes fuel loading in the center cell. The structural evaluation is based on the poisoned TRIGA basket configuration, so that the structural evaluation bounds transportation of the nonpoisoned configuration with the center cell blocked. Intact fuel elements are loaded directly into the module cells, while intact fuel cluster rods are loaded into fuel rod inserts that are placed into the basket cells prior to fuel loading. For the poisoned basket design, an alternative is provided that utilizes one base module and four intermediate modules, along with a spacer to fill the space differential resulting from the use of an additional intermediate module, rather than a top module.

The top and bottom modules are designed to hold up to 4 intact TRIGA fuel elements in screened cans, or failed or damaged TRIGA fuel elements or fuel cluster rods in screened or sealed cans in each of the open cells. Up to four intact fuel elements may be confined within a screened failed fuel can. The screened can is a square tube of 14-gage Type 304 stainless steel, closed on its bottom end with a screen to allow water draining. It is closed with a lid.

Up to two failed TRIGA fuel elements or up to 6 failed TRIGA fuel cluster rods may be transported in a sealed failed fuel can. The sealed can has a circular cross-section and is fabricated from Type 304 stainless steel tubing with a 0.065-inch thick wall. The bottom end includes a check valve and drain plug to facilitate draining. The top end is closed with a metal seal and a lid that is bolted in place.

Each basket module is a Type 304 stainless steel weldment made up of two 1/2-inch thick, 13.27-inch diameter, circular plates at each end of longitudinal divider plates. The divider plates create seven compartments or cells. The outside wall of the four symmetric outermost fuel cells is fabricated from 11-gage Type 304 stainless steel sheet. The 1/2-inch plate at the top end of the module is welded to the exterior surfaces of the divider plates using a continuous 1/8-inch weld on the under side of the top plate and a continuous fillet weld on the top side. The 1/2-inch thick baseplate is continuously welded to the 1/2-inch thick divider plates and the 5/16-inch thick

web plates. The top module has an additional 1-inch thick support plate midway between the top and bottom circular plates that has a continuous fillet weld on the bottom side and a continuous seal weld on the top side. The 11-gage sheet metal, and the 5/16-inch thick (0.28-inches, min) intermediate webs, end 1/2-inch above the top surface of the baseplate to provide for module drainage. In addition, a 1-inch diameter hole is located in the module base plate, at the center of each of the cells. The bottom module sits on a 1.5-inch section of 10-inch diameter, schedule 80S, pipe welded to the baseplate. The pipe carries the total weight of the TRIGA basket assembly, and bears directly on the cask bottom forging. As previously noted, the center cell of each nonpoisoned basket module is blocked with an 11 gage plate welded to the cell walls. This plate prevents loading fuel elements in the center cell. The center cell is open at the bottom to ensure water draining.

Four of the seven cells in each poisoned basket module have a plate of borated stainless steel neutron absorber material on one side to ensure criticality control in transport. The borated plate extends over the active length of the TRIGA fuel assemblies, and covers the width and length of the cell face within the limits of the attachment welds. The configuration of the borated plate is shown in the license drawings in Section 1.4.

The bottom and intermediate modules have guide pins fixed to the surface of the top support plate. The pins fit into holes in the baseplate provided for that purpose to achieve alignment. A cutout in the baseplate and top plate is provided for clearance of the cask drain tube, and for circumferential alignment of the TRIGA basket assembly.

The weights of the TRIGA basket assembly and modules are shown below. The weight includes the heaviest fuel element that could be installed in the module, and failed fuel containers in the top and bottom modules. The calculated weight of each top and bottom module is increased by 70 lbs to account for the poison plates and to conservatively bound the structural analysis.

Similarly, the calculated weight of the intermediate module is increased by 140 lbs.

Component	Weight of Fuel (lb) 140 Elements	Weight of Module(s)¹ (lb)	Total Weight (lb)	Length of Module(s) (in)
Bottom Module	247 ²	356	603	34.70
3 Intermediate Modules	741 ²	957	1,698	31.50
Top Module	370 ³	460	830	48.30
Weight of Empty Basket		1,773		
Loaded Weight of Basket			3,131	

Notes:

1. Includes the weight of failed fuel cans plus additional weight added for conservative design evaluation.
2. TRIGA fuel element design-basis weight is 8.82 pounds.
3. TRIGA fuel element design-basis weight is 13.2 pounds for top module.

The weight of TRIGA fuel cluster rods in a basket cell, including the weight of the fuel rod insert, is bounded by that of the TRIGA fuel elements. As reported in Section 1.2.3.1, the design basis weight of a TRIGA fuel element is 8.8 lbs, while the design basis weight of a TRIGA fuel cluster rod is 1.4 lbs and the weight of the insert is 11.2 lbs. Thus, four fuel elements in a cell weigh 35.2 lbs, while 16 fuel cluster rods and an insert in a cell weigh 33.6 lbs. Additionally, the active fuel cluster rod length is slightly longer than the length of the fuel elements, producing a smaller bearing load along the length of the fuel cluster rod and insert.

Therefore, the analyses of TRIGA basket modules and payload presented in the following sections are bounding for both nonpoisoned and poisoned basket configurations, and for all TRIGA fuel types.

2.6.12.7.1 NAC-LWT Inner Shell Bearing Stress Analysis

The nominal radial gap between the TRIGA fuel basket and the cask inner shell is 0.0531 inch at the calculated, steady state, normal conditions fuel temperature. As defined for other NAC-LWT fuel specific basket designs, it is assumed that there is no relative motion between the basket and the cask, and that the basket is in bearing contact with the cask cavity inner shell in the side drop. Bearing loads of the intact fuel, and the screened and sealed failed fuel cans, are thus transmitted directly to the inner shell and cask structure.

Bearing stress is calculated using Case 2C (Young) which models the cylindrical basket in a circular groove. The maximum compressive stress, for two elastic bodies with a similar elastic modulus, is:

$$S_c = 0.798 \left\{ \frac{gp(D_1 - D_2)}{D_1 D_2} \frac{2(1 - \nu^2)}{E} \right\}^{1/2} = 15,305 \quad \text{psi}$$

where:

g = 24.3, Dynamic load factor for the one-foot side drop

p = 1,256 lb/in., 1 g bearing load

D₁ = 13.405 inches, Cask cavity diameter

D₂ = 13.265 inches, Basket outside diameter.

ν = 0.275, Poisson's ratio for SS 304

E = 28.3 x 10⁶ psi, Elastic modulus (conservatively use E at 70°F)

The bounding bearing load, p , is determined using the weight of the bottom module bearing on the inner shell of the cask at the top and bottom circular plates. The bearing surface considers the chamfer at the edge of the circular plates.

The allowable stress $S_y = 18,200$ psi at 600°F . Therefore:

$$MS = \frac{18,200}{15,305} - 1 = +0.19$$

2.6.12.7.2 NAC-LWT Bottom Forging Bearing Stress

The TRIGA basket assembly, when in the vertical position, is supported by a 0.5-inch thick, 10-inch nominal diameter schedule 80S pipe. The 1.5-inch long pipe is welded to the baseplate of the base unit. The compressive stress is:

$$S_c = \frac{g \times W}{A} = 3,073 \quad \text{psi}$$

where:

$g = 15.8$ Dynamic load factor for the one-foot end drop

$W = 3,131$ lbs, Total weight of the basket

$A = 16.1 \text{ in}^2$, Area of 10-inch diameter Schedule 80S pipe

The allowable stress, $S_y = 18,200$ psi at 600°F .

Therefore:

$$MS = \frac{18,200}{3,073} - 1 = +\underline{\text{Large}}$$

2.6.12.7.3 TRIGA Basket Compressive Stress Analysis

The TRIGA fuel basket is designed to ensure that the longitudinal movement of the basket relative to the cask inner cavity is limited. The fuel, and screened or sealed can contents are not attached to the basket, and do not impart any longitudinal structural load on the basket body. However, the basket must support itself during an end drop accident. The basket is analyzed as a column, acted upon by a structural (weight) compressive load.

The compressive stress developed in the basket compartment wall is:

$$S_c = \frac{g \times W}{A} = 6,033 \quad \text{psi}$$

where:

$g = 15.8$ Dynamic load factor for the one-foot end drop

$W = 3,131$ lbs, Total weight of the basket

$A = 8.20$ in², Total compartment cross-section area at base plate.

The allowable stress, $S_m = 16,400$ psi at 600°F.

Therefore:

$$MS = \frac{16,400}{6,033} - 1 = \underline{+1.72}$$

The Euler elastic buckling load formulation is used to determine the critical buckling load (P_{cr}) of the 10-inch diameter Schedule 80S pipe and the base module. The pipe and base module are conservatively treated as simply supported, which results in an effective length that is twice the actual length, reducing the critical buckling load by a factor of 4.0. For the 10-inch pipe, the critical buckling load is:

$$P_{cr} = \frac{\pi^2 EI}{L_e^2} = 5.88 \times 10^9 \text{ lbs}$$

where:

$E = 25.3 \times 10^6$ psi at 600°F

$I = 212$ in⁴, inertia moment

$L_e = 2 \times 1.5 = 3.0$ in., effective length (2L)

The calculated compressive load is:

$$P_c = W \times g = 3,131 \times 15.8 = 49,470 \text{ lbs}$$

where:

$g = 15.8$ Dynamic load factor for the one-foot end drop

$W = 3,131$ lbs, Total weight of the basket

Therefore:

$$M.S. = \frac{P_{cr}}{P_c} - 1 = \frac{5.88 \times 10^9}{49,470} - 1 = \underline{+Large}$$

The critical buckling load for the base module is calculated using the same equation as above, by applying the moment of inertia of the fuel support structure. The fuel web and divider support structure is shown in the figure in the section titled "Baseplate Stress Due to End Drop."

The moment of inertia for the support structure is:

Item	$(I_o)_{yy}$	A	h	Ah ²	$(I_o)_{xx}$
2-11.57" x 0.28" web plate	0.0	6.48	1.86	22.42	72.28
2-3.44" x 0.25" divider plate	1.7	1.72	3.72	23.80	0.0
Total	1.7			46.22	72.28

$$(I_o)_{yy} = I_o + \Sigma Ah^2 = 1.7 + 46.22 = 47.92 \text{ in}^4$$

$$(I_o)_{xx} = \Sigma I_o = 72.28 \text{ in}^4$$

Choosing the smaller moment of inertia, $(I_o)_{yy}$, as I:

$$I = 47.92 \text{ in}^4$$

$$P_{cr} = \frac{\pi^2 EI}{L_e^2} = \frac{\pi^2 \times 25.3 \times 10^6 \times 47.92}{(2 \times 33.2)^2} = 2.11 \times 10^6 \text{ lbs}$$

where:

$$L_e = 2 \times 33.2 \text{ inches}$$

$$P_c = W \times g = 3,131 \times 15.8 = 49,470 \text{ lbs}$$

where:

$$g = 15.8, \text{ Dynamic load factor for 1 foot end drop}$$

$$W = 3,131 \text{ lbs, Total weight of the basket}$$

$$\text{M.S.} = \frac{P_{cr}}{P_c} - 1 = \frac{2.11 \times 10^6}{49,470} - 1 = \underline{\text{+Large}}$$

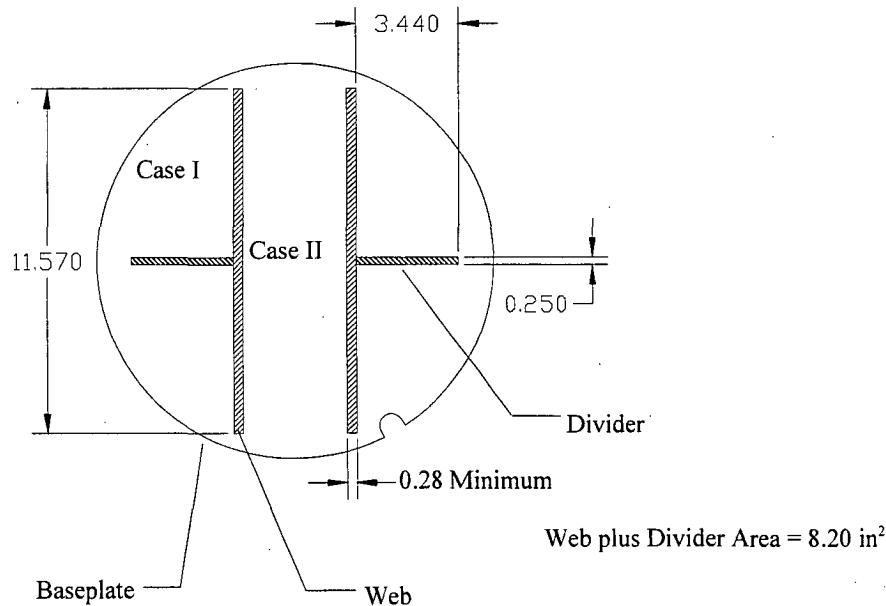
2.6.12.7.4 TRIGA Basket Lateral Stress Analysis

The base plate at the end of a typical TRIGA basket module supports the weight of up to 28 TRIGA fuel elements, or the loaded screened or sealed failed fuel cans, when the cask is in the vertical orientation (0 degree drop). With the cask in the horizontal orientation (90 degree drop), the fuel cell divider plates support the entire length of the TRIGA fuel. The base plate and the divider plates share in the support of the TRIGA fuel at drop orientations between 0 and 90 degrees.

Baseplate Stress Due to End Drop

The support plate at the top end of the modules is continuously welded to the outside periphery of the plates, including the support plates that form the fuel cells. The baseplate of the basket module is continuously welded to the two 11.57-inches wide, 5/16-inch thick (0.28-inch min)

web plates, and to the two 3.44-inches wide, 1/4-inch thick divider plates as shown in the following sketch:



The baseplate supports 28 TRIGA fuel elements and is conservatively assumed to be supported by the main longitudinal support plates during a cask end drop. Two separate load cases are evaluated. The maximum stress for each case is combined to obtain the total stress on the baseplate.

The first case (Case I), evaluates a 3.44-inches square plate with adjacent sides fixed and the other sides free. The applied pressure over the entire plate is uniform (Young, page 471, case 11). The second case, Case II, examines a rectangular plate, 11.57 inches by 3.44 inches, fixed along the long edges, free along the short edges and uniform pressure (Young, page 462, case 6).

For Case I, the 3.44-inches square plate is analyzed as a cantilevered plate supported at two adjacent sides with the other two sides free. Load is assumed uniform over the area of the plate. The bounding fuel weight is applied. The maximum stress is expressed as (Young, page 471, case 11):

$$S_1 = \frac{-g \times B_1 \times P \times b^2}{A \times t^2} = -8,944 \text{ psi}$$

where:

$g = 15.8$, Dynamic load factor for the one-foot end drop

$B_1 = 1.769$, Boundary condition stress factor

P = 80 lbs, Bounding module fuel weight

b = 3.44 inches, Width of plate

A = (3.44)² sq. in., Plate area

t = 0.5 in, Plate thickness

Case II, evaluates a plate 3.44-inches by 3.44-inches (width x length), fixed on two opposite sides, with the other two sides free. The maximum stress is expressed as (Young, page 462, case 6):

$$S_{II} = \frac{-g \times B_{II} \times P \times b^2}{A \times t^2} = -2,528 \text{ psi}$$

where:

g = 15.8, Dynamic load factor for the one-foot end drop

B_{II} = 0.5, Boundary condition stress factor

P = 80 lbs, Bounding module fuel weight

b = 3.44 inches, Width of plate

A = (3.44)² sq. in., Plate area

t = 0.5 in., Plate thickness

The total bending stress from Case I and Case II is:

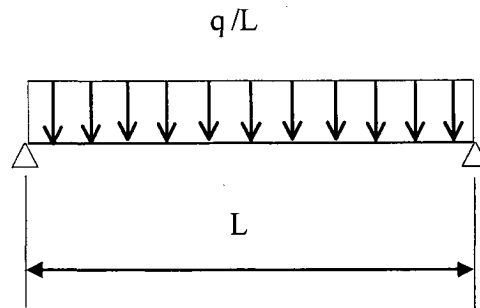
$$S_{\text{total}} = S_I + S_{II} = -11,472 \text{ psi} < 1.5 S_m = 24,600 \text{ psi}$$

Therefore:

$$MS = \frac{24,600}{11,472} - 1 = +1.14$$

Support Plate Stress Due to Side Drop With Intact Fuel or the Screened Failed Fuel Can

The maximum stress in the support plates that form the fuel cells occurs in the 0.12-inch thick 11 gage sheet metal tubes which support the entire length of the TRIGA fuel elements, or the length of the loaded screened failed fuel can. The weight of the TRIGA fuel element is transmitted through the can walls to the support plates that form the fuel cell. This load path creates a uniform pressure load over the entire area as shown in the following sketch.



As stated in Section 2.6.12.7, the loading of TRIGA fuel cluster rods is bounded by the TRIGA fuel elements. The fuel weight per unit length for the bounding TRIGA fuel elements is:

Fuel Type	Max. Weight, W (lb)	Max. Length, L (in)	W/L (lb/in)
Aluminum Clad	6.4	28.53"	0.22
Stainless Steel Clad	8.82	29.88"	0.30
Fuel Follower Control Element	13.2	45"	0.29

The intact fuel bounding load, q_i , along the length of the tube is:

$$q_i = \frac{W_i}{L_s} = 1.850 \text{ lb/in}$$

The uniform pressure load for the shorter (L_s) failed fuel in the screened can is:

$$q_f = \frac{W_f}{L_s} = 1.950 \text{ lb/in}$$

The uniform pressure load of the longer (L_L) failed fuel in the screened can is:

$$q_f = \frac{W_f}{L_L} = 1.778 \text{ lb/in}$$

where:

$L_s = 29.88$ inches, length of short fuel element

$L_L = 45$ inches, length of long fuel element

Weight of long failed fuel can = 17 lbs

Weight of short failed fuel can = 13 lbs

Added weight for fuel can calculation = 10 lbs

The weight calculation below includes 4 fuel elements, added weight, plus fuel can.

$$W_f = 58.28 \text{ lbs for fuel can with fuel elements having a length of 29.88 inches (L}_s)$$

$$W_f = 80 \text{ lbs for fuel can with fuel elements having a length of 45 inches (L}_L)$$

$$W_i = 55.28 \text{ lbs for fuel can with intact fuel}$$

The bounding load for TRIGA fuel is 1.950 lb/in.

The maximum bending moment is:

$$M_{\max} = \frac{(q_f + w) \times gL}{8} = 21.6 \text{ in-lb}$$

where:

$$q_f = 1.950 \text{ lb/in}$$

$$g = 24.3, \text{ dynamic load factor for one foot side drop}$$

$$t = 0.12\text{-inches (11 gage)}$$

$$L = 3.44 = \text{width of side support plate (11 gage)}$$

$$w = 0.288 \times 3.44 \times t = 0.1185 \text{ lb/in, steel beam weight}$$

$$S = \frac{6 \times M_{\max}}{t^2} = 9,065 \text{ psi}$$

Therefore,

$$MS = \frac{24,600}{9,065} - 1 = +1.71$$

The 11 gage sheet metal is continuously welded to the adjacent divider plates with a 1/8-inch fillet weld. This weld resists the shear developed in the simple beam analysis above.

$$V = \frac{(W_f + wL_s) \times g}{2 \times L_s} = 25.14 \text{ lbs}$$

where:

$$W_f = 58.28 \text{ lbs}$$

$$L_s = 29.88 \text{ inches}$$

$$S_v = \frac{V}{t \times 1} = 210 \text{ psi}$$

The throat thickness of 1/8-inch fillet weld is $0.707 \times 0.125 = 0.088\text{-inches}$. The square of the ratio of the plate thickness (0.12-inch) to the weld throat thickness (0.088-inches) is 1.86.

ASME Code Subsection NG-3352 recommends that the calculated stress in a fillet weld be increased by a factor of $1/0.35 = 2.86$. The maximum weld stress is:

$$S_w = S_v (1.86) (2.86) = 1,117 \text{ psi}$$

The allowable stress is $0.6S_m = 9,840 \text{ psi}$ at 600°F .

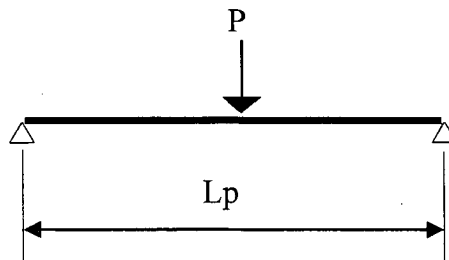
Therefore:

$$MS = \frac{9,840}{1,117} - 1 = \underline{+Large}$$

Support Plate Stress Due To Side Drop For the Sealed Failed Fuel Can

The total bounding weight of the long sealed can is 59.6 lbs, which includes 20 lbs for the can and a bounding weight of 39.6 lbs for the follower control elements.

The maximum stress in the support plates occurs in the 0.12-inch thick (11 gage) sheet metal tubes which supports the entire length of the sealed can. Since the sealed can is cylindrical, its weight is transmitted as a line load over the length to the supporting plate. For a unit cross-section of the supporting plate, the line load is treated as a concentrated load over the supporting plate as shown in the following loading diagram.



The load of the sealed can and its contents is represented by a uniformly distributed line load along the basket length that is in contact with the sealed can. For a unit length, the concentrated load due to the longer can is:

$$P = \frac{W_f \times g}{L} = 37.71 \text{ lb/in}$$

where:

$W_f = 59.6 \text{ lbs}$, weight of the long sealed can (20 lbs) and the follower control elements (39.6 lbs)

$g = 24.3$, dynamic load factor for one-foot side drop

$L = 38.41 \text{ inches}$, length of the longer body sealed can tube

For the shorter can:

$$P = \frac{W_f \times g}{L} = 45.24 \text{ lb/in.}$$

where:

$W_f = 43.4$ lbs, weight of the shorter sealed can (17 lbs) and bounding fuel element (26.4 lbs)

$g = 24.3$, dynamic load factor for one-foot side drop

$L = 23.31$ inches, length of the shorter body sealed can tube

The concentrated load from the shorter can, $P = 45.24$ lb/in., enveloping both the longer can and short can, is used to calculate the maximum bending moment. The unit length of the basket support plate with the 45.24 lbs concentrated force in the middle is treated as a simply supported beam. The maximum bending moment is:

$$M_{\max} = \frac{P \times L_p}{4} = 38.91 \text{ in-lb}$$

where:

$P = 45.24$ lbs, concentrated load

$L_p = 3.44$ inches, width of the 11 gage support plate

The maximum bending stress is:

$$S = \frac{6 \times M_{\max}}{t^2} = 16,321 \text{ psi}$$

where:

$M_{\max} = 38.91$ in-lb, maximum bending moment

$t = 0.12$ in., thickness of the 11-gage support plate

The margin of safety is:

$$\text{M.S.} = \frac{1.5S_m}{S} - 1 = \frac{24,600}{16,321} - 1 = +0.51$$

The 11 gage sheet metal is continuously welded to the adjacent divider plates with a 1/8-inch fillet weld. This weld resists shear developed in the simple beam analyzed above.

$$S_v = \frac{P}{t \times 1} = 378 \text{ psi}$$

where:

$$P = 45.24 \text{ lbs, load of unit length}$$

$$t = 0.12 \text{ in, thickness of the 11 gage support plate}$$

The throat thickness of 1/8-inch fillet weld is $0.707 \times 0.125 = 0.088$ in. The square of the ratio of the plate thickness (0.12 in) to the weld throat thickness (0.088 in) is 1.86. ASME Code Subsection NG-3352 recommends that the calculated stress in a fillet weld be increased by a factor of $1/0.35 = 2.86$.

Maximum weld stress is the calculated stress in the material times the above factors.

$$S_w = S_v (1.86) (2.86) = 378 \times 1.86 \times 2.86 = 2,011 \text{ psi}$$

The allowable stress is:

$$0.6S_m = 9,840 \text{ psi @ } 600^\circ\text{F,}$$

The margin of safety is:

$$MS = \frac{9,840}{2,011} - 1 = \underline{+3.9}$$

Maximum Basket Stress Due To Oblique Drop

As shown in the previous sections, the sealed can imposes the largest stress in the basket support plate due to its cylindrical cross-section. Therefore, the maximum stress in the basket is bounded by the stress induced by the sealed failed fuel can.

The maximum stress in the basket during oblique drop is found by combining the absolute value of the maximum stresses found in the basket during side drop and end drop determined in the previous sections. Although the stresses in the two different drop configurations do not occur in the same location, the stress combination method conservatively envelopes the maximum possible stress states during the oblique drop.

The maximum calculated stresses for the 1-foot end drop and the 1-foot side drop are:

$$\text{Maximum stress} = 6,033 \text{ psi for end drop}$$

$$\text{Maximum stress} = 16,321 \text{ psi for side drop}$$

Adding the two stress values to obtain the total oblique drop stress = $6,033 + 16,321 = 22,354$ psi.

$$\text{Allowable stress} = 1.5 S_m = 1.5 \times 16,400 = 24,600 \text{ psi @ } 600^\circ\text{F,}$$

$$MS = \frac{24,600}{22,354} - 1 = \underline{+0.10}$$

2.6.12.7.5 Screened Failed Fuel Can

This section evaluates the stresses in the screened failed fuel can as a result of the normal condition one-foot drop. The screened failed fuel can is described in Section 2.6.12.7. The screened failed fuel can is analyzed for side and end drops during transportation.

Screened Failed Fuel Can Compressive Stress Analysis

The fuel contents are not attached to the screened can and do not impart any longitudinal structural load on the can. The screened can must support itself during an end drop accident. The can is analyzed as a column acted upon by a structural (weight) compressive load consisting of the weight of the can and its contents. The screened can for fuel follower control rods is used since it is heavier, carries a heavier load and has the same properties as the screened can for the fuel rods.

The compressive stress developed in the screened can wall is:

$$S_c = Wg/A = 1,145 \text{ psi}$$

where:

W = 71 lbs, weight of screened can and contents

g = 15.8, dynamic load factor for one foot end drop (normal condition)

A = 0.98 in², cross-section area of screened can

The allowable stress,

$$S_m = 16,400 \text{ psi at } 600^\circ\text{F.}$$

Therefore:

$$MS = (16,400/1,145) - 1 = +\underline{\text{Large}}$$

Buckling of the screened failed fuel can is evaluated using hypothetical accident loading conditions in Section 2.7.7.9.4. The loading conditions presented in that section bound normal condition loads.

Screened Failed Fuel Can Plate Stress Due to Side Drop

The plate making up the sides of the screened failed fuel can is analyzed for bending as a result of loads applied during a side drop. To bound the analysis, the weight of the longer failed fuel can is used and this load is distributed over the length of the shorter fuel can to determine the load acting on a one-inch wide strip (along the axial length of the can) of the fuel can cross section. This total load on a one-inch strip is conservatively applied to the area between fuel elements (1.5 inches), resting inside of the can. This is the longest span of plate subject to

bending from a side drop and the 1.5-inch long plate section (which is one-inch wide) is considered to be simply supported.

The bending moment in the plate due to a uniform load is:

$$M = gPL/8 = 10.3 \text{ in-lb}$$

where:

$$g = 24.3, \text{ dynamic load factor for one foot side drop}$$

$$P = 2.26 \text{ lbs.}, \text{ Total load on one inch wide strip}$$

$$L = 1.5 \text{ inches}, \text{ spacing between fuel elements}$$

The section modulus, s , of the cross section resisting the bending moment is:

$$s = t^2/6 = 0.00093 \text{ in.}^3$$

where:

$$t = 0.0747 \text{ in.}, \text{ thickness of plate making up the screened failed fuel can}$$

The bending stress is:

$$S_b = M/s = 11,075 \text{ psi}$$

The allowable stress is: $1.5S_m = 24,600 \text{ psi}$

Therefore:

$$MS = (24,600/11,075) - 1 = +1.22$$

2.6.12.7.6 Sealed Failed Fuel Can

This section evaluates the stresses in the sealed failed fuel can as a result of the normal condition one-foot side and end drops. The sealed can is described in Section 2.6.12.7.

Sealed Failed Fuel Can Compressive Stress Analyses Due to End Drop

This section analyzes the compressive stress and buckling load in the fuel tube, bottom tube and lifting lugs. The bounding weight of the sealed can used in this analysis is 59.6 lbs, which includes 20 lbs for the can and conservatively 39.6 lbs for the follower control elements. Actual operational capacity is controlled to the weight of two fuel elements.

Fuel Tube

The fuel elements are not attached to the round tube that forms the wall of the can. However, it is conservatively assumed that the shell of the sealed can carries the entire weight of the can and contents. The compressive stress is:

$$\sigma_c = \frac{W \times g}{A} = 1,448 \text{ psi}$$

where:

W = 59.6 lbs, conservative weight of the can and contents

g = 15.8, dynamic load factor for one foot end drop

A = $\pi(1.625^2 - 1.56^2) = 0.6504 \text{ in.}^2$ cross section area of the can

The margin of safety is:

$$MS = \frac{S_m}{\sigma_c} - 1 = \frac{16,400}{1,448} - 1 = +\underline{\text{Large}}$$

Bottom Tube

The compressive stress for the bottom tube is:

$$\sigma_c = \frac{W \times g}{A} = 1,010 \text{ psi}$$

where:

W = 59.6 lbs, conservative weight of the can and contents

g = 15.8, dynamic load factor for one foot end drop

A = $\pi(1.25^2 - 1.125^2) = 0.9327 \text{ in.}^2$ cross section area of bottom tube

The margin of safety is:

$$MS = \frac{S_m}{\sigma_c} - 1 = \frac{16,400}{1,010} - 1 = +\underline{\text{Large}}$$

Lifting Lug

The sealed can lifting lugs may be subject to compressive or buckling loads in drop accident events. The load is considered evenly distributed to both lugs.

The compressive stress for two lift lugs is:

$$\sigma_c = \frac{W \times g}{A} = 3,657 \text{ psi}$$

where:

W = 59.6 lbs, conservative weight of the can and contents

g = 15.8, dynamic load factor for one foot end drop

A = $2 \times 0.515 \times 0.25 = 0.2575 \text{ in.}^2$ smallest cross section area of the two lift lugs

The margin of safety is:

$$MS = \frac{S_m}{\sigma_c} - 1 = \frac{16,400}{3,657} - 1 = +\underline{3.48}$$

Considering the lifting lug as a cantilever beam with a fixed end, the load is carried by an equivalent moment, M:

$$M = (P/2) \times d \times g = 114.2 \text{ in-lbs}$$

where:

$g = 15.8$, g load factor for the one foot end drop

$P = 59.6$ lbs, conservative weight of can and contents

$d = 0.2425$ in, the length of moment arm, measured from the center of the section to the point of load application (.5 - .515/2)

The total stress acting on the neck section is:

$$\sigma = \frac{(M \times c)}{I} + \sigma_c = 13,975 \text{ psi}$$

where:

$\sigma_c =$ compressive stress, 3,657 psi

$W = 114.2$ in-lbs, equivalent moment

$c = 0.515/2$ inches, distance from center of neck section to the edge

$I = 0.25 \times (0.515)^3/12 = 2.85 \times 10^{-3} \text{ in}^4$, moment of inertia of the cross section

The margin of safety is:

$$MS = \frac{1.5S_m}{\sigma_c} - 1 = \frac{24,600}{13,975} - 1 = +\underline{0.76}$$

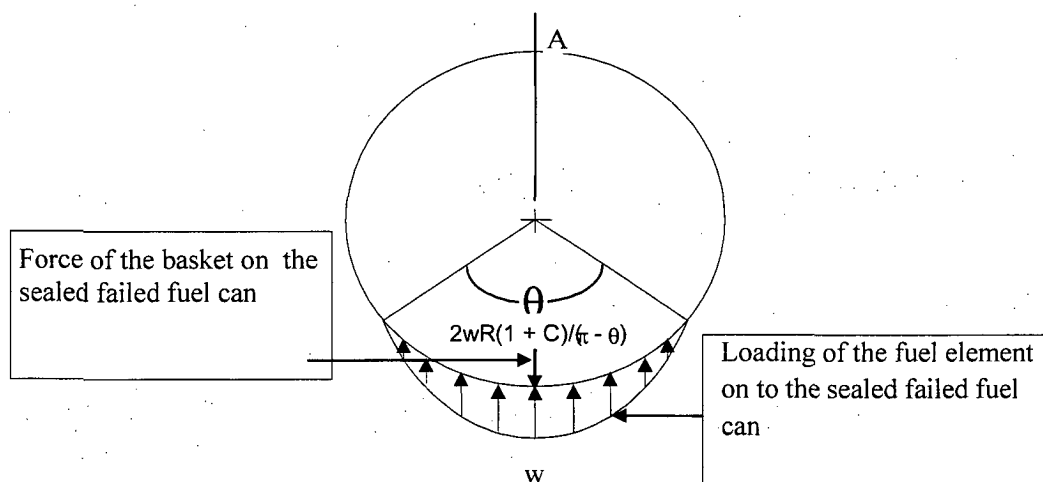
Buckling of the Sealed Failed Fuel Can

Buckling of the sealed failed fuel can, the bottom tube and the lifting lug is evaluated in Section 2.7.7.9.5. The loading conditions presented in that section bound the normal condition loads.

Sealed Failed Fuel Can Plate Stress Due to Side Drop

In the one-foot side drop, the sealed can supports the load applied by its contents.

The load applied to the can is considered as a linearly distributed load over the bottom 120° arc. The radial pressure w_x varies linearly from 0 at the beginning, to w at the bottom point of the can, as shown in the following sketch:



The load is uniformly distributed along the length of the can. For a unit length it is calculated as:

For the longer can:

$$p = \frac{W_f \times g}{L} = 25.05 \text{ lb / in.}$$

where:

$W_f = 39.6$ lbs, conservative fuel weight of three fuel follower control elements

$g = 24.3$, dynamic load factor for a one-foot side drop

$L = 38.41$ inches, length of the longer tube body

For the shorter can:

$$p = \frac{W_f \times g}{L} = 27.52 \text{ lb / in.}$$

where:

$W_f = 24.4$ lbs, conservative fuel weight of three fuel elements

$g = 24.3$, dynamic load factor for a one-foot side drop

$L = 23.31$ inches, length of the shorter tube body

To bound both the longer can and short can, $p = 27.52$ lb/in. is used to calculate the maximum distributed load.

Since (Young, 6th Edition, Table 17, Case 13):

$$p = 2wR(1+C) / (\pi - \theta)$$

$$w = \frac{p \times (\pi - \theta)}{2R \times (1 + C)} = 17.73 \text{ lb/in}$$

where:

$p = 27.52$ lbs, load on this unit length of the can tube

$\theta = 120^\circ = 2\pi/3$, angle

$C = \cos(\theta) = -0.5$

$R = 3.25/2$, radius of the can

The bending moment occurring at location A and C are respectively (Young, 6th Edition, Table 17, Case 13):

$$M_A = \frac{-wR^2}{\pi(\pi - \theta)} \left\{ 2 + 2C - s(\pi - \theta) + k_2 \left[1 + C - \frac{(\pi - \theta)^2}{2} \right] \right\} = -1.273 \text{ in-lb}$$

$$M_C = \frac{-wR^2}{\pi(\pi - \theta)} \left\{ \pi(\pi - \theta) - 2 - 2C - s\theta + k_2 \left[1 + C - \frac{(\pi - \theta)^2}{2} \right] \right\} = -6.507 \text{ in-lb}$$

where:

$w = 17.73$ lb/in, maximum distributed load

$R = 3.25/2 - 0.625/2$, curvature

$\theta = 120^\circ = 2\pi/3$, angle

$C = \cos(\theta) = -0.5$

$s = \sin(\theta) = 0.866$

$$k_2 = 1 - \alpha = 1 \quad \text{and} \quad \alpha = \frac{I}{AR^2} = \frac{2.289e-5}{0.6504 \times 1.593^2} = 1.388 \times 10^{-5}$$

$$I = \frac{1 \times 0.065^3}{12} = 2.289 \times 10^{-5} \text{ in}^4, \text{ moment of inertia of ring cross section}$$

$$A = \pi(1.625^2 - 1.56^2) = 0.6504 \text{ in}^2$$

The bending stress at location C, for unit length, is:

$$\sigma_c = \frac{M_C}{t^2/6} = 9,241 \text{ psi}$$

where:

$M_C = 6.507$ lb-in., bending moment at location C

$t = 0.065$ in., thickness of the can

Margin of safety is:

$$MS = \frac{S_m}{\sigma_c} - 1 = \frac{16,400}{9,241} - 1 = +0.77$$

Sealed Failed Fuel Can Bolt Evaluation

The sealed failed fuel can bolts are evaluated using the worst case loading conditions. For analysis purposes, the maximum differential thermal expansion (from accident conditions), lifting loads, and bolt preload are combined to calculate the maximum bolt stresses.

Bolt Thread Stress

The shear stress caused by lifting is:

$$\tau_L = \frac{1.1 \times W}{A_s} = 170 \text{ psi}$$

where:

1.1 = dynamic load factor for lifting

W = total weight of the canister and contents, 59.6 lbs

A_s = shear area of the external thread, 0.3859 in.²

The load caused by pre-load on each bolt is:

$$F_T = (\pi \times D \times P) / 4 = 1,721 \text{ lbs}$$

where:

P = 700 lb/in., conservative linear load required to crush the seal

D = 3.131 inches, diameter of the seal

The linear load, P, considers both the load to seat the metal seal as well as the internal pressure of the gas in the failed fuel canister. The contribution of the pressure to the linear load is:

$$\frac{P_{\text{gas}} D}{4} = \frac{(3 \text{ atm})(14.7 \text{ psi / atm})(3.131 \text{ in.})}{4} = 34.5 \text{ lb / in.}$$

Three (3) atm is conservatively used for the internal gas pressure during the fire. The linear load to seat the metal seal is 514 lbs. Combining the linear loads due to the pressure and seal gives a total value of 548.5 lb/inch. For analysis purposes, a conservative value of 700 lb/in. is used.

The shear stress caused by pre-loads in the bolts is:

$$\tau_t = \frac{F_t}{A_s} = 4,460 \text{ psi}$$

where:

$$F_t = 1,721 \text{ lbs, bolt pre-load}$$

$$A_s = \text{shear area for } 3/8 \text{ -16 UNC 2A thread} = 0.3859 \text{ sq. inch}$$

Total shear caused by lifting and pre-load is obtained by conservatively adding the shear stresses:

$$\tau = \tau_L + \tau_t = 4,630 \text{ psi}$$

The margin of safety is:

$$MS = \frac{0.6S_m}{\tau} - 1 = \frac{0.6 \times 45,200}{4,630} - 1 = +4.86$$

The average tensile stress due to pre-load in the bolts is:

$$S_t = \frac{F_t}{A_t} = 23,039 \text{ psi}$$

where:

$$F_t = 1,721 \text{ lbs, bolt pre-load}$$

$$A_t = \text{tensile stress area for } 3/8\text{-14 UNC 2A thread} = 0.0747 \text{ in}^2$$

The tensile stress due to the differential expansion of the bolt and the top plate is:

$$S_{dt} = \Delta T(\alpha_L - \alpha_{637})E_{637} = 26,912 \text{ psi}$$

where:

$$\Delta T = (600 - 70)^\circ\text{F} = 530^\circ\text{F} \text{ (The actual maximum temperature of the can during the fire accident is } 551^\circ\text{F.)}$$

$$\alpha_L = 9.53 \times 10^{-6} \text{ (in/in/}^\circ\text{F), coefficient of thermal expansion of top plate (S.S.304) at } 600^\circ\text{F}$$

$$\alpha_{637} = 7.67 \times 10^{-6} \text{ (in/in/}^\circ\text{F), coefficient of thermal expansion of bolt (SB - 637) at } 600^\circ\text{F}$$

$$E_{637} = 27.3 \times 10^6 \text{ psi at } 600^\circ\text{F, bolt material elastic modulus at } 600^\circ\text{F}$$

The total stress due to pre-load and differential expansion of the bolt and the top plate is:

$$S = S_{dt} + S_t = 49,951 \text{ psi}$$

The margin of safety is:

$$M.S = \frac{2S_m}{S} - 1 = \frac{2 \times 45,200}{49,951} - 1 = +0.81$$

The relation between the torque value and tensile force is:

$$T = \left[\left(\frac{d_m}{2d} \right) \left(\frac{\tan \lambda + \mu \sec \alpha}{1 - \mu \tan \lambda \sec \alpha} \right) + 0.625\mu \right] (F_T)(d) \quad (\text{Machinery's})$$

$$T = (0.2096) \times F_T \times d = 135 \text{ in-lb}$$

where:

T = applied torque in inch-pounds

F_T = pre-load force in pounds

d = 3/8 in, bolt diameter

$\tan \lambda = L/(\pi d_m)$

L = 1/16 in

$d_m = 0.3911$ in, mean diameter of threads

$\alpha = 30^\circ$, one-half the thread angle

$\mu = 0.15$, coefficient of friction

The torque required to engage the bolt is 135 in-lb. However, the maximum torque is 160 in-lb.

The torsional stress due to this torque value is:

$$\tau_t = \frac{T \times r}{J} = \frac{160 \times 0.1875}{1.94 \times 10^{-3}} \text{ psi} = 15,464 \text{ psi}$$

where:

T = 160 in-lb, the torque on a bolt

r = (3/8)/2 = 0.1875 in, radius of bolt

J = $(\pi r^4)/2 = (\pi \times 0.1875^4)/2 = 1.94 \times 10^{-3} \text{ in}^4$, polar moment of inertia

The margin of safety is:

$$MS = \frac{0.8S_m}{\tau_t} - 1 = \frac{0.8 \times 45,200}{15,464} - 1 = +1.34$$

Top Plate Thread Stress

The effect of Heli-Coil is conservatively ignored. The shear stress consists of two parts; one is caused by the lifting load; the other is caused by the combination of pre-load P (700 lbs/in.) and differential thermal expansion. The shear stress due to the lifting load is:

$$t_L = \frac{1.1 \times W}{A_n} = 118 \text{ psi}$$

where:

1.1 = the dynamic load factor for lifting

W = 59.6 lbs, total weight of the canister and contents

$A_n = 0.5548 \text{ in}^2$, shear area of the inner thread

The shear stress due to pre-load and differential thermal expansion in the top plate is:

$$S = \frac{F_t}{A_n} = 6,725 \text{ psi}$$

where:

$F_t = 1,721 + 26,912 \times 0.0747 = 3,731 \text{ lbs}$, bolt pre-load

$A_n = 0.5548 \text{ in}^2$, shear area for 3/8 -16 UNC 2A thread

Total shear caused by lifting, pre-load and differential expansion is obtained by conservatively adding the separate shear stresses:

$$\tau = \tau_L + S = 6,843 \text{ psi}$$

The margin of safety is:

$$MS = \frac{0.6S_m}{\tau} - 1 = \frac{0.6 \times 16,400}{6843} - 1 = +0.44$$

Top Plate Bearing Stress

Top plate bearing stress is developed from the combination of pre-load and the differential thermal expansion of the bolt and the top plate. The pre-load is 1,721 lbs on one bolt and thermal load is 2,010 lbs ($0.0747 \text{ in}^2 \times 26,912 \text{ psi}$). The total bearing is 3,731 lbs. Then, the bearing stress on the top plate is:

$$S_b = \frac{P_b}{A_b} = \frac{3731}{0.2311} = 16,145 \text{ psi}$$

where:

$$P_b = 3,731 \text{ lbs, total bearing force}$$

$$A_b = \pi(0.68^2 - 0.41^2)/4 = 0.2311 \text{ in}^2, \text{ bearing area}$$

The margin of safety for top plate is:

$$MS = \frac{1.0S_y}{S_b} - 1 = \frac{18,200}{16,145} - 1 = +0.13$$

2.6.12.7.7 Borated Stainless Steel Plate Weld Stress

The borated stainless steel plate utilized in the poisoned TRIGA baskets is assumed to be welded on two sides to the divider plates using a 1/16-inch fillet weld. This assumption is conservative since the borated plate is welded completely around its periphery. For the end drop condition, the only load applied on the weld is the self weight of the plate, which results in a shear stress. For side drop, the load applied on the weld is the self weight of plate, which also results in shear stress. The plate also carries the weight of the fuel, which results in compressive stress.

The welded area for one stainless steel plate is:

Parameter	Base Module	Intermediate Module	Top Module
Weight of Plate (lb)*	14.44	13.64	21.61
Length of Plate (in)	30.45	28.75	45.55
Cross Section Area (in ²)	99.27	93.73	148.49
Weld Area (in ²)	3.81	3.59	5.69

Using the smallest area, 3.59 in² and largest weight, 21.61 lbs, the end drop shear stress is:

$$S_{se} = \frac{g \times W}{A} = \frac{15.8 \times 21.61}{3.59} = 95.11 \text{ psi}$$

where:

$$g = 15.8 \text{ one-foot end drop load factor}$$

$$W = 21.61 \text{ lbs bounding poison plate weight}$$

$$A = 3.59 \text{ in}^2 \text{ bounding weld area}$$

The allowable shear stress for normal condition is $0.6 S_m = 9840 \text{ psi}$. The margin of safety is:

$$\text{Margin of Safety} = \frac{0.6S_m}{S_{se}} - 1 = \frac{9840}{95.11} - 1 = +\text{Large}$$

Using the smallest area, 3.59 in² and largest weight, 21.61 lbs, the side drop shear stress is:

$$S_{ss} = \frac{g \times W}{A} = \frac{24.3 \times 21.61}{3.59} = 146.27 \text{ psi}$$

where:

- g = 24.3 one-foot side drop load factor
- W = 21.61 lbs bounding poison plate weight
- A = 3.59 in² bounding weld area

The allowable shear stress for normal condition is $0.6 S_m = 9840$ psi. The margin of safety is:

$$\text{Margin of Safety} = \frac{0.6 S_m}{S_{ss}} - 1 = \frac{9840}{146.27} - 1 = + \text{Large}$$

The compressive stress is evaluated using a bounding fuel cell weight of 80 lbs. The minimum cross section area is 93.73 in².

$$S_c = \frac{g \times W}{A} = \frac{24.3 \times 80}{93.73} = 20.74 \text{ psi}$$

where:

- g = 24.3 one-foot side drop load factor
- W = 80 lbs bounding fuel cell weight
- A = 93.73 in² bounding cross section area

The allowable stress is $1.0 S_m = 16,400$ psi. The margin of safety is:

$$\text{Margin of Safety} = \frac{1.0 S_m}{S_c} - 1 = \frac{16,400}{20.74} - 1 = + \text{Large}$$

This evaluation shows that the weld has large margins of safety for the stresses that could occur in normal conditions.

2.6.12.7.8 TRIGA Fuel Spacer Evaluation

A spacer fabricated from Type 304 stainless steel is used in poisoned TRIGA basket Configuration 2 (base module and 4 intermediate modules). The spacer consists of 8-inch diameter pipe with a 1-inch thick plate welded to the bottom, and a 0.5-inch thick plate welded to the top. The top plate is attached to the underside of the NAC-LWT cask lid using four 1/2-inch diameter SA-193, Grade B6, bolts. It has a calculated weight of 85 lbs.

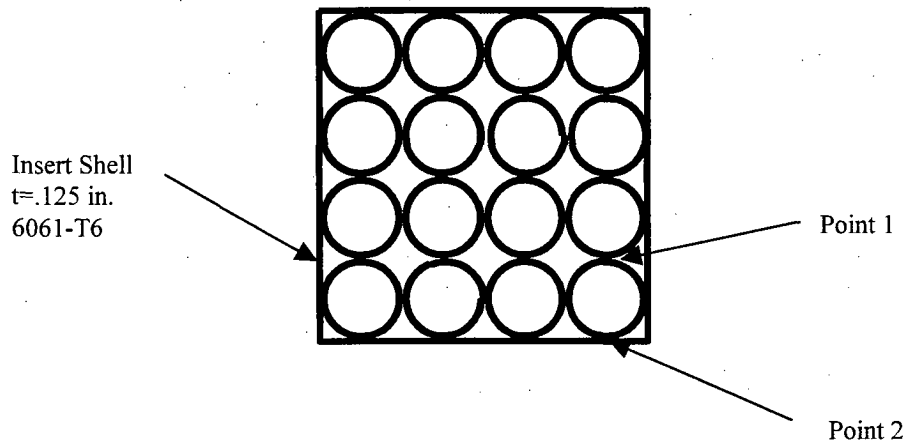
The spacer and bolts are analyzed for the effects of a normal condition 1-foot side and end drop. The material temperatures and properties are the same as those imposed on the fuel baskets. The compression load is calculated as 50,813 lbs, which results in a calculated stress of 6,049 psi

(Margin of Safety = +1.71). The stress on the bolts in combined shear and tension is 11,881 psi. All margins of safety are positive with a minimum Margin of Safety of +0.21 for the bolts in shear and tension as a result of the side drop condition.

2.6.12.7.9 TRIGA Fuel Cluster Rods Basket One Foot Drop Evaluation

The fuel cluster rod is restrained from motion by the aluminum tube, which has a 0.75-inch outer diameter and a 0.62-inch inner diameter. An array of four by four is inserted into an aluminum shell of 0.125-inch thickness, which is loaded into the stainless steel basket.

The bearing stress between the aluminum tubes is required to be less than the yield stress of the 6061-T6 aluminum. The yield stress is evaluated at the maximum aluminum temperature of 300°F, corresponding to a yield stress of 27.5 ksi. The maximum bearing load would occur between the aluminum tube and the 0.125 aluminum shell (Point 2 in the following sketch), but the maximum bearing stress would occur between two adjacent cylinders (Point 1 in the following sketch).



Using Roark, 6th edition, Table 33, Case 2a, which is the bearing stress between two adjacent cylinders, the bearing stress (S_{brg}) is:

$$S_{brg} = .789 \times \sqrt{\frac{P}{K_D C_E}}$$

$$P = \text{the line load} = (3 \text{ tubes}) \left(\frac{1.44}{27.5} + \frac{\pi}{4} (0.75^2 - 0.62^2)(0.098) \right)$$

$$P = 0.198 \text{ lbs/in (for dead weight only)}$$

where:

$$\text{TRIGA fuel cluster rod weight} = 1.44 \text{ lbs}$$

$$\text{rod length} = 27.5 \text{ inches}$$

aluminum density	=	0.098 lb/in ³
aluminum tube OD	=	0.75 in
aluminum tube ID	=	0.62 in

$$C_E = \frac{1-\nu_1^2}{E_1} + \frac{1-\nu_2^2}{E_2} = 1.937e-7$$

where for 6061-T6 Aluminum at 300°F:

$$E = 9.2 \times 10^6 \text{ psi}$$

$\nu = 0.33$ and the subscripts 1 and 2 refer to each of the cylinders

where:

$$K_D = \frac{D_1 D_2}{D_1 + D_2} = .375$$

where D is the outer diameter of the tube, .75 in (the subscripts 1 and 2 refer to the individual tubes). The bearing stress corresponding to 24.3 g is:

$$S_{brg} = .798 \times \sqrt{\frac{24.3 \times 0.198}{0.375 \times 1.937e-7}} = 6495 \text{ psi}$$

$$MS = \frac{27400}{6495} - 1 = +3.21$$

The bending stress in the aluminum insert tube is evaluated as a curved beam using the diametrical point forces, as contained in Roark's, 6th Edition, Table 17, Case 1.

Conservatively using 400°F to evaluate the aluminum properties, and the weight of four tubes (which results in a line load of $1.33 \times 0.198 = 0.263$ lbs/in), the maximum bending stress in the aluminum tube is:

$$S_b = \frac{6M}{bt^2}$$

Where $b = 1.0$ in, which is the axial length for the purpose of the calculation.

$$M = 0.3183 \cdot P \cdot R \cdot k_2$$

$$k_2 = 1 - \alpha$$

$$\alpha = \frac{I}{AR^2}$$

$$t_{\text{ring}} = \frac{.75 - .62}{2} = 0.065 \text{in} \quad I = \frac{0.065^3 \times 1}{12} = 2.29 \text{e} - 5 \text{in}^4 \quad A = .065 \times 1 = 0.065 \text{in}^2$$

$$R = \frac{0.62}{2} + \frac{0.065}{2} = 0.343 \text{in} \quad \alpha = \frac{2.29 \text{e} - 5}{0.065 \times 0.343^2} = 0.003 \quad k_2 = 1 - 0.003 = 0.997$$

$$M = 0.3183 \times (4 \times 0.263) \times 0.343 \times 0.997 = 0.115 \text{ in} \cdot \text{lb/in}$$

$$S_b = \frac{6 \times 0.115 \times 24.3}{1 \times 0.065^2} = 3969 \text{ psi}$$

$$MS = \frac{1.5S_m}{S_b} - 1 = \frac{8250}{3969} - 1 = + \underline{1.07}$$

Where 24.3 g corresponds to the side drop accelerations.

This verifies that the aluminum insert tube is acceptable for the normal operational conditions.

2.6.12.8 DIDO Fuel Basket Construction

The DIDO modular basket assembly consists of a top module, four intermediate modules, and a base module. The top module is 29.8 inches long and the intermediate modules are each 29.3 inches long and all have an outer diameter of 13.27 inches. The base module has a length of 29.8 inches and an outer diameter of 13.27 inches. Each module is capable of holding seven DIDO fuel assemblies. Each module is a weldment made up of a 13.27 inch diameter 1/2-inch thick base plate and two 13.27 inch diameter 1/2-inch thick support plates scalloped on the inner diameter to fit around six peripheral fuel tubes. The weldment structure, fuel tubes and base and support plates are fabricated from Type 304 stainless steel. Each fuel tube has an inner diameter of 4.01 inches and a wall thickness of 0.12 inches. The bottom of each fuel tube is welded to the 1/2-inch thick base plate. At the bottom of each fuel tube, where it is welded to the base plate, there is a 0.3-inch slot to permit water to drain from the tube. The base plate supports the fuel in the end drop orientation. The base module sits on a 0.5-inch long, 10-inch diameter schedule 80S pipe that is welded to the base plate. The total weight of the DIDO basket assembly bears directly on the bottom forging of the cask through the schedule 80S pipe. The two scalloped 1/2-inch thick support plates and the base plate of each basket module provide lateral support and maintain the fuel configuration in the side drop orientation.

Heat rejection from the DIDO fuel and basket structure is augmented by six aluminum shunts and two heat transfer shells. Each shunt is mechanically attached to the center stainless steel fuel

tube. The heat transfer shell wraps around the 6 outer fuel tubes and is mechanically attached to the drain tube guide bars. The heat shunts are machined to match the outer diameter of the center fuel tube and are held in place by two shunt posts and shunt retainers. The shunt post at the bottom of each basket module is assembled with a tight fit between the shunt post, shunt retainer and base plate to provide a good conductive heat transfer path. The shunt post at the top of the basket is assembled with a slotted hole in the shunt to permit unrestricted differential thermal expansion between the fuel tube and thermal shunt. The aluminum sheet heat transfer shell is held in place against the outside fuel tubes by bolting the edge of the aluminum sheet to the drain tube guide bars. The heat shunts and heat transfer shell are not structural components and are not included in the structural analysis as load carrying components. The mass of the heat shunts and heat transfer shell have been included as loads in the structural analysis.

2.6.12.8.1 DIDO Fuel Basket Cask Interface Analysis

Structural analysis of the DIDO modular fuel basket and the MTR modular fuel basket are similar. DIDO fuel baskets and MTR fuel baskets are made from the same type of stainless steel. The contact points between the basket structure and the cask inner shell and between the basket structure and the cask bottom forging are similar. DIDO fuel baskets have an additional lateral support ring, reducing the side drop bearing stresses. A loaded DIDO fuel basket base module weighs approximately 250 lbs, assuming each DIDO assembly weighs 15 lbs. Loaded top and intermediate modules weigh approximately 247.4 lbs each. A full cask load of six DIDO basket modules represents a total contents weight of 1,487 lbs. The weight of a loaded 28-element MTR basket module is 289 lbs, which bounds the loaded weight of the loaded base DIDO basket module. Therefore, the bearing stress between the basket and the cask inner shell created by the DIDO basket module is bounded by the 28-element MTR fuel basket interface analysis.

The cask contents weight for the loaded 42-element MTR basket is 2,262 lbs, which bounds the cask contents weight of 1,487 lbs for the loaded DIDO basket. Therefore, the bearing stresses between the basket and cask bottom forging and between the basket and the cask lid created by the DIDO fuel baskets, are bounded by the 42-element MTR fuel basket interface analysis.

2.6.12.8.2 DIDO Fuel Basket Structural Analysis

Structural analyses of the DIDO fuel basket for the 1-foot end drop and the 1-foot side drop are performed using a finite element model of one basket module, as shown in Figure 2.6.12-1 and Figure 2.6.12-2, and the ANSYS general purpose computer program. Eight node brick elements (SOLID45) are used to construct the model. Each solid element has the material properties of stainless steel. In each basket module, the elements representing the seven 4.01-inch inner diameter tubes are joined to the base plate and to the two support plates at locations where the

welds are specified to connect the tubes to the plates. By design, the center tube is not connected to any of the six outer tubes. In this evaluation, the center tube is not considered to have any interaction with the outer six tubes, which is conservative, particularly in the side drop orientation where the tube is cantilevered from the base plate.

DIDO Fuel Basket 1-Foot Side Drop Orientation Analysis

The 1-foot side drop analysis of the DIDO fuel basket considers the weight of the center tube and fuel to be transferred to the circular base plate. A bounding fuel assembly weight of 15 pounds is used in the side drop analysis. To model the interaction of the two support plates and the base plate with the 13.375-inch cask inner shell diameter, CONTACT52 elements are used. The CONTACT52 element consists of two nodes, which corresponds to a 3D-line element, limiting transmitted loads to compression. One node of the CONTACT52 element is located on a circular plate, while the second node represents the inner shell, and is constrained in all three degrees of freedom. This boundary condition is considered to be conservative, since it models the inner shell as a rigid surface and minimizes the angle of contact between a circular plate and the cask inner shell, resulting in a more concentrated load at the point of contact. The aluminum heat shunts and aluminum heat transfer shell are not considered to be structural components. The shunts and shells are represented as lumped masses using the MASS21 element. These lumped masses are distributed along the outside of the center tube to represent the distributed weight of the heat shunt. The heat transfer shell is represented with lumped masses distributed along the outer six fuel tubes at the points of contact with the heat transfer shell.

The 1-foot side drop normal condition event is analyzed using an acceleration of 24.3g applied in each of three orientations: 0°, -60°, and -90° with respect to the model's X-axis. Maximum primary membrane stresses for each of the side drop orientations are shown in Table 2.6.12-1. The minimum margin of safety is calculated to be +2.5 for the 0° and 60° orientations. The maximum primary membrane plus bending stresses for each of the side drop orientations are shown in Table 2.6.12-2. The minimum margin of safety is calculated to be + 0.003 for the 60° orientation. Figure 2.6.12-3 presents the location of the maximum primary membrane and the primary membrane plus bending stresses for the side drop load.

DIDO Fuel Basket 1-Foot End Drop Analysis

For the end drop analysis, the finite element model load orientation and boundary conditions are specified to represent axial loading and consideration of the base basket module supporting five stacked modules above it. Equivalent pressure was applied to the area inside of the fuel tube at the top surface of the base plate to represent the fuel in each of the fuel tube locations in each basket module. The weight of the five loaded fuel basket modules, which rest on the base fuel basket module, multiplied by the equivalent acceleration, is applied as an equivalent pressure to

the top edges of the fuel tubes in the base module. A bounding DIDO fuel assembly weight of 15 pounds is used in the end drop analysis. The bounding assembly weight accounts for the fuel assembly and the tube spacer and variations in the weight of either. The total weight resting on the top of the base module is approximately 1,237 pounds. This load was applied as a pressure load on the ends of the fuel tubes.

$$\text{Total end area of tubes} = 7 \times \pi/4 \times (4.25^2 - 4.01^2) = 10.9 \text{ in}^2$$

$$\text{Equivalent pressure} = 1237 \text{ lbs}/10.9 \text{ in}^2 = 113.5 \text{ psi}$$

The end drop finite element model reflects the base basket design shown on the drawings provided in Section 1.0. The height of the base skirt below the bottom support is 0.5 inch. Four full height drain slots are cut into the base skirt.

For the 1-foot end drop condition, the equivalent pressure load is increased to represent the maximum acceleration of 15.8 g. The maximum primary membrane stress for the end drop orientation is 11.4 ksi (shown in Table 2.6.12-1) resulting in a minimum margin of safety of +0.75. The maximum primary membrane plus bending stress is 13.2 ksi (shown in Table 2.6.12-2) resulting in a minimum margin of safety of + 1.27. Figure 2.6.12-6 presents the location of the maximum primary membrane and the primary membrane plus bending stresses for the end drop load.

Based on these results, it is concluded that the DIDO fuel basket is structurally adequate for normal transport conditions.

2.6.12.8.3 Fuel Assembly Spacer Structural Evaluation

During a top end drop, the spacer would be loaded by the weight of the fuel and the tube spacer. A bounding analysis of the DIDO fuel spacer post and top disk, based on hypothetical accident condition g-loads, is performed. The DIDO fuel assembly weight of 15 lbs is considered to include the weight of the tube spacer. The post is analyzed by determining the membrane stress due to the weight of the fuel assembly and tube spacer acting concentrically on the post. The top disk of the spacer is analyzed as a circular plate with a uniform load acting over the entire surface of the disk. The results, showing the spacer design is adequate to sustain the hypothetical accident top end drop analysis, are:

Component	Primary Membrane Stress (psi)	Allowable Stress (psi) @ Temp.	Margin of Safety	Primary Membrane + Bending (psi)	Allowable Stress (psi) @ Temp.	Margin of Safety
Pin	1,140	46,200	Large	5,082	66,000	12.0
Disk	N/A	46,200	N/A	10,980	66,000	5.0

Figure 2.6.12-3 DIDO Fuel Basket Module Structural Model – Top View

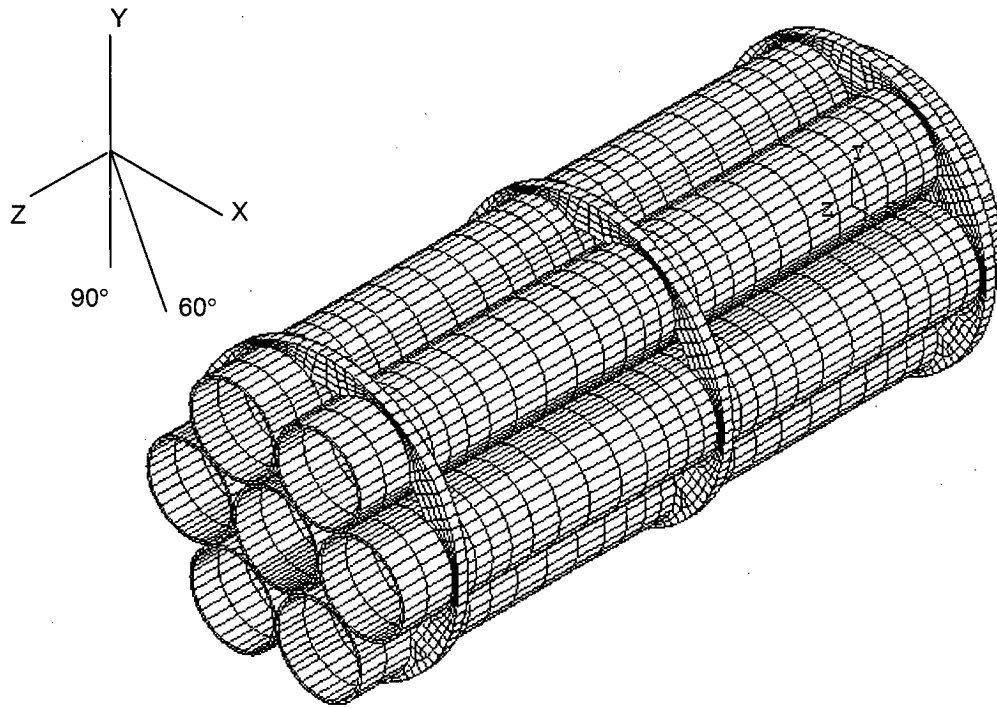


Figure 2.6.12-4 DIDO Fuel Basket Module Structural Model – Bottom View

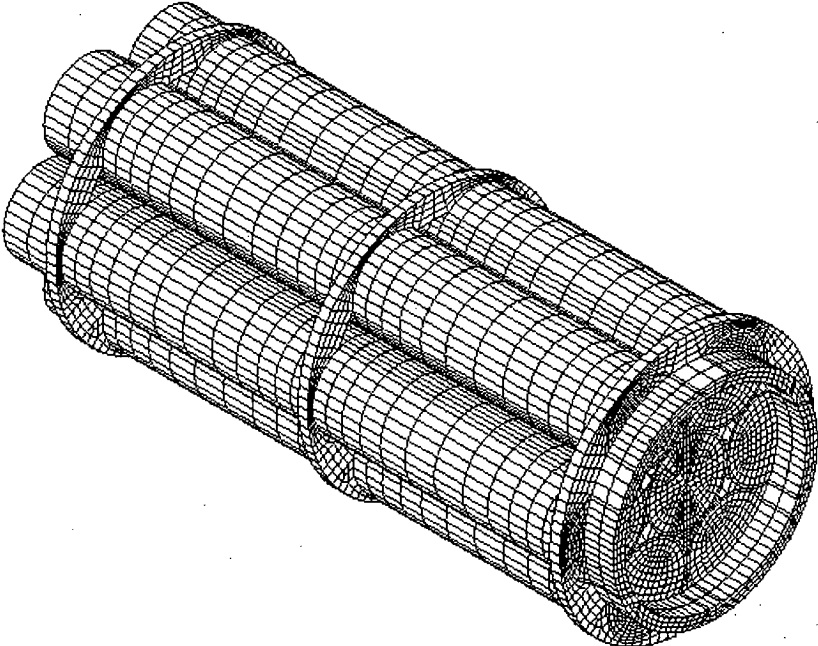


Figure 2.6.12-5 DIDO Fuel Basket Module Maximum Stress Locations for the Side Drop Orientation

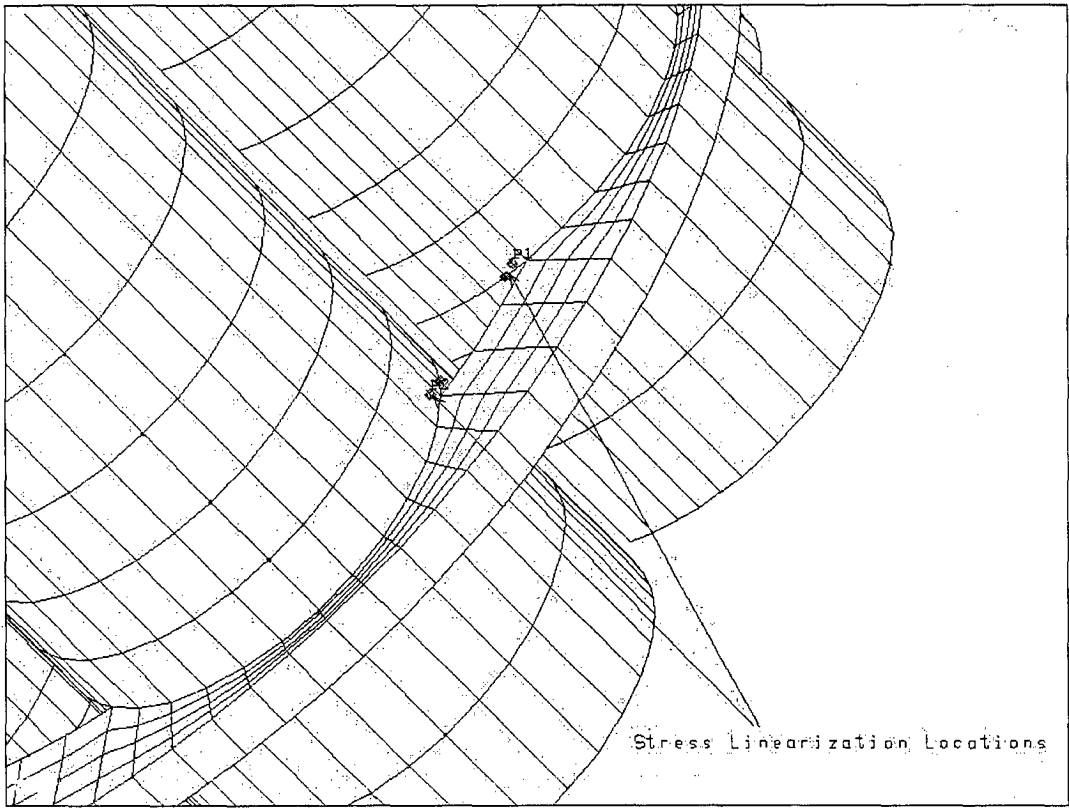


Figure 2.6.12-6 DIDO Fuel Basket Module Maximum Stress Locations for the End Drop Orientation

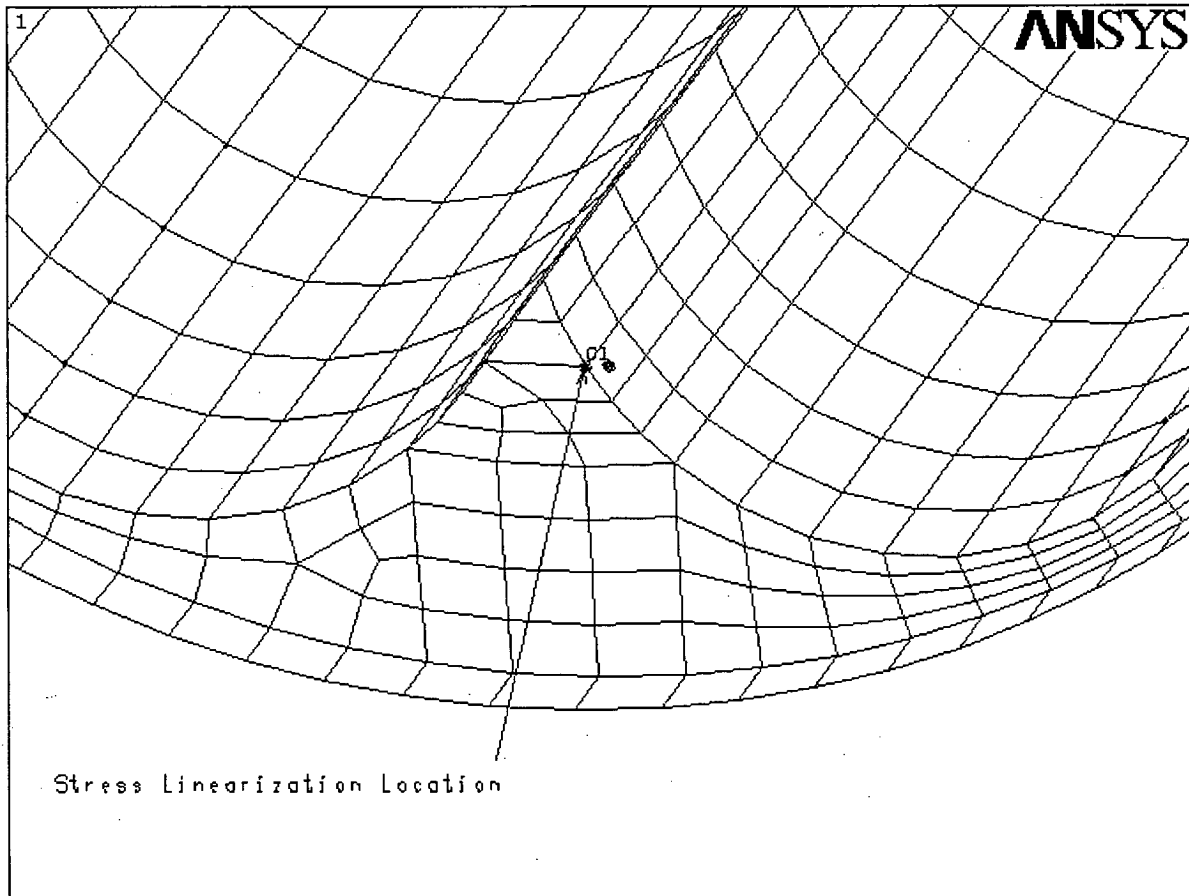


Table 2.6.12-1 Maximum Primary Membrane Stress for the 1-Foot Drop (DIDO Basket)

Location	Load Case 1-ft drop	Membrane (ksi)	Allowable (ksi) ¹	Margin of Safety ²
Fuel Tube Wall	Side @ 0 Deg ³	5.7	20.0	2.5
Fuel Tube Wall	Side @ 60 Deg ³	5.7	20.0	2.5
Fuel Tube Wall	Side @ 90 Deg ³	5.2	20.0	2.8
Fuel Tube Wall	End drop	11.4 ⁴	20.0	0.75

Table 2.6.12-2 Maximum Primary Membrane Plus Bending Stress for the 1-Foot Drop (DIDO Basket)

Location	Load Case 1-ft drop	Membrane + Bending (ksi)	Allowable (ksi) ⁵	Margin of Safety ²
Fuel Tube Wall	Side @ 0 Deg ³	29.6 ⁶	30.0	0.01
Fuel Tube Wall	Side @ 60 Deg ³	29.9 ⁶	30.0	0.003
Fuel Tube Wall	Side @ 90 Deg ³	24.4 ⁶	30.0	0.23
Fuel Tube Wall	End drop	13.2 ⁴	30.0	1.27

¹ $P_m \leq S_m$.

² Margin of safety = (Allowable-Stress/Actual Stress) - 1.

³ Angle orientation shown on Figure 2.6.12-1.

⁴ The linearized stresses for the end drop case are scaled by the ratio of 360/178.65, which is the full arc-to-arc length of the tube welded to the base plate.

⁵ $P_m + P_b \leq 1.5S_m$.

⁶ These stresses are maximum local tube wall stresses and may be considered secondary stresses. They are conservatively considered primary membrane plus bending stresses and are located as shown in Figure 2.6.12-3.

2.6.12.9 General Atomics IFM Basket Construction

The General Atomics Irradiated Fuel Material (IFM) basket consists of a top module assembly designed to carry two IFM Fuel Handling Units (FHUs). Each IFM FHU is associated with RERTR or HTGR fuel materials. A spacer assembly is used to permit the top module assembly to be positioned next to the transport cask lid.

The top module is 43.7 inches long and is made up of two fuel tubes and three support plates. All components are made from ASME SA240 Type 304 stainless steel. The fuel tubes have a 6.0-inch outer diameter and a 0.25-inch wall thickness. Two of the support plates are 0.50-inch thick and the third, center plate, is 1.0-inch thick. The support plates are welded to the fuel tubes with 1/8-inch bevel welds.

Two types of IFM FHU are carried by the top module. One FHU carries irradiated HTGR fuel material and is 5.25 inches in diameter (0.12-inch thick wall) and 39.0 inches long. The other FHU contains irradiated RERTR fuel material, is 4.75 inches in diameter (0.12-inch thick wall), and is 37.25 inches long.

Each end of the FHU is comprised of a 0.25-inch thick plate welded to the container shell. The weld connecting the end plate to the container shell is labeled as a full-penetration butt weld. The dimensions of the end plate and the container shell provide a minimal gap (2 mils when considering maximum tolerances) to permit the end plate to be inserted into the container end. The close tolerances ensure that the two components are effectively in contact along the 0.5-inch common interface length of the end plate and the container. Once the end plate is inserted, a fusion weld procedure is employed to weld the lip of the end plate to the wall of the container. The depth of the weld along the interface between the end plate and the container is equal to approximately 70% of the thickness of the end plate lip or the container lip.

Due to the location of the weld for the end plate, the weld does not transfer any load for the drop conditions. Additionally, since the heat loads are insignificant (13w) and the backfill for the FHU and the cask cavity are limited to atmospheric pressure, the pressure differential across the welded plates is insignificant. Each of these FHUs also has an additional smaller container, which holds the fuel. In these evaluations, the inner container is neglected.

The spacer assembly is 133.0 inches in length, excluding guide pins. The assembly is comprised of one spacer tube and five support plates. The spacer tube consists of a Type 304 stainless steel 8-inch Schedule 80S pipe. The tube has an outside diameter of 8.63 inches and a wall thickness of 0.50 inch. The spacer plates are 1.0-inch thick and are welded to the tube with 1/8-inch bevel welds. Two guide pins are located at the top of the spacer assembly to facilitate alignment with the top module.

2.6.12.9.1 General Atomics IFM Basket Interface Analysis

The structural evaluation of the top module assembly is performed using classical hand calculations. The weight of the top module is bounded by 200 lbs, and the maximum weight of one FHU and its fuel contents is 76 lbs. Therefore, the total weight of a loaded top module system is $200 + 2(76)$ or 352 lbs. The weight of the spacer assembly is 760 lbs. The total loaded system weight is 1,112 lbs, and this weight is bounded by the design basis contents weight for the LWT system. Therefore, no analysis of the LWT cask body is required.

2.6.12.9.2 General Atomics Top Module Structural Analysis

Structural analyses for the top module for the 1-foot end drop and 1-foot side drop are performed using classical hand calculations.

General Atomics 1-Foot Side Drop Analysis

Top Module:

During a 1-foot side drop, the distributed load on one fuel tube is:

$$W = \frac{\left(76 + 0.291 \times \frac{\pi(6.0^2 - 5.5^2)}{4} \times 43.7 \right)}{43.7} = 3.1 \text{ lb/in}$$

where:

weight of fuel = 76 lbs

length of tube = 43.7 inches

outer diameter = 6.0 inches

inner diameter = 5.5 inches

The maximum bending moment in tube is:

$$M = \frac{3.1 \times 20.35^2}{8} = 160 \text{ in-lbs}$$

The maximum bending stress in the fuel tube for 1g loading is:

$$I = \frac{\pi(6.0^4 - 5.5^4)}{64} = 18.7 \text{ in}^4$$
$$S_b = \frac{160 \times 3}{18.7} = 26 \text{ psi}$$

The margin of safety for tube bending for a 1-foot side drop (25g) is:

$$MS = \frac{1.5S_m}{S_b} - 1 = \frac{1.5 \times 19350}{25 \times 26} - 1 = + \text{Large}$$

During a 1-foot side drop, the support plates bear up against the inner shell of the LWT cask. The center plate will carry the maximum weight. The bearing load on the center plate is:

$$W = \frac{10 \times \frac{[(2 \times 76) + 200]}{40.7} \times 20.35}{8} = 220 \text{ lbs} \quad (\text{Page 2-299, \#12, Manual of Steel Construction})$$

The bearing stress is maximum for the center disk.

The bearing stress is (Item 2c, Table 33, Young):

LWT cask cavity diameter, $D_1 = 13.375$ inches

Support plate diameter, $D_2 = 13.265$ inches

$$K_D = \frac{D_1 D_2}{D_1 - D_2} = 1,613$$

$$C_E = \frac{1 - 0.31^2}{26.75e6} + \frac{1 - 0.31^2}{8.29e6} = 1.42e-7$$

$$S_c = 0.798 \sqrt{\frac{p}{K_D C_E}} = 0.798 \sqrt{\frac{220}{1613 \times 1.42e-7}} = 782 \text{ psi, 1g loading}$$

where:

$$p = 220 / (1.0) = 220 \text{ lbs/in}$$

$$E = 26.75e6 \text{ psi @ } 350^\circ\text{F}$$

Effective 'E' of LWT shells with lead:

$$E = \frac{0.75 \times 26.75e6 + 1.25 \times 26.75e6 + 5.75 \times 1.87e6}{7.75} = 8.29e6 \text{ psi}$$

The margin of safety for bearing for a 1-foot side drop (25g) is:

$$MS = \frac{S_y}{25 \times S_c} - 1 = \frac{21600}{25 \times 782} - 1 = +0.10$$

During a side drop, the top and bottom support plate welds are in shear. The load on the weld due to 1g is:

$$W = \frac{3 \times \frac{[(2 \times 76) + 200]}{40.7} \times 20.35}{8} = 66 \text{ lbs} \quad (\text{Page 2-299, \#12, Manual of Steel Construction})$$

The weld length is:

$$\begin{aligned} L &= 2(\pi d_{\text{tube}} - r_{\text{tube}} \theta) \\ &= 2(\pi \times 6.0 - 3.0 \times 1.57) = 28.3 \text{ inches} \\ \theta &= \text{non welded arc length} = 90 \text{ deg} = 1.57 \text{ radians} \end{aligned}$$

The support disk/ tube weld is a 1/8-inch bevel weld. The stress in the weld for 1g is:

$$S = \frac{66}{(28.3 \times 0.125 \times 0.7071)} = 26.4 \text{ psi, 1g loading}$$

For visual inspection, the weld factor is 0.25 per ASME Section III, Subsection NG-3352. The margin of safety for shear is:

$$MS = \frac{0.25 \times 0.6 S_m}{25S} - 1 = \frac{0.25 \times 0.6 \times 19350}{25 \times 26.4} - 1 = +3.4$$

Spacer Assembly:

During a 1-foot side drop, the distributed load on the tube is:

$$W = \frac{760}{129.5} = 5.9 \text{ lb/in, use 6.0 lb/in}$$

The maximum bending moment in tube, conservatively assuming a simply supported beam, is:

$$M = \frac{6 \times 32.0^2}{8} = 768 \text{ in - lbs}$$

The bending stress in tube for a 1g loading is:

$$\begin{aligned} I &= \frac{\pi(8.63^4 - 7.63^4)}{64} = 106 \text{ in}^4 \\ S_b &= \frac{768 \times (8.63/2)}{106} = 31 \text{ psi} \end{aligned}$$

The margin of safety for bending in the 1-foot side drop (25g) is:

$$MS = \frac{1.5 S_m}{S_b} - 1 = \frac{1.5 \times 19350}{25 \times 31} - 1 = + \text{Large}$$

During a 1-foot side drop, the support plates bear up against the inner shell of the LWT cask. The maximum load on a support plate during a side drop is:

$$W = 1.143 \times \frac{760}{128.0} \times 32.0 = 217 \text{ lbs} \quad (\text{Page 2-309, \#39, Manual of Steel Construction})$$

The bearing stress is (Item 2c, Table 33, Young):

$$\text{LWT cask cavity diameter} \quad D_1 = 13.375 \text{ inches}$$

$$\text{Support plate diameter} \quad D_2 = 13.265 \text{ inches}$$

$$K_D = \frac{D_1 D_2}{D_1 - D_2} = 1,613$$

$$C_E = \frac{1 - 0.31^2}{26.75e6} + \frac{1 - 0.31^2}{8.29e6} = 1.42e-7$$

$$S_c = 0.798 \sqrt{\frac{p}{K_D C_E}} = 0.798 \sqrt{\frac{217}{1613 \times 1.42e-7}} = 777 \text{ psi}$$

where:

$$p = 217 / 1.0 = 217 \text{ lb/in}$$

$$E = 26.75e6 \text{ psi @ } 350^\circ\text{F}$$

Effective 'E' of LWT shells with lead:

$$E = \frac{0.75 \times 26.75e6 + 1.25 \times 26.75e6 + 5.75 \times 1.87e6}{7.75} = 8.29e6 \text{ psi}$$

The margin of safety for bearing is:

$$MS = \frac{S_y}{25 \times S_c} = \frac{21600}{25 \times 777} - 1 = +0.11$$

During a side drop, the top and support plate weld is in shear. The load on the weld is:

$$W = 0.393 \times \frac{760}{128.0} \times 32.0 = 75 \text{ lbs} \quad (\text{Page 2-309, \#39, Manual of Steel Construction})$$

The weld length is:

$$L = \pi \times 8.63 = 27.1 \text{ inches}$$

The weld between the support disk and tube is a 1/8-inch bevel weld. The stress in the weld for 1g is:

$$S = \frac{75}{(27.1 \times 0.125 \times 0.7071)} = 31 \text{ psi, 1g loading}$$

For visual inspection, the weld factor is 0.25 per ASME Section III, Subsection NG-3352. The margin of safety for shear is:

$$MS = \frac{0.25 \times 0.6 S_m}{25S} - 1 = \frac{0.25 \times 0.6 \times 19350}{25 \times 31} - 1 = 2.7$$

Fuel Handling Units (FHU)

The FHUs are analyzed in accordance with ASME Section III, Subsection NG. The bounding weight of a loaded fuel container is 76 lbs.

The side drop is analyzed assuming a circular ring under an external compressive load using Roarks Table 17, Item 1 (Young). The stress in the container shell is:

$$\alpha = \frac{I}{AR^2} = \frac{\pi(2.125^3) \times (0.12)}{\pi(2.125^2 - 2.0^2) \times 2.125^2} = 0.49$$

$$k_2 = 1 - \alpha = 1 - 0.49 = 0.51$$

$$M = (0.5 - 0.3183k_2)WR = [0.5 - 0.3183(0.51)] \frac{76}{35.5} 2.125 = 1.5 \text{ in} \cdot \text{lb}$$

$$S = \frac{6(1.5)}{0.12^2} = 0.63 \text{ ksi}$$

The margin of safety is:

$$MS = \frac{1.5 S_m}{25S} - 1 = \frac{1.5 \times 19.35}{25 \times 0.63} - 1 = +0.84$$

General Atomics 1-Foot End Drop Analysis

Top Module:

During an end drop, the stress in the fuel tubes is calculated as follows.

The cross-sectional area of a tube is:

$$A = \frac{\pi(6.0^2 - 5.5^2)}{4} = 4.52 \text{ in}^2$$

Using a top module weight of 200 lbs, fuel weight not included, the stress in the two fuel tubes is:

$$S = \frac{200}{2 \times 4.52} = 22 \text{ psi}$$

The margin of safety is:

$$MS = \frac{S_m}{20S} - 1 = \frac{19350}{20 \times 22} - 1 = +\underline{\text{Large}}$$

Since the axial compression stress in the tubes is minimal, no buckling evaluation is required.

The top end drop is the bounding end drop because the top end has significantly less bearing area than the bottom end, and the weight of the spacer is included.

The bearing area for the top end is assumed to be the two fuel tubes, conservatively neglecting the lifting components. The cross-sectional area is:

$$A = 2 \left[\frac{\pi(6.0^2 - 5.5^2)}{4} - 3.22 \times 0.25 \right] = 7.42 \text{ in}^2$$

where:

outer diameter = 6.0 inches

inner diameter = 5.5 inches

cut out arc length = 3.22 inches

$$S = r\theta = 2.875 \times 1.12 = 3.22 \text{ inches}$$

$$\theta = 2 \times \tan^{-1} \left(\frac{1.72}{2.75} \right) = 64.05^\circ = 1.12 \text{ radians}$$

The bearing stress, fuel weight not included, in the module for a 1g loading is:

$$S_{\text{brg}} = \frac{200 + 760}{7.42} = 129 \text{ psi}$$

The margin of safety is:

$$S_{\text{brg}} = 20 \times 129 = 2.58 \text{ ksi}$$

$$MS = \frac{S_y}{S_{\text{brg}}} - 1 = \frac{21.6}{2.58} - 1 = +7.37$$

During an end drop, the self-weight of the center support plate has to be carried by the welds.

The weight of the center support plate is:

$$W = 0.291 \left\{ 1.0 \left[\frac{\pi \times 13.265^2}{4} - 2 \left(\frac{\pi \times 6.0^2}{4} \right) \right] \right\} = 24 \text{ lbs (use 30 lbs)}$$

where:

0.291 lbs/in³ is the density of 304 stainless steel

1.0 inch is the disk thickness

13.265 inches is the disk diameter

6.0 inches is the cutout diameter

The weld length is:

$$\begin{aligned} L &= 2(\pi d_{\text{tube}} - r_{\text{tube}} \theta) \\ &= 2(\pi \times 6.0 - 3.0 \times 1.57) = 28.3 \text{ in.} \\ \theta &= \text{nonwelded arc length} = 90 \text{ deg} = 1.57 \text{ radians} \end{aligned}$$

The welds are 1/8-inch bevel welds on both sides of the disk. The stress in the weld for 1g is:

$$S = \frac{30}{2(28.3 \times 0.125 \times 0.7071)} = 6.0 \text{ psi}$$

For visual inspection, the weld factor is 0.25 per ASME Section III, Subsection NG-3352. The margin of safety for normal conditions is:

$$MS = \frac{0.25 \times 0.6 S_m}{20S} - 1 = \frac{0.25 \times 0.6 \times 19350}{20 \times 6} - 1 = +\text{Large}$$

Spacer Assembly:

During an end drop, the stress in the tube is calculated as follows.

The cross-sectional area of a tube is:

$$A = \frac{\pi(8.63^2 - 7.63^2)}{4} = 12.77 \text{ in}^2$$

The stress in the tube is:

$$S = \frac{760 + 200 + 2 \times 76}{12.77} = 87 \text{ psi}$$

The margin of safety is:

$$MS = \frac{S_m}{20S} - 1 = \frac{19350}{20 \times 87} - 1 = +\text{Large}$$

Since the axial stress in the tube is minimal, no buckling evaluation is required.

For a top and bottom end drop, the bearing stresses for 1g are:

$$\begin{aligned} A_{\text{top}} &= 2(9.9 \times 0.3125) = 6.19 \text{ in}^2 \\ S_{\text{brg}} &= \frac{760}{6.19} = 123 \text{ psi} \\ A_{\text{bot}} &= \frac{\pi(8.63^2 - 7.63^2)}{4} - (4 \times 1.0 \times 0.5) = 10.77 \text{ in}^2 \end{aligned}$$

$$S_{\text{brg}} = \frac{760 + 200 + 2 \times 76}{10.77} = 103 \text{ psi}$$

The margin of safety is:

$$S_{\text{brg}} = 20 \times 123 = 2.46 \text{ ksi}$$

$$MS = \frac{S_y}{S_{\text{brg}}} - 1 = \frac{21.6}{2.46} - 1 = +7.78$$

During an end drop, the weight of a support plate has to be carried by the welds to the tube.

The weight of the support plate is:

$$W = 0.291 \left(\frac{\pi(13.265^2 - 8.63^2)}{4} \times 1.0 \right) \approx 25 \text{ lbs}$$

The weld length is:

$$L = \pi \times 8.63 = 27.1 \text{ inches}$$

$$S = \frac{25}{2(27.1 \times 0.125 \times 0.7071)} = 5.2 \text{ psi}$$

Since the weld stress is less than the weld stress in the support disks in the top module, no additional analysis is required.

Fuel Handling Unit:

The maximum bearing stress occurs in the top end drop orientation. The bearing area for the handle supports is:

$$A = 2 \times 0.5^2 = 0.5 \text{ in}^2$$

The bearing stress is:

$$S_{\text{brg}} = \frac{76}{0.5} = 152 \text{ psi}$$

$$S_{\text{brg}} = 20 \times 152 = 3.0 \text{ ksi}$$

The margin of safety is

$$MS = \frac{S_y}{S_{\text{brg}}} - 1 = \frac{21.6}{3.0} - 1 = +6.2$$

The top lid and bottom plates sit on a lip in the container shell. The cross-sectional area of the lip is:

$$A = \frac{\pi(4.124^2 - 4.0^2)}{4} = 0.79 \text{ in}^2$$

Since the area is greater than the handle support area above, no additional analysis is required.

The cross-sectional area of the tube is:

$$A = \frac{\pi(4.25^2 - 4.0^2)}{4} = 1.62 \text{ in}^2$$

For a 20g end drop, normal conditions, the stress in the tube is:

$$S = \frac{20 \times 76}{1.62} = 0.94 \text{ ksi}$$

$$MS = \frac{S_m}{S} - 1 = \frac{19.35}{0.94} - 1 = +\text{Large}$$

Since the axial compression stresses in the tube are minimal, no buckling evaluation is required.

2.6.12.10 TPBAR Basket Analysis

The TPBAR basket is a modified NAC-LWT PWR basket with increased free volume that is fabricated from 6061-T651 aluminum alloy. Figure 2.6.12-7 shows the cross-section of the TPBAR basket. A 13.25-inch outside diameter, 8.25-inch long stainless steel alternate upper fitting is bolted to the top of the basket body. This fitting provides lifting points for removing the basket from the cask. Additionally, this alternate upper fitting prevents the basket from applying load to the TPBAR contents during the top-end drop. A stainless steel lower fitting is bolted to the bottom of the basket body. The lower fitting assembly supports the fuel basket and contents longitudinally. An additional spacer assembly is bolted to the cask lid to prevent the TPBAR contents from shifting axially and rotationally within the basket. A groove on the periphery of the basket body provides for the cask drain tube. The drain tube is connected to a fitting on the cask body for draining or filling the cask during wet cask loading or unloading operations.

The TPBAR basket accommodates two TPBAR content configurations. The first TPBAR content configuration is the shipment of up to 300 production TPBARs (of which two can be prefailed) contained in an open consolidation canister with optional top insert. The consolidation canister body is fabricated from Type 304 stainless steel and the bail is fabricated from Type 7-4 precipitation hardened stainless steel. The consolidation canister is used to load and unload the TPBARs into and from the NAC-LWT cask configured with a TPBAR basket assembly.

The second TPBAR content configuration is the shipment of up to 55 segmented TPBARs, following post-irradiation examinations (PIE), contained in a welded sealed waste container. The waste container is welded to an extension weldment to provide the identical length as the consolidation canister to assure fit-up in the TPBAR basket assembly. The waste container and extension are fabricated from Type 316L stainless steel.

Following placement of the consolidation canister or the waste container with extension in the TPBAR basket, and installation and bolting of the lid, the TPBAR basket and contents are evaluated without consideration of the strength of the consolidation canister or waste container. The TPBAR basket provides a boundary for support on all sides of the consolidation canister and TPBARs for the full length of the canister. The cylindrical TPBAR waste container (external diameter 8.6 inches) is sized to fit within the square cross-section (8.8 inches) of the TPBAR basket. The TPBAR upper end-fitting spacer guides do not permit the consolidation canister to be loaded by the TPBAR basket in any drop orientation. The TPBAR spacer assembly attached to the bottom of the cask lid restricts the movement of the TPBARs in the axial direction and prevents rotation of the TPBAR waste container. Therefore, no additional evaluations are required for the TPBAR consolidation canister or TPBAR waste container and extension weldment.

2.6.12.10.1 TPBAR Basket Body

Structural analyses of the TPBAR basket for 1-foot side and end drops are performed using classical hand calculations. The analyzed weight of the loaded TPBAR consolidation canister is 1,000 lbs, which bounds the loaded weight of the TPBAR waste container and extension of 700 lbs. Therefore, the analyses provided for the consolidation canister are bounding.

TPBAR Basket Body 1-Foot Side Drop Analysis

The TPBAR basket body is constructed of four machined segments held together with aluminum bands at five locations along the axial length of the basket; as well as the top and bottom fittings, which are bolted to the aluminum basket. During a side drop, the TPBAR basket is subjected to bending and bearing stresses. The maximum bending stress occurs at Location 'A' as shown in the following sketch and is due to the content weight. The maximum bending stress is calculated using a cantilevered beam. This is conservative, since it neglects any support of the load due to the edges of the basket being supported by the cask inner shell. The maximum bending stress is:

$$S_b = \frac{6M}{t^2} = \frac{6 \times 152}{0.5^2} = 3.6 \text{ ksi}$$

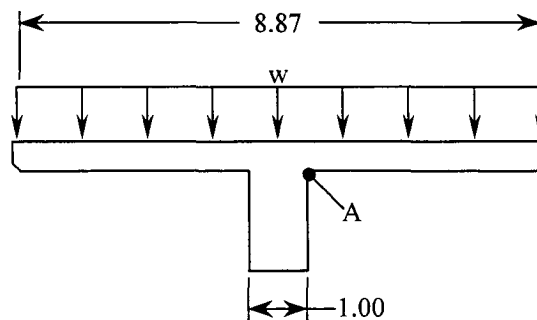
where:

$$w = \frac{W_c \times g}{L \times b} = \frac{1000 \times 25}{144 \times 8.87} = 19.6 \text{ psi}$$

(distributed load of the TPBAR consolidation canister)

$W_c = 1,000$ lbs, bounding TPBAR canister weight (with TPBARs)

$L = 144$ inches, length of consolidation canister



b = 8.87 inches, TPBAR basket opening width

g = 25g, bounding side drop acceleration

$$M = w \times \left(\frac{b}{2} - \frac{1}{2} \right) \times \frac{1}{2} \left(\frac{b}{2} - \frac{1}{2} \right)$$
$$= 19.6 \times \left(\frac{8.87}{2} - \frac{1}{2} \right) \times \frac{1}{2} \left(\frac{8.87}{2} - \frac{1}{2} \right) = 152 \text{ in-lb/in, the maximum bending moment}$$

t = 0.5 in, thickness of the flange

The margin of safety is:

$$MS = \frac{1.5S_m}{S_b} - 1 = \frac{1.5 \times 8.4}{3.6} - 1 = +2.5$$

where:

$S_m = 8.4$ ksi, stress intensity of 6061-T651 aluminum @300°F

The bearing stress in the basket is:

$$S_{\text{brg}} = \frac{P}{A} = \frac{47,500}{1.00 \times 161.5} = 294 \text{ psi} \approx 0.3 \text{ ksi}$$

where:

$P = g \times (W_c + W_b) = 25 \times (1,000 \text{ lbs} + 900 \text{ lbs}) = 47,500 \text{ lbs}$, total side drop load

$W_b = 900 \text{ lbs}$, the bounding weight of the TPBAR basket

$A =$ is the minimum bearing area of the basket

The margin of safety is:

$$MS = \frac{S_y}{S_{\text{brg}}} = \frac{26.9}{0.3} - 1 = +\text{Large}$$

where:

$S_y = 26.9$ ksi, yield strength of 6061-T651 aluminum @300°F

TPBAR Basket 1-Foot End-Drop Analysis

During an end drop, the maximum compressive stress on the minimum cross-section of the basket body is:

$$S_{\text{comp}} = \frac{g \times W_b}{A} = \frac{20 \times 900}{32.26} = 558 \text{ psi} \approx 0.6 \text{ ksi}$$

where:

$$A = 9.87^2 - 8.87^2 + 4(1.00 \times (13.25 - 9.87)) = 32.26 \text{ in}^2, \text{ the minimum cross-sectional area of the basket (see Figure 2.6.12-7)}$$

$$g = 20g, \text{ bounding end drop acceleration}$$

$$W_b = 900 \text{ lbs, bounding weight of the TPBAR basket}$$

The margin of safety is:

$$MS = \frac{S_y}{S_{\text{comp}}} - 1 = \frac{26.9}{0.6} - 1 = +\text{Large}$$

where:

$$S_y = 26.9 \text{ ksi, yield strength of 6061-T651 aluminum @300°F}$$

2.6.12.10.2 TPBAR Basket Upper Fitting

The upper fitting prevents the basket from loading the consolidation canister and TPBARs during a top-end drop. Four (4) spacer guides of the upper fitting are provided for this purpose. The spacer guides have a length of 7.63 inches, a width of 2.0 inches, and a thickness of 1.00 inch with a 45° × 0.25-inch chamfer. A bounding weight of 900 lbs is used for the TPBAR basket analysis. The temperature of the lid and upper region of the NAC-LWT cask body during TPBAR shipment is conservatively assumed to be 300°F. From Chapter 3, a temperature of 300°F bounds the maximum temperature of the upper LWT region for a maximum heat load of 1.05 kW. Since the maximum heat load for the TPBAR shipment is less than 1.0 kW, using 300°F for the analysis of the TPBAR upper fitting is conservative.

TPBAR Basket Upper Fitting 1-Foot Side Drop

During a side drop, the welds that hold the spacer guides to the top fitting are in shear and bending. The shear load on the welds is:

$$P = (b \times t \times L) \times \rho \times g = (2.0 \times 1.0 \times 7.63) \times 0.288 \times 25 = 110 \text{ lbs}$$

where:

$$b = 2.0 \text{ inches, spacer guide width}$$

$$t = 1.0 \text{ in, spacer guide thickness}$$

$$L = 7.63 \text{ inches, spacer guide length}$$

$$\rho = 0.288 \text{ lb/in}^3, \text{ density of Type 304 stainless steel}$$

$$g = 25g, \text{ side drop acceleration}$$

The welds for the spacer are 1/8-inch fillet welds on three sides. The shear stress in the welds is:

$$\tau = \frac{P}{A} = \frac{110}{0.354} = 311 \text{ psi} = 0.3 \text{ ksi}$$

where:

$$A = 0.125 \times 0.707 \times (2.0 + 2 \times 1.0) = 0.354 \text{ in}^2, \text{ weld area}$$

The bending moment is:

$$M = \frac{wL^2}{2} = \frac{(b \times t \times \rho \times g) \times L^2}{2} = \frac{(2 \times 1 \times 0.288 \times 25) \times 7.63^2}{2} = 419 \text{ in-lb}$$

The stress in the weld due to bending is:

$$S = \frac{M}{t \times S_w} = \frac{419}{(0.125 \times 0.707) \times 0.56} = 8.5 \text{ ksi}$$

where:

$$S_w = \frac{d^2(2b + d^2)}{3(b + d)} = \frac{1^2(2 \times 2 + 1^2)}{3(2 + 1)} = 0.56 \text{ in}^2, \text{ section modulus of weld (Blodgett)}$$

The maximum shear stress, τ_{\max} , in the weld which, is equivalent to the stress intensity divided by two is:

$$\tau_{\max} = \frac{\sqrt{S^2 + 4\tau^2}}{2} = \frac{\sqrt{8.5^2 + 4 \times 0.3^2}}{2} = 4.26 \text{ ksi}$$

The margin of safety is:

$$MS = \frac{0.6S_y}{\tau_{\max}} - 1 = \frac{0.6 \times 22.5}{4.26} - 1 = +2.17$$

where:

$$S_y = 22.5 \text{ ksi, yield strength of Type 304 stainless steel @300°F}$$

TPBAR Basket Upper Fitting 1-Foot Top-End Drop

For a top-end drop the weight of the TPBAR basket will load the four spacer guides. The membrane stress in the spacer guide is:

$$S = \frac{W_b \times g}{A} = \frac{900 \times 20}{(2.0 \times 1.0) \times 4} = 2.3 \text{ ksi}$$

where:

$$W_b = 900 \text{ lbs, bounding TPBAR basket weight}$$

$$A = (2.0 \times 1.0) \times 4 = 8 \text{ in}^2, \text{ cross sectional area of the spacer guide}$$

$$g = 20g, \text{ bounding end drop acceleration}$$

The margin of safety is:

$$MS = \frac{S_y}{S} - 1 = \frac{22.5}{2.3} - 1 = +8.8$$

where:

$$S_y = 22.5 \text{ ksi, yield strength of Type 304 stainless steel @300°F}$$

The bearing stress is:

$$S = \frac{W_b \times g}{A} = \frac{900 \times 20}{6} = 3.0 \text{ ksi}$$

where:

$$A = (2.0 \times 0.75) \times 4 = 6 \text{ in}^2, \text{ bearing area of the spacer guide}$$

The margin of safety is:

$$MS = \frac{S_y}{S} - 1 = \frac{22.5}{3.0} - 1 = +6.5$$

The critical buckling load for the spacer is determined by using Euler's buckling equation. The critical buckling load is:

$$W_{cr} = K_c \frac{EI}{L^2} = 2.47 \frac{27 \times 10^6 (0.1667)}{7.63^2} \approx 190.9 \text{ kip}$$

where:

$$E = 27 \times 10^6 \text{ psi, modulus of elasticity of Type 304 stainless steel @ 300°F}$$

$$K_c = 2.47, \text{ buckling constant (Blake, Table 10.3)}$$

$$I = \frac{bt^3}{12} = 0.1667 \text{ in}^4, \text{ minimum moment of inertia for cross section}$$

$$b = 2.0 \text{ inches, spacer guide width}$$

$$t = 1.0 \text{ in, spacer guide thickness}$$

$$L = 7.63 \text{ inches, length of spacer guide}$$

The margin of safety against buckling of the four spacer guides is:

$$MS = \frac{190,900}{20 \times 900/4} - 1 = + \underline{\text{Large}}$$

2.6.12.10.3 TPBAR Basket Lower Fitting

The TPBAR basket lower fitting is identical to the lower fitting of the PWR basket. The weight of the loaded TPBAR basket is less than the weight of the loaded PWR basket. Therefore, no further analysis is required.

2.6.12.10.4 TPBAR Spacer

The TPBAR Spacer is designed to limit the movement of the TPBAR contents during transport and to prevent the consolidation canister from loading the TPBARs during a top-end drop. The spacer is constructed of a circular base plate, two triangular spacer bases, two tubes, and two triangular top plates. The circular base plate forms the attachment of the spacer to the lower surface of the NAC-LWT cask closure lid. The circular base plate is attached with Type 304 stainless steel bolts. The two triangular spacer bases are bolted to the circular base plate. The tubes, constructed of 3-inch schedule 80 pipes, are welded to the spacer base and the triangular top plates that provide the interface with the TPBAR contents. The triangular top plates are arranged to form a square with a gap that fits over the consolidation canister or waste container bail and above the consolidation canister contents or the welded top of the waste container. Figure 2.6.12-8 shows the top view of the triangular top plate and tube. The calculated weight of the spacer assembly is 115 lbs. The analyzed loaded weight of the consolidation canister is 1,000 lbs, which bounds the loaded weight of the waste container (700 lbs). During the top-end drop condition, the weight of the consolidation canister is supported by the bail and directly transmitted into the NAC-LWT cask lid. Therefore, only the weight of the TPBARs is supported by the spacer for top-end drop conditions. The temperature of the lid and upper region of the NAC-LWT cask body during TPBAR transport is conservatively assumed to be 300°F. From Chapter 3, a temperature of 300°F bounds the maximum temperature of the upper LWT region for a maximum heat load of 1.05 kW. Since the maximum heat load for the transport of the TPBAR consolidation canister shipment is less than 0.7 kW, using 300°F for the analysis of the TPBAR spacer is conservative. The heat load of the TPBAR waste container is 0.127 kW and, therefore, the evaluated temperatures for the consolidation canister are bounding.

TPBAR Spacer 1-Foot Side Drop

Bolts

During 1-foot side-drop conditions, the weight of the spacer applies a shearing and tensile load to the bolts. The tensile load is due to the moment generated by the cantilever action of the spacer.

The shear stress is:

$$\tau = \frac{P}{A_t} = \frac{719}{0.1419} = 5.1 \text{ ksi}$$

where:

$$P = \frac{W \times g}{4} = \frac{115 \times 25}{4} = 719 \text{ lbs}$$

W = 115 lb, spacer assembly weight abbreviations

g = 25g, side-drop acceleration

$$A_t = 0.7854 \left(D - \frac{0.9743}{n} \right)^2 = 0.7854 \left(0.5 - \frac{0.9743}{13} \right)^2 = 0.1419 \text{ in}^2, \text{ tensile area of screw thread with ultimate strength up to 100 ksi}$$

For 1/2-13UNC bolts (Machinery's Handbook)

n = 13, number of threads per inch

D = 0.50 in, bolt diameter

Kn_{\max} = 0.434 in, maximum minor diameter of internal thread

ES_{\min} = 0.4435 in, minimum major diameter of external thread

En_{\max} = 0.4565 in, maximum pitch diameter of internal thread

DS_{\min} = 0.4876 in, minimum major diameter of external thread

L_e = 1.0 in, Thread engagement

$$P = \frac{M}{d} = \frac{16,891}{2 \times 4.95} = 1,706 \text{ lbs, the tensile load}$$

d = 9.9 in, maximum distance between bolts

$$M = \frac{wL^2}{2} \times g = \frac{\left(\frac{115}{11.75} \right) (11.75^2)}{2} \times 25 = 16,891 \text{ in} \cdot \text{lb}, \text{ the prying moment generated by the cantilever action of the spacer}$$

The bolt tensile stress due to the moment, M, is:

$$S = \frac{P}{A_t} = \frac{1706}{0.1419} = 12.0 \text{ ksi}$$

The membrane stress intensity on the fastener is:

$$SI = \sqrt{S^2 + 4\tau^2} = \sqrt{12.0^2 + 4 \times 5.1^2} = 15.7 \text{ ksi}$$

The margin of safety is:

$$MS = \frac{S_y}{SI} - 1 = \frac{22.5}{15.7} - 1 = +0.43$$

where:

$$S_y = 22.5 \text{ ksi, yield strength of Type 304 stainless steel @300°F}$$

The shear stress on the external threads is:

$$\tau = \frac{P}{A_s} = \frac{1706}{0.7789} = 2.2 \text{ ksi}$$

where:

$$\begin{aligned} A_s &= 3.1416nL_e K_{n_{max}} \left[\frac{1}{2n} + 0.57735(Es_{min} - Kn_{max}) \right] \\ &= 3.1416(13)(1.00)(0.434) \left[\frac{1}{2(13)} + 0.57735(0.4435 - 0.434) \right] \\ &= 0.7789 \text{ in}^2, \text{ shear area of the bolt threads} \end{aligned}$$

The margin of safety is:

$$MS = \frac{0.6S_y}{\tau} - 1 = \frac{0.6 \times 22.5}{2.2} - 1 = +6.14$$

Spacer Welds

Using a bounding weight (W) of 25 pounds for the tube and triangular plates, the shear load on the welds is:

$$P = W \times g = 25 \times 25 = 625 \text{ lbs}$$

where:

$$g = 25 \text{ g, side-drop acceleration}$$

The welds for the spacer are ¼-inch fillet weld. The shear stress in the weld is:

$$\tau = \frac{P}{t_w 0.707 \pi d} = \frac{625}{0.25 \times 0.707 \times (\pi \times 3.5)} = 322 \text{ psi}$$

where:

$$t_w = 0.25 \text{ in, weld size}$$

$$d = 3.5 \text{ inches, outside diameter of 3-inch schedule-80 pipe}$$

The stress in the weld due to bending is:

$$S = \frac{M}{t \times S_w} = \frac{5,263}{(0.25 \times 0.707) 9.62} = 3.1 \text{ ksi}$$

where:

$$M = wL = 25 \times 25 \times 8.42 = 5,263 \text{ in} \cdot \text{lb}, \text{ the bending moment}$$

$$S_w = \frac{\pi d^2}{4} = \frac{\pi \times 3.5^2}{4} = 9.62 \text{ in}^2, \text{ section modulus of the weld (Blodgett)}$$

The maximum shear stress (τ_{\max}) in the weld, which is equivalent to the stress intensity divided by two, is:

$$\tau_{\max} = \frac{\sqrt{S^2 + 4\tau^2}}{2} = \frac{\sqrt{3.1^2 + 4 \times 0.3^2}}{2} = 1.6 \text{ ksi}$$

The margin of safety is:

$$MS = \frac{0.6S_y}{\tau_{\max}} - 1 = \frac{0.6 \times 22.5}{1.6} - 1 = +7.4$$

where:

$$S_y = 22.5 \text{ ksi}, \text{ yield strength of Type 304 stainless steel @300}^\circ\text{F}$$

TPBAR Spacer 1-Foot Top-End Drop

When loaded in the consolidation canister, the TPBARs (held in the shape of a square) load the spacer tubes via the triangular top plates during top-end drop conditions. The compressive load applied to the tubes during the top-end drop is the weight of the TPBARs, 795 lbs (300 TPBARs at a bounding weight of 2.65 lbs per TPBAR), times the bounding acceleration of 20g (actual 15.8 g). For this analysis, $W=1,000$ lbs, is conservatively used.

Tube

The compressive stress in the tubes is:

$$S = \frac{W \times g}{A} = \frac{1000 \times 20}{2 \times \left(\frac{\pi}{4} (3.5^2 - 2.9^2) \right)} = 3.3 \text{ ksi}$$

where:

$$A = \text{the cross sectional area of a 3-inch schedule-80 pipe with an outer diameter of 3.5 inches and a thickness of 0.3 inch}$$

The margin of safety is:

$$MS = \frac{S_y}{S} - 1 = \frac{22.5}{3.3} - 1 = +5.8$$

where:

$$S_y = 22.5 \text{ ksi, yield strength of Type 304 stainless steel @300°F}$$

Triangular Top Plate

Referring to the dimensions provided in Figure 2.6.12-8, the pressure applied to a triangular plate is

$$P_{TP} = \frac{1}{2} \times \frac{1000}{0.5 \times 7.43 \times 7.43} \times 20 = 362 \text{ psi}$$

The bending moment in the top plate is (see Line A in Figure 2.6.12-6)

$$M = 362 \times (0.5 \times 4.18^2) \times \left(\frac{1}{3} \times 4.18 \right) = 4406 \text{ in-lb}$$

The bending stress in the plate is:

$$S = \frac{6M}{bt^2} = \frac{6 \times 4,406}{4.18 \times 0.75^2} = 11.2 \text{ ksi}$$

The margin of safety is:

$$MS = \frac{1.5S_m}{S} - 1 = \frac{1.5 \times 20.0}{11.2} - 1 = +1.68$$

where:

$$S_m = 20.0 \text{ ksi, stress intensity of Type 304 stainless steel @300°F}$$

TPBAR Spacer 1-Foot Bottom-End Drop

During the one-foot bottom-end drop, the inertial load of the spacer is applied to the bolts that affix the spacer to the NAC-LWT cask lid and the welds used to fabricate the spacer assembly. The maximum bottom-end drop acceleration is 20g.

Bolts

Four bolts (½-13UNC, Type 304 stainless steel) hold the spacer assembly to the bottom of the NAC-LWT cask lid and six bolts hold the spacer base to the circular base plate. For this evaluation, only the four spacer assembly bolts are considered since the individual bolt load is higher and the thread engagement length is shorter. The Internal lid thread evaluation is not required since high strength Helicoil inserts are utilized. Using the spacer assembly weight of 115 lbs and an acceleration of 20g, the critical bolt load is:

$$P = \frac{115 \times 20}{4} = 575 \text{ lbs}$$

The tensile stress is:

$$S = \frac{P}{A_t} = \frac{575}{0.1419} = 4.1 \text{ ksi}$$

The margin of safety is:

$$MS = \frac{S_y}{S} - 1 = \frac{22.5}{4.1} - 1 = +4.49$$

where:

$$S_y = 22.5 \text{ ksi, yield strength of Type 304 stainless steel @300°F}$$

The shear stress in the bolt thread is:

$$\tau = \frac{P}{A_s} = \frac{575}{0.7789} = 0.74 \text{ ksi}$$

The margin of safety is:

$$MS = \frac{0.6S_y}{\tau} - 1 = \frac{0.6(22.5)}{0.74} - 1 = + \text{Large}$$

Spacer Welds

During a 1-foot bottom-end drop (20g), the spacer weld is loaded by the inertial load of the spacer tube and the triangular top plate (25 lbs bounding). The weld is a ¼-inch fillet weld. The weld stress is:

$$S_w = \frac{W \times g}{t(0.707)(\pi d)} = \frac{25 \times 20}{0.25 \times 0.707 \times (\pi \times 3.5)} = 257 \text{ psi} = 0.3 \text{ ksi}$$

where:

$$d = 3.5 \text{ in, outside diameter of 3-inch schedule 80 pipe}$$

$$t = 0.25 \text{ in, weld size}$$

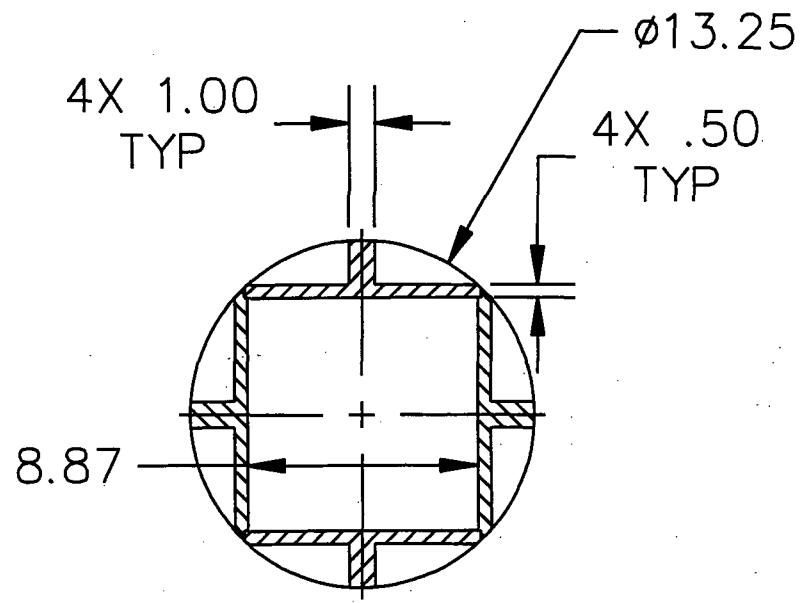
The margin of safety is:

$$MS = \frac{0.6S_y}{S_w} - 1 = \frac{0.6(22.5)}{0.3} - 1 = + \text{Large}$$

where:

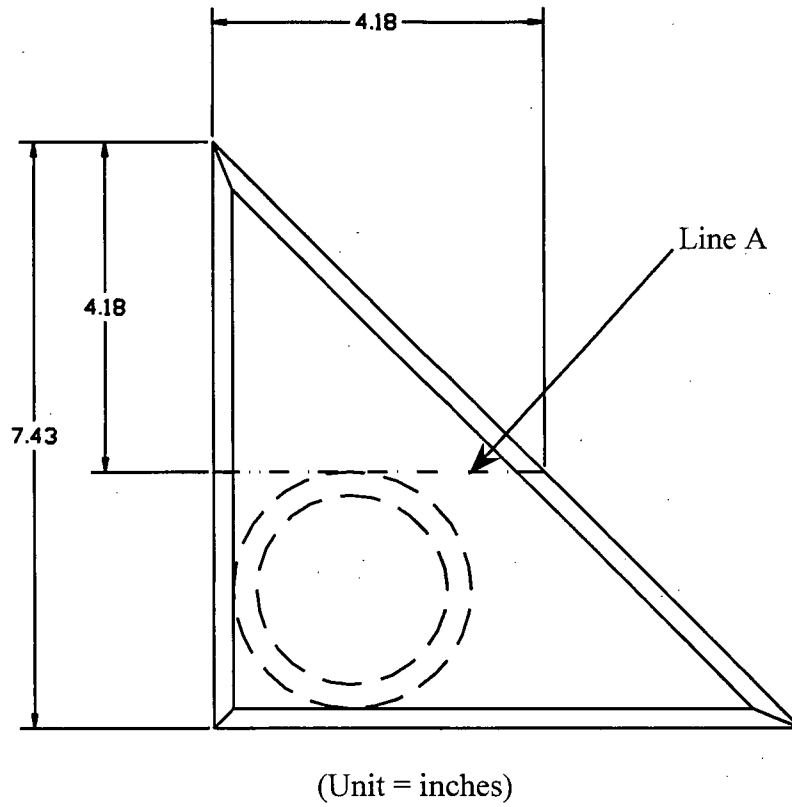
$$S_y = 22.5 \text{ ksi, yield strength of Type 304 stainless steel @300°F}$$

Figure 2.6.12-7 Cross-Section of TPBAR Basket



(Unit = inches)

Figure 2.6.12-8 TPBAR Spacer Schematic Triangular Top Plate and Tube



2.6.12.11 ANSTO Basket Analysis

The ANSTO modular basket assembly consists of a top module, four intermediate modules, and a base module. The top and base modules are each 29.8 inches long; each of the four intermediate modules is 29.3 inches long (not including guide pins); and all six modules have an outer diameter of 13.27 inches. Each module is capable of holding up to seven spiral fuel assemblies or MOATA plate bundles. Each module is a weldment made up of a 13.27-inch-diameter, 1/2-inch-thick base plate and six 13.27-inch-diameter, 1/2-inch-thick support plates scalloped on the inner diameter to fit around six peripheral fuel tubes. The weldment structure, fuel tubes, and base and support plates are fabricated from Type 304 stainless steel. Each of the seven fuel tubes in each module has an outer diameter of 4.375 inches and a wall thickness of 0.125 inch. The bottom of each fuel tube is welded to the 1/2-inch-thick base plate. At the bottom of each fuel tube, where it is welded to the base plate, there is a 0.3-inch slot to permit water to drain from the tube. The base plate supports the fuel assembly/bundle in the end drop orientation. The base module sits on a 0.5-inch-high, 10-inch-diameter ring that is welded in segments to the base plate. The total weight of the ANSTO basket assembly bears directly on the bottom forging of the cask through the ring. The six scalloped 1/2-inch-thick support plates and the base plate of each basket module provide lateral support and maintain the fuel configuration in the side drop orientation.

2.6.12.11.1 ANSTO Basket Body 1-Foot Side Drop Analysis

Structural analyses of the ANSTO basket for 1-foot side and end drops are performed using classical hand calculations.

The inertia load of the LWT cask for a 1-foot side drop is 25g. A conservative loading condition of a diametrically loaded ring (Table 17, Case 1, Roark) is considered, which neglects any load distribution. Also, it is conservative to assume that there are three loaded fuel tubes acting on the top of a fuel tube since, in reality, there are only two of them. The stresses in the circumferential direction and in the longitudinal direction are added without regard to their signs. Since the circumferential direction and the longitudinal direction also correspond to the direction of the principal stresses, the addition of the two magnitudes reflects the possibility of the principal stresses being of opposite signs.

The maximum applied load to a fuel tube for the circumferential bending stress is:

$$P_s = (3W_{FT} + 3W) \times 25 = 2,415 \text{ lbs}$$

where:

$$W_{FT} = 14.2 \text{ lbs, maximum fuel tube weight}$$

$$W = 18.0 \text{ lbs, maximum average fuel assembly weight}$$

The bending moment in the fuel tube is:

$$M = \frac{wRk_2}{\pi} = \frac{84 \times 2.13 \times 1.00}{\pi} = 57 \text{ in-lb/in} \quad (\text{Table 17, Case 1, Roark})$$

where:

$$w = \frac{P_s}{L_t} = 84 \text{ lb/in}$$

$$L_t = 28.81 \text{ inches, shortest fuel tube length}$$

$$R = 2.13 \text{ inches, mean radius of fuel tube}$$

$$k_2 = 1 - \alpha = 1.00$$

$$\alpha = \frac{I}{A \times R^2} = \frac{bt^3 / 12}{b \times t \times R^2} = 2.87 \times 10^{-4}$$

$$b = 1.0 \text{ in, unit length}$$

$$t = 0.125 \text{ in, tube wall thickness}$$

The circumferential bending stress in the fuel tube is:

$$\sigma_c = \frac{6M}{bt^2} = \frac{6 \times 57}{1 \times 0.125^2} = 21.9 \text{ ksi}$$

The stress in the fuel tube in the longitudinal direction is calculated assuming the fuel tube acts like a beam. The maximum bending moment occurs at the top of the basket where the fuel tube acts like a cantilever beam. (The maximum moment for a cantilevered beam with a uniform loading of w (lb/in) and length (l) is $wl^2/2$, as compared to the maximum moment $wl^2/8$ for a simply supported beam.) The bending moment in the tube is:

$$M = \frac{wl^2}{2} = \frac{84 \times 4.0^2}{2} = 672 \text{ in-lb}$$

where:

$$l = 4.0 \text{ inches, the length of the tube extending beyond the support plates}$$

The bending stress is:

$$\sigma_l = F \frac{Mc}{I} = \frac{672 \times 2.19}{3.77} \approx 1.1 \text{ ksi}$$

where:

$c = 2.19$ inches, distance to extreme outer fiber of tube from centroid of tube

$I = 3.77 \text{ in}^4$, tube moment of inertia

$F = 2.725$, factor to account for the effect of the small diameter-to-length ratio on bending for a cantilevered tube. This is obtained for a uniformly loaded beam in Article 7.10 in Roark.

The maximum stress in the tube is:

$$\sigma_b = 21.9 + 1.1 = 23.0 \text{ ksi}$$

The margin of safety is:

$$MS = \frac{1.5S_m}{\sigma_b} - 1 = +0.26$$

where:

$S_m = 19.4$ ksi, design stress intensity, Type 304 stainless steel, 350°F

The bearing stress on the support plate is calculated using Table 33, Case 2c from Roark.

The maximum weight of a loaded module is the weight of the base module, $W_{BM} = 280$ lbs. The weight of the loaded basket is supported by the six support plates and the base plate (i.e., total of seven). The bearing stress on a support plate is:

$$\sigma_{brg} = 0.591 \sqrt{\frac{pE}{K_D}} = 3.6 \text{ ksi}$$

where:

$$p = \frac{W}{7t_d} g = \frac{280}{7 \times 0.5} \times 25 = 2,000 \text{ lb/in, bearing load for 25g side drop}$$

$t_d = 0.5$ in, support disk thickness

$g = 25g$, side drop inertia load

$$K_D = \frac{D_1 D_2}{D_1 - D_2} = 1,366.81$$

$D_1 = 13.395$ inches, LWT cask inner diameter

$D_2 = 13.265$ inches, support disk diameter

$E = 25.7 \times 10^6$ psi, modulus of elasticity, Type 304 stainless steel, 350°F

The margin of safety is:

$$MS = \frac{S_y}{\sigma_{brg}} - 1 = +5.06$$

where:

$S_y = 21.8$ ksi, yield strength, Type 304 stainless steel, 350°F

2.6.12.11.2 ANSTO 1-Foot End Drop Evaluation

The inertia load for the LWT for a 1-foot end drop is 20g. The applied load to the ANSTO basket is:

$$P = W_{total} \times 20 = 35,400 \text{ lbs}$$

where:

$W_{total} = 1,770$ lbs, total weight of loaded basket, which bounds the calculated weight of 1,667 lbs

The minimum cross-sectional area is at the base of the fuel tubes where the cutouts for water drainage are located. The cross-sectional area is:

$$A = \frac{\left[\frac{\pi}{4} (D_o^2 - D_i^2) \times 6 \right]}{2} + \left[\frac{\pi}{4} (D_o^2 - D_i^2) - 6 \times l_c \times t_t \right] = 5.93 \text{ in}^2$$

where:

$D_o = 4.375$ inches, tube outer diameter

$D_i = 4.125$ inches, tube inner diameter

$l_c = 1.00$ in, cutout length in center tube

$t_t = 0.125$ in, tube wall thickness

The membrane stress in the basket is:

$$\sigma = \frac{P}{A} = \frac{35,400}{5.93} = 5.97 \text{ ksi}$$

The margin of safety is:

$$MS = \frac{S_m}{\sigma} - 1 = +2.2$$

where:

$$S_m = 19.4 \text{ ksi, design stress intensity, Type 304 stainless steel, } 350^\circ\text{F}$$

The support plates are welded to the fuel tube with 1/16-inch bevel welds on both sides of the plate. The area of the weld is:

$$A_w = \frac{6(\pi D_o)}{2} \times 2t_w = 5.15 \text{ in}^2$$

where:

$$D_o = 4.375 \text{ inches, outer diameter of tube}$$

$$t_w = 1/16 \text{ in, weld thickness}$$

The bounding weight of the support plates is 20.1 lbs; and the bounding g-load factor is 60. A weld quality factor of 0.25 for a surface visual examination is divided into the calculated stress. This factor corresponds to the largest stress reduction factor in Table NG-3352-1 of the ASME Code. Therefore, the stress in the weld is:

$$\sigma_w = \frac{20.1 \times 60}{A_w (0.25)} = 936 \text{ psi}$$

The margin of safety using normal conditions allowable is:

$$MS = \frac{0.6S_m}{\sigma_w} - 1 = +\underline{\text{Large}}$$

where:

$$S_m = 19.4 \text{ ksi, design stress intensity, Type 304 stainless steel, } 350^\circ\text{F}$$

2.6.12.11.3 ANSTO Thermal Stress Evaluation

Thermal stress caused by a temperature gradient in the basket is calculated in this section. The thermal stress is minimal since the basket is free to expand. The thermal stress occurs as the hotter tubes expand radially against the basket support plates, which are at a lower temperature.

The maximum thermal stress of the fuel tube is back-calculated from the displacement computed using equations for circular rings from Table 17, Case 1, Roark.

The diametrical displacements caused by the thermal expansions for the center tube (Δ_1) and the tube adjacent to it (Δ_2) are calculated as:

$$\Delta_1 = \alpha \times \Delta T \times R_t = 4.58 \times 10^{-3} \text{ in}$$

where:

$\alpha = 9.1 \times 10^{-6} / ^\circ\text{F}$, coefficient of thermal expansion, Type 304 stainless steel, 350°F

$\Delta T = 230^\circ\text{F}$ (300-70), T_{max} of the basket is conservatively considered to be 300°F

70°F is room temperature

$R_t = 2.19$ inches (4.375/2), radius of the fuel tube outer surface

$$\Delta_2 = \alpha \times \Delta T \times D_t = 9.17 \times 10^{-3} \text{ in}$$

where,

$\alpha = 9.1 \times 10^{-6} / ^\circ\text{F}$, coefficient of thermal expansion, Type 304 stainless steel, 350°F

$\Delta T = 230^\circ\text{F}$ (300-70), T_{max} of the basket is conservatively considered to be 300°F

70°F is room temperature

$D_t = 4.375$, diameter of the fuel tube

The displacement caused by the thermal expansions for the outer surface of the support plate (Δ_s) is calculated as:

$$\Delta_s = \alpha \times \Delta T \times R_s = 8.58 \times 10^{-3} \text{ in}$$

where,

$\alpha = 9.1 \times 10^{-6} / ^\circ\text{F}$, coefficient of thermal expansion, Type 304 stainless steel, 350°F

$\Delta T = 144^\circ\text{F}$ (214-70), T_{max} of the inner shell

70°F is room temperature

$R_s = 6.55$ inches (13.1/2), radius of the support plate

Note: 214°F is conservatively used to result in a minimum Δ_s in order to maximize the thermal stress.

The deformation that results in thermal stress is -5.17×10^{-3} inch ($\Delta_S - \Delta_1 - \Delta_2$). Therefore, the fuel tube will experience a reduction in diameter due to the differential thermal expansion of the fuel tubes and support plates. It is conservative to assume that all deformation occurs at the center tube. Using Case 1 in Table 17 of Roark, the change in the diameter of the circular ring, D_V , and the moment, M_A , are given by:

$$D_V = 0.1488 \times \frac{WR^3}{EI} \quad \text{and} \quad M_A = \frac{WR \times k_2}{\pi}$$

therefore:

$$M_A = \frac{D_V \times EI}{0.1488 \times R^2} \times \frac{k_2}{\pi}$$

where:

W is the load due to differential thermal expansion

$D_V = 5.17 \times 10^{-3}$ inch, change in the diameter due to thermal stress

R = 2.13 inches, mean radius of fuel tube

E = 25.7×10^6 psi, modulus of elasticity, Type 304 stainless steel, 350°F

I = $bt^3/12$, inertial of the cross-section

b = 1.0 in, unit length

t = 0.125 in, tube wall thickness

$k_2 = 1 - \alpha = 1.00$

$$\alpha = \frac{I}{A \times R^2} = \frac{bt^3/12}{b \times t \times R^2} = 2.87 \times 10^{-4}$$

The thermal stress is:

$$\sigma = \frac{6M_A}{bt^2} = \frac{D_V E t k_2}{0.2976 \pi R^2} = \frac{5.17 \times 10^{-3} \times 25.7 \times 10^6 \times 0.125 \times 1.0}{0.2976 \times \pi \times 2.13^2} = 3,916 \text{ psi}$$

The maximum P+Q stress in the basket is conservatively calculated by combining the bending stress and thermal stress in the basket. The P+Q stress is:

$$\sigma_{pq} = \sigma_b + \sigma_{th} = 23.0 + 3.9 = 26.9 \text{ ksi}$$

The margin of safety is:

$$MS = \frac{3S_m}{\sigma_{pq}} - 1 = +1.16$$

where:

$$S_m = 19.4 \text{ ksi, design stress intensity, Type 304 stainless steel, } 350^\circ\text{F}$$

2.6.12.12 Conclusion

Loads generated during normal operations conditions for each basket assembly design result in total equivalent stresses, which each basket body can adequately sustain. Analyses show that all basket-bearing stresses during a side drop are much less than the material yield strength.

Column analyses demonstrate that each basket assembly is self-supporting during an end drop. The minimum Margin of Safety, for all basket designs, is +0.10 as reported in Section 2.6.12.7.4 for the TRIGA basket; +0.003 as shown in Table 2.6.12-2 for the DIDO basket; +0.10 as reported in Section 2.6.12.9.2 for the GA fuel basket; and +0.26 as reported in Section 2.6.12.11.1 for the ANSTO basket. Therefore, it can be concluded that all basket designs have sufficient structural integrity for adequate service during normal conditions of transport.

Chapter 3

Table of Contents

3.0	THERMAL EVALUATION.....	3.1-1
3.1	Discussion	3.1-1
3.2	Thermal Properties of Materials.....	3.2-1
3.2.1	Conductive Properties	3.2-1
3.2.2	Radiative Properties	3.2-2
3.2.3	Convective Properties.....	3.2-3
3.3	Technical Specifications of Components	3.3-1
3.4	Thermal Evaluation for Normal Conditions of Transport.....	3.4-1
3.4.1	Thermal Model	3.4-1
3.4.2	Maximum Temperatures	3.4-31
3.4.3	Minimum Temperatures	3.4-31
3.4.4	Maximum Internal Pressures.....	3.4-32
3.4.5	Maximum Thermal Stresses.....	3.4-45
3.4.6	Evaluation of Package Performance for Normal Conditions of Transport	3.4-46
3.5	Hypothetical Accident Thermal Evaluation	3.5-1
3.5.1	Finite Element Models	3.5-1
3.5.2	Package Conditions and Environment	3.5-4
3.5.3	Package Temperatures.....	3.5-5
3.5.4	Maximum Internal Pressure	3.5-12
3.5.5	Maximum Thermal Stresses.....	3.5-16
3.5.6	Evaluation of Package Performance for Hypothetical Accident Thermal Conditions	3.5-17
3.5.7	Assessment of the Effects of the Fission Gas Release in the Fire Accident Condition.....	3.5-17
3.6	Failed Metallic Fuel Basket – SCOPE Evaluations	3.6-1

List of Figures

Figure 3.4-1	HEATING5 Normal Transport Conditions Thermal Model	3.4-47
Figure 3.4-2	Design Basis PWR Fuel Assembly Axial Flux Distribution	3.4-48
Figure 3.4-3	ANSYS MTR Fuel Design Basis Heat Load Thermal Model (Uniform 30-Watt/Element Configuration Heat Load)	3.4-49
Figure 3.4-4	MTR Fuel Variable Decay Heat ANSYS Thermal Model	3.4-50
Figure 3.4-5	Thermal Resistance Model for TRIGA Fuel Elements	3.4-51
Figure 3.4-6	Modeling Details for the MTR Fuel Assembly Resting on the Surface of the NAC-LWT MTR Basket	3.4-52
Figure 3.4-7	Finite Element Thermal Model for TRIGA Fuel Cluster Rods	3.4-53
Figure 3.4-8	Details of the TRIGA Fuel Cluster Rods in the Finite Element Model.....	3.4-54
Figure 3.4-9	Individual TRIGA Fuel Cluster Rod Finite Element Model Details	3.4-55
Figure 3.4-10	PWR and BWR High Burnup Fuel Rods Normal Condition ANSYS Thermal Model (Condition 1).....	3.4-56
Figure 3.4-11	Close-up of PWR and BWR High Burnup Fuel Rods Normal Condition ANSYS Thermal Model	3.4-57
Figure 3.4-12	PWR and BWR High Burnup Fuel Rods Normal Condition ANSYS Thermal Model (Condition 2).....	3.4-58
Figure 3.4-13	Finite Element Thermal Model for MTR Fuel Element.....	3.4-59
Figure 3.4-14	Detailed DIDO Basket Module Finite Element Model	3.4-60
Figure 3.4-15	Detailed DIDO Fuel Assembly Model	3.4-61
Figure 3.4-16	ANSYS Model for BWR 7 × 7 Fuel Lattice with 25 High Burnup Fuel Rods	3.4-62
Figure 3.4-17	Fuel Rod Locations in the Thermal Model for Damaged Fuel	3.4-63
Figure 3.4-18	Finite Element Model for TPBARs	3.4-64
Figure 3.4-19	Finite Element Model for MOATA Plate Fuel – ANSTO	3.4-65
Figure 3.4-20	Finite Element Model for Mark III Spiral Fuel - ANSTO	3.4-66
Figure 3.5-1	Transient Thermal Analysis Finite Element Model of the NAC-LWT	3.5-19
Figure 3.5-2	Top Region of the ANSYS Model.....	3.5-20
Figure 3.5-3	Bottom Region of the ANSYS Model	3.5-21
Figure 3.5-4	Temperature History of NAC-LWT O-Rings and Valves in the Hypothetical Fire Event	3.5-22
Figure 3.5-5	Temperature History of NAC-LWT Components in the Hypothetical Fire Event.....	3.5-23
Figure 3.5-6	MTR Fuel Design Basis Heat Load Fire Accident ANSYS Thermal Model (Uniform 30-Watt/Element Configuration Heat Load)	3.5-24
Figure 3.5-7	MTR Fuel Variable Heat Load Fire Accident ANSYS Thermal Model (120-Watt/70-Watt/20-Watt Configuration Heat Load).....	3.5-25
Figure 3.5-8	Temperature History in the MTR Fuel Variable Heat Load Fire Accident Analysis	3.5-26
Figure 3.5-9	Location of the Maximum Temperature in the MTR Fuel Variable Heat Load	3.5-27
Figure 3.5-10	Temperature History for the TRIGA Fuel Cluster Rods Design Basis Heat Load Fire Accident Analysis	3.5-28

List of Figures (continued)

Figure 3.5-11	Temperature History of NAC-LWT Cask Components with PWR and BWR High Burnup Fuel Rods in the Hypothetical Fire Event.....	3.5-29
Figure 3.5-12	End of Fire Temperatures of the Alternate Port Cover Components	3.5-30
Figure 3.5-13	Transient Temperatures of the Alternate Port Cover Components.....	3.5-31
Figure 3.6-1	Failed Fuel Basket SCOPE Input.....	3.6-2
Figure 3.6-2	Failed Fuel Basket SCOPE Output.....	3.6-3
Figure 3.6-3	Nine Failed Metallic Fuel Rods SCOPE Input	3.6-7
Figure 3.6-4	Nine Failed Metallic Fuel Rods SCOPE Output	3.6-8

List of Tables

Table 3.2-1	Thermal Properties of Type 304 Stainless Steel	3.2-7
Table 3.2-2	Thermal Properties of 6061-T6 Aluminum Alloy	3.2-7
Table 3.2-3	Thermal Properties of Dry Air	3.2-8
Table 3.2-4	Thermal Properties of Chemical Copper Lead	3.2-8
Table 3.2-5	Thermal Properties of 56 Percent Ethylene Glycol Solution	3.2-9
Table 3.2-6	Thermal Properties of BISCO FPC (Fireblock Silicone Foam)	3.2-10
Table 3.2-7	Thermal Properties of Helium	3.2-10
Table 3.2-8	Fiberfrax Ceramic Fiber Paper, Grades 550, 880, and 970	3.2-11
Table 3.4-1	Temperatures for Metallic Fuel Transport	3.4-67
Table 3.4-2	Maximum Component Temperatures – Design Basis PWR Fuel	3.4-68
Table 3.4-3	Limiting Cold Case Component Temperatures – Design Basis PWR Fuel	3.4-69
Table 3.4-4	Fission Product Gas Inventories and Pressures for Design Basis PWR Fuel Assembly	3.4-70
Table 3.4-5	NAC-LWT Cask Thermal Performance Summary	3.4-70
Table 3.4-6	MTR Fuel Maximum Component Temperatures – Normal Transport Condition	3.4-71
Table 3.4-7	PWR Rods (25 Total) Maximum Component Temperatures – Normal Transport Condition	3.4-72
Table 3.4-8	TRIGA Fuel Element Maximum Component Temperatures - Normal Conditions of Transport	3.4-73
Table 3.4-9	TRIGA Fuel Cluster Rod Temperatures – Normal Conditions of Transport	3.4-74
Table 3.4-10	PWR and BWR High Burnup Fuel Rods Maximum Component Temperatures – Normal Transport Condition	3.4-75
Table 3.4-11	Fission Product Gas Inventories and Pressures for the Exxon 7 × 7 BWR Fuel Assembly	3.4-76
Table 3.4-12	DIDO Fuel Maximum Component Temperatures – Normal Transport Condition	3.4-77
Table 3.4-13	General Atomics IFM Maximum Component Temperatures – Normal Transport Condition	3.4-78
Table 3.4-14	PWR and BWR High Burnup Fuel Rods in a Fuel Assembly Lattice Maximum Component Temperatures—Normal Transport Condition	3.4-79
Table 3.4-15	Maximum Component Temperatures for High Burnup Fuel Rods with Damaged Fuel Rods in a Rod Holder	3.4-79
Table 3.4-16	Maximum Component Temperatures for TPBAR Shipment – Normal Conditions of Transport	3.4-80
Table 3.4-17	Maximum Component Temperatures - PULSTAR Fuel in MTR Basket ...	3.4-81
Table 3.4-18	PULSTAR Fuel Dimensions	3.4-82
Table 3.4-19	PULSTAR Payload Volume Summary	3.4-82
Table 3.4-20	PULSTAR Fuel Assembly Fission Product Gas Inventory	3.4-83
Table 3.4-21	PULSTAR Fuel Element Normal Condition Internal Pressure Summary...	3.4-83

List of Tables (continued)

Table 3.4-22	Maximum Component Temperatures – MOATA Plate Fuel and Mark III Spiral Fuel in ANSTO Basket.....	3.4-84
Table 3.5-1	Maximum Component Temperatures (°F) During the Fire Accident Design Basis PWR Fuel, 2.5 kW Heat Load).....	3.5-32
Table 3.5-2	MTR Fuel Fire Accident Maximum Temperatures (°F), 10 Fuel Plate/ 120W Element Case (Bounding Configuration).....	3.5-33
Table 3.5-3	TRIGA Fuel Fire Accident Maximum Temperatures (°F)	3.5-33
Table 3.5-4	PWR and BWR High Burnup Fuel Rods Fire Accident Maximum Temperatures (°F).....	3.5-34
Table 3.5-5	Maximum Component Temperatures for High Burnup Fuel Rods in a Rod Holder with Damaged Fuel Rods for the Fire Accident	3.5-34
Table 3.5-6	TPBAR Fire Accident Maximum Temperatures.....	3.5-35

3 THERMAL EVALUATION

3.1 Discussion

This chapter summarizes the thermal analyses, which are performed to demonstrate fulfillment of the thermal capability requirements established in 10 CFR 71.

The NAC-LWT cask is designed to safely contain irradiated nuclear fuel and other radioactive materials under a variety of normal transport conditions (as described in 10 CFR 71.71) and accident conditions (as described in 10 CFR 71.73). In order to verify the adequacy of the design, detailed analyses of a reference design PWR shipment are performed considering extreme normal transport and hypothetical accident conditions. The NAC-LWT cask is designed to transport one intact PWR fuel assembly; up to 2 intact BWR fuel assemblies; up to 25 individual PWR or BWR rods (including up to 14 fuel rods classified as damaged); up to 16 PWR MOX fuel rods (or a combination of PWR MOX and UO₂ PWR fuel rods); up to 42 MTR and DIDO fuel elements; up to 140 TRIGA fuel elements or 560 TRIGA fuel rod clusters; up to 300 TPBARs (of which two can be prefailed); up to 55 segmented TPBARs; or up to 700 PULSTAR fuel elements (intact or damaged); and metallic fuel. The PULSTAR fuel will be loaded in the 28 MTR basket and consist of intact fuel assemblies, intact fuel rods loaded in fuel rod inserts or fuel cans, or intact or damaged fuel and nonfuel components or fuel assemblies loaded in fuel cans.

High burnup PWR/BWR/PWR MOX fuel rods are placed in a rod holder (a rod holder is the term generally used in this chapter to describe a PWR/BWR Rod Transport Canister with a 4 × 4 or a 5 × 5 insert as presented on the drawings provided in Section 1.4). The high burnup PWR and BWR rods may also be placed in a fuel assembly lattice. Damaged PWR/BWR fuel rods must be placed in a rod holder. The 16 PWR MOX fuel rods are required to be placed in a rod holder with a 5 × 5 insert. Along with the maximum 16 PWR MOX rod contents (or combination of PWR MOX and UO₂ PWR fuel rods), the remaining tubes may be loaded with burnable poison rods or other intact components with negligible heat loads (total additional heat load of less than 10 watts).

An intact PWR fuel assembly with a maximum decay heat load of 2.5 kW is used in a majority of the thermal analyses. The failed fuel basket analysis in Section 3.6 uses a decay heat load of 30 Watts. The 42 MTR fuel assembly basket in Section 3.4.1.3 uses a decay heat load of 1.26 kW. A decay heat load of 1.05 kW is conservatively used for the TRIGA fuel basket analysis and a decay heat load of 0.693 kW is used for the TPBAR basket analysis. The maximum heat load for the PULSTAR fuel is 0.840 kW per cask. The maximum heat load for the maximum

number of 16 PWR MOX fuel rods is 2.3 kW per cask (143 W per PWR MOX rod). As long as the decay heat load is within the design limit of 2.5 kW, any of the fuel types and other radioactive material that the NAC-LWT cask is analyzed to transport are bounded by the cask body thermal analyses of the design basis PWR assembly.

The primary heat rejection design criteria for the NAC-LWT cask are that:

1. Components important to safety shall not be subjected to temperatures outside their safe operating ranges.
2. Thermally induced stresses in the cask containment (in combination with pressure and various load condition stresses) shall not cause degradation of the cask containment capability.

The first criterion is fulfilled by thermal analysis results, which show that components important to safety are maintained within their safe operating ranges. In the event that the temperatures of the components important to safety fall outside the safe operating ranges, it is assumed that the component has failed. Temperatures of components important to safety may not fall outside the safe operating range during normal transport conditions. There are three important safety components that are subject to this thermal criterion – the tetrafluoroethylene (TFE), Viton[®], and metallic O-ring seals; the lead gamma shield; and the 56 % ethylene glycol and water neutron shield.

An additional thermal consideration is associated with the liquid neutron shield tank – the reduction in neutron shielding capability caused by thermal contraction. An expansion tank is provided to ensure that the neutron shield tank remains full despite worst case contraction of the liquid in the tank during cooling. The method used by the expansion tank to keep the neutron shield tank full is described in Section 2.6.7.7.1.

The second criterion is fulfilled by the structural analysis of Chapter 2, which shows that combined load stresses (including thermally induced stresses) are less than the limits stated in Section 2.1.2.

The thermal analyses were performed for a 0.25-inch thick neutron shield tank shell, while the actual fabricated thickness is only 0.24 inch (6mm). The shell thickness difference of 0.01 inch equates to only a 0.009°F ΔT ; therefore, the analyses reported in this chapter are valid.

3.4 Thermal Evaluation for Normal Conditions of Transport

The temperatures of each of the components of the NAC LWT cask must be evaluated during normal transport conditions. The NAC-LWT cask must prevent components from exceeding their allowable temperatures by rejecting sufficient decay heat to the environment when the design basis, 2-year cooled, Westinghouse 15×15 fuel assembly is being transported. Since the neutron shield may be empty when metallic fuel is being transported, cask temperatures are also evaluated for this configuration. Components important to safety, identified in Section 3.3, must be maintained within their safe operating ranges. Also, the thermally induced stresses, in combination with pressure and mechanical load stresses, must be maintained below allowable stress levels.

3.4.1 Thermal Model

The temperatures of the NAC-LWT cask are evaluated for normal transport conditions. The cask is analyzed for two different cases referred to as the Heat Case and the Cold Case.

The Heat Case consists of an ambient temperature of 130°F, still air, and direct solar heating of 737 Btu/ft² on the vertical flat surfaces and 1,475 Btu/ft² on the curved surfaces for a period of 12 out of every 24 hours.

The Cold Case uses an ambient temperature of -40°F, still air, and shade (no solar heat load). This case requires no thermal analysis when a 0.0 kW decay heat load is considered because a uniform cask temperature of -40°F results. The more limiting decay heat load, from a thermal stress standpoint, is the design fuel assembly maximum decay heat load of 2.5 kW.

3.4.1.1 PWR Analytical Model

The temperatures of the NAC-LWT cask were evaluated using the HEATING5 computer code (Turner). The model used to evaluate the temperature distribution is shown in Figure 3.4-1. The model consists of the fuel basket section and the cask body.

The fuel basket section consists of several regions. These are the active fuel region, the non-power producing portion of the fuel region, the end-fittings, the spacer, an air region above the upper end-fitting, an air gap surrounding the fuel region, and an aluminum annulus (the basket wall) surrounding the gap. The fuel region is modeled as a cylinder 9.5 inches in diameter. (This diameter is actually an effective diameter for an 8.426-inch square fuel assembly.) The active fuel region is broken up into six regions of varying heat generation to closely approximate the axial power distribution shown in Figure 3.4-2. The effective diameter of the air gap is determined based on the 8.875-inch square cavity area minus the 8.426-inch

square fuel assembly area. The effective diameter of the aluminum annulus is obtained by taking the area of the basket and subtracting the area of the cavity. The cask cavity is modeled axially with an active fuel length of 144 inches, 6 inches on either side of the active fuel length as the non-power producing portion of the fuel region, a 4-inch end-fitting on the top and a 3-inch endfitting on the bottom, a 7-inch spacer at the bottom and an 8-inch air gap at the top.

The cask body is modeled based on the nominal dimensions of the license drawings in Section 1.4 with the exception of the radial lead region. The method used to obtain the dimensions of the lead region is described in Section 3.2. Because the calculation of the gap is conservative, the effect of the thermal insulator can be ignored during normal transport conditions. The resulting temperatures will still be conservative.

For ease of designing the analytical model, some of the methods of heat transfer within the NAC-LWT cask are not modeled. The effect of this simplification is an additional conservative small overestimation of overall temperatures within the cask. The heat generated by the fuel rods is transferred within the fuel assembly by conduction and to the air gap surrounding the assembly by convection. Conduction is the only axial means of heat transfer from the fuel assembly to the stainless steel at the top and bottom of the fuel basket. Heat is conducted through the aluminum surrounding the fuel assembly and then transferred by means of convection through the air gap between the fuel basket and the cask body. Heat is then conducted through the inner stainless steel wall, the air gap assumed in the lead region, the lead itself, and the outside stainless steel wall. In the liquid neutron shield, heat is transferred by both convection and conduction. It is then conducted through the stainless steel to the surface of the cask where it is transferred to the environment by means of convection and radiation. The solar heat load is evaluated using a steady-state HEATING5 analysis based on one-half of the maximum hourly solar heat load. The factor of one-half is based on the maximum insolation being applied to all cask surfaces for a period of 12 out of every 24 hours. For this report, this steady-state value for the solar heat load is referred to as full insolation.

3.4.1.2 Metallic Fuel Analytical Model

A HEATING5 computer analysis is performed for the NAC-LWT cask containing metallic fuel. When loaded with this fuel, the neutron shield tank (which is not required for neutron shielding of metallic fuel) is empty. This configuration reduces the heat transfer through the neutron shield region requiring further evaluation. The analysis is performed on the NAC-LWT cask containing the design basis metallic fuel producing 540 watts of decay heat.

This thermal analysis shows that the design basis PWR is the more limiting fuel. The results of the metallic fuel thermal analysis are presented in Table 3.4-1 and show that the temperatures are

lower at all locations (except the neutron shield region) than the corresponding temperatures for the design basis PWR fuel presented in Table 3.4-2.

3.4.1.3 MTR Fuel Analytical Models

Heat transfer analysis of the NAC-LWT containing MTR fuel is performed using two separate two-dimensional planar finite element models and the general purpose ANSYS computer code. The first model represents the entire cask and uses a nominal, effective thermal conductivity to represent the fuel element in each basket location. This cask model is used to determine the maximum temperatures throughout the cask, including the temperature of the fuel element side plates. The second model represents the detailed construction of the fuel element itself. The detailed fuel model uses the results from the cask model to specify the boundary condition temperature of the fuel element side plate. This model is used to determine the maximum fuel temperature for each case. Note that the loose fuel plate configuration in the MTR canister is bounded by the assembled fuel element because the stacked loose plates have a much greater contact area for heat transfer to the basket walls. Therefore, the loose fuel plate configuration is not evaluated. Two transport conditions are evaluated:

Condition 1:

The NAC-LWT is supported in an ISO container with solar insolation applied on the surface of the ISO container, and the NAC-LWT is considered to be insulated from the environment (only for normal conditions of transport steady state conditions). The gas inside the ISO container is air. The cavity of the NAC-LWT is backfilled with helium as required by operational procedures.

Condition 2:

The NAC-LWT is not located in an ISO container and solar insolation is applied to the NAC-LWT cask surface. For the purpose of performing the thermal analyses, the cavity of the NAC-LWT is considered to be filled with air.

Of these two conditions, Condition 2 (air in cavity case) produces the higher temperatures as shown in Table 3.4-6. Therefore, the detailed fuel model is used to evaluate Condition 2 only. For each of the two conditions listed above, two different fuel configurations are considered for evaluation for steady-state normal transport conditions.

- (1) Uniform design basis heat load of 30 watts per MTR fuel assembly:

This configuration consists of seven MTR fuel elements with design basis heat loads (30 watts per element) corresponding to a total MTR package contents heat load of 1.26 kilowatts (42 fuel elements).

(2) MTR fuel with variable decay heat:

As described in Section 5.3.4, MTR fuel may also be shipped in a variable decay heat configuration. In this case, a basket module may be loaded with only three elements, each having a maximum decay heat of 70 watts, or with three elements with maximum decay heats of 120 watts, 70 watts, and 20 watts. The total decay heat load for the basket must not exceed 210 watts. The same detailed heat transfer model described in Section 3.4.1.3.1 is also used for this analysis.

The fuel decay heat is modeled using uniform volumetric heat generation terms defined by administrative controls from Section 7.1.5. The administrative controls define bounding basket loading configurations that:

- Limit the combined basket heat load to 210 watts per basket module.
- Exclude MTR elements having decay heat loads in excess of 120 watts.
- Require MTR elements having decay heat loads between 120 watts and 70 watts to be loaded into the center basket module position.
- Require MTR elements with decay heat loads between 30 watts and 70 watts to be loaded in the center in-line row of the basket module.
- Limit decay heat loads of MTR elements placed in peripheral basket tubes, not on the center line, to a 30-watt decay heat load (per element).

These constraints result in two bounding loading configurations of MTR fuel elements.

Assuming that individual elements have maximum decay heats of 70 watts and 120 watts, the two bounding configurations are:

1. Three 70-watt fuel elements
2. One 120-watt fuel element, one 70-watt fuel element, and one 20-watt fuel element

These combinations are depicted in Figure 3.5-7. Of these two configurations, the second configuration will produce the highest temperatures, as the center assembly contains a 120-watt MTR fuel element. This is the fuel configuration, which is analyzed for the variable decay heat loading. The thermally limiting configuration is also depicted in Figure 3.4-4, which conservatively bounds any fuel loading configuration permitted by the operating procedure presented in Section 7.1.5.

3.4.1.3.1 MTR Fuel Thermal Model of the NAC-LWT (Transported in an ISO Container)

For Condition 1, the detailed fuel model is not used because this condition is bounded by Condition 2, as shown in Section 3.4.1.3.2. Thermal analyses of the NAC-LWT cask for Condition 1 are performed using a half-symmetry, cross-sectional model of the cask in an ISO container positioned along the container centerline. Heat transfer to the environment is limited to surface convection and radiation on both horizontal and vertical surfaces of the ISO container with an emissivity of 0.36. Solar insolation is applied to the vertical surfaces and the top horizontal surface of the ISO container. Heat transfer from the cask to the ISO container is modeled as conduction, convection and radiation. Convective and conductive heat transfer are modeled in the liquid neutron shield, while heat transfer in the cask cavity is limited to conduction and radiation. Axial heat transfer is conservatively ignored in the model. The MTR fuel elements are represented in the model with homogenized fuel elements. The conductive heat flow path from the cask through the saddle support to the bottom surface of the ISO container is conservatively ignored.

Thermal conductivity for 6061-T6 aluminum alloy is based on ASME Code, Section II, Part D, Table TCD. The finite element model for the uniform 30 watts per MTR fuel element is shown in Figure 3.4-3, while the finite element model for the variable decay heat of 120 watts, 70 watts and 20 watts is shown in Figure 3.4-4. For the basket slots, which are empty for the variable decay heat, only conduction through the cavity gas is modeled. In each of these fuel models, the fuel is considered to rest on the surface of each basket slot. The details of this modeling are shown in Figure 3.4-6. While the MTR fuel assemblies are considered to rest on the surface of the basket, the basket is conservatively modeled as being in the center of the cask cavity. Conduction (through helium) and radiation (using emissivity of stainless steel for both surfaces) are modeled from the inner shell of the cask to the basket.

The heat transfer analysis model represents the cask cavity free space using the conductivity of helium. (see Table 3.2-7). The properties for the remaining materials are contained in Table 3.2-1 through Table 3.2-6.

The air space between the NAC-LWT cask and the ISO container is modeled using air with an effective conductivity. This effective conductivity (Incropera) is:

$$\frac{k_{\text{eff}}}{k} = 0.386 \left(\frac{\text{Pr}}{0.861 + \text{Pr}} \right)^{1/4} (\text{Ra}_c^*)^{1/4}$$

$$Ra_c^* = \frac{[\ln(D_o/D_i)]^4}{L^3 (D_i^{-3/5} + D_o^{-3/5})^5} Ra_L$$
$$Ra_L = \frac{g\beta(T_i - T_o)L^3}{\alpha v}$$

where:

Pr = Prandtl number (Krieth)

v = kinematic viscosity (Krieth)

α = thermal diffusivity (Krieth)

β = $1/T_f$

T_f = $(T_i + T_o)/2$

T_i = inner surface temperature

T_o = outer surface temperature

D_i = inner diameter (cask surface)

D_o = outer diameter (height of the ISO container)

L = $(D_o - D_i)/2$

The effective conductivity for the neutron shield and expansion tank as well as the convection from the surface of the ISO container to an ambient temperature of 100°F are presented in Section 3.2.3.

Decay heat for the different MTR package configurations is conservatively enveloped for the heat transfer analysis. Each fuel element of the maximum capacity MTR package configuration, 42 elements, is modeled with a heat generation of 30 watts. Total MTR package contents heat load is 1.26 kilowatts, approximately half of the NAC-LWT cask maximum decay heat load of 2.5 kilowatts. The decay heat is modeled as uniformly generated within the homogenized fuel regions.

The Condition 1 models of the NAC-LWT cask with uniform and variable decay heat MTR fuel element loadings are shown in Figure 3.4-3 and Figure 3.4-4, respectively.

3.4.1.3.2 MTR Fuel Thermal Model of the NAC-LWT (Transported via Truck Trailer)

Thermal analyses of the NAC-LWT cask for Condition 2 are performed using two separate models. The first is a half-symmetry cross-sectional model of the cask in which the outer surface of the expansion tank is the boundary of the model. This model is used to determine the temperatures throughout the cask up to and including the maximum fuel element side plate temperatures. The second is a half-symmetry cross-sectional model of the fuel element. This model is used to determine the maximum fuel temperature within the element for the worst-case fuel plate dimensions. The worst case dimensions are based on the limiting design dimensions combined with the limiting manufacturing tolerances that result in the maximum resistance to heat transfer from the fuel to the side plates.

Cask Model

The modeling of the normal steady state condition of the NAC-LWT from the center of the cask to the outer surface of the expansion tank is identical to the model described in Section 3.4.1.3.1 with the following exceptions:

1. The gas in the NAC-LWT cask cavity is considered to be air.
2. The MTR basket is shifted downward towards the inner shell leaving a minimum gap of 0.07 inch between the outer diameter of the basket end plate and the cask inner shell surface. This is an effective representation of the normal condition of transport (i.e. cask horizontal).
3. The solar insolation and convection to the ambient temperature of 100°F is applied to the outer shell of the expansion tank.

The Condition 2 models of the NAC-LWT cask with uniform and with variable decay heat MTR fuel element loadings are shown in Figure 3.5-6 and Figure 3.5-7, respectively. These same models are used to calculate both normal and accident condition temperatures for the cask.

Fuel Element Model

The fuel element model includes the side plate, the fuel, cladding, and the air between the plates and surrounding the side plate. The total element heat load is uniformly distributed throughout the fuel. Based on symmetry, only one-half of the fuel element assembly is modeled. Figure 3.4-13 shows the model for both the minimum 10-plate and maximum 23-plate cases. These two configurations bound fuel elements with any intermediate number of plates. The boundary condition for this model is the applied side plate temperature at the lower right corner of the model. This assumes that the basket is oriented such that only the ends of the element side plates are in contact with the basket. The lateral surfaces of the side plates are assumed to be adiabatic, which results in a conservative calculation of the maximum temperature of the fuel.

Temperature, °F	K, BTU/hr-in-°F		
	Aluminum	UO ₂	Fuel Matrix 75% UO ₂
100	8.08	0.42	2.33
200	8.25	0.37	2.34
300	8.38	0.33	2.35
400	8.49	0.30	2.35

The worst-case fuel effective thermal conductivity occurs for the maximum UO₂ percentage of 75% and corresponds to the LEU fuel plates.

The fuel in the center of each fuel plate is a matrix of aluminum and uranium or aluminum and uranium oxide (UO₂) combined in various ratios. The effective thermal conductivity is calculated using a mass-weighted average of the conductivity of the individual materials. The fuel plates are modeled using worst-case dimensions as shown:

1. Fuel plate thickness = 0.045 inch (< 0.05 inch)
2. Cladding thickness = 0.008 inch (< 0.015 inch)

A sensitivity analysis shows that variation of the active fuel width within the fuel plate has a negligible effect. A constant value of 6.6 cm is used in the analysis. This corresponds to the worst case for reactivity considerations. Note that the case of the loose fuel plates in the MTR canister is bounded by that of the assembled fuel element and, therefore, is not evaluated.

3.4.1.3.3 MTR Fuel Heat Transfer Analyses Results

The thermal analysis is performed to demonstrate that the temperature of the MTR fuel is maintained within acceptable limits. A conservative temperature of 400°F is established as the maximum allowable MTR fuel cladding temperature for normal conditions of transport. The aluminum retains its capability to function as a mechanical component in this temperature range, and it is not close to the 1,220°F melting temperature of aluminum (Table 6.4.1, pg. 6-60, Marks' Standard Handbook for Mechanical Engineers). The material properties presented in MIL-HDBK-5F indicate that 6061-T6 aluminum alloy retains over 40% of its room temperature yield and ultimate strengths at a long-term temperature of 400°F.

Maximum temperatures for package components with the NAC-LWT configured for MTR fuel are summarized in Table 3.4-6. The reported temperatures are lower at all locations than the corresponding temperatures for the design basis PWR fuel presented in Table 3.4-2.

Temperatures of the MTR fuel element cladding are maintained below 400°F for both the design basis uniform decay heat loading and the variable heat loading.

3.4.1.4 PWR Rod

Heat transfer of the NAC-LWT containing 25 PWR rods with a total heat load of 1.41 kW configured in the PWR/BWR aluminum basket in the NAC-LWT cask enclosed in an International Shipping Organization (ISO) container was evaluated using ANSYS. The model presented in Figure 3.4-3 was revised to include the PWR/BWR aluminum basket and 25 PWR rods. Results from this evaluation are summarized in Table 3.4-7.

These results show that the temperatures are lower at all locations (except the neutron shield region) than the corresponding temperatures for the design basis PWR fuel presented in Table 3.4-2. Similar to the discussion presented in Section 3.4.1.3.3 for the MTR heat transfer analysis, temperature results from the two dimensional heat transfer analysis are conservative based on the imposed limitations of the model and can be used to evaluate acceptability of component temperatures outside the modeled section. Temperature of components in the lid closure region is less than the hottest basket temperature which is directly influenced by the decay heat of the fuel. It is concluded that the temperature of the safety related O-ring seals is within the allowable range of temperature of -40°F to +735°F. The maximum temperature of the lead gamma shield in the base of the LWT cask is less than the cask inner shell and much lower than the maximum of +600°F.

3.4.1.5 Thermal Evaluation for TRIGA Fuel

The thermal evaluation for TRIGA fuel is performed using classical analysis employing a thermal resistance model. The TRIGA fuel is transported in a basket assembly consisting of 5 modules - a base module, a top module, and three intermediate modules. During transport all 5 modules must be installed in the cask. The three intermediate modules are interchangeable, but the top and base modules are not. Each module contains 7 cells, and each open cell holds up to 4 TRIGA fuel elements. The top module is sized to accept fuel follower control elements, which are longer than the typical element. The center cell of each module is blocked with an 11-gage stainless steel plate so that fuel cannot be loaded in the center cell. The thermal evaluation conservatively assumes that the center cell also contains 4 fuel elements, so although only 120 fuel elements may be loaded into the cask, the thermal evaluation assumes 140 elements. Consequently, the total heat load in the thermal evaluation is conservatively considered to be 1.05 kW ($7.5 \text{ watt/fuel element} \times 140 = 1.05 \text{ kW}$).

TRIGA fuel elements may be transported directly in a basket module cell, in a screened failed fuel can, or in a sealed failed fuel can. The fuel cans fit in either a top or base module cell. The screened failed fuel cans hold up to four (4) TRIGA fuel elements, while the sealed failed fuel can holds up to two (2) damaged elements or equivalent fuel debris.

As described in Section 1.2.3.1, TRIGA fuel elements with minor cladding defects are loaded into screened failed fuel cans (screened cans). The screened can precludes gross particulate material from escaping the cell. The screened failed fuel cans are provided in two lengths. The screened failed fuel can is a square tube of 14-gage, Type 304 stainless steel, that holds four fuel elements. It is provided with a closure lid and an end plate that is screened to allow water draining.

TRIGA fuel debris and damaged fuel elements, which do not have structural integrity, are loaded into sealed failed fuel cans (sealed cans). The sealed cans are used to containerize the TRIGA fuel debris. The cans are provided in two lengths. The shorter can may be used in the base or top basket modules. The longer can may only be used in the top module. The cans are vacuum dried and leak tested prior to loading into a TRIGA fuel basket.

The TRIGA fuel thermal evaluation determines the maximum fuel cladding temperatures based on the maximum basket temperatures determined for the design basis heat load MTR thermal analysis presented in Section 3.4.1.3.1. An intermediate basket module with the shortest TRIGA fuel, which provides the highest heat load density, is used to obtain a bounding evaluation. Based on the maximum basket temperature and heat load density, the maximum fuel cladding temperatures are determined using a thermal resistance model.

The cross-section of the TRIGA and MTR fuel baskets are identical. As shown in Section 1.2.3 and Table 1.2-4, the maximum decay heat load for MTR fuel is 1.26 kW per cask. The maximum decay heat load for TRIGA fuel is 1.05 kW per cask. Therefore, it is conservative to use the maximum basket temperature for MTR fuel as a boundary condition for the thermal resistance model for TRIGA fuel.

Since the total decay heat load for MTR fuel bounds that for TRIGA fuel, the temperatures for cask components for the MTR fuel also bound those for the TRIGA fuel. The cask body temperatures for the MTR fuel are shown in Table 3.4-6.

3.4.1.5.1 TRIGA Model Description

The heat generated from the TRIGA fuel in the basket is transferred to the basket module by thermal conduction and radiation, and then transferred to the cask inner shell from the basket surface by the same heat transfer modes. The heat is finally transferred through the cask and International Shipping Organization (ISO) container to ambient. The thermal resistance model and thermal analysis of TRIGA fuel considers the regions inside a single basket opening of the TRIGA fuel basket. This analysis bounds transport in the cask without an ISO container.

The thermal resistance model is shown in Figure 3.4-5. The maximum temperature of the basket (T_{basket}) is taken from the MTR design basis heat loading thermal analysis. The temperatures for

the TRIGA fuel are determined by stepping through each of the resistors in the thermal circuit, from the basket to the fuel cladding. All temperatures calculated are maximums, based on the basket temperature. Each successive maximum temperature calculated is then applied uniformly over the next surface in the resistance model. Fuel may be shipped directly in a basket cell, in a screened failed fuel can, or in a sealed failed fuel can. Since the model assumes the presence of the can, the model is conservative for configurations in which a can is not used.

The gas in the cask cavity is considered to be air in the thermal resistance model. Thermal conductivities of air and stainless steel are obtained from "Fundamentals of Heat and Mass Transfer" (Incropera). Emissivities of stainless steel (basket) and aluminum (fuel clad) are obtained from the Nuclear Systems Material Handbook and from "Scoping Design Analyses for Optimized Shipping Casks Containing 1-, 2-, 3-, 5-, or 10-Year-Old PWR Spent Fuel" (Bucholz), respectively.

Assuming the maximum temperature of the basket (T_{basket}) occurs at all inside surfaces of the webs forming the central cell in the basket module, the temperature of the can (T_{can}) is then determined by considering heat conduction and radiation between the can surface and the inside surface of the basket central cell. Convection in the gap between these surfaces is conservatively ignored.

The heat transfer rate across the gap per unit length (q_{gap}) between the can surface and the inside surface of the basket central cell wall can be represented as follows:

$$q_{\text{gap}} = q_{\text{cond}} + q_{\text{rad}}$$

$$q_{\text{gap}} = \frac{A(K_{\text{cond}})(T_1 - T_2)}{L_{\text{gap}}} + \frac{A(\sigma)(T_1^4 - T_2^4)}{\left(\frac{1}{\mathcal{E}_1} + \frac{1}{\mathcal{E}_2} - 1\right)}$$

where:

$$q_{\text{gap}} = 7.5 \text{ watt} \times 4/14 = 2.14 \text{ watt} = 7.302 \text{ Btu/hr}$$

$$A = \text{Can surface area} = 3.33 \times 4 = 13.32 \text{ inch}^2$$

$$K_{\text{cond}} = \text{Air conductivity @ } 260^\circ\text{F (400}^\circ\text{K)} = 1.628 \times 10^{-3} \text{ Btu/hr-in-}^\circ\text{F}$$

$$L_{\text{gap}} = \text{Gap size between can and basket} = (3.44 - 3.33)/2 = 0.055 \text{ inch}$$

$$T_1 = \text{temperature at can surface (} T_{\text{can}} \text{)}$$

$$T_2 = \text{temperature at inside surface of the basket central cell (} T_{\text{basket}} \text{)} = 267^\circ\text{F}$$

$$\sigma = 1.19 \times 10^{-11} \text{ Btu/hr-in}^2\text{-}^\circ\text{R}$$

ϵ_1 = emissivity of web of basket central cell (stainless steel) = 0.36

ϵ_2 = emissivity of can (stainless steel) = 0.36

The temperature at the can (T_{can}) is calculated to be 287°F.

The maximum temperature of the can (T_{can}) is then applied to all can surfaces for determining the cladding temperature of the fuel. It is assumed that there are four (4) fuel elements inside the can surrounded by air. In the equivalent resistor analogy, the fuel elements do not contact each other, neglecting heat conduction between fuel elements. For a specific fuel element, an assumed circular region equivalent to 1/4 of the area inside the can, is developed to contain a fuel element, which results in a uniform air gap. The fuel cladding temperature is determined using the formula representing a hollow cylinder. Note that convective heat transfer in the gap between the fuel clad and the can is conservatively ignored.

Heat transfer rate per unit length of the basket (Q_{leng}) can be represented as:

$$Q_{leng} = q_{cond} + q_{rad}$$

$$Q_{leng} = \frac{2\pi (K_{cond})(T_1 - T_2)}{\ln\left(\frac{r_2}{r_1}\right)} + \frac{\sigma(2\pi r_1)(T_1^4 - T_2^4)}{\left(\frac{1}{\epsilon_1}\right) + \left(\frac{1 - \epsilon_2}{\epsilon_2}\right)\left(\frac{r_1}{r_2}\right)}$$

where:

r_1 = fuel cladding outer radius = 0.675 inch

r_2 = radius of equivalent circular region representing 1/4 of the area inside a can
= 0.93 inch

K_{cond} = Air conductivity @ 260°F (400°K) = 1.628×10^{-3} Btu/hr-in-°F

σ = 1.19×10^{-11} Btu/hr-in²-°R

ϵ_1 = emissivity of fuel cladding (aluminum) = 0.22

ϵ_2 = emissivity of the can (stainless steel) = 0.36

T_1 = fuel cladding temperature (T_{clad})

T_2 = can temperature (T_{can}) = 287°F

The fuel cladding temperature (T_{clad}) is solved to be 326°F.

3.4.1.5.2 TRIGA Fuel Thermal Evaluation Results

Using the model described above, and the assumed boundary condition of 267°F for the maximum basket temperature (from Table 3.4-6), the maximum normal transport conditions temperature of the TRIGA fuel is determined as shown in Table 3.4-8.

A conservative temperature of 400°F is established as the maximum allowable temperature for aluminum-clad TRIGA fuel, as described in Section 3.4.1.3.3 for MTR fuel. Stainless steel clad TRIGA fuel is allowed a significantly higher cladding temperature, since the melting temperature of stainless steel is 2,600°F (Mark's) and stainless steel retains its capability to function as a mechanical component at temperatures up to the 800°F range. Therefore, the temperatures calculated for the TRIGA fuel cladding are acceptable.

3.4.1.6 TRIGA Fuel Cluster Rods

The TRIGA fuel cluster rods are 0.542 inches OD with 0.016-inch thick Incoloy 800 cladding. Each rod is inserted into a 6061-T6 aluminum tube (0.75 inch OD, 0.62 inch ID) that is part of the fuel rod insert. Up to sixteen rods and a fuel rod insert are placed into a single cell of the seven cell basket. This TRIGA basket has the same cross sectional dimensions and basket material as the MTR basket presented in Section 3.4.1.3. The thermal evaluation for the TRIGA fuel cluster rods is performed using two-dimensional planar finite element analyses and the general purpose ANSYS computer code. Two transport conditions are evaluated:

Condition 1:

The NAC-LWT is supported in an ISO container with solar insolation applied on the surface of the ISO container, and the NAC-LWT is considered to be insulated from the environment (only for the normal conditions of transport steady state conditions). The gas inside the ISO container is air. The cavity of the NAC-LWT is actually backfilled with helium as required by operational procedures.

Condition 2:

The NAC-LWT is not located in an ISO container and solar insolation is applied to the NAC-LWT cask surface.

For the purpose of performing these thermal analyses, the cavity of the NAC-LWT is considered to be filled with air.

For each of the two conditions listed above, only a single fuel configuration is evaluated: 16 rods in a fuel rod insert in each of the seven cells comprising a basket section. This corresponds to a total heat load of 210 watts for each basket section (30 watts per cell of a basket section which

corresponds to 30/16 or 1.875 watts per rod). Therefore, the heat load in the cask cavity corresponding to five basket sections is 5 times 210 watts or 1.05 kW.

Since the finite element model corresponds to a one inch axial length, the heat generation applied to each rod in the model was 1.875 watts divided by the length of the rod or 22 inches. Although the aluminum inserts will conduct heat in the axial direction, this was conservatively ignored.

3.4.1.6.1 Condition 1 Analysis of TRIGA Fuel Cluster Rods

Thermal analyses of the NAC-LWT cask for Condition 1 are performed using a half symmetry cross sectional model of the cask in an ISO container positioned along the container centerline. The model employed for the ISO container, cask body and the seven-celled basket is the same finite element model used in Section 3.4.1.3.1 for the MTR fuel thermal model (Condition 1). The similarity in modeling includes the finite element mesh and the material properties for conduction, convection and radiation. The 16 rods and fuel rod inserts are modeled in each of the seven cells, as shown in Figure 3.4-7. Figure 3.4-8 and Figure 3.4-9 show details of the fuel region model. The TRIGA fuel cluster rods were conservatively modeled in the center of the aluminum fuel tube, and the fuel rod inserts were modeled without any contact with the sides of the basket. The 0.13 inch aluminum shell, which surrounds the TRIGA fuel cluster, provides a heat transfer path from the rods to the basket surface. This aluminum shell was conservatively not considered in the analysis. The space between the aluminum tubes and the stainless steel basket surface was modeled with the cavity gas, and the modes of heat transfer from fuel rod insert to the basket surface included conduction through the gas and radiation from the surface of the insert to the basket surface.

3.4.1.6.2 Condition 2 Analysis of TRIGA Fuel Cluster Rods

Thermal analyses of the NAC-LWT cask for Condition 2 are performed using a half symmetry cross sectional model of the cask in which the outer surface of the expansion tank is the boundary of the model. The modeling of the normal steady state conditions of the NAC-LWT from the center of the cask to the outer surface of the expansion tank is identical to the model described in Section 3.4.1.3.1 with the following exceptions:

1. The gas in the NAC-LWT cask cavity is considered to be air.
2. The solar insolation and convection to the ambient temperature of 100°F is applied to the outer shell of the expansion tank.

3.4.1.6.3 TRIGA Fuel Cluster Rods Heat Transfer Results

The thermal analysis is performed to demonstrate that the temperature of the TRIGA fuel cluster rod is maintained within acceptable limits. A conservative temperature of 800°F is established as

the maximum allowable TRIGA fuel cladding temperature for normal conditions of transport. For aluminum 6061-T6 aluminum alloy, the allowable temperature is considered to be 400°F.

Temperatures for package components with the NAC-LWT configured for the TRIGA fuel are summarized in Table 3.4-9. In this table, the maximum fuel clad temperature is 295°F, which is significantly below the 800°F value. For the aluminum, the maximum reported temperature is 292°F, which is also well below the 400°F limit.

3.4.1.7 High Burnup PWR or BWR Rods in a Rod Holder

The high burnup rods may be either BWR rods or PWR rods. The decay heat for the PWR is 2.3 kW with a corresponding peaking factor of 1.1 and for the BWR the decay heat per rod is 2.1 kW with a peaking factor of 1.22. The thermal evaluation employs a two-dimensional planar model to ensure that the peaking factor is conservatively included and the heat load applied to the finite element model is the total heat load factored by the peaking factor. The bounding product of the heat load and the peaking factor corresponds to the BWR. The evaluation of the BWR rod is considered to bound the temperatures corresponding to the PWR rod configuration. All of the fuel rods are considered to be intact for this evaluation. The evaluation of damaged fuel rods is provided in Section 3.4.1.11.

The rod holder for the high burnup rod transport can accommodate two configurations: a 4 × 4 matrix of pin tubes containing 16 rods and a 5 × 5 matrix of pin tubes containing 25 rods. Since the decay heat per rod is considered to be the same, the maximum heat load is bounded by the 25-rod configuration. For the 4 × 4 matrix of pin tubes, an additional stainless steel insert, .31-inch thick, is placed in the can weldment. This permits the can weldment to be employed for the 16-rod transport or the 25-rod transport configuration. For the can weldment, the aluminum basket and the remainder of the cask, the additional insert has a negligible affect on their temperatures. Therefore, the bounding configuration is the 25-rod configuration, since it produces 56% more heat load in the cask basket than the 16-rod configuration. The bounding configuration for the clad temperatures and the pin tubes supporting the fuel rods is also the 25-rod configuration due to the 56% additional heat load. While the additional insert increases the thermal resistance, this is significantly offset by the additional 56% additional decay heat.

Heat transfer analysis of the NAC-LWT containing high burnup rods is performed using two-dimensional planar finite element analyses and the general purpose ANSYS computer code. Two transport conditions are evaluated:

Condition 1:

The NAC-LWT is supported in an ISO container with solar insolation applied on the surface of the ISO container, and the NAC-LWT is considered to be insulated from the environment (only for normal conditions of transport steady state conditions). The gas inside the ISO container is air.

The cavity of the NAC-LWT is backfilled with helium as required by operational procedures.

Condition 2:

The NAC-LWT is not located in an ISO container and solar insolation is applied to the NAC-LWT cask surface.

For the purpose of performing the thermal analyses, the cavity of the NAC-LWT is considered to be filled with air.

3.4.1.7.1 High Burnup PWR and BWR Fuel Rods Thermal Model of the NAC-LWT (Transported in an ISO Container)

Thermal analyses of the NAC-LWT cask for Condition 1 are performed using a half-symmetry, cross-sectional model of the cask in an ISO container. Heat transfer to the environment is limited to surface convection and radiation on both horizontal and vertical surfaces of the ISO container with an emissivity of 0.36. Solar insolation is applied to the vertical surfaces and the top horizontal surface. Heat transfer from the cask to the ISO container is modeled as conduction, convection and radiation. Convective and conductive heat transfer are modeled in the liquid neutron shield, while heat transfer in the cask cavity is limited to conduction and radiation. Axial heat transfer is conservatively ignored in the model.

Bounding configuration of BWR fuels used in analyses is based on U.S. Department of Energy, Office of Civilian Radioactive Waste Management, "Characteristics of Spent Fuel, High-Level Waste, and Other Radioactive Wastes Which May Require Long -Term Isolation," Appendix 2A, December 1987. Thermal properties of UO_2 and zirconium alloy cladding are from 1) Hagrman, D.L., Reymann, G.A., "Matpro-Version 11, A Handbook of Material Properties for Use in the Analysis of Light Water Reactor Rod Behavior," Idaho Falls, ID, EG&G Idaho, Inc., 1997; 2) Rust, J.H., "Nuclear Power Plant Engineering," Atlanta, GA, S.W., Holland Company, 1979. Thermal conductivity for 6061-T651 aluminum alloy is based on ASME Code, Section II, Part D, Table TCD.

The finite element model for the condition 1 is shown in Figure 3.4-10. The fuel cladding and the inner surface of the pin tube are considered to be in point-to-point contact. The outer surface

of the fuel cladding only contacts the pin tube in one point in the model. The pin tubes are conservatively considered separated and a gap of 0.0005 inch between pin tubes is modeled. This condition neglects any pin tube contact due to dead weight loading of the contents. One of the can weldment sides is modeled in contact with the aluminum insert. For the other three sides, a gap 0.042/0.084/0.042 inch between the aluminum insert and the tube of the can weldment is modeled. The details of this modeling are shown in Figure 3.4-11. Likewise, only one surface between the PWR aluminum insert and the PWR basket is considered to be in contact.

Conduction (through helium) and radiation (using emissivity of stainless steel for both surfaces) are modeled from the inner shell of the cask to the basket.

The heat transfer analysis model uses conduction in the remaining volume of the cask cavity. The conductivity of this material corresponds to helium. (see Table 3.2-7). The properties for the remaining materials are contained in Table 3.2-1 through Table 3.2-8.

The air space between the NAC-LWT cask and the ISO container is modeled using air with an effective conductivity. This effective conductivity (Incropera) is:

$$\frac{k_{\text{eff}}}{k} = 0.386 \left(\frac{\text{Pr}}{0.861 + \text{Pr}} \right)^{1/4} (\text{Ra}_c^*)^{1/4}$$

$$\text{Ra}_c^* = \frac{[\ln(D_o/D_i)]^4}{L^3 (D_i^{-3/5} + D_o^{-3/5})^5} \text{Ra}_L$$

$$\text{Ra}_L = \frac{g\beta(T_i - T_o)L^3}{\alpha\nu}$$

where:

Pr = Prandtl number (Krieth)

ν = kinematic viscosity (Krieth)

α = thermal diffusivity (Krieth)

β = $1/T_f$

T_f = $(T_i + T_o)/2$

T_i = inner surface temperature

T_o = outer surface temperature

D_i = inner diameter (cask surface)

D_o = outer diameter (height of the ISO container)

$L = (D_o - D_i) / 2$

3.4.1.7.2 High Burnup PWR and BWR Fuel Rods Thermal Model of the NAC-LWT (Transported via Truck Trailer)

Thermal analyses of the NAC-LWT cask for Condition 2 are performed using a half-symmetry planar cross-sectional model of the cask in which the inner surface of the inner shell is the boundary of the model. The maximum temperature of 274°F (PWR design basis fuel with 2.5 kW heat load and a peaking factor of 1.2 under normal transport condition [Table 3.4-2]) is applied to the boundary of the model. The modeling of the normal steady state condition of the NAC-LWT from the center of the cask to the inner surface of the inner shell is identical to the model described in Section 3.4.1.7.1 with the following exceptions:

1. The gas in the NAC-LWT cask cavity is considered to be air.
2. The constant temperature of 274°F is applied to the outer surface of the model, which corresponds to the inner surface of the cask inner shell. This temperature corresponds to the condition, which imposes solar insolation and convection/radiation boundary at the outer shell of the expansion tank. This is also described in Section 3.4.1.1.

The Condition 2 model of the NAC-LWT cask with high burnup PWR and BWR fuel rods is shown in Figure 3.4-12. This model is also used to calculate both normal and accident condition temperatures for the cask.

3.4.1.7.3 High Burnup PWR and BWR Fuel Rods Heat Transfer Analyses Results

The thermal analysis is performed to demonstrate that the component temperature of NAC-LWT cask loaded with high burnup PWR and BWR rods is maintained within acceptable limits.

Maximum temperatures for package components with the NAC-LWT configured for high burnup PWR and BWR rods are summarized in Table 3.4-10. As shown in Table 3.4-10, component temperatures are all maintained within their allowable temperatures.

3.4.1.8 Thermal Evaluation for DIDO Fuel

3.4.1.8.1 Analytical Models for the DIDO Fuel Contents

Heat transfer analysis of the NAC-LWT containing DIDO fuel is performed using a two-dimensional planar finite element analysis and the general purpose ANSYS computer code. Two transport conditions are evaluated:

Condition 1:

The NAC-LWT is supported in an ISO container with solar insolation on the surface of the ISO container, and the NAC-LWT is considered to be insulated from the environment (only for the normal conditions of transport steady state conditions). The gas inside the ISO container is air. The cavity of the NAC-LWT is backfilled with helium as required by operational procedures.

Condition 2:

The NAC-LWT is not located in an ISO container and solar insolation is applied to the NAC-LWT cask surface. For the purpose of performing the thermal analysis, the cavity of the NAC-LWT is considered to be filled with air.

A single fuel configuration is considered for this evaluation. Each DIDO fuel assembly is limited to having a heat load of 25 W per assembly. The total contents of the NAC-LWT for the DIDO fuel are limited to having six basket modules and each module is limited to having seven DIDO fuel assemblies. This limits the heat load of a basket module to 175 W, and a total NAC-LWT heat load of 1.05 kW. The 1.05 kW total heat load is enveloped by the 1.26 kW total heat load for the NAC-LWT MTR fuel contents contained in Section 3.4.1.3. Since the NAC-LWT cask ambient conditions are the same for the DIDO fuel as for the MTR fuel, the maximum temperature of all cask body components for the DIDO contents are enveloped by the maximum temperatures for the MTR fuel contents. Therefore, the cask inner shell temperature for the MTR fuel contents bounds the maximum cask inner shell temperature for the DIDO fuel contents. The maximum cask inner shell temperature is used as the boundary condition for the finite element model for the DIDO thermal evaluation. For Condition 1 and Condition 2, the maximum inner shell temperatures are 214°F and 181°F, respectively. These values correspond to the design basis heat load values obtained from Table 3.4-6.

Two finite element models are used in the evaluation of the DIDO fuel basket and the DIDO fuel assemblies.

The evaluation of the maximum basket component temperatures for these conditions is performed using a finite element model, which is shown in Figure 3.4-14. This model is used to evaluate both conditions. This model corresponds to the 4.01-inch inside diameter stainless steel tubes, the 1/2-inch thick plates, the 3/4-inch × 3/8-inch aluminum bars (thermal shunts) and the 0.19-inch thick aluminum sheet (heat transfer shell) on the outside of the tubes. The SOLID70, eight-noded brick element is used to represent stainless steel components, the heat transfer shell and the cavity gas between the surfaces of the circular plates and the heat transfer shell and the

inner shell of the cask body. To account for the axial conductance of the thermal shunts, they are modeled as conduction elements using an area corresponding to the dimensions of the aluminum bars. Radiation is conservatively neglected from the outer surface of the heat transfer shell and the inner surface of the cask inner shell. The center tube is assumed not to be in contact with any of the six outer tubes. During transport, the NAC-LWT is in a horizontal position in which the basket modules are in contact with the inner shell of the cask. To represent the contact of the basket module with the cask inner shell, the inner shell temperature was applied to two nodes of the circular plates and the remaining nodes corresponding to the inner surface of the inner shell of the cask body. The 25 W per assembly heat load is represented by applying the heat flux along a concentrated area at the inner tube surface, which would correspond to the contact of the fuel assembly with the 4.01-inch inside diameter stainless steel tube.

For Condition 1, the elements representing the cavity gas between the basket and the inner shell correspond to helium, whereas for Condition 2, these elements use properties for air.

To determine the maximum temperature for the fuel, a separate detailed model of a DIDO fuel assembly is constructed. This model is shown in Figure 3.4-15, which consists of four circular cylinders in contact at a corresponding single point to be transported in the horizontal position. Each cylinder is comprised of a layer of fuel of 0.64 mm (0.025 in.) thickness between two aluminum shells, each being 0.46 mm (0.018 in.) thick. The boundary condition of this model is the maximum basket temperature determined from the detailed basket model and the volumetric heat generation corresponding to 25 W per assembly.

3.4.1.8.2 DIDO Fuel Heat Transfer Analyses Results

The thermal analysis is performed to demonstrate that the temperature of the DIDO fuel is maintained within acceptable limits. A conservative temperature of 400°F is established as the maximum allowable DIDO fuel cladding temperature for normal conditions of transport. The aluminum retains its capability to function as a mechanical component in this temperature range and it is not close to the 1,220°F melting temperature of aluminum (Table 6.4.1, p. 6-60, Marks' Mechanical Handbook for Mechanical Engineers). The material properties presented in MIL-HDBK-5F indicate that 2000 series aluminum retains over 40% of its room temperature yield and ultimate strengths at a long-term temperature of 300°F.

Maximum temperatures for package components with the NAC-LWT configured for DIDO fuel are summarized in Table 3.4-12. The reported temperatures are lower at all locations than the corresponding temperatures for the design basis PWR fuel presented in Table 3.4-2. The DIDO fuel assembly cladding temperatures are maintained below 400°F.

3.4.1.9 Thermal Evaluation for General Atomics IFM

The heat generated from the General Atomics IFM in the Fuel Handling Unit (FHU) is transferred to the basket by thermal conduction and radiation, and is then transferred to the cask inner shell from the basket surface by the same heat transfer modes. The heat is finally transferred through the cask and International Shipping Organization (ISO) container to ambient. The thermal resistance model and thermal analysis of General Atomics IFM consider a single FHU of the fuel. The maximum temperature from the resistor model corresponds to the FHU's stainless steel shell, while the minimum temperature corresponds to the inner surface of the transport cask inner shell. The fuel is actually stored in two FHUs, but the evaluation conservatively considers the total heat load of 13 W to be placed into a container at the center of the cask cavity. The evaluation does not consider the reduction in thermal resistance due to the contact of the FHU with the basket or of the basket with the inner shell of the transport cask. Additional conservatism is included by ignoring heat transfer by radiation across any of the gaps in the system. To ensure that a bounding temperature for the basket is calculated, air properties are used in the analysis for the gas in the cavity. Also, conservatism is included by using the inner shell temperature corresponding to the 1.26 kW condition for the cask body as opposed to 13 W. This analysis, therefore, bounds transport in the cask with and without an ISO container.

A thermal evaluation of the top module is performed by considering a heat load of 13 W in the center of the basket with only one 6.0-inch diameter top module tube. This is conservative because it maximizes the gap between the tube and the cask inner shell. Air is used as the cavity gas as an additional conservatism. The maximum temperature is computed using the resistor analogy.

For concentric cylinders, the thermal resistance (R) for the heat flow through the cylinders is taken from Krieth as:

$$R = \frac{\ln\left(\frac{r_2}{r_1}\right)}{2\pi K L}$$

where:

r_2 = outer radius of cylinder (inch)

r_1 = inner radius of cylinder (inch)

K = thermal conductivity (BTU/hr/in/°F)

The effective resistance from the secondary enclosure can be expressed as to the cask inner shell:

$$R_T = R_1 + R_2 + R_3 + \frac{1}{\frac{1}{R_4} + \frac{1}{R_5}}$$

where:

R_1 = resistor of the outer canister

R_2 = resistor of the gap between outer canister and the basket shell

R_3 = resistor basket shell

R_4 = resistor of the air from the basket shell to inner shell surface (outside of the basket disks)

R_5 = resistor of stainless steel disks supporting the basket shell in series with the air gap between the basket disks and the inner shell

The maximum temperature of the secondary enclosure can be determined by the following equation:

$$T_i = R_t Q + T_{\text{cask}}$$

where:

Q = total heat load

T_{cask} = temperature of cask inner shell

The following parameters will be used for this evaluation:

Q = 13 Watts

L = 37.0 inches – length of shortest secondary fuel closure

r_1 = 2.255 inches – minimum inner radius of secondary closure

r_2 = 2.375 inches – minimum outer radius of secondary closure

r_3 = 2.75 inches – inner radius of module fuel cell

r_4 = 3.00 inches – outer radius of module fuel cell

r_5 = 6.688 inches – inner radius of LWT

r_6 = 6.6325 inches – outer radius of the basket disks

K_{ss} = 0.7143 Btu/hr/in/F at 70°F for stainless steel

K_{air} = 0.00161 Btu/hr/in/F at 300°F for air

From Table 3.4-6, the maximum temperature of the LWT inner shell for a 1.26 kW heat load is 214°F, with 100°F ambient temperature with solar insolation. This is used as a bounding temperature for the cask inner shell (T_{cask}) for this evaluation.

$$R_{\text{eff}} = \frac{1}{\frac{1}{R_4} + \frac{1}{R_5}} \qquad R_4 = \frac{\ln(6.688/3.0)}{2\pi(0.00161)(37.0-2)}$$

$$R_4 = 2.264$$

$$R_5 = \frac{\ln(6.8125/3.0)}{2\pi(0.7143)(2)} + \frac{\ln(6.688/6.6325)}{2\pi(0.00161)(2)}$$

$$R_5 = 0.503$$

(Stainless steel disk in series with the air between the basket disk and the inner shell)

$$R_{\text{eff}} = \frac{1}{\frac{1}{R_4} + \frac{1}{R_5}}$$

$$R_{\text{eff}} = 0.412$$

$$R_T = R_1 + R_2 + R_3 + R_{\text{eff}}$$

$$R_T = \frac{\ln(2.375/2.255)}{2\pi(0.7143)(37.0)} + \frac{\ln(2.75/2.375)}{2\pi(0.00161)(37.0)} + \frac{\ln(3.0/2.75)}{2\pi(0.7143)(37.0)} + 0.412$$

$$R_T = 0.0003 + 0.392 + 0.0005 + .412 = 0.805$$

The maximum temperature of the secondary enclosure (T_i) is :

$$T_i = 0.805(13 \times 3.415) + 214 = 250^\circ \text{F}$$

The maximum temperature of the basket is conservatively considered to be the same as the temperature of the secondary enclosure (250°F). Temperatures of individual components are summarized in Table 3.4-13.

The maximum content temperature for the GA IFM shipment is considered to be bounded by the TRIGA maximum fuel cladding temperature of 326°F contained in Table 3.4-8, which corresponds to a bounding heat load of 1.05 kW (as compared to the approximately 13 watts for the GA IFM).

A conservative temperature of 800°F is established as the maximum allowable temperature for the stainless steel basket and the contents, which is comprised of the steel-clad TRIGA fuel and the HTGR pellets. The steel cladding of the TRIGA fuel is actually an inconel alloy. Mil HDBK-5G (1 November 1994), Section 6.3.2, identifies that alloys of inconel are used for parts

requiring strength for temperatures exceeding 1,000°F, which significantly exceeds 800°F. The HTGR pellets were designed for operational exposure to reactor core temperatures exceeding 1,000°F, which also exceeds 800°F. Therefore, the maximum temperatures for the contents for the GA IFM are acceptable.

3.4.1.10 High Burnup PWR or BWR Fuel Rods in a Fuel Assembly Lattice

The NAC-LWT cask may transport up to 25 intact high burnup PWR or BWR fuel rods that are in a fuel assembly lattice. The decay heat for the PWR rods is 2.3 kW with a corresponding peaking factor of 1.1, and the decay heat for the BWR rods is 2.1 kW with a corresponding peaking factor of 1.22.

The thermal evaluation employs two-dimensional planar half-symmetry models of the fuel lattice with 25 fuel rods, fuel channel (for BWR fuel), PWR insert (for BWR fuel), fuel basket, and the gas inside the cask cavity. The model extends to the inner surface of the cask inner shell. The model for a 7×7 BWR fuel lattice with 25 fuel rods is shown in Figure 3.4-16. BWR arrays of 7×7 , 8×8 , 9×9 , and 10×10 are analyzed. PWR arrays of 14×14 , 15×15 , 16×16 , and 7×17 are analyzed. The BWR model includes a fuel channel and insert, which are absent from the PWR model.

To determine the worst-case fuel rod arrangement, the 25 fuel rods are analyzed in five different arrangements:

1. Centered (top and bottom) in the two-dimensional model (as shown in Figure 3.4-16).
2. Centered horizontally and concentrated at the bottom of the lattice cross-section.
3. Spread out horizontally and concentrated at the bottom of the lattice cross-section.
4. Centered horizontally and concentrated at the top of the lattice cross-section.
5. Spread out horizontally and concentrated at the top of the lattice cross-section.

For the even numbered fuel arrays (i.e., 8×8 , 10×10 , 14×14 , and 16×16), only 24 fuel rods are modeled due to the use of the half-symmetry models. For these cases, a higher heat generation rate is applied at each fuel rod so that the total heat load of 2.3 kW for PWR and 2.1 kW for BWR is maintained. The empty fuel rod locations in the lattice are modeled as air. The maximum inner shell temperature (274°F) for the PWR design basis fuel with 2.5 kW heat load (Table 3.4-2) is applied to the boundary of the model.

For each fuel array and fuel rod location configuration, a steady-state thermal analysis is performed using the general purpose ANSYS computer code. The Condition 2 transport case, with the NAC-LWT not located in an ISO container is evaluated. As shown in Table 3.4-10, this

results in higher maximum temperatures for the fuel cladding than transport Condition 1 where the cask is assumed to be inside of the ISO container. Transport Conditions 1 and 2 are described in Section 3.4.1.3.

3.4.1.11 High Burnup PWR and BWR Fuel Rods in a Rod Holder with Damaged Fuel Rods

The NAC-LWT may transport up to 25 PWR or BWR high burnup fuel rods in a rod holder, with up to 14 of the fuel rods classified as damaged. The maximum decay heat for these configurations is 2.3 kW for PWR and 2.1 kW for BWR. The finite element model for the evaluation of the 25 intact fuel rods in a rod holder is described in Section 3.4.1.7. This section provides the thermal evaluation for the configuration containing damaged fuel rods. The analysis conservatively assumes 15 damaged fuel rods, with the remainder of the rod holder containing intact fuel. The model used for this analysis is based on the two-dimensional half-symmetry model described in Section 3.4.1.7 (Condition 2 configuration), as shown in Figure 3.4-12. Modifications were made to the fuel regions to simulate the damaged fuel rods.

The basket design for the high burnup fuel rod transport can accommodate two configurations: a 4×4 matrix of fuel tubes containing 16 rods and a 5×5 matrix of fuel tubes containing 25 rods. Since the decay heat per rod is considered the same, the maximum heat load occurs with the 5×5 matrix and is the configuration evaluated. Thermal analysis is performed for three cases with different locations of the 15 damaged fuel rods. The fuel rod locations are shown in Figure 3.4-17, which shows the matrix region of the thermal model shown in Figure 3.4-12. The nine locations in the half-symmetry model correspond to 15 actual fuel rod locations. The three cases evaluated are:

Case 1: Damaged fuel rods in locations 4 through 12

Case 2: Damaged fuel rods in locations 7 through 15

Case 3: Damaged fuel rods in locations 1 through 9

The inner surface of the inner shell is the boundary of the model. From Table 3.4-2, the maximum inner shell temperature of 274°F for PWR design basis fuel with 2.5 kW heat load for normal transport conditions is applied to the boundary of the model. The maximum temperature of 274°F results from the condition of solar insolation and convection/radiation to surroundings.

To simulate the damaged fuel rods, a 50% compaction of the fuel material in the fuel tubes is considered. It is assumed that the interior region of the fuel rod tube consists of 50% fuel debris and 50% gas. One half of the heat generation rate for the intact fuel rod is conservatively applied to the entire interior region of the fuel rod tube. Since the volume of the interior of the fuel rod

tube is four times that of the volume of an intact fuel rod, the applied heat load for the damaged fuel is two times that of the heat load for an intact fuel rod. In addition, the heat generation rate is multiplied by a peaking factor of 1.22. The material properties in the entire interior of the fuel rod tubes for the damaged fuel are conservatively considered to be the thermal properties of the fuel (rather than 50% fuel and 50% gas), since this results in higher temperatures in the fuel rod tube walls and the surrounding components.

3.4.1.12 Thermal Evaluation for TPBARs

Heat transfer analysis of the NAC-LWT containing TPBARs is performed using a two-dimensional planar finite element analysis and the general purpose ANSYS computer code. The NAC-LWT is transported in an ISO container with solar insolation on the surface of the ISO container during normal conditions of transport. The gas inside the ISO container is air. The cavity of the NAC-LWT is backfilled with helium as required by operational procedures.

There are two TPBAR content conditions requested for certification: the first is for the transport of up to 300 production TPBARs (of which two can be prefailed) in an open consolidation canister; the second is for the transport of up to 55 segmented TPBARs in a welded closed waste container. The 55 segmented TPBARs and debris resulting from PIE are limited to a total heat load of 127 W, based on a minimum of 90 days of cooling (2.31 watts/rod). Therefore, the loaded TPBAR consolidation canister with 300 rods is considered the bounding content condition for this thermal evaluation with each TPBAR limited to a heat load of 2.31 W, which corresponds to a 90-day cooling period (see Appendix 1-C of Chapter 1). This limits the maximum heat load of the NAC-LWT with TPBAR contents to 0.693 kW. The 0.693 kW total heat load is enveloped by the 1.05 kW total heat load for the NAC-LWT TRIGA fuel contents as described in Section 3.4.1.6. Since the NAC-LWT cask ambient conditions are the same for the TPBAR contents as for the TRIGA fuel contents, the maximum temperature of all cask body components for the TPBAR contents are enveloped by the maximum temperatures for the TRIGA fuel contents. Therefore, the cask inner shell temperature of 222°F (Table 3.4-9) for the TRIGA fuel contents bounds the cask inner shell temperature for the TPBAR contents and is used as the bounding condition for the TPBAR thermal evaluation.

The evaluation of the maximum component temperatures for TPBARs is performed using a finite element model as shown in Figure 3.4-18. This model corresponds to the aluminum basket, the consolidation canister containing 300 TPBARs, and the helium inside the cask. The loaded TPBAR consolidation canister bounds the maximum decay heat of the TPBAR waste container containing 55 segmented TPBARs and, therefore, the thermal evaluation bounds all TPBAR content conditions.

Any axial conductance of the contents is conservatively neglected in this two dimensional planar model. The ANSYS PLANE55 and MATRIX50 elements are used. Radiation is considered using radiation matrix elements while convection is conservatively ignored in the following regions.

- Between the outer surfaces of TPBARs.
- Between the inner surface of the consolidation canister and the adjacent TPBARs.
- Between the outer surface of the consolidation canister and the inner surface of the basket.
- Between the outer surface of the basket and the inner surface of the cask inner shell.

A constant temperature of 222°F (Table 3.4-9, Condition 1) was applied to the outer surface of the model, which corresponds to the inner surface of the cask inner shell. During transport, the NAC-LWT is in a horizontal position in which the TPBAR contents are in contact with the inner surface of the basket, while the basket plates are in contact with the inner shell of the cask.

The heat generated by the 300 TPBARs is applied via a heat generation rate to the stainless steel cladding of the TPBARs. A peaking factor of 1.15 is used in the heat generation rate calculation based on a heat load of 2.31 W for each TPBAR.

The thermal analysis demonstrates that the temperature of the TPBARs is maintained within a conservative limit of 300°F for normal conditions of transport. At 300°F, the aluminum retains its capability as a mechanical component.

Maximum component temperatures for the NAC-LWT containing TPBAR contents are summarized in Table 3.4-16. Maximum cask component temperatures for normal conditions are conservatively obtained from the analysis results corresponding to the TRIGA fuel contents, as shown in Table 3.4-9 (Condition 1).

3.4.1.13 PULSTAR Fuel Elements in 28 MTR Basket

Three loading patterns for PULSTAR fuel elements are postulated for the 28 MTR basket configuration.

- Intact fuel assemblies will be directly loaded into 28 MTR basket;
- Intact fuel elements (rods) will be loaded in the fuel rod insert or the PULSTAR cans;
- Damaged fuel elements (rods) or debris will be loaded in the PULSTAR cans.

The heat load in each basket cell is limited to 30 watts. This corresponds to a maximum heat load of 210 watts for each of the four basket modules. The cask cavity is back-filled with helium.

The thermal analysis for the PULSTAR fuel contents in the 28 MTR basket is bounded by the thermal analysis for the TRIGA fuel cluster rods as presented in Section 3.4.1.6. The MTR basket (Section 3.4.1.3) has the same cross-sectional dimensions and basket material as the basket for TRIGA fuel cluster rods. The maximum modular heat load for TRIGA fuel cluster rods is identical to the maximum modular heat load of the PULSTAR fuel contents (210 watts). The bounding condition for the thermal evaluation for the TRIGA fuel cluster rods is "Condition 2" as described in Section 3.4.1.6.2. In the two-dimensional planar model for the TRIGA fuel cluster, the cask cavity is modeled as air. The model conservatively includes an air gap between the fuel cladding and the aluminum tube and between fuel tube assembly and the inner surface of the basket cell, as shown in Figure 3.4-8 and Figure 3.4-9. This is conservative since there is contact between these components, which provides a significant heat transfer path from the fuel to the basket. Note that the aluminum tubes have an insignificant effect on heat transfer, since the air gap controls the heat conduction in the in-plane direction and the model is a two-dimensional planar model, which neglects any heat transfer in axial direction. Since the PULSTAR fuel rod insert is identical to the TRIGA rod insert, the thermal analysis results for TRIGA fuel cluster rods, Condition 2, as presented in Table 3.4-9, are used as the temperature results for the PULSTAR fuel. These temperatures are summarized in Table 3.4-17 for the PULSTAR fuel. The cask body component maximum temperatures with the NAC-LWT configured for the PULSTAR fuel conservatively use the temperatures from Condition 1 and Condition 2 in Table 3.4-17. The maximum temperatures for the cask body and basket are 222°F and 278°F, respectively, which are significantly below the allowable for stainless steel. For the configuration with intact rods or failed rods loaded in a PULSTAR can, the maximum fuel cladding temperature from Table 3.4-17 is conservatively used as the maximum temperature of the fuel can. The maximum fuel cladding temperature is 295°F, which is significantly below the allowable temperature limit of 1,058°F during transport.

3.4.1.14 Thermal Evaluation for ANSTO Fuel

Two types of ANSTO fuel may be loaded in the ANSTO basket in the NAC-LWT cask:

- MOATA plate fuel elements
- Mark III spiral fuel elements

The ANSTO basket consists of six modules with seven fuel tubes in each module. Each fuel tube may be loaded with a MOATA plate bundle or a Mark III spiral fuel assembly. The maximum heat load for a MOATA plate bundle is 0.4 watt (3 watts per assembly is conservatively considered in the thermal evaluation in this section). The maximum heat load is

18 watts per assembly for the Mark III spiral fuel. The corresponding maximum heat load per cask is 0.126 kW for the MOATA plate bundles and 0.756 kW for the Mark III spiral fuel.

The NAC-LWT is supported in an ISO container with solar insolation applied on the surface of the ISO container. The gas inside the ISO container is air. The cavity of the NAC-LWT is actually backfilled with helium as required by operational procedures.

The thermal evaluation for the MOATA plate fuel elements and Mark III spiral fuel is performed using finite element analysis with the ANSYS program. The finite element models for the MOATA plate bundles and Mark III spiral fuel are shown in Figure 3.4-19 and Figure 3.4-20, respectively. Each model corresponds to a quarter-symmetry cross-section of the fuel, the basket and the helium inside the cask cavity. The models are constructed using ANSYS PLANE55 two-dimensional planar elements. The maximum cask inner shell temperature of 222°F for the LWT cask loaded with the TRIGA fuel cluster rods (see Table 3.4-9) is conservatively used as the boundary condition for both models. The heat load used in the evaluation of the TRIGA fuel cluster rods is 1.05 kW per cask (see Section 3.4.1.6), which is significantly higher than the heat load for the MOATA fuel and Mark III spiral fuel. The MOATA plate fuel elements are explicitly modeled with aluminum cladding on both sides of the fuel meat. A volumetric heat generation rate corresponding to 3 watts per assembly is applied to the elements for fuel meat for the MOATA plate fuel.

The MARK III spiral fuel assemblies are modeled as straight plates with effective orthotropic properties. The longitudinal (radial) properties are decreased to reflect the reduction of the length (from the actual curved plates to the straight plates in the model). The material properties for the fuel meat are conservatively used in the transverse (circumferential) direction of the fuel elements in the model (conductivity of the aluminum clad is higher than that for the fuel meat). A volumetric heat generation rate corresponding to 18 watts per assembly is applied to the fuel elements for the Mark III spiral fuel.

The thermal conductivities of the fuel matrix for MTR fuel from Section 3.4.1.3 are used as the conductivities for the fuel meat for the MOATA plate and MARK III spiral fuel elements in the thermal models. These thermal conductivities are conservative since the fuel meat for the MOATA plate fuel and Mark III spiral fuel is composed of uranium and aluminum alloy, which are significantly more conductive than the fuel matrix material for the MTR fuel. Radiation between the basket tube and the cask inner shell is conservatively not considered in the models. For the MOATA fuel, radiation is only considered between fuel plates. For the Mark III spiral fuel, radiation is modeled across the helium gap between the fuel outer tube and the basket tube.

Steady-state thermal analysis is performed to demonstrate that the temperature of the MOATA plate fuel and Mark III spiral fuel is maintained within acceptable limits. A conservative temperature of 400°F is established as the maximum allowable temperature for these aluminum-clad fuel elements, as discussed in Section 3.4.1.3.3 for the MTR fuel.

3.4.1.15 High Burnup PWR MOX Rods in a PWR/BWR Rod Transport Canister

A maximum of 16 PWR MOX fuel rods (or a combination of PWR MOX and standard PWR fuel rods) may be placed in the PWR/BWR Rod Transport Canister, including a 5 × 5 insert. Along with the maximum 16 PWR MOX rod contents, the remaining tubes may be loaded with burnable poison rods or other zirconium alloy-based hardware components with negligible activation and heat load. The maximum decay heat for the PWR MOX rods is 2.3 kW (or 143 W/rod), with a corresponding peaking factor of 1.1.

The thermal evaluation described in Section 3.4.1.7 for the high burnup PWR and BWR rods is a two-dimensional planar model in which the heat load applied to the model is based on the BWR rod decay heat load factored by the peaking factor. The bounding product of the heat load and the peaking factor for the PWR MOX rods is (2.3)(1.1) or 2.53 kW, as compared to (2.1)(1.22) or 2.56 kW for the BWR high burnup rods. The evaluation performed in Section 3.4.1.7 using the BWR high burnup rods is considered to bound the heat load for the 16 PWR MOX rods.

As described in Section 3.4.1.7, the model for the 25-rod configuration (in a 5 × 5 insert) uses a heat load of (25/16) times the product of the BWR rod decay heat and associated peaking factor. With this bounding heat load, it is, therefore, not necessary to evaluate the 16-rod configuration in the Rod Transport Canister with a 5 × 5 insert.

The thermal conductivities of the UO₂ and MOX from MATPRO-Version 11 at 600°F are 0.26 Btu/hr-in-°F and 0.22 Btu/hr-in-°F, respectively. The thermal resistance to the heat rejection of the rod canister is due to the thin tube walls and the gaps modeled between the tubes and rods and the basket insert. The reduction in the conductivity of the rod material has an insignificant effect on the thermal resistance incorporated in the gaps and thin tube walls in the model. The thermal resistance internal to each rod does not affect the rejection of the heat from other rods in the basket. Since the maximum number of PWR MOX rods is limited to 16, there are nine or more other vacant positions in the basket without the heat generation of the PWR MOX rods. The evaluation of any arbitrary configuration of tubes, with and without the PWR MOX rods, is bounded by an evaluation of the model having all tubes containing the design basis heat load of 143 W for each PWR MOX rod.

The evaluation using BWR rods in Section 3.4.1.7 is considered to bound all configurations of PWR MOX rods.

Maximum temperatures for package components with the NAC-LWT cask configured for high burnup PWR and BWR fuel rods are summarized in Table 3.4-10. Since the BWR rod configuration is bounding, the temperatures presented in Table 3.4-10 are bounding temperatures for the PWR MOX rod configuration. As shown in Table 3.4-10, component temperatures are all maintained within their allowable limits.

3.4.2 Maximum Temperatures

Using the models described, temperatures for the cask body and fuel rod cladding are determined for maximum normal operation conditions (2.5 kW decay heat load, 130°F ambient temperature, still air, full insolation). The maximum cask component and fuel rod cladding temperatures for PWR fuel (2.5 kW) are listed in Table 3.4-2. Not all of the cask components are explicitly modeled; their temperatures are obtained by evaluating the analytical model at the component location. Maximum normal operating temperatures for the 1.26 kW MTR fuel and the 1.05 kW TRIGA fuel configurations are shown in Table 3.4-6 and Table 3.4-8, respectively. Maximum normal operating temperatures for high burnup PWR and BWR fuel rods in a rod holder are shown in Table 3.4-10. The maximum component temperatures for DIDO fuel and General Atomics IFM for normal conditions of transport are shown in Table 3.4-12 and Table 3.4-13, respectively. The maximum component temperatures for 25 high burnup PWR and BWR fuel rods in a fuel assembly lattice are shown in Table 3.4-14. The maximum component temperatures for high burnup PWR or BWR fuel with up to 14 damaged fuel rods in a rod holder are shown in Table 3.4-15. Maximum operating component temperatures for the NAC-LWT containing TPBARs are shown in Table 3.4-16. The maximum operating temperatures for the PULSTAR fuel contents in the MTR basket are shown in Table 3.4-17. The maximum component temperatures for the NAC-LWT containing MOATA plate fuel and Mark III spiral fuel are presented in Table 3.4-22.

3.4.3 Minimum Temperatures

As stated in Section 3.4.1, the minimum temperatures in the cask occur with a 0.0 kW decay heat load and the minimum ambient conditions. Under these conditions, a uniform temperature of -40°F will exist in the cask. The maximum thermal stresses in the cask, during normal operations conditions, occur when the design basis decay heat load of 2.5 kW exists in the cask along with the minimum ambient conditions (-40°F ambient temperature and no insolation). The cask component and fuel rod clad temperatures for the 2.5 kW decay heat load with minimum ambient conditions are listed in Table 3.4-3.

3.4.4 Maximum Internal Pressures

3.4.4.1 Maximum Internal Pressure for Design Basis Fuel in Normal Conditions

The NAC-LWT cask is filled to one atmosphere (14.7 psia) upon loading. It is necessary to evaluate the internal pressure of the cask after thermal equilibrium has been attained. Assuming a maximum normal fuel cladding temperature of 472°F (932°R) from Table 3.4-2, 3 percent fuel rods rupture, and 30 percent of the fission gas and 100 percent of the rod backfill gas escape from the ruptured fuel rods, the cask internal pressure is calculated. Table 3.4-4 reports the fission gas inventories for the design basis PWR fuel assembly. Table 5.1-2 reports the design parameters of the design basis PWR fuel. Using information from Table 5.1-2, the void volume of a single fuel rod is calculated as 2.43 in³ (39.82 cm³) by subtracting the volume of the fuel pellets from the volume of an empty fuel rod (the plenum spring volume is disregarded). The total fuel assembly void volume is calculated as 495.16 in³ (8,123.28 cm³) by multiplying the single fuel rod volume by 204, the number of fuel rods in the fuel assembly. The total fuel assembly void volume, the fission gas inventory information in Table 3.4-4, and the maximum normal transport temperature (472°F) are applied to the ideal gas law ($PV = nRT$) to obtain the pressure in the unruptured fuel rods due to the fission gases. This fission gas pressure, 1,771.5 psia, is also reported in Table 3.4-4, based on 100% availability of fission gases, later adjusted to 30%. The releasable fission gas pressure and rod backfill pressure (assumed 565 psia) are summed to obtain the total fuel rod pressure.

The cask pressure is obtained using Dalton's Law of Partial Pressures:

$$P = P_A + P_B$$

where:

P = total pressure

P_A = partial pressure of gas A (cask cavity helium gas backfill)

P_B = partial pressure of gas B (fuel rod backfill and fission gas)

The reported cask and fuel rod backfill pressures are at standard temperature (72°F) and must be corrected to the normal transport temperature. Given that the internal volumes of the NAC-LWT Cask and the fuel rods remain constant, the resultant pressure is proportional to the temperature change according to the ideal gas law:

$$P_2 = P_1 \left(\frac{T_2}{T_1} \right)$$

where:

$$P_1 = 14.7 \text{ psia (cask backfill pressure)}$$

$$T_1 = 72^\circ\text{F (532}^\circ\text{R) (cask backfill temperature)}$$

$$T_2 = 472^\circ\text{F (932}^\circ\text{R) (maximum normal operating condition cavity gas temperature)}$$

Thus, the cask backfill pressure at normal operating temperature equals:

$$P_2 = 14.7 \text{ psia} \left(\frac{932^\circ\text{R}}{532^\circ\text{R}} \right)$$

$$P_2 = 25.8 \text{ psia}$$

For the fuel rod backfill pressure at normal operating temperature:

$$P_1 = 565 \text{ psia (fuel rod backfill pressure)}$$

$$T_1 = 72^\circ\text{F (532}^\circ\text{R) (fuel rod backfill temperature)}$$

$$T_2 = 472^\circ\text{F (932}^\circ\text{R) (maximum normal operating condition cavity gas temperature)}$$

and:

$$P_2 = 565 \text{ psia} \left(\frac{932^\circ\text{R}}{532^\circ\text{R}} \right)$$

$$P_2 = 989.8 \text{ psia}$$

The partial pressure of the cask backfill distributed over the cask free volume (including 3% failed rods) is calculated by:

$$P_{\text{cask backfill}} = P_{\text{initial}} \left(\frac{V_{\text{cask}}}{V_{\text{total}}} \right)$$

where:

$$P_{\text{initial}} = 25.8 \text{ psia (temperature adjusted cask backfill pressure)}$$

$$V_{\text{cask}} = 5.196 \text{ ft}^3 \text{ (147,134 cm}^3 \text{)}$$

$$V_{\text{rod void}} = 244 \text{ cm}^3 \text{ (volume of 3\% failed fuel rods)}$$

$$V_{\text{total}} = V_{\text{cask}} + V_{\text{rod void}}$$

$$V_{\text{total}} = 147,378 \text{ cm}^3$$

Thus, the cask backfill partial pressure at normal operating temperature, including the volume of failed fuel rods equals:

$$P_{\text{cask backfill}} = 25.8 \text{ psia} \left(\frac{147,134 \text{ cm}^3}{147,378 \text{ cm}^3} \right)$$

$$P_{\text{cask backfill}} = 25.8 \text{ psia}$$

The partial pressure of the failed fuel rod gases in the cask cavity is calculated by:

$$P_{\text{fuelrods}} = P_{\text{initial}} \left(\frac{V_{\text{rodvoid}}}{V_{\text{total}}} \right)$$

where:

$$P_{\text{initial}} = 1,521.3 \text{ psia} \quad (\text{fission gas pressure } (0.30 \times 1,771.5 \text{ psia}) \text{ plus rod backfill pressure } (989.8 \text{ psia}))$$

$$V_{\text{rod void}} = 244 \text{ cm}^3$$

$$V_{\text{total}} = 147,378 \text{ cm}^3$$

Thus, the failed fuel rod partial pressure at normal operating temperature, including fission gases and the volume of cask cavity void equals:

$$P_{\text{fuelrods}} = 1,521.3 \text{ psia} \left(\frac{243.7 \text{ cm}^3}{147,378 \text{ cm}^3} \right)$$

$$P_{\text{fuelrods}} = 2.5 \text{ psia}$$

Summing the two partial pressures yields the total cask pressure.

$$P_{\text{Total}} = P_{\text{cask backfill}} + P_{\text{fuelrods}}$$

$$P_{\text{Total}} = 25.8 \text{ psia} + 2.5 \text{ psia}$$

$$P_{\text{Total}} = 28.3 \text{ psia}$$

3.4.4.2 High Burnup Fuel Rod Canister Maximum Normal Conditions Internal Pressure

The high burnup fuel sealed canister is filled to one atmosphere (14.7 psia) upon loading. The canister internal pressure is calculated assuming that the average helium backfill gas temperature is 600°F (1060 R) and that 3 percent of the fuel rods fail in normal conditions of transport. The temperature of the canister gas is selected to conservatively bound the temperatures given in Table 3.4-10, Table 3.4-14 and Table 3.4-15. On failure, the fuel rods are assumed to release 30% of the fission gas and 100% of the rod backfill gas. To bound both the PWR and BWR analysis, the fuel type with the highest fission source, on a per rod basis, and smallest free gas volume inside the sealed canister is selected. This fuel type is the Exxon 7 × 7 BWR fuel. The fission gas inventory for this fuel is shown in Table 3.4-11, which reports the fission gas inventory for the assembly, and on a per rod basis. The design parameters for the Exxon 7 × 7 fuel rod are:

Parameter	Value
Number of Rods	49
Rod Diameter (in)	0.570
Clad Thickness (in)	0.036
Pellet Diameter (in)	0.4900
Active Fuel Length (in)	150
Rod Length (in)	170

From the values shown, the void volume of a single fuel rod is calculated as 4.82 in³ (78.99 cm³) by subtracting the volume of the fuel pellets from the volume of an empty fuel rod (the plenum spring volume is disregarded). For the analysis, 3% of 25 rods is taken to fail, which is 0.75 rods. Conservatively, the number of failed rods is defined as one, which is equal to a 4% fuel rod failure. The equivalent void volume is then equal to one rod, or 4.82 in³. The fission gas inventory, provided in Table 3.4-11, and the maximum normal transport temperature (600°F) are applied to the ideal gas law ($PV = nRT$) to obtain the pressure in the unruptured fuel rods due to the fission gases. This fission gas pressure, 4,251 psia (Table 3.4-11), is based on 100% availability of fission gases, which is adjusted to account for the 30 percent release of the fission gas. The releasable fission gas and rod backfill pressures are summed to obtain the total fuel rod pressure.

The ideal gas law is used to analyze the effects of pressure, temperature, volume, and gas inside the cask the ideal gas law states:

$$pV = nRT$$

where:

p = pressure (atm)

V = volume (liters)

n = gram-moles of material

R = gas constant (0.0831 atm-liters/K g-mole)

T = temperature (K)

After the rods rupture, the resultant internal cask pressure is impacted by three sources: the 1-atm inert gas backfill of the canister, the fission product gas escaping from the fuel rods, and the fuel rod inert gas backfill escaping from the ruptured fuel rods. To calculate the resultant internal cask pressure after the fuel rods rupture, partial pressures are calculated using Dalton's law:

$$P = P_a + P_b$$

where:

P = total pressure

P_a = partial pressure of gas A

P_b = partial pressure of gas B

The void volume of the fuel rod is simply the volume contained within the cladding less the fuel volume. The rod is modeled as a cylinder with a 0.570-in outside diameter, a 0.036-in. wall thickness, and a 150-in. active fuel length. The volume of the plenum spring is disregarded. The void volume, which includes the plenum volume, is 4.82 in³ per rod.

The partial pressure of the canister is calculated by:

$$P_{\text{canister}} = P_{\text{initial}} \left(\frac{V_{\text{canister}}}{V_{\text{total}}} \right)$$

where:

$$P_{\text{initial}} = P_{\text{atm}} * \frac{T_{\text{norm}}}{T_{\text{stand}}} = 14.7 \text{ psia} * \frac{588.7 \text{ K}}{295.35 \text{ K}} = 29.3 \text{ psia}$$

$$P_{\text{initial}} = 29.3 \text{ psia}$$

The minimum free gas volume is calculated as:

$$V_{\text{canister}} = 2,800 \text{ in}^3 - \pi * r_{\text{OD}}^2 * L_{\text{rod}} * 25 \text{ rods} = 2,800 \text{ in}^3 - \pi * \left(\frac{0.57 \text{ in}}{2} \right)^2 * 170 \text{ in.} * 25 \text{ rods}$$

$$= 2,800 \text{ in}^3 - 1085 \text{ in}^3 = 1715 \text{ in}^3$$

$$V_{\text{canister}} = 28.1 \text{ liters}$$

$$V_{\text{void}} = 4.82 \text{ in}^3 * (2.54 \text{ cm/in})^3 * 0.001 \text{ liters/cc} = 0.079 \text{ liters}$$

$$V_{\text{total}} = V_{\text{canister}} + 25 * 0.04 * V_{\text{void}} = 28.1 \text{ liters} + 0.04 * 25 * 0.079 \approx 28.2 \text{ liters}$$

$$V_{\text{total}} = \sim 28.2 \text{ liters}$$

This results in a P_{canister} of 29.3 psia.

Fission product gas inventories were obtained from Table 3.4-11. Using the ideal gas law, the initial pressure of each fission product gas is calculated based upon these inventories, the normal condition temperature (600°F), and the calculated void volume of the fuel (25 rods). The partial pressure of the fuel rod volume is calculated by:

$$P_{\text{fuel rods}} = P_{\text{initial}} \left(\frac{V_{\text{fuel rods}}}{V_{\text{total}}} \right)$$

where:

$$P_{\text{initial}} = 0.3 * P_{\text{fission}} + P_{\text{backfill}}$$

$$P_{\text{fission}} = 4251 \text{ psia}$$

$$P_{\text{backfill}} = P_{\text{initial}}^{\text{backfill}} * \frac{T_{\text{norm}}}{T_{\text{stand}}} = 75 \text{ psia} * \frac{588.7 \text{ K}}{295.35 \text{ K}} = 150 \text{ psia}$$

$$P_{\text{initial}} = \sim 1,425 \text{ psia}$$

$$V_{\text{fuel rods}} = \sim 0.079 \text{ liter (at 4\% of the total fuel rod volume)}$$

$$V_{\text{total}} = 28.2 \text{ liters} = V_{\text{canister}} + 25 * 0.04 * (V_{\text{void}})$$

$$P_{\text{fuel rods}} = 1425 \text{ psia} \left(\frac{0.079 \text{ liter}}{28.2 \text{ liters}} \right) = \sim 4.00 \text{ psia}$$

then:

$$P_{\text{total}} = P_{\text{canister}} + P_{\text{fuel rods}} = 29.3 \text{ psia} + \sim 4.00 \text{ psia} \approx 33.3 \text{ psia (2.3 atm)}$$

An additional analysis was performed for BWR high burnup rods (>45 GWd/MTU) with a 56% failure fraction to envelope damaged fuel rod shipments. This evaluation is conservative since damaged rods are likely to have released their gas inventory prior to shipment.

Following the methodology used for calculating the pressure given above and the calculated canister free gas volume of 29.2 liters, the resulting internal canister pressure from a 56% failed fuel fraction is 82.3 psia (~ 5.6 atm). The calculation follows.

$$\begin{aligned}
 P_{\text{canister}} &= P_{\text{initial}} * V_{\text{canister}} / V_{\text{total}} \\
 P_{\text{initial}} &= 29.3 \text{ psia} \\
 V_{\text{canister}} &= 28.1 \text{ liters} \\
 V_{\text{total}} &= V_{\text{canister}} + 14 * V_{\text{void}} = (28.1 \text{ liters}) + 14 * (0.079 \text{ liter}) = 29.2 \text{ liters} \\
 P_{\text{canister}} &= (29.3 \text{ psia}) * (28.1 \text{ liters}) / (29.2 \text{ liters}) = 28.2 \text{ psia} \\
 P_{\text{fuel rods}} &= P_{\text{initial}} * V_{\text{fuel rods}} / V_{\text{total}} \\
 P_{\text{initial}} &= 1,425 \text{ psia} \\
 V_{\text{fuel rods}} &= 14 * V_{\text{void}} = 1.108 \text{ liters} \\
 P_{\text{fuel rods}} &= (1,425 \text{ psia}) * (1.108 \text{ liters}) / (29.2 \text{ liters}) = 54.1 \text{ psia} \\
 P_{\text{total}} &= P_{\text{canister}} + P_{\text{fuel rods}} = 28.2 \text{ psia} + 54.1 \text{ psia} = 82.3 \text{ psia} = 5.6 \text{ atm}
 \end{aligned}$$

3.4.4.3 25-Rod Maximum Cask Cavity Internal Pressure-Normal Conditions

Following the methodology used for calculating pressure in Section 3.4.4.2, the cask free gas volume is calculated as:

$$\begin{aligned}
 V_{\text{cask}} &= 6,534 \text{ in}^3 - \pi * r_{\text{OD}}^2 * L_{\text{rod}} * 25 \text{ rods} = 6,534 \text{ in}^3 - \pi * \left(\frac{0.57 \text{ in}}{2} \right)^2 * 170 \text{ in} * 25 \text{ rods} \\
 &= 6,534 \text{ in}^3 - 1,085 \text{ in}^3 \\
 &= 5,449 \text{ in}^3
 \end{aligned}$$

$$V_{\text{cask}} = 89.32 \text{ liters}$$

Using this free gas volume in place of V_{canister} and the temperatures in Section 3.4.4.2, the cask cavity pressure resulting from a 3% fuel rod failure is 31 psia (~2.1 atm). This pressure is based on the assumption that the gases in the canister are released to the cask cavity. There are no design basis events that could result in the release of the gas in the canister to the cask cavity.

An additional analysis was performed for a bounding 25 BWR high burnup rod configuration (>45 GWd/MTU) containing up to 14 damaged rods. The damaged fuel rods are conservatively assumed to release the rod gas inventory during transport.

Following the methodology used for calculating the pressures given above and the cask free gas volume of 90.4 liters, the resulting internal cask pressure from a 56% failed fuel fraction is 46.4 psia (~ 3.2 atm). The calculation is outlined below.

$$\begin{aligned}
 P_{\text{cask}} &= P_{\text{initial}} * V_{\text{cask}} / V_{\text{total}} \\
 P_{\text{initial}} &= 29.3 \text{ psia} \\
 V_{\text{cask}} &= 89.3 \text{ liters} \\
 V_{\text{total}} &= V_{\text{cask}} + 14 * V_{\text{void}} = (89.3 \text{ liters}) + 14 * (0.079 \text{ liter}) = 90.4 \text{ liters} \\
 P_{\text{cask}} &= (29.3 \text{ psia}) * (89.3 \text{ liters}) / (90.4 \text{ liters}) = 28.9 \text{ psia} \\
 P_{\text{fuel rods}} &= P_{\text{initial}} * V_{\text{fuel rods}} / V_{\text{total}} \\
 P_{\text{initial}} &= 1,425 \text{ psia} \\
 V_{\text{fuel rods}} &= 14 * V_{\text{void}} = 1.108 \text{ liters} \\
 P_{\text{fuel rods}} &= (1,425 \text{ psia}) * (1.108 \text{ liters}) / (90.4 \text{ liters}) = 17.5 \text{ psia} \\
 P_{\text{total}} &= P_{\text{cask}} + P_{\text{fuel rods}} = 28.9 \text{ psia} + 17.5 \text{ psia} = 46.4 \text{ psia} = 3.2 \text{ atm}
 \end{aligned}$$

3.4.4.4 Maximum Cask Cavity Internal Pressure for the General Atomics IFM

The combined heat load of the two GA IFM FHUs is 13 watts. This heat load is distributed between two separate canisters, which have a length of approximately 40 inches. As a result, the heat generation, which would result in a temperature differential between the cavity and ambient, is insignificant.

The internal pressure in the LWT cask cavity is due to the fission gas release from the TRIGA fuel or HTGR fuel pellets in conjunction with the cavity being heated by solar insolation. No credit is taken for the pressure retention capability of the FHUs. The internal pressure that may result from the 20 TRIGA fuel rods in the GA IFM is significantly enveloped by that of the 120 TRIGA fuel rods, which are authorized for transport in the NAC-LWT cask. Likewise, the fission gas release by the HTGR elements is considered to be bounded by the current design basis PWR fuel. Since the free volume for the GA IFM shipment is significantly larger than for the design basis PWR fuel assembly with the PWR basket, the pressure increase in the cavity gas due to the GA IFM shipment is considered to be significantly bounded by the design basis condition in the current NAC-LWT cask. Therefore, the current design pressure of 50 psig for the cask cavity envelopes the cask cavity pressure for the GA IFM contents.

3.4.4.5 TPBAR Shipment Cask Cavity Internal Pressure-Normal Conditions

The method employed in the TPBAR (Tritium Producing Burnable Absorber Rod) shipment evaluation is similar to that employed in the fuel rod evaluations where the cask cavity free volume and molar gas quantities are combined with the ideal gas law ($PV=nRT$) to determine system pressure. The bounding TPBAR content condition consists of up to 300 production TPBARs (of which two can be prefailed) placed in a consolidation canister and loaded into a NAC-LWT with a TPBAR basket installed in the cavity.

A typical TPBAR is composed of a steel clad rod 0.381 inch in diameter, with a maximum length of 154.15 inches, and a minimum internal free volume of 5.727 inch³. The TPBARs are located in a consolidation canister composed of three primary pieces: canister body, top insert, and bail. A spacer, attached to the NAC-LWT cask lid, assures that rods remain within the canister envelope and provides support to both the basket and canister under end-drop conditions. The TPBAR basket is a modified NAC-LWT PWR basket that increases the cavity free volume from that provided by a standard PWR basket design.

For conservatism in determining the cask internal pressure, the 298 TPBARs that are not prefailed at loading are assumed to undergo cladding failure during normal transport conditions. Prefailed rods have cladding damage that allows reactor coolant or spent fuel pool water to enter the rod cavity. Cladding failure during transport results in the release of the rod helium backfill gas, helium gas generated during the tritium production, and a portion of the tritium gas produced. For rods not prefailed, the majority of the tritium is locked in the TPBAR structure and is not released during normal or accident conditions of cask transport. Tritium release from intact or in-cask prefailed rods is limited to 55 Ci/rod (0.0019 mole – See Chapter 1, Appendix 1-B) versus a helium release of 0.42 mole per rod after the 90-day cool-down period. A conservative tritium release of 100 Ci per rod is applied in this calculation. After the 90-day cool-down period, the helium release increases according to the decay of tritium.

$${}^3\text{He}[\text{moles}](t) = 0.398 \times \left(1 - \exp\left(\frac{-\ln(2)t}{12.33}\right) \right)$$

The remaining two rods in the 300 TPBAR shipment are assumed to be prefailed and waterlogged. These rods contain a maximum of 7.5 moles of H₂O and 0.199 moles of T₂O (1.2 grams H₂), 2% of which dissociate into their constituent gases due to elevated temperatures in the cask cavity (see Chapter 1 appendices). The NAC-LWT is vacuum dried prior to transport, removing water from the cask cavity. This process is expected to remove water from the prefailed rod. The water content is conservatively assumed to remain in the rods for the pressure

calculated. After dissociation, the total gaseous inventory in each prefailed TPBAR is 7.78 moles.

Cask cavity gases after rod failure are therefore comprised of the cask helium backfill (one atmosphere at loading); the combined helium rod backfill, helium generated during the tritium production, helium production from tritium decay, and the tritium release itself (298 rods); and the molar inventory of the two prefailed, waterlogged rods. The total free volume available for the gas is the cask cavity volume plus the internal free volume of the failed rods, minus the canister, spacer, basket, and rod volumes.

Description (Based on 300 Rods Failing)	Volume [cm ³]
Cavity (Empty)	4.10E+05
TPBAR Rod (Based on Exterior Rod Dimension)	-8.64E+04
TPBAR Minimum Free Interior	2.82E+04
TPBAR Consolidation Canister	-1.40E+04
TPBAR Basket	-8.49E+04
Cask Cavity Spacer	-5.55E+03
Cask Free volume (300 Rods Failed)	2.47E+05

The free volume in the canister cavity for intact rods is $2.19 \times 10^5 \text{ cm}^3$. Applying a conservative volume $2.4 \times 10^5 \text{ cm}^3$ to calculate the cask backfill molar quantity yields 9.98 moles of helium. The backfill conditions at sealing used in the calculation are one atmosphere pressure and a temperature of 68°F. The backfill pressure is specified in the operating procedure, while 68°F is conservative for the cask with a heat-generating payload.

Again employing the ideal gas law with a total 152 moles of gas (298 rods releasing 0.42 moles of helium and 0.003 mole of tritium, two waterlogged rods releasing 7.78 moles each, plus the 10.27 moles cask backfill), a conservative free volume of $2.47 \times 10^5 \text{ cm}^3$, and the normal condition average gas temperature of 246°F, yields an operating pressure of 276 psig at the end of a 90-day cooldown. For a period of one year following the 90-day cooldown and considering a fixed gas temperature of 246°F, the pressure increases to 289 psig (MNOP). System pressure at cool times greater than 90 days will be lower due to the decreased heat loads associated with the radioactive decay of the payload.

The TPBAR content condition of 55 segmented TPBARs contained in a sealed waste container is bounded by the pressure analyses performed for the fully loaded TPBAR consolidation canister. The contents include segments, debris and vented shrouds, all placed in a vented inner storage container within the welded waste container. Due to the condition of the TPBAR segments and

the cooling period since irradiation, the heat load of the waste container is 0.127 kW, significantly less than the 0.693 kW analyzed for the production TPBAR content condition of 300 TPBARs in an open consolidation canister.

Each of the 55 TPBARs is assumed to contain a maximum of 1.2 grams of tritium at the time of sealing the waste container, and all backfill gases have been vented. For the purpose of the maximum pressure analysis, all of the contained tritium is assumed to decay to He^3 , resulting in a total of 66 grams of He^3 . Note that the confinement boundary of the welded waste container is assumed to fail during normal transport conditions. Due to the state of the TPBAR segments and the loading of the materials in dry loading conditions, no water will be present in the waste container. Conservatively assuming that the cask free volume and gas temperature for the transport of the waste container is the same as that for the production TPBAR contents listed previously ($2.47 \times 10^5 \text{ cm}^3$), the calculated maximum normal operating pressure (MNOP) for the 55 segmented TPBARs in the waste container is less than 65 psia. Therefore, the MNOP for the 55 segmented TPBAR content condition is conservatively bounded by the MNOP of the 300 production TPBARs in the consolidation canister of 289 psig.

Combustible Hazard Assessment

Hydrogen may be released by prefailed, waterlogged TPBARs (TPBARs damaged during in-core use or in-pool storage) primarily in the form of water, tritiated water, and potentially some tritiated methane. Each prefailed TPBAR has the potential to release the tritium assumed to dissociate from tritiated water (0.004 moles) as well as up to 0.15 moles hydrogen gas dissociated from 7.5 moles of H_2O . Both the hydrogen and the tritium gas, as well as the water and tritiated water, will be removed from the cask during vacuum drying prior to helium backfill.

The flammability/ignitability characteristics of tritium (T_2) in the presence of oxygen are substantially the same as for hydrogen (H_2). Hydrogen in air reaches a lower flammability limit at 4% volume.

Tritium escapes intact TPBARs in the form of molecular tritium gas at a rate of less than 0.12 mCi/hr/TPBAR. For a one-year transport period and a 300 TPBAR payload this rate results in a release of less than 0.01 moles of T_2 gas. Given a helium gas back-fill of approximately 10 moles helium (1 atmosphere) no flammability hazard exists for intact TPBARs.

Tritium may be released by event-failed (in-cask failed) TPBARs in the form of tritiated methane (CH_4) or tritiated water. Event-failed TPBARs may release up to 55 Ci of tritium. This translates to approximately 0.002 mole of tritium that may be released from a TPBAR in conjunction with 0.42 mole of helium.

The 55 equivalent TPBARs, in segments and debris, may release up to 100% of the tritium contained in the pellets during transport. The pellets contain approximately 40% of the tritium quantity in the TPBAR. At NAC-LWT normal and accident conditions temperatures, the TPBAR components release tritium primarily as tritiated water with only a small fraction (maximum 2%) as gaseous tritium (see Appendix 1-B of Chapter 1). During a one-year transport, an additional maximum 1% of the tritiated water may undergo radiolysis and dissociate. Conservatively applying a maximum 3% release rate to the 55 equivalent TPBAR total inventory of 66 grams (1.2 grams per rod) yields an inventory of 0.33 moles T_2 . Based on an inert gas cask backfill in excess of 10.3 moles, a bounding estimated maximum hydrogen (T_2) volume fraction of 3.1% is calculated. Therefore, no flammability hazard will exist for the 55 segmented TPBAR content condition.

3.4.4.6 Maximum Internal Pressure for PULSTAR Fuel Element Payload

Based on the allowable loading configurations for PULSTAR fuel elements, cask internal pressures are calculated for a payload of 28 intact assemblies and a mixed payload of 14 intact assemblies and the equivalent of 14 canned assemblies. A payload of 28 4×4 intact rod inserts is bounded by either of these evaluated payloads.

The ideal gas law and Dalton's law of partial pressures are used to calculate internal pressures. Cask, can, and element backfill initial conditions are taken as a pressure of 1 atm and a temperature of 68°F.

PULSTAR fuel element and fuel assembly dimensions are summarized in Table 3.4-18. Elements are UO_2 pellets clad with zirconium alloy. A PULSTAR fuel assembly is a 5×5 rectangular array of elements with aluminum upper and lower fittings.

Based on the PULSTAR fuel element, PULSTAR failed fuel can, MTR basket stack, and NAC-LWT cavity dimensions, volumes are calculated and summarized in Table 3.4-19.

The remaining two inputs to the pressure calculation are the temperature and fission gas inventory. For conservatism, the average gas temperature applied is the maximum TRIGA fuel clad temperature of 295°F. The TRIGA temperatures are applicable to the PULSTAR fuel element evaluation as discussed in Section 3.4.1.13. The fission gas inventory is taken from the SAS2H results discussed in Chapter 5 and is shown in Table 3.4-20.

For a payload of 28 intact PULSTAR fuel assemblies, the partial pressures of the cask, element (rod) backfill, and fission gases are summed. The cask free volume is 217 liters and is calculated by subtracting the basket stack volume and the assembly envelope volume (multiplied by 28)

from the cavity volume. The partial pressure of the cask, P_{Cask} , is simply the initial backfill pressure multiplied by the temperature ratio:

$$P_{\text{Cask}} = 1 \text{ atm} \frac{419.26 \text{ K}}{293.15 \text{ K}} = 1.430 \text{ atm}$$

The cask partial pressure due to a 100% release of element backfill, $P_{\text{RodBackfill}}$, is the initial backfill pressure multiplied by the temperature ratio and the backfill-to-cask volume ratio:

$$P_{\text{RodBackfill}} = 1 \text{ atm} \frac{419.26 \text{ K}}{293.15 \text{ K}} \frac{2.7 \text{ liters}}{217.0 \text{ liters}} = 0.018 \text{ atm}$$

Only 3% of this pressure contributes to the total pressure under normal conditions.

The cask partial pressure due to a 100% release of the element fission gases, $P_{\text{FissionGas}}$, is calculated using the Ideal Gas Law:

$$P_{\text{FissionGas}} = \frac{28 \cdot 0.448 \cdot 0.08205 \cdot 419.26}{217} = 1.989 \text{ atm}$$

Only 30% of the fission gases are released, and only 3% of the resultant pressure contributes to the total pressure under normal conditions.

The total cask pressure is the sum of the partial pressures, adjusted by the relevant release fractions:

$$P_{\text{Total}} = P_{\text{Cask}} + 0.03 \cdot P_{\text{RodBackfill}} + 0.03 \cdot 0.30 \cdot P_{\text{FissionGas}}$$

$$P_{\text{Total}} = 1.430 + 0.03 \cdot 0.018 + 0.03 \cdot 0.30 \cdot 1.989 = 1.449 \text{ atm}$$

Cask internal pressure for a mixed payload is calculated in a similar fashion, with a smaller cask free volume due to the difference in can and assembly envelope volume, and an assumed 100% failure rate of PULSTAR elements in either the screened or sealed can. The calculated maximum cavity pressure is 1.8 atm. Pressure in the sealed can is based on a 100% failure rate, the can cavity volume, and a payload equivalent in volume to 25 intact PULSTAR fuel elements. Normal condition pressure in the sealed can is 4.4 atm.

A summary of the pressure calculations is given in Table 3.4-21.

3.4.4.7 Maximum Internal Pressure for 16 PWR MOX/UF₆ Fuel Rods in a Rod Holder

Based on the allowable loading of up to 16 PWR MOX/UF₆ fuel rods, cask internal pressures are calculated. Bounding cask free volume, gas temperatures, and rod backfill pressure are directly obtained from the BWR high burnup rod evaluations in Section 3.4.4.3.

Variable	Unit	Value
Cask Free Volume (PWR Basket with Insert/Canister/Rod Holder)	in ³	5908
Normal Condition Cask Average Gas Temperature	°F	600
Normal Condition Cask Backfill Partial Pressure (at temperature)	psia	29.3
PWR Fuel Rod Backfill Pressure	psia	565

These values are combined with a conservative 2.9 in³ fuel rod free volume and SAS2H calculated fission and actinide gas inventories to determine system pressure. The 2.9 in³ free rod volume applied here is larger than the UO₂ rod volume previously employed (2.5 in³) to account for additional volume designed into the MOX rods to counter any potential increase in fission gas release from the PuO₂ / UO₂ MOX fuel mixture.

The ideal gas law and Dalton's law of partial pressures are used to calculate internal pressures by combining cask backfill, rod backfill, and fission/actinide gases. Fill temperature applied to the rod gases is 22°C (standard temperature). Maximum fission and actinide gas inventories were obtained from 80 GWd/MTHM fuel rod, 3% enriched ²³⁵U or 3 wt % fissile Pu, SAS2H output sets. The fuel rod corresponds to the maximum fissile mass defined in the shielding source term calculations. SAS2H runs produced a total gas inventory of 0.29 moles per rod (99+% fission gas), with bounding values obtained from the UO₂ rods (MOX rods produce approximately 98% of the UO₂ rod fission gas). Gas inventories increase as a function of reduced initial fissile material content. A 3% enrichment and/or 3% fissile Pu content is significantly below levels required to reach an 80 GWd/MTHM burnup level.

The resulting normal condition pressure for a failure fraction of 1/16 (bounds the 3% normal condition PWR rod failure fraction in the Standard Review Plan, NUREG-1617, Supplement 1) and 30% fission gas release is 17.2 psig (31.9 psia, or 2.2 atm).

Parametric studies are performed on the number of rods failing and the release fraction under normal conditions with an applied limit of 50 psig (normal condition structural analysis input value). Normal condition failure of up to 13 rods, at 100% gas release, remains below 50 psig. A similar analysis results in a maximum normal condition pressure of 48.5 psig for a normal condition failure of all 16 rods at a 75% fission gas release fraction (100% of backfill gas is released). Given that each of the rods is individually located within a support tube, no normal condition rod failures are expected during transport.

3.4.5 Maximum Thermal Stresses

The conditions within the range of normal transport conditions and fabrication that result in the limiting combination of thermal gradient and isothermal stresses have been evaluated. The

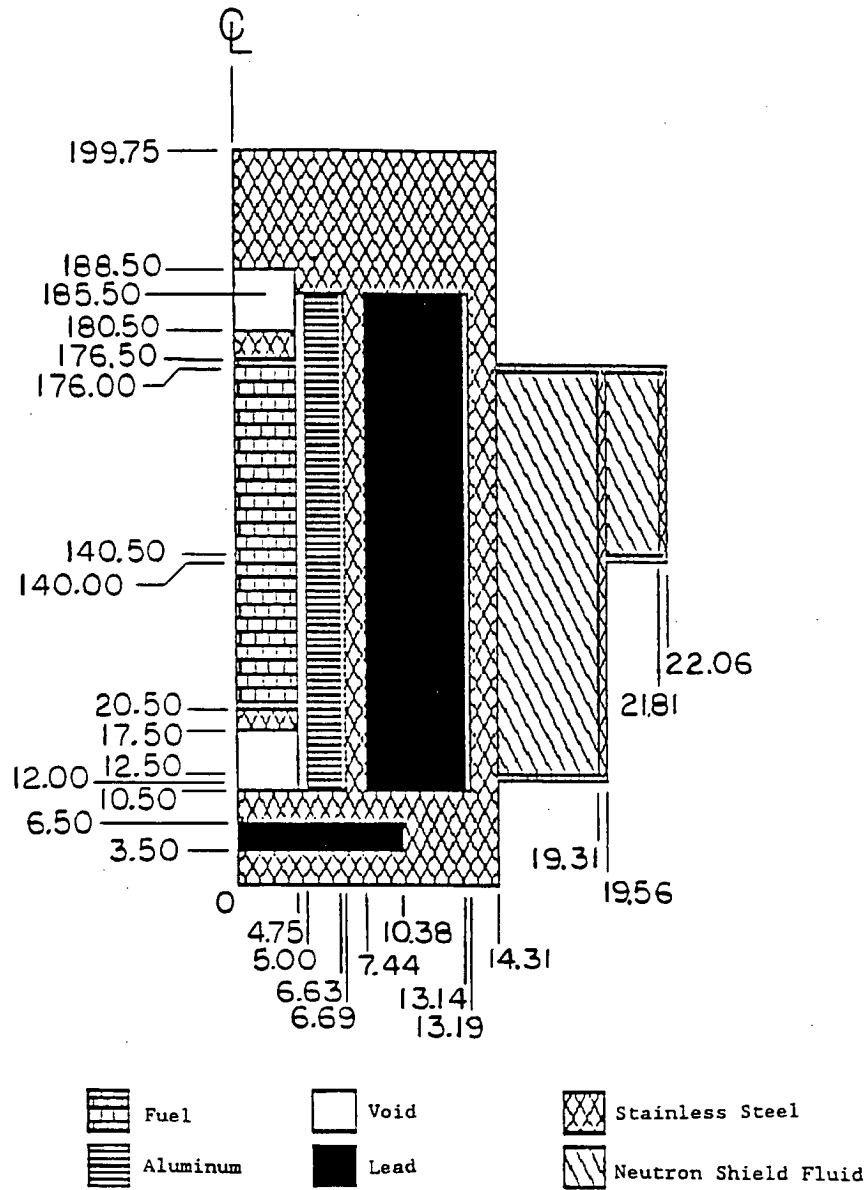
analyses are performed in Sections 2.5 through 2.7. The resulting isothermal temperature plots are presented in Section 2.10.3.

3.4.6 Evaluation of Package Performance for Normal Conditions of Transport

Section 3.4 provides analyses of the NAC-LWT cask thermal performance for normal transport conditions. The analyses demonstrate that the NAC-LWT cask thermal performance meets the criteria of 10 CFR 71 for normal transport conditions.

The maximum fuel rod cladding temperature under normal transport conditions is 472°F. This is well below the temperatures that can cause fuel rod cladding deterioration. Components important to safety remain within their safe operating ranges (Section 3.3) during normal transport conditions. Thermally induced stresses (in combination with pressure and mechanical load stresses) are less than allowable stresses as shown in Section 2.6. Thus, the analyses of Section 3.4 demonstrate that the NAC-LWT cask fulfills the heat rejection criteria established in Section 3.1 for normal transport conditions.

Figure 3.4-1 HEATING5 Normal Transport Conditions Thermal Model



(Dimensions in inches)

Figure 3.4-2 Design Basis PWR Fuel Assembly Axial Flux Distribution

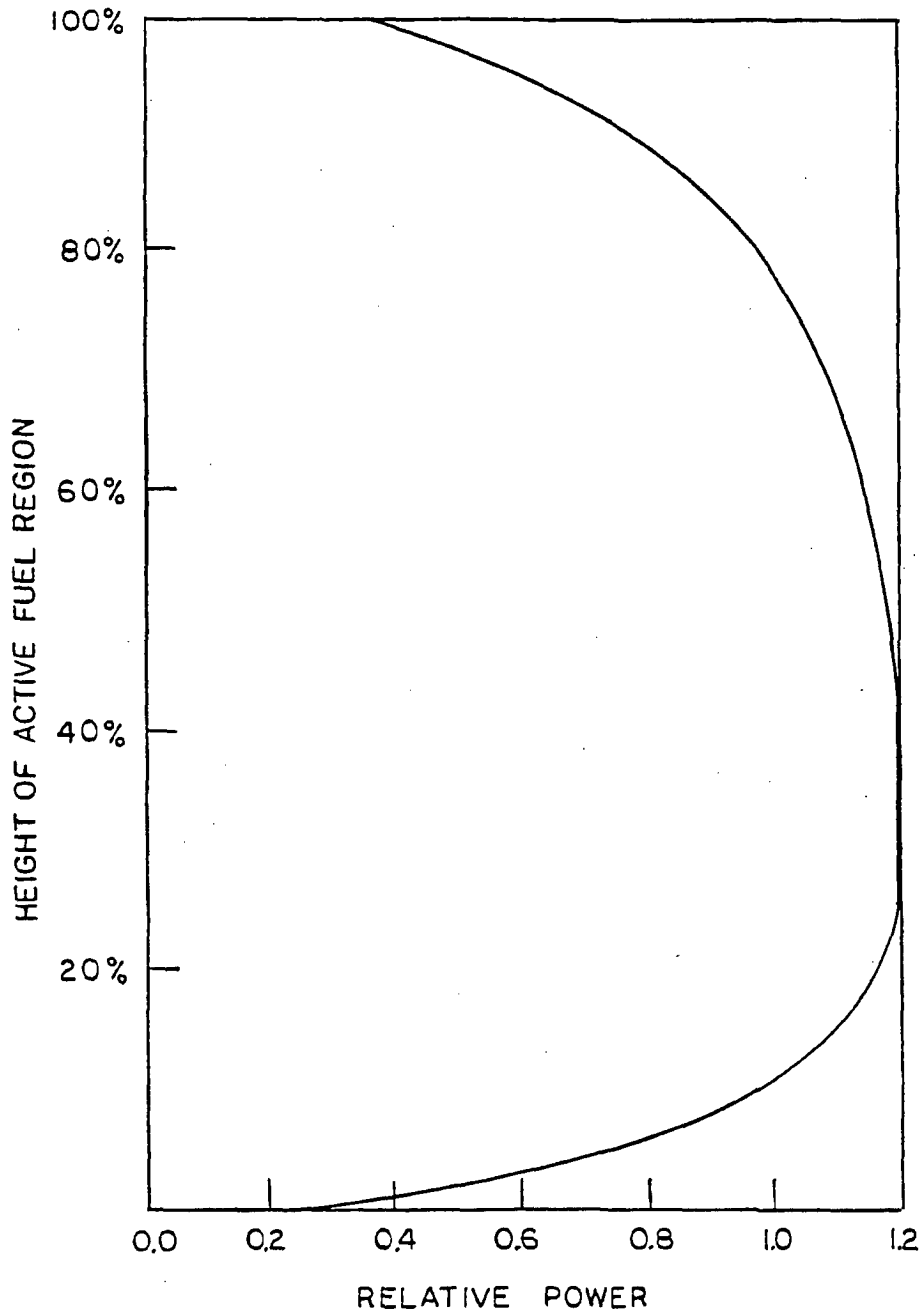


Figure 3.4-3 ANSYS MTR Fuel Design Basis Heat Load Thermal Model
(Uniform 30-Watt/Element Configuration Heat Load)

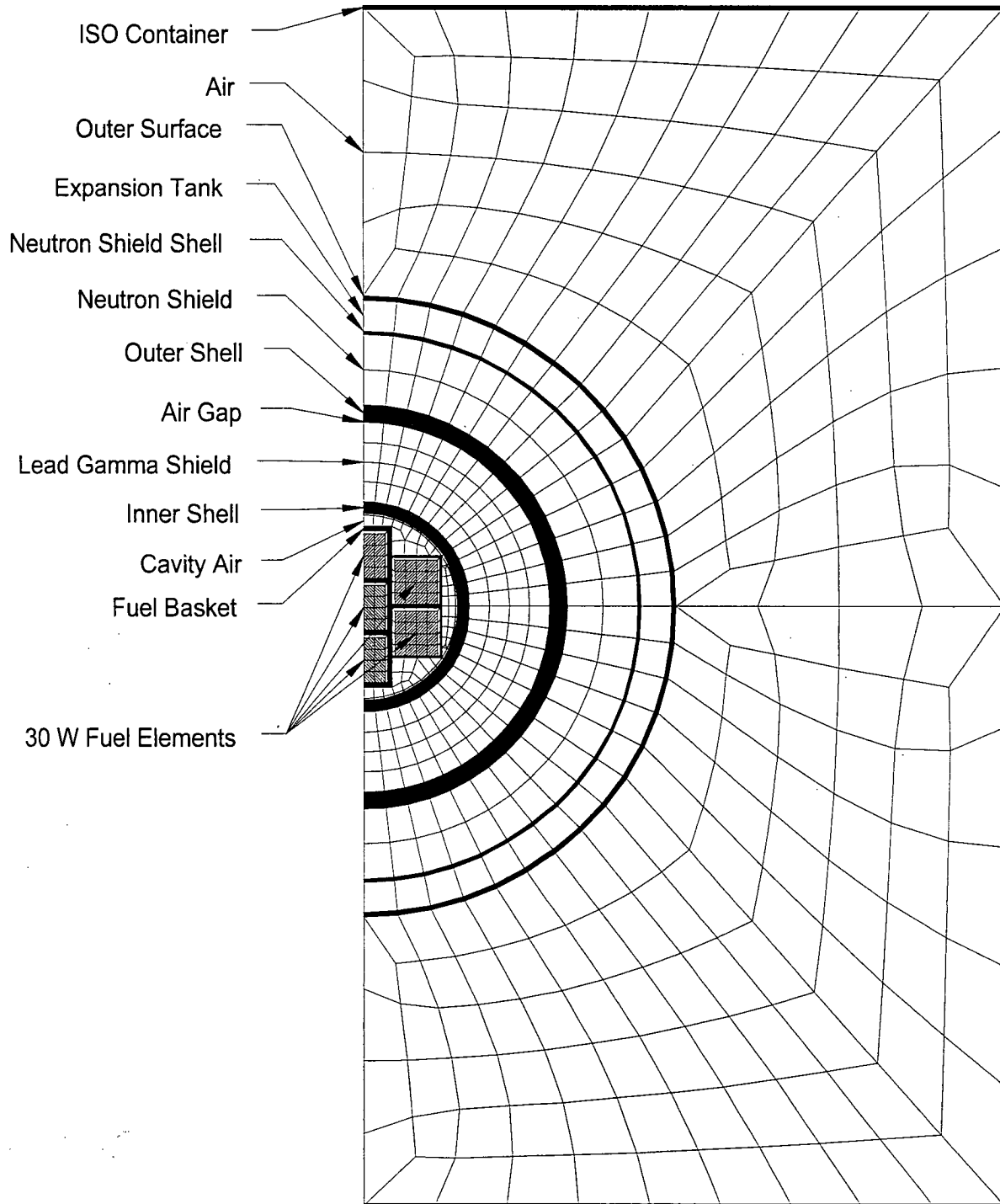


Figure 3.4-4 MTR Fuel Variable Decay Heat ANSYS Thermal Model
(120-Watt / 70-Watt / 20-Watt Configuration Heat Load)

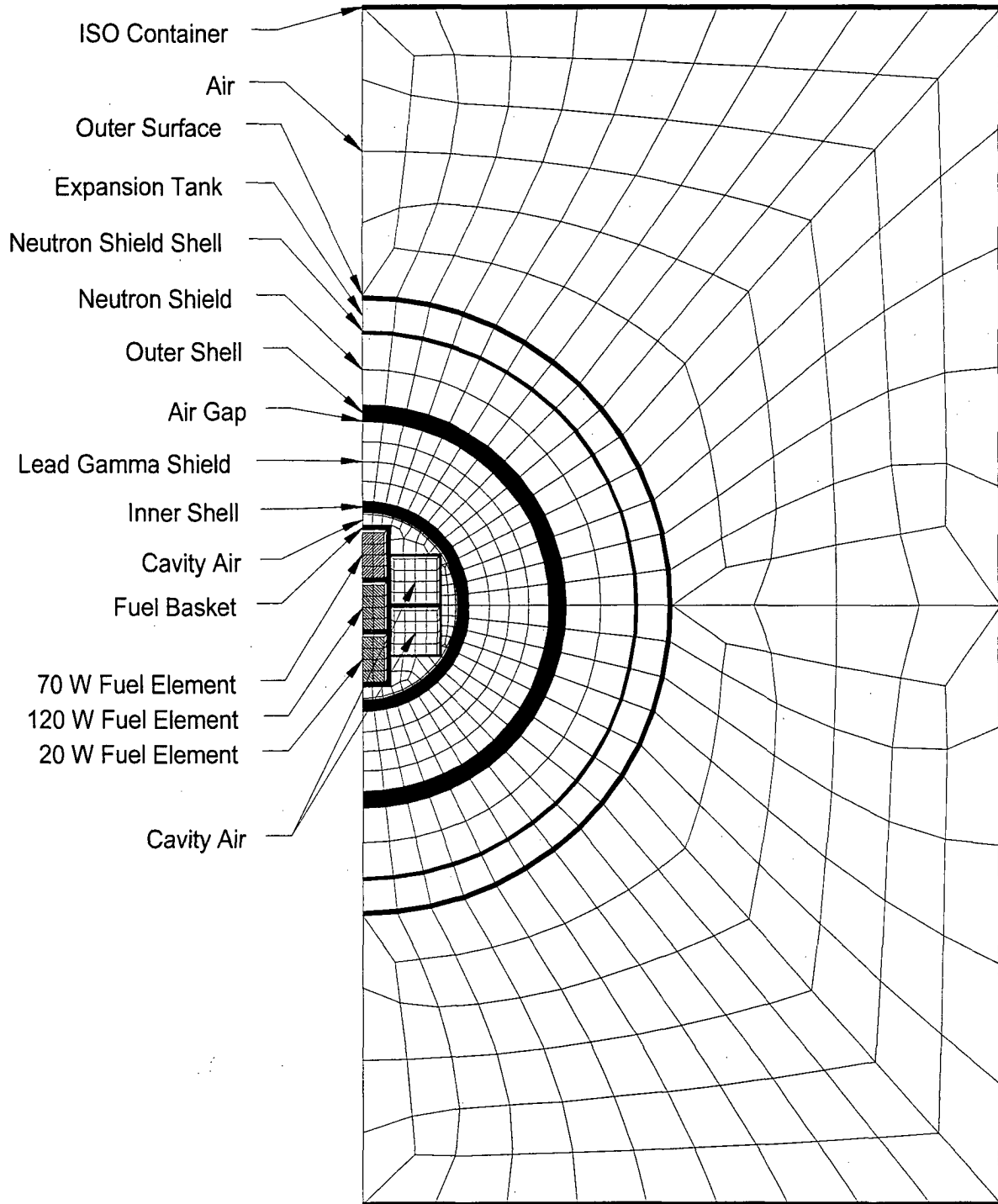
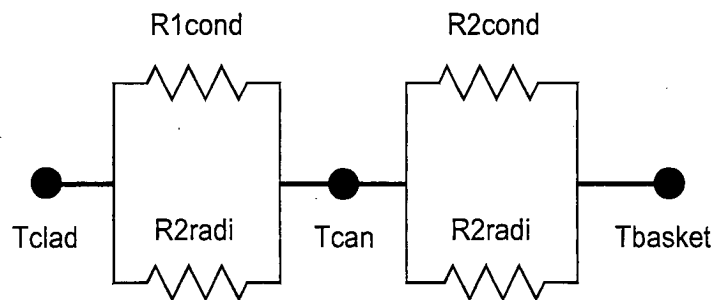
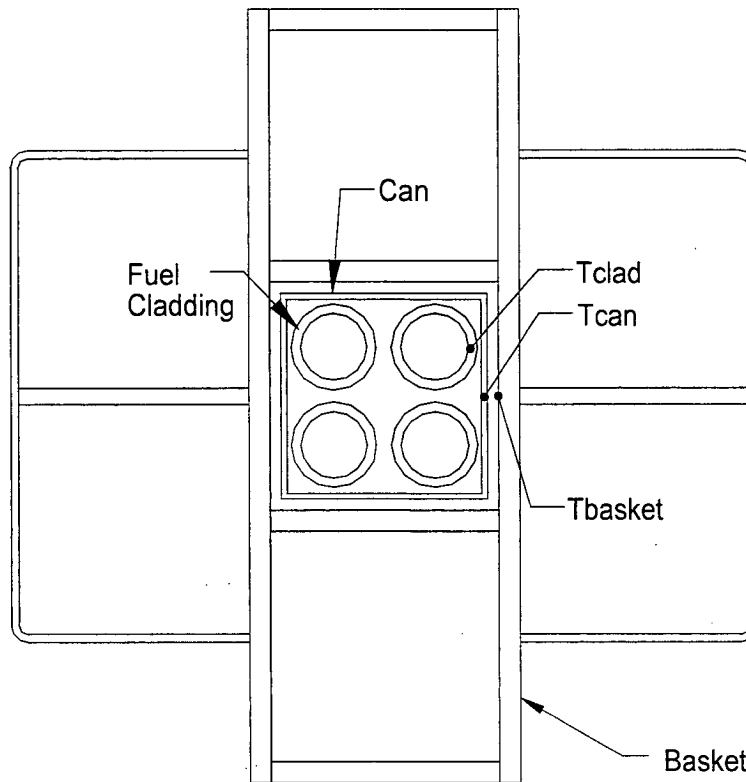


Figure 3.4-5 Thermal Resistance Model for TRIGA Fuel Elements



Where:

- R_{cond} = Thermal resistance for conduction
- R_{radi} = Thermal resistance for radiation
- T_{basket} = Maximum basket temperature
- T_{can} = Maximum can temperature
- T_{clad} = Maximum fuel cladding temperature

Figure 3.4-6 Modeling Details for the MTR Fuel Assembly Resting on the Surface of the NAC-LWT MTR Basket

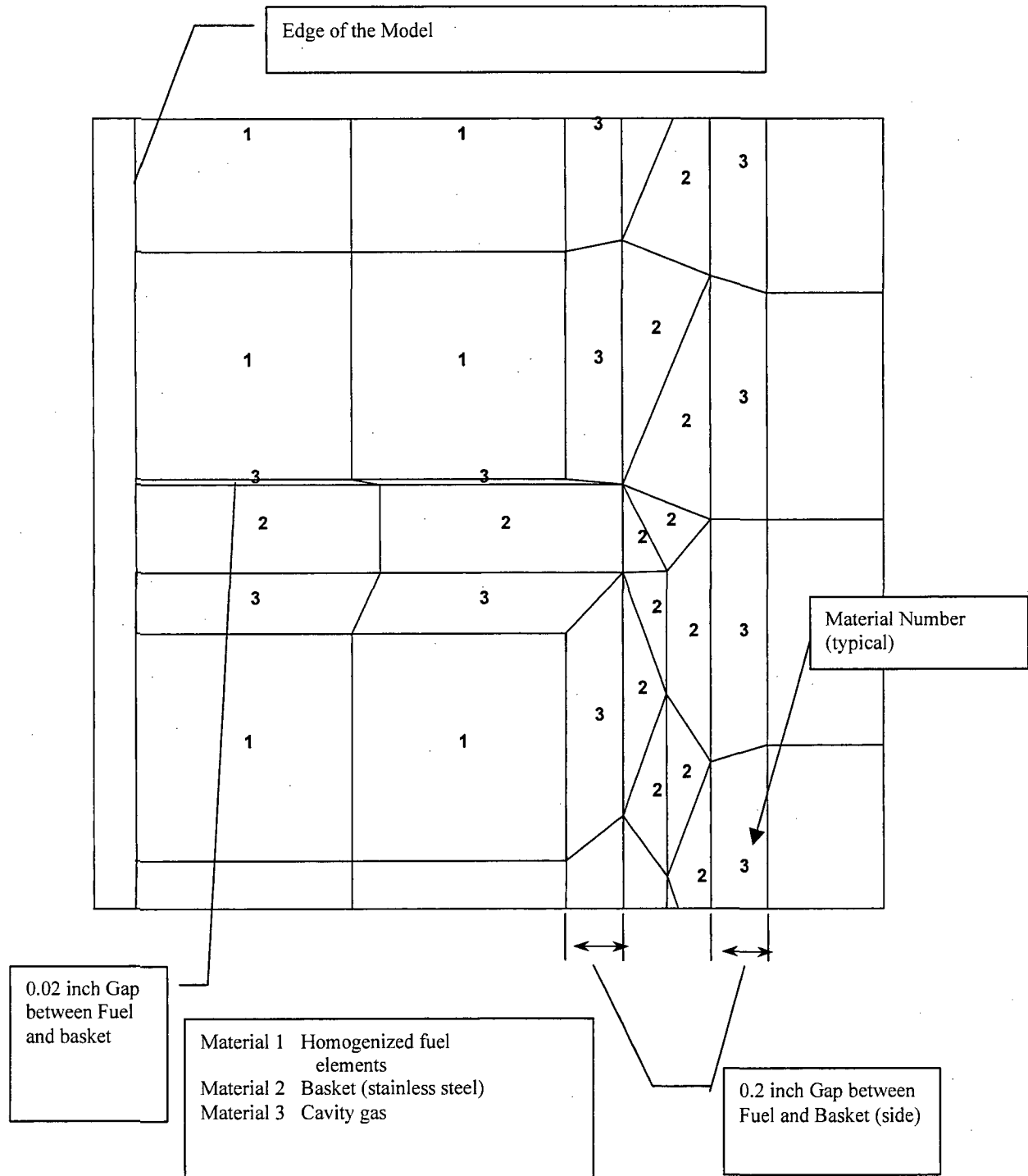


Figure 3.4-7 Finite Element Thermal Model for TRIGA Fuel Cluster Rods

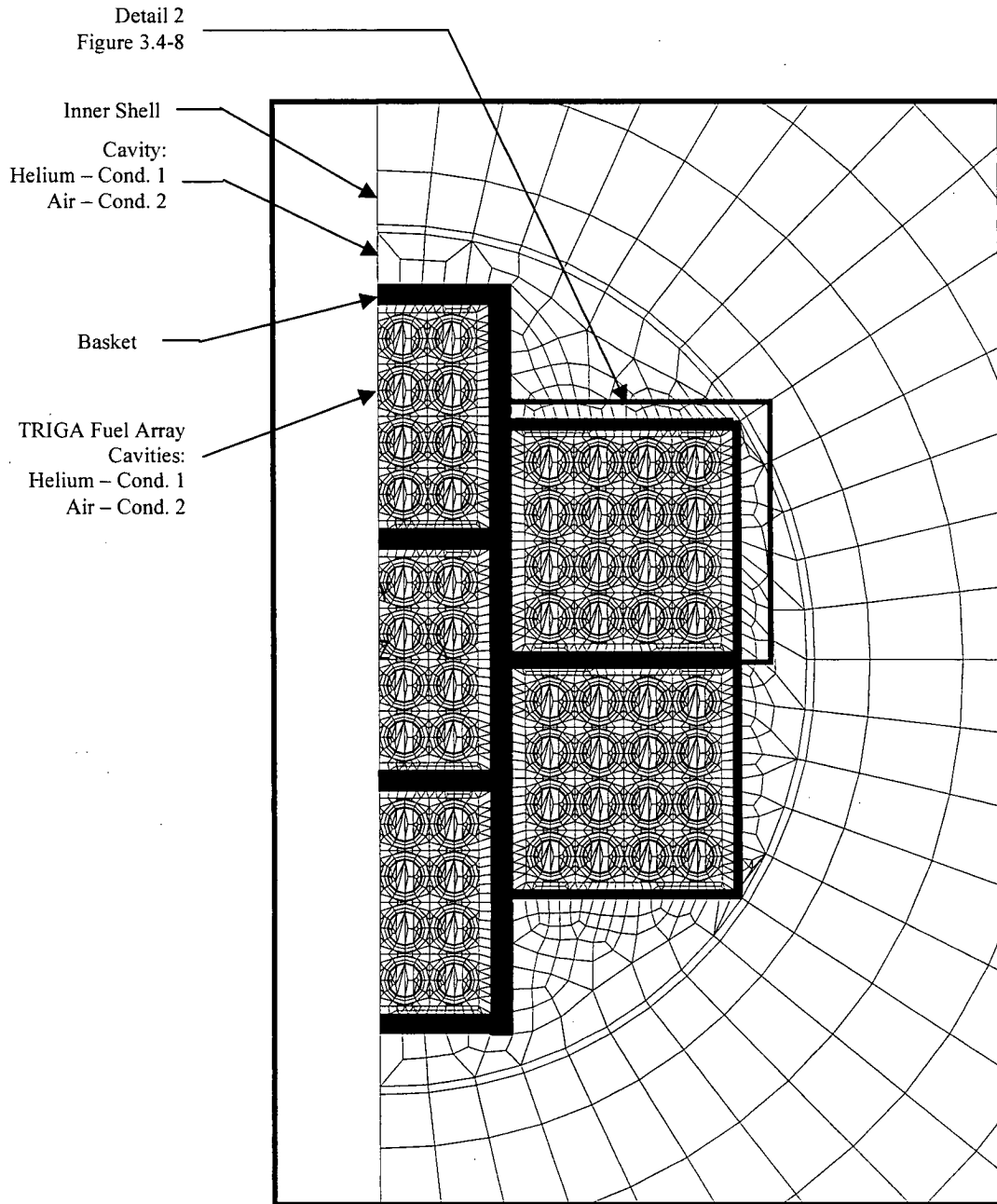


Figure 3.4-8 Details of the TRIGA Fuel Cluster Rods in the Finite Element Model

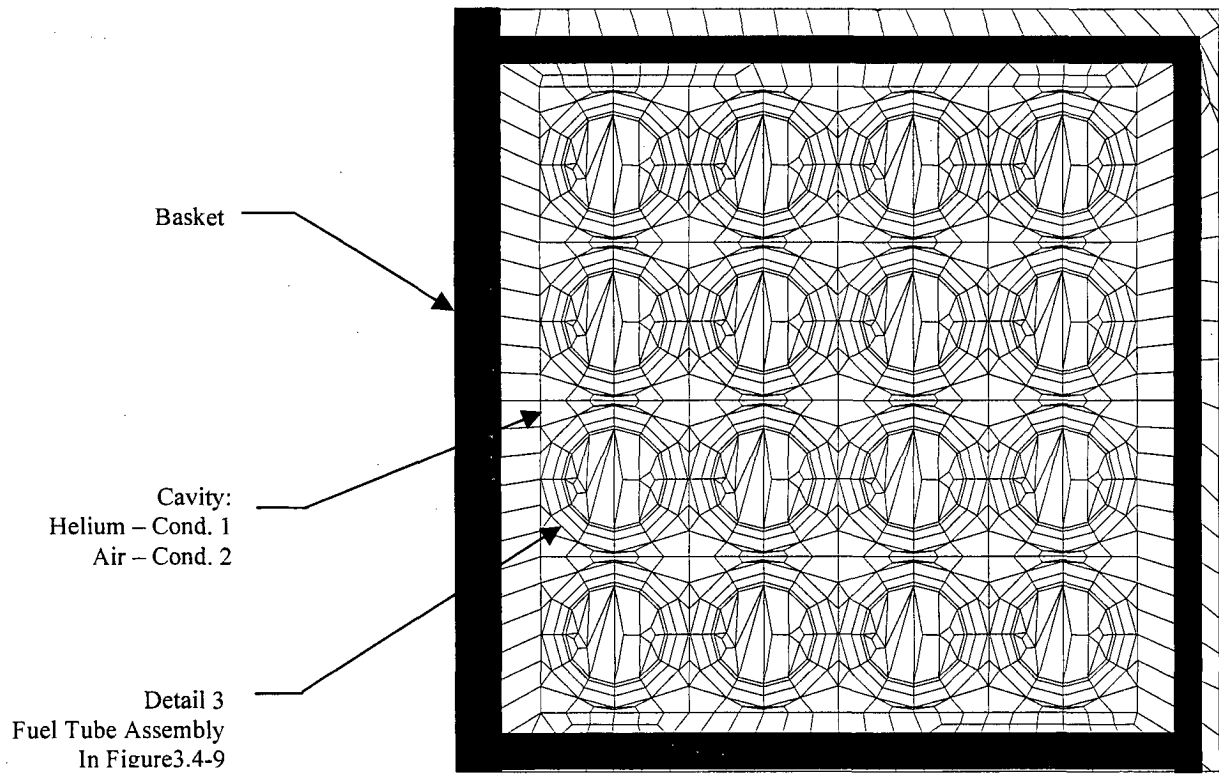


Figure 3.4-9 Individual TRIGA Fuel Cluster Rod Finite Element Model Details

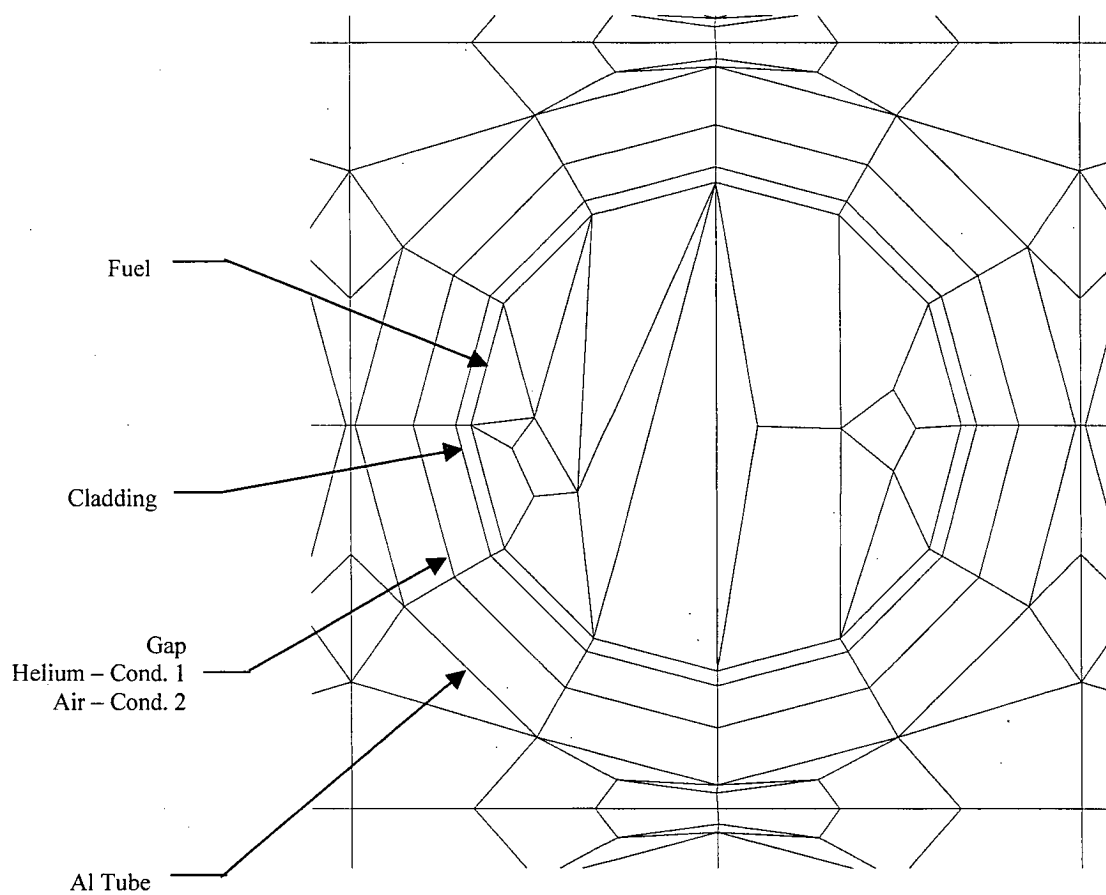


Figure 3.4-10 PWR and BWR High Burnup Fuel Rods Normal Condition ANSYS
Thermal Model (Condition 1)

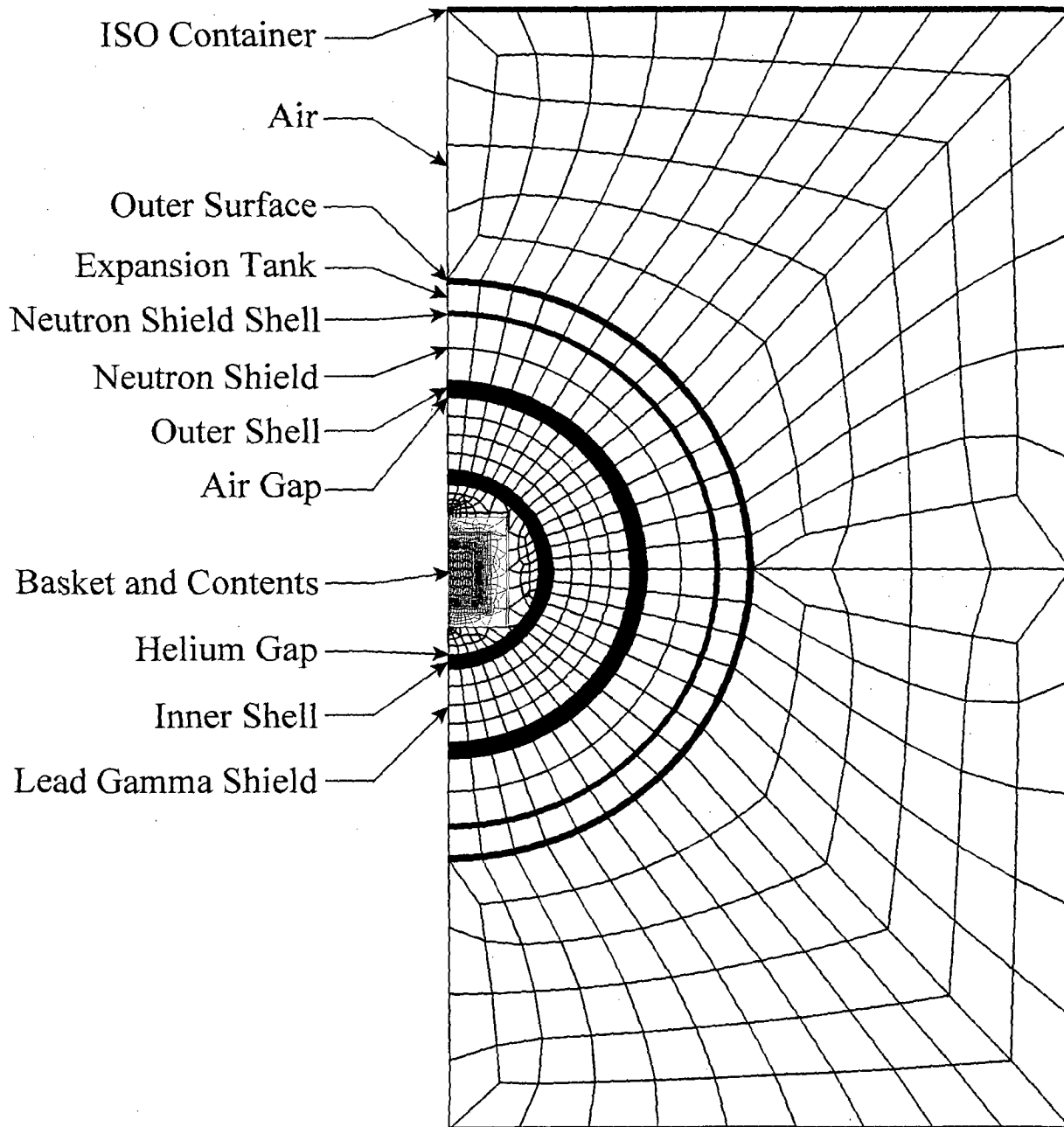
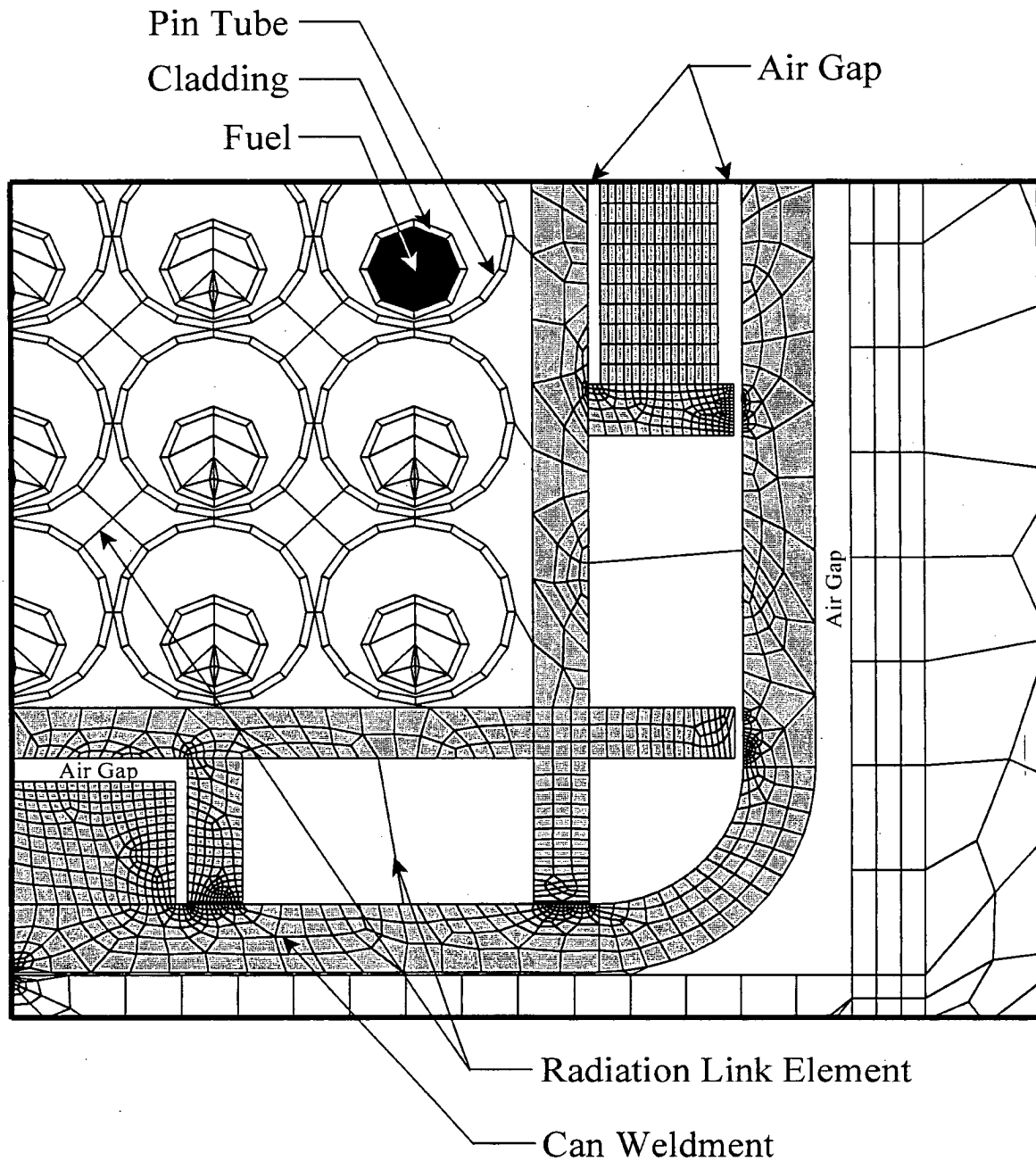


Figure 3.4-11 Close-up of PWR and BWR High Burnup Fuel Rods Normal Condition
ANSYS Thermal Model



Note: air elements are not shown for clarity.

Figure 3.4-12 PWR and BWR High Burnup Fuel Rods Normal Condition ANSYS Thermal Model (Condition 2)

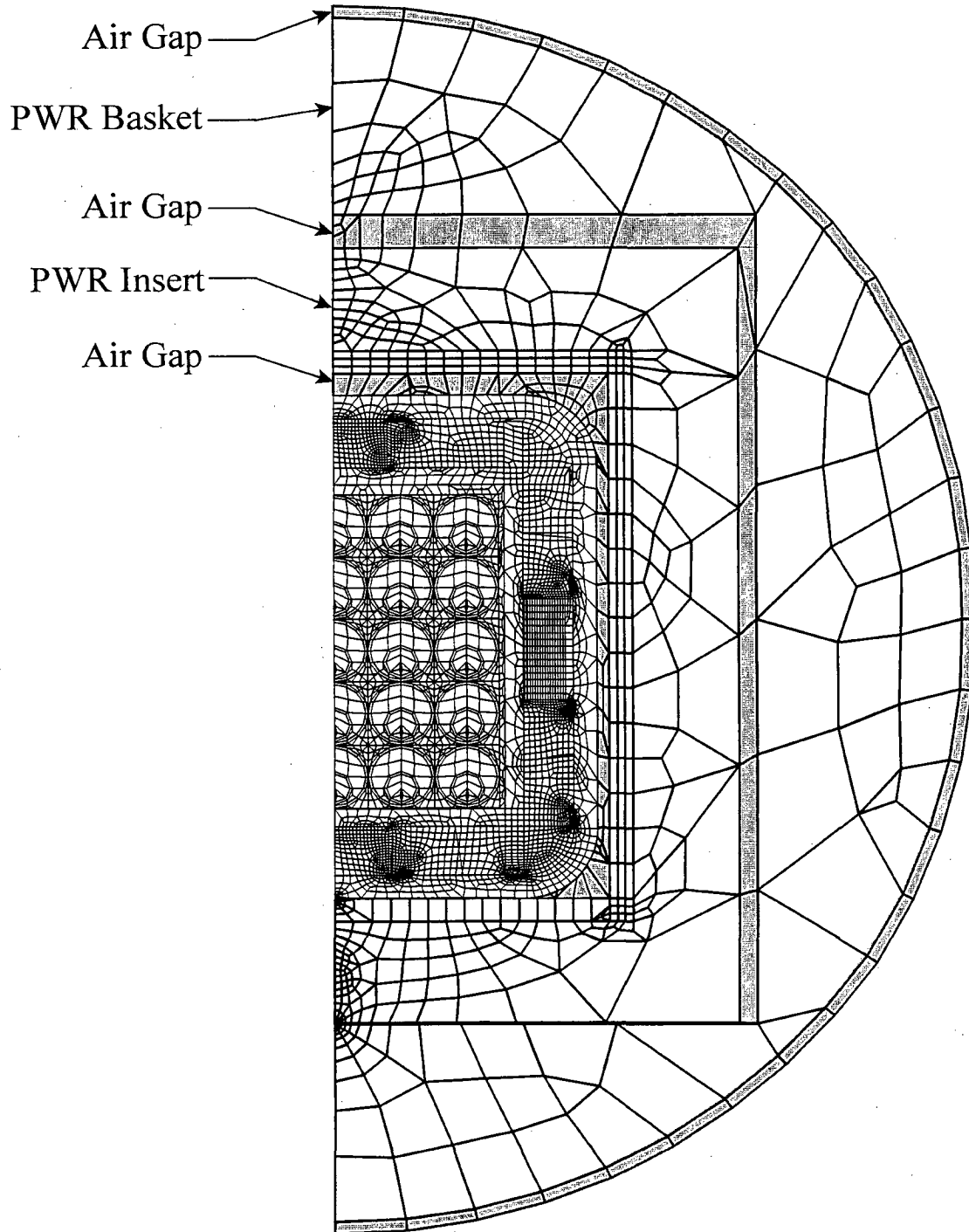
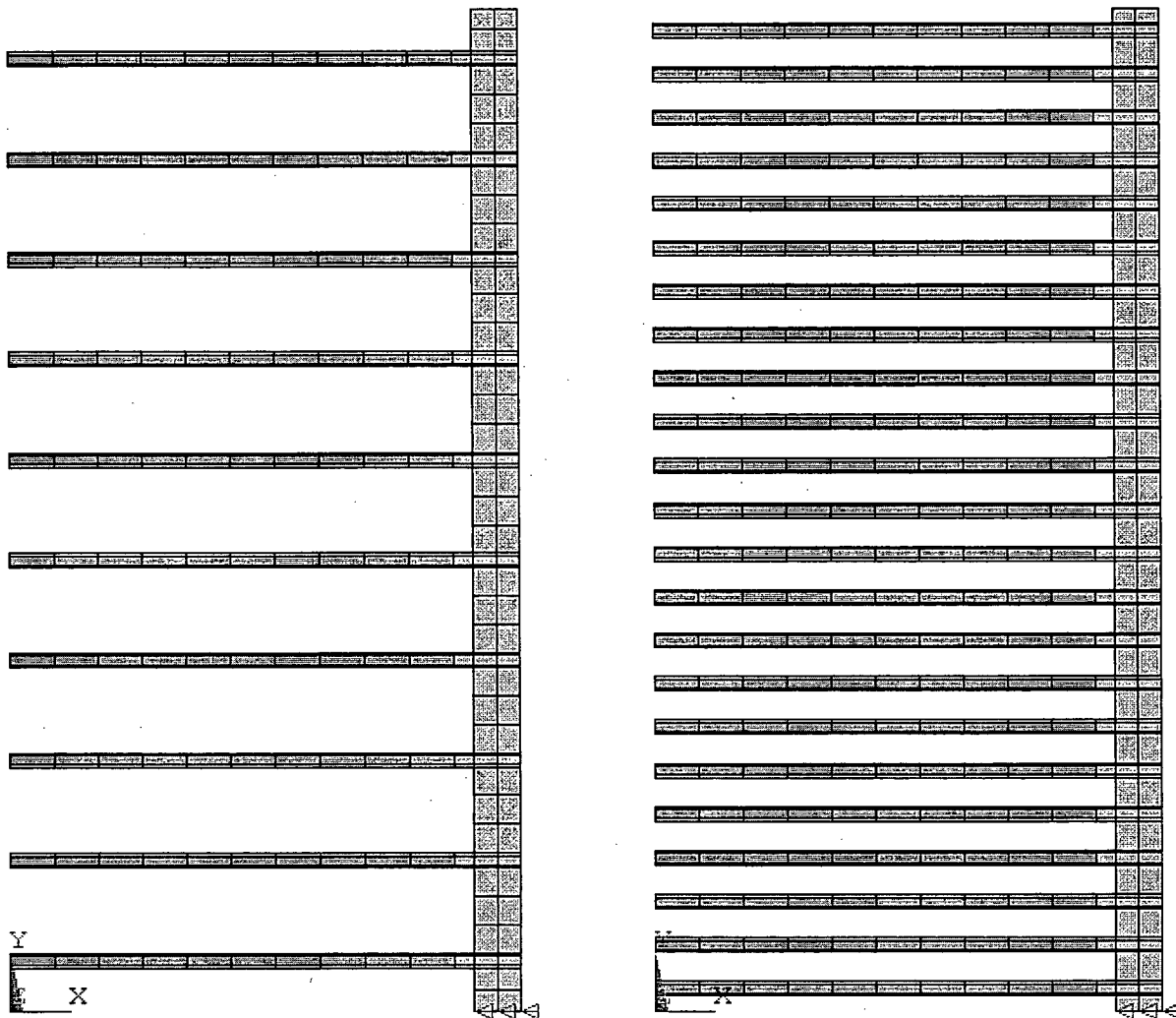


Figure 3.4-13 Finite Element Thermal Model for MTR Fuel Element



10 Fuel Plates

23 Fuel Plates



Application of temperature
boundary condition

(Air elements omitted for clarity)

Figure 3.4-14 Detailed DIDO Basket Module Finite Element Model

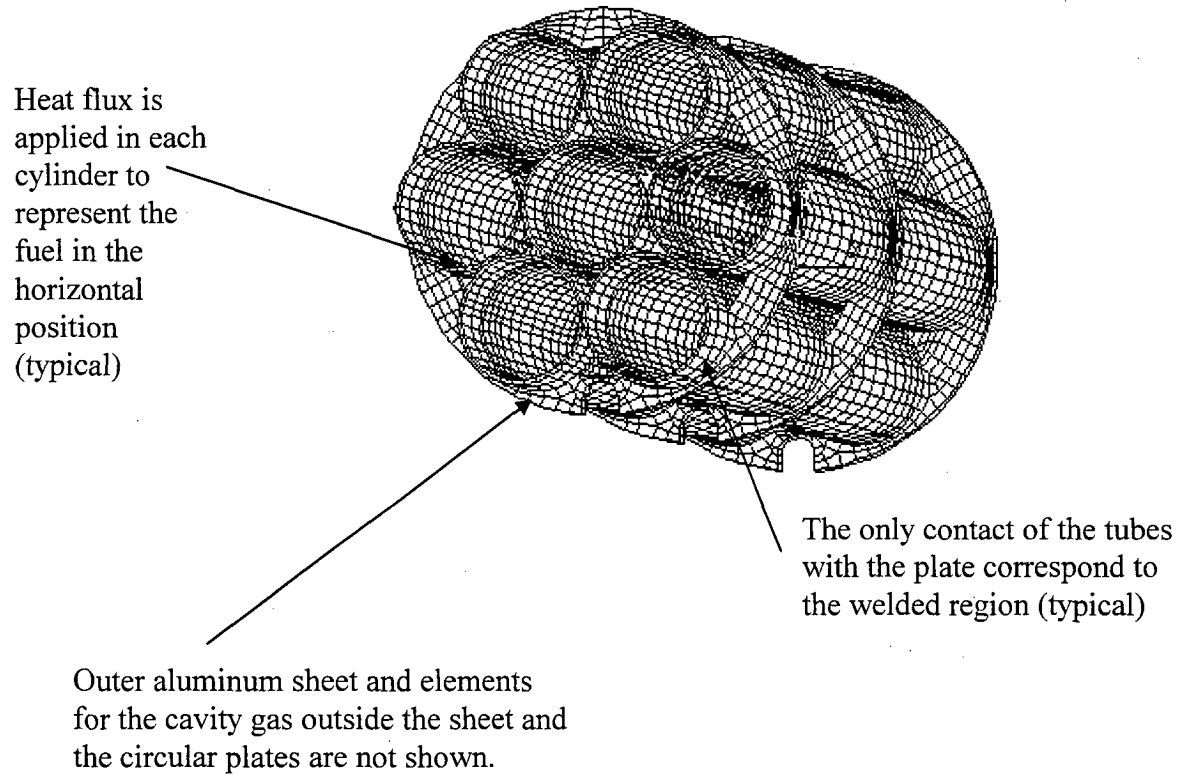


Figure 3.4-15 Detailed DIDO Fuel Assembly Model

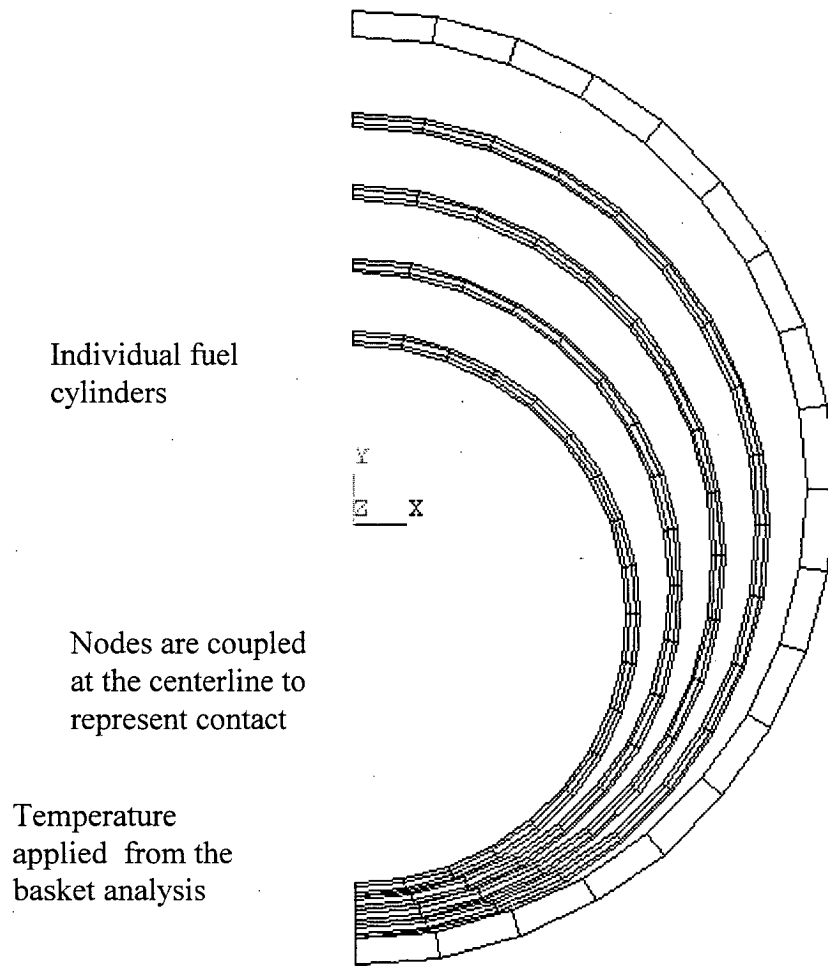


Figure 3.4-16 ANSYS Model for BWR 7x7 Fuel Lattice with 25 High Burnup Fuel Rods

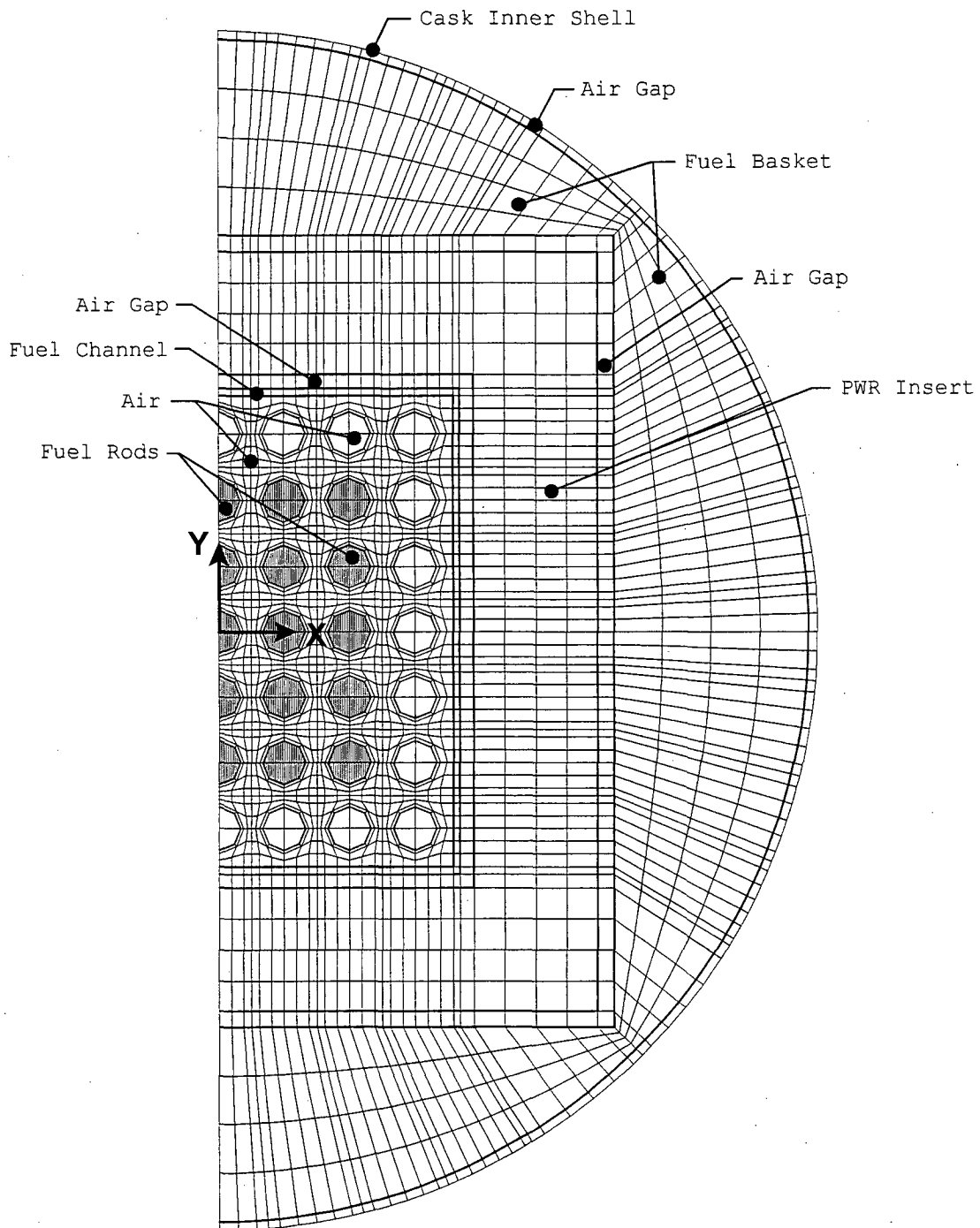


Figure 3.4-17 Fuel Rod Locations in the Thermal Model for Damaged Fuel

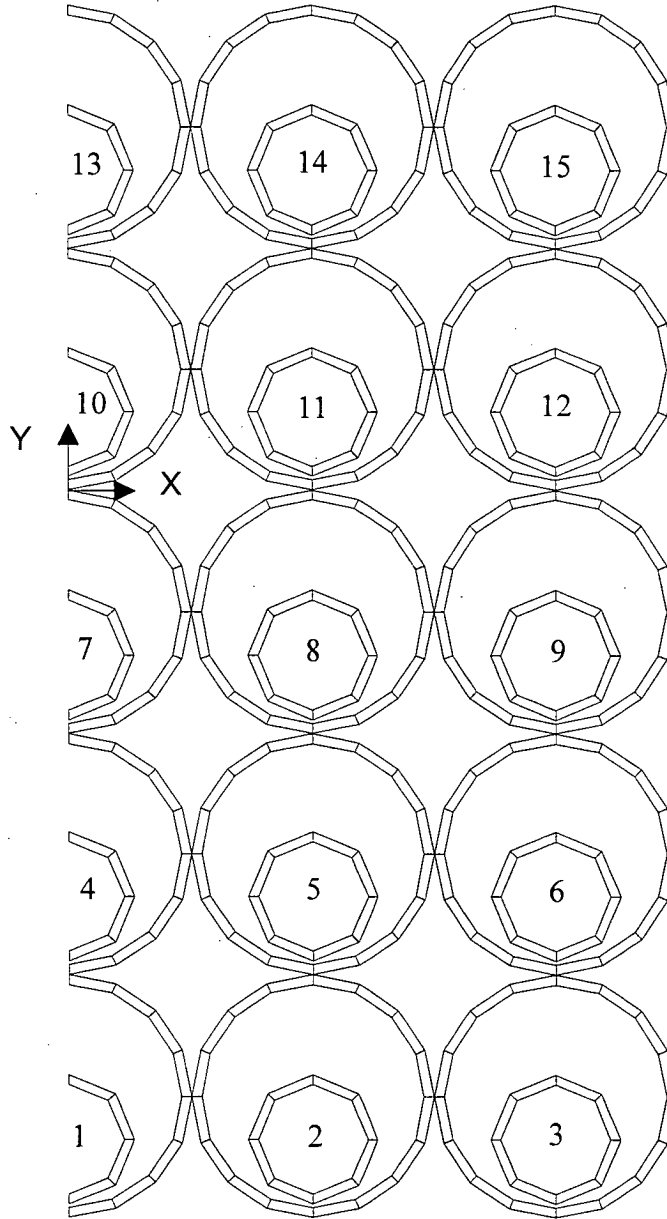
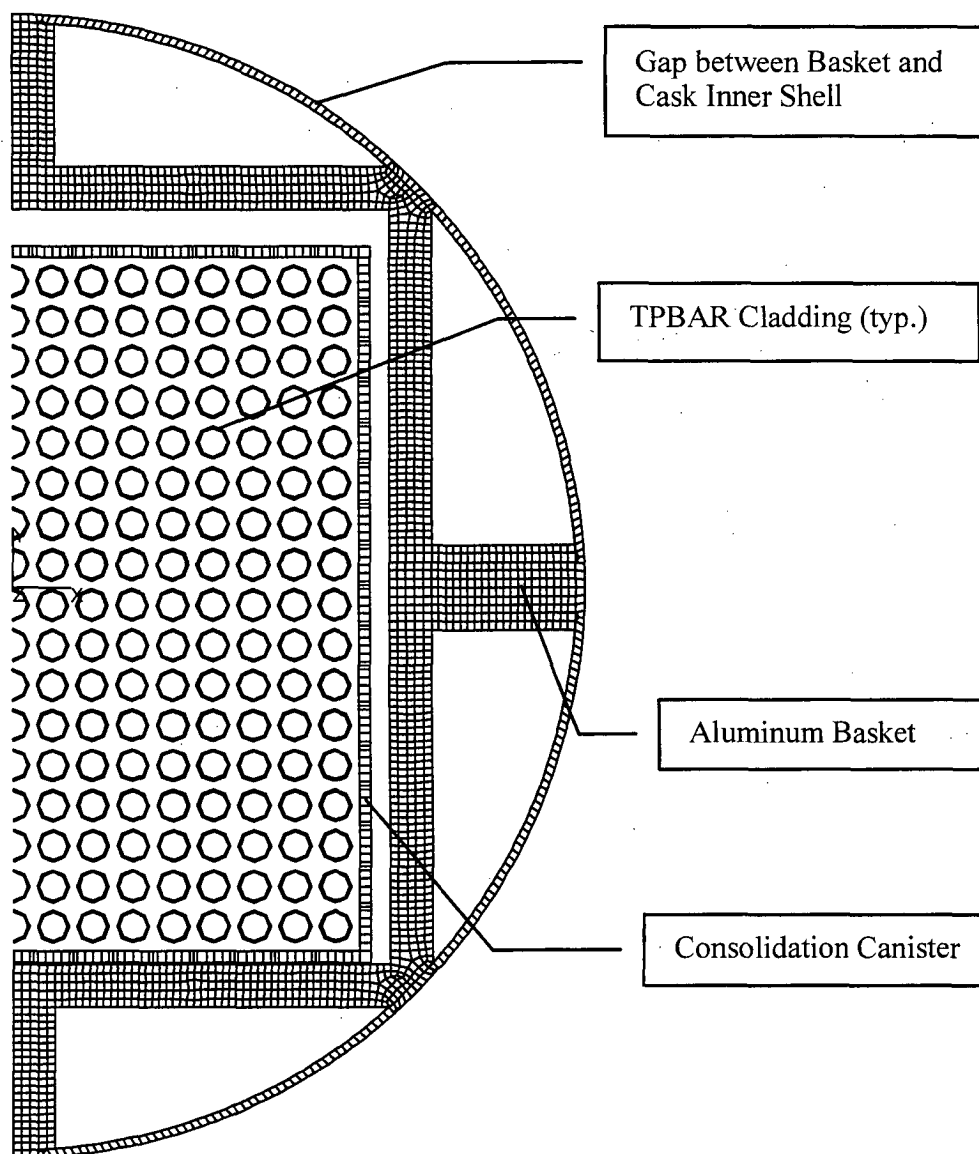


Figure 3.4-18 Finite Element Model for TPBARs



Note: Helium elements, except the gap between the basket and cask inner shell, are not shown for clarity.

Figure 3.4-19

Finite Element Model for MOATA Plate Fuel – ANSTO

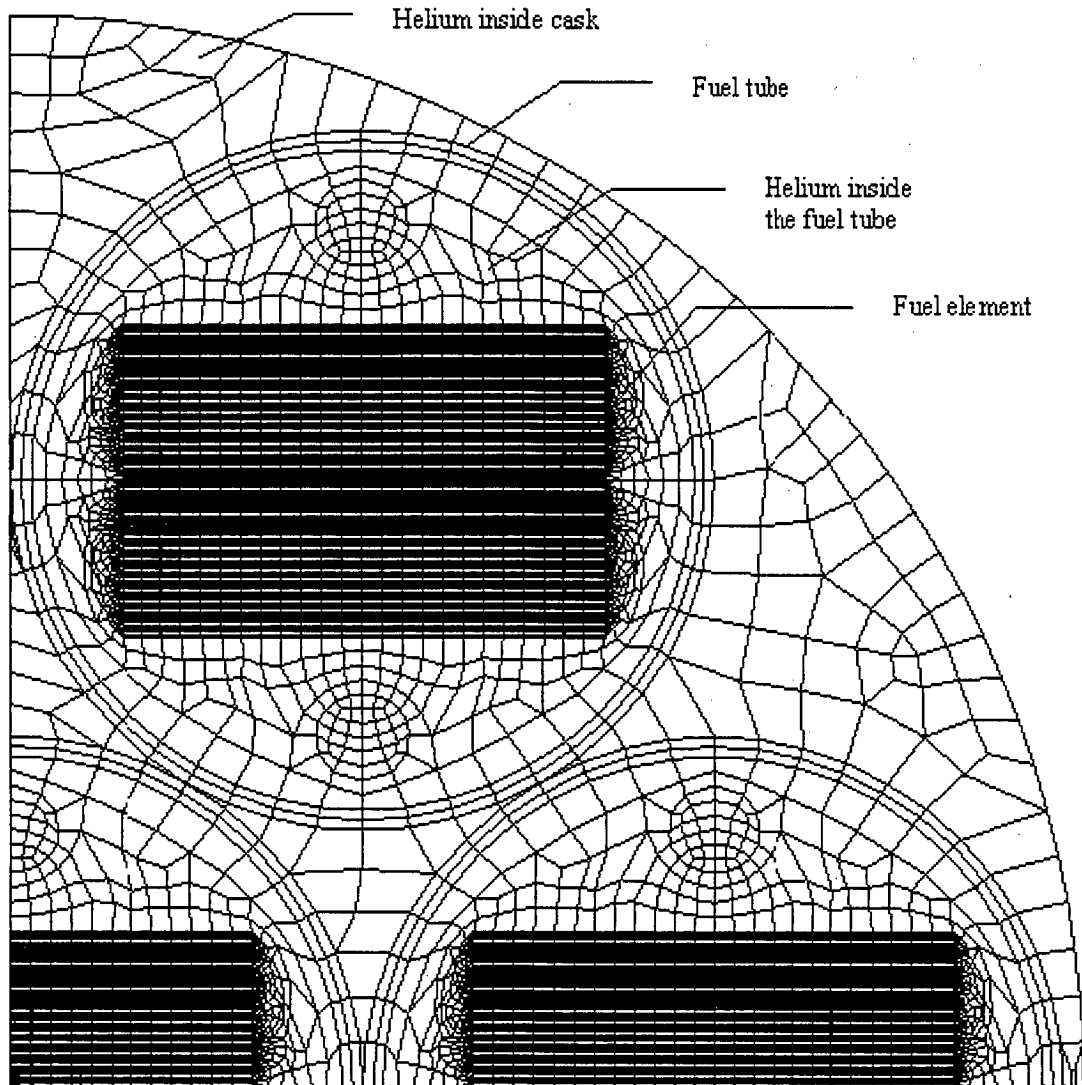


Figure 3.4-20 Finite Element Model for Mark III Spiral Fuel - ANSTO

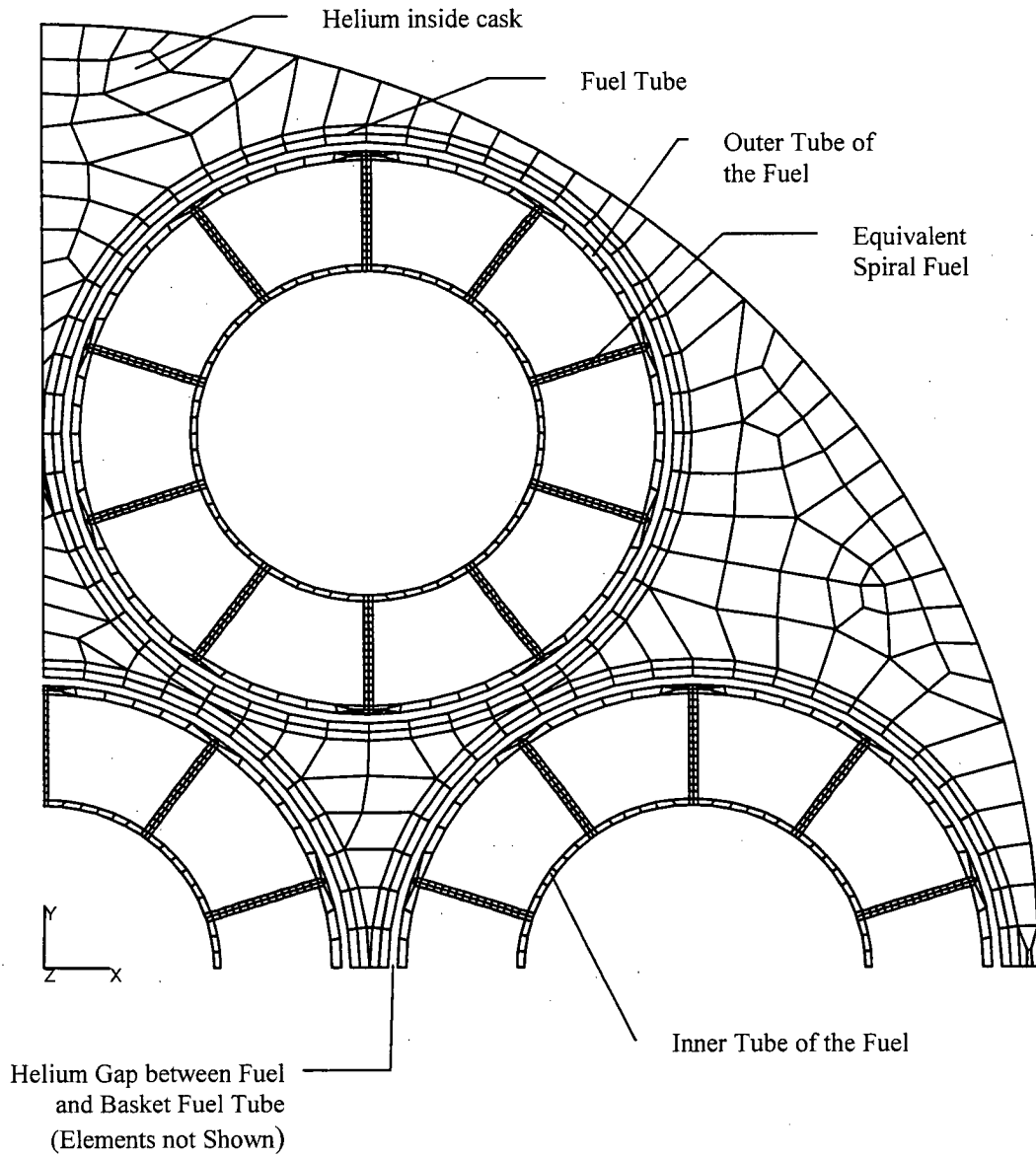


Table 3.4-1 Temperatures for Metallic Fuel Transport

Normal Transport Conditions

Component	Temperature (°F)
O-rings	200
Valves	201
Cask Radial Outer Surface	173
Neutron Shield	252
Radial Lead Gamma Shield	254
Bottom Lead Gamma Shield	210
Inner Stainless Steel Shell	255
Fuel Basket Outer Wall	255
Maximum Fuel Rod Cladding	270

Table 3.4-2 Maximum Component Temperatures – Design Basis PWR Fuel

Normal Transport Conditions

Component	Temperature (°F)
O-rings	227
Valves	231
Cask Radial Outer Surface	229
Neutron Shield	238
Radial Lead Gamma Shield	273
Bottom Lead Gamma Shield	239
Inner Stainless Steel Shell	274
Fuel Basket Outer Wall	276
Maximum Fuel Rod Cladding	472

Table 3.4-3 Limiting Cold Case Component Temperatures – Design Basis PWR Fuel

Normal Transport Conditions

Maximum Decay Heat Load, Minimum Ambient

Component	Temperature (°F)
O-rings	124
Valves	129
Cask Radial Outer Surface	128
Neutron Shield	110
Radial Lead Gamma Shield	167
Bottom Lead Gamma Shield	150
Inner Stainless Steel Shell	167
Fuel Basket Outer Wall	170
Maximum Fuel Rod Cladding	336

Table 3.4-4 Fission Product Gas Inventories and Pressures for Design Basis PWR Fuel Assembly

Fission Product	Inventory per Fuel Assembly (moles)	Initial Pressure (psia)
H-3	0.008	0.615
Kr-80	0.000	0.000
Kr-81	0.000	0.000
Kr-82	0.004	0.308
Kr-83	0.234	17.989
Kr-84	0.687	52.814
Kr-85	0.129	9.917
Kr-86	1.060	81.489
I-127	0.167	12.838
Xe-128	0.010	0.769
I-129	0.704	54.121
Xe-129	0.000	0.000
Xe-130	0.032	2.460
Xe-131	1.641	126.154
Xe-132	4.159	319.728
Xe-134	5.679	436.580
Xe-136	8.529	655.678
Total	23.044	1,771.5

Table 3.4-5 NAC-LWT Cask Thermal Performance Summary
Normal Transport Conditions

Component	Minimum Temperature °F	Maximum Temperature °F	Safe Operating Range °F
TFE O-rings	-40	227	-40 to +735 ¹
Metallic O-rings	-40	227	-40 to +800
Viton [®] O-rings	-40	227 ²	-40 to +550 ³
Lead gamma shield	-40	273	-40 to +600
Liquid neutron shield	-40	238	-40 to +350

¹ Verified through testing (Certified Test Report D9-3362-1, Applied Technical Services, Inc., Marietta, GA, February 8, 1989)

² Normal Transport Condition maximum O-ring temperatures were not calculated. The Viton[®] O-rings are located in close proximity to the TFE O-rings and there is substantial thermal margin, a new O-ring temperature is not calculated

³ Verified through testing (Certified Test Report 43939-01, Wyle Laboratories, Inc., Huntsville, AL, February 21, 2000).

Table 3.4-6 MTR Fuel Maximum Component Temperatures – Normal Transport Condition

Conditions: 100°F Ambient Temperature
Solar Insolation
1.26 Kilowatts Decay Heat Load

Condition 1: NAC-LWT (Transported in an ISO Container)
Cavity gas: Helium

Component	Temperature (°F)	
	Design Basis Decay Heat Load ¹	Variable Decay Heat Load ²
Liquid Neutron Shield	198	198
Outer Shell	199	199
Lead Gamma Shield	212	214
Inner Shell	214	215
Basket (maximum)	256	292
Fuel (maximum)	< 363 ³	< 363 ³

Condition 2: NAC-LWT (Transported via Truck Trailer)
Cavity gas: Air

Component	Temperature (°F)	
	Design Basis Decay Heat Load ¹	Variable Decay Heat Load ²
Liquid Neutron Shield	160	160
Outer Shell	161	160
Lead Gamma Shield	180	180
Inner Shell	181	180
Basket (maximum)	267	312
Fuel (maximum)	< 363 ³	363

¹ Uniform 30-Watt/Element Configuration Heat Load.

² 120-Watt / 70-Watt / 20-Watt Configuration Heat Load.

³ Fuel not modeled for this condition. Fuel temperature is bounded by the variable decay heat load in air case.

Table 3.4-7 PWR Rods (25 Total) Maximum Component Temperatures – Normal Transport Condition

Conditions: 100°F Ambient Temperature
Cask Inside ISO Container
Solar Insolation
1.41 Kilowatts Decay Heat Load

Component	Temperature (°F)
O-rings	< 249
Valves	< 249
Cask Radial Outer Surface	185
Lead Gamma Shield	248
Inner Shell	249
Outer Shell	235
Basket	252
Liquid Neutron Shield	235
Maximum Cladding Temperature	358

Table 3.4-8 TRIGA Fuel Element Maximum Component Temperatures - Normal Conditions of Transport

Conditions: 100°F Ambient Temperature
Solar Insolation
1.05 Kilowatts Decay Heat Load

Condition 2: NAC-LWT (Transported via Truck Trailer)
Cavity Gas: Air

Component	Temperature (°F)
Liquid Neutron Shield	< 160
Outer Shell	< 161
Lead Gamma Shield	< 180
Inner Shell	< 181
Basket (maximum)	267 ¹
Cladding (maximum)	326 ¹

¹ As shown in Table 3.4-6, the Condition 2 analysis produces higher basket temperatures than Condition 1. Therefore, the Condition 2 analysis for TRIGA fuel bounds transport of the cask in an ISO container.

Table 3.4-9 TRIGA Fuel Cluster Rod Temperatures – Normal Conditions of Transport

Conditions: 100°F Ambient Temperature
Solar Insolation
1.05 Kilowatts Decay Heat Load

Condition 1: NAC-LWT (Transported in an ISO Container)
Cavity gas: Helium

Component	Temperature (°F)
Liquid Neutron Shield	207
Outer shell	207
Lead Gamma shield	221
Inner shell	222
Basket (maximum)	263
Aluminum insert tube	265
Cladding (maximum)	266

Condition 2: NAC-LWT (Transported via Truck Trailer)
Cavity gas: Air

Component	Temperature (°F)
Liquid Neutron Shield	159
Outer shell	160
Lead Gamma shield	177
Inner shell	178
Basket (maximum)	278
Aluminum insert tube	292
Cladding (maximum)	295

Table 3.4-10 PWR and BWR High Burnup Fuel Rods Maximum Component Temperatures – Normal Transport Condition

Conditions: 100°F Ambient Temperature Solar Insolation
2.1 Kilowatts Decay Heat Load

Condition 1: NAC-LWT (Transported in an ISO Container)
Cavity gas: Helium

Component	Temperature (°F)
Liquid Neutron Shield	306
Outer Shell	308
Lead Gamma Shield	375
Inner Shell	385
Basket (maximum)	387
Cladding (maximum)	671
Aluminum PWR Insert	394
Stainless Steel Can Weldment	500
Average Cavity Gas	506

Condition 2: NAC-LWT (Transported via Truck Trailer)
Cavity gas: Air

Component	Temperature (°F)
Inner Shell	274
Basket (maximum)	280
Aluminum PWR Insert	286
Stainless Steel Can Weldment	538
Cladding (maximum)	896
Average Cavity Gas	541

Table 3.4-11 Fission Product Gas Inventories and Pressures for the Exxon 7 × 7 BWR Fuel Assembly

Fission Product	Inventory per Fuel Assembly (moles)	Initial Partial Pressure per Rod (psia)
H-3	7.670E-03	1.408E+00
Kr-80	0.000E+00	0.000E+00
Kr-81	0.000E+00	0.000E+00
Kr-82	8.110E-03	1.489E+00
Kr-83	1.270E-01	2.331E+01
Kr-84	7.060E-01	1.296E+02
Kr-85	9.590E-02	1.760E+01
Kr-86	9.330E-01	1.713E+02
I-127	1.770E-01	3.249E+01
Xe-128	3.000E-02	5.507E+00
I-129	7.030E-01	1.290E+02
Xe-129	4.260E-04	7.819E-02
Xe-130	9.040E-02	1.659E+01
Xe-131	9.710E-01	1.782E+02
Xe-132	5.030E+00	9.233E+02
Xe-134	5.690E+00	1.044E+03
Xe-136	8.590E+00	1.577E+03
Total	2.32E+01	4.251E+03

Table 3.4-12 DIDO Fuel Maximum Component Temperatures – Normal Transport Condition

Conditions: 100°F Ambient Temperature
Solar Insolation
1.05 Kilowatts Decay Heat Load

Condition 1: NAC-LWT (Transported in an ISO Container)
Cavity gas: Helium

Component	Temperature (°F)
	Design Basis Decay Heat Load
Liquid Neutron Shield	198 ^{1,2}
Outer Shell	199 ^{1,2}
Lead Gamma Shield	212 ^{1,2}
Inner Shell	214 ^{1,2}
Basket (maximum)	299 ³
Fuel (maximum)	306 ³

- 1 Uniform 30-Watt/Assembly Configuration Heat Load for MTR fuel.
- 2 Bounding values obtained from Table 3.4-6 for MTR fuel.
- 3 Uniform 25-Watt/Assembly Configuration Heat Load for DIDO fuel.

Condition 2: NAC-LWT (Transported via Truck Trailer)
Cavity gas: Air

Component	Temperature (°F)
	Design Basis Decay Heat Load
Liquid Neutron Shield	160 ^{1,2}
Outer Shell	161 ^{1,2}
Lead Gamma Shield	180 ^{1,2}
Inner Shell	181 ^{1,2}
Basket (maximum)	327 ³
Fuel (maximum)	338 ³

- 1 Uniform 30-Watt/Assembly Configuration Heat Load for MTR fuel.
- 2 Bounding values obtained from Table 3.4-6 for MTR fuel.
- 3 Uniform 25-Watt/Assembly Configuration Heat Load for DIDO fuel.

Table 3.4-13 General Atomics IFM Maximum Component Temperatures – Normal Transport Condition

Conditions: 100°F Ambient Temperature
Solar Insolation
13 W Decay Heat Load

NAC-LWT (Transported in an ISO Container)

Component	Temperature (°F)
	Design Basis Decay Heat Load
Liquid Neutron Shield	198 ¹
Outer Shell	199 ¹
Lead Gamma Shield	212 ¹
Inner Shell	214 ¹
Basket (maximum)	250 ²
FHU contents (maximum)	326 ³

¹ Bounding values obtained from Table 3.4-6 for MTR fuel.

² 13-Watt Configuration Heat Load for General Atomics fuel.

³ Bounding value obtained from Table 3.4-8 for the 1.05 kW TRIGA fuel.

**Table 3.4-14 PWR and BWR High Burnup Fuel Rods in a Fuel Assembly Lattice
Maximum Component Temperatures—Normal Transport Condition**

Conditions: 100°F Ambient Temperature
Solar Insolation
2.1 Kilowatts Decay Heat Load (BWR)
2.3 Kilowatts Decay Heat Load (PWR)
Transport Condition 2 (no ISO container) with air in the cavity

Component	Temperature (°F)
Inner Shell	274
Basket (maximum)	276
Aluminum PWR Insert	336
Cladding (maximum)	664
Average Cavity Gas	430

**Table 3.4-15 Maximum Component Temperatures for High Burnup Fuel Rods with
Damaged Fuel Rods in a Rod Holder**

Case ¹	Maximum Temperatures (°F)					
	Basket	Aluminum Insert	Rod Holder Weldment	Fuel Rod Tube ²	Fuel Cladding ³	Cavity Gas Average
Damaged Rods at Locations #4, 5, 6, 7, 8, 9, 10, 11, 12	280	285	523	835	809	479
Damaged Rods at Locations #7, 8, 9, 10, 11, 12, 13, 14, 15	280	286	567	866	653	482
Damaged Rods at Locations #1, 2, 3, 4, 5, 6, 7, 8, 9	280	284	474	743	749	465

¹ See Figure 3.4-17 for fuel rod locations. The nine locations in the half-symmetry model correspond to fifteen actual fuel rod locations.

² The structural analysis of the fuel tubes in Section 2.6.7.10.2 uses a maximum temperature of 925°F.

³ Maximum temperatures are reported for intact fuel rods only.

Table 3.4-16 Maximum Component Temperatures for TPBAR Shipment – Normal Conditions of Transport

Component	Temperature (°F)
Liquid Neutron Shield	207 ¹
Outer Shell	207 ¹
Lead Gamma Shield	221 ¹
Inner Shell	222 ¹
TPBARs	290
Aluminum Basket	228
Consolidation Canister	245
Gas (average)	246

¹ Cask component temperature conservatively obtained from Table 3.4-9, Condition 1 for TRIGA Fuel Cluster Rod.

Table 3.4-17 Maximum Component Temperatures - PULSTAR Fuel in MTR Basket

Conditions: 100°F Ambient Temperature
Solar Insolation
840 watts Decay Heat Load
(30 watts in Each Basket Cell)

Condition 1: NAC-LWT (Transported in an ISO Container)
Cavity gas: Helium

Component	Temperature (°F)
Liquid Neutron Shield	207
Outer shell	207
Lead Gamma shield	221
Inner shell	222
Basket (maximum)	263
Aluminum insert tube	265
Cladding (maximum)	266

Condition 2: NAC-LWT (Transported via Truck Trailer)
Cavity gas: Air

Component	Temperature (°F)
Liquid Neutron Shield	159
Outer shell	160
Lead Gamma shield	177
Inner shell	178
Basket (maximum)	278
Aluminum insert tube	292
Cladding (maximum)	295

- Notes:
1. The temperatures in this table correspond to the temperatures in Table 3.4-9.
 2. PULSTAR fuel can (if used) = 295°F (assume same as fuel cladding temperature).

Table 3.4-18 PULSTAR Fuel Dimensions

Description	Value
Fuel Assembly Height (inch)	38
Fuel Assembly Width (inch)	3.15 × 2.74
Active Fuel Region Height (inch)	24.1
Fuel Rod Diameter (inch)	0.47
Fuel Clad Thickness (inch)	0.0185
Fuel Pellet Diameter (inch)	0.423
Rod Length (inch)	26.2
Plenum Length (inch)	0.5
Number of Fuel Rods	25

Table 3.4-19 PULSTAR Payload Volume Summary

Description	Dimension[cm ³]
Fuel Volume (25 Elements)	1,860
Pellet to Clad Volume (25 Elements)	97
PULSTAR Can Free Volume	1,440
PULSTAR Can Total Volume	4,230
Assembly Envelope Volume	5,370
LWT Cavity Volume	409,300
MTR Basket Stack Volume	41,900

Table 3.4-20 PULSTAR Fuel Assembly Fission Product Gas Inventory

Isotope	Moles
⁴ He	2.28E-03
³ H	1.30E-04
⁸² Kr	6.32E-05
⁸³ Kr	7.03E-03
⁸⁴ Kr	1.66E-02
⁸⁵ Kr	2.41E-03
⁸⁶ Kr	2.81E-02
¹²⁷ I	2.87E-03
¹²⁸ Xe	1.27E-04
¹²⁹ I	1.42E-02
¹³⁰ Xe	3.11E-04
¹³¹ Xe	3.91E-02
¹³² Xe	8.49E-02
¹³⁴ Xe	1.27E-01
¹³⁶ Xe	1.23E-01
Total	4.48E-01

Table 3.4-21 PULSTAR Fuel Element Normal Condition Internal Pressure Summary

Description	Free Volume	Pressure		
	(liters)	(atm)	(psia)	(psig)
Cask Pressure -28 Intact Assemblies	217.0	1.4	21.3	6.6
Cask Pressure -14 Intact Assemblies and 14 Cans	233.0	1.8	27.2	12.5
Can Pressure - PULSTAR Failed Fuel Can	1.53	4.4	65.4	50.7

Table 3.4-22 Maximum Component Temperatures – MOATA Plate Fuel and Mark III Spiral Fuel in ANSTO Basket

Conditions: 100°F Ambient Temperature

Solar Insolation

Heat Load: 126 Watts – MOATA Plate Fuel; 756 Watts – Mark III Spiral Fuel

Component	Temperature (°F)
Liquid Neutron Shield ¹	207
Outer Shell ¹	207
Lead Gamma Shield ¹	221
Inner Shell ¹	222
Basket - MOATA Plate Fuel	230
Fuel Cladding – MOATA Plate Fuel	233
Basket – Mark III Spiral Fuel	248
Fuel Cladding – Mark III Spiral Fuel	250

¹ The cask component temperatures are conservatively obtain from Table 3.4-9 for the TRIGA Fuel Cluster Rod.

3.5 Hypothetical Accident Thermal Evaluation

The hypothetical accident scenario is a series of accidents that occur in a specified order as described in 10 CFR 71.73. The only thermal consequence as a result of the drop and puncture portions of the hypothetical accident is the assumption that the neutron shield is lost prior to the start of the fire. The remainder of the thermal analysis in this section consists of an evaluation of the thermal consequences of the fire portion of the hypothetical accident.

3.5.1 Finite Element Models

There are two finite element models used to evaluate the hypothetical fire accident condition. The axisymmetric thermal model, as described in Section 3.5.1.1, is used to evaluate all configurations except for the PWR and BWR high burnup fuel rod configuration. For the PWR and BWR high burnup fuel rod configuration, a two-dimensional planar finite element model is used. The planar model is described in Section 3.5.1.2.

3.5.1.1 Axisymmetric Thermal Model

The finite element code ANSYS (Revision 5.5) is used to generate a two-dimensional (2-D) axisymmetric finite element model and to perform thermal analyses for the pre-fire, fire and post-fire (cool down) conditions. The ANSYS finite element model is shown in Figure 3.5-1. Figure 3.5-2 and Figure 3.5-3 show the detail of the model at the locations where the thermal insulator is installed in the top and bottom regions. The ANSYS model uses thermal conductivity values for the thermal insulators that are conservative in that they are higher than the values shown in Table 3.2-6 and Table 3.2-8. The thermal insulator protects the lead gamma shield against localized melting during the fire event. As shown, the main components in the radial direction consist of the inner shell, the radial lead, the outer shell, the neutron shield tank and the expansion tank.

The model is constructed using the ANSYS thermal PLANE55 element. Thermal radiation and convection heat transfer at the cask surface is modeled using the PLANE55 and SURF19 elements. Radiation heat transfer across the neutron shield tank and neutron shield expansion tank is modeled using the ANSYS radiation LINK31 element.

The pre-fire condition is defined as the normal transport condition, and a steady-state analysis is performed to determine the temperature field of the cask body. This temperature field is used as the initial condition for the 30 minute fire transient analysis (fire condition), which is followed by a 50-hour cool down period (post-fire condition). Analysis of the 50-hour cool down period ensures that the maximum component temperatures are determined.

The pre-fire analysis considers the convection heat transfer of the liquid neutron shielding inside the shell, but convection heat transfer of the air inside the expansion tank is conservatively neglected. During the fire and post-fire conditions, the liquid neutron shielding is considered to be lost, due to either the pin puncture accident or the failure of the relief valve in the neutron shield tank resulting from high pressure steam produced by the fire. The convection heat transfer of the air in the tank is negligible compared to the radiation heat transfer. The radiation heat transfer across the air-filled tank, and expansion tank, is explicitly modeled using the ANSYS radiation LINK31 element. An emissivity of 0.36 is used for all inner surfaces of the stainless steel neutron shield tank and the expansion tank.

The impact limiters are not discretely modeled, but are represented as thermal boundary conditions. Before the fire accident, adiabatic thermal boundary conditions are conservatively applied to the interface regions between the cask and the impact limiters so that no heat is transferred out of the cask through the impact limiters. During the fire and post-fire periods, the impact limiters are assumed to be removed. In this time period, heat transfer by convection and radiation are modeled in the regions previously covered by the impact limiters. Solar insolation is considered in the model during the pre-fire and post-fire conditions, but neglected during the fire.

The heat input from the fire considers thermal radiation and convection heat transfer. A convection heat transfer coefficient of $0.02446 \text{ Btu/hr-in}^2\text{-}^\circ\text{F}$ is applied to account for heat transfer to the cask surface. This value is twice the theoretical value (W_{ix}) to account for uncertainties in the fire accident condition and the data from which the recommended value is derived. These assumptions lead to maximizing the material temperatures and are conservative.

The cask contents (basket and fuel) are not directly modeled. The decay heat generated from the fuel region inside the cask is simulated using an equivalent non-uniform heat flux applied to the inner surface of the cask cavity inner shell, corresponding to the height of the active fuel region. The analysis considers the bounding fuel heat load, 2.5 kW for PWR fuel, and applies the power distribution curve shown in Figure 3.4-2 with a peaking factor of 1.2.

ANSYS 5.5 was used to calculate the maximum post-fire accident temperatures at four new locations for the alternate port cover design. Temperatures calculated for comparable locations on the port cover body vary from those temperatures presented in Table 3.5-1. Changes in the ANSYS 5.5 version and computational solvers account for the differences in calculated results. The transient temperature analysis results are presented in Figure 3.5-12 and Figure 3.5-13.

Exactly the same model described above was rerun using ANSYS 5.5 for the alternate port cover to determine the bolt head and thread temperatures and the temperatures at both O-ring locations. The output is post-processed to determine the maximum average temperatures at specific locations of interest. The temperatures calculated are presented in Table 3.5-1.

3.5.1.2 Two-Dimensional Planar Thermal Model

Thermal analysis of the NAC-LWT cask loaded with PWR and BWR high burnup fuel rods is performed using a two-dimensional planar thermal model. The thermal model is identical to the model utilized to perform the steady state analysis (condition 2, Section 3.4.1.7) for the NAC-LWT cask loaded with PWR and BWR high burnup fuel rods. The detailed model description is contained in Section 3.4.1.7.2.

The Condition 2 model was selected since it initiates the thermal transient with clad temperatures 225°F higher (from Table 3.4-10, 896°F-671°F) than the Condition 1 model steady-state condition. This increase in the initial condition temperature for the cask cavity air-filled condition overcompensates for the higher conductivity of helium as the cavity gas. The effect of the higher helium conductivity heat input during the period of fire exposure is significantly less due to the influence of the parallel heat transfer paths by conduction through the metal contents and by radiation across the gas-filled space. This influence is seen in the transient maximum temperature difference from the higher steady-state temperature of 896°F to the maximum transient temperature of 1,014°F (a change of 118°F), which is significantly bounded by the steady-state temperature condition difference of 225°F, as stated previously. In addition to the conservative modeling introduced by the initial steady-state temperature, during the cooldown portion of the transient, the use of air thermal conductivity in the cavity retards the heat removal from the fuel (as compared to helium conductivity). This also results in a maximum transient temperature higher than when modeling helium as the cavity gas.

A thermal transient analysis for the design basis fuel is performed using the two-dimensional planar thermal model (see Figure 3.4-12). To impose the fire accident condition on this model, a temperature time history was applied to the outer surface of the model, which corresponds to the inner surface of the inner shell. This temperature time history at the inner shell inner surface near the axial midplane is obtained from the fire accident analysis (heat load of 2.5 kW and a peaking factor of 1.2, as described in Section 3.5.2) using the axisymmetric two-dimensional model described in Section 3.5.1.1.

Using a two-dimensional planar model of the cross-section, a 50.5-hour transient analysis is performed with a heat load of 2.1 kW with a peaking factor of 1.22. This represents the bounding heat load for the high burnup PWR and BWR fuel rods.

3.5.2 Package Conditions and Environment

The fire accident is preceded by the cask drop and cask puncture portions of the hypothetical accident. The only damage that occurs as a result of the drop and puncture accident events that are of importance to the cask thermal performance is the damage to the NAC-LWT cask neutron shield. As a result of these events, it is assumed that the integrity of the neutron shield has been damaged to such an extent that the entire contents of the neutron shield are no longer present.

The fuel heat load of 2.5 kW is applied using a nonuniform heat flux with a peaking factor of 1.2. Solar insolation is applied to the outer surfaces of the cask, including the area covered by the impact limiters, during the post-fire conditions, and neglected during the fire condition. The value of solar insolation, based on a 24-hour average to curved surfaces, is:

$$Q_{\text{sun}} = 1,475 / (24 \times 144) = 0.4268 \text{ BTU/hr-in}^2$$

Convection and radiation heat transfer at the outer surfaces of the cask were considered in the analysis. During the pre-fire (normal) and post-fire periods, the ambient temperature assumed is 100°F, and the cask outer surface emissivity is 0.36. During the fire, the ambient temperature is 1,475°F, and the cask surface emissivity is 0.9. The convection coefficient applied is 0.02446 Btu/hr-in²-°F.

Using a decay heat of 2.5 kW, the conditions for the hypothetical fire accident are:

Analysis Condition	Loads and Boundary Conditions
Initial steady-state (pre-fire)	<ul style="list-style-type: none"> • Solar Insolation • Combined convection (using the film coefficient for the cask surface, 0.00125ΔT^{0.33} Btu/hr-in²-°F) and radiation heat transfer (as defined in Section 3.2.3) between the cask exterior (ε=0.36) and the ambient (100°F) • The surface of the cask in contact with the impact limiter is adiabatic
Fire transient (during fire)	<ul style="list-style-type: none"> • Ambient temperature 1,475°F with no solar insolation • Combined convective (additional coefficient of 0.02446 Btu/hr-in²-°F) and radiative heat transfer using a film coefficient (as defined in Section 3.2.3) between the cask exterior (ε=0.9), including the area normally covered by impact limiters, and the fire • Neutron shield fluid lost
Cool down (post-fire)	<ul style="list-style-type: none"> • Ambient temperature 100°F with solar insolation • Combined convection (using the film coefficient for the cask surface, 0.00125ΔT^{0.33} Btu/hr-in²-°F) and radiation heat transfer (as defined in Section 3.2.3) between the cask exterior (ε=0.36), including the area covered by the impact limiters, and ambient • Neutron shield fluid lost

3.5.3 Package Temperatures

The temperatures of the cask body resulting from the fire are determined using ANSYS. The heat load used in the transient thermal analysis corresponds to the PWR fuel, since its heat load envelopes all other fuel types that can be transported in the NAC-LWT cask.

The maximum temperatures of the basket and fuel for the different fuel types are determined using the results of the fire transient analysis of the cask body and the maximum temperature differences between the basket and fuel and the inner shell of the cask body as computed in the steady state thermal evaluations.

3.5.3.1 Evaluation for PWR Fuel Contents

The maximum temperatures of the cask body and principal components are evaluated using the ANSYS model described in Section 3.5.1.1. A radial temperature profile is obtained during the postulated 30-minute fire and for a cooldown period of 50 hours. The maximum cask component temperatures for the hypothetical accident are presented in Table 3.5-1.

Maximum time dependent temperatures of different cask components, before, during and after the fire, are shown in Figure 3.5-4 and Figure 3.5-5. The temperatures of the components show a sharp increase during the fire and a sharp decrease that begins right after the fire. After the 50 hour cooling period, the temperatures of the components do not return to the normal conditions of transport values. This is attributed to the loss of the liquid neutron shield during the accident, which results in the loss of the (liquid) convection heat transfer across the tank.

As noted above, the fuel and the fuel basket were not directly modeled in the ANSYS analysis. To determine the maximum temperature of the components inside the basket, the following method is applied:

$$T_{\max} = T_{iS_{\max}} + \Delta T_{\text{comp}}$$

where:

$T_{iS_{\max}}$ is the maximum temperature of the inner shell, obtained in the ANSYS transient thermal analysis.

ΔT_{comp} is the difference in maximum temperatures from Table 3.4-2 between the inner shell and the fuel basket outer wall or the fuel rod cladding during normal transport.

The maximum temperatures of fuel cladding and basket wall are:

Component	ΔT_{comp} (°F) ¹	$T_{is_{max}}$ (°F) ²	T_{max} (°F)
Fuel basket outer wall	2 (276-274)	505	507
Fuel cladding	198 (472-274)	505	703

¹ Temperatures from Table 3.4-2.

² Temperatures obtained in the ANSYS evaluation.

As a result, the maximum average cavity gas temperature can be taken as the average of the maximum basket wall and maximum fuel cladding temperatures. This produces an average cavity gas temperature of 605°F.

As shown in Table 3.5-1, all of the cask component temperatures are within the allowable temperature limit during the fire accident event.

3.5.3.2 Evaluation of MTR Fuel Contents

The temperatures in the MTR fuel basket and MTR fuel plates produced during the fire accident were determined using the two ANSYS finite element models of the NAC-LWT cask for MTR fuel element discussed in Section 3.4.1.3.2. The gas in the NAC-LWT cask cavity is considered to be air. Other conditions applied to the model are the same as those described in Sections 3.5.1 and 3.5.2 for the axisymmetric fire transient model with respect to the liquid neutron shield and outer surface boundary conditions. The accident thermal models for MTR fuel are shown in Figure 3.5-6 and Figure 3.5-7, for the design basis decay heat loading and the variable decay heat loading, respectively. The type, form, design or enrichment of the MTR fuel assemblies has no effect as long as the decay heat load and other fuel characteristics are in compliance with the requirements of Table 1.2-4. The presence and/or use of axial fuel spacers and spacer plates to position the fuel assemblies for ease of handling have no effect on the thermal analyses of the MTR basket assembly.

The transient calculation is performed to determine the maximum temperatures in the MTR fuel elements only for the variable decay heat loading because this is the worst-case condition. The cask model is used to determine the temperature history of the cask components, including the basket. The fuel element model is used to determine the temperature rise between the basket and the hottest point in the fuel element. The capacitance of the fuel element is negligible compared to the very large capacitance of the cask assembly. Therefore, a constant ΔT between basket and fuel is used. The temperature history for the MTR fuel variable heat load fire accident analysis is

shown Figure 3.5-8. The temperature profile within the cask model at the time of the maximum fuel temperature is shown in Figure 3.5-9. The bounding case is an element with 10 fuel plates, a decay heat of 120W and with worst-case dimensions. The maximum temperatures of the components are presented in Table 3.5-2. These results demonstrate that the maximum MTR fuel plate temperature for the variable decay heat loading is 473°F. The MIL-HDBK-5F Specification for 6061-T6 aluminum alloy indicates that the material retains more than 35% of its room temperature yield and ultimate strengths during transient exposure to temperatures as high as 500°F. Therefore, the reduction in strength for the fuel cladding as a result of the fire transient is minor when compared to the values presented in Section 3.4.1.3.3 for aluminum at 400°F. Since the fuel cladding temperatures are maintained significantly below 500°F, it is concluded that the structural integrity of the fuel cladding is maintained. Furthermore, the aluminum cladding of the MTR fuel elements is heated to a temperature of approximately 900°F during the fabrication process and it is clear that the cladding integrity is maintained during that process.

3.5.3.3 Evaluation of TRIGA Fuel Contents

The accident condition temperatures are obtained by applying the temperature differential calculated for the MTR fuel configuration to the TRIGA fuel configuration. To determine the TRIGA accident condition maximum cladding temperature, the temperature difference between the maximum basket temperatures for the normal and accident component temperatures calculated for MTR fuel in Section 3.5.3.2, is added to the maximum cladding temperature calculated for TRIGA fuel in Section 3.4.1.5.

The maximum basket temperature for the MTR fuel design basis heat load fire accident analysis is 374°F, as reported in Table 3.5-2. This temperature is 107°F higher than the normal condition maximum temperature (267°F) reported in Table 3.4-6. The corresponding maximum TRIGA fuel cladding temperature for the fire accident condition is reported in Table 3.5-3 to be 433°F. The MIL-HDBK-5F Specification for 6061-T6 aluminum alloy indicates that the material retains more than 35% of its room temperature yield and ultimate strengths during transient exposure to temperatures as high as 500°F. Therefore, the reduction in strength for the aluminum-clad TRIGA fuel cladding as a result of the fire transient is minor when compared to the values presented in Section 3.4.1.3.3 for aluminum at 400°F. Since the fuel cladding temperatures are maintained significantly below 500°F, it is concluded that the structural integrity of the aluminum-clad TRIGA fuel is maintained. The allowable temperature for stainless steel-clad TRIGA fuel is significantly higher.

The TRIGA fuel generates small amounts of fission gases during reactor operations, but it contains no initial charge of helium gas. Consequently, the internal pressure developed in the accident condition is less for TRIGA fuel than for the design basis PWR fuel.

3.5.3.4 Evaluation of TRIGA Fuel Cluster Rod Contents

The temperatures in the TRIGA fuel cluster rod basket and cladding produced during the fire accident were determined using the ANSYS finite element model of the NAC-LWT for the TRIGA fuel discussed in Section 3.4.1.6 for Condition 2 (air in the cavity and without the ISO container). The gas in the NAC-LWT cask cavity is considered to be air. Other conditions applied to the model are the same as those described in Sections 3.5.1 and 3.5.2 for the axisymmetric fire transient model with respect to the liquid neutron shield and outer boundary conditions.

The temperatures in the basket are bounded by the maximum temperatures of the fuel region. The temperature time history for the fuel region is shown in Figure 3.5-10. The maximum temperature of the clad was determined to be 394°F. This value is below the 800°F limit for the clad or the 400°F limit for the aluminum specified in Section 3.4.1.6. Therefore, the components are determined to be acceptable for the fire accident condition.

3.5.3.5 Evaluation for PWR and BWR High Burnup Fuel Rod Contents in a Rod Holder

The maximum temperatures of the principal components are evaluated using the ANSYS model described in Section 3.5.1.2. The maximum cask component temperatures for the hypothetical accident are identical to those presented in Table 3.5-1 since the bounding temperature history from the analysis of NAC-LWT PWR contents is used as a boundary condition for the analysis for PWR and BWR high burnup fuel rod contents.

Maximum time dependent temperatures of different components, before, during and after the fire, are shown in Figure 3.5-11. For the maximum time dependent temperatures of cask components see Figure 3.5-4 and Figure 3.5-5.

As a result, the maximum average cavity gas temperature for fire accident is calculated as the average of the air contained inside the basket. This produces an average cavity gas temperature of 695°F.

Table 3.5-4 shows the can weldment and fuel rod cladding temperatures during the fire accident event.

3.5.3.6 Evaluation of DIDO Fuel Contents

The DIDO fuel maximum heat load is bounded by the maximum heat load of the MTR fuel. Therefore, in the accident condition, the maximum temperatures of the cask components for the MTR contents will bound the maximum temperatures for the cask components for the DIDO

contents. It is conservative to use the results of the fire transient evaluated in Section 3.5.3.2 for the cask inner shell temperature. The maximum basket and fuel temperatures (T_{max}) for the DIDO fuel for the accident conditions are determined by adding the increase in steady state temperature from the cask inner shell to the maximum temperature of the component ($\Delta T_{component}$) to the maximum cask inner shell temperature ($T_{inner\ shell}$) obtained from the MTR evaluation. The maximum temperatures of the fuel cladding and basket wall are:

Component	$\Delta T_{component}$ (°F)	$T_{inner\ shell}^1$ (°F)	T_{max} (°F)
Fuel basket	146 = 327 ² -181	334	480
Fuel cladding	157 = 338 ² -181	334	491

¹ Obtained from Table 3.5-2 for the uniform heat distribution.

² Obtained from Table 3.4-12, Condition 2.

The fuel cladding temperature previously listed is bounded by those determined for the MTR contents. It is concluded that the structural integrity of the fuel cladding is maintained for the fire accident condition.

3.5.3.7 Evaluation for General Atomics Fuel Contents

The General Atomics fuel maximum heat load is bounded by the maximum heat load of the DIDO and MTR fuels. Therefore, in the accident condition, the maximum temperatures of the cask components for the MTR contents will bound the maximum temperatures for the cask components with General Atomics fuel. It is conservative to use the results of the fire transient calculation evaluated in Section 3.5.3.2 for the cask inner shell temperature. The maximum basket temperature (T_{max}) for the General Atomics fuel for accident conditions is determined by adding the increase in steady-state temperature from the cask inner shell to the maximum temperature of the component ($\Delta T_{component}$) to the maximum cask inner shell temperature ($T_{inner\ shell}$) obtained from the MTR evaluation. The maximum temperature of the basket is:

$$T_{max} = (250 - 214) + 334 = 370^{\circ}F$$

where:

334°F is the maximum temperature of the LWT inner shell during a fire accident

This temperature is bounded by those determined for the MTR contents. It is concluded that the structural integrity of the General Atomics basket and contents is maintained for the fire accident condition.

3.5.3.8 Evaluation of PWR and BWR High Burnup Fuel Rods in Fuel Assembly Lattice

The total heat load of the PWR and BWR high burnup fuel rods (up to 25 rods) in a fuel assembly lattice is bounded by that for the PWR and BWR high burnup fuel in a rod holder as evaluated in Section 3.5.3.5. Therefore, in the accident condition, the maximum temperatures of the cask components for the design basis PWR configuration bound the maximum temperatures for the PWR or BWR high burnup fuel rods in the fuel assembly lattice. The fuel cladding is expected to have the same difference in temperature between normal conditions and the accident fire conditions as determined in Section 3.5.3.5. The temperature difference for the fuel cladding between normal and accident conditions for the high burnup fuel in a rod holder is 118°F (1,014°F – 896°F). The maximum fuel cladding temperature is 664°F for high burnup fuel rods in a fuel assembly lattice for normal conditions of transport as evaluated in Section 3.4.1.10 (Table 3.4-14). Therefore, the maximum temperature of the fuel cladding for the 25 fuel rods in the fuel assembly lattice for accident conditions is 782°F (664°F + 118°F).

3.5.3.9 Evaluation of PWR and BWR High Burnup Fuel in a Rod Holder with Damaged Rods

The damaged fuel maximum heat load is equal to the maximum heat load of the PWR and BWR high burnup fuel rods. To determine maximum temperatures of the fuel configuration with damaged fuel rods in the fire accident condition, temperatures from the normal and accident conditions for the PWR and BWR high burnup intact fuel rods (Table 3.4-10 and Table 3.5-4) are used to determine the temperature differentials that are caused by the fire accident. The increase in temperatures is added to the maximum normal conditions temperature for the fuel rods in a rod holder with damaged rods (Table 3.4-15) to compute the maximum fire temperatures. The maximum temperatures of the fuel cladding and stainless steel rod holder are shown in Table 3.5-5. The maximum temperatures for the cask components are bounded by those for the design basis PWR fuel assembly configuration.

3.5.3.10 Evaluation of TPBAR Contents

The maximum heat load of TPBARs is bounded by the maximum heat load of the MTR fuel. Therefore, in the accident condition, the maximum temperatures of the cask components for the MTR contents will bound the maximum temperatures for the cask components for the TPBAR contents. It is conservative to use the results of the fire transient evaluated in Section 3.5.3.2 for the cask inner shell temperature. The maximum component temperatures (T_{\max}) for the TPBARs for the accident conditions are determined by adding the temperature difference ($\Delta T_{\text{component}}$)

between the cask inner shell and the maximum component temperature for normal conditions to the maximum accident cask inner shell temperature ($T_{\text{inner shell}}$) obtained from the MTR evaluation. The maximum component temperatures are computed as follows.

Component	$\Delta T_{\text{component}}$ (°F)	$T_{\text{inner shell}}^2$ (°F)	T_{max} (°F)
TPBAR	68 (290 ¹ -222 ¹)	334	402
Aluminum Basket	6 (228 ¹ -222 ¹)	334	340
Consolidation Canister	23 (245 ¹ -222 ¹)	334	357
Gas (average)	24 (246 ¹ -222 ¹)	334	358

¹ See Table 3.4-16

² See Table 3.5-2

The maximum temperatures of the components are presented in Table 3.5-6.

3.5.3.11 Evaluation of PULSTAR Fuel Elements in 28 MTR Basket

As described in Section 3.4.1.13, the thermal performance of the configuration of PULSTAR fuel elements in the 28 MTR basket is bounded by the thermal performance of the TRIGA fuel cluster rods, condition 2. The temperatures in the TRIGA fuel cluster rod basket and cladding produced during the fire accident were determined and described in Section 3.5.3.4. The temperatures in the basket are bounded by the maximum temperatures of the fuel region. The temperature time history for the fuel region is shown in Figure 3.5-11. The maximum temperature of the cladding was determined to be 394°F. This value is below the 1,058°F limit for the fuel cladding. Therefore, the components for PULSTAR fuel elements in the 28 MTR baskets are determined to be acceptable for the fire accident condition.

3.5.3.12 Evaluation of ANSTO Fuels

The maximum heat load of the spiral fuel assemblies (0.756 kW per cask) is bounded by the maximum heat load of the MTR fuel (1.05 kW per cask). Therefore, in the accident condition, the maximum temperatures of the cask components for the MTR contents will bound the maximum temperatures for the cask components for the ANSTO basket contents. It is conservative to use the results of the fire transient evaluated in Section 3.5.3.2 for the cask inner shell temperature. The maximum basket and fuel temperatures (T_{max}) for the ANSTO fuel contents for the accident condition are determined by adding the temperature difference ($\Delta T_{\text{component}}$) between the maximum temperature of the cask inner shell and the component (basket or fuel) for the normal condition to the maximum cask inner shell temperature ($T_{\text{innershell}}$)

for the accident condition obtained from the MTR evaluation. The maximum temperatures of the fuel cladding and basket are computed as follows.

Component	$\Delta T_{\text{component}}$ (°F)	$T_{\text{innershell}}^1$ (°F)	T_{max} (°F)
Fuel basket – MOATA Plate Fuel	8 = 230 ² -222 ²	334	342
Fuel cladding – MOATA Plate Fuel	11 = 233 ² -222 ²	334	345
Fuel basket – Mark III Spiral Fuel	26 = 248 ² -222 ²	334	360
Fuel cladding – Mark III Spiral Fuel	28 = 250 ² -222 ²	334	362

¹ Obtained from Table 3.5-2 for the uniform heat distribution

² Obtained from Table 3.4-22

3.5.3.13 Evaluation of 16 PWR MOX High Burnup Rods

The PWR/BWR Rod Transport Canister and 5 × 5 insert used for the transport of 16 PWR MOX high burnup rods is the same design as the one used for the BWR and PWR high burnup rods. The heat load used in the evaluation of the BWR high burnup rods, which includes the effect of the peaking factor, bounds that of the PWR MOX high burnup rods (see Section 3.4.1.15). As presented in Section 3.4.1.15, the reduced conductivity of the PWR MOX fuel rods does not affect the heat transfer through the canister or insert or, in the case of the transient, it does not affect the ability to absorb and retain heat. The initial temperatures of the fuel rods are conservative since the heat load used in the steady-state evaluation is for 25 rods of the design basis heat load (see Section 3.4.1.7), rather than the 16 PWR MOX high burnup rods. The temperatures summarized in Section 3.5.3.5, referencing Table 3.5-4, provide bounding temperatures for the PWR MOX fuel rod contents.

3.5.4 Maximum Internal Pressure

3.5.4.1 Maximum Internal Pressure for Design Basis Fuel in Accident Conditions

The accident internal pressure is calculated assuming an accident with 100 percent fuel rod failure combined with the design basis fire described in 10 CFR 71. The fuel rod failure assumes 30 percent of the fission gas and 100 percent of the backfill gas escapes the ruptured fuel rods.

The internal pressure due to the 100 percent fuel rod rupture is calculated using the method described in Section 3.4.4. The total cask pressure of the cask backfill and failed fuel rods is calculated by a two step procedure. First, the pressures documented under normal conditions in Section 3.4.4 are adjusted to include the increased total free volume associated with 100% fuel.

rod failure. Then, the revised cask pressure at normal operating temperature is adjusted to accident condition temperatures.

Adjusting the partial pressure of the cask backfill:

$$P_{\text{cask}} = P_{\text{initial}} \left(\frac{V_{\text{cask}}}{V_{\text{total}}} \right)$$

where:

$$P_{\text{initial}} = 25.8 \text{ psia (normal condition temperature adjusted cask backfill pressure)}$$

$$V_{\text{cask}} = 5.196 \text{ ft}^3 (147,134 \text{ cm}^3) \text{ [Section 3.4.4]}$$

$$V_{\text{rod void}} = 8,123 \text{ cm}^3 \text{ [Section 3.4.4]}$$

$$V_{\text{total}} = 155,257 \text{ cm}^3 (V_{\text{cask}} + V_{\text{rod void}})$$

$$P_{\text{cask}} = 25.8 \text{ psia} \left(\frac{147,134 \text{ cm}^3}{155,257 \text{ cm}^3} \right)$$

$$P_{\text{cask}} = 24.4 \text{ psia}$$

Adjusting the partial pressure of the fuel rod backfill and fission gases:

$$P_{\text{fuel rods}} = P_{\text{initial}} \left(\frac{V_{\text{rod void}}}{V_{\text{total}}} \right)$$

where:

$$P_{\text{initial}} = 1,521.3 \text{ psia (fuel rod backfill pressure of 989.8 psia plus fission gas pressure of } 0.30 \times 1771.5 \text{ psia)}$$

$$V_{\text{rod void}} = 8,123 \text{ cm}^3$$

$$V_{\text{total}} = 155,257 \text{ cm}^3$$

$$P_{\text{fuel rods}} = 1,521.3 \text{ psia} \left(\frac{8,123.28 \text{ cm}^3}{155,257 \text{ cm}^3} \right)$$

$$P_{\text{fuel rods}} = 79.6 \text{ psia}$$

Summing the two partial pressures yields the total cask pressure at normal operating condition temperature:

$$P_{\text{Total}} = P_{\text{cask}} + P_{\text{fuel rods}}$$

$$P_{\text{Total}} = 24.4 \text{ psia} + 79.6 \text{ psia}$$

$$P_{\text{Total}} = 104.0 \text{ psia}$$

The fuel cladding has the highest temperature of any barrier with which the gas comes in contact during a design basis fire. As shown in Section 3.5.3.1, the maximum average cavity gas temperature is 605°F during the fire accident condition. For conservatism, a temperature of 667°F is used in the calculation of the maximum accident condition internal pressure. Given that the internal volume of the NAC-LWT Cask remains constant during the fire, the resultant pressure is proportional to the temperature change according to the ideal gas law:

$$P_2 = P_1 \left(\frac{T_2}{T_1} \right)$$

Thus, for the design basis fire:

$$P_{\text{fire}} = 104.0 \text{ psia} \left(\frac{1127^\circ \text{R}}{932^\circ \text{R}} \right)$$

$$P_{\text{fire}} = 125.8 \text{ psia}$$

3.5.4.2 High Burnup Fuel Rod Canister Maximum Internal Pressure

The high burnup fuel rod canister maximum internal pressure in the accident conditions is calculated assuming 100 percent fuel rod failure combined with the design basis fire maximum temperature. The fuel rod failure assumes release of 30 percent of the fission gas and 100 percent of the backfill gas.

The canister internal pressure is calculated using the method described in Section 3.4.4.2, with the BWR used as the bounding fuel type for the analysis. The total canister pressure is calculated in two steps. First, the pressures documented under normal conditions in Section 3.4.4.2 are adjusted to include the increased total free volume associated with 100 percent fuel rod failure. Then, the canister pressure is adjusted to account for the accident condition temperature.

The partial pressure of the canister volume is calculated by:

$$P_{\text{canister}} = P_{\text{initial}} \left(\frac{V_{\text{canister}}}{V_{\text{total}}} \right)$$

where:

$$P_{\text{initial}} = 29.3 \text{ psia (from earlier)}$$

$$\begin{aligned} V_{\text{canister}} &= 28.2 \text{ liters (from earlier)} \\ V_{\text{void}} &= 0.079 \text{ liter (from earlier)} \\ V_{\text{void}} &= 25 * V_{\text{void}} + V_{\text{canister}} = 30.2 \text{ liters} \\ V_{\text{total}} &= 30.2 \text{ liters} \end{aligned}$$

Therefore, P_{canister} is equal to 27.4 psia. The partial pressure of the fuel rods is calculated by:

$$P_{\text{fuel rods}} = P_{\text{initial}} \left(\frac{V_{\text{fuel rods}}}{V_{\text{total}}} \right)$$

where:

$$\begin{aligned} P_{\text{initial}} &= 1,425 \text{ psia (earlier from Section 3.4.4.2)} \\ V_{\text{fuel rods}} &= 25 * V_{\text{void}} \\ V_{\text{fuel rods}} &= \sim 1.97 \text{ liters (at 100\% of the total fuel rod volume)} \\ V_{\text{total}} &= 30.2 \text{ liters (} V_{\text{canister}} + (25 * V_{\text{void}}) \text{)} \end{aligned}$$

then:

$$P_{\text{fuel rods}} = 1,425 \text{ psia} \left(\frac{1.97 \text{ liters}}{30.2 \text{ liters}} \right) = \sim 94 \text{ psia}$$

and

$$P_{\text{total}} = P_{\text{canister}} + P_{\text{fuel rods}} = 27.4 \text{ psia} + \sim 94 \text{ psia} = \sim 121 \text{ psia} (\sim 8.2 \text{ atm})$$

For the 100% fuel rod failure and the design basis fire accident temperature of 725°F, the pressure is calculated by multiplying the 100% rod failure pressure by the inverse ratio of the normal condition temperature (588.7 K) to the accident temperature (658.15 K). The pressure thus calculated is 135 psia (~9.2 atm)

3.5.4.3 25-Rod Maximum Internal Pressure-Cask Cavity

Using the same methodology used to calculate the cavity pressure in Section 3.5.4.2, the pressure from the 100% fuel rod failure and the design basis fire accident temperature of 725°F is calculated using the cask cavity free gas volume (89.32 liters from earlier). The resulting pressure in the cask cavity, assuming that the gases within the canister are released to the cask cavity, is 67 psia (~4.5 atm).

3.5.4.4 TPBAR Shipment Cask Cavity Internal Pressure-Accident Conditions

Employing the normal condition TPBAR result in Section 3.4.4.5 of 276 psig for the 300 production TPBAR content condition and adjusting system pressure to the average accident gas temperature of 358°F yields a maximum accident condition pressure of 322 psig. For a period of one year following the 90-day cooldown, the pressure for this content condition increases to 337 psig.

Utilizing the same assumptions as presented in Section 3.4.4.5 and the post-accident thermal conditions discussed above, the pressure for the 55 segmented TPBARs in the waste container will be less than 75 psia and, therefore, bounded by the 300 TPBAR content condition.

3.5.4.5 Maximum Internal Pressure for PULSTAR Fuel Payload

Maximum internal pressures under accident conditions are calculated using the same methodology as that employed in Section 3.4.4.6. The accident condition temperature is set to 394°F, and 100 percent of the fuel rods are assumed to fail. The resulting calculated pressures are summarized as follows.

Description	Free Volume	Pressure		
	(liters)	(atm)	(psia)	(psig)
Cask Pressure -28 Intact Assemblies	217.0	2.3	34.0	19.3
Cask Pressure -14 Intact Assemblies and 14 Cans	233.0	2.4	35.4	20.7
Can Pressure - PULSTAR Failed Fuel Can	1.53	5.0	73.9	59.2

3.5.4.6 Maximum Internal Pressure for 16 PWR MOX/UO₂ Fuel Rods in a Rod Holder

Using the same methodology used to calculate the cavity pressure in Section 3.4.4.4, the pressure from the 100% fuel rod failure with 100% gas release and the design basis fire accident temperature of 725°F is calculated. The resulting pressure in the cask cavity is 65.3 psig (80.0 psia, 5.4 atm).

3.5.5 Maximum Thermal Stresses

The most severe thermal stress conditions that occur during the fire test and subsequent cooldown have been evaluated. For conservatism, an internal pressure of 168 psig is used, in the analysis that is performed in Section 2.7.3. The temperatures corresponding to the maximum thermal stresses are reported in Table 3.5-1.

3.5.6 Evaluation of Package Performance for Hypothetical Accident Thermal Conditions

The NAC-LWT cask thermal performance has been assessed for the hypothetical accident, as specified in 10 CFR 71. The O-rings and the lead gamma shields remain within their safe operating ranges. The cask does not suffer any adverse structural consequences as a result of the thermal considerations of the hypothetical accident. The NAC-LWT cask maintains containment and does not exceed the dose rate limits of 49 CFR 173 as a result of the hypothetical accident.

3.5.7 Assessment of the Effects of the Fission Gas Release in the Fire Accident Condition

During the fire, the release of the fission gas is expected to reduce the effective thermal conductivity of the gas in the cavity or inside the sealed canisters. To assess the reduction of the thermal conductivity, the helium conductivity is factored by the ratio of the conservative initial fill pressure of 565 psia (Section 3.4.4) for the PWR fuel assemblies and the end of life pressure (which contains the fill gas plus the fission gas release) of 1,521 psia (Section 3.5.4). This ratio is computed to be 0.37. A conservative ratio of 0.24 is applied to the conductivity of helium, assuming that all fission product gases have a conductivity of zero.

For the temperatures shown, which envelope the maximum temperatures of the cavity gas in the accident condition, the reduced helium properties are larger than the thermal conductivity of air. This is bounding because, as shown in Table 4.2-2, the volume of fission product gas produced by the design basis PWR assembly is higher than that for any other fuel loading.

The data below (Krieth) reflects the comparison of the air conductivity and the factored helium conductivity.

Temperature (°F)	Air Conductivity (K _{air}) (Btu/hr-in-F)	Helium Conductivity (Btu/hr-in-F)	Factored Helium Conductivity (K _{He}) (Btu/hr-in-F)	Ratio K _{He} / K _{air}
300	0.00161	0.00883	0.00212	1.32
400	0.00177	0.00958	0.00230	1.30
500	0.00193	0.01017	0.00244	1.26
600	0.00208	0.01075	0.00258	1.24
700	0.00223	0.01113	0.00267	1.20
800	0.00238	0.01150	0.00276	1.16

The analyses performed for the contents employed air as the gas in the cavity and containers for the accident condition. This demonstrates that the evaluation of the accident condition using air bounds the “reduced helium properties” case.

Figure 3.5-1 Transient Thermal Analysis Finite Element Model of the NAC-LWT

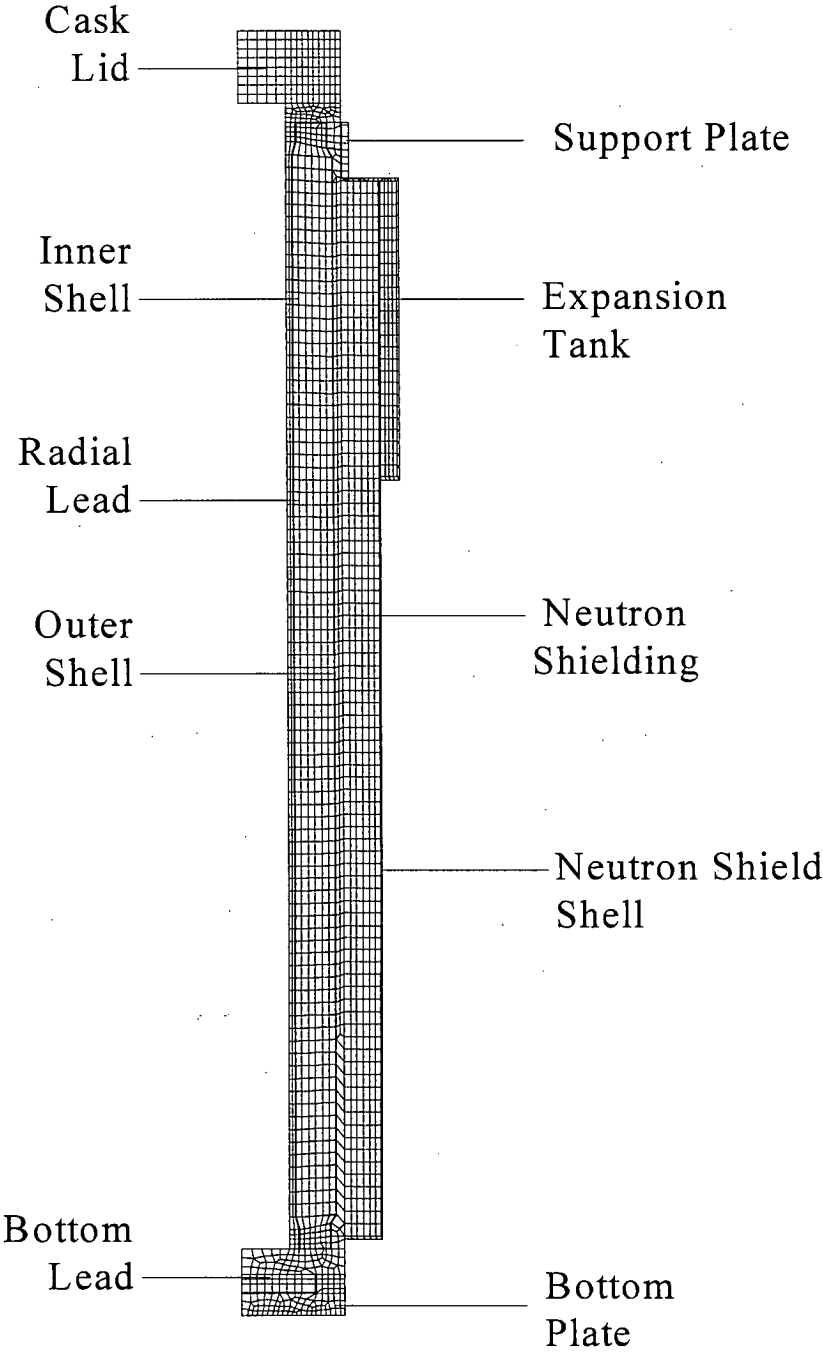
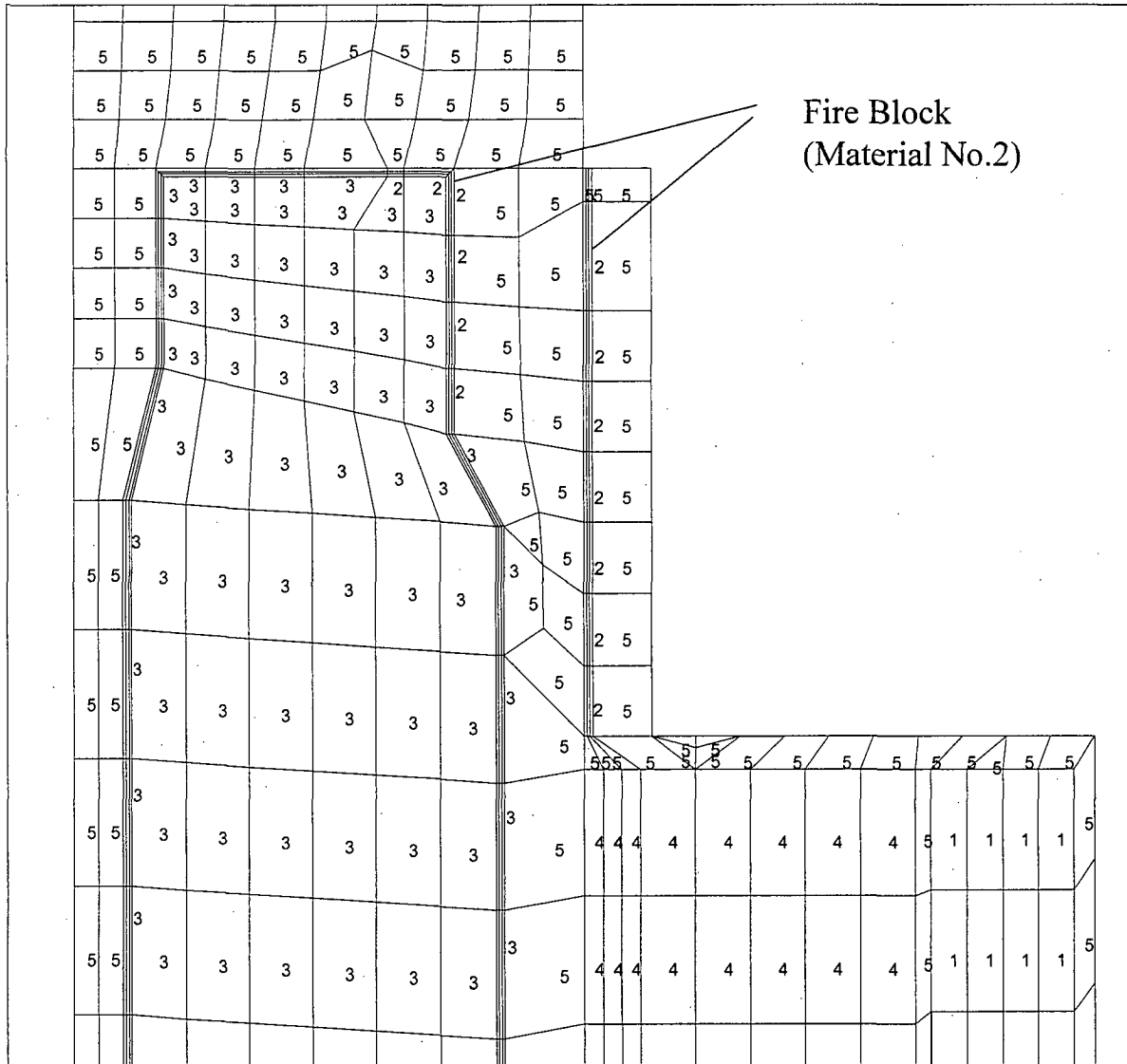
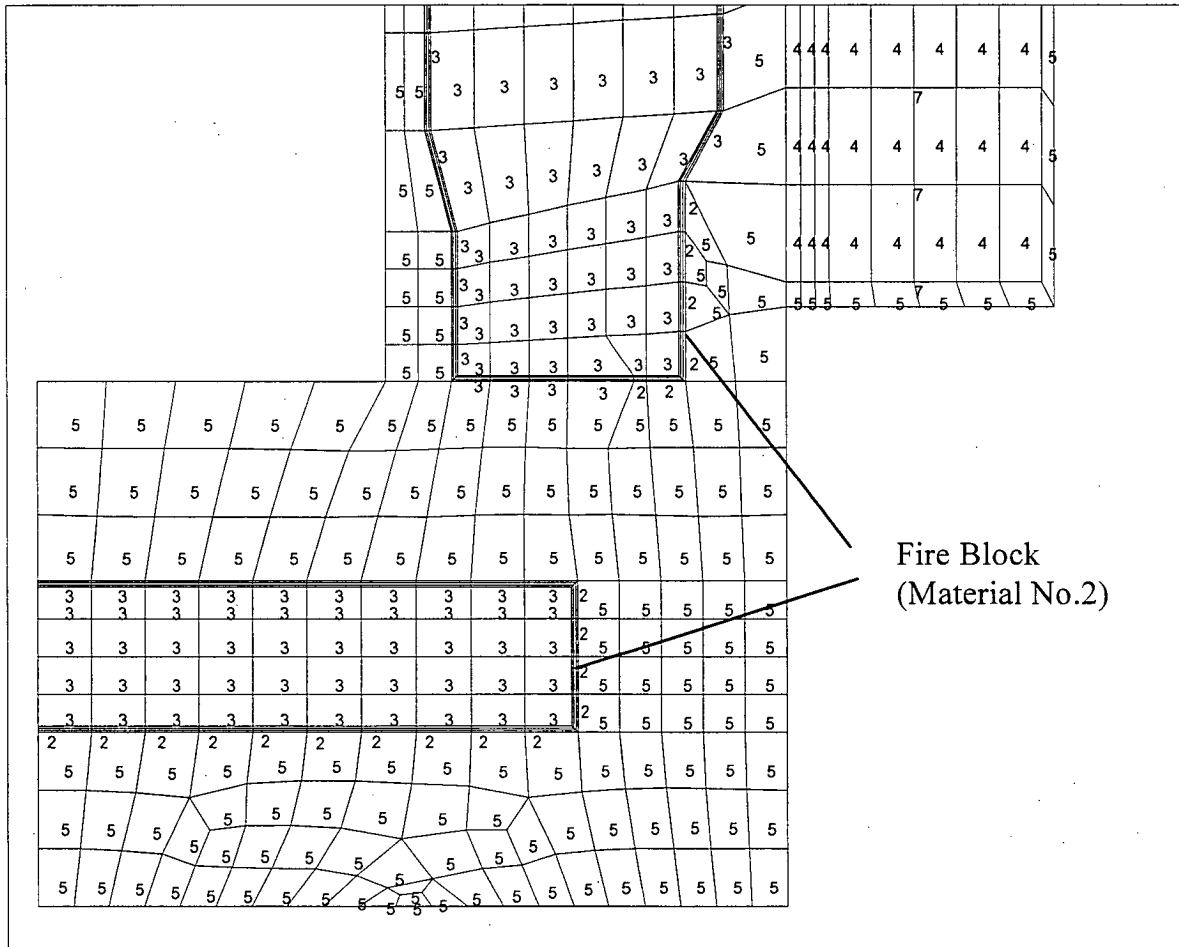


Figure 3.5-2 Top Region of the ANSYS Model



Note: Fire Block is either BISCO FPC or UNIFRAX Fiberfrax Ceramic Fiber Paper

Figure 3.5-3 Bottom Region of the ANSYS Model



Note: Fire Block is either BISCO FPC or UNIFRAX Fiberfrax Ceramic Fiber Paper

Figure 3.5-4 Temperature History of NAC-LWT O-Rings and Valves in the Hypothetical Fire Event

1. Temperature of the Valves
2. Temperature of the O-Rings

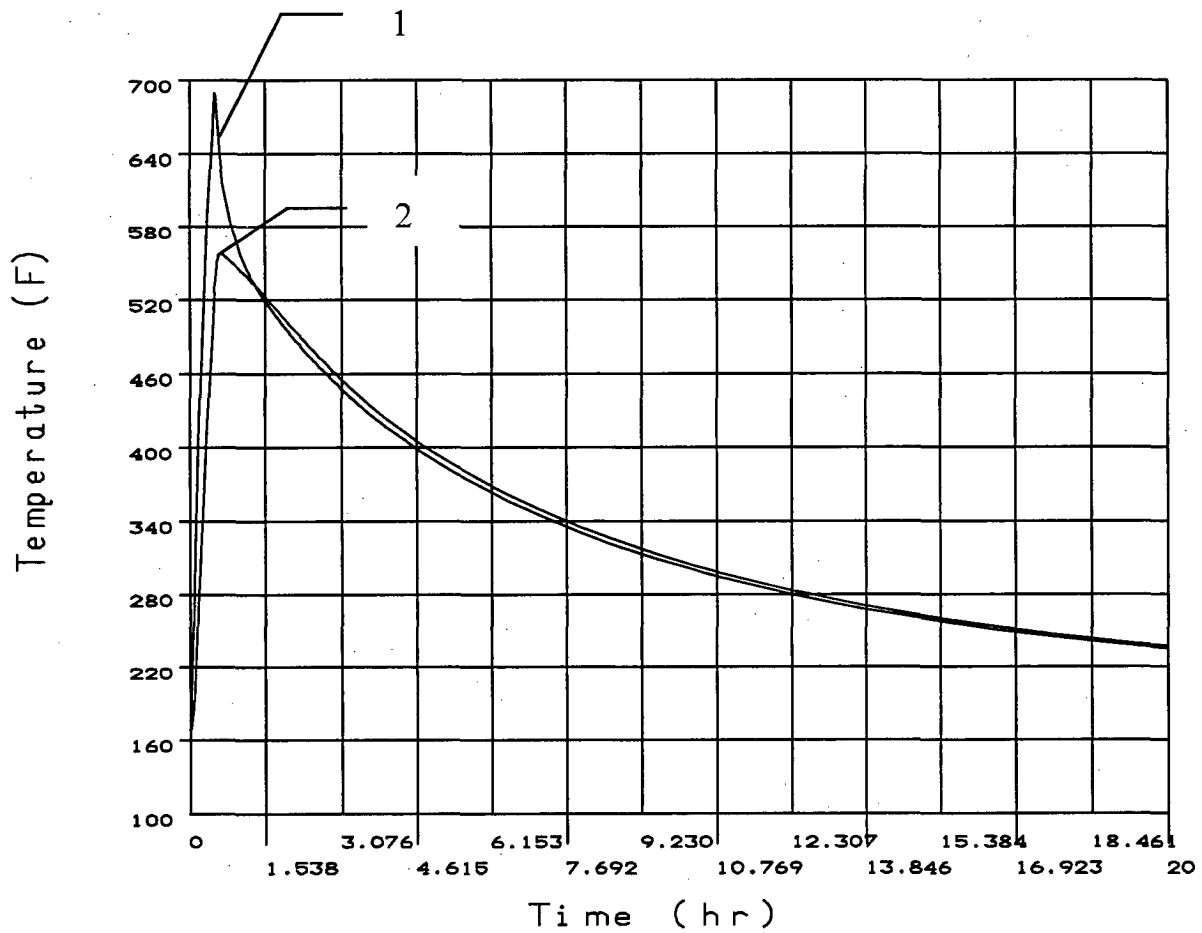


Figure 3.5-5 Temperature History of NAC-LWT Components in the Hypothetical Fire Event

1. Temperature of the Cask Outer Surface
2. Temperature of the Neutron Shield
3. Temperature of the Radial Lead Gamma Shield
4. Temperature of the Bottom Lead Gamma Shield
5. Temperature of the Inner Stainless Steel Shell

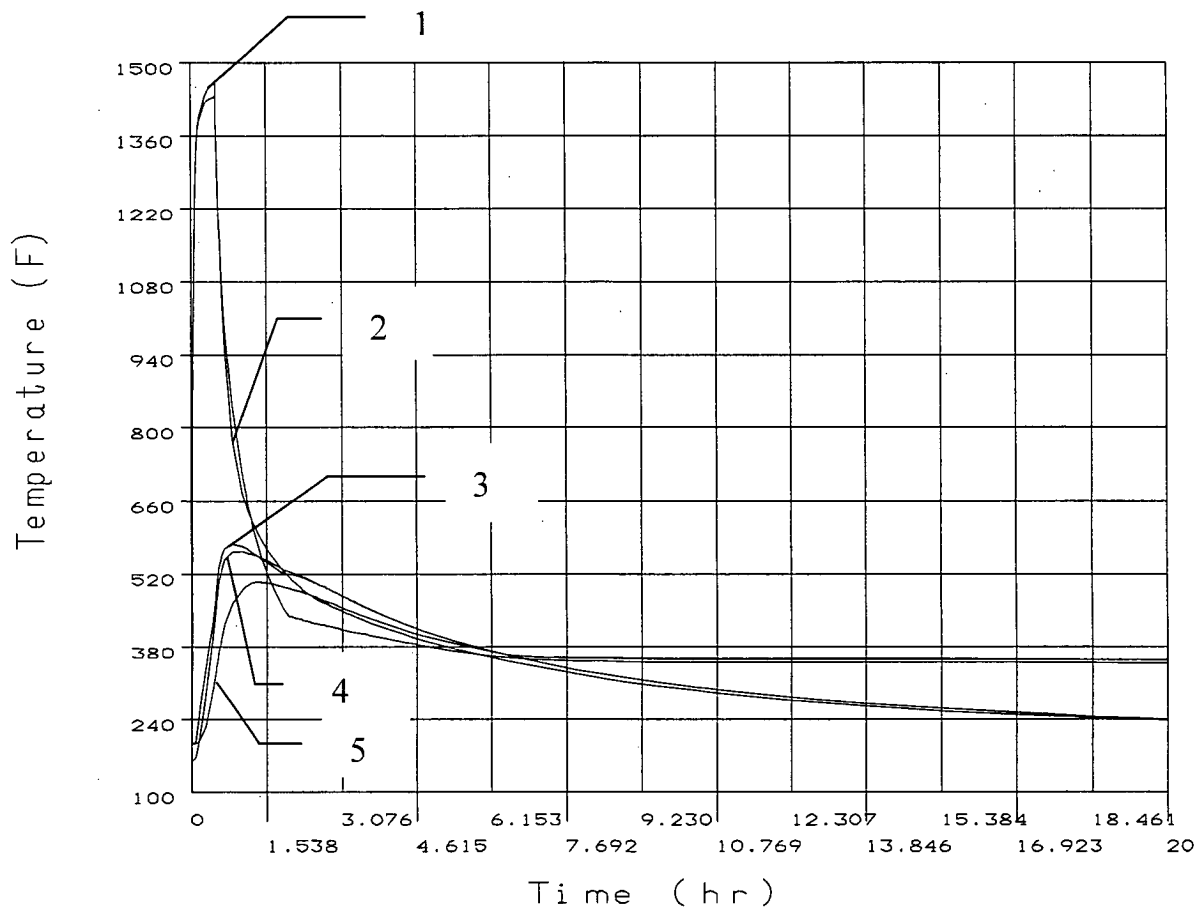


Figure 3.5-6 MTR Fuel Design Basis Heat Load Fire Accident ANSYS Thermal Model
(Uniform 30-Watt/Element Configuration Heat Load)

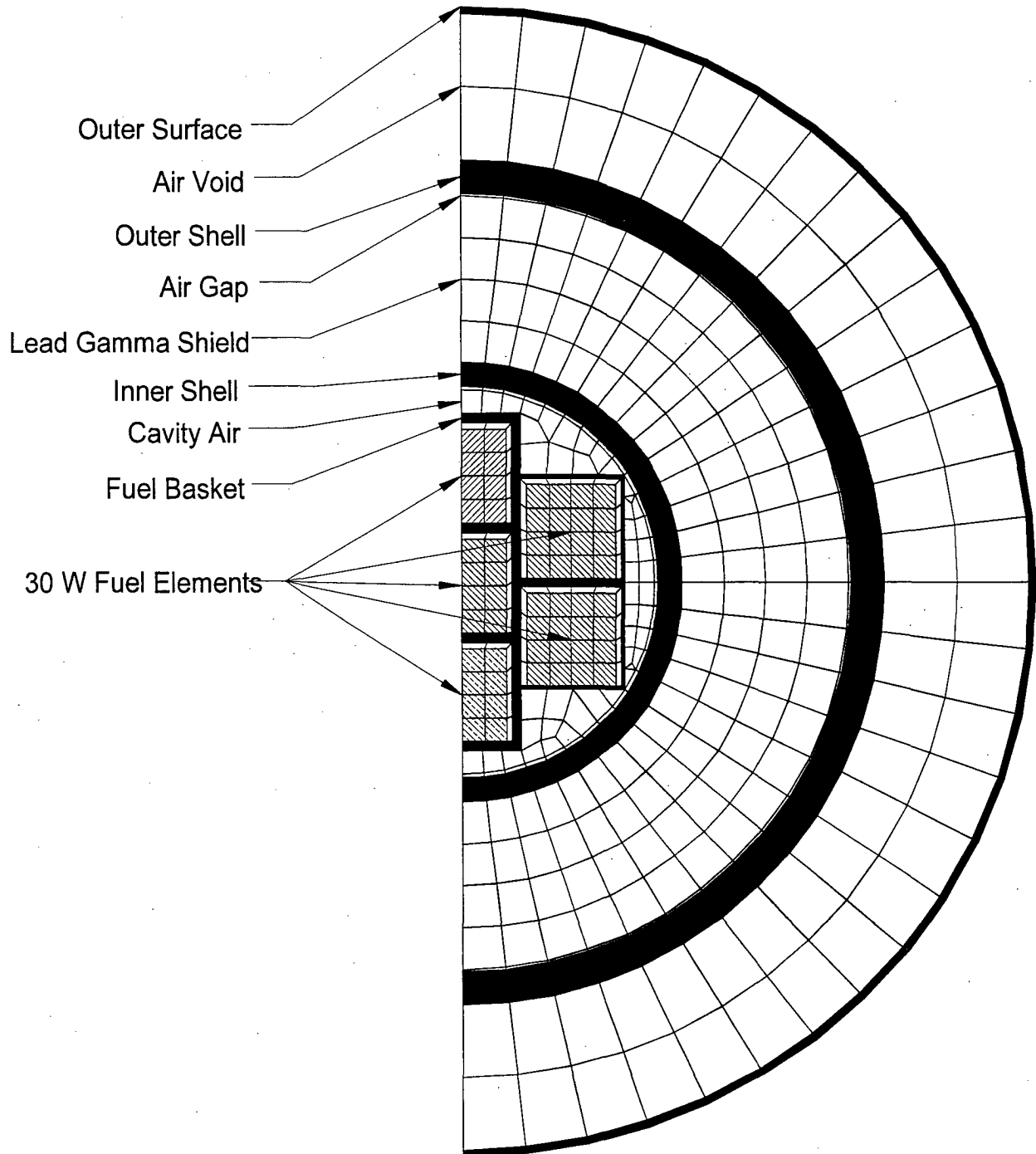


Figure 3.5-7 MTR Fuel Variable Heat Load Fire Accident ANSYS Thermal Model
(120-Watt/70-Watt/20-Watt Configuration Heat Load)

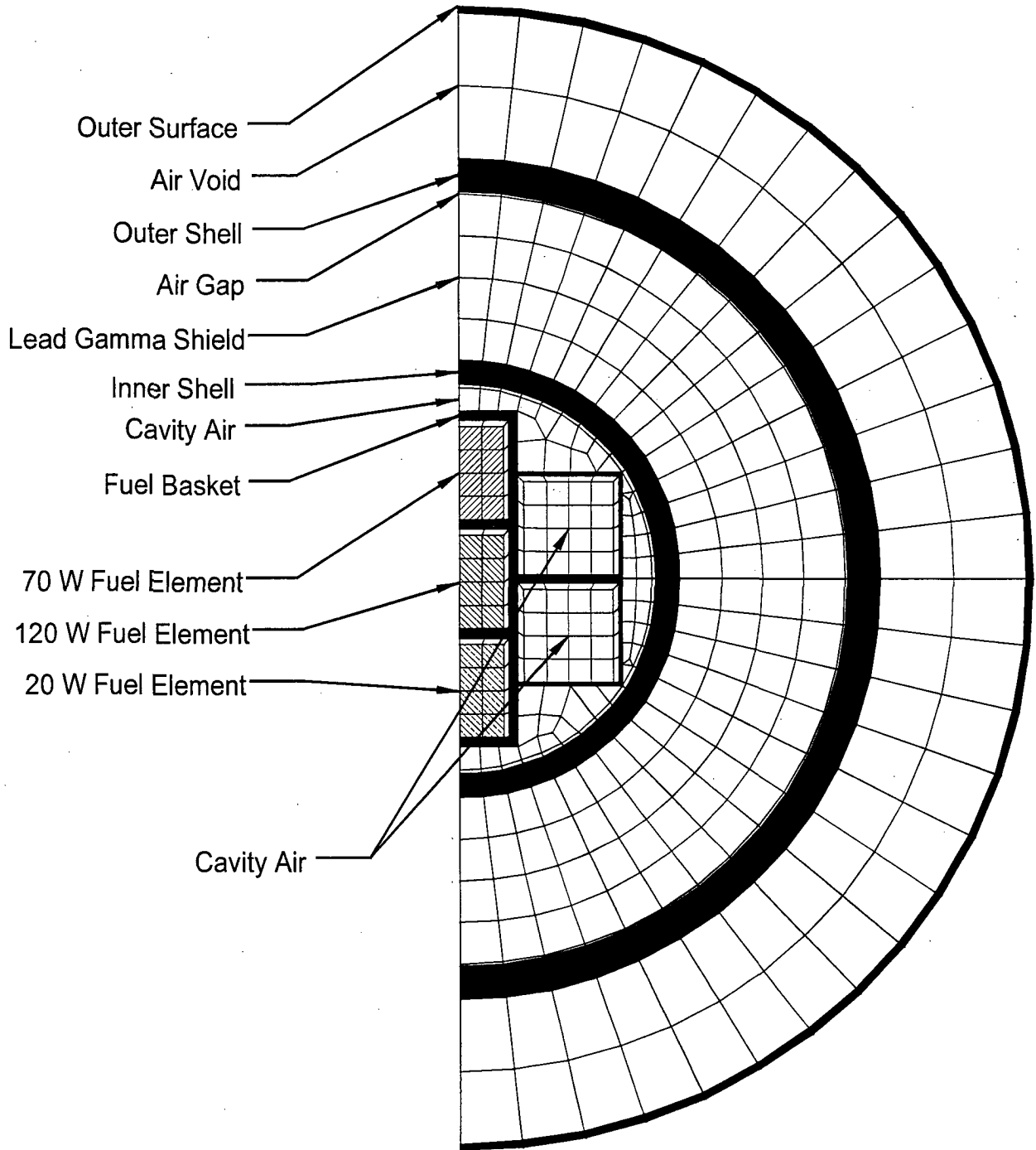
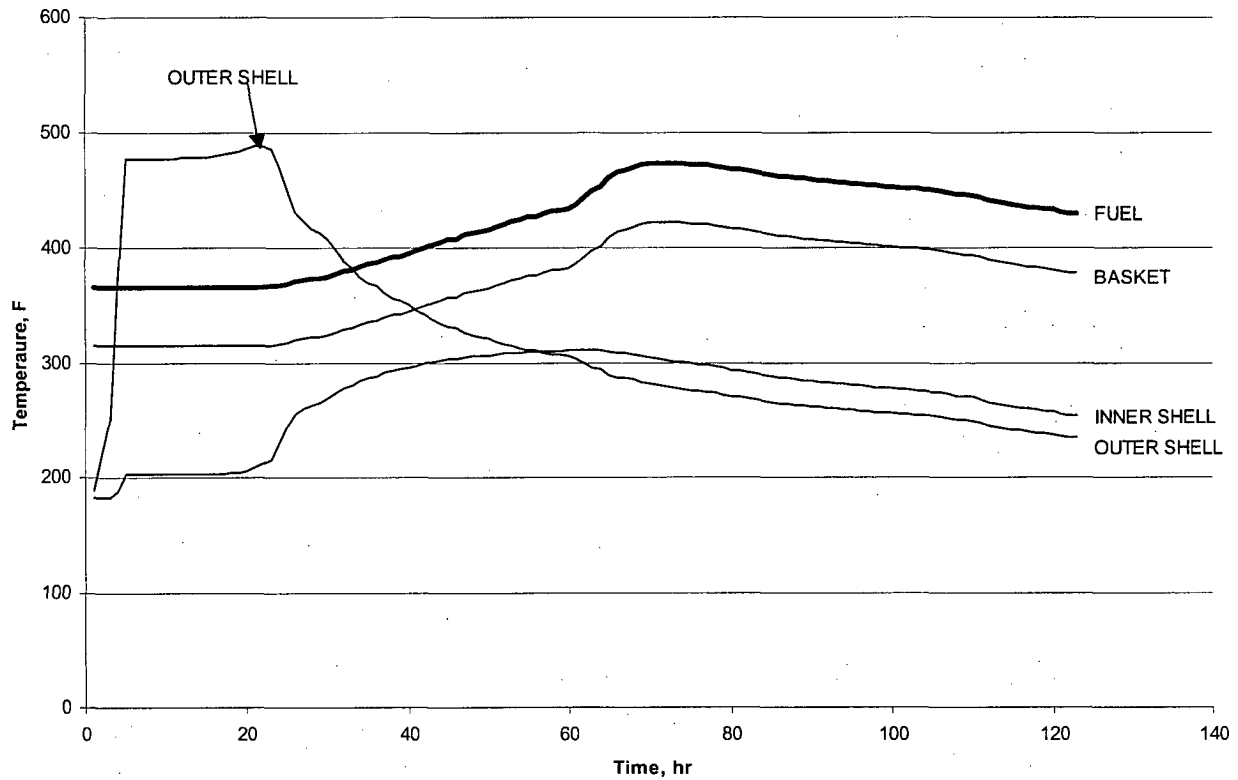
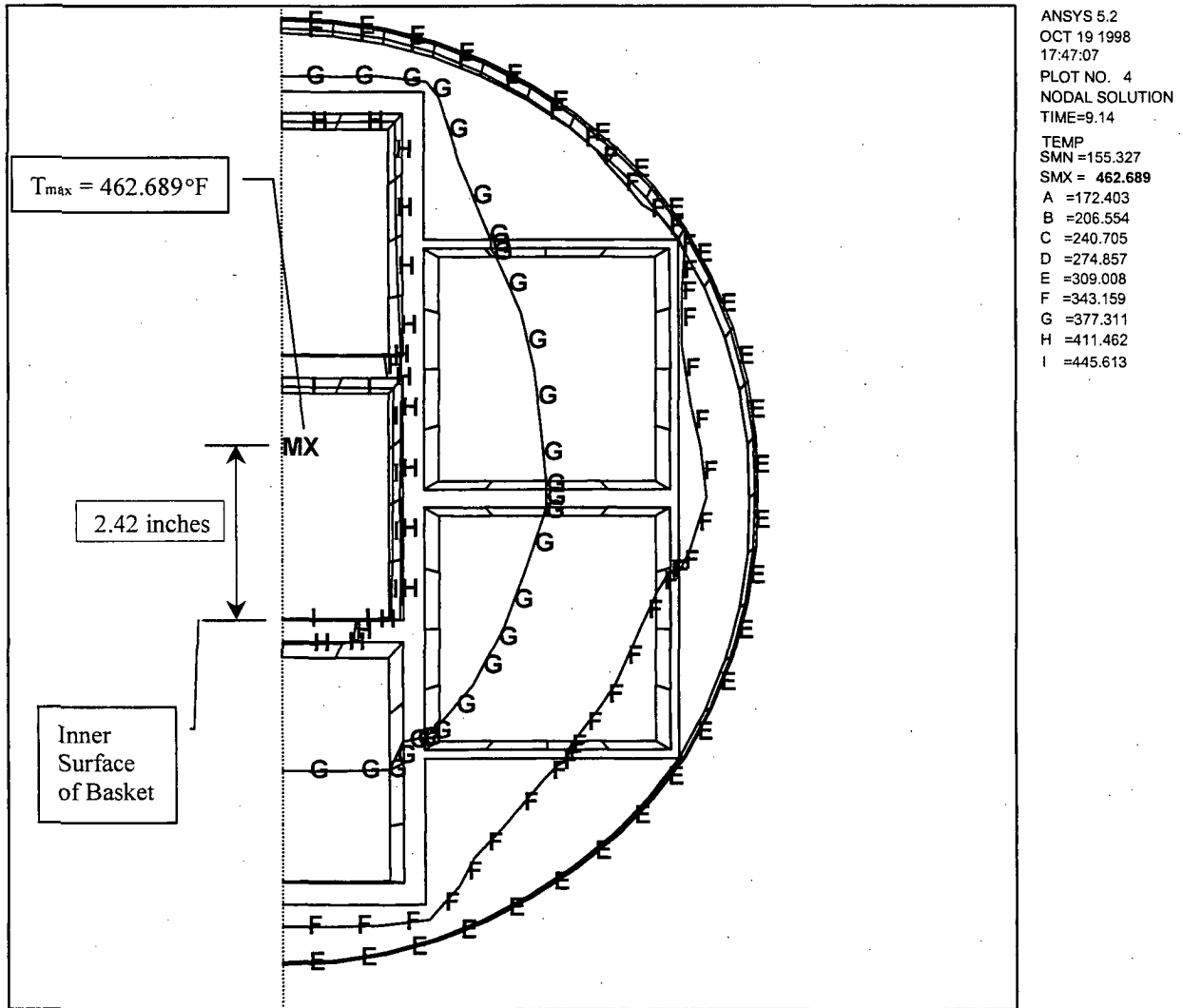


Figure 3.5-8 Temperature History in the MTR Fuel Variable Heat Load Fire Accident Analysis



Note: 120-Watt / 70-Watt / 20-Watt Configuration Heat Load. Cavity gas is air with fire applied to cask surface.

Figure 3.5-9 Location of the Maximum Temperature in the MTR Fuel Variable Heat Load



**Figure 3.5-10 Temperature History for the TRIGA Fuel Cluster Rods Design Basis
Heat Load Fire Accident Analysis**

(Uniform 30 watt/basket cell or 210 watt/basket section or 1.05 kW total heat load)
(Cavity gas: Air, Fire is Applied to the Cask Surface)

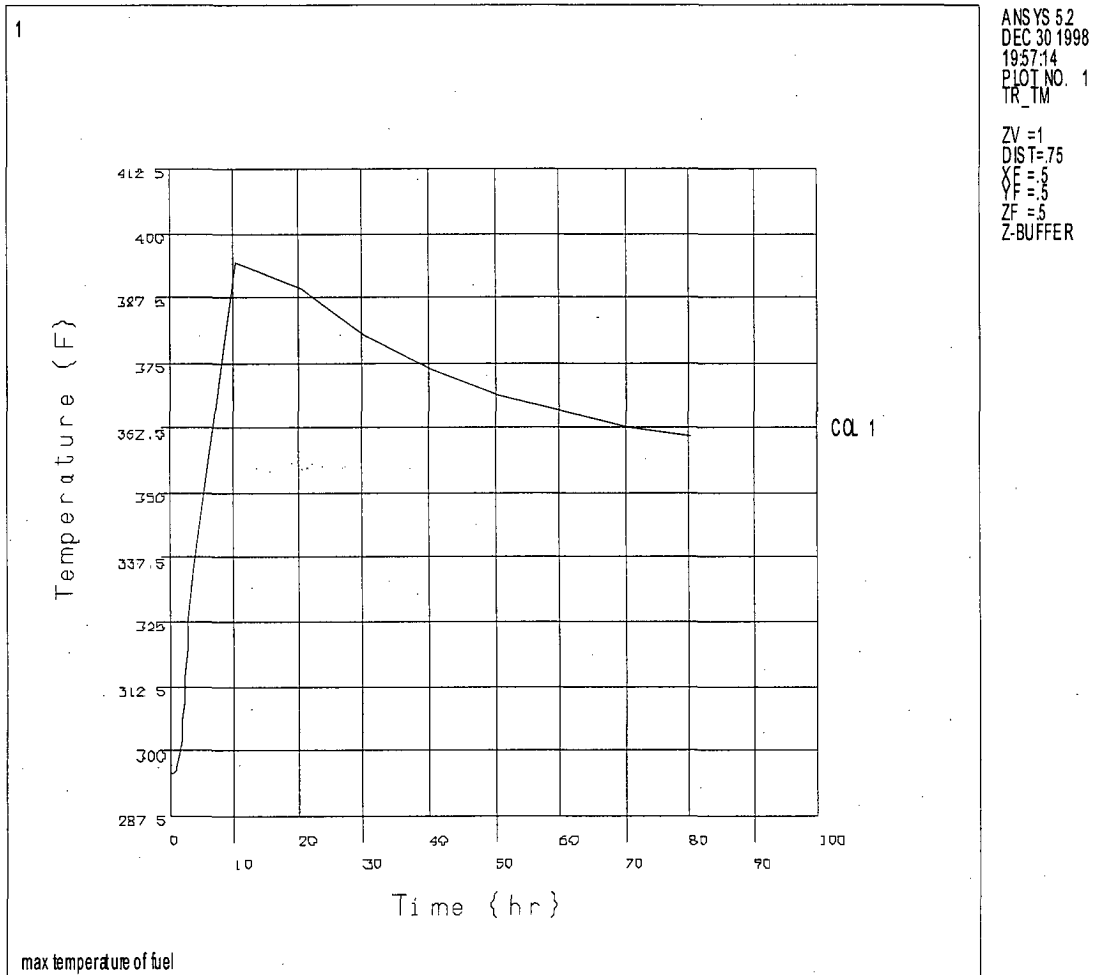


Figure 3.5-11 Temperature History of NAC-LWT Cask Components with PWR and BWR High Burnup Fuel Rods in the Hypothetical Fire Event

1. Average Temperature of Cask Cavity Gas
2. Temperature of the Fuel Cladding
3. Temperature of the Can Weldment
4. Temperature of the Aluminum Structural Component
5. Temperature of the Pin Tube

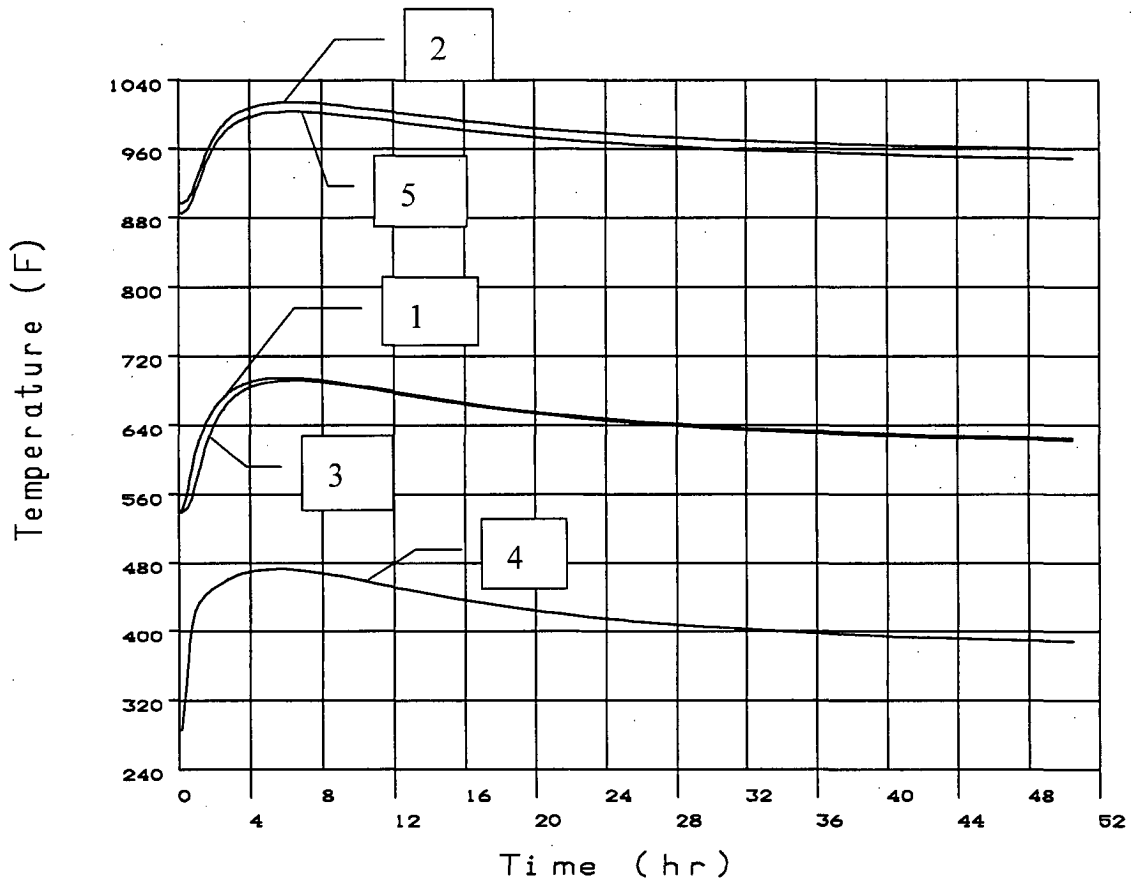


Figure 3.5-12 End of Fire Temperatures of the Alternate Port Cover Components

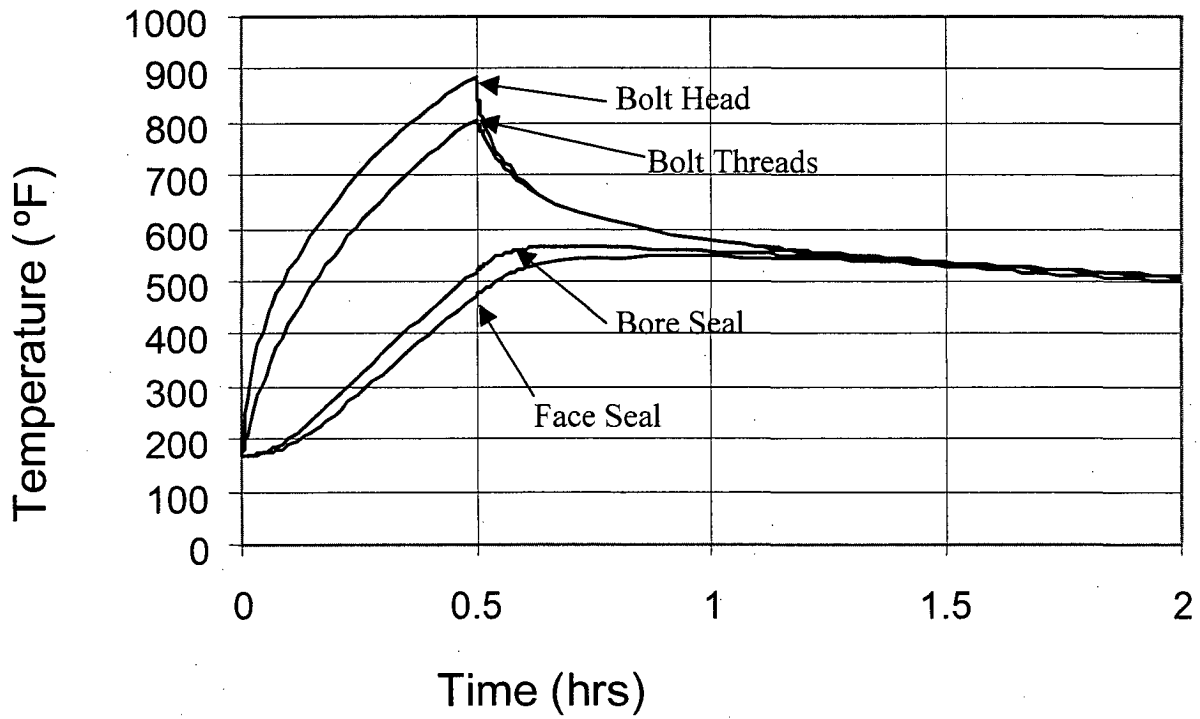
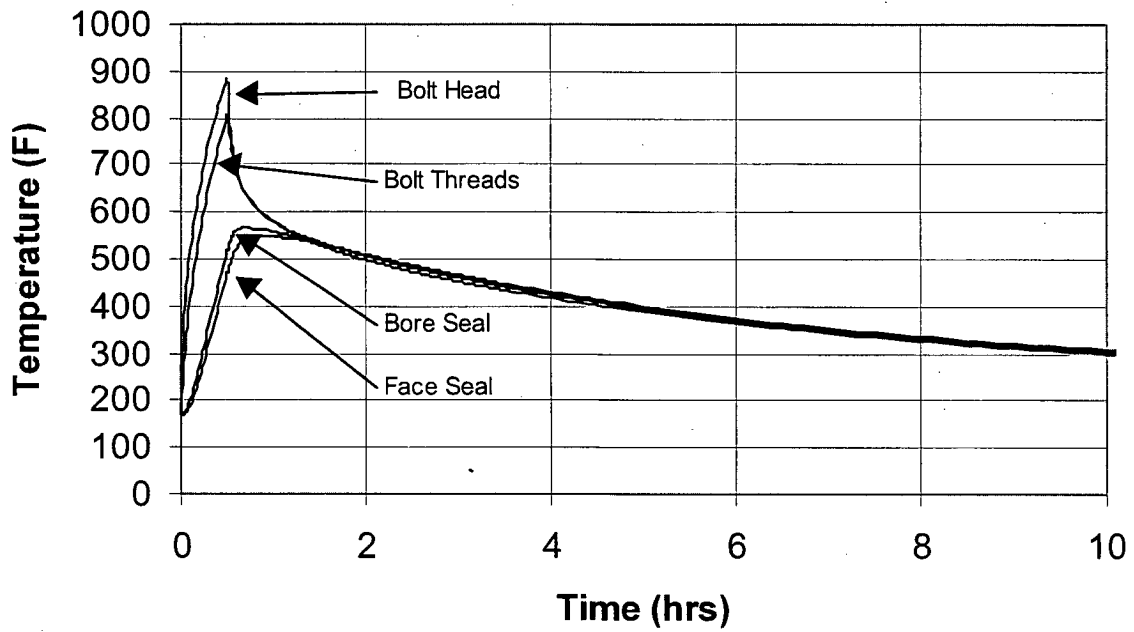


Figure 3.5-13 Transient Temperatures of the Alternate Port Cover Components



**Table 3.5-1 Maximum Component Temperatures (°F) During the Fire Accident
(Design Basis PWR Fuel, 2.5 kW Heat Load)**

Component	Calculated Temperature	Temperature Limit
O-rings: TFE	558	735
Metallic	571 ³	800
Cask radial outer surface	1460	---- ¹
Neutron shield region	1435	---- ¹
Radial lead gamma shield	578	600
Bottom lead gamma shield	564	600
Inner stainless steel shell	505	800
Fuel basket outer wall	507	700 ²
Fuel rod cladding	703	1058
Alternate Port Cover	--	--
Bolt head	886	900
Bolt threads	807	900
Port cover O-ring – bore	565 ⁴	550
Port cover O-ring – face	547	550

- Notes:
1. No upper limit established.
 2. The primary consideration in establishing the safe operating range of the aluminum is maintaining the integrity of the aluminum. According to MIL-HDBK-5F, it can be shown that aluminum at 700°F retains component performance.
 3. The maximum port cover seal temperature is conservatively used to bound the maximum temperature of the metallic seal.
 4. Should the bore seal fail post-fire accident, containment would not be breached.

Table 3.5-2 MTR Fuel Fire Accident Maximum Temperatures (°F), 10 Fuel Plate/120W Element Case (Bounding Configuration)

Condition 2: NAC-LWT (Transported via Truck Trailer)
Cavity Gas: Air

Component	Design Basis Heat Loading [*]	Variable Decay Heat Loading ^{**}
Cask Radial Outer Surface	***	***
Lead Shield	***	***
Inner Shell	334	337
Fuel Basket	374	420
Fuel Cladding	385	473

* Uniform 30-Watt/Element Configuration Heat Load.

** 120-Watt/70-Watt/20-Watt Configuration Heat Load.

*** The maximum temperatures for these components are bounded by the design basis reported.

Table 3.5-3 TRIGA Fuel Fire Accident Maximum Temperatures (°F)

Component	Temperature
Fuel Basket	374
Fuel Cladding	433

Table 3.5-4 PWR and BWR High Burnup Fuel Rods Fire Accident Maximum Temperatures (°F)

NAC-LWT (Transported via Truck Trailer)
Cavity Gas: Air

Component	Temperature
Stainless steel Can Weldment	692
Fuel rod cladding	1,014

Table 3.5-5 Maximum Component Temperatures for High Burnup Fuel Rods in a Rod Holder with Damaged Fuel Rods for the Fire Accident

Component	Normal Conditions Temperature ¹ (T _{norm})(°F)	Temperature Difference (ΔT) (°F)	Accident Temperature T _{acc} = T _{norm} + ΔT(°F)
Rod Holder Weldment	567	692 ² - 538 ³ = 154	721
Fuel Cladding	809	1014 ² - 896 ³ = 118	927

¹ Table 3.4-14.

² Table 3.5-4.

³ Table 3.4-10, Condition 2.

Table 3.5-6 TPBAR Fire Accident Maximum Temperatures

Component	Temperature (°F)
TPBARs	402
Aluminum Basket	340
Consolidation Canister	357

January 2008

Revision LWT-08A

NAC-LWT

Legal Weight Truck Cask System

SAFETY ANALYSIS REPORT

Volume 2 of 2

Docket No. 71-9225



Atlanta Corporate Headquarters: 3930 East Jones Bridge Road, Norcross, Georgia 30092 USA
Phone 770-447-1144, Fax 770-447-1797, www.nacintl.com

List of Effective Pages

LIST OF EFFECTIVE PAGES

Chapter 1

1-i thru 1-iv Revision LWT-08A
1-1 thru 1-5 Revision LWT-08A
1.1-1 thru 1.1-3 Revision LWT-08A
1.2-1 thru 1.2-49 Revision LWT-08A
1.3-1 Revision 38
1.4-1 Revision 38
1.5-1 Revision 38

76 drawings in the
Chapter 1 List of Drawings

Chapter 1 Appendices 1-A
through 1-G

Chapter 2

2-i thru 2-xxiv Revision LWT-08A
2-1 Revision 38
2.1.1-1 thru 2.1.1-2 Revision 38
2.1.2-1 thru 2.1.2-3 Revision 38
2.1.3-1 thru 2.1.3-8 Revision 38
2.2.1-1 thru 2.2.1-3 Revision 38
2.3-1 Revision 38
2.3.1-1 thru 2.3.1-13 Revision 38
2.4-1 Revision 38
2.4.1-1 Revision 38
2.4.2-1 Revision 38
2.4.3-1 Revision 38
2.4.4-1 Revision 38
2.4.5-1 Revision 38
2.4.6-1 Revision 38
2.5.1-1 thru 2.5.1-11 Revision 38
2.5.2-1 thru 2.5.2-17 Revision 38
2.6.1-1 thru 2.6.1-7 Revision 38
2.6.2-1 thru 2.6.2-7 Revision 38
2.6.3-1 Revision 38

2.6.4-1 Revision 38
2.6.5-1 thru 2.6.5-2 Revision 38
2.6.6-1 Revision 38
2.6.7-1 thru 2.6.7-136 Revision 38
2.6.8-1 Revision 38
2.6.9-1 Revision 38
2.6.10-1 thru 2.6.10-15 Revision 38
2.6.11-1 thru 2.6.11-12 Revision 38
2.6.12-1 thru 2.6.12-91 ... Revision LWT-08A
2.7-1 Revision 38
2.7.1-1 thru 2.7.1-117 Revision 38
2.7.2-1 thru 2.7.2-23 Revision 38
2.7.3-1 thru 2.7.3-5 Revision 38
2.7.4-1 Revision 38
2.7.5-1 thru 2.7.5-5 Revision 38
2.7.6-1 thru 2.7.6-4 Revision 38
2.7.7-1 thru 2.7.7-70 Revision 38
2.8-1 Revision 38
2.9-1 thru 2.9-13 Revision 38
2.10.1-1 thru 2.10.1-3 Revision 38
2.10.2-1 thru 2.10.2-49 Revision 38
2.10.3-1 thru 2.10.3-18 Revision 38
2.10.4-1 thru 2.10.4-11 Revision 38
2.10.5-1 Revision 38
2.10.6-1 thru 2.10.6-19 Revision 38
2.10.7-1 thru 2.10.7-66 Revision 38
2.10.8-1 thru 2.10.8-67 Revision 38
2.10.9-1 thru 2.10.9-9 Revision 38
2.10.10-1 thru 2.10.10-97 Revision 38
2.10.11-1 thru 2.10.11-10 Revision 38
2.10.12-1 thru 2.10.12-31 Revision 38
2.10.13-1 thru 2.10.13-17 Revision 38
2.10.14-1 thru 2.10.14-38 Revision 38
2.10.15-1 thru 2.10.15-10 Revision 38

LIST OF EFFECTIVE PAGES (Continued)

Chapter 3

3-i thru 3-v	Revision LWT-08A	5.3.13-1 thru 5.3.13-17.....	Revision 38
3.1-1 thru 3.1-2	Revision LWT-08A	5.3.14-1 thru 5.3.14-21	Revision 38
3.2-1 thru 3.2-11	Revision 38	5.3.15-1 thru 5.3.15-9.....	Revision 38
3.3-1	Revision 38	5.3.16-1 thru 5.3.16-5.....	Revision 38
3.4-1 thru 3.4-84	Revision LWT-08A	5.3.17-1 thru 5.3.17-9.....	Revision 38
3.5-1 thru 3.5-35	Revision LWT-08A	5.3.18-1 thru 5.3.18-29...	Revision LWT-08A
3.6-1 thru 3.6-12	Revision 38	5.4.1-1 thru 5.4.1-6.....	Revision 38

Chapter 4

4-i thru 4-iv	Revision LWT-08A
4.1-1 thru 4.1-3	Revision LWT-08A
4.2-1 thru 4.2-12	Revision LWT-08A
4.3-1 thru 4.3-7	Revision LWT-08A
4.4-1 thru 4.4-2	Revision 38
4.5-1 thru 4.5-85	Revision 38

Chapter 5

5-i thru 5-xi	Revision LWT-08A
5-1 thru 5-3	Revision LWT-08A
5.1.1-1 thru 5.1.1-17 ...	Revision LWT-08A
5.2.1-1 thru 5.2.1-7	Revision 38
5.3.1-1 thru 5.3.1-2	Revision 38
5.3.2-1	Revision 38
5.3.3-1 thru 5.3.3-8	Revision 38
5.3.4-1 thru 5.3.4-19	Revision 38
5.3.5-1 thru 5.3.5-4	Revision 38
5.3.6-1 thru 5.3.6-18	Revision 38
5.3.7-1 thru 5.3.7-11	Revision 38
5.3.8-1 thru 5.3.8-25	Revision 38
5.3.9-1 thru 5.3.9-26	Revision 38
5.3.10-1 thru 5.3.10-14	Revision 38
5.3.11-1 thru 5.3.11-48	Revision 38
5.3.12-1 thru 5.3.12-26	Revision 38

Chapter 6

6-i thru 6-xiii	Revision LWT-08A
6-1	Revision LWT-08A
6.1-1 thru 6.1-5	Revision LWT-08A
6.2-1	Revision 38
6.2.1-1 thru 6.2.1-3	Revision 38
6.2.2-1 thru 6.2.2-3	Revision 38
6.2.3-1 thru 6.2.3-7.....	Revision 38
6.2.4-1	Revision 38
6.2.5-1 thru 6.2.5-5.....	Revision 38
6.2.6-1 thru 6.2.6-3.....	Revision 38
6.2.7-1 thru 6.2.7-2.....	Revision 38
6.2.8-1 thru 6.2.8-3.....	Revision 38
6.2.9-1 thru 6.2.9-4.....	Revision 38
6.2.10-1 thru 6.2.10-3.....	Revision 38
6.2.11-1 thru 6.2.11-3.....	Revision 38
6.2.12-1 thru 6.2.12-4.....	Revision 38
6.3.1-1 thru 6.3.1-6.....	Revision 38
6.3.2-1 thru 6.3.2-4.....	Revision 38
6.3.3-1 thru 6.3.3-9.....	Revision 38
6.3.4-1 thru 6.3.4-9.....	Revision 38
6.3.5-1 thru 6.3.5-12.....	Revision 38
6.3.6-1 thru 6.3.6-9.....	Revision 38
6.3.7-1 thru 6.3.7-4.....	Revision 38
6.3.8-1 thru 6.3.8-7.....	Revision 38

LIST OF EFFECTIVE PAGES (Continued)

6.3.9-1 thru 6.3.9-7Revision 38
6.4.1-1 thru 6.4.1-10Revision 38
6.4.2-1 thru 6.4.2-10Revision 38
6.4.3-1 thru 6.4.3-34Revision 38
6.4.4-1 thru 6.4.4-24Revision 38
6.4.5-1 thru 6.4.5-32Revision 38
6.4.6-1 thru 6.4.6-17Revision 38
6.4.7-1 thru 6.4.7-14Revision 38
6.4.8-1 thru 6.4.8-14Revision 38
6.4.9-1 thru 6.4.9-10Revision 38
6.4.10-1 thru 6.4.10-18Revision 38
6.5.1-1 thru 6.5.1-13Revision 38
6.5.2-1 thru 6.5.2-4Revision 38
6.5.3-1 thru 6.5.3-2Revision 38
6.7.1.1 thru 6.7.1-18.....Revision LWT-08A
6.7.2.1 thru 6.7.2-47.....Revision LWT-08A

6.6.15-1 thru 6.6.15-43..Revision LWT-08A

Chapter 7

7-i thru 7-iiRevision LWT-08A
7.1-1 thru 7.1-56.....Revision LWT-08A
7.2-1 thru 7.2-14.....Revision LWT-08A
7.3-1 thru 7.3-2..... Revision 38

Chapter 8

8-iRevision LWT-08A
8.1-1 thru 8.1-11Revision LWT-08A
8.2-1 thru 8.2-4.....Revision LWT-08A
8.3-1 thru 8.3-4..... Revision 38

Chapter 9

9-iRevision LWT-08A
9-1 thru 9-10.....Revision LWT-08A

Appendix 6.6

6.6-i thru 6.6-iii Revision LWT-08A
6.6-1Revision 38
6.6.1-1 thru 6.6.1-111Revision 38
6.6.2-1 thru 6.6.2-56Revision 38
6.6.3-1 thru 6.6.3-73Revision 38
6.6.4.-1 thru 6.6.4-77Revision 38
6.6.5-1 thru 6.6.5-101Revision 38
6.6.6-1 thru 6.6.6-76Revision 38
6.6.7-1 thru 6.6.7-84Revision 38
6.6.8-1 thru 6.6.8-183Revision 38
6.6.9-1 thru 6.6.9-52Revision 38
6.6.10-1 thru 6.6.10-33Revision 38
6.6.11-1 thru 6.6.11-47Revision 38
6.6.12-1 thru 6.6.12-20Revision 38
6.6.13-1 thru 6.6.13-22Revision 38
6.6.14-1 thru 6.6.14-7Revision 38

Chapter 4

Table of Contents

4	CONTAINMENT	4.1-1
4.1	Containment Boundary	4.1-1
4.1.1	Containment Penetrations	4.1-1
4.1.2	Seals and Welds	4.1-1
4.1.3	Closure	4.1-3
4.2	Containment Requirements for Normal Conditions of Transport	4.2-1
4.2.1	Containment of Radioactive Material	4.2-1
4.2.2	Pressurization of Containment Vessel	4.2-8
4.2.3	Containment Criteria.....	4.2-9
4.3	Containment Requirements for Hypothetical Accident Conditions.....	4.3-1
4.3.1	Fission Gas Products.....	4.3-1
4.3.2	Containment of Radioactive Materials	4.3-1
4.3.3	Tritium Contamination Issues.....	4.3-5
4.4	Special Requirements.....	4.4-1
4.5	Appendices.....	4.5-1
4.5.1	Tetrafluoroethylene O-Rings.....	4.5-1
4.5.2	Metallic O-Rings.....	4.5-10
4.5.3	Viton® O-Rings	4.5-23
4.5.4	SAS2H Output and Group A ₂ Values for Design Basis PWR, BWR, TRIGA, MTR and DIDO Fuel.....	4.5-29
4.5.5	Containment Analysis of MTR Fuel Elements	4.5-51
4.5.6	Evaluation of Normal Conditions Allowable Leakage Rate for 25 BWR High Burnup Rods with up to 14 Damaged Rods.....	4.5-57
4.5.7	Containment Analysis of DIDO Fuel Assemblies	4.5-62
4.5.8	Containment Analysis for PULSTAR Fuel Elements.....	4.5-67
4.5.9	Metallic Face Seal.....	4.5-73
4.5.10	Containment Analysis of ANSTO Basket Payloads	4.5-85

List of Figures

Figure 4.5-1 SAE International Aerospace Standard AS8791 4.5-2
Figure 4.5-2 Metallic O-Rings Technical Bulletin 4.5-11
Figure 4.5-3 Parker Seals Material Report on the Viton® Material..... 4.5-25

List of Tables

Table 4.2-1	Release Fractions: Normal and Accident Conditions	4.2-10
Table 4.2-2	Allowable Release Rates for NAC-LWT Cask Contents: Normal Conditions	4.2-10
Table 4.2-3	Cask Free Volumes and Pressures	4.2-11
Table 4.2-4	Leak Rate and Leak Test Sensitivity - Normal Conditions	4.2-12
Table 4.3-1	A ₂ Calculation for PWR Spent Fuel	4.3-6
Table 4.3-2	Standard Leak Rates for Accident Conditions.....	4.3-6
Table 4.3-3	A ₂ Calculation for 25 High Burnup PWR Spent Fuel Rods.....	4.3-7
Table 4.3-4	A ₂ Calculation for 25 High Burnup BWR Spent Fuel Rods	4.3-7
Table 4.4-1	Transport Conditions for the TRIGA Sealed Failed Fuel Can	4.4-2
Table 4.4-2	A ₂ Calculation for Two Canned FLIP-LEU II Elements.....	4.4-2
Table 4.4-3	Normal and Accident Condition Leak Rates for the TRIGA Failed Fuel Can	4.4-2
Table 4.5-1	Westinghouse 15×15 SAS2H Output and Group A ₂ Value (Gas).....	4.5-30
Table 4.5-2	Westinghouse 15×15 SAS2H Output and Group A ₂ Value (Volatiles).....	4.5-30
Table 4.5-3	Westinghouse 15×15 SAS2H Output and Group A ₂ Value (Fuel Fines)	4.5-31
Table 4.5-4	General Electric 7×7 SAS2H Output and Group A ₂ Value (Gas).....	4.5-33
Table 4.5-5	General Electric 7×7 SAS2H Output and Group A ₂ Value (Volatiles)	4.5-33
Table 4.5-6	General Electric 7×7 SAS2H Output and Group A ₂ Value (Fuel Fines).....	4.5-34
Table 4.5-7	TRIGA (FLIP-LEU II) SAS2H Output and Group A ₂ Value (Gas)	4.5-36
Table 4.5-8	TRIGA (FLIP-LEU II) SAS2H Output and Group A ₂ Value (Volatiles)	4.5-36
Table 4.5-9	TRIGA (FLIP-LEU II) SAS2H Output and Group A ₂ Value (Fuel Fines).....	4.5-37
Table 4.5-10	MTR HEU SAS2H Output and Group A ₂ Value (Gas).....	4.5-39
Table 4.5-11	MTR HEU SAS2H Output and Group A ₂ Value (Volatiles).....	4.5-39
Table 4.5-12	MTR HEU SAS2H Output and Group A ₂ Value (Fuel Fines)	4.5-40
Table 4.5-13	25 High Burnup BWR-Rod SAS2H Output and Group A ₂ Value (Gas).....	4.5-42
Table 4.5-14	25 High Burnup BWR-Rod SAS2H Output and Group A ₂ Value (Volatiles) ..	4.5-42
Table 4.5-15	25 High Burnup BWR-Rod SAS2H Output and Group A ₂ Value (Fuel Fines)	4.5-43
Table 4.5-16	25 High Burnup PWR-Rod SAS2H Output and Group A ₂ Value (Gas).....	4.5-45
Table 4.5-17	25 High Burnup PWR-Rod SAS2H Output and Group A ₂ Value (Volatiles)...	4.5-45
Table 4.5-18	25 High Burnup PWR-Rod SAS2H Output and Group A ₂ Value (Fuel Fines)	4.5-46
Table 4.5-19	DIDO LEU SAS2H Output and Group A ₂ Value (Gas)	4.5-48
Table 4.5-20	DIDO LEU SAS2H Output and Group A ₂ Value (Volatiles)	4.5-48
Table 4.5-21	DIDO LEU SAS2H Output and Group A ₂ Value (Fuel Fines).....	4.5-49
Table 4.5-22	Pressure Summary for PULSTAR Fuel	4.5-69
Table 4.5-23	PULSTAR Fuel SAS2H Output and Group A ₂ Value (Gas).....	4.5-69
Table 4.5-24	PULSTAR Fuel SAS2H Output and Group A ₂ Value (Volatiles).....	4.5-69

List of Tables (continued)

Table 4.5-25	PULSTAR Fuel SAS2H Output and Group A ₂ Value (Fuel Fines)	4.5-70
Table 4.5-26	PULSTAR Fuel Containment Release Fractions.....	4.5-72
Table 4.5-27	Containment Analysis Results for PULSTAR Fuel Payloads.....	4.5-72
Table 4.5-28	PULSTAR Fuel Leakage Rate Calculation	4.5-72

4 CONTAINMENT

4.1 Containment Boundary

The containment boundary for the NAC-LWT cask consists of the 0.75-inch thick inner shell, the 4.0-inch thick bottom end plate, the 11.25-inch thick lid, and the upper ring forging. The inner shell is Type XM-19 stainless steel and the other components are Type 304 stainless steel. The valves used for filling and draining the cask cavity are not considered to be part of containment; this function is provided by the valve port covers. There are two port cover designs: alternate and Alternate B. The alternate port cover is fabricated from SA-705, Grade 630, condition H1150 precipitation-hardened stainless steel. The Alternate B port cover is fabricated from XM-19 stainless steel and is designed to withstand a higher MNOP and to provide a leaktight containment boundary. The closure lid's metallic O-ring seal and the port cover's Viton[®] O-ring (alternate port cover) or metallic face seal (Alternate B port cover) are also part of the containment boundary. The sealing surfaces for O-rings and seals are machined in accordance with seal manufacturers' recommendations to a finish suitable to achieve reliable sealing of the containment. The metal face seal, located on the Alternate B port cover face, is in a 0.125-inch counterbore with a suitable surface finish, and provides a leaktight containment boundary seal when the Alternate B port cover design is used.

4.1.1 Containment Penetrations

The only containment penetrations in the NAC-LWT cask are the cask cavity vent and drain ports, and the cask lid.

4.1.2 Seals and Welds

4.1.2.1 Seals

The O-rings of the cask lid and valve port covers are the seals that affect containment for the radioactive contents of the NAC-LWT cask, as described in Section 4.1. Appendix 4.5.1 contains the military specification that prescribes the physical and chemical properties of the TFE O-rings. Appendix 4.5.2 is the manufacturer's technical bulletin for the metallic O-rings. Seal testing, prior to cask acceptance from the manufacturer, during routine maintenance, and upon assembly for transportation, includes the fabrication leakage rate test, the periodic maintenance leakage rate test, and the preshipment leakage rate test in accordance with the requirements of ANSI N14.5-1997. Appendix 4.5.3 contains a description of the leakage testing performed using the Viton[®] O-rings on the alternate port cover design at temperatures exceeding the

manufacturer's elevated temperature limit. Appendix 4.5.3 also contains the O-ring manufacturer's material report on the Viton[®] material. Appendix 4.5.9 contains the technical specification on the Alternate B port cover HELICOFLEX[®] metallic face seal.

4.1.2.1.1 Fabrication Leakage Rate Test

Upon completion of fabrication, the cask containment shall be tested as described in Section 8.1.3. There are two leakage rates defined for the NAC-LWT containment boundary: one for radioactive material contents that do not require a leaktight containment, and a second for radioactive material contents requiring a leaktight containment boundary—e.g., TPBARs, PWR MOX fuel rods, etc. The standard helium leakage rate test verifies the containment boundary integrity of the package, including the closure lid and alternate port covers, to a leakage rate of less than or equal to 5.5×10^{-7} cm³/s (helium). The leaktight helium leakage rate test verifies the containment boundary integrity of the package, including cask lid and Alternate B port covers, to a leakage rate of less than or equal to 2×10^{-7} cm³/s (helium). The leakage rate tests are further described in Chapter 8.

4.1.2.1.2 Fabrication Pressure Test

During acceptance testing, the cask containment boundary shall be hydrostatically tested using the pressure test described in Section 8.1.2. This test verifies the sealing integrity of the package with a hydrostatic test pressure of 209 psig for fissile material shipments.

As an additional post-fabrication test, prior to performing the first TPBAR shipment in a specific NAC-LWT cask, the hydrostatic test described in Section 8.1.2 shall be performed with the Alternate B port covers installed. The test pressure for the hydrostatic test shall be 450 psig, which is 150% MNOP. The hydrostatic tests are further described in Chapter 8.

4.1.2.1.3 Preshipment Leakage Rate Test

Prior to shipment of a loaded NAC-LWT cask, the containment seals of the closure lid and the vent and drain port covers shall be individually leakage tested. For the alternate port covers, a pressure drop test is performed by pressurizing the volume between the containment seal and the test seal. This preshipment leakage rate test assures that the port covers and seals are properly installed and that there is no leakage in excess of the minimum test sensitivity of 1×10^{-3} cm³/s.

If the alternate port cover Viton[®] containment O-ring is replaced, a maintenance leakage rate test is required to be performed per Section 8.1.3.

The closure lid and the Alternate B port cover both utilize metallic O-rings for the containment boundary seal. Metallic O-rings are designed for a single use and must be replaced prior to each loaded transport. Following installation of the closure lid and Alternate B port covers, maintenance leakage rate tests are performed on each component in accordance with the helium leak test procedures in Section 8.1.3.

4.1.2.2 Welds

All containment vessel welds are full penetration bevel or groove welds to ensure structural and containment integrity.

4.1.3 Closure

Closure of the containment vessel is provided by the twelve 1-8 UNC closure lid bolts, each tightened to 260 ± 20 ft-lb of torque. The lid bolts are SA-453, Grade 660 high alloy steel bolting material. The lid bolts are preloaded so that the lid seals remain fully compressed for all load conditions. The structural adequacy of the lid bolts is documented in Sections 2.1.3.2.2, 2.6.7.6 and 2.10.9. The closure lid O-ring seals are specified on Drawing No 315-40-02 in Section 1.4. The O-ring seals and grooves are selected based on the manufacturer's specifications to satisfy the pressure and temperature conditions incurred by the NAC-LWT cask. The leakage test described in Section 8.1.3 verifies that the lid seal leakage rate does not exceed 5.5×10^{-7} cm³/sec (helium) for packages that do not require a leaktight containment boundary. Packages requiring a leaktight containment boundary are tested per Section 8.1.3 to a lid seal leakage rate of less than or equal to 2×10^{-7} cm³/s (helium).

Alternate port covers are retained by three $\frac{3}{8}$ - 16 UNC bolts, each tightened to 100 ± 10 in-lb of torque. The bolt material for these ports covers is SA-193, Grade B6 high alloy steel. The Alternate B port cover is retained by three $\frac{3}{8}$ - 16 UNC bolts, made from SB-637 Grade N07718 nickel alloy steel, each tightened to 285 ± 15 in-lb of torque. The Alternate B port covers are required for the transport of PWR MOX fuel rods, TPBAR contents and other contents that require a leaktight containment configuration.

4.2 Containment Requirements for Normal Conditions of Transport

The NAC-LWT cask must maintain a radioactivity release rate less than 10^{-6} A₂/hr under normal conditions of transport, as required by 10 CFR 71.51 and IAEA Transportation Safety Standards (TS-R-1). For any of the evaluated fuels, except for those requiring a leaktight containment, this condition is satisfied by maintaining a maximum allowable leak rate of 6.39×10^{-7} ref. cm³/sec (air) at standard temperature and pressure conditions for normal conditions of transport as shown in Table 4.2-4. The equivalent maximum allowable helium leak rate is 1.06×10^{-6} std cm³/sec (helium). To ensure that the maximum allowable leak rate is not exceeded, the cask is conservatively leak tested to 5.5×10^{-7} std cm³/sec (helium). As shown in Table 4.3-2, the allowable leak rate for accident conditions is larger. For the transport of PWR MOX fuel rods and TPBARs, a leaktight containment boundary is required. Leaktight is defined per ANSI N14.5-1997 to be 1×10^{-7} ref cm³/sec (2×10^{-7} std cm³/sec helium).

The limiting contents for the containment analysis for the non-leaktight containment boundary condition are 25 BWR high burnup fuel rods, assuming that 56%, or 14, of the fuel rods are classified as damaged. The analysis is based on the assumption that the fuel rods fail in transport, which is considered to bound the condition in which the fuel is already damaged. This is conservative since fuel classified as damaged is likely to have already lost its initial helium backfill charge and fission gases prior to loading in the transport cask. The calculated allowable leak rate for the 14 failed rod configuration is 1.06×10^{-6} std cm³/sec (helium). This value is greater than the helium leak test condition of 5.5×10^{-7} cm³/sec (helium). Therefore, transport of 25 high burnup PWR or BWR fuel rods, with up to 14 of the fuel rods classified as damaged, is acceptable.

The PULSTAR fuel element containment evaluations, compliant with a 10 CFR 71 B(U)F-96 designation as specified in the TS-R-1 compliance document, are presented in Section 4.5.8. Both intact and damaged fuel payloads are acceptable per the revised 10 CFR 71.63, as the plutonium produced in the PULSTAR fuel elements is in solid form.

The structural and thermal evaluations of the NAC-LWT are provided in Chapters 2 and 3, respectively. Results of these evaluations demonstrate that cask containment is maintained during normal conditions of transport and hypothetical accident conditions. Therefore, the package satisfies the containment requirements of 10 CFR 71.51

4.2.1 Containment of Radioactive Material

The 10 CFR 71 limit for the release of radioactive material under normal conditions of transport is 10^{-6} A₂/hr. The A₂ value for a mixture of isotopes is determined by using the method

described in 10 CFR 71, Appendix A. The assumed release fractions for the cask contents, with the exception of MTR and DIDO fuel assemblies, are obtained from NUREG/CR-6487 (Anderson) and are summarized in Table 4.2-1. The isotope curie contents for the cask design basis PWR and BWR fuel assemblies, 25 PWR or BWR high burnup rods, and TRIGA and MTR fuel elements and DIDO fuel assemblies are provided in Section 4.5.4. The isotopic curie content and displaced volume associated with TRIGA fuel cluster rods are bounded by that of the design basis TRIGA fuel element. As shown below, the allowable leak rate for TRIGA fuel characterized as failed bounds the allowable leak rate for the TRIGA spent fuel described in Table 1.2-1. The containment analyses for MTR and DIDO fuel are presented in Sections 4.1.1 and 4.5.7 and are performed in accordance with the methodology presented in "Bases for Containment Analysis for Transportation of Aluminum-Based Spent Nuclear Fuel," WSRC-TR-98-00317, October 1998. Spiral fuel and MOATA plate bundle ANSTO basket payloads are comprised of MTR/DIDO type fuel plates and rely on the bounding containment evaluations performed for the similar DIDO basket. Further discussions of the ANSTO basket payloads are included in Section 4.5.10.

The allowable leak rate for BWR fuel is primarily determined by the postulated concentration of ^{60}Co in crud that is assumed to coat the external surface of the fuel rods and channel of the BWR fuel assemblies. Crud is a mixture of impurities that are deposited on the exterior of the fuel assembly by reactor cooling water during power generation. NUREG/CR-6487 estimates the maximum ^{60}Co concentrations on spent fuel assemblies to be $140 \mu\text{Ci}/\text{cm}^2$ for PWR assemblies and $1,254 \mu\text{Ci}/\text{cm}^2$ for BWR assemblies at initial discharge. The calculated concentration, based on assembly surface area, is decayed 2 years based on the required cool time for design basis PWR and BWR fuel.

The combined payload isotopic content of the two General Atomics (GA) Irradiated Fuel Material (IFM) Fuel Handling Units (FHUs) is 3403 Ci, 86% of which is for the TRIGA elements in the RERTR/IFM FHU. Based on the FLIP-LEU II TRIGA element data in Table 4.5-7 through Table 4.5-9, the design basis activity inventory for a single TRIGA element is 2094 Ci. However, since up to 140 design basis elements can be loaded in the poisoned TRIGA basket, the cask inventory is 293,174 Ci. This bounds the 3403 Ci of the combined GA IFM payload (by a factor of more than 80). Thus, no containment evaluation is necessary for the NAC-LWT loaded with GA IFM.

4.2.1.1 Calculation of Permissible Leak Rates

The maximum permissible leak rate from the cask under normal conditions of transport is determined from the 10 CFR 71 limit of $10^{-6} \text{ A}_2/\text{hr}$:

$$R_N = L_N C_N \leq A_2 \times 10^{-6} \text{ hr}^{-1} \text{ or } 2.78 \times 10^{-10} \text{ sec}^{-1}$$

where:

L_N = allowable volumetric gas leakage rate [cm^3/s]

C_N = curies per unit volume (termed "activity density") of the radioactive material that passes through the leak path [Ci/cm^3]

R_N = Release rate for normal transport conditions [Ci/sec]

Activity Density of Radioactive Material (C_N)

The total inventory of fission product gases, volatiles, fines and crud for the design basis PWR and BWR spent fuel are shown in Table 4.5-1 through Table 4.5-6. The inventories are calculated using the source terms produced by the SAS2H sequence (Hermann) and applying the release fractions (Table 4.2-1) and the postulated ^{60}Co content of the crud. The ^{60}Co content is decayed 2 years from discharge to the design basis fuel cool time. The PWR crud analysis is based on a single design basis fuel assembly, while the BWR crud analysis is based on 2 design basis fuel assemblies. The total inventories for metallic fuels are calculated in the same way, conservatively applying the release fractions for PWR and BWR spent fuel. Crud does not contribute to the source term for metallic fuels, as crud formation is not considered to be a significant contaminant for MTR, research reactor, and other metallic fuels. The radionuclide inventory of the bounding TRIGA fuel element, the FLIP LEU with type II end fittings, is shown in Table 4.5-7 through Table 4.5-9, for gases, volatiles and fines, respectively. The radionuclide inventory of the TRIGA fuel cluster rods is bounded by that of the design basis TRIGA fuel element. The radionuclide inventory of the bounding MTR fuel element is similarly shown in Table 4.5-10 through Table 4.5-12. The radionuclide inventory of the bounding DIDO fuel assembly is shown in Table 4.5-19 through Table 4.5-21. As indicated by the bounding source described in Chapter 5 and further discussed in Section 4.5.10, the spiral fuel assemblies and MOATA plate bundles in the ANSTO basket are bounded by DIDO evaluations.

As shown in Table 4.2-2, the allowable leak rate for TRIGA fuel characterized as failed bounds the allowable leak rate of the design basis PWR and BWR fuel, the intact high burnup 25 PWR or BWR rod configuration, and other MTR, research reactor, and the other metallic fuels considered. However, the 56% failed, high burnup 25 PWR or BWR fuel rod configuration allowable release rates are the most restrictive, as shown in Section 4.5.6.

The total activity density for the contents of the cask, C_N , is:

$$C_N = C_{\text{Crud}} + C_{\text{Volatiles}} + C_{\text{Fission Gas}} + C_{\text{Fines}}$$

The activity density for crud is:

$$C_{\text{Crud}} = \frac{f_C M_T}{V} = \frac{f_C S_C N_A (N_R S_{AR} + S_{Ch})}{V}$$

where:

C_{crud} = activity density inside containment vessel resulting from crud spallation [Ci/cm³]

M_T = total crud activity inventory [Ci]

f_C = crud spallation factor

V = free volume inside containment vessel [cm³]

S_C = crud surface activity [Ci/cm²]

N_R = number of fuel rods per assembly

N_A = number of assemblies

S_{AR} = surface area per rod [cm²]

S_{Ch} = channel surface area [cm²] (BWR fuel only).

The activity density for fuel fines (particulates) is:

$$C_{\text{fines}} = \frac{f_F W_R A_R N_R N_A f_B}{V}$$

where:

C_{fines} = activity concentration inside containment vessel resulting from fines released from cladding breaches [Ci/cm³]

f_F = fraction of fuel rod's mass released as fines resulting from cladding breach

f_B = fraction of fuel rods that develop cladding breach

W_R = mass of the fuel in fuel rod [g]

N_R = number of fuel rods per assembly

N_A = number of assemblies

A_R = specific activity of fines emitted from cladding breach in fuel rod [Ci/g]

V = containment vessel void volume [cm³].

The activity density for isotopes characterized as volatile and gaseous is:

$$C_{\text{vol\&gas}} = C_{\text{vol}} + C_{\text{gas}} = \frac{N_R N_A f_B W_R (A_V f_V + A_G f_G)}{V}$$

where:

$C_{\text{vol\&gas}}$ = releasable activity concentration inside the containment vessel resulting from gases and volatiles released from cladding breaches [Ci/cm³]

- C_{vol} = releasable activity concentration inside the containment vessel resulting from volatiles released from cladding breaches [Ci/cm³]
- C_{gas} = releasable activity concentration inside the containment vessel resulting from gases released from cladding breaches [Ci/cm³]
- W_R = mass of the fuel in a fuel rod [g]
- N_R = number fuel rods per assembly
- N_A = number of assemblies
- f_B = fraction of rods that develop cladding breaches
- A_V = specific activity of volatiles in fuel rod [Ci/g]
- f_V = fraction of volatiles in fuel rod released if rod develops cladding breach
- A_G = specific activity of gas in fuel rod [Ci/g]
- f_G = fraction of gas that would escape from fuel rod that develops cladding breach
- V = is the void volume inside containment vessel [cm³].

Activity Values for Radionuclides

A_2 values for the design basis PWR and BWR fuel crud, gases and volatiles, and fuel fines are shown in Section 4.5.4, and summarized in Table 4.5-1 through Table 4.5-6. For those isotopes for which no specific A_2 value is specified, the generic values listed in 10 CFR 71, Table A-2, are applied. The A_2 value for mixtures of isotopes is calculated from:

$$A_2 = \frac{1}{\sum \frac{F_i}{A_2^i}}$$

where:

$$F_i = \frac{S_i}{S_n}$$

F_i = The fraction of isotope i with respect to the entire mixture

S_i = The activity isotope i (Curies)

S_n = The total group activity (Curies)

A mixture A_2 value is determined for gases, volatiles, fines, and crud. These A_2 values are then combined, using the same formula, to obtain a total cask mixture A_2 value. Based on the releasable curie content and the cask contents A_2 value, the allowable leak rate for the various spent fuel contents are summarized in Table 4.2-2.

Maximum Allowable Leak Rates

Using the methodology described above, the bounding maximum allowable leak rate for all of the NAC-LWT cask contents is calculated to be 1.32×10^{-6} cm³/sec. This leak rate analysis is based on the conservative assumption that 56% of the 25 high burnup fuel rods, or 14 fuel rods, fail in transport.

The results of the leak rate analysis of the high burnup fuel rods and the other NAC-LWT fuel contents are shown in Table 4.2-2. The allowable release rate for HEU MTR fuel is specified as it bounds the allowable release rate for MEU and LEU MTR fuel. Similarly, the allowable release rate for LEU DIDO fuel is specified, since it bounds the allowable release rate for HEU and MEU DIDO fuel. The evaluations of MTR and DIDO fuel are presented in Sections 4.1.1 and 4.5.7, respectively. Based on these results, a helium leak test value of 5.5×10^{-7} cm³/sec is used to demonstrate containment of the NAC-LWT spent fuel contents. As shown in Table 4.2-4, this test leak rate is conservative with respect to the calculated maximum allowable leak rate for the cask contents. A leaktight containment boundary is required for the transport of TPBAR contents.

The allowable release rate of the TRIGA fuel is more restrictive than for the design basis PWR or BWR assemblies because of the application of the postulated release fractions for light water reactor fuel to the metallic TRIGA fuel. This application is highly conservative as the metallic fuel is less subject to the release of volatile isotopes and fuel fines due to fabrication methods employed in making the fuel. Based on a report by General Atomics for Lockheed Martin Idaho Technologies Company, "Uranium-Zirconium Hydride Fuels for TRIGA Reactors," (UZR-28, June 1997) fission gas release from an unclad TRIGA element is less than 0.01% at a temperature of 400°C. The maximum accident temperature for the TRIGA cask is conservatively assumed to be 756°F (402°C) with air in the cask. The maximum calculated accident average cavity gas temperature is 574°F (301°C) as shown in Section 3.5.3.2. A conservative release fraction of 1% is employed in the containment evaluation. A 1% release represents the release fraction of the fuel at 800°C.

For certain content conditions, including PWR MOX fuel rods and TPBARs, a leaktight containment boundary configuration is required. For this containment configuration, Alternate B port covers with metallic containment seals are installed. Each of the containment penetrations (i.e., closure lid and the vent and drain Alternate B port covers) are individually leakage tested to leaktight acceptance criteria prior to transport.

4.2.1.2 Correlation of Permissible Leak Rates to Air Standard

The maximum allowable release must be correlated to air standard leak rates, which depend on gas temperatures, pressures, and leak path. This correlation requires calculation of the capillary opening diameter through which the flow occurs. Depending on pressure and condition of the flow, two flow regimes are evaluated: continuum and molecular flow. Continuum flow and molecular flow equations are obtained from NUREG/CR-6487, Section 2. Continuum and molecular flow can occur simultaneously and are so treated in this analysis. Both continuum and molecular flow rate equations presented below are adjusted to upstream flow rate.

The continuum volumetric flow rate of the gas (cm^3/sec), L_c , is given by:

$$L_c = \frac{2.48 \times 10^6 D^4}{am} (P_u - P_d) \frac{P_a}{P_u} = F_c (P_u - P_d) \frac{P_a}{P_u}$$

where:

L_c = continuum flow rate of gas at P_u [cm^3/sec]

F_c = coefficient for continuum flow [$\text{cm}^3/\text{atm-s}$]

D = capillary diameter [cm]

A = capillary length [cm]

μ = fluid viscosity [cP]

P_u = upstream pressure [atm] - pressure inside containment

P_d = downstream pressure [atm] - pressure outside containment

The molecular volumetric flow rate of the gas (cm^3/sec), L_m , is given by:

$$L_m = \frac{3.81 \times 10^3 D^3 \sqrt{\frac{T}{M}}}{aP_a} (P_u - P_d) \frac{P_a}{P_u} = F_m (P_u - P_d) \frac{P_a}{P_u}$$

where:

L_m = molecular volumetric flow rate of gas at P_u [cm^3/sec]

F_m = coefficient for molecular flow [$\text{cm}^3/\text{atm-s}$]

D = capillary diameter [cm]

T = gas temperature [K]

M = gas molecular weight [g/mole]

P_a = average pressure $(P_u + P_d)/2$ [atm]

P_u = upstream pressure [atm]

P_d = downstream pressure [atm]

A = capillary diameter [cm]

For this analysis, the gas temperature used for molecular flow analysis is identical to the upstream temperature.

Based on the maximum allowable leakage rate, the flow rate equations are solved for the capillary diameter. Air standard (reference) properties for air are then substituted into the flow equations to arrive at the air standard leakage rate (L_R) and leak test sensitivity. Standard conditions represent leakage at 298K, flowing from an upstream pressure of 1 atmosphere, to a downstream pressure of 0.01 atmospheres. To complete the analysis, helium leak rates are calculated for the NAC-LWT limiting contents at standard conditions.

The cask pressure, P_u , is determined based on the pressure conditions for the design basis PWR fuel as described in Section 4.2.2. This pressure is conservative because the metallic fuel, including MTR, TRIGA and DIDO fuel, does not contain an initial charge of helium gas. The temperature applied is that for the type of fuel considered in the leak rate evaluation as shown in Table 4.2-3.

4.2.2 Pressurization of Containment Vessel

The maximum pressure in the cask during normal conditions of transport for the fissile material payloads is calculated by using the methodology presented in Section 3.4.4. Assumptions underlying this calculation are that during normal conditions of transport, 3% of the fuel rods may fail and that 30% of the fission gases in the rods are releasable. In addition, for LWR high burnup rods, 56% of the rods with oxide layers greater than 70 micrometers (14 rods) are assumed to fail during transport. This is conservative since fuel rods classified as damaged may have released fission and charge gases prior to transport. Failed rods are assumed to have released the fission gas prior to transport. The cask cavity is backfilled to 1 atm with 99.9% pure helium gas.

The gas volume (e.g., plenum and pellet to cladding gap) inside the fuel rods is conservatively neglected when calculating the cask free volume. The maximum normal conditions cavity pressure for the PWR fuel configuration is 1.99 atm. This pressure is conservatively applied to all the fuels (except in the 25 PWR/BWR high burnup fuel rod analysis) to establish the allowable leak rate. The pressure is conservative since the metallic fuels contain no initial charge of helium gas and release a lower percentage of fission product gases. The maximum normal condition cavity pressure used for the 25 intact PWR/BWR high burnup fuel rod analysis is 2.1 atm. For the 25 BWR/PWR rod analysis with 56% fuel rod failure, the maximum normal

condition cavity pressure is 3.2 atm for the BWR analysis, and 3.0 atm for the PWR analysis, respectively.

Normal condition system maximum normal operating pressure (MNOP) for the transport of up to 300 production TPBARs (including up to 2 prefailed rods) is conservatively determined in Section 3.4.4.5 as 289 psig. The TPBAR normal condition pressure assumed clad failure of all 300 TPBARs during transport. The pressure for the second TPBAR content condition of 55 segmented TPBARs contained in a waste container is bounded by the 300 TPBAR MNOP.

4.2.3 Containment Criteria

The standard leak rate provided in Table 4.2-4 for fissile material shipments represents the maximum leak rate allowed if the seals were to be tested with air at an upstream pressure of 1 atm and a downstream pressure of 0.01 atm at a temperature of 25°C. This is the maximum allowable leak rate for the containment system fabrication verification and periodic verification leak tests described in Section 4.1, and in Chapter 8.

As specified in Section 4.1.2, the containment boundary for contents not requiring a leaktight containment is leak tested to 5.5×10^{-7} std cm³/sec (helium). The sensitivity for these tests is required by ANSI N14.5-1997 to be one-half the test leak rate, or 2.75×10^{-7} std cm³/sec (helium).

The leakage rate for contents requiring a leaktight containment (e.g., PWR MOX fuel rods, TPBARs, etc.) per ANSI N14.5-1997 is 1×10^{-7} ref cm³/sec, which is equivalent to a helium leak rate of less than or equal to 2×10^{-7} std cm³/sec. The minimum test sensitivity is 1×10^{-7} cm³/sec (helium).

Table 4.2-1 Release Fractions: Normal and Accident Conditions

Radionuclide Origin	Fraction: Normal Conditions	Fraction: Accident Conditions
Fuel Assumed to Fail	0.03 ¹	1.0
Fission Gas Released ²	0.3	0.3
Volatiles Released	0.0002	0.0002
Fuel Mass Released as Fines	0.00003	0.00003
Crud Spallation ³	0.15	1.0

¹ 56% for > 70 micrometer oxide layer rod shipment.

² The release fraction from TRIGA and NRX fuel is taken as 0.01.

³ Applied only to BWR and PWR spent fuel.

Table 4.2-2 Allowable Release Rates for NAC-LWT Cask Contents: Normal Conditions

Fuel Type	Crud (Ci)	Gas (Ci)	Volatiles (Ci)	Fines (Ci)	Total (Ci)	A ₂ (Ci)	L _N (cm ³ /sec)
WE 15x15	4.397	36.144	1.173	0.400	42.114	36.603	3.56E-05
GE 7x7	42.808	24.611	0.827	0.275	68.521	15.525	6.41E-06
Metallic (NRX - 15 Intact Rods)	---	0.103	0.106	0.095	0.304	2.793	2.60E-04
Metallic (NRX -9 Failed Rods)	---	2.059	2.129	1.894	6.082	2.793	1.30E-05
25 PWR Rods	0.602	7.930	0.456	0.242	9.231	12.295	5.45E-05
MTR ¹	0.019	108.851	0.012	1.829	110.711	24.745	1.42E-05
DIDO ²	0.011	53.613	0.005	8.161	61.789	7.996	1.32E-05
TRIGA (Intact)	---	1.011	0.697	0.156	1.864	6.161	1.58E-04
TRIGA ³ (Failed)	---	14.086	9.711	2.179	25.976	6.161	1.13E-05
25 PWR Rods – 56% Failed	0.773	194.727	37.154	23.708	256.362	17.473	1.83E-06
25 BWR Rods – 56% Failed	9.236	293.314	44.234	26.349	373.133	19.828	1.32E-06

¹ As evaluated in Section 4.5.5, the listed values are for HEU MTR elements, which bound the LEU and MEU MTR fuel elements.

² As evaluated in Section 4.5.7, the listed values are for LEU DIDO assemblies, which bound the MEU and HEU DIDO fuel assemblies.

³ Assumes 84 intact elements and 56 failed elements in sealed cans.

Table 4.2-3 Cask Free Volumes and Pressures

Fuel Type	Pressure (atm)		Temperature (K)	Free Volume (10 ⁵ cm ³)
	Normal	Accident		
PWR	1.99 ¹	11.4 ¹	517.4	1.471
BWR	1.99 ²	11.4 ²	517.4	1.018
Metallic Fuel	1.99 ²	11.4 ²	405.2	1.018
MTR	1.99 ²	11.4 ²	470.2	2.293
DIDO	1.99 ²	11.4 ³	433.2	3.681
TRIGA	1.99 ²	11.4 ²	571.4 ²	1.717
GA IFM	N/A ⁶	N/A ⁶	403.2	3.354
25 PWR Rods – 56% Failed Fuel Fraction	3.0	4.3 ⁵	588.7 ⁴	0.9681
25 BWR Rods – 56% Failed Fuel Fraction	3.2	4.5 ⁵	588.7 ⁴	0.8932

¹ Based on Sections 3.4.4 and 3.5.4, the maximum calculated pressures for the PWR payload are 1.93 atm (28.3 psia) normal condition and 8.56 atm (125.8 psia) accident conditions. The higher pressures used in the analyses are conservative since a higher pressure will result in a smaller leak diameter and reduced leak test requirements.

² The maximum pressure for the PWR fuel is conservatively applied.

³ The temperature employed is approximately 4K lower than the maximum fuel clad temperature calculated. The fuel clad temperature is significantly higher than the average gas temperature in the cask. By combining the listed temperature with the cask maximum pressure (PWR fuel) conservative leak rates are calculated.

⁴ The normal condition temperature is conservatively applied to the 25 PWR and BWR high burnup rod analysis.

⁵ These pressures result from the 100% fuel rod failure plus the design basis fire accident.

⁶ Based on the lower temperature and larger free volume of the GA IFM, as compared to the other contents, the pressure, although not explicitly calculated, is lower than that calculated for PWR and BWR fuel.

Table 4.2-4 Leak Rate and Leak Test Sensitivity - Normal Conditions

Fuel Type ¹	Assembly Type	Volumetric Activity (Ci/cm ³)	Leak Rate (cm ³ / sec)			
			Allowable (L _N)	Allowable (air) (L _R)	Allowable (helium)	Test (helium) ²
BWR	GE 7x7	6.73E-04	6.41E-06	5.35E-06	7.66E-06	5.50E-07
TRIGA (Failed) ³	FLIP-LEU II	1.51E-04	1.13E-05	9.90E-06	1.36E-05	5.50E-07
MTR	HEU	4.83E-04	1.42E-05	1.19E-05	1.62E-05	5.50E-07
DIDO	LEU	1.68E-04	1.32E-05	1.46E-05	4.54E-06	5.50E-07
25 BWR Rods – 56% Failed Fuel Fraction	Exxon 7x7	4.18E-03	1.32E-06	6.39E-07	1.06E-06	5.50E-07

¹ The bounding TRIGA fuel element is the FLIP-LEU II.

² Containment Verification Leak Test. Test Sensitivity is 2.75E-07 std. cm³/sec (helium).

³ Assumes 84 intact TRIGA elements and 56 failed elements in sealed cans.

4.3 Containment Requirements for Hypothetical Accident Conditions

The 10 CFR 71 requirement for the release of radioactive material under hypothetical accident conditions is met by ensuring that the requirement is met for the bounding fissile material contents, 140 TRIGA fuel elements, 56 of which are characterized as failed. Calculation of the allowable release rate is provided in Section 4.3.2.

The structural integrity of the cask containment during hypothetical accident conditions is demonstrated in Section 2.7. Therefore, the cask containment is maintained under hypothetical accident conditions.

As shown in Table 4.3-2, the allowable release rate in the hypothetical accident condition is significantly larger than that for normal conditions of transport. Consequently, the bounding allowable leak rate is that for the failed TRIGA fuel as calculated in Section 4.2.1.

The containment boundary for the transport of contents requiring a leaktight containment (e.g., PWR MOX fuel rods, TPBARs, etc.) is demonstrated by leakage testing to a leakage rate of less than or equal to 1×10^{-7} ref cm³/sec. Per ANSI N14.5-1997, the equivalent helium leakage rate for leaktight conditions is less than or equal to 2×10^{-7} cm³/sec.

PULSTAR fuel element specific analyses are compliant with B(U)F-96 requirements as documented in Section 4.5.8.

4.3.1 Fission Gas Products

The accident conditions for maximum fission gas release assumes 100% rod failure and also assume that 30% of the tritium and 30% of the ⁸⁵Kr are available for release to the cask cavity. In addition, 100% of the ⁶⁰Co in the crud on the design basis PWR and BWR fuel assemblies is conservatively assumed to be available for release as an aerosol. Due to the crud contamination of the BWR assembly, its allowable leak rate bounds that of the PWR fuel. The metallic fuels do not contain significant amounts of fission gas that are available for immediate release and do not have significant levels of crud. TRIGA fuel elements are assumed to release 1% of their fission gas products under accident conditions.

4.3.2 Containment of Radioactive Materials

The NAC-LWT cask is designed to maintain a release rate of less than 1 A₂/week for the hypothetical accident conditions, as required by 10 CFR 71.51. The A₂ for the mixed radionuclides considered to be available for release is determined by using the method described in 10 CFR 71, Appendix A. The release fractions for the various radionuclides found in the cask

are obtained from NUREG/CR-6487 and are summarized in Table 4.2-1. The A_2 per week limit is not exceeded for any NAC-LWT contents, based on the leak test described in Section 4.1.3.

4.3.2.1 Calculation of Allowable Leak Rates

The allowable leak rates under hypothetical accident conditions are calculated by using the method described in Section 4.2.1.1 for normal conditions of transport. The total inventory of fission product gases, volatiles, fines, and crud are calculated by using the source terms generated by SAS2H. The assumed release fractions are shown in Table 4.2-1. Using the A_2 values from 10 CFR 71, Appendix A, the mixture A_2 values are determined for gas, volatile, fine, and crud mixtures for the bounding accident condition fuel contents (WE 15 × 15 PWR) as shown in Table 4.3-1. For the 25 PWR and BWR high burnup rod analysis, A_2 values were also determined and are reported in Table 4.3-3 (PWR) and Table 4.3-4 (BWR). The maximum allowable release rates are calculated by using the hypothetical accident condition allowable release limit:

$$R_A = L_A C_A \leq A_2 \times \text{week}^{-1} = A_2 \times 1.65 \times 10^{-6} \text{ sec}^{-1}$$

where:

L_A = volumetric gas leak rate [cm^3/s]

C_A = curies per unit volume (termed “activity density”) of the radioactive material that passes through the leak path [Ci/cm^3]

R_A = release rate for accident transport conditions

Assumptions underlying the calculations for the hypothetical accident conditions are that 100% of the fuel cladding fails and 100% of the crud is released. The mixture A_2 value for the hypothetical accident conditions is calculated using the methodology of Section 4.2.1.1, applying the accident condition release fractions of Table 4.2-1.

The calculated maximum allowable hypothetical accident condition leak rate for the design basis PWR and BWR spent fuel, and for metallic fuel rods and TRIGA fuel characterized as failed, are tabulated in Table 4.3-2. The calculated maximum allowable hypothetical accident condition leak rate for the 25 PWR and BWR high burnup rod analysis is also reported in Table 4.3-2.

4.3.2.2 Correlation of Allowable Leak Rates to Standard Leak Rates

The maximum allowable leak rates for the hypothetical accident conditions are corrected to standard leakage rates using the methodology described in Section 4.2.1.2. The results are tabulated in Table 4.3-2 for the design basis PWR and BWR spent fuel, MTR HEU elements,

DIDO LEU assemblies and 140 TRIGA fuel elements, with 56 elements characterized as failed prior to loading in the cask.

4.3.2.3 Containment Criteria

For fissile material payloads evaluated, the allowable leak rates for the hypothetical accident conditions are much greater than those for the normal conditions of transport calculated in Section 4.2.1. Because the cask containment is demonstrated to be maintained under hypothetical accident conditions (Section 2.7), the maximum permissible leak rates for normal conditions of transport are more limiting and are, therefore, used for the establishment of the maximum allowable leak rates for the containment system fabrication and periodic verification leak tests. For PWR MOX fuel rods and TPBAR contents, a leaktight containment boundary is maintained during transport.

4.3.2.4 Tritium Permeation Rate of Seals for TPBAR Shipment

The release of tritium into the cask cavity from all 300 rods, 298 rods that are event-failed and 2 rods defined to be prefailed, has the potential of releasing a significant quantity of tritium ($> 1A_2$) into the cask cavity. As shown in the structural analysis, the lid and port cover seals retain their ability to provide cask closure during all accident conditions. To assure that the accident release limit of $1A_2/\text{week}$ is not exceeded under accident conditions the port and lid seal permeation rates are evaluated.

The formula for permeation through metal is:

$$PR = \Phi \times A / l \times (P_p)^{1/2}$$

where:

PR = equilibrium (steady-state) permeation rate in std cc (permeate) per sec

Φ = permeability in std cc (permeate) per second per material surface area per permeate partial pressure $^{1/2}$ through a unit material thickness

A = material surface area that is "exposed" to the permeate

l = material thickness through which the permeate "passes"

P_p = upstream permeate partial pressure

The formula for permeability is:

$$\Phi = \Phi_0 \times \exp\left(-\frac{E_\Phi}{RT}\right)$$

where:

Φ = permeability as stated previously

Φ_0 = pre-exponential permeation factor in the same units as Φ

E_Φ/R = the activation energy of the permeation process, which has been 'normalized' by the universal gas constant

T = absolute temperature of the metal (K).

Combining the permeation equations with an activity density of 0.16 Ci/cc, resulting from the release of 55 Ci per event failed rod and 0.199 moles of tritiated water for each prefailed rods, and

T = 572K – Maximum accident temperature for the seals per Table 3.5-1

Φ_0 = 7.42×10^{-2} [LLNL Report UCRL-53441] (stainless steel port seal),
 2.10×10^{-2} [Fusion Science and Technology] (inconel lid seal)

E_Φ/R = 7,700 (stainless steel port seal), 7490 [Fusion Science and Technology] (inconel lid seal)

l = 0.012 inch for the port cover seal (only considering the stainless steel portion of the seal) and 0.032 inch for the lid seal

P_p = 0.15 atm – tritium partial pressure in the cask cavity based on the cask free volume, accident condition temperature, and a release of 55 Ci of tritium per event failed rod (conservative modeled as isotope not molecular tritium) and 0.199 moles of tritiated water from the prefailed rods)

yields an approximate release through seal permeation of 5 Ci/week compared to the allowable accident release rate of 1.1×10^3 Ci/week ($1A_2$ /week based on an A_2 value for tritium of 1.1×10^3 Ci).

Actual permeation release rates would be significantly lower as the accident temperatures are short term, with elevated temperatures at the seal locations returning to normal condition temperatures within an hour of the fire.

Similar calculations are performed for the 55 equivalent TPBARs, in segments and debris, which may release up to 100% of the tritium contained in the pellets during transport. The pellet tritium content represents approximately 40% of the tritium quantity in the TPBAR. At NAC-LWT normal and accident conditions temperatures, the TPBAR components release tritium primarily as tritiated water with only a small fraction (maximum 2%) as gaseous tritium (see Appendix 1-B of Chapter 1). Gaseous tritium represents the basis for the seal permeation evaluation. During a one-year transport, an additional maximum 1% of the tritiated water may undergo radiolysis and dissociate. Conservatively applying a maximum 3% release rate to the 55 equivalent TPBAR total inventory of 66 grams (1.2 grams per rod) yields an inventory of 0.33 moles T_2 . Seal permeation rates based on the conservative temperatures discussed in the previous paragraphs and a 3% tritium gas release are 6.5×10^{-6} Ci/hr, normal conditions, and 1.06 Ci/week, accident conditions. A gaseous release of over 90% of the 1.2 grams per rod tritium inventory is required

to exceed normal condition allowables at the conservative seal temperature of 222°F. A 100% gaseous release and resulting tritium permeation through the cask seals meets accident condition limits. Reducing seal temperatures less than 5°F, to account for a significantly lower decay heat payload (0.127 kW for the waste container TPBARs versus 1.05 kW on which the 222°F temperature is based), permits a normal condition release of 100% of the tritium in gaseous form while meeting the 10⁻⁶ A2/hr allowable.

4.3.3 Tritium Contamination Issues

Precautions will be taken to minimize the risk of excessive contamination of NAC-LWT casks during the loading and unloading of TPBAR contents to ensure the reusability of the NAC-LWT casks for transport of non-TPBAR contents. In addition to ensuring the safe handling of TPBAR contents, additional cavity gas and internal and external removable contamination surveys for tritium contamination will be implemented at all TPBAR loading and unloading facilities. The specific monitoring methods and levels of contamination to which the cask surfaces must be decontaminated are defined in the TPBAR loading and unloading procedures in Chapter 7. In addition, the TPBAR procedures also include precautions for users to observe when loading, unloading and handling TPBARs.

The procedures and precautions comply with the recommended practices of NUREG-1609, Supplement 2. The results of previous loading and unloading experiences regarding the measurement of tritium gas and contamination levels are provided in the PNNL letter in Section 1.5, Appendix 1-G of this SAR.

NAC-LWT cask units used for TPBAR transports shall comply with the specified contamination levels, or other non-TPBAR users will be advised to incorporate tritium monitoring requirements into their survey procedures and radiological control program.

Table 4.3-1 A₂ Calculation for PWR Spent Fuel

	Crud	Gas	Volatiles	Fines	Total
Total Activity per Assembly (Ci)	2.931E+01	4.016E+03	1.955E+05	4.446E+05	6.441E+05
Releasable Activity per Cask (Ci)	2.931E+01	1.205E+03	3.910E+01	1.334E+01	1.287E+03
Cask Volumetric Activity (Ci/cm ³)	1.992E-04	8.188E-03	2.658E-04	9.065E-05	8.744E-03
A ₂ Value (Ci)	11.00000	281.42094	8.72766	0.81991	3.020E+02
Fraction of Activity	0.02278	0.93646	0.03039	0.01037	---
Fraction of Activity / A ₂ (1/Ci)	0.00207	0.00333	0.00348	0.01264	0.02152
Mixture A ₂ Value (Ci)					46.458

Table 4.3-2 Standard Leak Rates for Accident Conditions

Fuel Type	Assembly Type	Volumetric Activity (Ci/cm ³)	Allowable Leak Rate (cm ³ / sec) ^{LA}
BWR	GE 7×7	1.12E-02	3.88E-03
PWR	WE 15×15	8.74E-03	8.77E-03
MTR	HEU	1.64E-02	1.35E-03
DIDO	LEU	6.33E-03	1.20E-03
TRIGA (Includes Cans)	FLIP-LEU II	3.62E-04	2.81E-02
25 High Burnup PWR rods	CE 14×14 ¹	4.77E-03	6.02E-03
25 High Burnup BWR rods	Exxon 7×7 ¹	7.97E-03	3.91E-03

¹ Based upon these assemblies, but the active fuel lengths and rod lengths are extended to 150 inches.

Table 4.3-3 A₂ Calculation for 25 High Burnup PWR Spent Fuel Rods

	Crud	Gas	Volatiles	Fines	Total
Total Activity per Assembly (Ci)	5.150E+00	1.159E+03	3.317E+05	1.411E+06	1.744E+06
Releasable Activity per Cask (Ci)	5.150E+00	3.477E+02	6.635E+01	4.234E+01	4.616E+02
Cask Volumetric Activity (Ci/cm ³)	5.320E-05	3.592E-03	6.853E-04	4.373E-04	4.768E-03
A ₂ Value (Ci)	11.00000	283.63841	13.58800	2.12043	3.103E+02
Fraction of Activity	0.01116	0.75337	0.14374	0.09172	1.000
Fraction of Activity / A ₂ (1/Ci)	0.00101	0.00266	0.01058	0.04326	0.05751
Mixture A ₂ Value (Ci)					17.389

Table 4.3-4 A₂ Calculation for 25 High Burnup BWR Spent Fuel Rods

	Crud	Gas	Volatiles	Fines	Total
Total Activity per Assembly (Ci)	6.157E+01	1.746E+03	3.949E+05	1.568E+06	1.965E+06
Releasable Activity per Cask (Ci)	6.157E+01	5.238E+02	7.899E+01	4.705E+01	7.114E+02
Cask Volumetric Activity (Ci/cm ³)	6.894E-04	5.864E-03	8.844E-04	5.268E-04	7.965E-03
A ₂ Value (Ci)	11.00000	283.89694	13.28843	1.93498	3.101E+02
Fraction of Activity	0.08655	0.73627	0.11104	0.06614	---
Fraction of Activity / A ₂ (1/Ci)	0.00787	0.00259	0.00836	0.03418	0.05300
Mixture A ₂ Value (Ci)					18.868

Chapter 5

Table of Contents

5	SHIELDING EVALUATION	5-1
5.1	Discussion and Results	5.1.1-1
5.1.1	NAC-LWT Contents	5.1.1-1
5.2	Gamma and Neutron Sources	5.1.1-1
5.2.1	ORIGEN 2	5.2.1-1
5.3	Model Specification	5.2.1-1
5.3.1	Description of Radial and Axial Shielding Configuration	5.3.1-1
5.3.2	Shield Regional Densities	5.3.2-1
5.3.3	Metallic Fuel Configuration	5.3.3-1
5.3.4	MTR Fuel Configuration	5.3.4-1
5.3.5	25 PWR Fuel Rods Configuration	5.3.5-1
5.3.6	TRIGA Fuel Element Model Specification and Shielding Evaluation	5.3.6-1
5.3.7	TRIGA Fuel Cluster Rod Model Specification and Shielding Evaluation	5.3.7-1
5.3.8	High Burnup PWR and BWR Rods Shielding Evaluation	5.3.8-1
5.3.9	DIDO Fuel Configuration	5.3.9-1
5.3.10	GA IFM Shielding Evaluation	5.3.10-1
5.3.11	High Burnup PWR and BWR Rods in a Fuel Assembly Lattice	5.3.11-1
5.3.12	Damaged High Burnup PWR and BWR Rods in a Rod Holder	5.3.12-1
5.3.13	TPBAR Shielding Evaluation	5.3.13-1
5.3.14	PULSTAR Fuel Configuration	5.3.14-1
5.3.15	Spiral Fuel Assembly Configuration	5.3.15-1
5.3.16	MOATA Plate Bundle Configuration	5.3.16-1
5.3.17	Irradiated Hardware Shielding Evaluation	5.3.17-1
5.3.18	PWR MOX Rod Fuel Configuration	5.3.18-1
5.4	Shielding Evaluation	5.4.1-1
5.4.1	Shielding Evaluation Codes	5.4.1-1

List of Figures

Figure 5.3.3-1	Three-Dimensional Radial Model	5.3.3-2
Figure 5.3.3-2	End-Fitting Model with Fuel.....	5.3.3-3
Figure 5.3.3-3	Lead Slump Accident – PWR Top End-Fitting.....	5.3.3-4
Figure 5.3.3-4	Lead Slump Accident – PWR Bottom End-Fitting.....	5.3.3-5
Figure 5.3.3-5	Lead Slump Accident – BWR Bottom End-Fitting.....	5.3.3-6
Figure 5.3.3-6	One-Dimensional Radial Computational Model	5.3.3-7
Figure 5.3.4-1	MTR Fuel Evaluated Configurations	5.3.4-5
Figure 5.3.4-2	SAS4 Shielding Model for the MTR Fuel Basket in the NAC-LWT (Upper Half)	5.3.4-6
Figure 5.3.4-3	Dose Rates 2 Meters from Transport Vehicle (30 W Uniform Loading)	5.3.4-7
Figure 5.3.6-1	TRIGA Fuel Element One-Dimensional Bounding Radial Dose Rate - Normal Conditions of Transport - Curves and Data Points	5.3.6-7
Figure 5.3.6-2	TRIGA Fuel Element One-Dimensional Bounding Radial Dose Rate - Accident Condition - Curves and Data Points	5.3.6-8
Figure 5.3.6-3	TRIGA SAS4A Radial Model Geometry	5.3.6-9
Figure 5.3.6-4	TRIGA SAS4A Basket Model Geometry.....	5.3.6-10
Figure 5.3.6-5	TRIGA SAS4A Upper Half Model Geometry (Normal Condition – Shifted Fuel).....	5.3.6-11
Figure 5.3.6-6	TRIGA SAS4A Upper Half Model Geometry (Normal Condition)	5.3.6-12
Figure 5.3.6-7	TRIGA SAS4A Lower Half Model Geometry (Normal and Accident Condition)	5.3.6-13
Figure 5.3.8-1	PWR Rod SAS2H Model.....	5.3.8-5
Figure 5.3.8-2	BWR 7×7 SAS2H Model Shown at 80,000 MWd/MTU	5.3.8-5
Figure 5.3.8-3	BWR 8×8 Rod SAS2H Model	5.3.8-6
Figure 5.3.8-4	PWR Rods Axial Burnup and Source Profiles.....	5.3.8-6
Figure 5.3.8-5	BWR Rods Axial Burnup and Source Profiles	5.3.8-7
Figure 5.3.9-1	SAS2H Input for HEU DIDO Fuel 70% ²³⁵ U Burnup and 18W Heat Load.....	5.3.9-5
Figure 5.3.9-2	SAS4 Fuel Gamma Input for HEU DIDO Fuel 70% ²³⁵ U Burnup and 18W Heat Load – Radial Biasing & Normal Transport Conditions	5.3.9-6
Figure 5.3.9-3	SAS4 Shielding Model for the DIDO Fuel Basket in the NAC-LWT (Upper Half)	5.3.9-12
Figure 5.3.9-4	SAS4 Shielding Model for the DIDO Fuel Basket in the NAC-LWT (Section through Fuel).....	5.3.9-13
Figure 5.3.9-5	DIDO LEU Cooling Time vs. Fuel Burnup Basket Module Loading Guidelines for Uniform Loading	5.3.9-14
Figure 5.3.9-6	DIDO MEU Cooling Time vs. Fuel Burnup Basket Module Loading Guidelines for Uniform Loading.....	5.3.9-14
Figure 5.3.9-7	DIDO HEU Cooling Time vs. Fuel Burnup Basket Module Loading Guidelines for Uniform Loading.....	5.3.9-15

List of Figures (continued)

Figure 5.3.9-8	DIDO LEU Element Cooling Time vs. ^{235}U % Depletion.....	5.3.9-15
Figure 5.3.9-9	DIDO MEU Element Cooling Time vs. ^{235}U % Depletion.....	5.3.9-16
Figure 5.3.9-10	DIDO HEU Element Cooling Time vs. ^{235}U % Depletion	5.3.9-16
Figure 5.3.9-11	Comparison of DIDO Element 25W Minimum Cool Time Curves as a Function of ^{235}U % Depletion	5.3.9-17
Figure 5.3.9-12	Bounding DIDO Element Minimum Cool Time vs. % ^{235}U Depletion.	5.3.9-17
Figure 5.3.9-13	18W DIDO HEU Fuel Predicted vs. Actual ^{235}U Depletion Loading Curve.....	5.3.9-18
Figure 5.3.10-1	ORIGEN-S Input for GA RERTR IFM	5.3.10-3
Figure 5.3.10-2	ORIGEN-S Input for GA HTGR IFM	5.3.10-4
Figure 5.3.10-3	SAS1 Input for GA RERTR IFM	5.3.10-5
Figure 5.3.10-4	SAS1 Input for GA HTGR IFM.....	5.3.10-6
Figure 5.3.10-5	GA IFM One-Dimensional Radial Model of NAC-LWT.....	5.3.10-7
Figure 5.3.10-6	One-Dimensional Radial Model of GA RERTR and HTGR IFM.....	5.3.10-8
Figure 5.3.11-1	PWR Lattice Axial Source Profiles	5.3.11-7
Figure 5.3.11-2	BWR Lattice Axial Source Profiles.....	5.3.11-7
Figure 5.3.11-3	MCBEND Model of NAC-LWT with Fuel Assembly Lattice – Axial Detail.....	5.3.11-8
Figure 5.3.11-4	MCBEND Model of NAC-LWT with Fuel Assembly Lattice – Radial Detail.....	5.3.11-9
Figure 5.3.11-5	Normal Condition Radial Surface Dose Rate Profile by Source Type – Fuel Assembly Lattice.....	5.3.11-10
Figure 5.3.11-6	Normal Condition Radial 2m Dose Rate Profile by Source Type – Fuel Assembly Lattice.....	5.3.11-10
Figure 5.3.11-7	Accident Condition Radial 1m Dose Rate Profile by Source Type – Fuel Assembly Lattice.....	5.3.11-11
Figure 5.3.11-8	MCBEND Input – High Burnup Fuel Lattice – Radial Fuel Gamma..	5.3.11-12
Figure 5.3.12-1	MCBEND Model of NAC-LWT with Damaged Fuel Rods – Axial Detail.....	5.3.12-6
Figure 5.3.12-2	MCBEND Model of NAC-LWT with Damaged Fuel Rods – Radial Detail.....	5.3.12-7
Figure 5.3.12-3	Normal Condition Axial Surface Dose Rate Profile by Source Type – Damaged Fuel Rods.....	5.3.12-8
Figure 5.3.12-4	Normal Condition Radial 2m Dose Rate Profile by Source Type – Damaged Fuel Rods.....	5.3.12-8
Figure 5.3.12-5	Accident Condition Radial 1m Dose Rate Profile by Source Type – Damaged Fuel Rods.....	5.3.12-9
Figure 5.3.12-6	Sample Input File for Damaged Fuel Evaluation.....	5.3.12-10
Figure 5.3.13-1	ORIGEN-S Input for TPBARs at 30 Days Cool Time	5.3.13-3
Figure 5.3.13-2	MCNP Input for 300 TPBARs at 30 Days Cool Time – Normal Conditions & Radial Biasing	5.3.13-4

List of Figures (continued)

Figure 5.3.13-3	MCNP Three-Dimensional Model of NAC-LWT with 300 TPBAR Payload – Radial Detail	5.3.13-8
Figure 5.3.13-4	MCNP Three-Dimensional Model of NAC-LWT with 300 TPBAR Payload - Axial Detail	5.3.13-9
Figure 5.3.13-5	Normal Condition Radial Surface Dose Rate Profile for 300 TPBAR Payload	5.3.13-10
Figure 5.3.13-6	Normal Condition Radial 2 Meter Dose Rate Profile for 300 TPBAR Payload	5.3.13-10
Figure 5.3.13-7	Accident Condition Radial 1 Meter Dose Rate Profile for 300 TPBAR Payload	5.3.13-11
Figure 5.3.14-1	PULSTAR Fuel Assembly	5.3.14-6
Figure 5.3.14-2	SAS2H Input for PULSTAR Fuel.....	5.3.14-7
Figure 5.3.14-3	MCNP Model of NAC-LWT with PULSTAR Fuel – Axial Detail.....	5.3.14-8
Figure 5.3.14-4	MCNP Model of NAC-LWT with PULSTAR Fuel – Radial Detail	5.3.14-9
Figure 5.3.14-5	Sample MCNP Input File for Minimum Height Canned PULSTAR Fuel.....	5.3.14-10
Figure 5.3.14-6	Normal Condition Axial Surface Dose Rate Profile by Source Type – Minimum Height Canned PULSTAR Fuel.....	5.3.14-14
Figure 5.3.14-7	Normal Condition Radial 2m Dose Rate Profile by Source Type – Minimum Height Canned PULSTAR Fuel.....	5.3.14-14
Figure 5.3.14-8	Accident Condition Radial 1m Dose Rate Profile by Source Type – Minimum Height Canned PULSTAR Fuel.....	5.3.14-15
Figure 5.3.15-1	SAS2H Input for Spiral Fuel 70% ²³⁵ U Depletion and 18-Watt Heat Load.....	5.3.15-3
Figure 5.3.15-2	Spiral Fuel versus MEU DIDO Gamma Spectrum Comparison (18 Watts, 70% Depletion)	5.3.15-4
Figure 5.3.15-3	Minimum Cool Time Curve for 18-Watt Heat Load (Spiral Fuel and MEU DIDO).....	5.3.15-5
Figure 5.3.16-1	SAS2H Input for the MOATA Plate Bundle.....	5.3.16-3
Figure 5.3.17-1	SAS2H Input for Irradiated Hardware (on a per kg Basis)	5.3.17-3
Figure 5.3.17-2	Sample SAS1 Input for Irradiated Hardware (Source 1 kg Material)	5.3.17-4
Figure 5.3.17-3	Irradiated Hardware One-Dimensional Radial Model of NAC-LWT....	5.3.17-5
Figure 5.3.17-4	Irradiated Hardware Normal Condition Surface Dose Rate as a Function of Irradiated Hardware Height	5.3.17-6
Figure 5.3.17-5	Irradiated Hardware Normal Condition 2 Meter Dose Rate as a Function of Irradiated Hardware Height	5.3.17-6
Figure 5.3.17-6	Irradiated Hardware Accident Condition 1 Meter Dose Rate as a Function of Irradiated Hardware Height	5.3.17-7
Figure 5.3.18-1	Sample SAS2H Input for PWR MOX Fuel	5.3.18-8
Figure 5.3.18-2	PWR Rods Axial Burnup and Source Profiles.....	5.3.18-9
Figure 5.3.18-3	MCNP Model of NAC-LWT with PWR MOX Fuel – Axial Detail ...	5.3.18-10
Figure 5.3.18-4	MCNP Model of NAC-LWT with PWR MOX Fuel – Radial Detail ..	5.3.18-11

List of Figures (continued)

Figure 5.3.18-5	Sample MCNP Input File for PWR MOX Fuel (Response Method Benchmark Case)	5.3.18-12
Figure 5.3.18-6	Normal Condition Axial Surface Dose Rate Profile by Source Type – Power Grade MOX at 70 GWd/MTHM, 2% Fissile Material, and 90 Days Cool Time	5.3.18-17
Figure 5.3.18-7	Normal Condition Radial 2m Dose Rate Profile by Source Type – Power Grade MOX at 70 GWd/MTHM, 2% Fissile Material, and 90 Days Cool Time.....	5.3.18-18
Figure 5.3.18-8	Accident Condition Radial 1m Dose Rate Profile by Source Type – Power Grade MOX at 70 GWd/MTHM, 2% Fissile Material, and 90 Days Cool Time.....	5.3.18-19

List of Tables

Table 5.1.1-1	Type, Form, Quantity and Potential Sources of Design Basis Fuel	5.1.1-7
Table 5.1.1-2	Design Basis Fuel for Shielding Evaluation	5.1.1-11
Table 5.1.1-3	Nuclear and Thermal Source Parameters.....	5.1.1-14
Table 5.1.1-4	Combined Dose Rates for Normal Operations Conditions	5.1.1-15
Table 5.1.1-5	Hypothetical Accident – Loss of Shielding Materials.....	5.1.1-16
Table 5.1.1-6	Hypothetical Accident –Lead Slump.....	5.1.1-17
Table 5.2.1-1	LOR-2 Input Data.....	5.2.1-3
Table 5.2.1-2	Photon Spectrum for Design Basis Fuel	5.2.1-5
Table 5.2.1-3	Fission Product Gas Inventory	5.2.1-6
Table 5.2.1-4	Design Basis Fuel Neutron Spectrum	5.2.1-7
Table 5.3.3-1	Source Material Compositions	5.3.3-8
Table 5.3.3-2	Shield Material Densities and Compositions	5.3.3-8
Table 5.3.4-1	Design Basis MTR Fuel Assembly Characteristics	5.3.4-8
Table 5.3.4-2	MTR Fuel Element Gamma Source Terms by Thermal Output – 380 grams ²³⁵ U	5.3.4-9
Table 5.3.4-3	MTR Fuel Element Neutron Source Terms by Thermal Output – 380 grams ²³⁵ U	5.3.4-10
Table 5.3.4-4	MTR Fuel Element Gamma Source Terms by Thermal Output – 460 grams ²³⁵ U	5.3.4-11
Table 5.3.4-5	MTR Fuel Element Neutron Source Terms by Thermal Output – 460 grams ²³⁵ U	5.3.4-12
Table 5.3.4-6	LEU MTR Hardware Source to Fuel Source Comparison.....	5.3.4-13
Table 5.3.4-7	HEU MTR Hardware Source to Fuel Comparison	5.3.4-14
Table 5.3.4-8	Material Densities for MTR Fuel Shielding Analysis.....	5.3.4-15
Table 5.3.4-9	LWT Cask Surface Total Dose Rates (Normal Conditions of Transport) .	5.3.4-16
Table 5.3.4-10	LWT Cask Plan of Conveyance Dose Rates (Normal Conditions of Transport)	5.3.4-16
Table 5.3.4-11	LWT Cask 2 Meter Off The Plane of Conveyance Dose Rates (Normal Conditions of Transport)	5.3.4-17
Table 5.3.4-12	LWT Cask 1 Meter From the Cask Surface Dose Rates (Normal Conditions of Transport)	5.3.4-17
Table 5.3.4-13	Axial Surface Dose Rates at Cask Lid (Normal Conditions of Transport)	5.3.4-18
Table 5.3.4-14	LWT Cask Dose Rates 5 Meters from the Cask Lid (Back of Tractor Cab) for Normal Conditions of Transport.....	5.3.4-19
Table 5.3.4-15	LWT Cask Dose Rates – 1 Meter from the Cask Surface (Hypothetical Accident Conditions)	5.3.4-19
Table 5.3.5-1	25 PWR Fuel Rods Design Basis Fuel Source Spectra.....	5.3.5-2
Table 5.3.5-2	Material Densities for 25 Design Basis PWR Rods Fuel Shielding Analysis	5.3.5-3
Table 5.3.5-3	Cask Radial Dose Rates with 25 Design Basis PWR Fuel Rods (mrem/hr)	5.3.5-4

List of Tables (continued)

Table 5.3.6-1	TRIGA Fuel Element Gamma Source Term - Normal Transport (ACPR, 86,100 MWd/MTU, 231 Days Cooling, 50% ²³⁵ U Depletion)....	5.3.6-14
Table 5.3.6-2	TRIGA Fuel Element Neutron Source Term - Normal Transport (ACPR, 86,100 MWd/MTU, 231 Days Cooling, 50% ²³⁵ U Depletion)....	5.3.6-15
Table 5.3.6-3	TRIGA Fuel Element Gamma Source Term - Accident Conditions (FLIP- LEU-II, 151,100 MWd/MTU, 908 Days Cooling, 80% ²³⁵ U Depletion)	5.3.6-16
Table 5.3.6-4	TRIGA Fuel Element Neutron Source Term - Accident Conditions (FLIP-LEU-II, 151,100 MWd/MTU, 908 Days Cooling, 80% ²³⁵ U Depletion)	5.3.6-17
Table 5.3.6-5	Material Densities for TRIGA Fuel Element Shielding Analysis.....	5.3.6-18
Table 5.3.7-1	TRIGA Fuel Cluster Rod Parameters	5.3.7-4
Table 5.3.7-2	Incoloy 800 Clad Composition	5.3.7-5
Table 5.3.7-3	Representative TRIGA Fuel Cluster Rod Gamma Spectra at 180 GWd/MTU and 1.849 Year Cool Time	5.3.7-6
Table 5.3.7-4	Representative TRIGA Fuel Cluster Rod Neutron Spectrum at 180 GWd/MTU and 1.849 Year Cool Time	5.3.7-7
Table 5.3.7-5	Fuel Basket Region Material Composition Used in Shielding Analysis	5.3.7-8
Table 5.3.7-6	Normal Condition Dose Response to Gammas for TRIGA Fuel Cluster Rods	5.3.7-9
Table 5.3.7-7	Normal Condition Dose Response to Neutrons for TRIGA Fuel Cluster Rods	5.3.7-9
Table 5.3.7-8	Accident Condition Dose Response to Gammas for TRIGA Fuel Cluster Rods.....	5.3.7-10
Table 5.3.7-9	Accident Condition Dose Response to Neutrons for TRIGA Fuel Cluster Rods.....	5.3.7-10
Table 5.3.7-10	TRIGA Fuel Cluster Rod Required Cool Time at Various Fuel Burnups..	5.3.7-11
Table 5.3.8-1	High Burnup Fuel Rod Model Parameters	5.3.8-9
Table 5.3.8-2	High Burnup Fuel Assembly Model Parameters	5.3.8-9
Table 5.3.8-3	SCALE 27N18G Neutron Group Structure and ANSI Dose Factors	5.3.8-10
Table 5.3.8-4	SCALE 27N18G Gamma Group Structure and ANSI Dose Factors.....	5.3.8-11
Table 5.3.8-5	LWT Cask Total Decay Heat [kW] for 25 Rods at Various Cool Times ...	5.3.8-11
Table 5.3.8-6	PWR 80,000 MWd/MTU Fuel Model Neutron Source Term [n/sec/assy].....	5.3.8-12
Table 5.3.8-7	PWR 80,000 MWd/MTU Fuel Model Gamma Source Term [γ/sec/assy].	5.3.8-12
Table 5.3.8-8	BWR 7×7 60,000 MWd/MTU Fuel Model Neutron Source Term [n/sec/assy].....	5.3.8-13
Table 5.3.8-9	BWR 7×7 60,000 MWd/MTU Fuel Model Gamma Source Term [γ/sec/assy].....	5.3.8-13
Table 5.3.8-10	BWR 7×7 70,000 MWd/MTU Fuel Model Neutron Source Term [n/sec/assy].....	5.3.8-14

List of Tables (continued)

Table 5.3.8-11	BWR 7×7 70,000 MWd/MTU Fuel Model Gamma Source Term [γ/sec/assy]	5.3.8-14
Table 5.3.8-12	BWR 7×7 80,000 MWd/MTU Fuel Model Neutron Source Term [n/sec/assy]	5.3.8-15
Table 5.3.8-13	BWR 7×7 80,000 MWd/MTU Fuel Model Gamma Source Term [γ/sec/assy]	5.3.8-15
Table 5.3.8-14	BWR 8×8 80,000 MWd/MTU Fuel Model Neutron Source Term [n/sec/assy]	5.3.8-16
Table 5.3.8-15	BWR 8×8 80,000 MWd/MTU Fuel Model Gamma Source Term [γ/sec/assy]	5.3.8-16
Table 5.3.8-16	Fuel Axial Source Profile Parameters	5.3.8-17
Table 5.3.8-17	PWR Fuel Axial Source Profile	5.3.8-17
Table 5.3.8-18	BWR Fuel Axial Source Profile	5.3.8-18
Table 5.3.8-19	Fuel Region Homogenized Material Description [atom/b-cm]	5.3.8-19
Table 5.3.8-20	Basket and Cask Shielding Material Composition [atom/b-cm]	5.3.8-19
Table 5.3.8-21	Basket Model Parameters	5.3.8-20
Table 5.3.8-22	LWT Cask One-Dimensional Model for LWR High Burnup Rod Analysis	5.3.8-20
Table 5.3.8-23	LWT Cask Surface Neutron Dose Response Function	5.3.8-21
Table 5.3.8-24	LWT Cask Surface Gamma Dose Response Function	5.3.8-21
Table 5.3.8-25	LWT Cask 2m Neutron Dose Response Function	5.3.8-22
Table 5.3.8-26	LWT Cask 2m Gamma Dose Response Function	5.3.8-22
Table 5.3.8-27	Surface Dose Responses [mrem/hr] and Cask Decay Heat [kW] for Various Decay Times	5.3.8-23
Table 5.3.8-28	2m Dose Responses [mrem/hr] and Cask Decay Heat [kW] for Various Decay Times	5.3.8-24
Table 5.3.8-29	Loading Table for PWR and BWR High Burnup Rods Showing Minimum Required Cool Time as a Function of Burnup and Enrichment	5.3.8-25
Table 5.3.9-1	Design Basis DIDO Fuel Assembly Characteristics	5.3.9-19
Table 5.3.9-2	DIDO Fuel Assembly Gamma Source Terms by Thermal Output	5.3.9-20
Table 5.3.9-3	DIDO Fuel Assembly Neutron Source Terms by Thermal Output	5.3.9-21
Table 5.3.9-4	Material Densities for DIDO Fuel Shielding Analysis	5.3.9-22
Table 5.3.9-5	LWT Cask Surface Total Dose Rates - DIDO Fuel (Normal Conditions of Transport)	5.3.9-23
Table 5.3.9-6	LWT Cask Plane of Conveyance Dose Rates – DIDO Fuel (Normal Conditions of Transport)	5.3.9-23
Table 5.3.9-7	LWT Cask 2 Meters Off the Plane of Conveyance Dose Rates – DIDO Fuel (Normal Conditions of Transport)	5.3.9-24
Table 5.3.9-8	LWT Cask 1 Meter from the Cask Surface Dose Rates – DIDO Fuel (Normal Conditions of Transport)	5.3.9-24

List of Tables (continued)

Table 5.3.9-9	Axial Surface Dose Rates at Cask Lid – DIDO Fuel (Normal Conditions of Transport).....	5.3.9-25
Table 5.3.9-10	LWT Cask Dose Rates - 5 Meters from the Cask Lid – DIDO Fuel (Back of Tractor Cab) for Normal Conditions of Transport.....	5.3.9-26
Table 5.3.9-11	LWT Cask Dose Rates - 1 Meter from the Radial Cask Surface – DIDO Fuel (Hypothetical Accident Conditions).....	5.3.9-26
Table 5.3.10-1	GA IFM Activity Inventory as of January 1, 1996	5.3.10-9
Table 5.3.10-2	GA IFM Neutron and Gamma Spectra in SCALE Format.....	5.3.10-10
Table 5.3.10-3	GA IFM Primary and Secondary Enclosure Dimensions	5.3.10-11
Table 5.3.10-4	Elemental Constituents of GA IFM.....	5.3.10-12
Table 5.3.10-5	Material Compositions of GA IFM and NAC-LWT	5.3.10-13
Table 5.3.10-6	Combined Payload Radial Dose Rates for GA IFM.....	5.3.10-14
Table 5.3.11-1	MCBEND Standard 28 Group Neutron Boundaries.....	5.3.11-25
Table 5.3.11-2	MCBEND Standard 22 Group Gamma Boundaries	5.3.11-26
Table 5.3.11-3	BWR Fuel Assembly Lattice Three-Dimensional Model Parameters	5.3.11-27
Table 5.3.11-4	PWR Fuel Assembly Lattice Three-Dimensional Model Parameters	5.3.11-28
Table 5.3.11-5	Fuel Assembly Lattice SAS2H Burnup Parameters at 80,000 MWd/MTU	5.3.11-29
Table 5.3.11-6	B&W 15×15 80,000 MWd/MTU, 150 Day Cool Time Source Terms in MCBEND Format.....	5.3.11-30
Table 5.3.11-7	B&W 17×17 PWR 80,000 MWd/MTU, 150 Day Cool Time Source Terms in MCBEND Format	5.3.11-31
Table 5.3.11-8	CE 14×14 PWR 80,000 MWd/MTU, 150 Day Cool Time Source Terms in MCBEND Format.....	5.3.11-32
Table 5.3.11-9	Westinghouse 14×14 PWR 80,000 MWd/MTU, 150 Day Cool Time Source Terms in MCBEND Format	5.3.11-33
Table 5.3.11-10	Westinghouse 15×15 PWR 80,000 MWd/MTU, 150 Day Cool Time Source Terms in MCBEND Format	5.3.11-34
Table 5.3.11-11	Westinghouse 17×17 PWR 80,000 MWd/MTU, 150 Day Cool Time Source Terms in MCBEND Format	5.3.11-35
Table 5.3.11-12	BWR 7×7 80,000 MWd/MTU, 210 Day Cool Time Source Terms in MCBEND Format.....	5.3.11-36
Table 5.3.11-13	BWR 8×8 80,000 MWd/MTU, 150 Day Cool Time Source Terms in MCBEND Format.....	5.3.11-37
Table 5.3.11-14	PWR Fuel Lattice Axial Source Profile.....	5.3.11-38
Table 5.3.11-15	BWR Fuel Lattice Axial Source Profile	5.3.11-39
Table 5.3.11-16	BWR Fuel Assembly Lattice Fuel Region Homogenization	5.3.11-40
Table 5.3.11-17	PWR Fuel Assembly Lattice Fuel Region Homogenization	5.3.11-41
Table 5.3.11-18	Fuel Assembly Lattice Activated Hardware Region Homogenization	5.3.11-43
Table 5.3.11-19	Fuel Lattice Accident Condition Damaged Fuel Material Heights.....	5.3.11-44
Table 5.3.11-20	BWR Fuel Assembly Lattice Fuel Region Homogenized Material Description.....	5.3.11-44

List of Tables (continued)

Table 5.3.11-21	PWR Fuel Assembly Lattice Fuel Region Homogenized Material Description	5.3.11-45
Table 5.3.11-22	Basket and Cask Shielding Material Composition.....	5.3.11-45
Table 5.3.11-23	ANSI/ANS 6.1.1-1977 Neutron Flux-to-Dose Conversion Factors.....	5.3.11-46
Table 5.3.11-24	ANSI/ANS 6.1.1-1977 Gamma Flux-to-Dose Conversion Factors	5.3.11-47
Table 5.3.11-25	Maximum Radial Dose Rates for PWR and BWR Fuel Rods in an Irradiated Fuel Assembly Lattice	5.3.11-48
Table 5.3.11-26	Maximum Axial Dose Rates for PWR and BWR Fuel Rods in an Irradiated Fuel Assembly Lattice	5.3.11-48
Table 5.3.12-1	PWR Rods 80,000 MWd/MTU, 150 Day Cool Time Source Terms in MCBEND Format	5.3.12-20
Table 5.3.12-2	BWR 7x7 Rods 80,000 MWd/MTU, 210 Day Cool Time Source Terms in MCBEND Format	5.3.12-21
Table 5.3.12-3	BWR 8x8 Rods 80,000 MWd/MTU, 150 Day Cool Time Source Terms in MCBEND Format	5.3.12-22
Table 5.3.12-4	Fuel Region Homogenization for PWR Fuel Rods	5.3.12-23
Table 5.3.12-5	Fuel Region Homogenization for BWR 7x7 Fuel Rods	5.3.12-23
Table 5.3.12-6	Region Homogenization for BWR 8x8 Fuel Rods	5.3.12-24
Table 5.3.12-7	Intact/Damaged Fuel Mixture Composition Determinations	5.3.12-24
Table 5.3.12-8	Fuel Region Homogenized Material Description.....	5.3.12-25
Table 5.3.12-9	Maximum Radial Dose Rates for Damaged PWR and BWR Fuel Rods	5.3.12-26
Table 5.3.12-10	Maximum Axial Dose Rates for Damaged PWR and BWR Fuel Rods ..	5.3.12-26
Table 5.3.13-1	Single TPBAR Activity Inventory at 30 Days Cool Time	5.3.13-12
Table 5.3.13-2	TPBAR 30-Day Gamma Source Spectrum	5.3.13-13
Table 5.3.13-3	TPBAR Elemental Constituents.....	5.3.13-14
Table 5.3.13-4	Material Compositions of NAC-LWT for 300 TPBAR Payload	5.3.13-15
Table 5.3.13-5	Dose Rate Summary for 300 TPBARs at 30 Days Cool Time.....	5.3.13-16
Table 5.3.13-6	Reactor Operating Conditions for TPBAR Source Term Generation.....	5.3.13-17
Table 5.3.14-1	PULSTAR Fuel Geometry	5.3.14-16
Table 5.3.14-2	Source Term Generation Parameters for PULSTAR Fuel	5.3.14-16
Table 5.3.14-3	PULSTAR Fuel Assembly Neutron Source Term for 1 Year Cool Time	5.3.14-17
Table 5.3.14-4	PULSTAR Fuel Assembly Gamma Source Term for 1 Year Cool Time	5.3.14-18
Table 5.3.14-5	Intact Assembly Fuel Homogenization for PULSTAR Fuel.....	5.3.14-19
Table 5.3.14-6	Nominal Height Can Fuel Homogenization for PULSTAR Fuel	5.3.14-19
Table 5.3.14-7	Minimum Height Can Fuel Homogenization for PULSTAR Fuel	5.3.14-19
Table 5.3.14-8	Fuel Region Homogenized Material Description for PULSTAR Fuel	5.3.14-20
Table 5.3.14-9	Cask/Basket Material Descriptions for PULSTAR Fuel.....	5.3.14-20
Table 5.3.14-10	Maximum Radial Dose Rates for PULSTAR Fuel	5.3.14-21
Table 5.3.14-11	Maximum Axial Dose Rates for PULSTAR Fuel.....	5.3.14-21
Table 5.3.15-1	Spiral Fuel Assembly Characteristics.....	5.3.15-6
Table 5.3.15-2	Spiral Fuel Assembly Neutron and Gamma Source (18 Watt Heat Load)	5.3.15-7

List of Tables (continued)

Table 5.3.15-3	Spiral Fuel Assembly Source Comparison to DIDO MEU Fuel (70% Depletion and 18 Watts).....	5.3.15-8
Table 5.3.15-4	Spiral Fuel Assembly Source Comparison to DIDO MEU Fuel (70% Depletion and Fixed 2.23-Year Cool Time).....	5.3.15-9
Table 5.3.16-1	MOATA Plate Bundle Characteristics	5.3.16-4
Table 5.3.16-2	MOATA Plate Bundle Source Comparison	5.3.16-5
Table 5.3.17-1	Irradiated Hardware Gamma Spectra in SCALE Format (1 kg Activated Stainless Steel)	5.3.17-8
Table 5.3.17-2	Material Compositions of the NAC-LWT.....	5.3.17-9
Table 5.3.18-1	High Burnup Fuel Rod Model Parameters	5.3.18-20
Table 5.3.18-2	High Burnup MOX Fuel Assembly Model Parameters.....	5.3.18-20
Table 5.3.18-3	MOX Fuel Material Compositions.....	5.3.18-21
Table 5.3.18-4	Uranium/Plutonium Fractions in MOX Fuel.....	5.3.18-21
Table 5.3.18-5	PWR Fuel Axial Source Profile	5.3.18-22
Table 5.3.18-6	Fuel Axial Source Profile Parameters	5.3.18-22
Table 5.3.18-7	MOX Source Term Magnitudes at 70 GWd/MTHM and 90 Days Cool Time (per Rod Basis).....	5.3.18-23
Table 5.3.18-8	MOX Fuel Cool Time to Reach 143.75 W/Rod (Days).....	5.3.18-24
Table 5.3.18-9	PWR Power Grade MOX Fuel Assembly Neutron Source Term for 70 GWd/MTHM, 2% Fissile Pu, and 90 Days Cooling (16 Rods)	5.3.18-25
Table 5.3.18-10	PWR Power Grade MOX Fuel Assembly Gamma Source Term for 70 GWd/MTHM, 2% Fissile Pu, and 90 Days Cooling (16 Rods)	5.3.18-26
Table 5.3.18-11	Homogenization for PWR MOX Fuel Rod Regions.....	5.3.18-27
Table 5.3.18-12	Cask/Basket Material Descriptions for PWR MOX Fuel.....	5.3.18-28
Table 5.3.18-13	Subcritical Multiplication Study for PWR MOX Fuel.....	5.3.18-28
Table 5.3.18-14	Maximum Radial Dose Rates for PWR MOX Fuel – 90 Days Cool Time, 2% Fissile Pu.....	5.3.18-29
Table 5.3.18-15	Detailed Dose Rates for Bounding Fuel – Power Grade PWR MOX Fuel, 2% Fissile Pu, 70 GWd/MTHM and 90 Days Cool Time.....	5.3.18-29
Table 5.4.1-1	Discrete Axial Source Distribution	5.4.1-4
Table 5.4.1-2	Flux to Dose Conversion Factors	5.4.1-6

5 SHIELDING EVALUATION

The NAC-LWT cask utilizes a concentric cylindrical arrangement of steel, lead, steel and water to provide gamma shielding for the design basis fuel. The water-glycol solution in the neutron shield tank also provides neutron shielding. The water contains 1 weight percent (wt %) boron, which absorbs neutrons without producing significant secondary gamma radiation.

The PWR and BWR design basis shielding analysis uses the LOR-2 version of the ORIGEN-2 code to calculate radiation sources. The QAD-CG (Cain) and XSDRNPM (NUREG/CR-0200, Vol, 2, F3) codes are used to calculate the cask dose rates for normal operations and hypothetical accident conditions. The shielding analysis shows that the dose rates are below regulatory limits specified in 10 CFR 71.47 and 71.51 as well as IAEA Transportation Safety Standards (TS-R-1).

The PWR and BWR design basis shielding analyses were performed for a 0.25-inch thick neutron shield tank shell, while the actual fabricated thickness is only 0.24 inch (6mm). The shell thickness difference of 0.01 inch yields a maximum dose rate increase of only 2.4 percent, which gives lower dose rates than worst case tolerance analysis in this chapter. The analyses of this chapter, therefore, are valid.

The MTR design basis shielding analysis used the SCALE package. This included SAS2H (Herman) for source terms, and SAS4 (Tang) for three-dimensional shielding analysis. This evaluation is presented in Section 5.3.4. This shielding analysis shows that dose rates are below regulatory limits when the NAC-LWT contains up to 42 design basis MTR fuel elements with less than 210 watts of decay heat per basket.

The MTR shielding analysis explicitly calculated dose rates for LEU, MEU and HEU MTR fuel for a range of burnups and cool times to meet decay heat and dose rate limits. HEU fuel source terms were higher and thus the HEU fuel provides the most limiting dose rates for fixed decay heat limits.

The 25 PWR rod design basis shielding analysis used the SCALE package. This included SAS2H for source terms and SAS1 for one-dimensional radial shielding analysis. This analysis is presented in Section 5.3.5. This shielding analysis shows that the dose rates are below regulatory limits when the NAC-LWT contains up to 25 design basis PWR rods. A shielding evaluation of high burnup PWR and BWR fuel rods in a rod holder is presented in Section 5.3.8. Up to 25 PWR and BWR fuel rods are evaluated at burnups up to 80,000 MWd/MTU.

The NAC-LWT is evaluated for the transport of up to 140 TRIGA fuel elements or up to 560 TRIGA fuel cluster rods arranged in five (5) basket modules. This shielding evaluation uses the SCALE package with the SAS2H sequence for source term identification, and SAS4, also from

the SCALE package, to perform a three-dimensional shielding analysis. The analysis is presented in Section 5.3.6. The analysis shows that the dose rates are below the regulatory limits when the cask contains up to 140 TRIGA fuel elements each having a maximum decay heat of 7.5 W, or up to 560 TRIGA fuel cluster rods each having a maximum decay heat of 1.875 W.

There are two TRIGA basket configurations, non-poisoned and poisoned, as described in Section 1.2.3.1.2. Each TRIGA basket module consists of seven cells. The center cell of each non-poisoned basket module is blocked with a stainless steel plate. Consequently, only six (6) cells of each non-poisoned basket module are loaded with fuel. Because the shielding analyses assumes the center cell contains the bounding TRIGA fuel elements or TRIGA fuel cluster rods during the normal and accident conditions of transport; the evaluation of 140 fuel elements or 560 fuel cluster rods bounds the 120 fuel element / 480 fuel cluster rod configurations.

The DIDO design basis shielding analysis used the SCALE package. This included SAS2H (Herman) for source terms, and SAS4 (Tang) for three-dimensional shielding analysis. This evaluation is presented in Section 5.3.9. This shielding analysis shows that dose rates are below regulatory limits when the NAC-LWT contains up to 42 design basis DIDO fuel assemblies with two allowable heat loads per basket module, either 175 watts or 126 watts, dependent on the axial position of the fuel elements in the top basket.

The DIDO shielding analysis explicitly calculated dose rates for LEU, MEU and HEU DIDO fuel for a range of burnups and cool times to meet decay heat and dose rate limits. HEU fuel source terms were higher and thus the HEU fuel provides the most limiting dose rates for fixed decay heat limits.

The analysis of General Atomics (GA) Irradiated Fuel Material (IFM) used the SCALE package. The GA IFM consists of two Fuel Handling Units, one containing RERTR (an Incoloy clad TRIGA type fuel) and the other containing HTGR graphite matrix fuel material. The analysis included ORIGEN-S for source terms and SAS1 for one-dimensional radial shielding analysis. This evaluation is presented in Section 5.3.10. The shielding evaluation shows that dose rates are well below regulatory limits for a combined payload of the two Fuel Handling Units.

Up to 25 high burnup intact PWR or BWR fuel rods loaded into a fuel assembly lattice are analyzed in Section 5.3.11. Source terms were calculated using SAS2H with three-dimensional dose rates calculated using the MCBEND Monte Carlo transport code. Up to 14 high burnup damaged fuel rods may be loaded in a shipment of 25 PWR or BWR fuel rods, as demonstrated in Section 5.3.12. Damaged rods must be loaded in the rod holder. Source terms were calculated using SAS2H with three-dimensional dose rates calculated using the MCBEND Monte Carlo transport code.

A combination of up to 16 high burnup undamaged PWR MOX or UO₂ fuel rods loaded into a 5×5 rod holder is analyzed in Section 5.3.18. Remaining slots in the 5×5 lattice may be occupied by zirconium alloy-based hardware components such as burnable poison rods (BPRs), provided they are not comprised of highly activated materials (e.g., steel or inconel). The rod lattice is located within a canister placed into an insert located within the NAC-LWT PWR basket. Source terms were calculated using SCALE 5.0 SAS2H, with three-dimensional dose rates calculated using the MCNP5 Monte Carlo transport code.

An analysis of the content condition of 300 production Tritium Producing Burnable Absorber Rods (TPBARs) in a consolidation canister used the ORIGEN-S module of the SCALE package for source terms and the MCNP code package to calculate three-dimensional dose rates. This evaluation is presented in Section 5.3.13 and shows that dose rates are well below regulatory limits for normal and accident conditions. The second TPBAR content condition of 55 segmented TPBARs cooled for a minimum of 90 days is evaluated using the source terms determined by the ORIGEN-S module of the SCALE package. This evaluation readily shows compliance with the previously calculated regulatory dose rates for 300 production TPBARs cooled a minimum of 30 days.

A payload of up to 700 PULSTAR fuel elements is analyzed in Section 5.3.14. Source terms were calculated using SAS2H with three-dimensional dose rates calculated using the MCNP code. PULSTAR fuel elements may be loaded as assemblies in a 5×5 rectangular array; intact elements in a 4×4 fuel rod insert; or intact or damaged elements and nonfuel components of fuel assemblies in a can. Four 7-element MTR basket modules are stacked to form a 28 MTR basket in the cask cavity. The maximum cell loading is 25 elements.

A payload of up to 42 spiral fuel assemblies or 42 MOATA plate bundles in the ANSTO basket is analyzed in Section 5.3.15. Six 7-element ANSTO basket modules are stacked to form a 42-assembly payload in the cask cavity. Source terms were calculated using SAS2H. Due to similarities in the basket design to the DIDO basket and bounding source terms in the DIDO shielding evaluation, no shielding evaluations are required to demonstrate regulatory compliance.

5.1 Discussion and Results

The NAC-LWT cask is designed for the safe transport of spent nuclear fuel from various commercial nuclear installations and research reactors.

5.1.1 NAC-LWT Contents

The following contents constitute the design basis for transport in the NAC-LWT cask:

- one Westinghouse 15 × 15 Pressurized Water Reactor (PWR) assembly
- up to 25 PWR rods
- up to two General Electric 7 × 7 Boiling Water Reactor (BWR) assemblies
- fifteen intact metallic fuel rods or six failed metallic fuel rods
- up to 42 Materials Test Reactor (MTR) research reactor fuel elements
- up to 140 TRIGA fuel elements or up to 560 TRIGA fuel cluster rods
- up to 25 PWR or BWR UO₂ fueled high burnup (up to 80,000 MWd/MTU) rods
- up to 16 PWR MOX or UO₂ rods in any combination (up to 62,500 MWd/MTHM)
- up to 42 DIDO research reactor fuel assemblies
- two General Atomics (GA) Irradiated Fuel Material (IFM) Fuel Handling Units
- up to 300 TPBARs (of which two can be prefailed)
- up to 55 TPBARs segmented during PIE and associated segmentation debris
- up to 700 PULSTAR fuel elements (intact or damaged)
- up to 42 spiral fuel assemblies
- up to 42 MOATA plate bundles

The 25 high burnup PWR and BWR rods may be transported in three configurations: 1) a maximum of 25 intact fuel rods loaded in the rod holder; 2) a maximum of 25 fuel rods with up to 14 damaged fuel rods or rod fragments loaded in the rod holder; and 3) a maximum of 25 intact fuel rods housed in a fuel assembly lattice within the NAC-LWT PWR basket. The fuel assembly lattice may be irradiated up to an equivalent burnup of 80,000 MWd/MTU.

The metallic fuel consists of a single rod of uranium metal clad with aluminum. The intact metallic fuel rods are placed into a transport canister that will hold five intact rods. The cask can hold three transport canisters for a total of 15 intact metallic fuel rods. In the event the metallic fuel has failed or is suspected of having failed, each fuel rod is sealed in its own container. The failed metallic fuel is loaded into either one of the three holes in the metallic fuel basket or into one of the six openings in the failed metallic fuel basket.

MTR research reactor fuel elements are typically 33 to 57 inches long, including lower nozzle and upper handle. The fuel plates typically consist of U-Al, U₃O₈-Al, or USi-Al clad with aluminum. The fuel plates are held in a parallel arrangement with two thick aluminum slotted pieces to form a fuel element. Standard fuel elements have between 10 and 23 fuel plates. The active fuel region is typically 22.75 inches in height, and the fuel meat is typically 0.023-inch thick. The highly enriched uranium (HEU) fuel has been analyzed conservatively with an enrichment of 90 wt % ²³⁵U and fuel loading per element up to 380 g ²³⁵U, with a separate analysis performed to accommodate up to 460 g ²³⁵U. The design basis fuel parameters are provided in Table 5.1.1-1. The fuel characteristics are presented in Table 5.1.1-2. The dose rates produced from the design basis 470 g ²³⁵U and 640 g ²³⁵U LEU and 380 g ²³⁵U MEU MTR fuel are bounded by the HEU MTR design basis fuel. Therefore, a mixed loading of LEU, MEU and HEU MTR fuel elements are also bounded by a full HEU MTR fuel element loading.

The source term characteristics of the design basis PWR fuel assembly, BWR fuel assembly, metallic rods, 25 PWR rods, 16 PWR MOX rods, and MTR fuels are given in Table 5.1.1-3. The design basis PWR and BWR fuels require two years of cooling after discharge to meet the neutron and gamma source, and decay heat limits of the cask. The MOX rods require 90 days of cooling. The design basis metallic fuel requires one year cooling. The design basis MTR fuel requires a variable number of years cooling, after discharge, to meet the decay heat limits of the cask. Loading configurations must conform to the limits stated in Section 7.1.5.

DIDO research reactor fuel elements typically consist of U-Al, U₃O₈-Al, or U₃Si₂-Al that is aluminum clad. The fuel elements are held in a concentric arrangement inside an outer aluminum cylinder to form a fuel assembly. Fuel assemblies have 4 fuel elements. The active fuel region is typically 23.6 inches in height, and the fuel meat is typically 0.026 inch thick. The highly enriched uranium (HEU) fuel has been analyzed with a minimum enrichment of 90 wt % ²³⁵U and fuel loading per assembly up to 190 g ²³⁵U. Low enriched (LEU) and medium enriched (MEU) assemblies are evaluated at 190 g ²³⁵U with minimum enrichments of 19 and 40 wt % ²³⁵U, respectively. The design basis fuel parameters are provided in Table 5.1.1-1. The fuel characteristics are presented in Table 5.1.1-2. As discussed in Section 5, the dose rates produced from the design basis LEU and MEU DIDO fuel are bounded by the HEU DIDO design basis fuel. Therefore, a mixed loading of LEU, MEU and HEU DIDO fuel assemblies is also bounded by a full HEU DIDO fuel assembly loading.

Two GA IFM Fuel Handling Units (packages) are intended for a single shipment in the NAC-LWT. The first package is composed of Reduced-Enrichment Research and Test Reactor (RERTR) type fuel, which is an Incoloy clad TRIGA fuel. The second is composed of High-Temperature Gas-Cooled Reactor (HTGR) type fuel. Each set of IFM is packaged into stainless

steel weld-encapsulated primary and secondary enclosures. Design basis fuel parameters are summarized in Table 5.1.1-1, with fuel characteristics presented in Table 5.1.1-2. Design basis source terms are provided in Table 5.1.1-3. NAC-LWT combined dose rates for GA IFM are bounded by the dose rates for PWR fuel shown in Table 5.1.1-4 through Table 5.1.1-6.

An inventory of up to 300 production TPBARs (of which two can be prefailed) is intended for multiple shipments in the NAC-LWT. A separate content condition is for the transport of up to 55 segmented TPBARs and associated segmentation debris from PIE contained in a waste container. Each TPBAR is a Type 316 stainless steel rod with a 0.381-inch outer diameter and a 0.336-inch inner diameter and a post-irradiation length of approximately 154 inches. Tritium is produced by irradiation of ^6Li . Design basis fuel parameters are summarized in Table 5.1.1-1 with characteristics presented in Table 5.1.1-2. Design basis source terms are provided in Table 5.1.1-3. NAC-LWT dose rates for the payloads of up to 300 production TPBARs in a consolidation canister, or up to 55 segmented TPBARs in the waste container, are bounded by the dose rates for PWR fuel shown in Table 5.1.1-4 through Table 5.1.1-6.

Source terms for the high burnup PWR and BWR rods are developed using the SCALE SAS2H code package. Cask dose rates are evaluated using the SCALE SAS1 shielding analysis sequence. Results presented in Section 5.3.8 give the required cool time for PWR and BWR rods as a function of burnup for up to 25 intact fuel rods loaded in the NAC-LWT rod holder. The results presented in Sections 5.3.11 and 5.3.12 demonstrate that dose rate limits are met for the shipment of fuel rods in an irradiated fuel assembly lattice and damaged fuel rods in a rod holder, respectively.

Source terms for the 62,500 MWd/MTHM MOX rods, and the UO_2 rods evaluated in the same section, are developed using the SCALE 5.0 SAS2H code package. Source terms were conservatively calculated for a 70,000 MWd/MTHM burnup. Cask dose rates are evaluated using the MCNP5 Monte Carlo code. Results presented in Section 5.3.18 require the MOX and UO_2 rods to be cooled 90 days prior to shipment (low quality, power grade, MOX fuel requires 120 days to meet heat load limits, but produces dose rates below limits at 90 days).

As can be seen from Table 5.1.1-3, the PWR fuel assembly has the largest source terms and was used as the design basis fuel for shielding analysis of PWR and BWR fuel in the NAC-LWT presented in this section. The metallic fuel shielding analysis is presented in Section 5.3.3. Metallic fuel is shipped with the neutron shield drained and the analysis reflects this. The MTR fuel shielding analysis is presented in Section 5.3.4. The design basis source terms for 25 PWR rods at 60,000 MWd/MTU are well below the design basis PWR fuel assembly. However, the self shielding of 25 PWR rods is less than the 204 rod design basis PWR fuel assembly. Thus, a shielding evaluation of 25 design basis PWR rods is presented in Section 5.3.5. Similarly, the

self-shielding for either the 25 high burnup PWR or BWR rods at 80,000 MWd/MTU is lower than that of the design basis assemblies. Shielding evaluations for these rods are presented in Sections 5.3.8, 5.3.11 and 5.3.12.

The transport of up to 140 TRIGA fuel elements is evaluated in Section 5.3.6. TRIGA fuel is a solid metal hydride, U-ZrH and may be high enriched (70%), or low enriched (20%). The fuel clad is either aluminum or stainless steel. TRIGA fuel is fabricated in several configurations, as described in Section 1.2.3.1, that vary in weight, active fuel length and overall length. The typical fuel element length and weight is 28.3 inches and 8.82 pounds. The fuel follower control rod element (FFCR) establishes the upper bound weight (13.2 pounds) and length (approximately 45 inches). These elements can only be loaded in the top module of the TRIGA fuel basket. The design basis TRIGA fuel parameters are presented in Table 5.1.1-1 and Table 5.1.1-2. Source term characteristics are presented in Table 5.1.1-3. Cooling time for TRIGA fuel is variable, down to a minimum of 90 days, based on the time required for the decay heat to reach 7.5 watts.

In addition, the transport of TRIGA fuel cluster rods is evaluated in Section 5.3.7. These rods are obtained from the disassembly of the 5×5 (25 rod) arrays comprising the cluster-type TRIGA fuel as shown in Figure 1.2-6. Only the shipment of the fuel cluster rods is analyzed here; no other activated components of the TRIGA cluster assembly are considered for shipment in this analysis. The TRIGA fuel cluster rod is considered to contain a maximum design-basis fuel mass of 452 g of U-ZrH with an H to Zr ratio of 1.6 and a total uranium mass fraction of 10%. The fuel is highly enriched (93 wt. % ²³⁵U). The rods are clad in Incoloy 800 and contain upper and lower stainless steel end plugs with a mass of approximately 60.5 g each. For shipment, each rod is placed inside an aluminum tube (ID 0.625 in, OD 0.750 in), with 16 rods occupying each LWT basket opening for a total of up to 112 rods per basket or 560 rods per cask.

The basis for the dose rate evaluation of the TRIGA fuel cluster rods is a source term and one-dimensional shielding analysis in which the minimum cooling time required for the dose rates produced by the TRIGA fuel cluster rods to fall below the dose rates produced by the design basis TRIGA fuel elements. Cooling time results are determined at a large number of fuel burnup values (at approximately every 2.5% increment in ²³⁵U depletion).

PULSTAR fuel elements are zirconium alloy-clad UO₂ pellets with a physical design characteristic as listed in Table 5.1.1-1 and Table 5.1.1-2. PULSTAR fuel assemblies are a 5×5 rectangular array of elements surrounded by a zirconium alloy box, with aluminum upper and lower fittings. The element pitch is nominally 0.524 × 0.606 inch. PULSTAR fuel elements are analyzed at a loading of 32 grams ²³⁵U per element, an initial enrichment of 6 wt % ²³⁵U, and 45% ²³⁵U burnup. For conservatism, a cool time of one year from discharge is employed in the

shielding analysis; a cool time of at least 1.5 years is required to meet the basket cell heat load limit of 30 W. Source term characteristics are presented in Table 5.1.1-3

Spiral fuel assemblies typically consist of 10 curved plates (also referred to as elements) of metallic U-Al fuel meat that is aluminum clad. The fuel elements are held in a spiral arrangement between an inner and outer aluminum cylinder to form a fuel assembly. The active fuel region is typically 60.325 cm in height, and the fuel meat is typically 0.061 cm thick. The elements are nominally enriched to 80 wt % ^{235}U and were conservatively evaluated at 75 wt % ^{235}U . Maximum fuel loading per assembly is evaluated at 160 g ^{235}U . The design basis fuel parameters are provided in Table 5.1.1-1. The fuel characteristics are presented in Table 5.1.1-2. Applying MEU DIDO fuel assembly minimum cool time curves, which are based on a 40 wt % ^{235}U enriched 190 g ^{235}U fuel assembly, to the spiral fuel elements produces source terms that are bounded by the DIDO MEU fuel. Given similar basket designs, the dose rates produced by the spiral fuel elements are bounded by the MEU DIDO evaluation set.

MOATA fuel bundles consist of a maximum of 14 flat MTR type fuel plates. The fuel plates are composed of a metallic U-Al fuel meat that is aluminum clad. The fuel elements are held in place with aluminum outer plates and pins through the top and bottom of the plate stack in their shipment configuration. The plates are held in a typical MTR plate (12 plates per assembly) with a comb side plate configuration during reactor operations. The active fuel region is typically 58.4 cm in height, and the fuel meat is typically 0.1016-cm thick. The elements are nominally enriched to 90 wt % ^{235}U and were conservatively evaluated at 80 wt % ^{235}U . Maximum fuel loading per plate is evaluated at 25 g ^{235}U (nominal loading is 22 g ^{235}U). The design basis fuel parameters are provided in Table 5.1.1-1. The fuel characteristics are presented in Table 5.1.1-2. The gamma radiation source for the 14 fuel plate bundle is approximately 2% of the DIDO MEU assembly. Since the basket designs are similar, the dose rates produced by the plate bundle are bounded by the MEU DIDO evaluation set.

The shield materials are selected and arranged to minimize cask weight while maintaining overall shield effectiveness. Lead and steel are chosen as effective gamma radiation shields, and a water tank on the outside of the cask is provided to efficiently moderate and absorb the neutron radiation.

The total neutron and gamma dose rates calculated for the normal operations conditions are shown in Table 5.1.1-4. Note that the maximum dose rate is on the cask lid surfaces at the top end of the cask and does not exceed the design limit of 200 mrem/hour for the surface of the cask. The 10 CFR 71 limits of 10 mrem/hour at two meters from the cask surface and the design limit of 200 mrem/hour on the cask surface are met. Table 5.1.1-4 contains the total dose rates for the hypothetical accident conditions. These dose rates are well under the 49 CFR 173 limit of

Revision LWT-08A

1000 mrem/hour at one meter from the cask surface. The dose rates for the lead slump accident are shown in Table 5.1.1-5. These dose rates show that even with the lead slumped, the hypothetical accident dose rate limits have not been exceeded and the cask is safe for transport.

The cask surface fuel centerline normal operations and hypothetical accident dose rates calculated include neutrons and gammas originating from the fuel, neutrons and gammas scattered from the ground and secondary gammas resulting from neutron capture in the neutron shield. All of the other dose locations also include the contribution from the ^{60}Co in the end-fittings.

Table 5.1.1-1 Type, Form, Quantity and Potential Sources of Design Basis Fuel

<u>Fuel Type</u>	- PWR, Westinghouse 15 × 15
	- 3.7 wt % ²³⁵ U maximum initial enrichment
	- 35,000 MWd/MTU maximum burnup
	- 2.5 kW per assembly maximum decay heat
	- 2 years (or more) decay time after reactor discharge
<u>Fuel Form</u>	- Intact assemblies
<u>Quantity</u>	- 1 design basis fuel assembly
<u>Source of Fuel</u>	- Commercial PWR nuclear power reactors
<u>Transport Index</u>	- 35
<u>Fuel Type</u>	- BWR, General Electric 7 × 7
	- 4.0 wt % ²³⁵ U maximum initial enrichment
	- 30,000 MWd/MTU maximum burnup
	- 1.1 kW per assembly maximum decay heat, 2.2 kW per cask for 2 assemblies
	- 2 years (or more) decay time after reactor discharge
<u>Fuel Form</u>	- Intact assemblies
<u>Quantity</u>	- 2 design basis fuel assemblies
<u>Source of Fuel</u>	- Commercial BWR nuclear power reactors
<u>Transport Index</u>	- 35
<u>Fuel Type</u>	- High Burnup PWR or BWR rods
	- 5.0 wt % maximum ²³⁵ U initial enrichment
	- 80,000 MWd/MTU maximum average burnup
	- 2.3 kW /cask maximum decay heat
	- Minimum cool time dependent on burnup (See Table 5.3.8-29)
<u>Fuel Form</u>	- Intact rods in a fuel assembly lattice or rod holder and intact rods with up to 14 fuel rods classified as damaged in a rod holder
<u>Quantity</u>	- Up to 25
<u>Source of Fuel</u>	- Commercial PWR or BWR nuclear power reactor
<u>Transport Index</u>	- 36 (intact rods)
	28 (intact rods in a fuel assembly lattice)
	37 (intact rods with 14 rods classified as damaged)
<u>Fuel Type</u>	- Uranium metal fuel rods
	- Natural wt % ²³⁵ U
	- 1,600 MWd/MTU maximum burnup
	- 0.0357 kW per sound rod maximum decay heat, 0.54 kW per cask for 15 sound fuel rods
	- 1 year (or more) decay time after reactor discharge
<u>Fuel Form</u>	- Intact or encapsulated failed fuel rods
<u>Quantity</u>	- 15 design basis fuel rods, or 6 design basis failed fuel rods
<u>Source of Fuel</u>	- Research reactors
<u>Transport Index</u>	- 25

Table 5.1.1-1 Type, Form, Quantity and Potential Sources of Design Basis Fuel (cont'd)

<u>Fuel Type</u>	- Material Test Reactor (MTR) Fuel Elements
	- HEU: 90 wt % ²³⁵ U, Maximum burnup variable up to 660,000 MWd/MTU for 380 g ²³⁵ U and 577,500 MWd/MTU for 460 g ²³⁵ U
	- MEU: 40 wt % ²³⁵ U, Maximum burnup variable up to 293,300 MWd/MTU for 380 g ²³⁵ U
	- LEU: 19 wt % ²³⁵ U, Maximum burnup variable up to 139,300 MWd/MTU for 470 g ²³⁵ U and 640 g ²³⁵ U
	- 210 W per basket decay heat
	- Variable cool time down to 90 days using the procedure in Section 7.1.5
<u>Fuel Form</u>	- Intact aluminum clad parallel plates
<u>Quantity</u>	- Up to 42 fuel elements
<u>Source of Fuel</u>	- Research and Material Test Reactors
<u>Transport Index</u>	- 45
<u>Fuel Type</u>	- TRIGA Fuel Element
	- 20 to 70 wt % ²³⁵ U
	- 80% ²³⁵ U depletion (approximately 151 GWd/MTU for LEU fuel and 460 GWd/MTU HEU fuel)
	- 7.5 watts per element decay heat
	- Variable cool time down to 90 days
<u>Fuel Form</u>	- Aluminum or stainless steel (304) clad rods, intact, failed or as debris
<u>Quantity</u>	- Up to 140 fuel elements
<u>Source of Fuel</u>	- Test, Research and Isotope Reactors
<u>Transport Index</u>	- 25
<u>Fuel Type</u>	- TRIGA Fuel Cluster Rods
	- 93 wt % ²³⁵ U
	- 80% ²³⁵ U depletion (approximately 600 GWd/MTU)
	- 1.875 watts per rod decay heat
	- Variable cool time down to 90 days
<u>Fuel Form</u>	- Incoloy 800 clad rods, intact, failed or as debris
<u>Quantity</u>	- Up to 560 fuel rods
<u>Source of Fuel</u>	- Test, Research and Isotope Reactors
<u>Transport Index</u>	- 25
<u>Fuel Type</u>	- DIDO Fuel Assemblies
	- HEU: 90 wt % ²³⁵ U, Maximum burnup variable up to 577,460 MWd/MTU or 70% ²³⁵ U depletion
	- MEU: 40 wt % ²³⁵ U, Maximum burnup variable up to 256,650 MWd/MTU or 70% ²³⁵ U depletion
	- LEU: 19 wt % ²³⁵ U, Maximum burnup variable up to 121,910 MWd/MTU or 70% ²³⁵ U depletion
	- 175 or 126 W per basket decay heat
	- Variable cool time down to 180 days using the procedure in Section 7.1.4

Table 5.1.1-1 Type, Form, Quantity and Potential Sources of Design Basis Fuel (cont'd)

<u>Fuel Form</u>	- Intact aluminum clad concentric fuel tubes
<u>Quantity</u>	- Up to 42 fuel assemblies
<u>Source of Fuel</u>	- Research Reactors
<u>Transport Index</u>	- 40.1
<u>Fuel Type</u>	- General Atomics (GA) Irradiated Fuel Material (IFM)
	- RERTR (see activity inventory in Table 5.3.10-1)
	- HTGR (see activity inventory in Table 5.3.10-1)
	- <13.05 W
	- Transport after 1/1/96
<u>Fuel Form</u>	- RERTR: 13 intact TRIGA elements, 7 sectioned elements
	- HTGR: Spherical loose fuel particles, cylindrical fuel rods, 2 fuel pebbles
<u>Quantity</u>	- 1 Fuel Handling Unit holding RERTR IFM and 1 Fuel Handling Unit holding HTGR IFM
<u>Source of Fuel</u>	- Research reactors, commercial LWR reactors
<u>Transport Index</u>	- <1
<u>Maximum Activity</u>	- 3403 Ci
<u>Material Type</u>	- Tritium Producing Burnable Absorber Rods (TPBARs)
	- 3.35 W/TPBARs; 1.005 kW total ¹
	- 30 days minimum cool time
<u>Material Form</u>	- Type 316 stainless steel clad TPBARs
<u>Quantity</u>	- Up to 300 TPBARs (of which two can be prefailed)
<u>Source of Material</u>	- Commercial LWR reactors
<u>Transport Index</u>	- 22
<u>Maximum Activity</u>	- 12,800 Ci/TPBAR; 3,840,000 Ci total ¹
<u>Material Type</u>	- Tritium Producing Burnable Poison Rods (TPBARs)
	- 2.31 W/TPBAR, 127 W total
	- 90 days
<u>Material Form</u>	- Type 316 stainless steel clad TPBARs segmented for PIE
<u>Quantity</u>	- Up to 55 segmented TPBARs
<u>Source of Material</u>	- Commercial LWRs
<u>Transport Index</u>	- 22 ²
<u>Maximum Activity</u>	- 12,000 Ci/TPBAR, 665,500 Ci total

¹ Conservatively calculated for 30-day minimum cooling time. Actual minimum cooling period for thermal requirements is 90 days.

² Conservatively applied 300 TPBAR shipment transport index.

³ Conservatively evaluated at a one-year cool time and 38 watts per basket cell.

Table 5.1.1-1 Type, Form, Quantity and Potential Sources of Design Basis Fuel (cont'd)

<u>Fuel Type</u>	- PULSTAR Fuel Elements
	- 6 wt % ²³⁵ U
	- 32 grams ²³⁵ U per element
	- 45% ²³⁵ U depletion (burnup)
	- 210 W per basket decay heat (30 watts per basket cell) × 4 = 840W
	Minimum cool time from discharge of 1.5 years ³
<u>Fuel Form</u>	- Intact assemblies; intact elements in fuel rod insert; canned intact or failed elements
<u>Quantity</u>	- Up to 700 elements (25 elements per cell)
<u>Sources of Fuel</u>	- Research reactors
<u>Transport Index</u>	- 25
<u>Fuel Type</u>	- Spiral Fuel Assemblies
	- 75 wt % ²³⁵ U, maximum burnup variable up to 70% ²³⁵ U depletion
	- 18 W per assembly , 126 W per basket (at given cool time and burnup limits, maximum heat load is 15.7 W per assembly or 110 W per basket)
	Variable cool time down to 270 days using the procedure in Section 7.1.4 for 18 W DIDO MEU fuel
<u>Fuel Form</u>	- Intact aluminum clad fuel plates within concentric aluminum inner and outer shells
<u>Quantity</u>	- Up to 42 fuel assemblies
<u>Sources of Fuel</u>	- Research reactors
<u>Transport Index</u>	- 40.1 (applied bounding MEU DIDO limit)
<u>Fuel Type</u>	- MOATA Plate Bundles
	- 80 wt % ²³⁵ U, maximum burnup variable up to a 30,000 MWd/MTU or 4.1% ²³⁵ U depletion
<u>Fuel Form</u>	- Intact aluminum-clad fuel plates
<u>Quantity</u>	- Up to 42 bundles
<u>Sources of Fuel</u>	- Research reactors
<u>Transport Index</u>	- 40.1 (applied bounding MEU DIDO limit)
<u>Fuel Type</u>	- PWR MOX or UO ₂ rods
	- 5.0 wt % maximum ²³⁵ U initial enrichment for UO ₂ rods
	7.0 wt % fissile Pu for MOX rods
	- 62,500 MWd/MTHM maximum average burnup
	- 2.3 kW/cask maximum decay heat
	- Minimum cool time 90 days (120 days for Power Grade MOX)
<u>Fuel Form</u>	- Undamaged rods in a rod holder
<u>Quantity</u>	- Up to 16 (any combination of UO ₂ or MOX fuel rods)
<u>Source of Fuel</u>	- Commercial PWR nuclear power reactor
<u>Transport Index</u>	- 28

Table 5.1.1-2 Design Basis Fuel for Shielding Evaluation

Parameter	PWR	BWR	Metallic	MTR (HEU)	MTR (MEU)	MTR (LEU)	DIDO
Assembly Array	15 x 15	7 x 7	N/A	Parallel Plates	Parallel Plates	Parallel Plates	Fuel Tubes
Assembly or Element Weight (lbs)	1650	750	1805 (15 rods)	13.0 (max)	13.0 (max)	13.0 (max)	15.0 (max)
Assembly/Element/Rod Length (in)	162	176	120.5	25.23 ⁵	26.14 ⁵	26.14 ⁵	24.6
Active Fuel Length (in)	144	144	120.0	24.80	25.59	25.59	23.6
No. Rods per Assembly	204	49	N/A	N/A	N/A	N/A	N/A
No. of Plates per Element	N/A	N/A	N/A	23	23	23	4
Fuel Rod Diameter/Plate Thickness (in)	0.422	0.563	1.36	0.050	0.050	0.050	0.059
Clad Material	Zr-4	Zr-4	Al	Al	Al	Al	Al
Clad Thickness (in)	0.0243	0.032	0.080	0.0150	0.0150	0.0150	0.0167
Pellet Diameter/Meat Thickness (in)	0.3659	0.487	1.36	0.020	0.020	0.020	0.026
Fuel Material	UO ₂	UO ₂	U metal	U ₃ O ₈ -Al; U-Al; or U ₃ Si ₂ -Al	U ₃ O ₈ -Al; U-Al; or U ₃ Si ₂ -Al	U ₃ O ₈ -Al; U-Al; or U ₃ Si ₂ -Al	U ₃ O ₈ -Al; U-Al; or U ₃ Si ₂ -Al
Percent Theoretical Density	95	95	100	N/A	N/A	N/A	N/A
Enrichment (wt % ²³⁵ U)	3.7	4.0	Natural	90 ⁸	40 ⁸	19 ⁸	90 (HEU) 400 (MEU) 199 (LEU)
Maximum Average Burnup (MWd/MTU)	35,000	30,000	1,600	Variable up to 660,000 ^{2,9}	Variable up to 293,300 ²	Variable up to 139,300 ²	Variable up to 577,460 (HEU) 256,650 (MEU) 121,910 (LEU)
Minimum Cool Time	2 Years	2 Years	1 Year	Variable down to 90 days ²	Variable down to 90 days ²	Variable down to 90 days ²	Variable down to 180 days ¹⁰
U Weight (kg/assembly)	475	198	N/A	N/A	N/A	N/A	N/A
U Weight (kg/element)	N/A	N/A	54.5	0.422 0.511	0.950	2.4737 3.3684	0.2111 (HEU) 0.4750 (MEU) 1.0000 (LEU)
UO ₂ Weight (kg/assembly)	538.9	224.3	N/A	N/A	N/A	N/A	N/A

Notes:

1. Up to 2 of the PWR rods may have a maximum average burnup of 65,000 MWd/MTU.
2. Variable cool time down to 90 days using the procedure in Section 7.1.4.
3. Design Basis normal condition source term is for ACPR fuel with 86,100 MWd/MTU (50% ²³⁵U depletion) and accident condition source term is for FLIP-LEU-II with 151,100 MWd/MTU (80% ²³⁵U depletion).
4. Detailed fuel data is presented in Tables 1.2-1 and 6.2.5-1. The values presented here are the physical values for the bounding source terms of the ACPR and FLIP-LEU-II fuel types.
5. For MTR fuel assemblies, which are cut to remove non-fuel bearing hardware prior to transport, a nominal 0.28 inch of non-fuel hardware will remain above and below the active fuel region to allow for fuel handling operations
6. Minimum cool time varies with burnup such that maximum decay heat is 1.875 watts/rod.
7. Varies with burnup – see Table 5.3.8-29.
8. For the shielding evaluation, lower values are conservatively assumed.
9. Maximum burnup of 660,000 MWd/MTU for 380 g ²³⁵U and 577,500 MWd/MTU for 460 g ²³⁵U.
10. Variable cool time down to 180 days using the procedure in Section 7.1.4.

Table 5.1.1-2 Design Basis Fuel for Shielding Evaluation (continued)

Parameter	PWR Rods	High B/U PWR Rods	High B/U BWR Rods	PWR MOX/UO ₂ Rods	TRIGA ⁴	TRIGA Fuel Cluster Rods	TPBARs
Assembly Array	N/A	N/A	N/A	N/A	N/A	N/A	N/A
Assembly or Element Weight (lbs)	N/A	N/A	N/A	N/A	8.82 (nominal) 13.2 (max)		2.655
Assembly/Element/Rod Length (in)	162	162	176.1	162	45	31.0	153.035 (pre-irradiation)
Active Fuel Length (in)	144	150	150	153.5	15	22.5	N/A
No. Rods per Assembly per Shipment	25	25	25	16	1	1	300 Production or 55 Segmented
No. of Plates per Element	N/A	N/A	N/A	N/A	N/A	N/A	N/A
Fuel Rod Diameter/Plate Thickness (in)	0.422	0.440	0.570 (7×7) 0.4961 (other)	0.440	1.478	0.542	0.381
Clad Material	Zr-4	Zr-4	Zr-2	Zirc Alloy	304SS	Incoloy 800	316 SS
Clad Thickness (in)	0.242	0.026	0.036 (7×7) 0.0343 (other)	0.026	0.02	0.016	0.0225
Pellet Diameter/Meat Thickness (in)	0.3659	0.3805	0.4900 (7×7) 0.4213 (other)	0.3805	1.435 (max)	0.510	N/A
Fuel Material	UO ₂	UO ₂	UO ₂	UO ₂ – PuO ₂ / UO ₂	U-ZrH	U-ZrH	N/A
Percent Theoretical Density	97	95	95	95	95	95	N/A
Enrichment (wt % ²³⁵ U)	5.0	5.0	5.0	5.0 (UO ₂) 7.0 fissile Pu (MOX))	20	93.3	N/A
Maximum Average Burnup (MWd/MTHM)	60,000 ¹	80,000	60,000 – 80,000	62,500	ACPR 86,100 (50% ²³⁵ U) ³ FLIP-LEU-II 151,100 (80% ²³⁵ U) ³	Variable up to 600,000	N/A
Minimum Cool Time	150 days	150 days	Varies with burnup ⁷	90 days (Power Grade MOX – 120 days)	ACPR 231 days FLIP-LEU-II 908 days	Varies with burnup ⁶	30 days for production TPBAR; 90 days for PIE TPBAR
U Weight (kg/assembly)	58.2	65.6	108.8 (7×7) 91.3 (other)	N/A	N/A	N/A	N/A
HM Weight (kg/element)	N/A	N/A	N/A	2.63 ¹¹	ACPR 0.280 FLIP-LEU-II 0.824	0.0452	N/A
UO ₂ Weight (kg/assembly)	66.0	66.0	74.5	N/A	N/A	N/A	N/A

Notes:

- Up to 2 of the PWR rods may have a maximum average burnup of 65,000 MWd/MTU.
- Variable cool time down to 90 days using the procedure in Section 7.1.4.
- Design Basis normal condition source term is for ACPR fuel with 86,100 MWd/MTU (50% ²³⁵U depletion) and accident condition source term is for FLIP-LEU-II with 151,100 MWd/MTU (80% ²³⁵U depletion).
- Detailed fuel data is presented in Tables 1.2-1 and 6.2.5-1. The values presented here are the physical values for the bounding source terms of the ACPR and FLIP-LEU-II fuel types.
- For MTR fuel assemblies, which are cut to remove nonfuel-bearing hardware prior to transport, a nominal 0.28 inch of nonfuel hardware will remain above and below the active fuel region to allow for fuel handling operations.
- Minimum cool time varies with burnup such that maximum decay heat is 1.875 watts/rod.
- Varies with burnup – see Table 5.3.8-29.
- For the shielding evaluation, lower values are conservatively assumed.
- Maximum burnup of 660,000 MWd/MTU for 380 g ²³⁵U and 577,500 MWd/MTU for 460 g ²³⁵U.
- Variable cool time down to 180 days using the procedure in Section 7.1.4.
- Heavy metal weight per rod.

Table 5.1.1-2 Design Basis Fuel for Shielding Evaluation (continued)

Parameter	GA IFM RERTR	GA IFM HTGR	PULSTAR Fuel	Spiral Fuel Assembly	MOATA Plate Bundle
Assembly Array	N/A	N/A	5x5	Spiral Plates	Parallel Plates
Assembly or Element Weight (lbs)	23.73	23.52	45 (assembly); 1.3 (element)	7.9	13.6 ¹²
Assembly/Element/Rod Length (in)	29.92	N/A	38 (assembly) 26.2 (element)	63.5 cm	58.4 cm ¹³
Active Fuel Length (in)	22.05	N/A	24.1	60.325 cm	58.4 cm
No. Rods per Assembly	13 intact; 7 sectioned	N/A	25	N/A	N/A
No. of Plates per Element	N/A	N/A	N/A	10	Maximum 14
Fuel Rod Diameter/Plate Thickness (in)	0.543	N/A	0.47	0.147 cm	0.203 cm
Clad Material	Incoloy	N/A	Zirconium alloy	Al	Al
Clad Thickness (in)	0.031	N/A	0.0185	0.043 cm	N/A
Pellet Diameter/Meat Thickness (in)	0.512	N/A	0.423	0.061 cm	0.1016 cm
Fuel Material	U-ZrH	UC ₂ ; UCO; UO ₂ ; (Th,U)C ₂ ; or (Th,U)O ₂	UO ₂	U-Al	U-Al
Percent Theoretical Density	N/A	N/A	94.9% (nominal); 99.5% (analyzed)	N/A	N/A
Enrichment (wt % ²³⁵ U)	19.7	93.15 (maximum)	6	75	80
Maximum Average Burnup (MWd/MTU)	N/A	N/A	45	70% ²³⁵ U depletion	30,000 MWd/MTU 4.1% ²³⁵ U depletion
Minimum Cool Time	None	None	1.0 Year	see MEU DIDO	10 yr
U Weight (kg/assembly)	8.49	0.45	13.33	0.213 ¹⁴	0.4375 ¹⁵
U Weight (kg/element)	0.42	N/A	0.53	0.0213 ¹⁶	0.03125 ¹⁷
UO ₂ Weight (kg/assembly)	N/A	N/A	15.13	N/A	N/A

Notes: (cont'd)

12. For 14-fuel plate bundle.
13. Not available for in-core configuration. Analysis input restricted to active fuel length.
14. Based on a 160 g ²³⁵U fissile material load and listed enrichment.
15. Based on fuel mass per plate multiplied by 14 plates.
16. Based on 10 plates per assembly.
17. Based on 25 g ²³⁵U and listed enrichment.

Table 5.1.1-3 Nuclear and Thermal Source Parameters

Payload	Decay Heat (kW)	Gamma Source (MeV/sec) (g/sec)	Neutron Source (n/sec)	Top End-Fitting (g/sec)	Bottom End-Fitting (g/sec)
1 PWR Assembly	2.5	7.78E+15 1.27E+16	2.21E+08	1.49E+13	1.25E+13
2 BWR Assemblies	2.2	6.35E+15 1.04E+16	1.34E+08	1.16E+12	2.78E+12
15 Sound Metallic Fuel Rods ²	0.532	8.81E+14 4.37E+15	1.61E+05	N/A	N/A
6 Failed Metallic Fuel Rods ¹	0.03	3.53E+14 1.75E+15	6.44E+04	N/A	N/A
42 HEU MTR Elements ^{3,9}	1.26	-- 7.42E+15	1.40E+08	N/A ¹⁵	N/A ¹⁵
42 MEU MTR Elements ^{3,8}	1.26	-- 7.86E+15	2.88E+07	N/A ¹⁵	N/A ¹⁵
42 LEU MTR Elements ^{3,8,14}	1.26	-- 7.51E+15	3.96E+07	N/A ¹⁵	N/A ¹⁵
42 DIDO Assemblies ¹⁰	1.05	-- 6.07E+15	9.73E+04	N/A	N/A
25 PWR Rods ²	1.41	3.47E+15 8.39E+15	1.40E+08	N/A	N/A
TRIGA (140 Elements) ⁷ Normal Condition	1.05	2.15E+15 ⁴ 6.52E+15 ⁴	1.57E+06	Note 6	Note 6
TRIGA (140 Elements) ⁷ Accident Condition	1.05	2.60E+15 ⁵ 5.97E+15 ⁵	1.06E+08	Note 6	Note 6
General Atomics Irradiated Fuel Material	0.013	-- 3.429E+13	1.279E+04	Note 11	Note 11
300 Production TPBARs	1.005	5.030E+15 6.681E+15	N/A	N/A	N/A
55 PIE TPBARs	0.127	-- 7.54E+14	N/A	N/A	N/A
PULSTAR Fuel	1.05 ¹²	6.206E+15	2.115E+07	N/A	N/A
Spiral Fuel Assembly ¹³	0.756	--- 1.07E +14	4.54E+3	N/A	N/A
MOATA Plate Bundle	0.042	--- 2.2E +12	< 1E+3	N/A	N/A
16 PWR MOX Rods	2.3	1.14E+16	1.17E+09	N/A	N/A

Notes:

- Gamma and neutron source terms conservatively calculated based on design basis sound metallic fuel rods.
- 23 rods with 60,000 MWd/MTU burnup and two rods with 65,000 MWd/MTU burnup. Source terms as a function of cool time for the 80,000 MWd/MTU burnup PWR and BWR rods are presented in Section 5.3.8.
- Bounding values of the gamma and neutron source terms presented for 30W uniform loading for 80% burnup.
- Based on TRIGA ACPR fuel (86,100 MWd/MTU, 231 days cooling, 50% ²³⁵U depletion).
- Based on TRIGA FLIP-LEU-II fuel (151,100 MWd/MTU, 908 days cooling, 80% ²³⁵U depletion).
- Total hardware gamma is 7.64E+14 gamma/second for ACPR fuel (86,100 MWd/MTU, 231 days cooling, 50% ²³⁵U depletion).
- TRIGA Fuel Elements are the bounding values used in dose determination for TRIGA cluster rods fuel type.
- Moderator used is light water, H₂O.
- Moderator used is heavy water, D₂O.
- Bounding values of the gamma and neutron source terms presented for 25W uniform loading for 70% burnup HEU fuel.
- Hardware activation, including end-fitting sources, for the TRIGA elements included in the total gamma source for GA IFM.
- Cool time required to meet 30 watt per cell heat load limit is 1.5 years.
- Based on 18 W per assembly heat load.
- Fuel source represents maximum magnitude gamma source obtained from the 470 g ²³⁵U analysis, and the maximum neutron source obtained from the 640 g ²³⁵U analysis.
- A maximum 100 grams of cadmium may be included as part of the MTR fuel element or plate construction. Activation of the cadmium produces no significant source per Section 5.3.4.

Table 5.1.1-4 Combined Dose Rates for Normal Operations Conditions

(1 PWR assembly, 35,000 MWd/MTU, 2-year cool time)

Location	Detector I.D.	Radiation	Normal Dose Rate (mrem/hr)
Radial at 2 m from personnel barrier, Fuel midplane	1	Neutron	1.25
		Secondary Gamma	0.18
		Primary Gamma	<u>6.71</u>
		TOTAL	8.14
Radial surface, Fuel midplane	2	Neutron	6.53
		Secondary Gamma	1.37
		Primary Gamma	<u>43.44</u>
		TOTAL	51.34
Bottom surface, Axial centerline	3	Neutron	0.33
		Primary Gamma	35.51
		End-fitting Gamma	<u>17.02</u>
		TOTAL	52.86
Bottom at 2 m from impact limiter, Axial centerline	4	Neutron	0.03
		Primary Gamma	2.19
		End-fitting Gamma	<u>0.79</u>
		TOTAL	3.01
Top surface, Axial centerline	5	Neutron	0.12
		Primary Gamma	54.17
		End-fitting Gamma	<u>41.45</u>
		TOTAL	95.74
Top at 2 m from impact limiter, Axial centerline	6	Neutron	0.01
		Primary Gamma	3.82
		End-fitting Gamma	<u>2.17</u>
		TOTAL	6.00
Top at Cab	7	Neutron	0.00135
		Primary Gamma	0.47
		End-fitting Gamma	<u>0.25</u>
		TOTAL	0.72

Table 5.1.1-5 Hypothetical Accident – Loss of Shielding Materials

(1 PWR assembly, 35,000 MWd/MTU, 2-year cool time)

Location	Detector I.D.	Radiation	Normal Dose Rate (mrem/hr)
Radial surface, Fuel midplane, With neutron shield	8	Neutron	6.53
		Secondary Gamma	1.37
		Primary Gamma	<u>43.44</u>
		TOTAL	51.34
Radial surface, Fuel midplane, Without neutron shield	9	Neutron	177.13
		Secondary Gamma	0.39
		Primary Gamma	<u>75.00</u>
		TOTAL	252.52
Radial at 1 m from surface, Fuel midplane, Without neutron shield	10	Neutron	50.93
		Secondary Gamma	1.52
		Primary Gamma	<u>54.59</u>
		TOTAL	107.04

Table 5.1.1-6 Hypothetical Accident –Lead Slump

Location	Detector I.D.	Radiation	Normal Dose Rate (mrem/hr)
Radial at 1 m from surface, PWR top end-fitting	11	End-fitting Gamma	3.60
		TOTAL	3.60
Radial at 1 m from surface, PWR top end-fitting	12	End-fitting Gamma	1.31
		TOTAL	1.31
Radial at 1 m from surface, PWR top end-fitting	13	End-fitting Gamma	0.80
		TOTAL	0.80
Radial at 1 m from surface, PWR bottom end-fitting	14	End-fitting Gamma	0.01
		TOTAL	0.01
Radial at 1 m from surface, PWR bottom end-fitting	15	End-fitting Gamma	0.35
		TOTAL	0.35
Radial at 1 m from surface, PWR bottom end-fitting	16	End-fitting Gamma	1.48
		TOTAL	1.48
Radial at 1 m from surface, BWR bottom end-fitting	17	End-fitting Gamma	0.10
		TOTAL	0.10
Radial at 1 m from surface, BWR bottom end-fitting	18	End-fitting Gamma	0.54
		TOTAL	0.54
Radial at 1 m from surface, BWR bottom end-fitting	19	End-fitting Gamma	0.84
		TOTAL	0.84

5.3.18 PWR MOX Rod Fuel Configuration

Results of a shielding and decay heat analysis for up to 16 high burnup PWR MOX fuel rods are presented in this section. The rods are conservatively evaluated with burnups up to 70 GWd/MTHM. MOX rods are limited in this licensing application to a burnup of 62.5 GWd/MTHM. The results are presented in terms of the cool time required for 16 rods to meet the cask total payload heat load limit of 2.3 kW established for PWR rods (including MOX rods). At this cool time, the package surface and 2-meter dose rate are calculated and shown to be below limits.

The shielding analysis is performed using the three-dimensional MCNP transport code. Source terms are generated based on a limiting description of PWR rods using the SCALE 5.0 SAS2H code. The limiting description of a PWR MOX fuel rod bounds MOX rods from all PWR assembly array sizes. Analyses compare various MOX plutonium compositions and the inclusion of UO₂ fuel rods (up to 80 GWd/MTHM burnup) to demonstrate licensing compliance for up to 16 MOX rods or UO₂ rods in any combination.

5.3.18.1 PWR MOX Rod Fuel Source Term

Source Term

Source terms are generated in a manner similar to those of the PWR rods described in Section 5.3.8. The limiting rod description is determined by developing a hybrid fuel rod model, which contains a conservatively bounding heavy metal loading. For a given burnup, the bounding heavy metal mass leads to bounding decay heat and radiation source terms. Fuel rod model parameters are shown in Table 5.3.18-1 in the "SAS2H" column. SAS2H models for the various MOX and UO₂ compositions are then developed based on the cycle parameters shown in Table 5.3.18-2. The rod exposure is conservatively assumed to occur over a typical number of reactor operating cycles: three for the PWR MOX rods. A down time of 60 days between cycles is assumed. Fuel rods are evaluated at an initial enrichment between 2 and 7 wt % ²³⁵U for the UO₂ rods and between 2 and 7 wt % fissile plutonium for the four MOX fuel compositions shown in Table 5.3.18-3. Based on these compositions and the range of fissile plutonium contents analyzed, the resulting fractions of uranium and plutonium in the SAS2H fuel mixture are shown in Table 5.3.18-4. A sample SAS2H model for the MOX Services plutonium composition is shown in Figure 5.3.18-1. The SAS2H model adjusts the weight fractions in Table 5.3.18-4 by the modeled theoretical density factor shown in Table 5.3.18-1.

The SCALE 44-group library is employed in the source generation. For use in the MCNP shielding analysis, the gamma and neutron sources are rebinned within ORIGEN-S into the group

structure of the ANSWERS MCBEND code package. Gamma energy lines in this structure better reflect the gamma source lines around 1 MeV than the default energy lines generated by ORIGEN-S.

Neutron and gamma sources and heat loads are summarized for the various compositions in Table 5.3.18-7. As the fissile plutonium content increases, heat loads increase and neutron source decreases. Minimum cool times required for the fuel rods to reach the maximum allowed heat load of 143.75 W/rod (2.3 kW/16 rods) are included in Table 5.3.18-8. The minimum cool time evaluated in the source term generation was 90 days. Therefore, any results indicating a less than 90-day cool time is permissible are listed as "< 90." The only evaluated material exceeding 90 days as the required cool time is Power Grade (low grade plutonium with a significant quantity of ^{240}Pu and ^{242}Pu). A minimum 120-day cool time for the Power Grade material ensures that heat load limits are met. For conservatism, shielding evaluations include the Power Grade material at 90 days' cool time source terms. Neutron and gamma source term spectra for a Power Grade MOX composition at the maximum burnup (70 GWd/MTHM), a 2% fissile plutonium content, and a cool time of 90 days are presented in Table 5.3.18-9 and Table 5.3.18-10, respectively.

The effect of subcritical neutron multiplication is directly computed in the MCNP analysis. As the k_{eff} of a dry transport configuration is extremely low ($k_{\text{eff}} < 0.1$), there is no significant subcritical multiplication in the system regardless of material composition. Comparison of k_{eff} as a function of fuel composition is included in Section 5.3.18.3. To simplify the analysis, all shielding results, with the exception of the subcritical multiplication studies, are based on using a standard uranium oxide fuel composition.

Axial Source Profile

The description of the axial source profile for PWR rods is based on bounding axial burnup profiles observed for fuel at much lower burnups. This description is conservative because the higher burned fuel of interest here will have a substantially lower axial peaking factor. The PWR axial source profiles are shown in Figure 5.3.18-2. Values are tabulated in Table 5.3.18-5.

The computed relation between source rate S and burnup B:

$$S = aB^b$$

implies that, in general, the average source rate is not equal to the source rate at the average burnup. The exponent b is determined based on SAS2H analyses of various fuel assemblies at different burnups. A value of 4.22 is used for neutron source rate variation. The exponent for photon source rates has been determined to be 1.0.

Since SAS2H analyses are conducted at the average assembly burnup, a scale factor is required to relate the assembly average source rate to the source rate at the average burnup:

$$r = \frac{\bar{S}}{S(\bar{B})} = \frac{\int B^b dz}{a\bar{B}^b}$$

With the burnup profile normalized to one, this becomes

$$r = \frac{1}{H} \int B^b dz$$

where H is the height of the fuel region.

The integral is evaluated numerically using the trapezoid rule, and the resulting scale factors are shown in Table 5.3.18-6. Because MCNP normalizes the axial source profile by default, the scale factors are included in the MCNP runs in the tally multiplier cards.

5.3.18.2 MOX Fuel Shielding Model

MCNP three-dimensional shielding analysis allows detailed modeling of the fuel, canister, basket, and cask shield configurations. The fuel rod lattice (5×5 array of tubes containing up to 16 fuel rods) detail is conservatively omitted in the model. The remaining principal canister components and all shielding-related basket and cask body details are explicitly modeled, including the axial extents described by the applicable License Drawings.

The geometric description of a MCNP model is based on the combinatorial geometry system embedded in the code. In this system, bodies such as cylinders and rectangular parallelepipeds, and their logical intersections and unions, are used to describe the extent of material zones.

Source Models

The combination of 16 fuel rods, either UO₂ or MOX fissile material based, are loaded into a 5×5 tube array insert constructed from stainless steel. The insert in turn is located within a canister, placed into the LWT PWR basket insert. The 16 fuel rods are homogenized within the cross sectional area of the canister internal spacer. No credit is taken for the stainless steel tubes in the fuel rod homogenization. While the array may contain additional material in the form of burnable poison rods (or other non-steel/inconel-based materials), these materials are not included in the homogenization and are not included as a source region as they are considered to have negligible activation when compared to the short cool time fuel source. Axial regions (elevations) are retained for the active fuel region, plenum region, and rod end-caps. The plenum region is modeled as a void for shielding purposes.

To minimize self-shielding, the MCNP fuel rod model has significantly less mass than the fuel rod model used to generate MOX source terms. Fuel rod parameters for this model are shown in Table 5.3.18-1 in the "MCNP" column. This column includes the axial extents of the active fuel, plenum and end-cap regions included in the three-dimensional model.

Canister and Basket Model

The canister model includes the steel internal spacer (represented as a steel box), steel can weldment (including can base, body and lid), the aluminum basket insert, and the aluminum PWR basket body. No credit is taken for canister internal aluminum shunts.

MCNP NAC-LWT Model

The three-dimensional model of the NAC-LWT cask is based on the following features.

Normal conditions:

- Radial neutron shield and shield shell
- Aluminum impact limiters with 0.5 g/cm^3 density (calculated based on the impact limiter weight and dimensions) and diameter equal to the neutron shield shell diameter

Accident conditions:

- Removal of radial neutron shield and shield shell
- Loss of upper and lower impact limiters

Common to both the normal and accident conditions models is a 0.1374 cm gap between the lead outer diameter and the cask outer shell. During normal conditions, the gap volume is represented as a radial uniform gap between the lead outer radius and the cask outer shell. During accident calculations, the lead is assumed to slump to form radial, top and bottom gaps. All three slump configurations are conservatively included in a single model. The use of an axial spacer prevents the fuel region source from approaching the top of the radial lead shield. Only the axial separation by the spacer is accounted for in the analysis. No credit is taken for spacer material.

Detailed model parameters used in creating the three-dimensional model are taken directly from the License Drawings. Elevations associated with the three-dimensional features are established with respect to the center bottom of the NAC-LWT cask cavity for the MCNP combinatorial model. The three-dimensional NAC-LWT models are shown in Figure 5.3.18-3 and Figure 5.3.18-4. A sample input file is provided in Figure 5.3.18-5. The sample input provides a complete source description used in the response function benchmark analysis.

Shield Regional Densities

Based on the homogenization described previously, fuel region material densities are shown in Table 5.3.18-11. The fuel region densities were conservatively calculated based on a minimum material mass fuel rod (1.62 kg HM, see Table 5.3.18-1) versus the maximum mass rod used in the source generation. Material compositions for the basket and cask materials are shown in Table 5.3.18-12.

5.3.18.3 MOX Fuel Shielding Evaluation

Calculational Methods

The shielding evaluation is performed using MCNP.

The MCNP shielding model described in Section 5.3.18.2 is utilized with the source terms described in Section 5.3.18.1 to estimate the dose rate profiles at various distances from the side, top and bottom of the cask for both normal and accident conditions. The method of solution is continuous energy Monte Carlo with a Monte Carlo based weight window generator to accelerate code convergence. Weight window and problem convergence is verified by the 10 statistical checks performed by MCNP. Radial or axial biasing is performed depending on the desired dose location.

Significant validation literature is available for MCNP as it is an industry standard tool for spent fuel cask evaluations. Available literature covers a range of shielding penetration problems ranging from slab geometry to spent fuel cask geometries. Confirmatory calculations against other validated shielding codes (SCALE and MCBEND) on NAC casks have further validated the use of MCNP for shielding evaluations.

MCNP Flux-to-Dose Conversion Factors

The ANSI/ANS 6.1.1-1977 flux-to-dose rate conversion factors are employed in the MCNP analysis. The ANSI/ANS neutron and gamma dose conversion factors are shown in Table 5.3.11-23 and Table 5.3.11-24.

Dose Response Method

In order to avoid the significant effort required to prepare and execute shielding runs for each material composition, a unique device is employed that permits the ready calculation of dose rates at a given location by use of a dose rate response function. The dose rate response function for a given source type at a given detector location is a collection of values, one for each energy group, each of which gives the contribution to the dose rate at a specific detector location from a unit source strength in that energy group. With this response function, the dose rate, d , at the

corresponding detector location is determined for any given fuel type simply by vector multiplying the unnormalized source spectrum, f , by the response function, r .

The dose rate response function is computed by solving a series of three-dimensional cases, one for each energy group, with a unit source strength in each energy group.

Subcritical Multiplication

MCNP results documented in the dose rate section include subcritical neutron multiplication based on a 4 wt % enriched UO_2 (LEU) fuel description. To investigate potential dose increases due to a higher multiplication factor associated with MOX material, dose rates are compared for a consistent source term of 4 wt % (4 wt % ^{235}U for UO_2 and 4 wt % fissile plutonium for MOX) at 80 GWd/MTHM (note that the burnup compared is above the 70 GWd/MTHM limit for MOX fuel and produces dose rates higher than 10 mrem/hr at 2 meters). Normal condition radial surface average neutron results are compared. As shown in Table 5.3.18-13, the difference between response function runs with UO_2 subcritical multiplication and direct solution runs with MOX subcritical multiplication is negligible. Therefore, use of UO_2 subcritical multiplication response function runs is appropriate for computing MOX fuel dose rates. Furthermore, given that maximum dose rates are computed for 2 wt % fissile plutonium, the use of a 4 wt % ^{235}U subcritical multiplication is conservative.

Three-Dimensional Dose Rates for MOX Fuel

Dose rates are generated at the bounding 90-day minimum cool time for the various MOX plutonium compositions (and UO_2 fuel) at 2 percent fissile fuel material. Dose summaries for key conditions are listed in Table 5.3.18-14. As indicated by the source term magnitude and bounding heat load, the Power Grade MOX fuel produces bounding dose rates.

A summary of the maximum and average dose rates for the bounding power grade MOX fuel is shown in Table 5.3.18-15. All dose rates are below 10 CFR 71 limits. High uncertainties in the axial results are associated with the difficulty in axial biasing for a cask with a large ratio of length to diameter. Because dose rates in the axial locations are significantly below limits, no attempt is made to reduce the uncertainty in the results.

The axial elevation of the maximum cask surface and 2 meter dose rates are at the active fuel region midplane elevation. The cask surface dose rate profile is shown in Figure 5.3.18-6, with the 2 meter profile plotted in Figure 5.3.18-7. The normal condition maximum radial 2 meter dose rate is 9.2 mrem/hr. Accident condition radial 1 meter dose rates are well below the 1000 mrem/hr limit, with the radial 1 meter dose profile shown in Figure 5.3.18-8. The transport index (TI) for the MOX rod shipments is 28 based on the 1 meter normal condition dose rate.

Table 5.3.18-14 demonstrates that dose rate results for UO₂ (LEU) fuel at 80 GWd/MTHM are bounded by the results for the bounding Power Grade MOX fuel at 70 GWd/MTHM. Therefore, a mixed loading of UO₂ and MOX fuel rods is an acceptable payload for the NAC-LWT cask.

Figure 5.3.18-1 Sample SAS2H Input for PWR MOX Fuel

```
=SAS2H      PARM=(HALT06,SKIPSHIPDATA)
Power Grade, 2% Fissile, 70 Gwd/MTHM, 90-150 days cooled
44GROUPNDF5 LATTICECELL
UO2         1 0.9254 811 92235 0.2 92238 99.8 END
PuO2        1 0.0246 811 94238 1 94239 62 94240 22 94241 12 94242 3 END
ZR          2 1.0 620 END
H2O         3 DEN=0.725 1.0 570 END
ARBM-BORMOD 0.725 1 1 0 0 5000 100 3 550.0E-6 570 END
END COMP
SQUAREPITCH 1.473 0.9665 1 3 1.118 2 0.986 0 END
NPIN/ASSM=176 FUELENGTH=389.9 NCYCLE=3 NLIB/CYC=2 PRINTLEVEL=6
LIGH=5 INPLEVEL=2 NUMZONES=4 END
3 1.3589 2 1.4605 3 1.6623 500 5.2039
POWER=19.36 BURN=556.8 DOWN=60 END
POWER=19.36 BURN=556.8 DOWN=60 END
POWER=19.36 BURN=556.8 DOWN=0 END
FE 0.6738 CR 0.1900 NI 0.1150 MN 0.0200 CO 0.0012
END
=ORIGENS
0$$ A4 21 A8 26 A10 51 71 E
1$$ 1 1T
COOLING 90 TO 150 DAYS AND FISSION PRODUCT GAMMA REBIN
3$$ 21 0.1 28 A33 22 E
54$$ A8 1 E T
35$$ 0 T
56$$ 0 7 A13 -2 4 3 E
57** 0.0 E T
COOLING 90 TO 150 DAYS AND FISSION PRODUCT GAMMA REBIN
SINGLE REACTOR ASSEMBLY
60** 90 100 110 120 130 140 150
65$$ A4 1 A7 1 A10 1 A25 1 A28 1 A31 1 A46 1 A49 1 A52 1 E
61** F.00000001
81$$ 2 51 26 1 E
82$$ F6
83** 1.40e+7 1.20e+7 1.00e+7 8.00e+6 6.50e+6 5.00e+6
      4.00e+6 3.00e+6 2.50e+6 2.00e+6 1.66e+6 1.44e+6
      1.22e+6 1.00e+6 0.80e+6 0.60e+6 0.40e+6 0.30e+6
      0.20e+6 0.10e+6 0.05e+6 0.02e+6 0.01e+6
84** 1.46e+7 1.36e+7 1.25e+7 1.125e+7 1.00e+7
      8.25e+6 7.00e+6 6.07e+6 4.72e+6 3.68e+6
      2.87e+6 1.74e+6 0.64e+6 0.39e+6 0.11e+6
      6.74e+4 2.48e+4 9.12e+3 2.95e+3 9.61e+2
      3.54e+2 1.66e+2 4.81e+1 1.60e+1 4.00e+0
      1.50e+0 5.50e-1 7.09e-2 1.00e-5 T
56$$ F0 T
END
```

Note: Only the fission product rebin section of the input file is shown. Identical rebins are performed for the actinide and light element sources.

Figure 5.3.18-2 PWR Rods Axial Burnup and Source Profiles

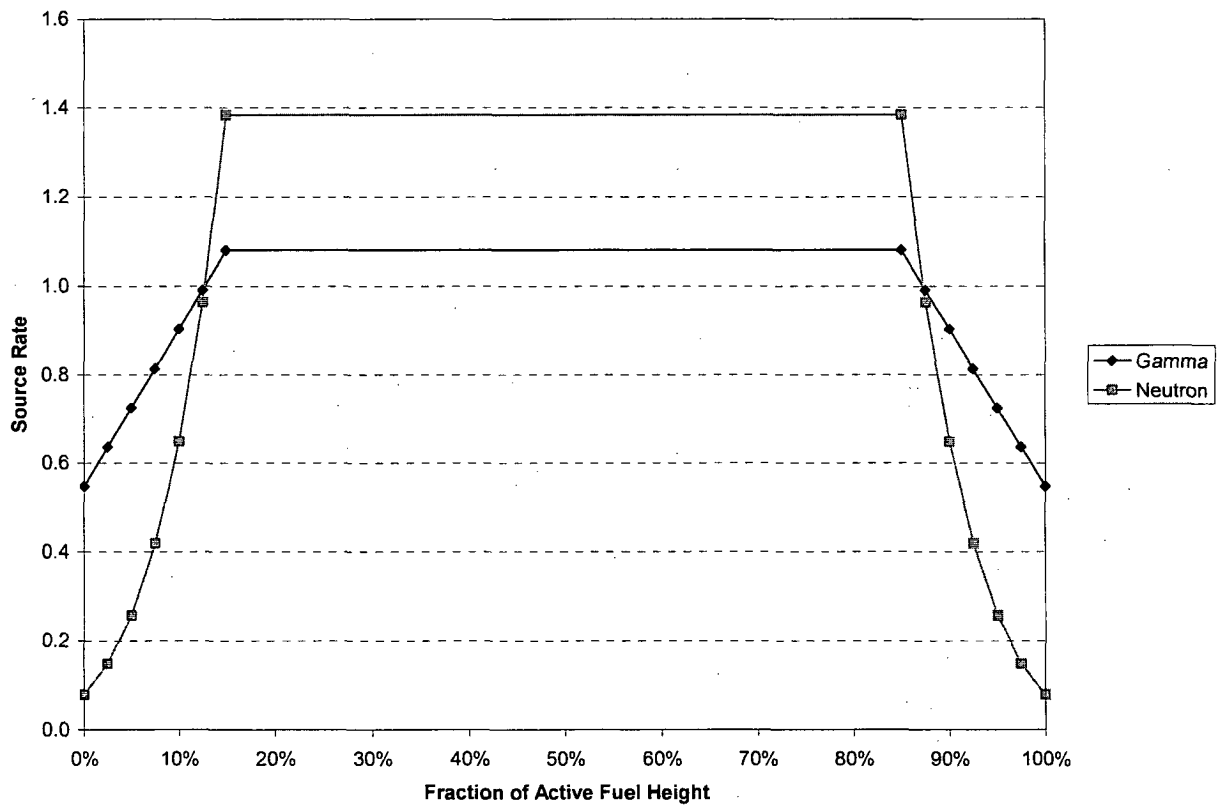
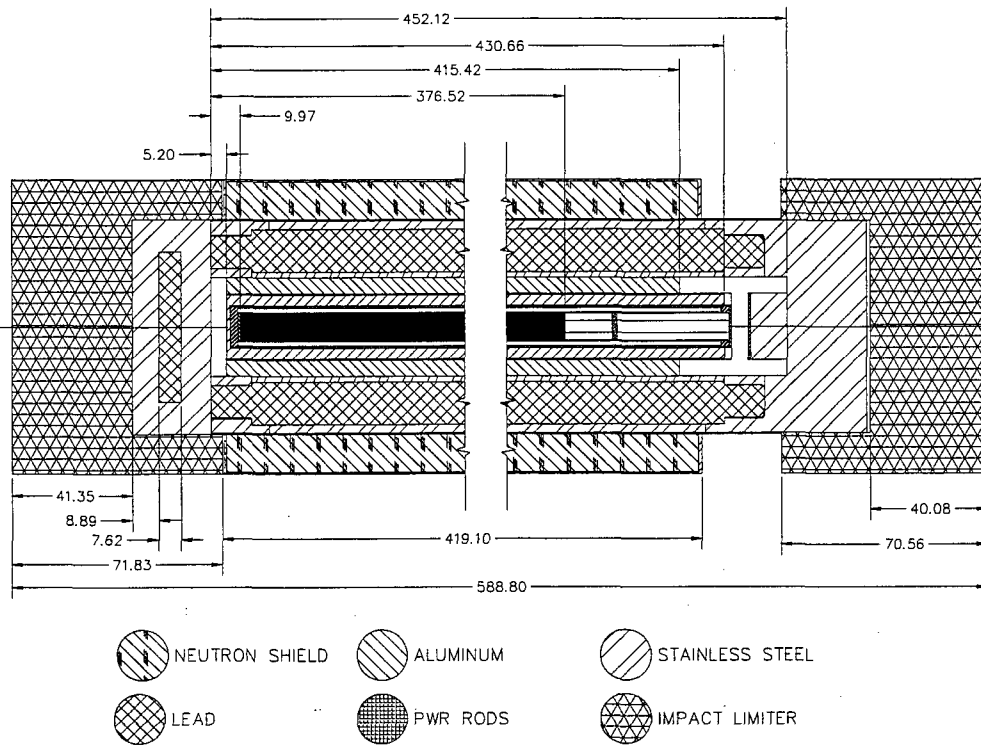
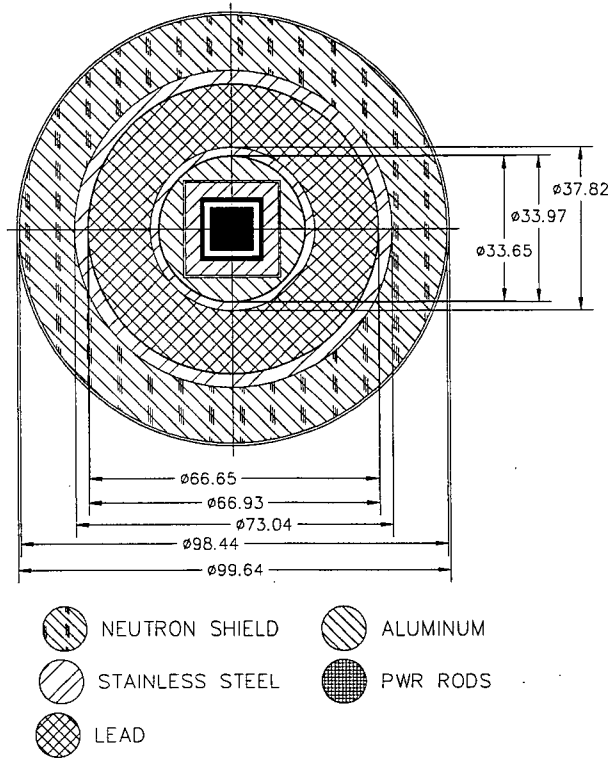


Figure 5.3.18-3 MCNP Model of NAC-LWT with PWR MOX Fuel – Axial Detail

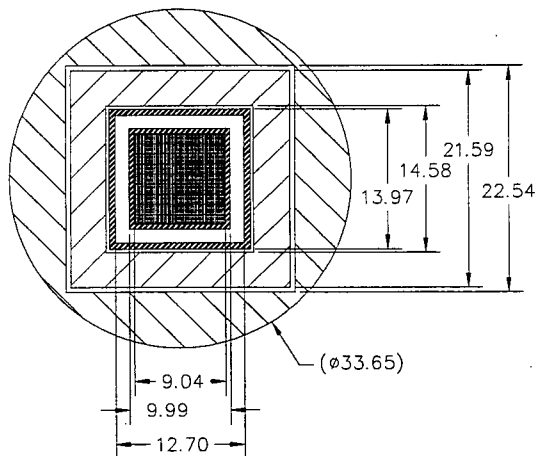


Note: Dimensions in cm

Figure 5.3.18-4 MCNP Model of NAC-LWT with PWR MOX Fuel – Radial Detail



Cask Cavity Detail:



Note: Dimensions in cm.

Figure 5.3.18-5 Sample MCNP Input File for PWR MOX Fuel
(Response Method Benchmark Case)

```
NAC-LWT Cask - wel7_leu_80b40e150d - Normal Transport Conditions
C Radial Biasing - Fuel Gamma Source
C 16 Rod Source & WE17x17 Fuel Homogenization
C Homogenized Rod Cells
1 2 -0.8430 -1 u=6 $ Bottom end cap
2 1 -1.2338 -2 +1 u=6 $ Fuel
3 0 -3 +2 u=6 $ Plenum
4 2 -0.8430 -4 +3 u=6 $ Top end cap
5 0 +4 u=6 $ Void
C Can Weldment Cells
10 0 -10 fill=6 ( 0.0000 0.0000 2.5400 ) u=5 $ Fuel Insert
11 5 -7.9400 -11 +10 u=5 $ Internal Spacer
12 0 -12 +11 +10 u=5 $ Can Weldment void
13 5 -7.9400 -13 u=5 $ Can Weldment base
14 5 -7.9400 -14 +13 +12 +10 u=5 $ Can Weldment body
15 5 -7.9400 -15 +14 +10 u=5 $ Can Weldment flange
16 5 -7.9400 -16 +15 u=5 $ Can Weldment lid
17 0 +16 u=5 $ Outside
C PWR Insert Cells
20 0 -20 fill=5 ( 0.0000 0.0000 1.2700 ) u=4 $ Can Weldment
21 7 -2.7020 -21 +20 u=4 $ PWR Insert Body
22 0 +21 +20 u=4 $ Outside
C PWR Basket Cells
30 0 -30 fill=4 ( 0.0000 0.0000 5.2070 ) u=3 $ PWR Insert
31 0 -32 -31 u=3 $ Offset
32 7 -2.7020 -32 +31 +30 u=3 $ Basket
33 0 +32 +30 u=3 $ Outside
C Cask Cavity Cells
40 0 -40 +41 fill=3 u=2 $ Cavity
41 5 -7.9400 -41 u=2 $ Spacer plate
42 0 +40 +41 u=2 $ Outside
C Cells - LWT Cask Normal Conditions
50 4 -11.344 -53 u=1 $ BotPb
51 0 -52 fill=2 u=1 $ Cavity
52 5 -7.9400 -50 -51 +53 u=1 $ Bottom
53 5 -7.9400 -50 +51 +55 +58 +52 u=1 $ OuterShell
54 5 -7.9400 -54 +57 +52 u=1 $ InnerShellTaper
55 5 -7.9400 -56 +52 u=1 $ InnerShell
56 4 -11.344 -57 +56 u=1 $ Lead
57 4 -11.344 -55 +54 +57 u=1 $ LeadTaper
58 0 -58 +57 u=1 $ LeadGap
59 3 -0.9669 -60 +50 u=1 $ NeutronShield
60 5 -7.9400 -59 +50 +60 u=1 $ NSShell
61 6 -0.4997 -61 +50 u=1 $ UpperLimiter
62 6 -0.4997 -62 +50 u=1 $ LowerLimiter
63 0 -63 +50 +59 +61 +62 u=1 $ Container
64 0 +63 u=1 $ Outside
C Detector Cells - Radial Biasing
100 0 -100 fill=1 $ Surface
150 0 -150 +100 $ SurfaceAzi
200 0 -200 +100 +150 $ 1ft
300 0 -300 +100 +150 +200 $ 1m
400 0 -400 +100 +150 +200 +300 $ 2m
500 0 -500 +100 +150 +200 +300 +400 $ 2m+Convey
600 0 +100 +150 +200 +300 +400 +500 $ Exterior

C Homogenized Rod Surfaces
1 PZ 1.7399 $ Bottom end cap
2 PZ 367.4999 $ Fuel
3 PZ 383.4003 $ Plenum
4 PZ 385.1402 $ Top end cap
C Can Weldment Surfaces
10 RPP -4.5212 4.5212 -4.5212 4.5212 2.5400 425.4500 $ Internal cavity
11 RPP -4.9975 4.9975 -4.9975 4.9975 2.5400 422.2750 $ Internal spacer
12 RPP -6.3500 6.3500 -6.3500 6.3500 2.5400 422.9100 $ Can weldment cavity
13 RPP -6.9850 6.9850 -6.9850 6.9850 0.0000 2.5400 $ Can weldment base
14 RPP -6.9850 6.9850 -6.9850 6.9850 0.0000 422.9100 $ Can weldment body
15 RPP -6.9850 6.9850 -6.9850 6.9850 0.0000 425.4500 $ Can weldment flange
16 RPP -6.9850 6.9850 -6.9850 6.9850 0.0000 426.7200 $ Can weldment lid
C PWR Insert Surfaces
20 RPP -7.2898 7.2898 -7.2898 7.2898 1.2700 427.9900 $ PWR Insert cavity
21 RPP -10.7950 10.7950 -10.7950 10.7950 0.0000 425.4500 $ PWR Insert body
C PWR Basket Surfaces
30 RPP -11.2713 11.2713 -11.2713 11.2713 5.2070 433.1970 $ Internal cavity
31 PZ 5.2070 $ Bottom offset
32 RCC 0.0000 0.0000 0.0000 0.0000 0.0000 415.4170 16.8273 $ Basket walls
C Cask Cavity Surfaces
40 RCC 0.0000 0.0000 0.0000 0.0000 0.0000 452.1199 16.9862 $ Cavity
41 RCC 0.0000 0.0000 438.7850 0.0000 0.0000 0.9525 11.1760 $ Spacer plate
C Surfaces - LWT Cask Normal Conditions
50 RCC 0.0000 0.0000 -26.6700 0.0000 0.0000 507.3650 36.5189 $ Lwt
51 RCC 0.0000 0.0000 -26.6700 0.0000 0.0000 26.6700 36.5189 $ Bottom
52 RCC 0.0000 0.0000 0.0000 0.0000 0.0000 452.1200 16.9863 $ Cavity
53 RCC 0.0000 0.0000 -17.7800 0.0000 0.0000 7.6200 26.3525 $ Bottom gamma shield
54 RCC 0.0000 0.0000 0.0000 0.0000 0.0000 444.5000 20.1740 $ Lead id - taper
55 RCC 0.0000 0.0000 0.0000 0.0000 0.0000 444.5000 31.5976 $ Lead od - taper
56 RCC 0.0000 0.0000 13.8176 0.0000 0.0000 416.8648 18.9103 $ Lead id
57 RCC 0.0000 0.0000 13.8176 0.0000 0.0000 416.8648 33.3271 $ Lead od
58 RCC 0.0000 0.0000 13.8176 0.0000 0.0000 416.8648 33.4645 $ Lead gap
59 RCC 0.0000 0.0000 3.8100 0.0000 0.0000 419.1000 49.8183 $ Neutron shield shell
60 RCC 0.0000 0.0000 5.0800 0.0000 0.0000 416.5600 49.2189 $ Neutron shield
61 RCC 0.0000 0.0000 450.2150 0.0000 0.0000 70.5612 49.8183 $ Upper limiter
62 RCC 0.0000 0.0000 -68.0212 0.0000 0.0000 71.8312 49.8183 $ Lower limiter
```

Figure 5.3.18-5 Sample MCNP Input File for PWR MOX Fuel
(Response Method Benchmark Case)

```

63 RCC 0.0000 0.0000 -68.0212 0.0000 0.0000 588.7974 49.8183 $ Container
C Radial Detector DRA (Surface)
100 RCC 0.0000 0.0000 -68.1212 0.0000 0.0000 588.9974 49.9184
101 PZ -38.6713
102 PZ -9.2215
103 PZ 20.2284
104 PZ 49.6783
105 PZ 79.1282
106 PZ 108.5780
107 PZ 138.0279
108 PZ 167.4778
109 PZ 196.9276
110 PZ 226.3775
111 PZ 255.8274
112 PZ 285.2772
113 PZ 314.7271
114 PZ 344.1770
115 PZ 373.6269
116 PZ 403.0767
117 PZ 432.5266
118 PZ 461.9765
119 PZ 491.4263
C Radial Detector DRAA (SurfaceAzi)
150 RCC 0.0000 0.0000 211.3775 0.0000 0.0000 30.0000 50.0184
151 PX 0.0000
152 1 PX 0.0000
153 2 PX 0.0000
154 3 PX 0.0000
155 4 PX 0.0000
156 5 PX 0.0000
157 6 PX 0.0000
158 7 PX 0.0000
159 8 PX 0.0000
160 PY 0.0000
161 9 PX 0.0000
162 10 PX 0.0000
163 11 PX 0.0000
164 12 PX 0.0000
165 13 PX 0.0000
166 14 PX 0.0000
167 15 PX 0.0000
168 16 PX 0.0000
C Radial Detector DRB (1ft)
200 RCC 0.0000 0.0000 -98.6012 0.0000 0.0000 649.9574 80.2984
201 PZ -66.1033
202 PZ -33.6055
203 PZ -1.1076
204 PZ 31.3903
205 PZ 63.8882
206 PZ 96.3860
207 PZ 128.8839
208 PZ 161.3818
209 PZ 193.8796
210 PZ 226.3775
211 PZ 258.8754
212 PZ 291.3732
213 PZ 323.8711
214 PZ 356.3690
215 PZ 388.8669
216 PZ 421.3647
217 PZ 453.8626
218 PZ 486.3605
219 PZ 518.8583
C Radial Detector DRC (1m)
300 RCC 0.0000 0.0000 -168.1212 0.0000 0.0000 788.9974 149.8184
301 PZ -135.2463
302 PZ -102.3714
303 PZ -69.4965
304 PZ -36.6216
305 PZ -3.7467
306 PZ 29.1282
307 PZ 62.0030
308 PZ 94.8779
309 PZ 127.7528
310 PZ 160.6277
311 PZ 193.5026
312 PZ 226.3775
313 PZ 259.2524
314 PZ 292.1273
315 PZ 325.0022
316 PZ 357.8771
317 PZ 390.7520
318 PZ 423.6269
319 PZ 456.5017
320 PZ 489.3766
321 PZ 522.2515
322 PZ 555.1264
323 PZ 588.0013
C Radial Detector DRD (2m)
400 RCC 0.0000 0.0000 -268.1212 0.0000 0.0000 988.9974 249.8184
401 PZ -226.9130
402 PZ -185.7048
403 PZ -144.4965
404 PZ -103.2883
405 PZ -62.0801
406 PZ -20.8719

```

Figure 5.3.18-5 Sample MCNP Input File for PWR MOX Fuel
(Response Method Benchmark Case)

```

407 PZ 20.3364
408 PZ 61.5446
409 PZ 102.7528
410 PZ 143.9611
411 PZ 185.1693
412 PZ 226.3775
413 PZ 267.5857
414 PZ 308.7940
415 PZ 350.0022
416 PZ 391.2104
417 PZ 432.4186
418 PZ 473.6269
419 PZ 514.8351
420 PZ 556.0433
421 PZ 597.2515
422 PZ 638.4598
423 PZ 679.6680
C Radial Detector DRE (2m+Convey)
500 RCC 0.0000 0.0000 -269.1212 0.0000 0.0000 990.9974 321.9200
501 PZ -227.8296
502 PZ -186.5381
503 PZ -145.2465
504 PZ -103.9550
505 PZ -62.6634
506 PZ -21.3719
507 PZ 19.9197
508 PZ 61.2113
509 PZ 102.5028
510 PZ 143.7944
511 PZ 185.0859
512 PZ 226.3775
513 PZ 267.6691
514 PZ 308.9606
515 PZ 350.2522
516 PZ 391.5437
517 PZ 432.8153
518 PZ 474.1269
519 PZ 515.4184
520 PZ 556.7100
521 PZ 598.0015
522 PZ 639.2931
523 PZ 680.5846

C
C Materials List
C
C Homogenized UO2 Fuel
m1 92235 -2.6740E-02
92238 -6.4177E-01
8016 -8.9904E-02
40000 -2.3730E-01
50000 -3.6238E-03
26000 -3.0198E-04
24000 -2.4158E-04
7014 -1.2079E-04
C Fuel Rod End Cap (Zircaloy)
m2 40000 -9.8225E-01
50000 -1.5000E-02
26000 -1.2500E-03
24000 -1.0000E-03
7014 -5.0000E-04
C Water/Glycol
m3 1001 -1.03651E-01
8016 -6.75619E-01
6000 -2.20730E-01
mt3 lwtr.01
C Lead
m4 82000 -1.0
C Stainless Steel 304
m5 24000 -0.190
25055 -0.020
26000 -0.695
28000 -0.095
C Aluminum (Impact Limiter)
m6 13027 -1.0
C Aluminum (Insert/Basket)
m7 13027 -1.0
phys:p 100 0 0 0 1
C
C Cell Importances
imp:p 1 43r 0
C
C Source Definition - Fuel Gamma
C LEU Basis - 80 GWD/MTM, 4 wt % Fissile, 150 days cooled
sdef x=d1 y=d2 z=d3 erg=d4 cell=100:51:40:30:20:10:2
si1 -4.5212 4.5212
sp1 0 1
si2 -4.5212 4.5212
sp2 0 1
si3 a 1.7399 10.8839 20.0279 29.1719 38.3159 47.4599 56.6039
312.6359 321.7799 330.9239 340.0679 349.2119 358.3559 367.4999
sp3 d 0.5470 0.6358 0.7247 0.8135 0.9023 0.9912 1.0800
1.0800 0.9912 0.9023 0.8135 0.7247 0.6358 0.5470
si4 1.000E-02 2.000E-02 5.000E-02 1.000E-01 2.000E-01 3.000E-01
4.000E-01 6.000E-01 8.000E-01 1.000E+00 1.220E+00 1.440E+00
1.660E+00 2.000E+00 2.500E+00 3.000E+00 4.000E+00 5.000E+00

```

Figure 5.3.18-5 Sample MCNP Input File for PWR MOX Fuel
(Response Method Benchmark Case)

```
6.500E+00 8.000E+00 1.000E+01 1.200E+01 1.400E+01
sp4 0.0000E+00 6.5335E+13 8.3523E+13 4.2132E+13 4.2987E+13 1.0861E+13
8.3438E+12 8.0750E+13 1.7401E+14 2.3085E+13 4.4177E+12 2.6664E+12
8.9233E+11 3.0024E+11 7.9369E+11 2.1689E+10 1.8203E+09 7.5273E+05
3.0209E+05 5.9261E+04 1.2582E+04 6.5057E+02 0.0000E+00
mode p
nps 40000000
C
C ANSI/ANS-6.1.1-1977 - Gamma Flux-to-Dose Conversion Factors
C (mrem/hr)/(photons/cm2-sec)
de0 0.01 0.03 0.05 0.07 0.1 0.15 0.2
0.25 0.3 0.35 0.4 0.45 0.5 0.55
0.6 0.65 0.7 0.8 1 1.4 1.8
2.2 2.6 2.8 3.25 3.75 4.25 4.75
5 5.25 5.75 6.25 6.75 7.5 9
11 13 15
df0 3.96E-03 5.82E-04 2.90E-04 2.58E-04 2.83E-04 3.79E-04 5.01E-04
6.31E-04 7.59E-04 8.78E-04 9.85E-04 1.08E-03 1.17E-03 1.27E-03
1.36E-03 1.44E-03 1.52E-03 1.68E-03 1.98E-03 2.51E-03 2.99E-03
3.42E-03 3.82E-03 4.01E-03 4.41E-03 4.83E-03 5.23E-03 5.60E-03
5.80E-03 6.01E-03 6.37E-03 6.74E-03 7.11E-03 7.66E-03 8.77E-03
1.03E-02 1.18E-02 1.33E-02
C
C Weight Window Generation - Radial
wwg 2 0 0 0 0
wwp:p 5 3 5 0 -1 0
mesh geom=cyl ref=0.0 6.3 193 origin=0.1 0.1 -568
imesh 6.4 12.2 17.0 18.9 33.3 36.5 49.2 49.8 549.8
lints 3 1 1 1 5 1 1 1 1
jmesh 500 541 550 558 568 575 579 964 1020 1049 1089 1589
jints 1 1 1 1 1 1 1 1 1 1 1
kmesh 1
kints 1
wwge:p 1e-3 1 20
fc2 Radial Surface Tally
f2:p +100.1
fm2 8.64200E+15
fs2 -101 -102 -103 -104 -105 -106
-107 -108 -109 -110 -111 -112
-113 -114 -115 -116 -117 -118
-119 T
tf2
fc12 Radial SurfaceAzi Tally Q1 (+x+y)
f12:p +150.1
fm12 8.64200E+15
fs12 -151 -160
+159 +158 +157 +156 +155 +154
+153 +152 T
sd12 4.7141E+03 2.3571E+03 2.6190E+02 8r 9.4282E+03
tf12
fc22 Radial SurfaceAzi Tally Q2 (-x+y)
f22:p +150.1
fm22 8.64200E+15
fs22 +151 -160
-168 -167 -166 -165 -164 -163
-162 -161 T
sd22 4.7141E+03 2.3571E+03 2.6190E+02 8r 9.4282E+03
tf22
fc32 Radial SurfaceAzi Tally Q3 (-x-y)
f32:p +150.1
fm32 8.64200E+15
fs32 +151 +160
-159 -158 -157 -156 -155 -154
-153 -152 T
sd32 4.7141E+03 2.3571E+03 2.6190E+02 8r 9.4282E+03
tf32
fc42 Radial SurfaceAzi Tally Q4 (+x-y)
f42:p +150.1
fm42 8.64200E+15
fs42 -151 +160
+168 +167 +166 +165 +164 +163
+162 +161 T
sd42 4.7141E+03 2.3571E+03 2.6190E+02 8r 9.4282E+03
tf42
fc52 Radial 1ft Tally
f52:p +200.1
fm52 8.64200E+15
fs52 -201 -202 -203 -204 -205 -206
-207 -208 -209 -210 -211 -212
-213 -214 -215 -216 -217 -218
-219 T
tf52
fc62 Radial 1m Tally
f62:p +300.1
fm62 8.64200E+15
fs62 -301 -302 -303 -304 -305 -306
-307 -308 -309 -310 -311 -312
-313 -314 -315 -316 -317 -318
-319 -320 -321 -322 -323 T
tf62
fc72 Radial 2m Tally
f72:p +400.1
fm72 8.64200E+15
fs72 -401 -402 -403 -404 -405 -406
-407 -408 -409 -410 -411 -412
-413 -414 -415 -416 -417 -418
```


Figure 5.3.18-5 Sample MCNP Input File for PWR MOX Fuel
(Response Method Benchmark Case)

```

-419 -420 -421 -422 -423 T
tf72
fc82 Radial 2m+Convey Tally
f82:p +500.1
fm82 8.64200E+15
fs82 -501 -502 -503 -504 -505 -506
-507 -508 -509 -510 -511 -512
-513 -514 -515 -516 -517 -518
-519 -520 -521 -522 -523 T
tf82
C
C Print Control
prdump -15 -30 1 2
print
C Random Number Generator
rand gen=2 seed=19073486328125 stride=152917 hist=1
C
C Rotation Matrix
C
*TR1 0.0 0.0 0.0 10 100 90 -80 10 90 90 90 0
*TR2 0.0 0.0 0.0 20 110 90 -70 20 90 90 90 0
*TR3 0.0 0.0 0.0 30 120 90 -60 30 90 90 90 0
*TR4 0.0 0.0 0.0 40 130 90 -50 40 90 90 90 0
*TR5 0.0 0.0 0.0 50 140 90 -40 50 90 90 90 0
*TR6 0.0 0.0 0.0 60 150 90 -30 60 90 90 90 0
*TR7 0.0 0.0 0.0 70 160 90 -20 70 90 90 90 0
*TR8 0.0 0.0 0.0 80 170 90 -10 80 90 90 90 0
*TR9 0.0 0.0 0.0 100 190 90 10 100 90 90 90 0
*TR10 0.0 0.0 0.0 110 200 90 20 110 90 90 90 0
*TR11 0.0 0.0 0.0 120 210 90 30 120 90 90 90 0
*TR12 0.0 0.0 0.0 130 220 90 40 130 90 90 90 0
*TR13 0.0 0.0 0.0 140 230 90 50 140 90 90 90 0
*TR14 0.0 0.0 0.0 150 240 90 60 150 90 90 90 0
*TR15 0.0 0.0 0.0 160 250 90 70 160 90 90 90 0
*TR16 0.0 0.0 0.0 170 260 90 80 170 90 90 90 0
    
```

Figure 5.3.18-6 Normal Condition Axial Surface Dose Rate Profile by Source Type – Power Grade MOX at 70 GWd/MTHM, 2% Fissile Material, and 90 Days Cool Time

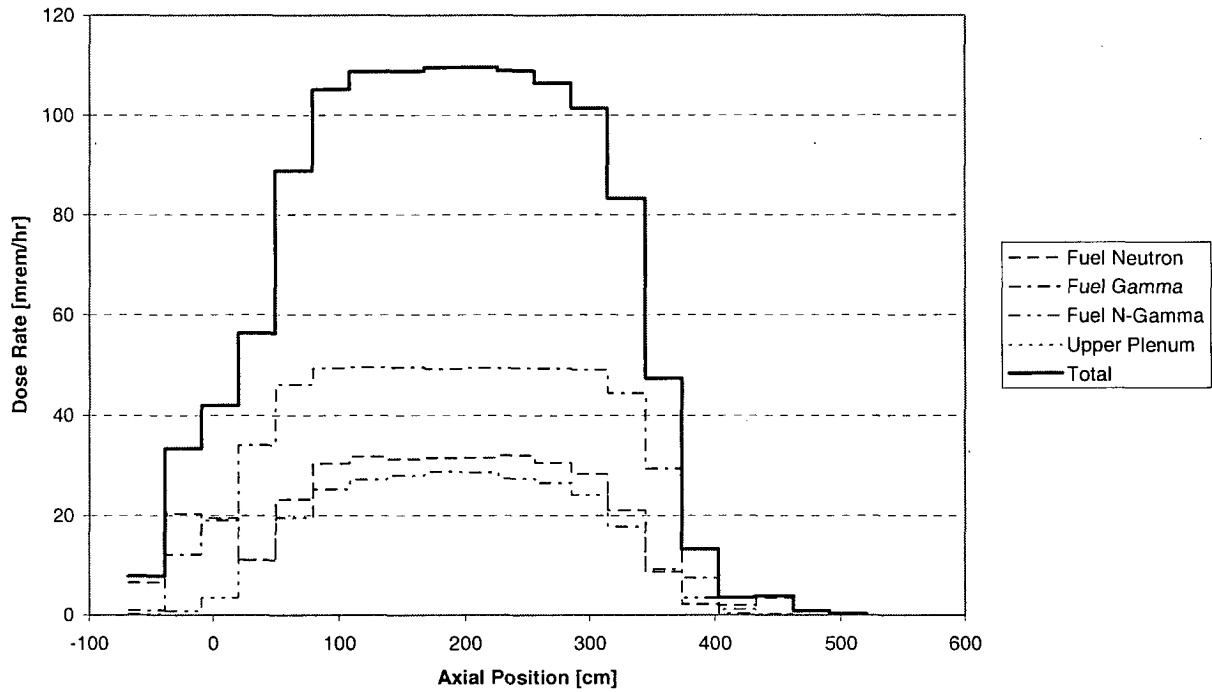


Figure 5.3.18-7 Normal Condition Radial 2m Dose Rate Profile by Source Type – Power Grade MOX at 70 GWd/MTHM, 2% Fissile Material, and 90 Days Cool Time

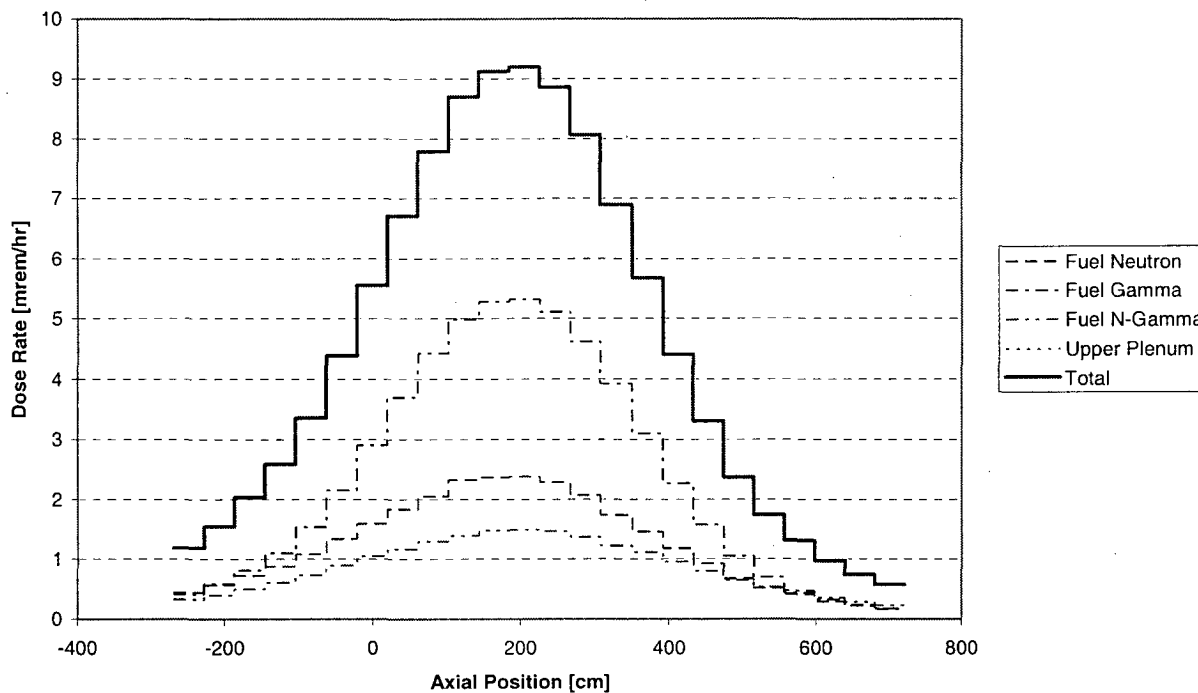


Figure 5.3.18-8 Accident Condition Radial 1m Dose Rate Profile by Source Type – Power Grade MOX at 70 GWd/MTHM, 2% Fissile Material, and 90 Days Cool Time

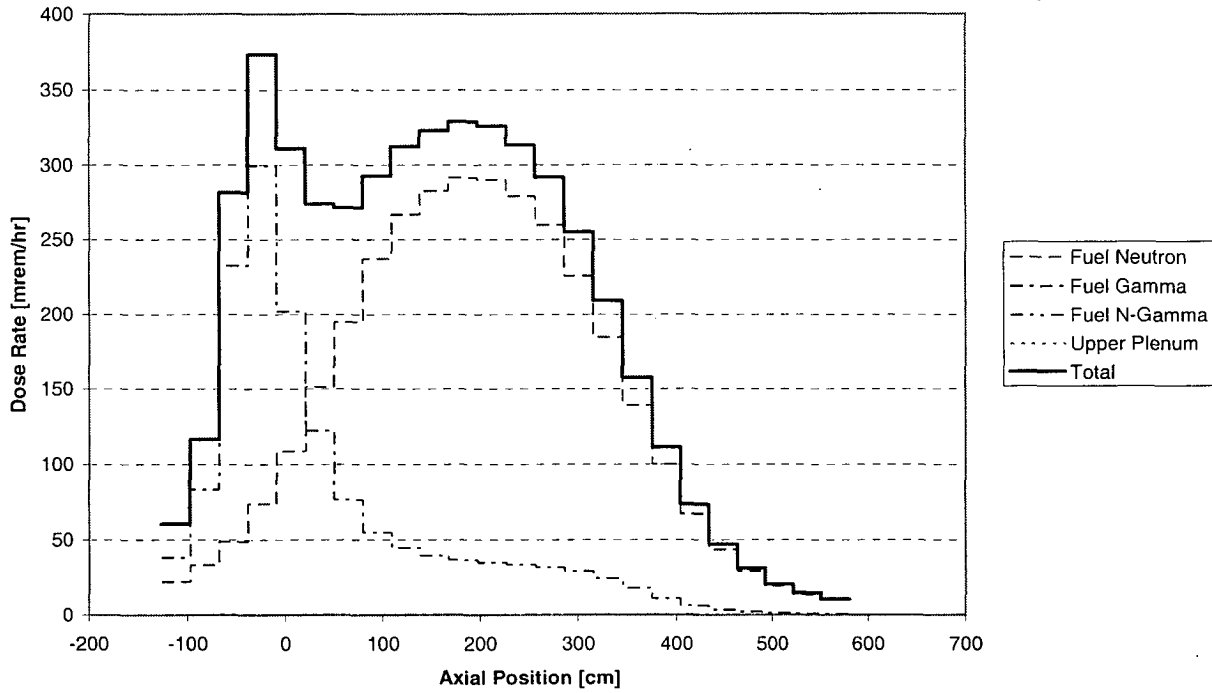


Table 5.3.18-1 High Burnup Fuel Rod Model Parameters

Parameter	Unit	SAS2H	MCNP
% Theoretical Density		95%	100%
Clad		Zirconium Alloy	Zirconium Alloy
Rod Diameter	[cm]	1.1180	0.9144
Clad Inner Diameter	[cm]	0.9860	0.8001
Pellet Diameter	[cm]	0.9665	0.7844
Active Length	[cm]	389.9	365.76
Heavy Metal Mass / Rod	[kg]	2.63 ¹	1.62
Fuel Rods ²		176	--
Pitch ²	[cm]	1.4730	--
Plenum Height	[cm]	--	15.9004
End Cap Height	[cm]	--	1.7399

Table 5.3.18-2 High Burnup MOX Fuel Assembly Model Parameters³

Burnup [MWd/MTHM]	Number Cycles	Assembly Power [MW]	Cycle Length [d]
70,000	3	19.36	556.8

¹ Slight variations exist between various fuel material compositions due to density changes associated with Pu content.

² Only used for source generation to generate full assembly.

³ UO₂ fuel evaluation employed same power density with increased cycle length (636.4 days) to achieve 80 GWd/MTHM burnup.

Table 5.3.18-3 MOX Fuel Material Compositions

Isotope	Isotopic Weight Fraction of U/Pu			
	Weapon Grade (WG)	Fuel Grade (FG)	Power Grade (PG)	MOX Services (MS)
²³⁵ U	0.2	0.2	0.2	0.2
²³⁸ U	99.8	99.8	99.8	99.8
²³⁸ Pu	0.05	0.1	1	0.05
²³⁹ Pu	93.5	86.1	62	89.85
²⁴⁰ Pu	6	12	22	9
²⁴¹ Pu	0.4	1.6	12	1
²⁴² Pu	0.05	0.2	3	0.1

Table 5.3.18-4 Uranium/Plutonium Fractions in MOX Fuel

Fissile Plutonium	Element	Element Weight Fraction in Fuel Composition			
		Weapon Grade (WG)	Fuel Grade (FG)	Power Grade (PG)	MOX Services (MS)
2%	U	97.96	97.82	97.41	97.89
	Pu	2.04	2.18	2.59	2.11
3%	U	96.94	96.72	96.12	96.84
	Pu	3.06	3.28	3.88	3.16
4%	U	95.92	95.63	94.82	95.77
	Pu	4.08	4.37	5.18	4.23
5%	U	94.90	94.53	93.52	94.72
	Pu	5.10	5.47	6.48	5.28
6%	U	93.87	93.44	92.22	93.67
	Pu	6.13	6.56	7.78	6.33
7%	U	92.85	92.34	90.92	92.61
	Pu	7.15	7.66	9.08	7.39

Table 5.3.18-5 PWR Fuel Axial Source Profile

% Active Fuel Height	Burnup Profile	Photon Source	Neutron Source
0.00%	0.5470	0.5470	7.840E-02
2.50%	0.6358	0.6358	1.479E-01
5.00%	0.7247	0.7247	2.569E-01
7.50%	0.8135	0.8135	4.185E-01
10.00%	0.9023	0.9023	6.481E-01
12.50%	0.9912	0.9912	9.633E-01
15.00%	1.0800	1.0800	1.384E+00
85.00%	1.0800	1.0800	1.384E+00
87.50%	0.9912	0.9912	9.633E-01
90.00%	0.9023	0.9023	6.481E-01
92.50%	0.8135	0.8135	4.185E-01
95.00%	0.7247	0.7247	2.569E-01
97.50%	0.6358	0.6358	1.479E-01
100.00%	0.5470	0.5470	7.840E-02

Table 5.3.18-6 Fuel Axial Source Profile Parameters

Burnup Peak to Average	Source	Exponent b	Average Source to Average Burnup
1.08	Neutron	4.22	1.1269
	Gamma	1.00	1.000

Table 5.3.18-7 MOX Source Term Magnitudes at 70 GWd/MTHM and 90 Days Cool Time (per Rod Basis)

Type	Heat [watts/rod]				
	LEU	WG	FG	PG	MS
2% Fissile	111.4	118.1	119.5	125.2	118.8
3% Fissile	109.6	122.4	124.8	134.5	123.5
4% Fissile	108.0	126.7	130.1	144.2	128.3
5% Fissile	106.6	129.0	133.2	151.9	131.0
6% Fissile	105.2	129.3	134.3	157.5	131.7
7% Fissile	104.0	128.6	134.3	161.6	131.3
Type	Neutron [n/sec/rod]				
	LEU	WG	FG	PG	MS
2% Fissile	3.02E+07	4.34E+07	4.68E+07	7.33E+07	4.50E+07
3% Fissile	2.05E+07	3.28E+07	3.59E+07	5.99E+07	3.43E+07
4% Fissile	1.42E+07	2.59E+07	2.92E+07	5.29E+07	2.74E+07
5% Fissile	1.01E+07	2.14E+07	2.50E+07	4.94E+07	2.31E+07
6% Fissile	7.37E+06	1.83E+07	2.21E+07	4.73E+07	2.01E+07
7% Fissile	5.56E+06	1.60E+07	2.00E+07	4.58E+07	1.78E+07
Type	Gamma [γ/sec/rod]				
	LEU	WG	FG	PG	MS
2% Fissile	7.02E+14	7.11E+14	7.12E+14	7.12E+14	7.12E+14
3% Fissile	6.96E+14	7.12E+14	7.12E+14	7.13E+14	7.12E+14
4% Fissile	6.90E+14	7.09E+14	7.09E+14	7.11E+14	7.09E+14
5% Fissile	6.84E+14	7.06E+14	7.06E+14	7.09E+14	7.06E+14
6% Fissile	6.79E+14	7.03E+14	7.04E+14	7.08E+14	7.03E+14
7% Fissile	6.76E+14	7.00E+14	7.01E+14	7.06E+14	7.01E+14

Table 5.3.18-8 MOX Fuel Cool Time to Reach 143.75 W/Rod (Days)

Burnup (GWd/MTHM)	80	70	70	70	70
Fissile Material Type	LEU	WG	FG	PG	MS
7% Fissile Content	<90	<90	<90	120	<90
6% Fissile Content	<90	<90	<90	120	<90
5% Fissile Content	<90	<90	<90	110	<90
4% Fissile Content	<90	<90	<90	100	<90
3% Fissile Content	<90	<90	<90	<90	<90
2% Fissile Content	<90	<90	<90	<90	<90

Table 5.3.18-9 PWR Power Grade MOX Fuel Assembly Neutron Source Term for 70 GWD/MTHM, 2% Fissile Pu, and 90 Days Cooling (16 Rods)

Group	E Lower [MeV]	E Upper [MeV]	Source [neutrons/sec]
1	1.360E+01	1.460E+01	5.558E+04
2	1.250E+01	1.360E+01	1.419E+05
3	1.125E+01	1.250E+01	4.110E+05
4	1.000E+01	1.125E+01	1.086E+06
5	8.250E+00	1.000E+01	4.941E+06
6	7.000E+00	8.250E+00	1.036E+07
7	6.070E+00	7.000E+00	1.661E+07
8	4.720E+00	6.070E+00	5.380E+07
9	3.680E+00	4.720E+00	9.000E+07
10	2.870E+00	3.680E+00	1.220E+08
11	1.740E+00	2.870E+00	2.806E+08
12	6.400E-01	1.740E+00	4.000E+08
13	3.900E-01	6.400E-01	9.264E+07
14	1.100E-01	3.900E-01	8.346E+07
15	6.740E-02	1.100E-01	8.475E+06
16	2.480E-02	6.740E-02	6.216E+06
17	9.120E-03	2.480E-02	1.412E+06
18	2.950E-03	9.120E-03	3.328E+05
19	9.610E-04	2.950E-03	6.121E+04
20	3.540E-04	9.610E-04	1.086E+04
21	1.660E-04	3.540E-04	2.125E+03
22	4.810E-05	1.660E-04	8.485E+02
23	1.600E-05	4.810E-05	1.268E+02
24	4.000E-06	1.600E-05	2.625E+01
25	1.500E-06	4.000E-06	2.891E+00
26	5.500E-07	1.500E-06	6.710E-01
27	7.090E-08	5.500E-07	1.829E-01
28	1.000E-11	7.090E-08	9.100E-03
Total			1.173E+09

Table 5.3.18-10 PWR Power Grade MOX Fuel Assembly Gamma Source Term for 70 GwD/MTHM, 2% Fissile Pu, and 90 Days Cooling (16 Rods)

Group	E Lower [MeV]	E Upper [MeV]	Fuel Gamma [photons/sec]	Hardware Gamma ¹ [photons/sec]
1	1.20E+01	1.40E+01	0.0000E+00	0.0000E+00
2	1.00E+01	1.20E+01	3.1246E+04	0.0000E+00
3	8.00E+00	1.00E+01	6.0432E+05	0.0000E+00
4	6.50E+00	8.00E+00	2.8462E+06	0.0000E+00
5	5.00E+00	6.50E+00	1.4508E+07	0.0000E+00
6	4.00E+00	5.00E+00	3.6147E+07	0.0000E+00
7	3.00E+00	4.00E+00	4.4686E+10	1.3138E-13
8	2.50E+00	3.00E+00	1.2211E+12	1.9460E+02
9	2.00E+00	2.50E+00	1.7739E+13	2.2777E+05
10	1.66E+00	2.00E+00	8.2987E+12	1.0318E+07
11	1.44E+00	1.66E+00	4.1253E+13	4.4657E+05
12	1.22E+00	1.44E+00	5.0438E+13	2.1733E+10
13	1.00E+00	1.22E+00	9.1018E+13	2.3000E+10
14	8.00E-01	1.00E+00	3.8442E+14	8.1955E+09
15	6.00E-01	8.00E-01	3.8492E+15	7.3117E+05
16	4.00E-01	6.00E-01	1.8316E+15	6.7064E+08
17	3.00E-01	4.00E-01	1.6843E+14	1.2419E+09
18	2.00E-01	3.00E-01	2.1407E+14	7.3205E+06
19	1.00E-01	2.00E-01	9.3336E+14	8.7699E+07
20	5.00E-02	1.00E-01	8.1935E+14	1.4913E+08
21	2.00E-02	5.00E-02	1.6657E+15	3.9420E+08
22	1.00E-02	2.00E-02	1.3199E+15	4.5530E+08
Total			1.1396E+16	5.5947E+10

¹ Reflects a 25 gram activated plenum spring. As indicated by the relative source magnitude differences between fuel and hardware gamma in any energy bin, there is no significant hardware source.

Table 5.3.18-11 Homogenization for PWR MOX Fuel Rod Regions

Material	Density [g/cm ³]	Element	Number Density [atom/b-cm]
Homogenized Fuel Region (UO ₂ /MOX plus Clad)	1.23	Uranium-235	8.4528E-05
		Uranium-238	2.0031E-03
		Oxygen-16	4.1762E-03
		Zirconium	1.9328E-03
		Tin	2.2681E-05
		Iron	4.0176E-06
		Chromium	3.4521E-06
		Nitrogen-14	6.4091E-06
Fuel Rod End-Cap	0.84	Zirconium	5.4662E-03
		Tin	6.4146E-05
		Iron	1.1363E-05
		Chromium	9.7634E-06
		Nitrogen-14	1.8127E-05
Plenum Region ¹	0.0	N/A	0.0

¹ Plenum region modeled as void in the shielding evaluation.

Table 5.3.18-12 Cask/Basket Material Descriptions for PWR MOX Fuel

Material	Element	Density [g/cm ³]	Number Density [atom/b-cm]
Stainless Steel 304	Fe	7.94	5.9505E-02
	Cr		1.7472E-02
	Ni		7.7392E-03
	Mn		1.7407E-03
Lead	Pb	11.34	3.2967E-02
Neutron Shield	H	0.97	5.9884E-02
	O		2.4595E-02
	C		1.0701E-02
Impact Limiter	Al	0.50	1.1153E-02
Aluminum	Al	2.70	6.0306E-02

Table 5.3.18-13 Subcritical Multiplication Study for PWR MOX Fuel

Fuel	Cool Time	Response (mrem/hr) Using UO ₂ Composition	Direct (mrem/hr) Using Actual Composition	Diff
LEU	150 days	5.74	5.83	1.6% ¹
FG	90 days	10.72	10.86	1.3%
MS	90 days	10.16	10.29	1.3%
PG	90 days	18.44	18.70	1.4%
WG	90 days	9.72	9.86	1.4%

¹ Difference due to direct solution using the full spectrum of source in a single run versus response solution derived at by multiplication of the source spectrum by per energy line run results.

Table 5.3.18-14 Maximum Radial Dose Rates for PWR MOX Fuel – 90 Days Cool Time, 2% Fissile Pu

Burnup (GWd/MTHM)	80	70	70	70	70
Fuel Material	LEU	WG	FG	PG	MS
Normal Surface	91.6	85.0	87.8	109.6	86.3
Normal 1 meter	23.6	22.1	22.7	27.5	22.4
Normal 2 meter	8.1	7.6	7.8	9.2	7.7
Accident 1 meter	362	344	347	373	345

Table 5.3.18-15 Detailed Dose Rates for Bounding Fuel – Power Grade PWR MOX Fuel, 2% Fissile Pu, 70 GWd/MTHM and 90 Days Cool Time

Transport Condition	Dose Rate Location	Maximum		Average	
		[mrem/hr]	FSD	[mrem/hr]	FSD
Normal	Side Surface of Cask	1.1E+02	0.5%	6.2E+01	0.2%
	Top Surface of Cask	8.6E-01	6.4%	4.3E-01	7.1%
	Bottom Surface of Cask	1.2E+01	8.2%	7.9E+00	6.3%
	Side 1m (Transport Index)	2.8E+01	0.4%	1.3E+01	0.1%
	2m from Truck - Radial	9.2E+00	0.3%	4.5E+00	0.1%
	2m from Top	3.3E-01	12.5%	2.1E-01	8.5%
	2m from Bottom	7.6E-01	8.5%	6.6E-01	5.9%
	Edge of Truck - Top	6.6E-02	30.6%	3.0E-02	13.7%
	Edge of Truck - Bottom	6.2E-01	21.2%	5.0E-01	7.0%
	Dose at Cab of Truck	2.3E-02	11.4%	1.6E-02	6.4%
Accident	Side Surface of Cask	4.1E+03	0.4%	1.4E+03	0.1%
	Top Surface of Cask	6.6E+00	16.7%	2.5E+00	11.9%
	Bottom Surface of Cask	6.5E+01	6.5%	3.8E+01	7.5%
	Side 1m	3.7E+02	0.3%	2.0E+02	0.1%
	Top 1m	1.3E+01	56.3%	5.5E+00	27.2%
	Bottom 1m	7.4E+01	29.5%	3.3E+01	17.6%

Chapter 6

Table of Contents

6	CRITICALITY EVALUATION	6-1
6.1	Discussion and Results	6.1-1
6.2	Package Fuel Loading	6.2-1
6.2.1	PWR Fuel Assemblies	6.2.1-1
6.2.2	BWR Fuel Assemblies	6.2.2-1
6.2.3	MTR Fuel Elements	6.2.3-1
6.2.4	PWR and BWR Rods in a Rod Holder or Fuel Assembly Lattice	6.2.4-1
6.2.5	TRIGA Fuel Elements	6.2.5-1
6.2.6	TRIGA Fuel Cluster Rods	6.2.6-1
6.2.7	Metallic Fuel Rods	6.2.7-1
6.2.8	DIDO Fuel Assemblies	6.2.8-1
6.2.9	General Atomics Irradiated Fuel Material	6.2.9-1
6.2.10	PULSTAR Fuel Elements	6.2.10-1
6.2.11	Spiral Fuel Assemblies	6.2.11-1
6.2.12	MOATA Plate Bundles	6.2.12-1
6.3	Criticality Model Specifications	6.2.12-1
6.3.1	PWR Fuel Assemblies	6.3.1-1
6.3.2	BWR Fuel Assemblies	6.3.2-1
6.3.3	MTR Fuel Elements	6.3.3-1
6.3.4	PWR and BWR Rods in a Rod Holder or Fuel Assembly Lattice	6.3.4-1
6.3.5	TRIGA Fuel Elements and Cluster Rods	6.3.5-1
6.3.6	DIDO Fuel Assemblies	6.3.6-1
6.3.7	General Atomics Irradiated Fuel Material	6.3.7-1
6.3.8	PULSTAR Fuel Contents	6.3.8-1
6.3.9	ANSTO Basket Payload	6.3.9-1
6.4	Criticality Calculations	6.3.9-1
6.4.1	PWR Fuel Assemblies	6.4.1-1
6.4.2	BWR Fuel Assemblies	6.4.2-1
6.4.3	MTR Fuel Elements	6.4.3-1
6.4.4	PWR and BWR Rods in a Rod Holder or Fuel Assembly Lattice	6.4.4-1
6.4.5	TRIGA Fuel Elements	6.4.5-1
6.4.6	TRIGA Fuel Cluster Rods	6.4.6-1
6.4.7	DIDO Fuel Assemblies	6.4.7-1
6.4.8	General Atomics Irradiated Fuel Material	6.4.8-1
6.4.9	PULSTAR Fuel Contents	6.4.9-1
6.4.10	ANSTO Basket Payloads	6.4.10-1
6.5	Critical Benchmarks	6.4.10-1
6.5.1	PWR and BWR Fuel Assemblies	6.5.1-1
6.5.2	MTR and DIDO Fuel Elements	6.5.2-1
6.5.3	TRIGA Fuel Elements	6.5.3-1
6.7	Payload Specific Details	6.7.1-1
6.7.1	PWR Mixed Oxide Fuel Rods	6.7.1-1
6.7.2	Critical Benchmarks	6.7.2-1

Note: See separate Section 6.6 for Appendices to this chapter.

List of Figures

Figure 6.2.3-1	Design Basis HFBR MTR Fuel Element.....	6.2.3-2
Figure 6.2.5-1	Aluminum Clad TRIGA Fuel Element.....	6.2.5-2
Figure 6.2.5-2	Stainless Steel Clad TRIGA Fuel Element	6.2.5-3
Figure 6.2.6-1	TRIGA Fuel Cluster Rod Details	6.2.6-2
Figure 6.2.8-1	DIDO Fuel Assembly	6.2.8-2
Figure 6.2.10-1	PULSTAR Fuel Assembly	6.2.10-2
Figure 6.2.11-1	Spiral Fuel Assembly Cross-Section Sketch	6.2.11-2
Figure 6.2.12-1	MOATA Plate Bundle Sketch	6.2.12-2
Figure 6.3.1-1	KENO-Va Model of the NAC-LWT Cask Model with PWR Basket and 15×15 PWR Assembly	6.3.1-4
Figure 6.3.1-2	KENO-Va Model of the NAC-LWT Cask with PWR Basket and Westinghouse 17×17 OFA Assembly	6.3.1-5
Figure 6.3.2-1	KENO-Va Model of the NAC-LWT Cask Model with BWR Basket and 2 Exxon 9×9-2/80 Assemblies.....	6.3.2-3
Figure 6.3.3-1	KENO-Va Fuel/Basket Unit Cell Model for MTR Fuel	6.3.3-4
Figure 6.3.3-2	KENO-Va Model of NAC-LWT Cask with MTR Fuel	6.3.3-5
Figure 6.3.3-3	Intermediate MTR 42 Basket Module	6.3.3-6
Figure 6.3.3-4	Full Length NAC-LWT Cask Model with 42 MTR Fuel Elements.....	6.3.3-7
Figure 6.3.3-5	MTR Fuel Basket Module Loading Pattern	6.3.3-8
Figure 6.3.4-1	Triangular Pitch Lattice Formation of 25 PWR Rods	6.3.4-4
Figure 6.3.4-2	KENO-Va Model of the NAC-LWT Cask with 25 PWR Rods.....	6.3.4-5
Figure 6.3.4-3	Maximum Reactivity Triangular Pitch Lattice Formation of Damaged Fuel Rods.....	6.3.4-6
Figure 6.3.4-4	KENO-Va Model of the NAC-LWT Cask with Damaged Fuel Rods – Radial Detail	6.3.4-7
Figure 6.3.4-5	KENO-Va Model of the NAC-LWT Cask with Damaged Fuel Rods – Axial Detail	6.3.4-8
Figure 6.3.5-1	Fuel Rod Handling Insert for TRIGA Fuel Cluster Rods.....	6.3.5-5
Figure 6.3.5-2	Fuel/Basket Unit Cell Model for TRIGA Fuel Elements	6.3.5-6
Figure 6.3.5-3	NAC-LWT Cask with TRIGA Fuel, Nonpoisoned Basket - Radial View	6.3.5-7
Figure 6.3.5-4	KENO-Va Model of NAC-LWT with Poisoned Basket - Radial View..	6.3.5-8
Figure 6.3.5-5	NAC-LWT Cask Model with TRIGA Fuel Elements, Nonpoisoned Basket - Axial View	6.3.5-9
Figure 6.3.5-6	Full Length NAC-LWT Cask Model with TRIGA Fuel Elements, Nonpoisoned Basket - Axial View	6.3.5-10
Figure 6.3.6-1	Intermediate DIDO 42 Basket Module.....	6.3.6-3
Figure 6.3.6-2	KENO-Va DIDO Fuel in Fuel Tube and Basket Cross-Section.....	6.3.6-4
Figure 6.3.6-3	KENO-Va Model of NAC-LWT Cask Cross-Section with DIDO Fuel .	6.3.6-5
Figure 6.3.6-4	Full Length NAC-LWT Cask Model with 42 DIDO Fuel Assemblies ...	6.3.6-6
Figure 6.3.7-1	PICTURE Representation of NAC-LWT Cavity with ‘Rectangular’ Array of GA IFM TRIGA Elements.....	6.3.7-2

List of Figures (continued)

Figure 6.3.7-2	PICTURE Representation of NAC-LWT Cavity with ‘Square’ Array of GA IFM TRIGA Elements.....	6.3.7-2
Figure 6.3.7-3	KENO-Va Model of NAC-LWT Cask Cross-Section with GA IFM	6.3.7-3
Figure 6.3.8-1	PICTURE Representation of NAC-LWT Cavity with PULSTAR Assemblies	6.3.8-3
Figure 6.3.8-2	PICTURE Representation of NAC-LWT Cavity with PULSTAR Elements in 4×4 Rod Insert	6.3.8-3
Figure 6.3.8-3	PICTURE Representation of NAC-LWT Cavity with Canned Discrete PULSTAR Elements	6.3.8-4
Figure 6.3.8-4	PICTURE Representation of NAC-LWT Cavity with Canned Homogenized PULSTAR Elements	6.3.8-4
Figure 6.3.8-5	KENO-Va Model of NAC-LWT Cask Cross-Section with 28 MTR 7-Element Basket.....	6.3.8-5
Figure 6.3.8-6	Finite Length KENO-Va Model of NAC-LWT Cask with 700 PULSTAR Fuel Elements	6.3.8-6
Figure 6.3.9-1	Intermediate ANSTO Basket Module	6.3.9-3
Figure 6.3.9-2	KENO-Va ANSTO Payloads and Basket Cross-Section	6.3.9-4
Figure 6.3.9-3	KENO-Va Model of NAC-LWT Cask Cross-Section with ANSTO Basket	6.3.9-5
Figure 6.4.3-1	Cask Interior Moderator Density and Blocked Cell Study Results	6.4.3-16
Figure 6.4.4-1	Maximum Reactivity Pitch Determination for Damaged BWR Rod Arrays – Water Exterior	6.4.4-8
Figure 6.4.4-2	Maximum Reactivity Pitch Determination for Damaged PWR Rod Arrays – Water Exterior	6.4.4-8
Figure 6.4.4-3	Maximum Reactivity Determination for Homogenized UO ₂ /Water Mixture	6.4.4-9
Figure 6.4.5-1	Finite Cask Array Reactivity versus Fuel Zirconium Mass (Dry Cask Cavity).....	6.4.5-14
Figure 6.4.5-2	Finite Cask Array Reactivity versus H/Zr Ratio (Dry Cask Cavity)	6.4.5-14
Figure 6.4.5-3	Finite Cask Array Reactivity versus Fuel Mass (Study of ZrH Displacement of Fissile Material for a Fixed Fuel Geometry).....	6.4.5-15
Figure 6.4.5-4	Intact Fuel Optimum Moderator Study – 70 wt % ²³⁵ U Various Zirconium Masses	6.4.5-15
Figure 6.4.5-5	Detailed Intact Fuel Optimum Moderator Study – H/Zr Ratio, Fuel Element Characteristics and Location Varied	6.4.5-16
Figure 6.4.5-6	Screened and Sealed Can Optimum Moderator Study – Maximum Reactivity Fuel Configuration – 70 wt% ²³⁵ U Steel Clad	6.4.5-16
Figure 6.4.5-7	Screened and Sealed Can Debris Height Study – Maximum Reactivity Fuel Configuration – 70 wt% ²³⁵ U Steel Clad.....	6.4.5-17
Figure 6.4.5-8	Screened Can – 4 Elements per Can – Maximum Reactivity Fuel Configuration – 70 wt% ²³⁵ U Steel Clad.....	6.4.5-17

List of Figures (continued)

Figure 6.4.9-1	PICTURE Schematic of Modified PULSTAR Fuel Assembly Alignment Configuration.....	6.4.9-5
Figure 6.4.9-2	PULSTAR Intact Assembly Model Moderator Density Study Graphical Results.....	6.4.9-6
Figure 6.4.10-1	Spiral Fuel - Moderator Density Plot	6.4.10-7
Figure 6.4.10-2	MOATA Plate Bundle -Moderator Density Plot.....	6.4.10-8
Figure 6.5.1-1	KENO-Va Validation—27 Group Library Results: Frequency Distribution of k_{eff} Values	6.5.1-6
Figure 6.5.1-2	KENO-Va Validation—27-Group Library Results: k_{eff} versus Enrichment	6.5.1-7
Figure 6.5.1-3	KENO-Va Validation—27-Group Library Results: k_{eff} versus Rod Pitch.....	6.5.1-8
Figure 6.5.1-4	KENO-Va Validation—27-Group Library Results: k_{eff} versus H/U Volume Ratio	6.5.1-9
Figure 6.5.1-5	KENO-Va Validation—27-Group Library Results: k_{eff} versus Average Group of Fission.....	6.5.1-10
Figure 6.7.1-1	MCNP Model Sketch of the NAC-LWT Cask with PWR MOX/ UO ₂ Rods.....	6.7.1-3
Figure 6.7.1-2	VISED Sketch of LWT Radial View – Hex Rod Array– Normal Conditions	6.7.1-4
Figure 6.7.1-3	VISED Sketch of LWT Radial View – Square Rod Pitch - Accident Conditions	6.7.1-5
Figure 6.7.1-4	VISED Sketch of LWT Axial View – Accident Conditions	6.7.1-6
Figure 6.7.1-5	PWR MOX Rod Shipment - Reactivity versus Rod Pitch	6.7.1-12
Figure 6.7.1-6	Moderator Density Study – UO ₂ Fuel Material – 3.0 cm Rod Pitch	6.7.1-12
Figure 6.7.1-7	Moderator Density Study – MS Fuel Material – 3.6 cm Rod Pitch	6.7.1-13
Figure 6.7.1-8	Moderator Density Study – PWR MOX ²⁴¹ Pu Fuel Material – 3.6 cm Rod Pitch	6.7.1-13
Figure 6.7.2-1	LEU USLSTATS Output for EALCF	6.7.2-5
Figure 6.7.2-2	k_{eff} versus Fuel Enrichment (LEU).....	6.7.2-10
Figure 6.7.2-3	k_{eff} versus Rod Pitch (LEU).....	6.7.2-10
Figure 6.7.2-4	k_{eff} versus Fuel Pellet Diameter (LEU).....	6.7.2-11
Figure 6.7.2-5	k_{eff} versus Fuel Rod Outside Diameter (LEU).....	6.7.2-11
Figure 6.7.2-6	k_{eff} versus Hydrogen/ ²³⁵ U Atom Ratio (LEU).....	6.7.2-12
Figure 6.7.2-7	k_{eff} versus Soluble Boron Concentration (LEU).....	6.7.2-12
Figure 6.7.2-8	k_{eff} versus Cluster Gap Thickness (LEU)	6.7.2-13
Figure 6.7.2-9	k_{eff} versus ¹⁰ B Plate Loading (LEU).....	6.7.2-13
Figure 6.7.2-10	k_{eff} versus Energy of Average Neutron Lethargy Causing Fission (LEU).....	6.7.2-14
Figure 6.7.2-11	PWR MOX USLSTATS Output for Water to Fuel Volume Ratio	6.7.2-37

List of Figures (continued)

Figure 6.7.2-12	Adjusted k_{eff} vs. Energy of Average Neutron Lethargy Causing Fission.....	6.7.2-42
Figure 6.7.2-13	Adjusted k_{eff} vs. $^{235}\text{U}/^{238}\text{U}$ Ratio.....	6.7.2-42
Figure 6.7.2-14	Adjusted k_{eff} vs. $^{238}\text{Pu}/^{238}\text{U}$ Ratio.....	6.7.2-43
Figure 6.7.2-15	Adjusted k_{eff} vs. $^{239}\text{Pu}/^{238}\text{U}$ Ratio.....	6.7.2-43
Figure 6.7.2-16	Adjusted k_{eff} vs. $^{240}\text{Pu}/^{238}\text{U}$ Ratio.....	6.7.2-44
Figure 6.7.2-17	Adjusted k_{eff} vs. $^{241}\text{Pu}/^{238}\text{U}$ Ratio.....	6.7.2-44
Figure 6.7.2-18	Adjusted k_{eff} vs. $^{242}\text{Pu}/^{238}\text{U}$ Ratio.....	6.7.2-45
Figure 6.7.2-19	Adjusted k_{eff} vs. Water-to-Fuel Volume Ratio.....	6.7.2-45

Note: See separate Section 6.6 for Appendices to this chapter, along with the List of Figures for the Appendices.

List of Tables

Table 6.2.1-1	B&W, CE and Westinghouse PWR Fuel Assembly Data.....	6.2.1-2
Table 6.2.1-2	Exxon/ANF PWR Fuel Assembly Data	6.2.1-3
Table 6.2.2-1	GE BWR Fuel Assembly Data	6.2.2-2
Table 6.2.2-2	Exxon BWR Fuel Assembly Data	6.2.2-3
Table 6.2.2-3	BWR Fuel Assembly Data	6.2.2-3
Table 6.2.3-1	Characteristics of Design Basis HEU MTR Fuels.....	6.2.3-3
Table 6.2.3-2	Characteristics of Design Basis LEU MTR Fuel.....	6.2.3-6
Table 6.2.3-3	Characteristics of Design Basis MEU MTR Fuel	6.2.3-7
Table 6.2.5-1	Characteristics of Design Basis TRIGA Fuels Elements	6.2.5-4
Table 6.2.5-2	Characteristics of Design Basis TRIGA Fuels -Fuel Compositions.....	6.2.5-5
Table 6.2.6-1	Characteristics of Design-Basis TRIGA Fuel Cluster Rods.....	6.2.6-3
Table 6.2.6-2	Characteristics of Design-Basis TRIGA Fuel Cluster Rods - Fuel Compositions.....	6.2.6-3
Table 6.2.7-1	Characteristics of Design-Basis Metallic Fuel Rods	6.2.7-2
Table 6.2.8-1	Characteristics of DIDO Fuel Assemblies.....	6.2.8-3
Table 6.2.8-2	DIDO Fuel Assembly Tolerances.....	6.2.8-3
Table 6.2.9-1	GA IFM RERTR/TRIGA Fuel Parameters	6.2.9-3
Table 6.2.9-2	GA IFM RERTR/TRIGA Fuel Composition	6.2.9-3
Table 6.2.9-3	GA IFM RERTR/TRIGA Clad Composition.....	6.2.9-3
Table 6.2.9-4	GA IFM Elemental Constituents	6.2.9-4
Table 6.2.9-5	GA IFM Primary and Secondary Enclosure Dimensions.....	6.2.9-4
Table 6.2.10-1	PULSTAR Fuel Characteristics.....	6.2.10-3
Table 6.2.11-1	Spiral Fuel Assemblies Characteristics	6.2.11-3
Table 6.2.11-2	Spiral Fuel Assemblies Tolerances Applied.....	6.2.11-3
Table 6.2.12-1	MOATA Plate Bundle Characteristics	6.2.12-3
Table 6.2.12-2	MOATA Plate Bundle Tolerances Applied.....	6.2.12-4
Table 6.3.1-1	Compositions and Number Densities Used in the Criticality Analysis of PWR Fuel Assemblies	6.3.1-6
Table 6.3.2-1	Compositions and Number Densities Used in the Criticality Analysis of BWR Fuel Assemblies	6.3.2-4
Table 6.3.3-1	Composition Densities Used in Criticality Analysis of MTR Fuel.....	6.3.3-9
Table 6.3.4-1	Compositions and Number Densities Used in the Criticality Analysis of PWR and BWR Rods.....	6.3.4-9
Table 6.3.5-1	Sample Compositions and Number Densities Used in Criticality Analysis of TRIGA Fuel Elements.....	6.3.5-11
Table 6.3.5-2	Compositions and Number Densities Used in Criticality Analysis of TRIGA Fuel Cluster Rods	6.3.5-12
Table 6.3.6-1	DIDO Fuel Parameters	6.3.6-7
Table 6.3.6-2	DIDO Basket and Cask Parameters	6.3.6-8
Table 6.3.6-3	Composition Densities Used in Criticality Analysis of DIDO Fuel.....	6.3.6-9
Table 6.3.7-1	Composition Densities Used in Criticality Analysis of GA IFM.....	6.3.7-4
Table 6.3.8-1	Composition Densities Used in Criticality Analysis of PULSTAR Fuel	6.3.8-7
Table 6.3.9-1	ANSTO Basket and Cask Parameters	6.3.9-6

List of Tables (continued)

Table 6.3.9-2	Composition Densities Used in Criticality Analysis of ANSTO Basket Payloads	6.3.9-7
Table 6.4.1-1	PWR Fuel Assembly at 3.7% Enrichment Most Reactive Assembly Results.....	6.4.1-5
Table 6.4.1-2	PWR Fuel Assembly at 3.5% Enrichment Most Reactive Assembly Results.....	6.4.1-6
Table 6.4.1-3	Westinghouse 17×17 OFA Assembly Geometric Tolerances and Mechanical Perturbations Results.....	6.4.1-7
Table 6.4.1-4	Exxon 15×15 Geometric Tolerances and Mechanical Perturbations Results.....	6.4.1-7
Table 6.4.1-5	Reactivity with Design Basis PWR Fuel vs. Basket Moderator Density, Normal Conditions	6.4.1-8
Table 6.4.1-6	Reactivity with Design Basis PWR Fuel vs. Basket Moderator Density, Accident Conditions	6.4.1-9
Table 6.4.1-7	PWR Single Package 10 CFR 71.55(b)(3) Evaluation k_{eff} Summary for 3.5% Enrichment.....	6.4.1-10
Table 6.4.1-8	PWR Single Package 10 CFR 71.55(b)(3) Evaluation k_{eff} Summary for 3.7% Enrichment.....	6.4.1-10
Table 6.4.2-1	BWR Most Reactive Assembly Analysis Results.....	6.4.2-5
Table 6.4.2-2	BWR Basket Tolerances	6.4.2-6
Table 6.4.2-3	BWR Fuel Assembly Geometric Tolerances and Mechanical Perturbations Results	6.4.2-7
Table 6.4.2-4	Reactivity with BWR Fuel vs. Basket Moderator Density, Normal Conditions, Array of 20 Casks	6.4.2-8
Table 6.4.2-5	Reactivity with BWR Fuel vs. Basket Moderator Density, Accident Conditions, Array of 20 Casks	6.4.2-9
Table 6.4.2-6	BWR Single Package 10 CFR 71.55(b)(3) Evaluation k_{eff} Summary...	6.4.2-10
Table 6.4.3-1	Fuel/Basket Unit Cell k_{eff} versus MTR Fuel Element Type	6.4.3-17
Table 6.4.3-2	Cask k_{eff} versus Fuel Plate Spacing.....	6.4.3-17
Table 6.4.3-3	MTR Basket Geometric Tolerances.....	6.4.3-18
Table 6.4.3-4	MTR Basket/Intact Fuel Element Geometric Tolerances and Mechanical Perturbations Results.....	6.4.3-18
Table 6.4.3-5	MTR Basket/Optimally Spaced Fuel Plates Geometric Tolerances and Mechanical Perturbations Results.....	6.4.3-18
Table 6.4.3-6	Reactivity with MTR Fuel vs. Basket Moderator Density, Normal Conditions, Dry Exterior, Infinite Array of Casks	6.4.3-19
Table 6.4.3-7	Reactivity with MTR Fuel vs. Basket Moderator Density, Accident Conditions, Dry Exterior, Infinite Array of Casks	6.4.3-20
Table 6.4.3-8	MTR Fuel Element Rotation Perturbation Study.....	6.4.3-21
Table 6.4.3-9	MTR Basket/Center Fuel Element Perturbation Study.....	6.4.3-21
Table 6.4.3-10	Mixed HEU/LEU MTR Fuel Perturbation Study	6.4.3-21
Table 6.4.3-11	MTR Single Package 10 CFR 71.55(b)(3) Evaluation k_{eff} Summary ...	6.4.3-21
Table 6.4.3-12	MTR Fuel Uranium Weight Percentage Perturbations	6.4.3-22

List of Tables (continued)

Table 6.4.3-13	MEU MTR Unit Cell k_{eff} Comparison (Enrichment Variation).....	6.4.3-22
Table 6.4.3-14	MEU MTR Basket k_{eff} Comparison (Plate Location)	6.4.3-23
Table 6.4.3-15	Physical Characteristics of McMaster MTR Fuels.....	6.4.3-23
Table 6.4.3-16	Reactivity of Various Parameter Variations for 10-Plate McMaster Element.....	6.4.3-24
Table 6.4.3-17	Reactivity of Various Parameter Variations for 18-Plate McMaster Element.....	6.4.3-24
Table 6.4.3-18	MTR Limiting Fuel Configurations	6.4.3-25
Table 6.4.3-19	Initial Fuel Configurations for MTR Bounding Evaluations.....	6.4.3-25
Table 6.4.3-20	Reactivity Impact of Parameter Variations in the Finite Cask Model...	6.4.3-26
Table 6.4.3-21	Baseline MTR Bounding Configurations	6.4.3-27
Table 6.4.3-22	High Fissile Mass MTR Fuel – Bounding Parameter Analysis.....	6.4.3-28
Table 6.4.3-23	MTR High Fissile Content Loading Evaluation (460 g ^{235}U)	6.4.3-29
Table 6.4.3-24	LEU MTR Active Fuel Width Increase Evaluation	6.4.3-29
Table 6.4.3-25	Summary of LEU MTR Bounding Configurations	6.4.3-30
Table 6.4.3-26	Summary of Previous Bounding Configurations for Use in High Mass LEU Calculations	6.4.3-31
Table 6.4.3-27	High Fissile Mass LEU (32 gram ^{235}U per Plate) Analysis Results	6.4.3-32
Table 6.4.3-28	LEU High Fissile Mass Bounding Configuration	6.4.3-33
Table 6.4.3-29	Cask Interior Moderator Density and Blocked Cell Study Results	6.4.3-34
Table 6.4.4-1	NAC-LWT Cask with 25 PWR Rods, k_{eff} versus Fuel Rod Pitch, 5.0 w/o ^{235}U Initial Enrichment.....	6.4.4-10
Table 6.4.4-2	Reactivity with 25 PWR Rods vs. Basket Moderator Density, Normal Conditions, Infinite Array of Casks.....	6.4.4-11
Table 6.4.4-3	Reactivity with 25 PWR Rods vs. Basket Moderator Density, Accident Conditions, Infinite Array of Casks.....	6.4.4-12
Table 6.4.4-4	PWR Rods, Single Package 10 CFR 71.55(b)(3) Evaluation k_{eff} Summary.....	6.4.4-13
Table 6.4.4-5	NAC-LWT Cask with 25 BWR rods, k_{eff} versus Fuel Rod Pitch, 5.0 w/o ^{235}U Initial Enrichment.....	6.4.4-13
Table 6.4.4-6	Reactivity with 25 BWR Rods vs. Basket Moderator Density, Normal Conditions, Infinite Array of Casks.....	6.4.4-14
Table 6.4.4-7	Reactivity with 25 BWR Rods vs. Basket Moderator Density, Accident Conditions, Infinite Array of Casks	6.4.4-15
Table 6.4.4-8	BWR Rods, Single Package 10 CFR 71.55(b)(3) Evaluation k_{eff} Summary.....	6.4.4-16
Table 6.4.4-9	Maximum Reactivity Pitch Determination for 25 BWR Rods – Water Exterior.....	6.4.4-16
Table 6.4.4-10	Maximum Reactivity Pitch Determination for 25 PWR Rods – Water Exterior.....	6.4.4-17
Table 6.4.4-11	Maximum Reactivity Pitch Determination for 37 BWR Rods – Water Exterior.....	6.4.4-17

List of Tables (continued)

Table 6.4.4-12	Maximum Reactivity Pitch Determination for 37 PWR Rods – Water Exterior.....	6.4.4-18
Table 6.4.4-13	Maximum Reactivity Pitch Determination for 61 BWR Rods – Water Exterior.....	6.4.4-18
Table 6.4.4-14	Maximum Reactivity Pitch Determination for 61 PWR Rods – Water Exterior.....	6.4.4-19
Table 6.4.4-15	Maximum Reactivity Pitch Determination for 61 BWR Rods – Void Exterior.....	6.4.4-19
Table 6.4.4-16	Maximum Reactivity Pitch Determination for 61 PWR Rods – Void Exterior.....	6.4.4-20
Table 6.4.4-17	Maximum Reactivity Pitch Determination for 61 BWR Rods – Void Exterior and Preferential Flooding of Cask Cavity	6.4.4-20
Table 6.4.4-18	Maximum Reactivity Pitch Determination for 61 PWR Rods – Void Exterior and Preferential Flooding of Cask Cavity	6.4.4-21
Table 6.4.4-19	Damaged Rod Array Area Calculation – Flooded Cask Cavity	6.4.4-21
Table 6.4.4-20	Damaged Rod Array Area Calculation – Preferential Flooding.....	6.4.4-22
Table 6.4.4-21	Maximum Reactivity Determination for Homogenized UO ₂ /Water Mixture	6.4.4-22
Table 6.4.4-22	Homogenized UO ₂ /Water Cask Cavity Moderator Density Study Results - Void Exterior.....	6.4.4-22
Table 6.4.4-23	Homogenized UO ₂ /Water Cask Cavity Moderator Density Study Results - Water Exterior.....	6.4.4-23
Table 6.4.4-24	Homogenized UO ₂ /Water Exterior Moderator Density Study Results – Void Cask Cavity	6.4.4-23
Table 6.4.4-25	Homogenized UO ₂ /Water Exterior Moderator Density Study Results – Water Cask Cavity.....	6.4.4-24
Table 6.4.4-26	Single Cask Containment Reflected Results Comparison for Homogenized UO ₂ /Water Model	6.4.4-24
Table 6.4.5-1	Parametric Study – Fuel / Basket k-infinity versus TRIGA Fuel Element Type, Nonpoisoned Basket.....	6.4.5-18
Table 6.4.5-2	Parametric Study – Cask k _{eff} versus TRIGA Fuel Element Type, Poisoned Basket	6.4.5-19
Table 6.4.5-3	Axially Infinite Cask k _{eff} with TRIGA Fuel Elements- Fuel Element Placement Perturbations, Nonpoisoned Basket.....	6.4.5-20
Table 6.4.5-4	Axially Infinite Cask k _{eff} with TRIGA Fuel Elements - Fuel Element Placement Perturbations, Poisoned Basket	6.4.5-20
Table 6.4.5-5	Axially Infinite Cask k _{eff} with TRIGA Fuel Elements – Basket Manufacturing Tolerance Perturbations, Nonpoisoned Basket	6.4.5-21
Table 6.4.5-6	Axially Infinite Cask k _{eff} with TRIGA Fuel Elements – Basket Manufacturing Tolerance Perturbations, Poisoned Basket	6.4.5-21

List of Tables (continued)

Table 6.4.5-7	Screened Can Preferential Flooding and Partial Loading Reactivity Evaluations for TRIGA Fuel Elements, Nonpoisoned and Poisoned Baskets	6.4.5-22
Table 6.4.5-8	Sealed Can Preferential Flooding and Partial Loading Reactivity Evaluations for TRIGA Fuel Elements, Nonpoisoned and Poisoned Baskets	6.4.5-23
Table 6.4.5-9	Summary of Most Reactive Configurations, TRIGA Fuel Elements, Nonpoisoned Basket.....	6.4.5-24
Table 6.4.5-10	Summary of Most Reactive Configurations, TRIGA Fuel Elements, Poisoned Basket.....	6.4.5-24
Table 6.4.5-11	Reactivity Results for TRIGA Fuel Elements, Sealed Cans, Normal Conditions, Nonpoisoned Basket.....	6.4.5-25
Table 6.4.5-12	Reactivity Results for TRIGA Fuel Elements, Sealed Cans, Accident Conditions, Nonpoisoned Basket.....	6.4.5-26
Table 6.4.5-13	Reactivity Results for TRIGA Fuel Elements, Screened Cans, Normal Conditions, Poisoned Basket	6.4.5-27
Table 6.4.5-14	Reactivity Results for TRIGA Fuel Elements, Screened Cans, Accident Conditions, Poisoned Basket.....	6.4.5-28
Table 6.4.5-15	Single Package 10 CFR 71.55(b)(3) Evaluation k_{eff} Summary, TRIGA Fuel Element, Nonpoisoned Basket.....	6.4.5-29
Table 6.4.5-16	Single Package 10 CFR 71.55(b)(3) Evaluation k_{eff} Summary, TRIGA Fuel Element, Poisoned Basket	6.4.5-29
Table 6.4.5-17	Fuel Element Physical Characteristics Evaluation	6.4.5-30
Table 6.4.5-18	Element Variation to Reduce k_s Below 0.95	6.4.5-31
Table 6.4.5-19	General Model Configuration – Dry to Wet System Reactivity Changes, 70 wt% ^{235}U Stainless Steel Clad Fuel - Nominal Fuel Parameters.....	6.4.5-31
Table 6.4.5-20	Primary Fuel Type Reactivity Comparison – Accident Conditions Eight-Cask Array (No Cans).....	6.4.5-32
Table 6.4.5-21	Normal Condition Maximum System Reactivities (No Cans) ²	6.4.5-32
Table 6.4.6-1	Cask k_{eff} with TRIGA Fuel Cluster Rods – Fuel Rod Placement Perturbations, Nonpoisoned Basket	6.4.6-7
Table 6.4.6-2	Cask k_{eff} with TRIGA Fuel Cluster Rods – Fuel Rod Placement Perturbations, Poisoned Basket.....	6.4.6-7
Table 6.4.6-3	Axially Infinite Cask k_{eff} with TRIGA Fuel Cluster Rods – Basket and Insert Manufacturing Tolerance Perturbations, Nonpoisoned Basket.....	6.4.6-8
Table 6.4.6-4	Axially Infinite Cask k_{eff} with TRIGA Fuel Cluster Rods – Basket and Insert Manufacturing Tolerance Perturbations, Poisoned Basket.....	6.4.6-9
Table 6.4.6-5	Sealed Can Preferential Flooding and Partial Loading Reactivity Evaluations for TRIGA Fuel Rod Clusters, Nonpoisoned Basket	6.4.6-10
Table 6.4.6-6	Sealed Can Preferential Flooding and Partial Loading Reactivity Evaluations for TRIGA Fuel Rod Clusters, Poisoned Basket	6.4.6-10

List of Tables (continued)

Table 6.4.6-7	Summary of Most Reactive Configurations, TRIGA Fuel Cluster Rods, Nonpoisoned Basket.....	6.4.6-11
Table 6.4.6-8	Summary of Most Reactive Configurations, TRIGA Fuel Cluster Rods, Poisoned Basket.....	6.4.6-11
Table 6.4.6-9	Reactivity Results for TRIGA Fuel Cluster Rods, Sealed Cans, Normal Conditions, Nonpoisoned Basket	6.4.6-12
Table 6.4.6-10	Reactivity Results for TRIGA Fuel Cluster Rods, Sealed Can, Accident Conditions, Nonpoisoned Basket.....	6.4.6-13
Table 6.4.6-11	Reactivity Results for TRIGA Fuel Cluster Rods, Sealed Cans, Normal Conditions, Poisoned Basket	6.4.6-14
Table 6.4.6-12	Reactivity Results for TRIGA Fuel Cluster Rods, Sealed Cans, Accident Conditions, Poisoned Basket	6.4.6-15
Table 6.4.6-13	Single Package 10 CFR 71.55(b)(3) Evaluation k_{eff} Summary, TRIGA Fuel Cluster Rod, Nonpoisoned Basket	6.4.6-16
Table 6.4.6-14	Single Package 10 CFR 71.55(b)(3) Evaluation k_{eff} Summary, TRIGA Fuel Cluster Rod, Poison Basket.....	6.4.6-16
Table 6.4.6-15	Increased Fuel Dimensional Parameter k_{eff} Summary, TRIGA Fuel Cluster Rod, Nonpoisoned Basket	6.4.6-17
Table 6.4.7-1	Normal Condition HEU, LEU, MEU DIDO Evaluation	6.4.7-7
Table 6.4.7-2	HEU DIDO Accident Evaluation – Radial Shift and Exterior Moderator Density Variation	6.4.7-8
Table 6.4.7-3	DIDO Heat Shunt and Aluminum Shell Evaluation Results	6.4.7-8
Table 6.4.7-4	DIDO Basket Geometric Tolerance Study Results.....	6.4.7-8
Table 6.4.7-5	DIDO Fuel Assembly Tolerance Study Results	6.4.7-9
Table 6.4.7-6	DIDO Fuel Maximum Reactivity Combinations.....	6.4.7-10
Table 6.4.7-7	Moderator Density Study for the Infinite Array of Casks (Nominal Fuel and Basket Configuration)	6.4.7-11
Table 6.4.7-8	DIDO Single Package 10 CFR 71.55(b)(3) Evaluation k_{eff} Summary..	6.4.7-12
Table 6.4.7-9	DIDO Fuel Assembly Tolerance Study Results (Reduced Clad Thickness).....	6.4.7-12
Table 6.4.7-10	DIDO Fuel Maximum Reactivity Combinations (Reduced Clad Thickness).....	6.4.7-12
Table 6.4.7-11	DIDO Fuel Maximum Reactivity Combinations (Reduced Clad and Maximum Pitch)	6.4.7-13
Table 6.4.7-12	DIDO Bounding Configurations	6.4.7-14
Table 6.4.8-1	GA IFM Payload Evaluation Result Summary	6.4.8-5
Table 6.4.8-2	GA IFM TRIGA Rectangular Array Pitch Evaluation Result Summary	6.4.8-6
Table 6.4.8-3	GA IFM TRIGA Square Array Pitch Evaluation Result Summary	6.4.8-6
Table 6.4.8-4	GA IFM Interior Moderator Density Evaluation Result Summary.....	6.4.8-7
Table 6.4.8-5	GA IFM HTGR Matrix Moderator Density Evaluation Result Summary	6.4.8-8
Table 6.4.8-6	GA IFM Exterior Moderator Density Evaluation Result Summary.....	6.4.8-9

List of Tables (continued)

Table 6.4.8-7	GA IFM Partial Flooding Comparison Result Summary	6.4.8-10
Table 6.4.8-8	GA IFM Partial Flooding Interior Moderator Density, Void Exterior Result Summary	6.4.8-10
Table 6.4.8-9	GA IFM Partial Flooding Interior Moderator Density, Water Exterior Result Summary	6.4.8-11
Table 6.4.8-10	GA IFM Partial Flooding Exterior Moderator Density, Void Interior Result Summary	6.4.8-12
Table 6.4.8-11	GA IFM Partial Flooding Exterior Moderator Density, Water Interior Result Summary	6.4.8-13
Table 6.4.8-12	GA IFM Partial Flooding Single Cask Result Comparison	6.4.8-13
Table 6.4.8-13	GA IFM Damaged TRIGA Fuel Result Summary	6.4.8-14
Table 6.4.9-1	PULSTAR Intact Assembly Shift Results.....	6.4.9-7
Table 6.4.9-2	PULSTAR Intact Assembly Mechanical Perturbation Results	6.4.9-7
Table 6.4.9-3	PULSTAR Intact Assembly Lattice Moderator Ratio Results	6.4.9-8
Table 6.4.9-4	PULSTAR Canned Intact Element Results	6.4.9-8
Table 6.4.9-5	PULSTAR Canned Homogenized Element Results.....	6.4.9-9
Table 6.4.9-6	PULSTAR Maximum Reactivity Summary.....	6.4.9-10
Table 6.4.10-1	Spiral Fuel Assembly - Base Data Comparisons.....	6.4.10-9
Table 6.4.10-2	Spiral Fuel Assembly - Basket Tolerance Evaluations.....	6.4.10-10
Table 6.4.10-3	Spiral Fuel Assembly – Fuel Tolerance Evaluations.....	6.4.10-11
Table 6.4.10-4	Spiral Fuel Assembly - Moderator Density Variations	6.4.10-12
Table 6.4.10-5	Spiral Fuel Assembly - Maximum Reactivity Case Summary	6.4.10-13
Table 6.4.10-6	MOATA Plate Bundle - Base Data Comparisons	6.4.10-14
Table 6.4.10-7	MOATA Plate Bundle – Basket Tolerance Evaluations	6.4.10-15
Table 6.4.10-8	MOATA Plate Bundle - Fuel Tolerance Evaluations.....	6.4.10-16
Table 6.4.10-9	MOATA Plate Bundle - Moderator Density Variations.....	6.4.10-17
Table 6.4.10-10	MOATA Plate Bundle - Maximum Reactivity Case Summary	6.4.10-18
Table 6.5.1-1	KENO-Va and 27-Group Library Validation Statistics.....	6.5.1-11
Table 6.5.2-1	Criticality Results for High Enrichment Uranium Systems	6.5.2-3
Table 6.7.1-1	PWR MOX Fuel Analysis Compositions and Number Densities	6.7.1-7
Table 6.7.1-2	PWR MOX Fuel Analysis Isotope Weight Fraction	6.7.1-7
Table 6.7.1-3	PWR MOX Rod Shipment - Reactivity as a Function of Geometry and Material.....	6.7.1-14
Table 6.7.1-4	PWR MOX Fuel Shipment – Fuel Rod Pitch Study	6.7.1-15
Table 6.7.1-5	PWR MOX Fuel Shipment – Optimum Moderator Study Maximum Reactivity Summary	6.7.1-15
Table 6.7.1-6	PWR MOX Fuel Shipment Reactivity Summary for Single Cask Containment Fully Reflected Cases	6.7.1-16
Table 6.7.1-7	PWR MOX Fuel Shipment Reactivity Summary for Normal Condition Array Cases.....	6.7.1-16
Table 6.7.1-8	PWR MOX Fuel Shipments – Summary of Maximum Reactivity Configurations	6.7.1-17

List of Tables (continued)

Table 6.7.1-9	PWR MOX Fuel Shipments – PWR MOX Comparison to Area of Applicability.....	6.7.1-17
Table 6.7.1-10	PWR MOX Fuel Shipments – UO ₂ Comparison to Area of Applicability.....	6.7.1-18
Table 6.7.1-11	Bounding Parameters for PWR MOX/UO ₂ Rod Shipments.....	6.7.1-18
Table 6.7.2-1	LEU Range of Applicability for Complete Set of 186 Benchmark Experiments	6.7.2-7
Table 6.7.2-2	LEU Correlation Coefficients and USLs for Benchmark Experiments ..	6.7.2-8
Table 6.7.2-3	LEU MCNP Validation Statistics	6.7.2-15
Table 6.7.2-4	PWR MOX Range of Applicability for Complete Set of 59 Benchmark Experiments	6.7.2-39
Table 6.7.2-5	PWR MOX Correlation Coefficients and USLs for Benchmark Experiments	6.7.2-40
Table 6.7.2-6	MCNP Validation Statistics.....	6.7.2-46

6 CRITICALITY EVALUATION

The NAC-LWT cask is designed to transport either 1 pressurized water reactor (PWR) assembly; up to 25 intact PWR or BWR rods in a rod holder or fuel assembly lattice; up to 25 PWR or BWR fuel rods with a maximum of 14 of the rods classified as damaged in a rod holder; up to 16 PWR UO₂ or MOX rods in a rod holder; 2 boiling water reactor (BWR) assemblies; 15 sound metallic fuel rods; 6 failed metallic fuel rods; up to 42 high enriched uranium (HEU), medium enriched uranium (MEU) or low enriched uranium (LEU) Materials Test Reactor (MTR) fuel elements, or DIDO fuel assemblies; up to 140 TRIGA fuel elements; two packages of General Atomics Irradiated Fuel Material (GA IFM); up to 560 TRIGA fuel cluster rods; 1 consolidation canister with up to 300 TPBARs (including up to 2 damaged TPBARs); up to 700 PULSTAR fuel elements; up to 42 spiral fuel assemblies; or up to 42 MOATA plate bundles. This chapter illustrates that all packages meet the requirements of parts 71.55, 71.59 and 71.71 of 10 CFR 71.

In accordance with the requirements of 10 CFR 71.59 (b), the NAC-LWT cask is assigned a Criticality Safety Index (CSI) for criticality control for the authorized contents as follows: 100 for PWR assemblies; 5 for BWR assemblies; 12.5 for DIDO assemblies; 0 for metallic fuel, TPBARs, spiral fuel assemblies; MOATA plate bundles, high burnup PWR (UO₂ or MOX) or BWR rods with up to 14 damaged rods, MTR elements, TRIGA fuel elements loaded into a poisoned basket, TRIGA fuel cluster rods, TRIGA payloads with screened cans containing up to four TRIGA elements in a nonpoisoned basket, and GA IFM packages. The CSI for PULSTAR fuel is 0 for a payload of intact elements and 33.4 for a mixed payload of intact and damaged elements.

6.1 Discussion and Results

Analyses are performed on the NAC-LWT cask for one PWR assembly and two BWR assemblies. Both PWR and BWR packages are examined for normal transport conditions and hypothetical accident conditions. The hypothetical accident conditions are modeled with the fuel at its most reactive credible configuration. The design of the cask and the fuel basket is such that, under all conditions, the highest neutron multiplication factor with correction for bias and uncertainty is less than 0.95. Analyses to demonstrate conformance to this criterion include (1) no dissolved boron in the neutron shield tank, thus improving the shield tank neutron reflection, (2) no structural material present in the assembly, and (3) no dissolved boron in the cask cavity or surrounding loading or storage area. No credit is included for burnup or for the buildup of fission product neutron poisons.

Analyses are performed for the NAC-LWT cask with the most limiting single PWR assembly and also for the most limiting BWR assemblies. Sections 6.3.1 and 6.3.2 present the methods (CSAS25) and KENO-Va models used in the analysis for each of these respective fuel assemblies. Sections 6.4.1 and 6.4.2 present the criticality analysis results for the PWR and BWR fuel assemblies, respectively. The maximum PWR fuel enrichment is set at 3.7 w/o ^{235}U , but it was found that certain PWR fuel assemblies were required to be limited to a maximum uranium enrichment of 3.5 w/o ^{235}U . Thus, two design-basis PWR assemblies were consequently selected. Namely, a design basis case with the uranium enrichment limited to 3.7 w/o ^{235}U and a second design basis case for those assemblies with the uranium enrichment limited to 3.5 w/o ^{235}U .

Analyses are performed on the NAC-LWT with fuel baskets designed to transport up to 42 MTR research reactor fuel elements. Shipment of MTR loose fuel plates is evaluated inside an MTR plate canister. Section 6.3.2 presents the methods (CSAS25) and KENO-Va models used in the analysis. Section 6.4.3 presents the criticality analysis results of the NAC-LWT loaded with MTR fuel. Section 6.5.2 presents the validation of CSAS25 for use in criticality evaluations of MTR fuel. Criticality of the NAC-LWT cask with the most limiting MTR fuel assembly type and basket configuration is evaluated. The fuel assemblies are assumed to be unburned. An infinite array of casks of infinite axial extent is analyzed. The cask/basket configuration is examined for normal transport and accident conditions. Both normal and accident conditions consider variation in moderator density inside and outside the cask as well as the spacing between casks. Reactivity penalties for mechanical perturbations are also considered. The results show that the k_{eff} of an infinite array of NAC-LWT casks with the most limiting MTR fuel and at optimum interspersed moderation is always below 0.95 including the method bias, method uncertainty, Monte Carlo uncertainty and penalties due to mechanical perturbations.

Analyses are performed on the NAC-LWT with up to 25 PWR or BWR fuel rods of 5.0 w/o ^{235}U initial enrichment. Separate evaluations are performed for a payload consisting of only intact rods in a rod holder, a payload including up to 14 damaged rods in a rod holder, and rods in a fuel assembly lattice. Section 6.3.3 presents the methods (CSAS25) and KENO-Va model used in the rod holder or fuel assembly lattice analyses. Section 6.4.4 presents the criticality analysis results of the NAC-LWT loaded with up to 25 PWR or BWR fuel rods in either a rod holder or a fuel assembly lattice. The system reactivity of the NAC-LWT with up to 25 PWR or BWR fuel rods in intact (rod holder or lattice) or damaged configurations is evaluated as a function of rod pitch. Damaged fuel evaluations include the removal of clad and fuel and moderator mixture studies. The fuel is assumed to be fresh, i.e., no burnup credit. An infinite array of casks is analyzed. Variation of moderator density inside and outside the cask also is considered. The results show that the k_{eff} of an infinite array of NAC-LWT casks at optimum fuel rod pitch and at optimum interspersed moderation is significantly below 0.95 including the method bias, method uncertainty and Monte Carlo uncertainty.

Poisoned and nonpoisoned basket configurations of the NAC-LWT cask are evaluated for TRIGA fuel elements with up to 70 w/o ^{235}U initial enrichment and TRIGA fuel cluster rods with up to 93.3 w/o ^{235}U initial enrichment. The placement of sealed canisters in the top and bottom baskets of the cask is also evaluated to permit the transport of failed TRIGA fuel. Section 6.3.4 presents the methods (CSAS25) and the models used in the analyses. Section 6.4.5 presents the criticality analysis results for the NAC-LWT cask loaded with TRIGA fuel elements, while Section 6.4.6 presents the results for TRIGA fuel cluster rods. The fuel is assumed to be fresh (unirradiated) and the effects of burnable absorbers are conservatively ignored. An infinite array of casks is analyzed. Variation of moderator density inside and outside the cask is considered. Variation of geometrical configurations are also analyzed, including the tolerances of the TRIGA basket materials and fuel element positioning, to determine the most reactive configuration. The results show that the k_{eff} of an array of NAC-LWT casks with TRIGA fuel at optimum fuel element pitch, geometrical configuration, and optimum moderation is always below 0.95, including corrections for bias and uncertainty. An infinite cask array is evaluated for the poisoned and nonpoisoned TRIGA cluster rod baskets and the poisoned TRIGA fuel element basket, while a finite cask array is applied to the nonpoisoned TRIGA fuel element evaluations.

Analyses are performed on the NAC-LWT with fuel baskets designed to transport up to 42 DIDO fuel assemblies. Section 6.1.1 presents the methods (CSAS25) and KENO-VA models used in the analysis. Section 6.4.7 presents the criticality analysis results of the NAC-LWT loaded with DIDO fuel. Section 6.5.2 presents the validation of CSAS25 for use in criticality evaluations of DIDO fuel. Criticality of the NAC-LWT cask with the most limiting DIDO fuel assembly type (HEU) and basket configuration is evaluated. The fuel elements are assumed to be unburned.

An infinite array of casks of infinite axial extent is analyzed. The cask/basket configuration is examined for normal transport and accident conditions. Variations in moderator density inside and outside the cask are evaluated. Reactivity penalties for mechanical perturbations are also considered. The results show that the bias adjusted k_{eff} of an infinite array of NAC-LWT casks with the most limiting DIDO fuel under accident conditions at optimum interspersed moderation (void) is above 0.95. Limiting the accident array to a maximum of eight casks results in a k_{eff} below 0.95 including the method bias, method uncertainty, Monte Carlo uncertainty and penalties due to mechanical perturbations.

Analyses are performed of the NAC-LWT with a fuel basket designed to transport two Fuel Handling Units (packages) of General Atomics (GA) Irradiated Fuel Material (IFM). The first IFM package is composed of Reduced-Enrichment Research and Test Reactor (RERTR) type TRIGA fuel and the second is composed of High-Temperature Gas-cooled Reactor (HTGR) type fuel. Each set of IFM is packaged into stainless steel weld-encapsulated primary and secondary enclosures. Section 6.3.8 presents the methods (CSAS25) and KENO-Va models used in the analyses. Section 6.4.8 presents the criticality analysis results of the two GA IFM packages in the NAC-LWT. Section 6.1.1 presents the validation of CSAS25 for use in criticality evaluations of TRIGA fuel, which is deemed relevant for the GA IFM as discussed in Section 6.4.8. Criticality of the NAC-LWT cask with GA IFM is evaluated using pre-irradiation material compositions. No credit is taken for the basket structure axially or radially, and an infinite array of casks of infinite axial extent is analyzed. Variations in moderator density inside and outside the cask are evaluated, as well as the partial flooding of the IFM packages. The results show that the bias adjusted k_{eff} of an infinite array of NAC-LWT casks under accident conditions at optimum internal and interstitial moderation is less than 0.95, including corrections for bias and uncertainty. Maximum reactivity is obtained with flooded IFM packages, a void NAC-LWT cavity, and a void exterior.

The metallic fuel rods are not analyzed because the metallic fuel is at natural enrichment, and cannot become critical without the presence of heavy water (Paxton).

Criticality evaluations for the NAC-LWT loaded with TPBARs (Tritium Producing Burnable Absorber Rods) are not required because the TPBARs do not contain fissile material and, therefore, cannot form a critical configuration.

Analyses are performed of the NAC-LWT with a stack of four 28 MTR 7-element modules with a PULSTAR fuel element payload. PULSTAR fuel assemblies are comprised of a 5×5 rectangular fuel element array surrounded by a Zircaloy box with aluminum upper and lower fittings. The fuel elements are Zircaloy-clad UO_2 pellets conservatively evaluated at an enrichment of 6.5 wt % ^{235}U . PULSTAR fuel assemblies may be loaded directly into the module

cells. Individual intact PULSTAR fuel elements may be loaded into either a 4×4 fuel rod insert, or one of two PULSTAR cans. The can loadings are only permissible in the top and base modules. Damaged PULSTAR fuel elements or debris must be loaded into either of the cans. Section 6.3.7 presents the methods (CSAS25) and KENO-Va models used in the analyses. Section 6.4.9 presents the criticality analyses results of the various permissible loading configurations. Section 6.5.1-1 presents the validation of CSAS25 for use in criticality evaluations of PWR and BWR fuel, which is deemed relevant for PULSTAR fuel as discussed in Section 6.4.9. Criticality is evaluated using pre-irradiation material compositions. The basket structure axial and radial extents are explicitly modeled in a cask of finite axial extent. Cask arrays analyzed are dependent on the payload of either intact fuel or a mixed loading of intact fuel and canned elements. Variations in moderator density inside and outside the cask are evaluated, as well as the preferential flooding of the cans. The results show that the bias adjusted k_{eff} under accident conditions at optimum internal and interstitial moderation is less than 0.95, including corrections for bias and uncertainty. Maximum reactivity is obtained for a preferentially flooded cask containing two modules baskets of intact fuel assemblies and two modules of cans (each can contains 25 damaged fuel elements). Preferential flooding in this case is a void NAC-LWT cavity, flooded fuel cans, and a void cask exterior (including a void neutron shield).

Analyses are performed on the NAC-LWT with ANSTO fuel baskets designed to transport up to 42 spiral fuel assemblies, 42 MOATA plate bundles, or a combination of spiral assembly baskets and plate bundle baskets. Section 6.3.8 presents the methods (CSAS25) and KENO-VA models used in the analysis. Section 6.4.10 presents the criticality analysis results of the NAC-LWT loaded with spiral fuel assemblies or plate bundles. Section 6.5.2 presents the validation of CSAS25 for use in criticality evaluations of the ANSTO basket. Criticality of the NAC-LWT cask with the most limiting fuel characteristics and basket configuration is evaluated. The fuel elements are assumed to be unburned. An infinite array of casks in both the radial and axial extent is analyzed. The cask/basket configuration is examined for normal transport and accident conditions. Variations in moderator density inside and outside the cask are evaluated. Reactivity penalties for mechanical perturbations are also considered. The results show that the bias adjusted k_{eff} of an infinite array of NAC-LWT casks with the most-limiting ANSTO basket payload under normal and accident conditions at optimum interspersed moderation (void) is below 0.95.

Analyses are performed on the NAC-LWT with up to 16 PWR (UO₂ or MOX) fuel rods. UO₂ fuel rods are permitted with up to 5.0 wt % ²³⁵U initial enrichment. Mixed oxide (MOX) rods are evaluated up to 7 wt % fissile plutonium (²³⁹Pu + ²⁴¹Pu). The payload consists of undamaged

fuel rods (i.e., no gross fuel failure, hairline cracks or pinholes are allowed). All evaluation detail, including input, method, analysis results and critical benchmarks, are included in Section 6.7.1. Included are the fuel rod geometry and material description, the MCNP model used in the rod holder analyses, and the criticality analysis results of the NAC-LWT loaded with up to 16 PWR rods (fueled with either UO_2 or MOX material). The system reactivity of the NAC-LWT with up to 16 undamaged PWR rods is evaluated as a function of rod pitch. The fuel is assumed to be fresh, i.e., no burnup credit. An infinite array of casks is analyzed. Variation of moderator density inside and outside the cask is considered. Also included in the analysis are preferential flooding evaluations of the canister that contains the rod array. The results show that the bias adjusted k_{eff} of an infinite array of NAC-LWT casks at optimum fuel rod pitch and at optimum interspersed moderation is significantly below the upper safety limit (USL) for MOX and UO_2 critical benchmarks.

6.7 Payload Specific Details

This section contains NAC-LWT cask payload specific evaluation detail.

6.7.1 PWR Mixed Oxide Fuel Rods

This section includes input, analysis method, results, and critical benchmark evaluations for the NAC-LWT cask containing a payload of up to 16 PWR rods. The PWR rods may be composed of uranium oxide fuel pellets or mixed oxide fuel pellets (depleted or natural uranium oxide with plutonium oxide contributing the primary quantity of fissile material).

6.7.1.1 Package Fuel Loading

The NAC-LWT cask may transport up to 16 undamaged PWR fuel rods in a fuel rod holder. To bound all PWR MOX rods that may be transported in the NAC-LWT cask, UO₂ rods are evaluated with enrichments up to 5.0 wt % ²³⁵U, while MOX rods were evaluated up to 7 wt % fissile plutonium. Characteristics of the design basis PWR rods are presented in Table 6.7.1-1 and Table 6.7.1-2. Given a fixed fissile material density, defined by a maximum UO₂ enrichment or fissile plutonium weight percent, the most reactive rod has the greatest fissile mass, i.e., the rod with the largest pellet radius. Therefore, the CE 14×14 pellet diameter of 0.3765 inch is chosen as the base radius for the most reactive PWR fuel rod evaluated here. A conservative maximum fissile material length of 153.5 inches is also applied. As a maximum reactivity fuel pitch is established, and the zirconium alloy is essentially transparent to neutrons, the clad thickness has no significant effect on the analysis.

6.7.1.2 Criticality Model Specifications

This section describes the models that are used in the criticality analyses for the NAC-LWT cask containing up to 16 PWR rods. PWR rods are either low enriched uranium oxide (maximum 5 wt % ²³⁵U) fueled or MOX fueled. The models are analyzed separately under normal conditions and hypothetical accident conditions to ensure that all possible configurations are subcritical.

The model uses the MCNP5 code package with the ENDF/B-VI cross-section set. No cross-section pre-processing is required prior to MCNP implementation. MCNP uses the Monte Carlo technique to calculate the k_{eff} of a system. In these analyses, approximately 530 cycles with 1,000 neutron histories per cycle are tracked through the system.

Description of Calculational Models

The MCNP model of the NAC-LWT cask with 16 undamaged PWR rods includes triangular and square lattice formation of design basis rods centered in the cask cavity. No credit is taken for geometry control provided by the rod holder. The fuel rods, cask cavity and radial shields are explicitly modeled as shown in the Figure 6.7.1-1 model sketch.

The model of the NAC-LWT cask takes advantage of the universe structure of MCNP. Each universe defines an infinite space, bounded after its insertion into a containing cell. Four universes are employed herein. The "0" universe defines the cask universe. The remaining universes are discussed in the following sections. Each universe is developed independently as surfaces and cells. Fuel rod array surfaces and cells are configured to place the rods in either a rectangular (square) pitch array or a hex (triangular) pitch array. The rod pitch is a variable input into the model and is modified to achieve a maximum reactivity configuration. In the basket universe, the rod array is placed into a square (RPP) body that allows the moderator density outside the rod array to be adjusted independently.

The modeled accident condition completely removes the neutron shielding, the neutron shield tank and the cask impact limiters. In the normal conditions model, the impact limiter diameter is modeled as identical to the neutron shield tank diameter. This allows for closer packing for the cask array than physically possible.

VISED sketches of the assembled geometry are shown in Figure 6.7.1-2 through Figure 6.7.1-4. The cask outer surface is surrounded by a rectangular body with reflecting boundary conditions. The boundary conditions are imposed on the sides, top and bottom, which simulates an infinite array of casks.

Package Regional Densities

The composition densities (g/cc) and nuclide number densities (atm/b-cm) used in the subsequent criticality analyses are shown in Table 6.7.1-1. The various isotope weight compositions used in the MOX/UO₂ rod analysis are listed in Table 6.7.1-2.

Figure 6.7.1-1 MCNP Model Sketch of the NAC-LWT Cask with PWR MOX/UO₂ Rods
(Dimensions in centimeters)

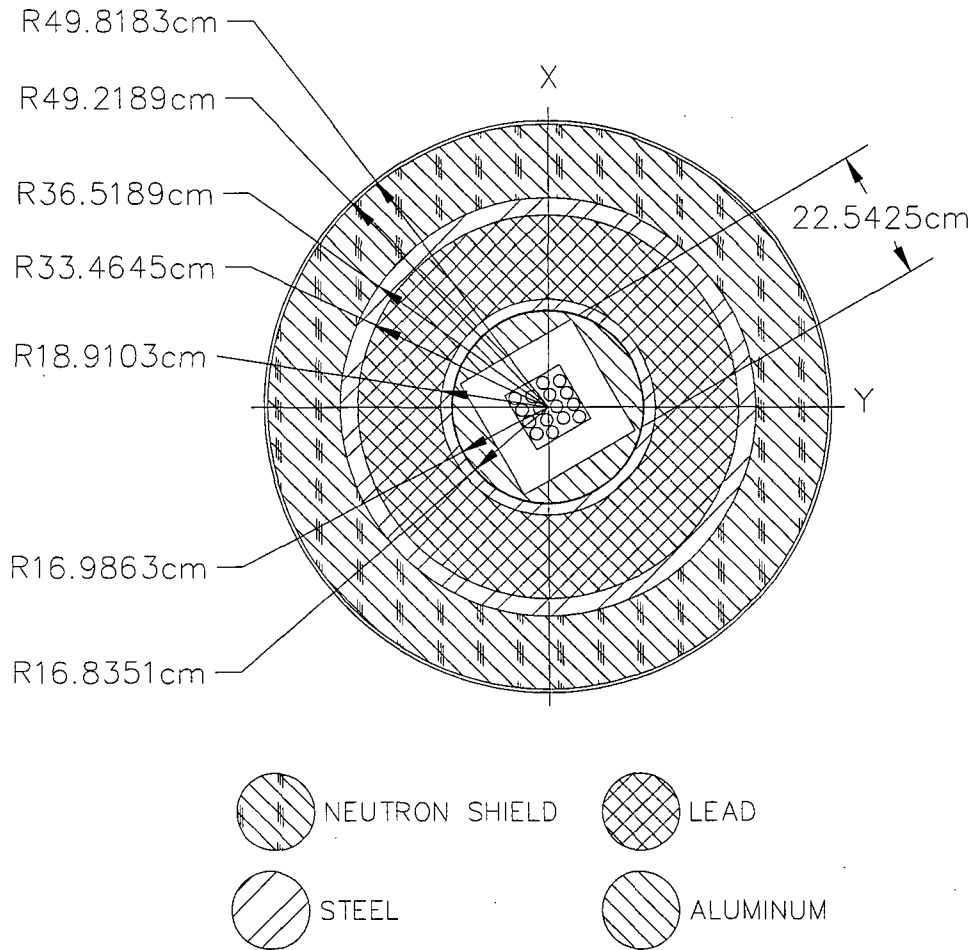


Figure 6.7.1-2 VISED Sketch of LWT Radial View – Hex Rod Array– Normal Conditions

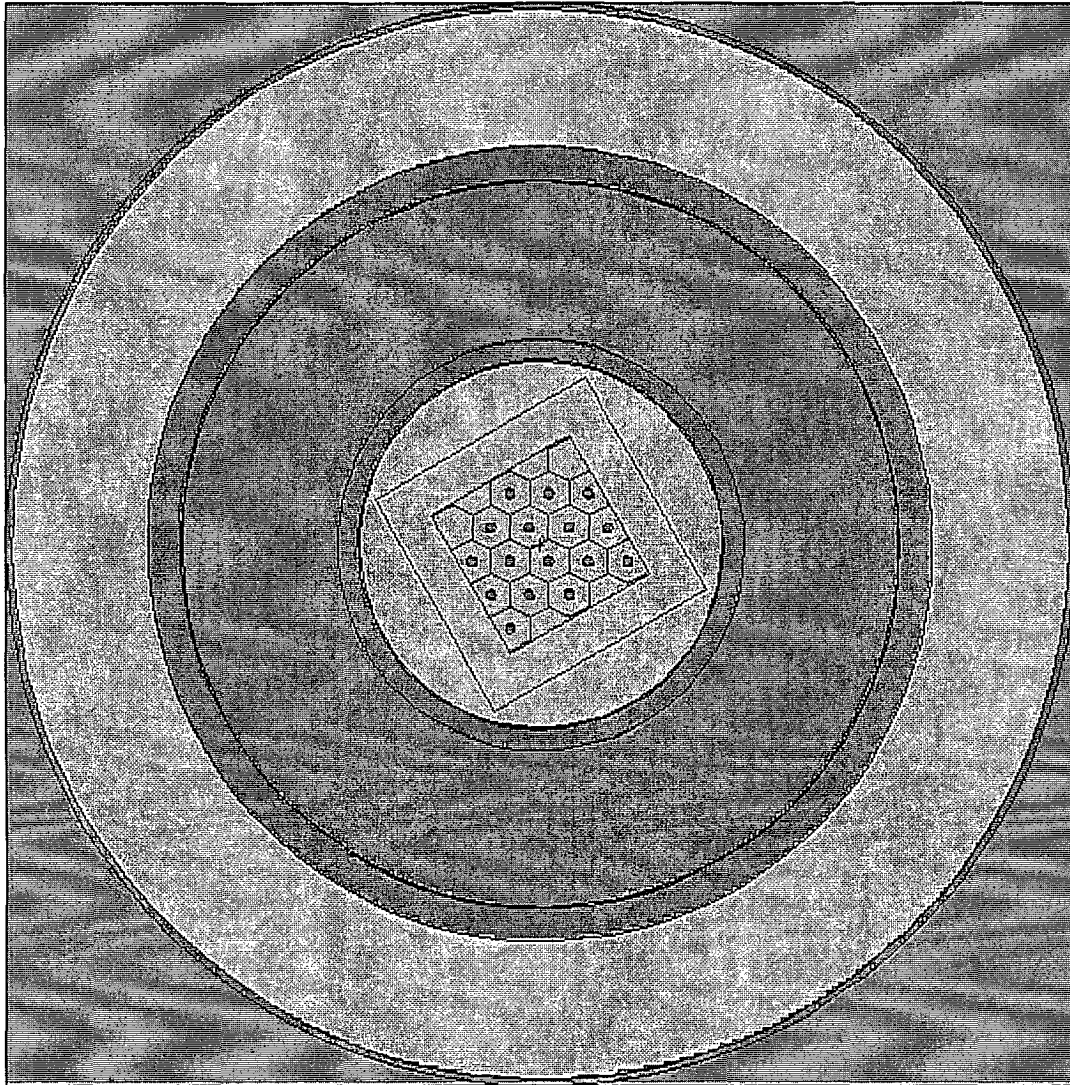


Figure 6.7.1-3 VISED Sketch of LWT Radial View – Square Rod Pitch -
Accident Conditions

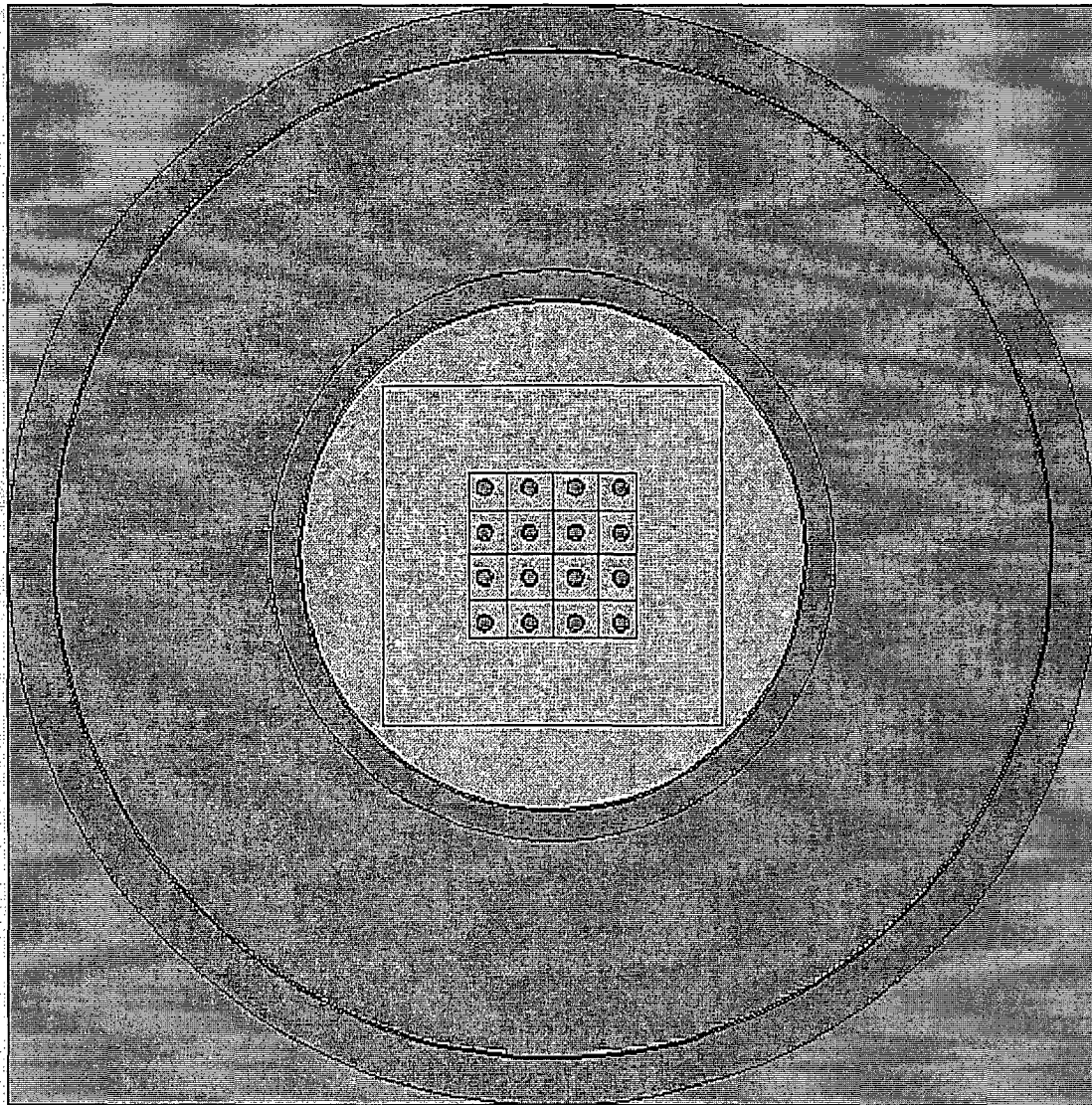


Figure 6.7.1-4 VISED Sketch of LWT Axial View – Accident Conditions

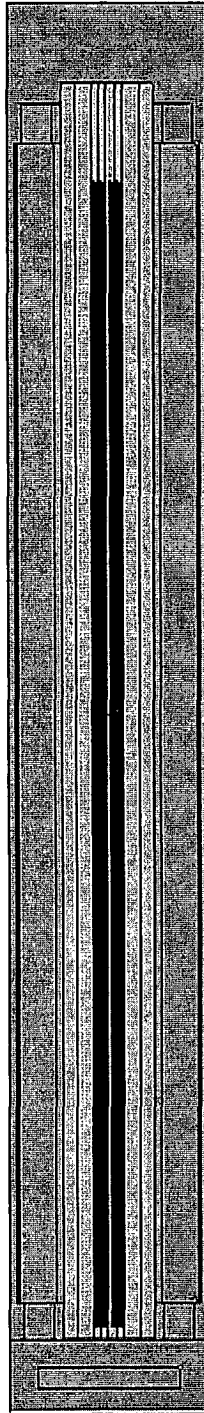


Table 6.7.1-1 PWR MOX Fuel Analysis Compositions and Number Densities

Material	5.0% Enriched UO ₂	Weapons Grade (7 wt % Fissile Pu) ¹	Zirconium Alloy	H ₂ O	304 Stainless Steel	Pb	Al
Density, g/cc	10.522	10.556	6.56	0.9982	7.920	11.344	2.702
Density	atoms/b-cm						
Uranium-235	1.19E-03	1.54E-04					
Uranium-238	2.23E-02	2.16E-02					
Plutonium-238		9.15E-07					
Plutonium-239		1.70E-03					
Plutonium-240		1.09E-04					
Plutonium-241		7.23E-06					
Plutonium-242		9.00E-07					
Oxygen	4.70E-02	4.70E-02		3.338E-2			
Hydrogen				6.677E-2			
Zirconium Alloy			4.331E-2				
Iron					5.936E-2		
Chromium					1.743E-2		
Nickel					7.721E-3		
Manganese					1.736E-3		
Lead						3.297E-2	
Aluminum							6.031E-2

Table 6.7.1-2 PWR MOX Fuel Analysis Isotope Weight Fraction²

Isotope	UO ₂	Weapon Grade	Fuel Grade	Power Grade	MOX Services
²³⁵ U	5	0.7	0.7	0.7	0.7
²³⁸ U	95	99.3	99.3	99.3	99.3
²³⁸ Pu	0	0.05	0.1	1	0.05
²³⁹ Pu	0	93.5	86.1	62	95
²⁴⁰ Pu	0	6	12	22	4.5
²⁴¹ Pu	0	0.4	1.6	12	0.4
²⁴² Pu	0	0.05	0.2	3	0.05

¹ Sample composition.

² Typical fresh fuel MOX material is composed of depleted uranium at 0.2 to 0.3 wt % ²³⁵U. A bounding natural uranium enrichment of 0.7 wt % ²³⁵U is used in the criticality evaluations.

6.7.1.3 Criticality Calculations

This section presents the criticality analysis for the NAC-LWT cask with up to 16 PWR UO₂ or MOX rods. UO₂ rods are enriched up to 5.0 wt % ²³⁵U initial enrichment, while MOX rods contain up to 7 wt % fissile plutonium. No credit is taken for geometry control that is provided by the rod holder and no rod positions are specified for the rods in the lattice. Since various fuel rod arrangements may be shipped, the criticality of the PWR MOX rods in the NAC-LWT cask cavity is studied to determine the optimum pitch and, therefore, the maximum k_{eff} for the cask.

Criticality results are divided into individual sets of analyses.

- Evaluate the NAC-LWT accident configuration to demonstrate that, at a fixed fissile plutonium content, the maximum fissile percentage material (MOX Services definition) produces the maximum reactivity configuration.
- Determine the maximum reactivity pitch of the most reactive fuel material.
- Run the optimum moderator density evaluation.
- Evaluate normal condition and single cask “containment reflected” cases.

Included in all analyses are hypothetical plutonium compositions solely to justify the removal of the plutonium compositions as a licensing limit.

Rod Geometry and Material Composition Studies

Each of the material compositions is evaluated for the maximum fissile material mass rod. Fissile material in the uranium oxide rods is limited by the 5 wt % ²³⁵U enrichment constraint, while the MOX material is limited by the 7 wt % fissile plutonium input. In addition to the physically realistic MOX material descriptions, three hypothetical MOX materials are evaluated: one containing all fissile plutonium (adding into ²⁴¹Pu the remaining plutonium weight fractions), an all ²³⁹Pu material and an all ²⁴¹Pu material. The following nomenclature is used to describe the various plutonium fuel materials.

Abbreviation	Material
PG	Power grade plutonium isotopic distribution
FG	Fuel grade plutonium isotopic distribution
WG	Weapons grade plutonium isotopic distribution
MS	MOX Services “WG type” material
FP	Plutonium is modeled as all fissile plutonium
P9	Plutonium is modeled as all ²³⁹ Pu
P1	Plutonium is modeled as all ²⁴¹ Pu

All cases are evaluated at a hexagonal pitch of 3.0 and 3.6 cm. Based on scoping evaluations, as validated in the following section, these fuel rod pitches approximate maximum reactivity configurations over a range of material composition.

As shown in later moderator density studies, maximum reactivity moderation is achieved by a preferentially flooded lattice with a void gap to the cask cavity. Fuel material and pitch studies are based on a flooded cask cavity. As these studies primarily rely on the interaction between rods in the lattice, rather than between casks, applying the results of the flooded cavity to the dry cavity/wet lattice is acceptable.

As seen in Table 6.7.1-3, maximum reactivity for physically realistic plutonium compositions is achieved by the MOX Services material. This result was expected as the MOX Services composition model contains the maximum fissile material within the plutonium oxide matrix. For the hypothetical compositions, the all ^{241}Pu case produces maximum reactivity. As the ^{241}Pu isotope has the highest fission cross-section, this result is to be expected.

Maximum Reactivity Rod Pitch Evaluation

The maximum fissile mass rod configuration is evaluated with uranium oxide, MOX Services (95 wt % ^{239}Pu in Pu), and 100% ^{241}Pu at a range of rod pitches to determine the maximum (optimum) pitch for a flooded cask cavity. This evaluation takes no credit for the actual pitch of the encapsulating stainless steel rod (11/16 inch at 1.75 cm OD) structure into which the rods are placed. As seen in Figure 6.7.1-5 and Table 6.7.1-4, the maximum reactivity pitch is approximately 3.4 to 3.6 cm for the MOX rods and around 3 cm for the uranium oxide rods, with a "flat" peak extending approximately 0.4 to 0.6 cm in width depending on material and configuration. Based on a three sigma uncertainty band, maximum reactivities do not statistically differ between hexagonal and square pitch configurations. The base case for the optimum moderator density studies will be the 3.6 cm hexagonal pitch for the MOX rods and the 3.0 cm hexagonal pitch for the UO_2 rods.

Optimum Moderator Density Evaluation

The maximum fissile mass rod is evaluated at various internal and external moderator densities, including preferential flooding of the fuel region. For the preferential flooding scenarios, the square container containing the rod array will be evaluated at a moderator density independent of that in the remainder of the cask cavity. Figure 6.7.1-6 through Figure 6.7.1-8 contain the moderator density plots of the uranium oxide, MOX Services, and all ^{241}Pu material configurations. All results produce identical trends in that maximum reactivity is achieved by a preferentially flooded fuel region and void cavity and cask exterior. This result was to be

expected as it provides maximum neutronic coupling within the reflective boundary (infinite array) model.

Maximum system reactivities are summarized in Table 6.7.1-5 for the UO₂ fuel composition, the MOX Services defined fuel composition, and the hypothetical fissile material composition (100% ²⁴¹Pu) at the bounding fissile configuration—a maximum fuel material rod (0.3765-in pellet OD, 153.5-in active fuel length).

Single Cask Containment (Fully Reflected) and Normal Condition Array Evaluations

A single cask evaluation is performed to comply with 10 CFR 71.55(b)(3).

The containment for the NAC-LWT is the cask inner shell. While no operating condition results in a removal of the cask outer shell and lead gamma shield, the most reactive preferential flooded and fully flooded cases are reevaluated by removing the lead and outer shells (including neutron shield), and reflecting the system by 20 cm water at full density on the X, Y, and Z faces. Single cask, containment fully reflected reactivities are summarized in Table 6.7.1-6.

A normal condition infinite cask array is also evaluated. As indicated by the evaluations of the accident conditions array, including the radial neutron shield reduces system reactivity by eliminating neutronic interaction between casks. Normal condition cask array results are summarized in Table 6.7.1-7.

Maximum Reactivities and Comparison to USL

The maximum $k_{\text{eff}} + 2\sigma$ results for three primary analysis groups (single cask, normal array and accident array) are summarized in Table 6.7.1-8. Two normal condition array cases are included as the cask remains dry through all operating conditions, while 10 CFR 71 requires a normal condition maximum reactivity moderator density case. The listed values represent the maximum system reactivity adjusted for Monte Carlo run uncertainty and are significantly below the lower of system USL.

Table 6.7.1-9 compares the physical and hypothetical rod/material combinations to the area of applicability for the MOX material and maximum reactivity ²⁴¹Pu material. The MOX Services fuel material is within the area of applicability. No pure ²⁴¹Pu benchmark exists; therefore, the hypothetical configuration is significantly outside the area of applicability of the benchmark calculation. Compliance with regulatory limits is assured, as there is no significant reactivity trend versus plutonium isotopic composition. There is a significant margin to limits (0.13 Δk) versus a typical code bias in the 1-2% range, and the results are obtained from a hypothetical (conservative) isotope composition (all ²⁴¹Pu).

As the shipment includes uranium oxide rods, the maximum reactivity uranium oxide rod configuration characteristics are compared to the area of applicability in Table 6.7.1-10. The USL for UO₂ evaluations is 0.9372. Exceeding the area of applicability for enrichment and fuel to moderator ratios (expressed as rod pitch and H/U ratio) in the UO₂ benchmark cases is acceptable as neither function has a trend that is statistically significant and the margin to limits is large (> 0.4). A similar argument is applied to slightly lower fission energy for the maximum reactivity case than covered by the benchmark analysis. There is no statistically significant trend of reactivity versus energy, and any relative changes in USL postulated from the extrapolation is not significant versus the subcritical margin of the UO₂ rod shipment.

Evaluations of a mixed shipment of enriched UO₂ rods and MOX rods are not required, as the reactivity of the evaluated MOX rods are significantly higher than those of the UO₂ rods. Mixed shipments are, therefore, permitted.

Table 6.7.1-11 lists the bounding characteristics for the MOX/UO₂ PWR fuel rods evaluated in this section.

Figure 6.7.1-5 PWR MOX Rod Shipment - Reactivity versus Rod Pitch

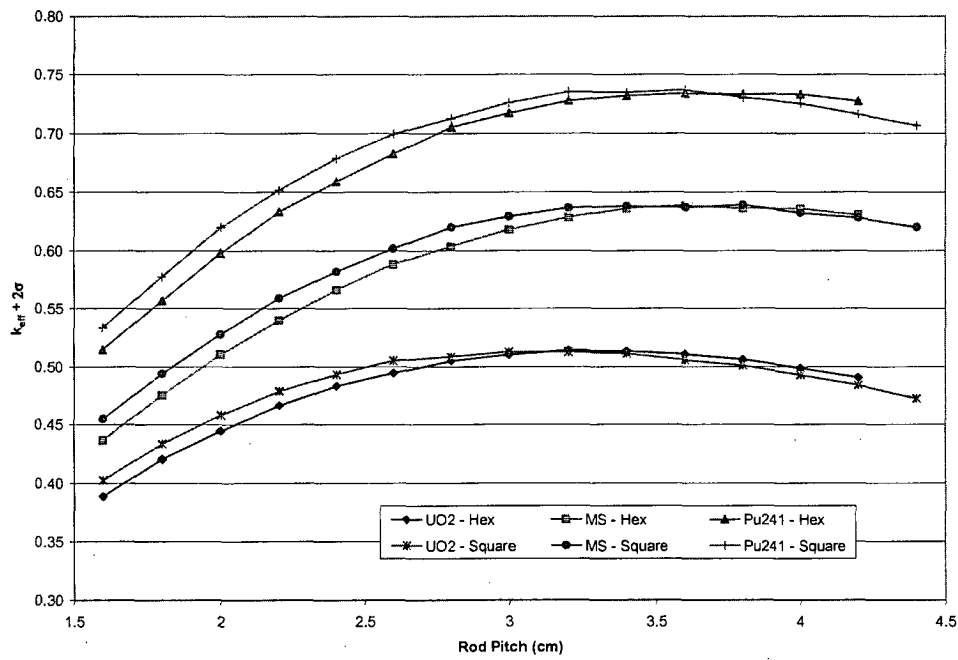


Figure 6.7.1-6 Moderator Density Study – UO₂ Fuel Material – 3.0 cm Rod Pitch

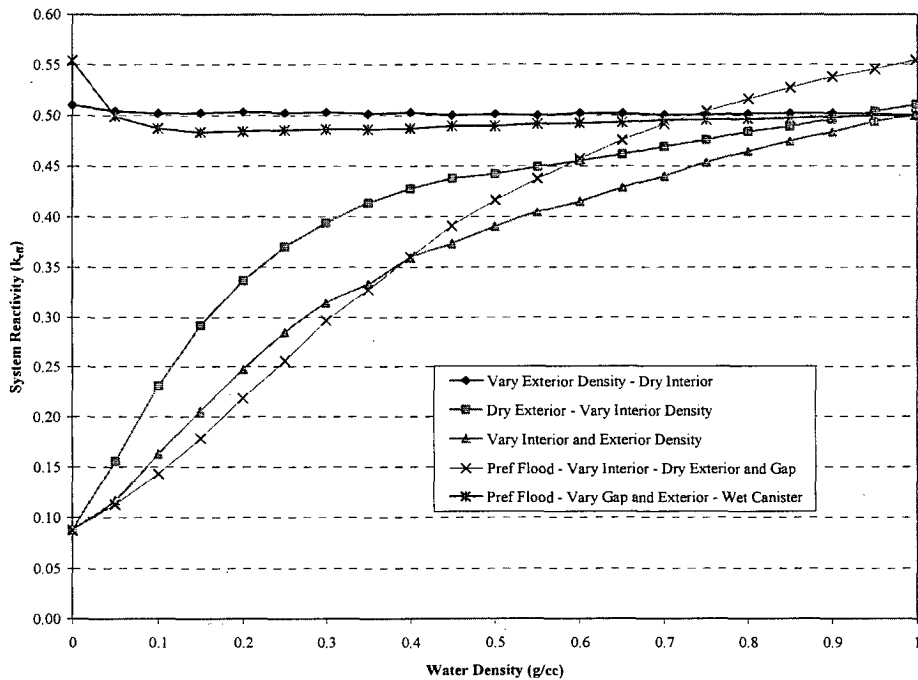


Figure 6.7.1-7 Moderator Density Study – MS Fuel Material – 3.6 cm Rod Pitch

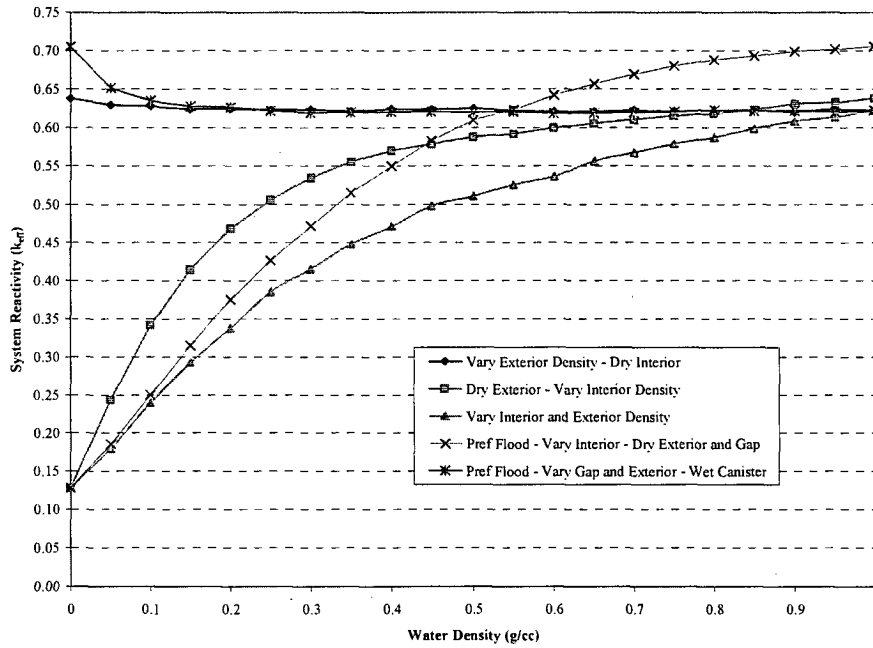


Figure 6.7.1-8 Moderator Density Study – PWR MOX ²⁴¹Pu Fuel Material – 3.6 cm Rod Pitch

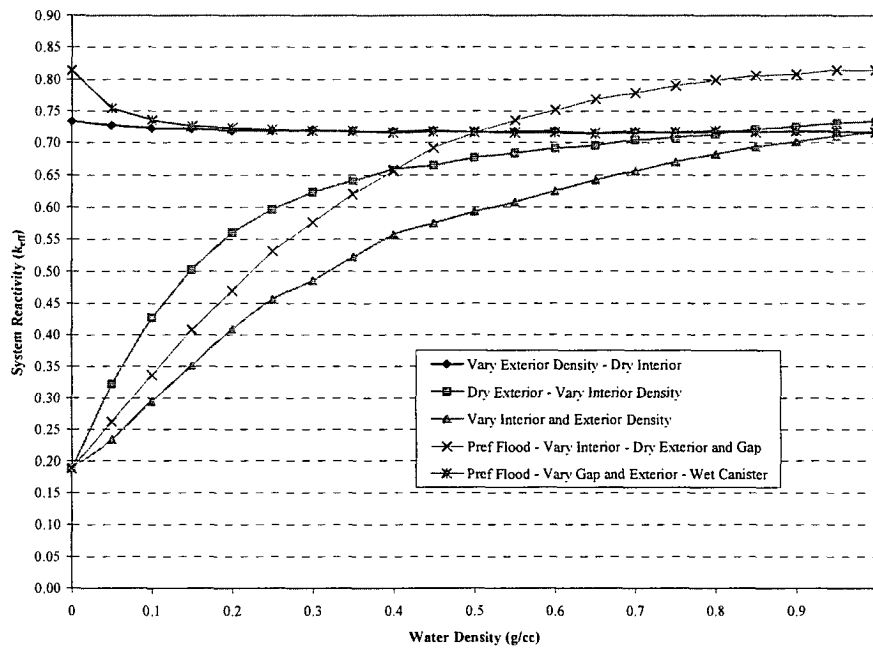


Table 6.7.1-3 PWR MOX Rod Shipment - Reactivity as a Function of Geometry and Material

Fuel Material	Rod Pitch	k_{eff}	σ	$k_{eff}+2\sigma$	vs. MS or P1 Composition	
					Δk_{eff}	$\Delta k_{eff}/\sigma$
UO ₂	3.0	0.50837	0.00087	0.51011	-0.10728	-81.4
WG	3.0	0.61442	0.00106	0.61654	-0.00123	-0.8
FG	3.0	0.60516	0.00097	0.60710	-0.01049	-7.6
PG	3.0	0.59390	0.00104	0.59598	-0.02175	-15.1
MS	3.0	0.61565	0.00099	0.61763	--	--
FP	3.0	0.63359	0.00107	0.63573	-0.08132	-51.8
P9	3.0	0.62715	0.00111	0.62937	-0.08776	-54.9
P1	3.0	0.71491	0.00115	0.71721	--	--
UO ₂	3.6	0.50911	0.00084	0.51079	-0.12688	-96.0
WG	3.6	0.63252	0.00098	0.63448	-0.00347	-2.5
FG	3.6	0.62282	0.00099	0.62480	-0.01317	-9.3
PG	3.6	0.61299	0.00105	0.61509	-0.02300	-15.7
MS	3.6	0.63599	0.00102	0.63803	--	--
FP	3.6	0.65225	0.00100	0.65425	-0.07909	-50.1
P9	3.6	0.64517	0.00107	0.64731	-0.08617	-53.1
P1	3.6	0.73134	0.00122	0.73378	--	--

Table 6.7.1-4 PWR MOX Fuel Shipment – Fuel Rod Pitch Study

Rod Pitch	Pitch Config	Fuel Material	k_{eff}	Fuel Material	k_{eff}	Fuel Material	k_{eff}
1.8	Hexagonal	UO ₂	0.41843	MS	0.47357	²⁴¹ Pu	0.55466
2.0	Hexagonal	UO ₂	0.44262	MS	0.50841	²⁴¹ Pu	0.59542
2.2	Hexagonal	UO ₂	0.46448	MS	0.53761	²⁴¹ Pu	0.63030
2.4	Hexagonal	UO ₂	0.48147	MS	0.56403	²⁴¹ Pu	0.65675
2.6	Hexagonal	UO ₂	0.49260	MS	0.58626	²⁴¹ Pu	0.68060
2.8	Hexagonal	UO ₂	0.50325	MS	0.60145	²⁴¹ Pu	0.70293
3.0	Hexagonal	UO ₂	0.50837	MS	0.61565	²⁴¹ Pu	0.71491
3.2	Hexagonal	UO ₂	0.51224	MS	0.62593	²⁴¹ Pu	0.72528
3.4	Hexagonal	UO ₂	0.51156	MS	0.63376	²⁴¹ Pu	0.72957
3.6	Hexagonal	UO ₂	0.50911	MS	0.63599	²⁴¹ Pu	0.73134
3.8	Hexagonal	UO ₂	0.50464	MS	0.63360	²⁴¹ Pu	0.73067
4.0	Hexagonal	UO ₂	0.49718	MS	0.63359	²⁴¹ Pu	0.73097
4.2	Hexagonal	UO ₂	0.48894	MS	0.62789	²⁴¹ Pu	0.72504
1.8	Square	UO ₂	0.43146	MS	0.49220	²⁴¹ Pu	0.57531
2.0	Square	UO ₂	0.45613	MS	0.52574	²⁴¹ Pu	0.61729
2.2	Square	UO ₂	0.47678	MS	0.55687	²⁴¹ Pu	0.64902
2.4	Square	UO ₂	0.49150	MS	0.57989	²⁴¹ Pu	0.67677
2.6	Square	UO ₂	0.50343	MS	0.59949	²⁴¹ Pu	0.69695
2.8	Square	UO ₂	0.50669	MS	0.61768	²⁴¹ Pu	0.71049
3.0	Square	UO ₂	0.51090	MS	0.62688	²⁴¹ Pu	0.72343
3.2	Square	UO ₂	0.51089	MS	0.63415	²⁴¹ Pu	0.73285
3.4	Square	UO ₂	0.50965	MS	0.63544	²⁴¹ Pu	0.73257
3.6	Square	UO ₂	0.50429	MS	0.63440	²⁴¹ Pu	0.73463
3.8	Square	UO ₂	0.49939	MS	0.63658	²⁴¹ Pu	0.72833
4.0	Square	UO ₂	0.49120	MS	0.63003	²⁴¹ Pu	0.72326
4.2	Square	UO ₂	0.48232	MS	0.62576	²⁴¹ Pu	0.71403

Table 6.7.1-5 PWR MOX Fuel Shipment – Optimum Moderator Study Maximum Reactivity Summary

Fuel Material	$k_{eff} + 2\sigma$
UO ₂	0.55404
MOX Services	0.70523
²⁴¹ Pu	0.81451

Table 6.7.1-6 PWR MOX Fuel Shipment Reactivity Summary for Single Cask Containment Fully Reflected Cases

Fuel Mat'l	Rod Gap (g/cc)	Array (g/cc)	Cavity (g/cc)	Exterior (g/cc)	k_{eff}	σ	$k_{eff} + 2\sigma$
UO ₂	0.0001	0.0001	0.0001	0.9982	0.03394	0.00018	0.03430
UO ₂	0.9982	0.9982	0.9982	0.9982	0.49629	0.00085	0.49799
UO ₂	0.9982	0.9982	0.0001	0.9982	0.43536	0.00091	0.43718
MS	0.0001	0.0001	0.0001	0.9982	0.04527	0.00028	0.04583
MS	0.9982	0.9982	0.9982	0.9982	0.61686	0.00100	0.61886
MS	0.9982	0.9982	0.0001	0.9982	0.58689	0.00102	0.58893
²⁴¹ Pu	0.0001	0.0001	0.0001	0.9982	0.04895	0.00036	0.04967
²⁴¹ Pu	0.9982	0.9982	0.9982	0.9982	0.71168	0.00115	0.71398
²⁴¹ Pu	0.9982	0.9982	0.0001	0.9982	0.67957	0.00121	0.68199

Table 6.7.1-7 PWR MOX Fuel Shipment Reactivity Summary for Normal Condition Array Cases

Fuel Mat'l	Rod Gap (g/cc)	Array (g/cc)	Cavity (g/cc)	Exterior (g/cc)	k_{eff}	σ	$k_{eff} + 2\sigma$
UO ₂	0.0001	0.0001	0.0001	0.0001	0.03393	0.00016	0.03425
UO ₂	0.9982	0.9982	0.9982	0.9982	0.49757	0.00089	0.49935
UO ₂	0.9982	0.9982	0.9982	0.0001	0.49624	0.00092	0.49808
UO ₂	0.9982	0.9982	0.0001	0.0001	0.43382	0.00087	0.43556
MS	0.0001	0.0001	0.0001	0.0001	0.04576	0.00025	0.04626
MS	0.9982	0.9982	0.9982	0.9982	0.61761	0.00101	0.61963
MS	0.9982	0.9982	0.9982	0.0001	0.61581	0.00102	0.61785
MS	0.9982	0.9982	0.0001	0.0001	0.58588	0.00099	0.58786
²⁴¹ Pu	0.0001	0.0001	0.0001	0.0001	0.04905	0.00032	0.04969
²⁴¹ Pu	0.9982	0.9982	0.9982	0.9982	0.71149	0.00112	0.71373
²⁴¹ Pu	0.9982	0.9982	0.9982	0.0001	0.71256	0.0012	0.71496
²⁴¹ Pu	0.9982	0.9982	0.0001	0.0001	0.68189	0.00118	0.68425

Table 6.7.1-8 PWR MOX Fuel Shipments - Summary of Maximum Reactivity Configurations

Fuel Material	Result	Accident Array – Preferentially Flooded	Normal Array – Preferentially Flooded	Normal Array – Dry	Single Cask Fully (Water) Reflected
UO ₂	k _{eff} + 2σ	0.55404	0.49808	0.03425	0.49799
	EALCF (eV)	9.79E-02	8.83E-02	2.95E+05	8.81E-02
MS	k _{eff} + 2σ	0.70523	0.61963	0.04626	0.61886
	EALCF (eV)	1.25E-01	1.17E-01	2.14E+05	1.17E-01
²⁴¹ Pu	k _{eff} + 2σ	0.81386	0.71496	0.04969	0.71398
	EALCF (eV)	1.33E-01	1.21E-01	8.72E+04	1.22E-01

Table 6.7.1-9 PWR MOX Fuel Shipments – PWR MOX Comparison to Area of Applicability

Parameter	Min	Max	MOX Services Materials	²⁴¹ Pu Materials
EALCF (eV)	8.10E-02	8.99E-01	0.13	0.13
²³⁵ U/ ²³⁸ U Weight Ratio	1.58E-03	1.51E+00	7.05E-03	7.05E-03
²³⁸ Pu/ ²³⁸ U Weight Ratio	1.88E-06	1.54E-04	4.17E-05	0.0
²³⁹ Pu/ ²³⁸ U Weight Ratio	1.39E-02	7.77E-01	7.92E-02	0.0
²⁴⁰ Pu/ ²³⁸ U Weight Ratio	1.20E-03	8.48E-02	3.75E-03	0.0
²⁴¹ Pu/ ²³⁸ U Weight Ratio	7.90E-05	7.59E-03	3.34E-04	7.94E-02
²⁴² Pu/ ²³⁸ U Weight Ratio	4.63E-06	6.38E-04	4.17E-05	0.0
Water to Fuel Volume Ratio	1.10E+00	2.07E+01	1.43E+01	

Table 6.7.1-10 PWR MOX Fuel Shipments – UO₂ Comparison to Area of Applicability

Parameter	Min	Max	UO ₂ Case
Enrichment (wt % ²³⁵ U)	2.35	4.738	5.0
Fuel rod pitch (cm)	1.3	2.54	3.0
Fuel pellet outer diameter (cm)	0.79	1.265	0.85/0.96
Fuel rod diameter (cm)	0.94	1.4172	0.93/1.12
H/ ²³⁵ U atom ratio	106.2	403.9	627 to 2140 ¹
EALCF (eV)	0.09781	0.3447	0.0874

Table 6.7.1-11 Bounding Parameters for PWR MOX/UO₂ Rod Shipments

Parameter	Value
Fuel Form	Clad UO ₂ or MOX rod
Number of Rods	16 ²
Clad Material	Zirconium Alloy
UO ₂ Rods – Max. Enrichment (wt % ²³⁵ U)	5
MOX Rods – Max. Fissile Pu Content (wt %)	7 ³
Maximum Heavy Metal Content Per Rod (kg)	2.60
Maximum Pellet Diameter (inch)	0.3765
Maximum Active Fuel Length (inch)	153.5

¹ Dependent on pitch configuration (square or hexagonal).

² Mixture of UO₂ and MOX rods is permitted.

³ Sum of ²³⁹Pu and ²⁴¹Pu.

6.7.2 Critical Benchmarks

The results of the criticality analyses presented in this chapter must be compared to the upper subcritical limit (USL). The USL accounts for bias and uncertainty resulting from the method using information obtained from the analysis of criticality benchmark experimental data.

Criticality code validation is performed for the Monte Carlo evaluation code and neutron cross-section libraries. Criticality validation is required by the criticality safety standard ANSI/ANS-8.1.

6.7.2.1 Benchmark Experiments and Applicability Discussion

NUREG/CR-6361, "Criticality Benchmark Guide for Light-Water-Reactor Fuel in Transportation and Storage Packages" (NUREG), provides a guide to LWR criticality benchmark calculations and the determination of bias and subcritical limits in critical safety evaluations. In Section 2 of the NUREG, a series of LWR critical experiments is described in sufficient detail for independent modeling. In Section 3, the critical experiments are modeled, and the results (k_{eff} values) are presented. The method utilized in the NUREG is KENO-Va with the 44-group ENDF/B-V cross-section library embedded in SCALE 4.3. In Section 4, a guide for the determination of bias and subcritical safety limits is provided based on ANSI/ANS-8.1 and statistical analysis of the trending in the bias. Finally, guidelines for experiment selection and applicability are presented in Section 5. The approach outlined in Section 4 of the NUREG is described in detail herein and is implemented for MCNP5 with continuous energy ENDF/B-VI cross-sections.

NUREG/CR-6361 implements ANSI/ANS-8.1 criticality safety criterion as follows.

$$k_s \leq k_c - \Delta k_s - \Delta k_c - \Delta k_m \quad (\text{Equation 1})$$

where:

- k_s = calculated allowable maximum multiplication factor, k_{eff} , of the system being evaluated for all normal or credible abnormal conditions or events.
- k_c = mean k_{eff} that results from a calculation of benchmark criticality experiments using a particular calculation method. If the calculated k_{eff} values for the criticality experiments exhibit a trend with an independent parameter, then k_c shall be determined by extrapolation based on best fit to calculated values. Criticality experiments used as benchmarks in computing k_c should have physical compositions, configurations and nuclear characteristics (including reflectors) similar to those of the system being evaluated.

Δk_s = allowance for the following:

- statistical or convergence uncertainties, or both, in computation of k_s
- material and fabrication tolerances
- geometric or material representations used in computational method

Δk_c = margin for uncertainty in k_c , which includes allowance for the following:

- uncertainties in critical experiments
- statistical or convergence uncertainties, or both, in computation of k_c
- uncertainties resulting from extrapolation of k_c outside range of experimental data
- uncertainties resulting from limitations in geometrical or material representations used in the computational method

Δk_m = arbitrary administrative margin to ensure subcriticality of k_s

The various uncertainties are combined statistically if they are independent. Correlated uncertainties are combined by addition.

Equation 1 can be rewritten as shown.

$$k_s \leq 1 - \Delta k_m - \Delta k_s - (1 - k_c) - \Delta k_c \quad (\text{Equation 2})$$

Noting that the definition of the bias is $\beta = 1 - k_c$, Equation 2 can be written as shown.

$$k_s + \Delta k_s \leq 1 - \Delta k_m - \beta - \Delta \beta \quad (\text{Equation 3})$$

where:

$$\Delta \beta = \Delta k_c$$

Thus, the maximum allowable value for k_{eff} plus uncertainties in the system being analyzed must be below 1 minus an administrative margin (typically 0.05), which includes the bias and the uncertainty in the bias. This can also be written as shown.

$$k_s + \Delta k_s \leq \text{Upper Subcritical Limit (USL)} \quad (\text{Equation 4})$$

where:

$$\text{USL} \equiv 1 - \Delta k_m - \beta - \Delta \beta \quad (\text{Equation 5})$$

This is the USL criterion as described in Section 4 of NUREG/CR-6361. Two methods are prescribed for the statistical determination of the USL. The "Confidence Band with Administrative Margin (USL-1)" approach is implemented here and is referred to generically as USL. A $\Delta k_m = 0.05$ and a lower confidence band are specified based on a linear regression of k_{eff} as a function of some system parameter. As recommended in NUREG/CR-6361, a simple linear regression is performed on each system parameter, and the line with the greatest correlation is used to functionalize β .

Application specific sections (e.g., low enriched uranium, MOX) contains the the list of critical benchmarks employed in the validation of MCNP with its continuous energy neutron cross-section libraries and the processing of the experimental results into the USL. Included in the subsequent sections are linear fits of reactivity (k_{eff}) to each of the system parameters. Experiments were chosen to reflect the fuel geometry and materials as closely as available.

6.7.2.2 LEU (Maximum 5 wt % ^{235}U in UO_2) Results of Benchmark Calculations

The range of parameters included in the low enriched uranium (LEU) benchmarks is shown in Table 6.7.2-1. Experiments are chosen to reflect the fuel evaluated for shipment. This includes the use of arrays of low enriched uranium oxide fuel rods with light water moderation. To cover potential borated water conditions within spent fuel pools or absorbers placed into the basket experiments with criticality control by spacing, borated moderator and/or borated absorber panels and tubes are included in the benchmarks effort. Trending in k_{eff} was evaluated for the following independent variables: wt % ^{235}U , rod pitch, H/U volume ratio, energy of the average neutron lethargy causing fission (EALCF), ^{10}B loading of the absorber sheet, and soluble boron loading. No statistically significant trends were found for any of the system parameters. USLs are, therefore, generated for each of the independent variables. A minimum USL covering the range of applicability of the benchmark set is determined.

To evaluate the relative importance of the trend analysis to the upper subcritical limits, correlation coefficients are required for all independent parameters. The linear correlation coefficient, R, is calculated by taking the square root of the R^2 value. In particular, the correlation coefficient, R, is a measure of the linear relationship between k_{eff} and a critical experiment parameter. If R is +1, a perfect linear relationship with a positive slope is indicated. If R is -1, a perfect linear relationship with a negative slope is indicated. When R is 0, no linear relationship is indicated.

Table 6.7.2-2 contains the correlation coefficient, R, for each linear fit of k_{eff} versus experimental parameter. Linear fits and correlation constants are based on the 183 data-point evaluation sets plotted in Section 6.7.2.3. The cluster gap plot is limited to the 137 data points for experiments containing multiple fuel rod clusters. Single fuel rod cluster experiments documented in LEU-COMP-THERM sets 06, 14, 35 and 50, in addition to LEU-COMP-THERM experiments 01-01, 02-01 to -03, and 08-01 to -15, were, therefore, excluded from the cluster gap study. The 183 data points evaluated for the remaining parameters represent the complete set of experiments listed in Section 6.7.2.3 minus the three high energy lethargy experiments above 0.35 eV (Experiments LEU-COMP-THERM 14-05, -06 and -07). The addition of these points, while not

resulting in a significant linear fit, produces a noticeable slope to the USL correlation not representative of the remaining data fits. As this increased slope results in a higher USL, it is acceptable to discard these data points. The three higher energy points are removed from all independent variables for consistency.

As there is no significant correlation to any of the independent variables, the USL for each independent variable is calculated and shown with its range of applicability in Table 6.7.2-2. A sample output for EALCF is shown in Figure 6.7.2-1. Uncertainties included in the USLSTATS evaluation are the Monte Carlo uncertainty associated with the reactivity calculation and experimental uncertainty that was provided in the literature for each of the cases.

Based on all the independent variable correlations, a lower limit constant USL of 0.9376 may be applied. The range of applicability (area of applicability) of this limit may be extended to 5 wt % enriched fuel, as the correlation shows no significant trend with enrichment between 2.35 and 4.74 wt %, and that the limited trending observed increases the USL. Extending the range of applicability for the average neutron lethargy is based on a minimal, but positive, trend of the USL versus EALCF. Studies, including additional data points up to 0.7722 eV, indicate that the trending continues to the higher energy levels.

Figure 6.7.2-1 LEU USLSTATS Output for EALCF

```

*****
Version 1.4, April 23, 2003
Oak Ridge National Laboratory
*****
Input to statistical treatment from file:enrich-183.in
Title: keff vs enrichment
Proportion of the population = .995
Confidence of fit = .950
Confidence on proportion = .950
Number of observations = 183
Minimum value of closed band = 0.00
Maximum value of closed band = 0.00
Administrative margin = 0.05

independent      dependent      deviation      independent      dependent      deviation
variable - x     variable - y   in y           variable - x     variable - y   in y
2.35000E+00      9.94910E-01   3.42000E-03   2.35000E+00      9.95090E-01   3.46000E-03
2.35000E+00      9.92830E-01   3.38000E-03   2.35000E+00      9.92520E-01   3.47000E-03
2.35000E+00      9.98060E-01   3.38000E-03   2.35000E+00      9.95620E-01   3.50000E-03
2.35000E+00      9.96550E-01   3.42000E-03   2.35000E+00      9.93130E-01   3.55000E-03
2.35000E+00      9.89310E-01   3.44000E-03   2.35000E+00      9.98130E-01   3.58000E-03
2.35000E+00      9.95340E-01   3.41000E-03   2.35000E+00      9.96700E-01   3.56000E-03
2.35000E+00      9.93880E-01   3.44000E-03   2.35000E+00      9.93830E-01   3.55000E-03
2.35000E+00      9.89690E-01   3.36000E-03   2.35000E+00      9.92770E-01   3.47000E-03
4.30600E+00      9.95160E-01   2.79000E-03   2.35000E+00      9.92920E-01   3.50000E-03
4.30600E+00      9.93670E-01   2.54000E-03   2.35000E+00      9.96410E-01   3.46000E-03
4.30600E+00      9.96340E-01   2.76000E-03   2.35000E+00      9.93060E-01   3.49000E-03
4.30600E+00      9.93110E-01   2.64000E-03   2.35000E+00      9.96500E-01   3.45000E-03
4.30600E+00      9.93000E-01   2.49000E-03   2.35000E+00      9.94680E-01   3.50000E-03
2.59600E+00      9.92680E-01   2.10000E-03   2.35000E+00      9.93300E-01   3.47000E-03
2.59600E+00      9.93190E-01   2.14000E-03   2.35000E+00      9.91810E-01   3.46000E-03
2.59600E+00      9.92990E-01   2.13000E-03   2.35000E+00      9.93920E-01   3.47000E-03
2.59600E+00      9.94790E-01   2.13000E-03   2.35000E+00      9.95560E-01   3.55000E-03
2.59600E+00      9.93100E-01   2.12000E-03   2.35000E+00      9.94540E-01   3.51000E-03
2.59600E+00      9.93240E-01   2.12000E-03   2.35000E+00      9.94490E-01   3.47000E-03
2.59600E+00      9.91990E-01   2.12000E-03   2.35000E+00      9.91300E-01   3.52000E-03
2.59600E+00      9.93820E-01   2.12000E-03   2.35000E+00      9.94800E-01   3.47000E-03
2.59600E+00      9.94450E-01   2.12000E-03   2.35000E+00      9.93500E-01   3.60000E-03
2.59600E+00      9.95440E-01   2.13000E-03   2.35000E+00      9.94000E-01   3.45000E-03
2.59600E+00      9.94410E-01   2.12000E-03   2.35000E+00      9.96280E-01   3.53000E-03
2.59600E+00      9.93920E-01   2.15000E-03   2.35000E+00      9.92620E-01   3.45000E-03
2.59600E+00      9.95090E-01   2.14000E-03   2.35000E+00      9.94100E-01   3.53000E-03
2.59600E+00      9.93780E-01   2.12000E-03   2.35000E+00      9.96470E-01   3.52000E-03
2.59600E+00      9.95040E-01   2.14000E-03   2.35000E+00      9.93600E-01   3.47000E-03
2.59600E+00      9.94380E-01   2.11000E-03   2.35000E+00      9.97020E-01   3.49000E-03
2.59600E+00      9.95730E-01   2.12000E-03   2.35000E+00      9.94970E-01   3.50000E-03
2.59600E+00      9.94270E-01   2.14000E-03   2.35000E+00      9.91950E-01   3.55000E-03
2.45900E+00      9.98350E-01   1.34000E-03   2.59600E+00      9.93410E-01   1.93000E-03
2.45900E+00      9.96860E-01   1.36000E-03   2.59600E+00      9.91310E-01   2.05000E-03
2.45900E+00      9.99310E-01   1.24000E-03   4.73800E+00      9.95860E-01   4.36000E-03
2.45900E+00      9.97950E-01   1.36000E-03   4.73800E+00      9.93580E-01   4.53000E-03
2.45900E+00      9.97650E-01   1.38000E-03   4.73800E+00      9.95390E-01   4.58000E-03
2.45900E+00      9.96990E-01   1.35000E-03   4.73800E+00      9.92370E-01   4.54000E-03
2.45900E+00      9.97230E-01   1.37000E-03   4.73800E+00      9.91440E-01   4.62000E-03
2.45900E+00      9.96590E-01   1.40000E-03   4.73800E+00      9.98780E-01   4.82000E-03
2.45900E+00      9.95260E-01   1.40000E-03   4.73800E+00      9.94180E-01   4.94000E-03
2.45900E+00      9.97450E-01   1.36000E-03   4.73800E+00      9.92400E-01   4.90000E-03
2.45900E+00      9.97590E-01   1.38000E-03   4.73800E+00      9.96930E-01   4.98000E-03
2.45900E+00      9.97650E-01   1.36000E-03   4.73800E+00      9.91370E-01   5.05000E-03
2.45900E+00      9.98880E-01   1.39000E-03   2.35000E+00      9.92500E-01   2.34000E-03
2.45900E+00      9.97350E-01   1.37000E-03   2.35000E+00      9.95140E-01   2.43000E-03
2.45900E+00      9.97580E-01   1.39000E-03   2.35000E+00      9.92190E-01   2.33000E-03
2.45900E+00      9.97720E-01   1.39000E-03   2.35000E+00      9.94760E-01   2.40000E-03
2.45900E+00      9.96910E-01   1.35000E-03   2.35000E+00      9.94690E-01   3.67000E-03
4.30600E+00      9.95480E-01   2.84000E-03   2.35000E+00      9.94340E-01   2.49000E-03
4.30600E+00      9.93430E-01   2.78000E-03   2.35000E+00      9.93190E-01   2.39000E-03
4.30600E+00      9.93300E-01   2.81000E-03   4.73800E+00      9.93300E-01   1.28000E-03
4.30600E+00      9.93710E-01   2.85000E-03   4.73800E+00      9.93400E-01   1.23000E-03
4.30600E+00      9.95930E-01   2.73000E-03   4.73800E+00      9.94890E-01   1.25000E-03
4.30600E+00      9.92950E-01   2.85000E-03   4.73800E+00      9.93190E-01   1.25000E-03
4.30600E+00      9.96160E-01   2.89000E-03   4.73800E+00      9.93060E-01   1.28000E-03
4.30600E+00      9.93890E-01   2.73000E-03   2.45900E+00      9.91330E-01   2.03000E-03
4.30600E+00      9.95710E-01   2.96000E-03   2.45900E+00      9.95970E-01   2.43000E-03
4.30600E+00      9.93190E-01   2.60000E-03   2.45900E+00      9.95550E-01   2.42000E-03
4.30600E+00      9.93780E-01   2.75000E-03   2.45900E+00      9.94860E-01   2.42000E-03
4.30600E+00      9.92630E-01   2.84000E-03   2.45900E+00      9.95040E-01   2.42000E-03
4.30600E+00      9.95660E-01   2.75000E-03   2.45900E+00      9.95420E-01   2.42000E-03
4.30600E+00      9.94310E-01   2.82000E-03   2.45900E+00      9.95300E-01   2.42000E-03
4.30600E+00      9.96390E-01   2.95000E-03   2.45900E+00      9.95070E-01   2.42000E-03
4.30600E+00      9.96860E-01   2.79000E-03   2.45900E+00      9.93680E-01   1.93000E-03
4.30600E+00      9.97160E-01   2.68000E-03   2.45900E+00      9.92100E-01   1.93000E-03
4.30600E+00      9.92370E-01   2.86000E-03   2.45900E+00      9.94470E-01   1.93000E-03

```

Figure 6.7.2-1 LEU USLSTATS Output for EALCF

4.30600E+00	9.97190E-01	2.81000E-03	2.45900E+00	9.90730E-01	1.93000E-03
4.30600E+00	9.94340E-01	2.76000E-03	2.45900E+00	9.86520E-01	2.23000E-03
4.30600E+00	9.96920E-01	2.79000E-03	2.45900E+00	9.86340E-01	1.93000E-03
4.30600E+00	9.96060E-01	2.83000E-03	2.45900E+00	9.90420E-01	2.42000E-03
4.30600E+00	9.97400E-01	2.94000E-03	2.45900E+00	9.89740E-01	2.03000E-03
4.30600E+00	9.92810E-01	2.69000E-03	2.45900E+00	9.91520E-01	2.72000E-03
4.30600E+00	9.92560E-01	2.88000E-03	2.45900E+00	9.90290E-01	2.13000E-03
4.30600E+00	9.93650E-01	2.88000E-03	2.45900E+00	9.89270E-01	1.93000E-03
4.30600E+00	9.94970E-01	2.85000E-03	2.60000E+00	9.95710E-01	1.42000E-03
2.45900E+00	9.94820E-01	3.21000E-03	2.60000E+00	9.96180E-01	1.42000E-03
2.45900E+00	9.94940E-01	3.21000E-03	2.60000E+00	9.95340E-01	1.52000E-03
2.45900E+00	9.95140E-01	3.21000E-03	2.60000E+00	9.95470E-01	1.52000E-03
2.45900E+00	9.95640E-01	3.21000E-03	2.60000E+00	9.96910E-01	1.42000E-03
2.45900E+00	9.95080E-01	3.21000E-03	2.60000E+00	9.96140E-01	1.42000E-03
2.45900E+00	9.95260E-01	3.21000E-03	2.60000E+00	9.95890E-01	1.42000E-03
2.45900E+00	9.95200E-01	3.21000E-03	2.60000E+00	9.96240E-01	1.62000E-03
4.30600E+00	9.94020E-01	1.92000E-03	2.60000E+00	9.96670E-01	1.52000E-03
4.30600E+00	9.94460E-01	1.91000E-03	2.60000E+00	9.96760E-01	1.62000E-03
4.30600E+00	9.93550E-01	1.91000E-03	2.60000E+00	9.96370E-01	1.62000E-03
4.30600E+00	9.94010E-01	1.91000E-03	2.60000E+00	9.96430E-01	1.72000E-03
4.30600E+00	9.92810E-01	3.27000E-03	2.60000E+00	9.97010E-01	1.62000E-03
4.30600E+00	9.94960E-01	1.91000E-03	2.60000E+00	9.96500E-01	1.62000E-03
4.30600E+00	9.93780E-01	1.90000E-03	2.60000E+00	9.96340E-01	1.62000E-03
4.30600E+00	9.96680E-01	1.95000E-03	2.60000E+00	9.96580E-01	1.71000E-03
4.30600E+00	9.85950E-01	7.71000E-03	2.60000E+00	9.96450E-01	1.62000E-03
2.35000E+00	9.94940E-01	3.54000E-03			

chi = 2.5464 (upper bound = 9.49). The data tests normal.

Output from statistical treatment

keff vs enrichment

Number of data points (n) 183
 Linear regression, k(X) 0.9950 + (-1.5719E-04)*X
 Confidence on fit (1-gamma) [input] 95.0%
 Confidence on proportion (alpha) [input] 95.0%
 Proportion of population falling above lower tolerance interval (rho) [input] 99.5%
 Minimum value of X 2.3500E+00
 Maximum value of X 4.7380E+00
 Average value of X 3.0597E+00
 Average value of k 0.99453
 Minimum value of k 0.98595
 Variance of fit, s(k,X)^2 5.0408E-06
 Within variance, s(w)^2 7.8633E-06
 Pooled variance, s(p)^2 1.2904E-05
 Pooled std. deviation, s(p) 3.5922E-03
 C(alpha,rho)*s(p) 1.5554E-02
 student-t @ (n-2,1-gamma) 1.64500E+00
 Confidence band width, W 5.9793E-03
 Minimum margin of subcriticality, C*s(p)-W 9.5746E-03

Upper subcritical limits: (2.3500 <= X <= 4.7380)

USL Method 1 (Confidence Band with Administrative Margin) USL1 = 0.9390 + (-1.5719E-04)*X

USL Method 2 (Single-Sided Uniform Width Closed Interval Approach) USL2 = 0.9795 + (-1.5719E-04)*X

USLs Evaluated Over Range of Parameter X:

X: 2.35E+0 2.69E+0 3.03E+0 3.37E+0 3.71E+0 4.06E+0 4.40E+0 4.74E+0

USL-1:	0.9387	0.9386	0.9386	0.9385	0.9385	0.9384	0.9383	0.9383
USL-2:	0.9791	0.9790	0.9790	0.9789	0.9789	0.9788	0.9788	0.9787

Table 6.7.2-1 LEU Range of Applicability for Complete Set of 186 Benchmark Experiments

Parameter	Minimum	Maximum
Enrichment (wt % ²³⁵ U)	2.350%	4.738%
Fuel rod pitch (cm)	1.30	2.54
Fuel pellet outer diameter (cm)	0.790	1.265
Fuel rod diameter (cm)	0.9400	1.4172
H/ ²³⁵ U atom ratio	72.7	403.9
Soluble boron (ppm by weight)	0	4986
Cluster Gap (cm)	1.206	13.750
Boron (¹⁰ B) plate loading (g/cm ²)	0.0000	0.0670
Energy of average neutron lethargy causing fission (eV)	0.09781	0.77219

Table 6.7.2-2 LEU Correlation Coefficients and USLs for Benchmark Experiments

Variable	R ²	R	Range of Applicability	USLSTATS Correlation	USL Low	USL High
Enrichment (wt % ²³⁵ U)	0.00410	0.064	2.35<=X<=4.738	0.9390-1.57E-04X	0.9382	0.9386
Fuel rod pitch (cm)	0.00150	0.039	1.3<=X<=2.54	0.9380+2.64E-04X	0.9383	0.9386
Fuel pellet outer diameter (cm)	0.00260	0.051	0.79<=X<=1.265	0.9376+8.25E-04X	0.9382	0.9386
Fuel rod diameter (cm)	0.00380	0.062	0.94<=X<=1.4172	0.9372+1.01E-03X	0.9381	0.9386
H/ ²³⁵ U atom ratio	3.00E-06	0.002	106.2<=X<=403.9	0.9386-4.74E-08X	0.9385	0.9385
Soluble boron (ppm by weight)	0.01730	0.132	0<=X<=4986	0.9379+3.96E-07X	0.9379	0.9398
Cluster gap (cm)	0.01940	0.139	1.2<=X<=13.8	0.9375+9.82E-05X	0.9376	0.9388
Boron (¹⁰ B) plate loading (g/cm ²)	0.00006	0.008	0<=X<=0.067	0.9382-1.37E-03X	0.9381	0.9382
Energy of average neutron lethargy causing fission (eV)	0.00900	0.095	0.09781<=X<=0.3447	0.9379+3.45E-03X	0.9382	0.9390

6.7.2.3 LEU (Maximum 5 wt % ^{235}U in UO_2) Critical Benchmarks

From the International Handbook of Evaluated Criticality Safety Benchmark Experiments, 186 experiments are selected as the basis of the MCNP benchmarking. Experiments were selected for compatibility of materials and geometry with the spent fuel casks. Of particular interest are benchmarks with arrays of low enriched uranium oxide fuel rods.

MCNP benchmark cases represent a collection of files composed of inputs directly obtained from references (with cross-section sets adjusted to those used in the cask analysis), NAC modified input files representing unique geometries based on reference input files, and input files constructed from the experimental material and geometry information. All cases were reviewed on a "preparer/checker" principle for modeling consistency with the cask models and the choice of code options. Due to large variations in the benchmark complexities, not all options employed in the cask models are reflected in each of the benchmarks (e.g., UNIVERSE structure). A review of the criticality results did not indicate any result trend due to particular modeling choices (e.g., using the UNIVERSE structure versus a single universe, or employing KSRC versus SDEF sampling).

Key system parameters, the experimental uncertainty, and calculated k_{eff} and σ for each experiment are shown in Table 6.7.2-3. Stochastic Monte Carlo error is kept within $\pm 0.2\%$ and each output is checked to assure that the MCNP built-in statistical checks on the results are passed and that all fissile material is sampled.

Scatter plots of k_{eff} versus system parameters for 183 data point sets (full set minus three high lethargy points above 0.35 eV) are created (see Figure 6.7.2-2 through Figure 6.7.2-10). Included in these scatter plots are linear regression lines with a corresponding correlation coefficient (R^2) to statistically indicate any trend or lack thereof. Scatter plates are created for k_{eff} versus the following.

- Enrichment in ^{235}U (wt % ^{235}U)
- Fuel rod pitch (cm)
- Fuel pellet outer diameter (cm)
- Fuel rod outer diameter (cm)
- Hydrogen/uranium (^{235}U) atom ratio
- Soluble boron (ppm by weight)
- Cluster gap spacing (spacing between assemblies in cm)
- Boron (^{10}B) plate loading (g/cm^2)
- Energy of average neutron lethargy causing fission (eV)

Figure 6.7.2-2 k_{eff} versus Fuel Enrichment (LEU)

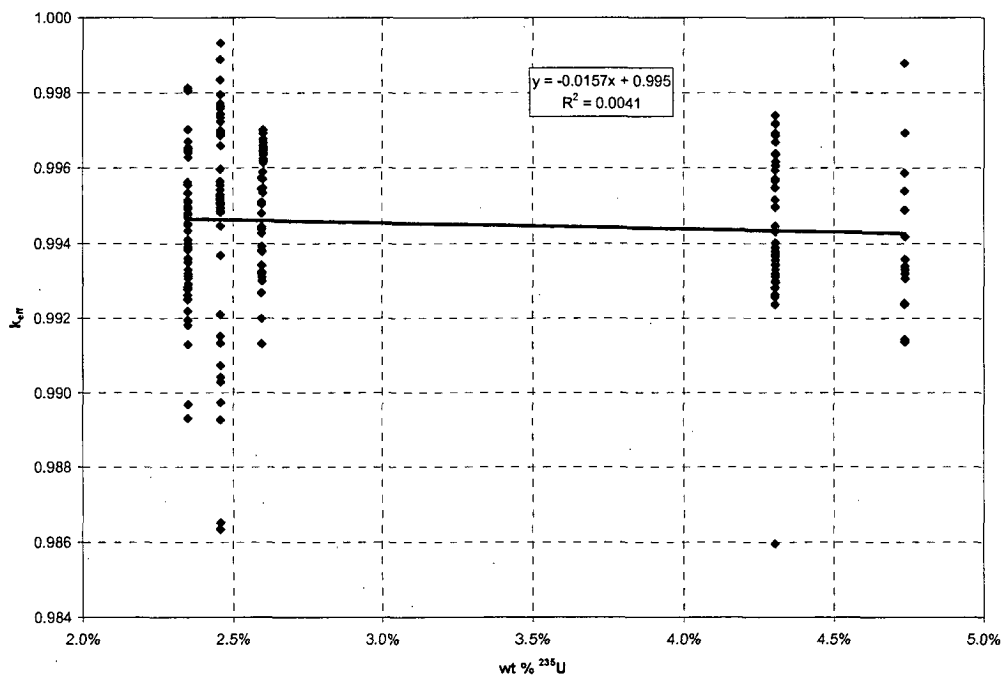


Figure 6.7.2-3 k_{eff} versus Rod Pitch (LEU)

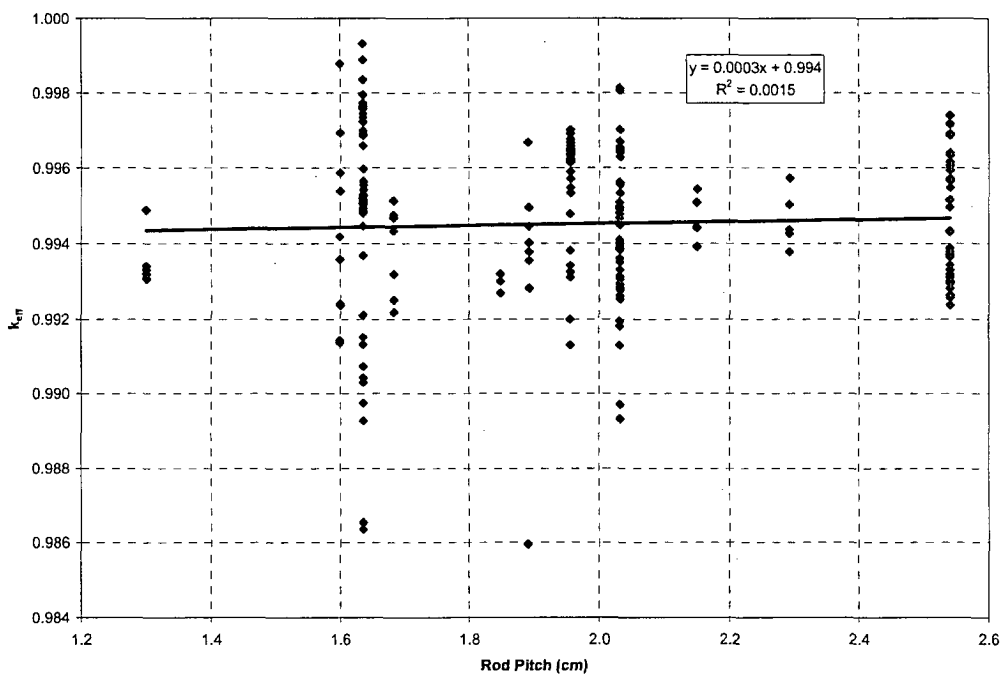


Figure 6.7.2-4 k_{eff} versus Fuel Pellet Diameter (LEU)

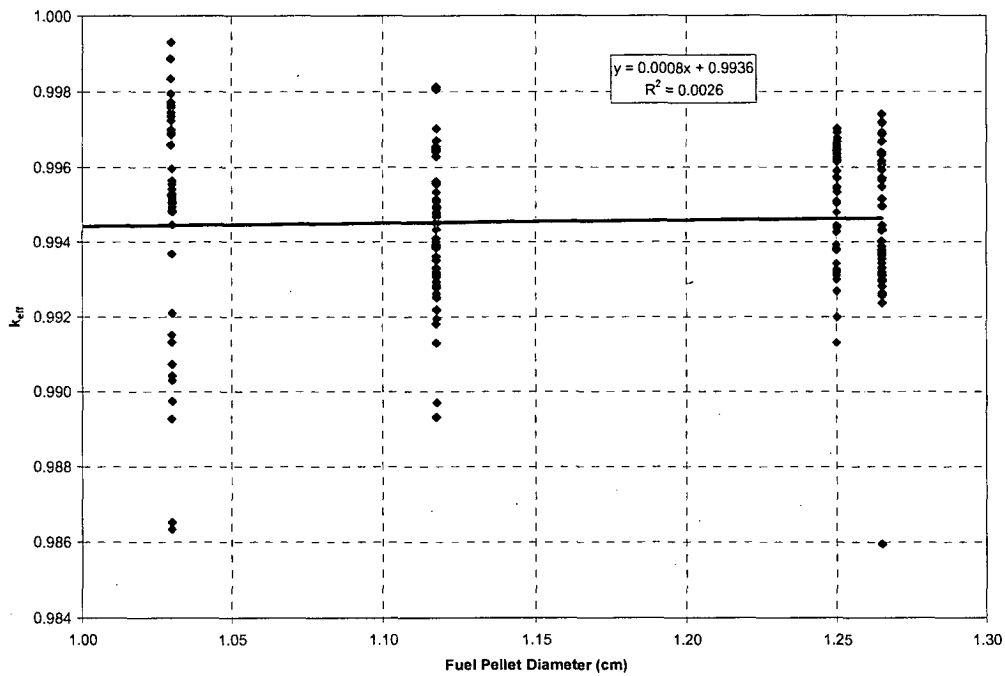


Figure 6.7.2-5 k_{eff} versus Fuel Rod Outside Diameter (LEU)

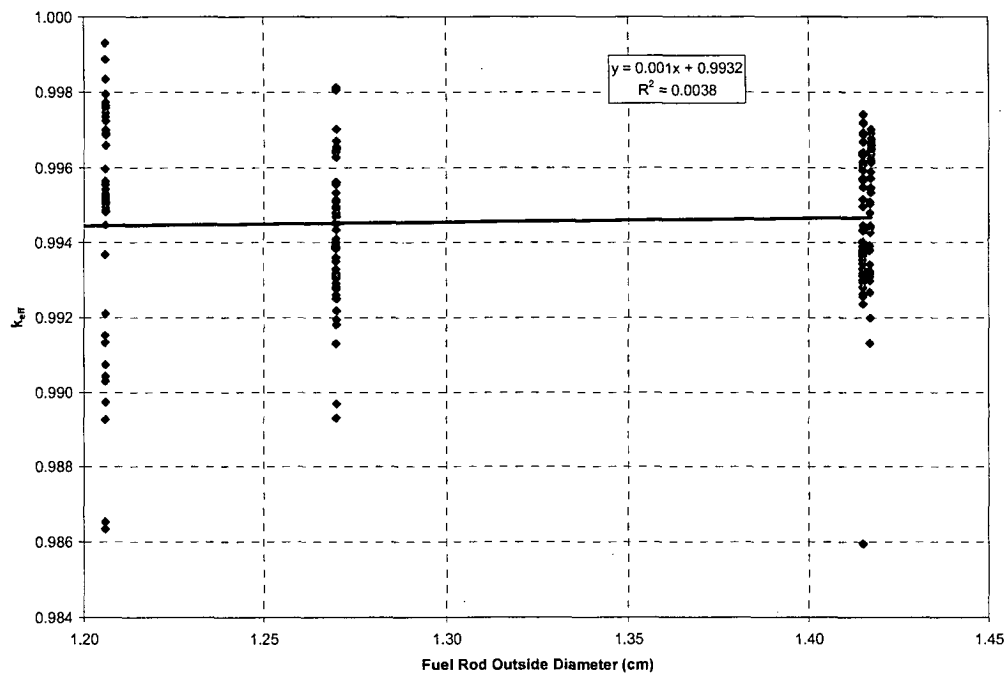


Figure 6.7.2-6 k_{eff} versus Hydrogen/²³⁵U Atom Ratio (LEU)

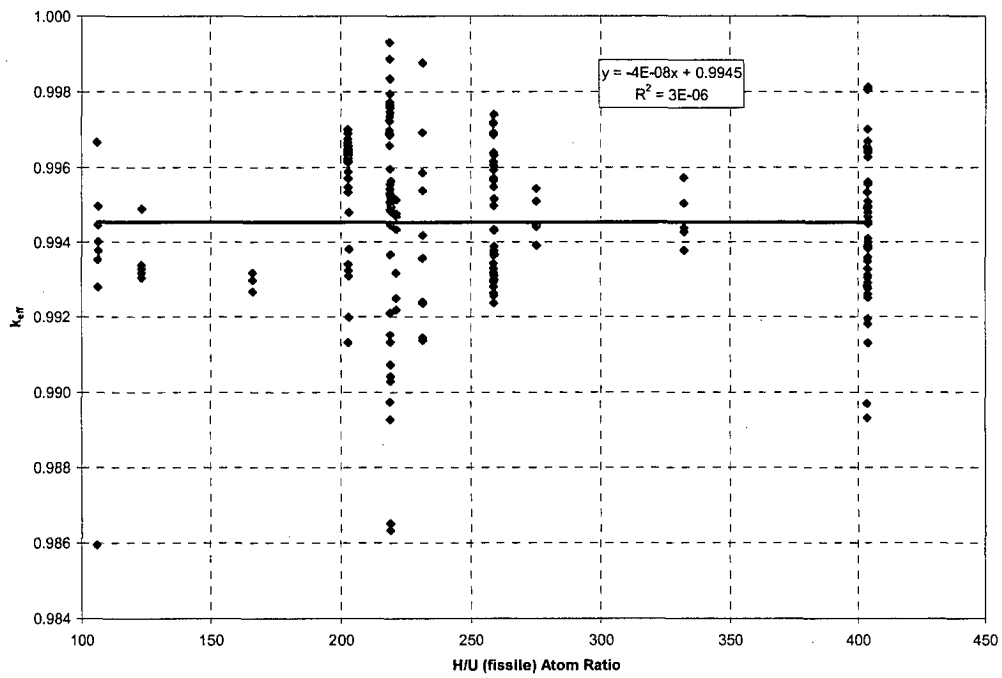


Figure 6.7.2-7 k_{eff} versus Soluble Boron Concentration (LEU)

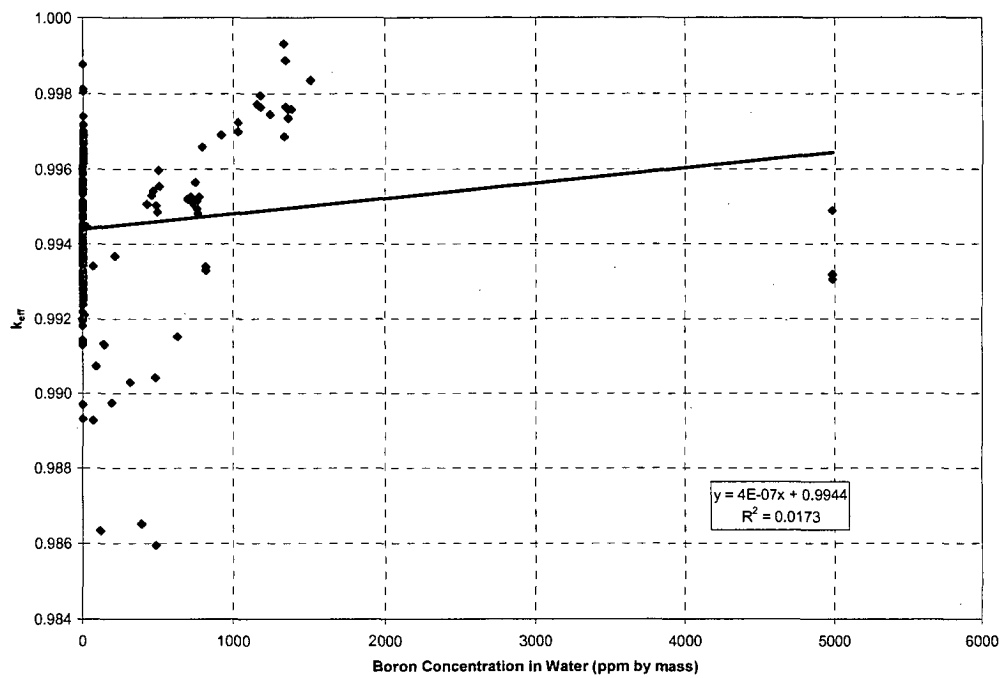


Figure 6.7.2-8 k_{eff} versus Cluster Gap Thickness (LEU)

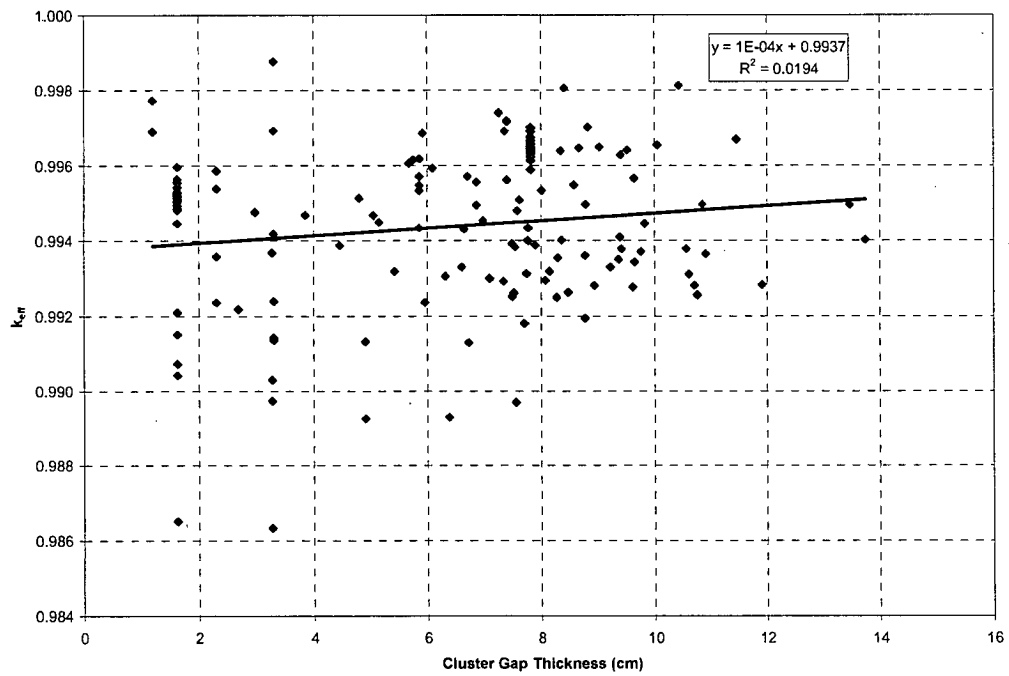


Figure 6.7.2-9 k_{eff} versus ^{10}B Plate Loading (LEU)

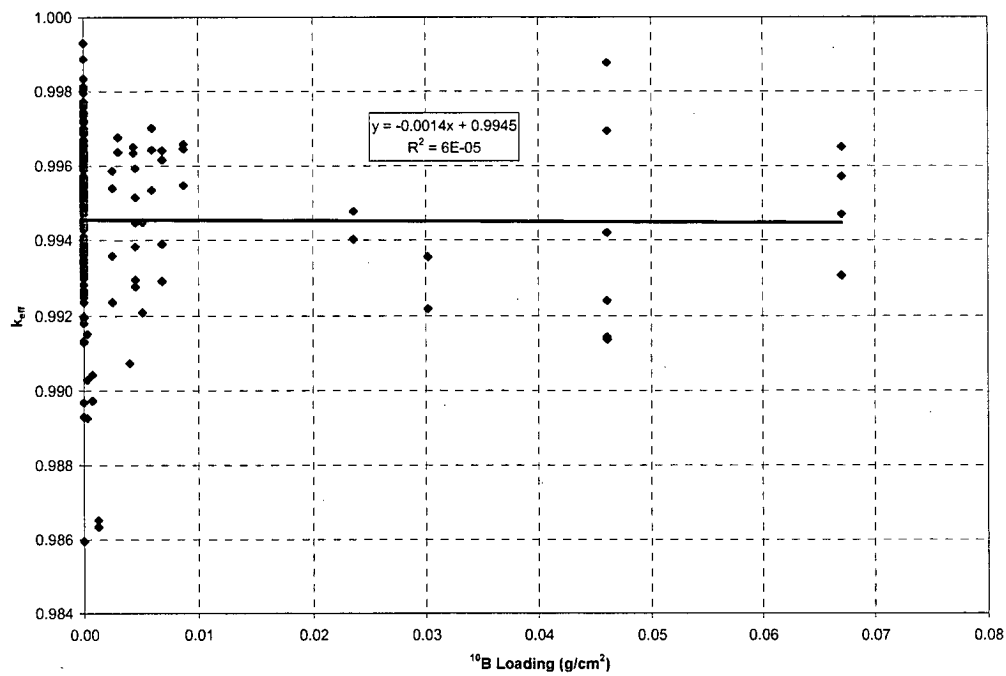


Figure 6.7.2-10 k_{eff} versus Energy of Average Neutron Lethargy Causing Fission (LEU)

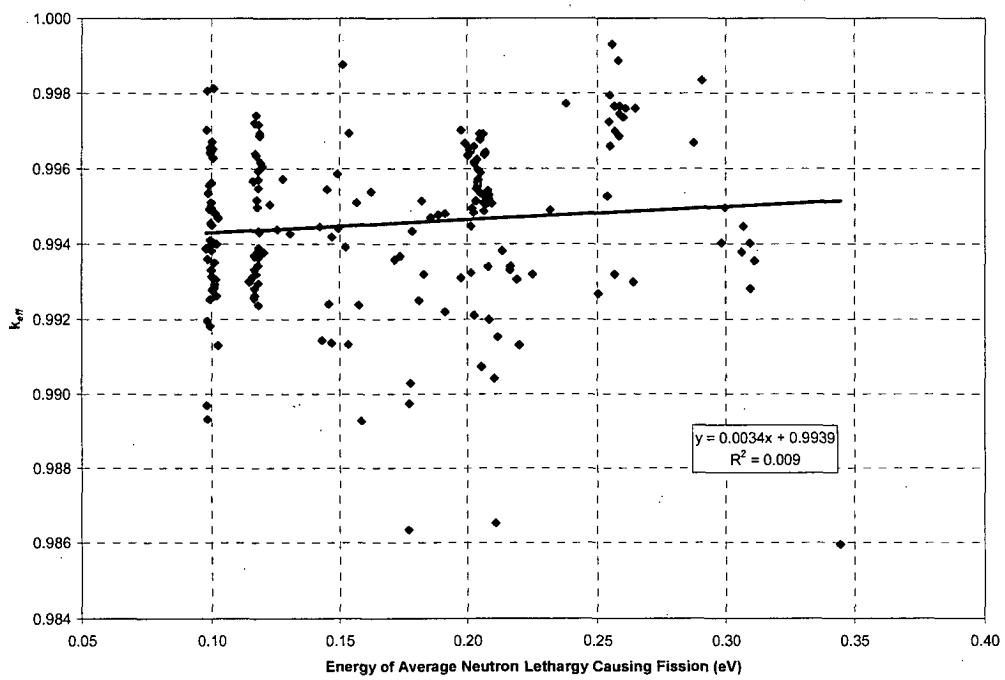


Table 6.7.2-3 LEU MCNP Validation Statistics

Case	1.01	1.02	1.03	1.04	1.05	1.06	1.07	1.08
Clusters	1	3	3	3	3	3	3	3
Enrichment (wt % ²³⁵ U)	2.35%	2.35%	2.35%	2.35%	2.35%	2.35%	2.35%	2.35%
Pitch (cm)	2.032	2.032	2.032	2.032	2.032	2.032	2.032	2.032
Fuel OD (cm)	1.118	1.118	1.118	1.118	1.118	1.118	1.118	1.118
Clad OD (cm)	1.270	1.270	1.270	1.270	1.270	1.270	1.270	1.270
Clad Material	Al	Al	Al	Al	Al	Al	Al	Al
H/U (fissile)	404	404	404	404	404	404	404	404
Soluble B (ppm)	--	--	--	--	--	--	--	--
Absorber Type	--	--	--	--	--	--	--	--
Cluster Gap (cm)	--	11.9	8.4	10.1	6.4	8.0	4.5	7.6
Reflector	H ₂ O	H ₂ O	H ₂ O	H ₂ O	H ₂ O	H ₂ O	H ₂ O	H ₂ O
Plate Loading (g ¹⁰ B/cm ²)	--	--	--	--	--	--	--	--
EALCF (MeV)	9.916E-8	1.010E-7	9.838E-8	9.933E-8	9.837E-8	9.874E-8	9.781E-8	9.826E-8
Exp. σ	0.0030	0.0030	0.0030	0.0030	0.0030	0.0030	0.0031	0.0030
k_{eff}	0.99491	0.99283	0.99806	0.99655	0.98931	0.99534	0.99388	0.98969
σ	0.00165	0.00155	0.00155	0.00165	0.00169	0.00162	0.00150	0.00152

Table 6.7.2-3 LEU MCNP Validation Statistics (cont'd)

Case	2.01	2.02	2.03	2.04	2.05
Clusters	1	1	1	3	3
Enrichment (wt % ²³⁵ U)	4.31%	4.31%	4.31%	4.31%	4.31%
Pitch (cm)	2.540	2.540	2.540	2.540	2.540
Fuel OD (cm)	1.265	1.265	1.265	1.265	1.265
Clad OD (cm)	1.415	1.415	1.415	1.415	1.415
Clad Material	Al	Al	Al	Al	Al
H/U (fissile)	259	259	259	259	259
Soluble B (ppm)	--	--	--	--	--
Absorber Type	--	--	--	--	--
Cluster Gap (cm)	--	--	--	10.6	7.1
Reflector	H ₂ O	H ₂ O	H ₂ O	H ₂ O	H ₂ O
Plate Loading (g ¹⁰ B/cm ²)	--	--	--	--	--
EALCF (MeV)	1.177E-7	1.164E-7	1.175E-7	1.161E-7	1.146E-7
Exp. σ	0.0020	0.0020	0.0020	0.0018	0.0019
k _{eff}	0.99516	0.99367	0.99634	0.99311	0.99300
σ	0.00195	0.00157	0.00190	0.00193	0.00161

Table 6.7.2-3 LEU MCNP Validation Statistics (cont'd)

Case	6.01	6.02	6.03	6.04	6.05	6.06	6.07	6.08	6.09
Clusters	1	1	1	1	1	1	1	1	1
Enrichment (wt % ²³⁵ U)	2.60%	2.60%	2.60%	2.60%	2.60%	2.60%	2.60%	2.60%	2.60%
Pitch (cm)	1.849	1.849	1.849	1.956	1.956	1.956	1.956	1.956	2.150
Fuel OD (cm)	1.250	1.250	1.250	1.250	1.250	1.250	1.250	1.250	1.250
Clad OD (cm)	1.417	1.417	1.417	1.417	1.417	1.417	1.417	1.417	1.417
Clad Material	Al	Al	Al	Al	Al	Al	Al	Al	Al
H/U (fissile)	166	166	166	203	203	203	203	203	275
Soluble B (ppm)	--	--	--	--	--	--	--	--	--
Absorber Type	--	--	--	--	--	--	--	--	--
Cluster Gap (cm)	--	--	--	--	--	--	--	--	--
Reflector	H ₂ O	H ₂ O	H ₂ O	H ₂ O	H ₂ O	H ₂ O	H ₂ O	H ₂ O	H ₂ O
Plate Loading (g ¹⁰ B/cm ²)	--	--	--	--	--	--	--	--	--
EALCF (MeV)	2.506E-7	2.568E-7	2.642E-7	1.915E-7	1.978E-7	2.018E-7	2.085E-7	2.136E-7	1.422E-7
Exp. σ	0.0020	0.0020	0.0020	0.0020	0.0020	0.0020	0.0020	0.0020	0.0020
k_{eff}	0.99268	0.99319	0.99299	0.99479	0.99310	0.99324	0.99199	0.99382	0.99445
σ	0.00065	0.00076	0.00074	0.00074	0.00069	0.00070	0.00071	0.00071	0.00069

Table 6.7.2-3 LEU MCNP Validation Statistics (cont'd)

Case	6.10	6.11	6.12	6.13	6.14	6.15	6.16	6.17	6.18
Clusters	1	1	1	1	1	1	1	1	1
Enrichment (wt % ²³⁵ U)	2.60%	2.60%	2.60%	2.60%	2.60%	2.60%	2.60%	2.60%	2.60%
Pitch (cm)	2.150	2.150	2.150	2.150	2.293	2.293	2.293	2.293	2.293
Fuel OD (cm)	1.250	1.250	1.250	1.250	1.250	1.250	1.250	1.250	1.250
Clad OD (cm)	1.417	1.417	1.417	1.417	1.417	1.417	1.417	1.417	1.417
Clad Material	Al	Al	Al	Al	Al	Al	Al	Al	Al
H/U (fissile)	275	275	275	275	332	332	332	332	332
Soluble B (ppm)	--	--	--	--	--	--	--	--	--
Absorber Type	--	--	--	--	--	--	--	--	--
Cluster Gap (cm)	--	--	--	--	--	--	--	--	--
Reflector	H ₂ O	H ₂ O	H ₂ O	H ₂ O	H ₂ O	H ₂ O	H ₂ O	H ₂ O	H ₂ O
Plate Loading (g ¹⁰ B/cm ²)	--	--	--	--	--	--	--	--	--
EALCF (MeV)	1.453E-7	1.496E-7	1.523E-7	1.568E-7	1.202E-7	1.227E-7	1.257E-7	1.280E-7	1.306E-7
Exp. σ	0.0020	0.0020	0.0020	0.0020	0.0020	0.0020	0.0020	0.0020	0.0020
k _{eff}	0.99544	0.99441	0.99392	0.99509	0.99378	0.99504	0.99438	0.99573	0.99427
σ	0.00073	0.00071	0.00078	0.00076	0.00070	0.00075	0.00067	0.00070	0.00076

Table 6.7.2-3 LEU MCNP Validation Statistics (cont'd)

Case	8.01	8.02	8.03	8.04	8.05	8.06	8.07	8.08
Clusters	3 x 3	3 x 3	3 x 3	3 x 3	3 x 3	3 x 3	3 x 3	3 x 3
Enrichment (wt % ²³⁵ U)	2.46%	2.46%	2.46%	2.46%	2.46%	2.46%	2.46%	2.46%
Pitch (cm)	1.636	1.636	1.636	1.636	1.636	1.636	1.636	1.636
Fuel OD (cm)	1.030	1.030	1.030	1.030	1.030	1.030	1.030	1.030
Clad OD (cm)	1.206	1.206	1.206	1.206	1.206	1.206	1.206	1.206
Clad Material	Al	Al	Al	Al	Al	Al	Al	Al
H/U (fissile)	219	219	219	219	219	219	219	219
Soluble B (ppm)	1511	1336	1336	1182	1182	1033	1033	794
Absorber Type	--	--	--	--	--	--	--	--
Cluster Gap (cm)	--	--	--	--	--	--	--	--
Reflector	H ₂ O	H ₂ O	H ₂ O	H ₂ O	H ₂ O	H ₂ O	H ₂ O	H ₂ O
Plate Loading (g ¹⁰ B/cm ²)	--	--	--	--	--	--	--	--
EALCF (MeV)	2.907E-7	2.583E-7	2.559E-7	2.548E-7	2.566E-7	2.568E-7	2.544E-7	2.548E-7
Exp. σ	0.0012	0.0012	0.0012	0.0012	0.0012	0.0012	0.0012	0.0012
k _{eff}	0.99835	0.99686	0.99931	0.99795	0.99765	0.99699	0.99723	0.99659
σ	0.00060	0.00063	0.00032	0.00063	0.00069	0.00061	0.00066	0.00073

Table 6.7.2-3 LEU MCNP Validation Statistics (cont'd)

Case	8.09	8.10	8.11	8.12	8.13	8.14	8.15	8.16	8.17
Clusters	3 x 3	3 x 3	3 x 3	3 x 3	3 x 3	3 x 3	3 x 3	5	5 x 5
Enrichment (wt % ²³⁵ U)	2.46%	2.46%	2.46%	2.46%	2.46%	2.46%	2.46%	2.46%	2.46%
Pitch (cm)	1.636	1.636	1.636	1.636	1.636	1.636	1.636	1.636	1.636
Fuel OD (cm)	1.030	1.030	1.030	1.030	1.030	1.030	1.030	1.030	1.030
Clad OD (cm)	1.206	1.206	1.206	1.206	1.206	1.206	1.206	1.206	1.206
Clad Material	Al	Al	Al	Al	Al	Al	Al	Al	Al
H/U (fissile)	219	219	219	219	219	219	219	219	219
Soluble B (ppm)	779	1245	1384	1348	1348	1363	1363	1158	921
Absorber Type	--	--	--	--	--	--	--	--	--
Cluster Gap (cm)	-	-	-	-	-	-	-	1.2	1.2
Reflector	H ₂ O	H ₂ O	H ₂ O	H ₂ O	H ₂ O	H ₂ O	H ₂ O	H ₂ O	H ₂ O
Plate Loading (g ¹⁰ B/cm ²)	--	--	--	--	--	--	--	--	--
EALCF (MeV)	2.538E-7	2.586E-7	2.647E-7	2.587E-7	2.582E-7	2.600E-7	2.609E-7	2.379E-7	2.063E-7
Exp. σ	0.0012	0.0012	0.0012	0.0012	0.0012	0.0012	0.0012	0.0012	0.0012
k _{eff}	0.99526	0.99745	0.99759	0.99765	0.99888	0.99735	0.99758	0.99772	0.99691
σ	0.00072	0.00065	0.00068	0.00065	0.00070	0.00067	0.00071	0.00070	0.00062

Table 6.7.2-3 LEU MCNP Validation Statistics (cont'd)

Case	9.01	9.02	9.03	9.04	9.05	9.06	9.07	9.08	9.09	9.10	9.11	9.12	9.13
Clusters	3	3	3	3	3	3	3	3	3	3	3	3	3
Enrichment (wt % ²³⁵ U)	4.31%	4.31%	4.31%	4.31%	4.31%	4.31%	4.31%	4.31%	4.31%	4.31%	4.31%	4.31%	4.31%
Pitch (cm)	2.540	2.540	2.540	2.540	2.540	2.540	2.540	2.540	2.540	2.540	2.540	2.540	2.540
Fuel OD (cm)	1.265	1.265	1.265	1.265	1.265	1.265	1.265	1.265	1.265	1.265	1.265	1.265	1.265
Clad OD (cm)	1.415	1.415	1.415	1.415	1.415	1.415	1.415	1.415	1.415	1.415	1.415	1.415	1.415
Clad Material	Al	Al	Al	Al	Al	Al	Al	Al	Al	Al	Al	Al	Al
H/U (fissile)	259	259	259	259	259	259	259	259	259	259	259	259	259
Soluble B (ppm)	-	-	-	-	-	-	-	-	-	-	-	-	-
Absorber Type	304L SS (no B)	304L SS (no B)	304L SS (no B)	304L SS (no B)	304L SS (1.05% B)	304L SS (1.05% B)	304L SS (1.62% B)	304L SS (1.62% B)	Boral	Cu	Cu	Cu	Cu
Cluster Gap (cm)	8.6	9.7	9.2	9.8	6.1	8.1	5.8	7.9	6.7	8.2	9.4	8.5	9.6
Reflector	H ₂ O	H ₂ O	H ₂ O	H ₂ O	H ₂ O	H ₂ O	H ₂ O	H ₂ O	H ₂ O	H ₂ O	H ₂ O	H ₂ O	H ₂ O
Plate Loading (g ¹⁰ B/cm ²)	0.00000	0.00000	0.00000	0.00000	0.00455	0.00455	0.00690	0.00690	0.06704	-	-	-	-
EALCF(MeV)	1.183E-7	1.181E-7	1.168E-7	1.179E-7	1.182E-7	1.182E-7	1.191E-7	1.182E-7	1.183E-7	1.173E-7	1.176E-7	1.169E-7	1.163E-7
Exp. σ	0.0021	0.0021	0.0021	0.0021	0.0021	0.0021	0.0021	0.0021	0.0021	0.0021	0.0021	0.0021	0.0021
k _{eff}	0.99548	0.99343	0.99330	0.99371	0.99593	0.99295	0.99616	0.99389	0.99571	0.99319	0.99378	0.99263	0.99566
σ	0.00191	0.00182	0.00187	0.00192	0.00174	0.00193	0.00198	0.00175	0.00209	0.00153	0.00178	0.00191	0.00177

Table 6.7.2-3 LEU MCNP Validation Statistics (cont'd)

Case	9.14	9.15	9.16	9.17	9.18	9.19	9.20	9.21	9.22	9.23	9.24	9.25	9.26	9.27
Clusters	3	3	3	3	3	3	3	3	3	3	3	3	3	3
Enrichment (wt % ²³⁵ U)	4.31%	4.31%	4.31%	4.31%	4.31%	4.31%	4.31%	4.31%	4.31%	4.31%	4.31%	4.31%	4.31%	4.31%
Pitch (cm)	2.540	2.540	2.540	2.540	2.540	2.540	2.540	2.540	2.540	2.540	2.540	2.540	2.540	2.540
Fuel OD (cm)	1.265	1.265	1.265	1.265	1.265	1.265	1.265	1.265	1.265	1.265	1.265	1.265	1.265	1.265
Clad OD (cm)	1.415	1.415	1.415	1.415	1.415	1.415	1.415	1.415	1.415	1.415	1.415	1.415	1.415	1.415
Clad Material	Al	Al	Al	Al	Al	Al	Al	Al	Al	Al	Al	Al	Al	Al
H/U (fissile)	259	259	259	259	259	259	259	259	259	259	259	259	259	259
Soluble B (ppm)	--	--	--	--	--	--	--	--	--	--	--	--	--	--
Absorber Type	Cu (0.989 wt % Cd)	Cu (0.989 wt % Cd)	Cd	Cd	Cd	Cd	Cd	Cd	Cd	Cd	Al (no B)	Al (no B)	Zircaloy-4	Zircaloy-4
Cluster Gap (cm)	6.7	8.4	5.9	7.4	6.0	7.4	5.9	7.4	5.7	7.3	10.7	10.8	10.9	10.9
Reflector	H ₂ O	H ₂ O	H ₂ O	H ₂ O	H ₂ O	H ₂ O	H ₂ O	H ₂ O	H ₂ O	H ₂ O	H ₂ O	H ₂ O	H ₂ O	H ₂ O
Plate Loading (g ¹⁰ B/cm ²)	--	--	--	--	--	--	--	--	--	--	0.00000	0.00000	--	--
EALCF(MeV)	1.186E-7	1.171E-7	1.186E-7	1.183E-7	1.183E-7	1.168E-7	1.182E-7	1.187E-7	1.199E-7	1.173E-7	1.167E-7	1.165E-7	1.181E-7	1.177E-7
Exp. σ	0.0021	0.0021	0.0021	0.0021	0.0021	0.0021	0.0021	0.0021	0.0021	0.0021	0.0021	0.0021	0.0021	0.0021
k _{eff}	0.99431	0.99639	0.99686	0.99716	0.99237	0.99719	0.99434	0.99692	0.99606	0.99740	0.99281	0.99256	0.99365	0.99497
σ	0.00188	0.00207	0.00183	0.00166	0.00194	0.00187	0.00179	0.00183	0.00189	0.00206	0.00168	0.00197	0.00197	0.00193

Table 6.7.2-3 LEU MCNP Validation Statistics (cont'd)

Case	11.03	11.04	11.05	11.06	11.07	11.08	11.09
Clusters	3	3	3	3	3	3	3
Enrichment (wt % ²³⁵ U)	2.46%	2.46%	2.46%	2.46%	2.46%	2.46%	2.46%
Pitch (cm)	1.636	1.636	1.636	1.636	1.636	1.636	1.636
Fuel OD (cm)	1.030	1.030	1.030	1.030	1.030	1.030	1.030
Clad OD (cm)	1.206	1.206	1.206	1.206	1.206	1.206	1.206
Clad Material	Al	Al	Al	Al	Al	Al	Al
H/U (fissile)	219	219	219	219	219	219	219
Soluble B (ppm)	769	764	762	753	739	721	702
Absorber Type	--	--	--	--	--	--	--
Cluster Gap (cm)	1.6	1.6	1.6	1.6	1.6	1.6	1.6
Reflector	H ₂ O	H ₂ O	H ₂ O	H ₂ O	H ₂ O	H ₂ O	H ₂ O
Plate Loading (g ¹⁰ B/cm ²)	--	--	--	--	--	--	--
EALCF [MeV]	2.027E-7	2.020E-7	2.035E-7	2.044E-7	2.065E-7	2.068E-7	2.085E-7
Exp. σ	0.0032	0.0032	0.0032	0.0032	0.0032	0.0032	0.0032
k _{eff}	0.99482	0.99494	0.99514	0.99564	0.99508	0.99526	0.99520
σ	0.00031	0.00030	0.00030	0.00030	0.00031	0.00030	0.00031

Table 6.7.2-3 LEU MCNP Validation Statistics (cont'd)

Case	13.01	13.02	13.03	13.04	13.05	13.06	13.07
Clusters	3	3	3	3	3	3	3
Enrichment (wt % ²³⁵ U)	4.31%	4.31%	4.31%	4.31%	4.31%	4.31%	4.31%
Pitch (cm)	1.892	1.892	1.892	1.892	1.892	1.892	1.892
Fuel OD (cm)	1.265	1.265	1.265	1.265	1.265	1.265	1.265
Clad OD (cm)	1.415	1.415	1.415	1.415	1.415	1.415	1.415
Clad Material	Al	Al	Al	Al	Al	Al	Al
H/U (fissile)	107	107	107	107	107	107	107
Soluble B (ppm)	--	--	--	--	--	--	--
Absorber Type	304L SS (no B)	304L SS (1.05% B)	Boral B	Boroflex	Cd	Cu	Cu (0.989 wt % Cd)
Cluster Gap (cm)	13.8	9.8	8.3	8.4	8.9	13.5	10.6
Reflector	Steel	Steel	Steel	Steel	Steel	Steel	Steel
Plate Loading (g ¹⁰ B/cm ²)	0.00000	0.00455	0.03022	0.02361	--	--	--
EALCF (MeV)	2.982E-7	3.068E-7	3.111E-7	3.094E-7	3.097E-7	2.998E-7	3.061E-7
Exp. σ	0.0018	0.0018	0.0018	0.0018	0.0032	0.0018	0.0018
k _{eff}	0.99402	0.99446	0.99355	0.99401	0.99281	0.99496	0.99378
σ	0.00068	0.00064	0.00064	0.00064	0.00066	0.00063	0.00062

Table 6.7.2-3 LEU MCNP Validation Statistics (cont'd)

Case	14.01	14.02	14.05	14.06	14.07
Clusters	1	1	1	1	1
Enrichment (wt % ²³⁵ U)	4.31%	4.31%	4.31%	4.31%	4.31%
Pitch (cm)	1.890	1.890	1.890	1.715	1.715
Fuel OD (cm)	1.265	1.265	1.265	1.265	1.265
Clad OD (cm)	1.415	1.415	1.415	1.415	1.415
Clad Material	Al	Al	Al	Al	Al
H/U (fissile)	106	106	106	73	73
Soluble B (ppm)	0	491	2539	0	1030
Absorber Type	--	--	--	--	--
Cluster Gap (cm)	--	--	--	--	--
Reflector	H ₂ O	H ₂ O	H ₂ O	H ₂ O	H ₂ O
Plate Loading (g ¹⁰ B/cm ²)	--	--	--	--	--
EALCF (MeV)	2.873E-7	3.447E-7	6.003E-7	5.175E-7	7.722E-7
Exp. σ	0.0019	0.0077	0.0069	0.0033	0.0051
k_{eff}	0.99668	0.98595	1.00221	1.00245	0.99973
σ	0.00044	0.00045	0.00043	0.00045	0.00044

Table 6.7.2-3 LEU MCNP Validation Statistics (cont'd)

Case	16.01	16.02	16.03	16.04	16.05	16.06	16.07	16.08	16.09	16.10
Clusters	3	3	3	3	3	3	3	3	3	3
Enrichment (wt % ²³⁵ U)	2.35%	2.35%	2.35%	2.35%	2.35%	2.35%	2.35%	2.35%	2.35%	2.35%
Pitch (cm)	2.032	2.032	2.032	2.032	2.032	2.032	2.032	2.032	2.032	2.032
Fuel OD (cm)	1.118	1.118	1.118	1.118	1.118	1.118	1.118	1.118	1.118	1.118
Clad OD (cm)	1.270	1.270	1.270	1.270	1.270	1.270	1.270	1.270	1.270	1.270
Clad Material	Al	Al	Al	Al	Al	Al	Al	Al	Al	Al
H/U (fissile)	404	404	404	404	404	404	404	404	404	404
Soluble B (ppm)	--	--	--	--	--	--	--	--	--	--
Absorber Type	304L SS (no B)	304L SS (no B)	304L SS (no B)	304L SS (no B)	304L SS (no B)	304L SS (no B)	304L SS (no B)	304L SS (1.05% B)	304L SS (1.05% B)	304L SS (1.62% B)
Cluster Gap (cm)	6.9	7.6	7.5	7.4	7.8	10.4	11.5	7.6	9.6	7.4
Reflector	H ₂ O	H ₂ O	H ₂ O	H ₂ O	H ₂ O	H ₂ O	H ₂ O	H ₂ O	H ₂ O	H ₂ O
Plate Loading (g ¹⁰ B/cm ²)	0.00000	0.00000	0.00000	0.00000	0.00000	0.00000	0.00000	0.00455	0.00455	0.00690
EALCF (MeV)	1.000E-7	9.983E-8	9.947E-8	1.001E-7	1.002E-7	1.009E-7	1.001E-7	9.993E-8	1.004E-7	1.012E-7
Exp. σ	0.0031	0.0031	0.0031	0.0031	0.0031	0.0031	0.0031	0.0031	0.0031	0.0031
k _{eff}	0.99494	0.99509	0.99252	0.99562	0.99313	0.99813	0.99670	0.99383	0.99277	0.99292
σ	0.00171	0.00153	0.00157	0.00162	0.00173	0.00179	0.00175	0.00172	0.00157	0.00162

Table 6.7.2-3 LEU MCNP Validation Statistics (cont'd)

Case	16.11	16.12	16.13	16.14	16.15	16.16	16.17	16.18	16.19	16.20	16.21	16.22
Clusters	3	3	3	3	3	3	3	3	3	3	3	3
Enrichment (wt % ²³⁵ U)	2.35%	2.35%	2.35%	2.35%	2.35%	2.35%	2.35%	2.35%	2.35%	2.35%	2.35%	2.35%
Pitch(cm)	2.032	2.032	2.032	2.032	2.032	2.032	2.032	2.032	2.032	2.032	2.032	2.032
Fuel OD (cm)	1.118	1.118	1.118	1.118	1.118	1.118	1.118	1.118	1.118	1.118	1.118	1.118
Clad OD (cm)	1.270	1.270	1.270	1.270	1.270	1.270	1.270	1.270	1.270	1.270	1.270	1.270
Clad Material	Al	Al	Al	Al	Al	Al	Al	Al	Al	Al	Al	Al
H/U (fissile)	404	404	404	404	404	404	404	404	404	404	404	404
Soluble B (ppm)	--	--	--	--	--	--	--	--	--	--	--	--
Absorber Type	304L SS (1.62% B)	Boral	Boral	Boral	Cu	Cu	Cu	Cu	Cu	Cu (0.989 wt % Cd)	Cd	Cd
Cluster Gap (cm)	9.5	6.3	9.0	5.1	6.6	7.7	7.5	6.9	7.0	5.2	6.7	7.6
Reflector	H ₂ O	H ₂ O	H ₂ O	H ₂ O	H ₂ O	H ₂ O	H ₂ O	H ₂ O	H ₂ O	H ₂ O	H ₂ O	H ₂ O
Plate Loading (g ¹⁰ B/cm ²)	0.00690	0.06704	0.06704	0.06704	--	--	--	--	--	--	--	--
EALCF (MeV)	9.962E-8	1.016E-7	1.006E-7	1.025E-7	1.000E-7	9.944E-8	9.904E-8	9.919E-8	9.971E-8	1.001E-7	1.024E-7	1.014E-7
Exp. σ	0.0031	0.0031	0.0031	0.0031	0.0031	0.0031	0.0031	0.0031	0.0031	0.0031	0.0031	0.0031
k _{eff}	0.99641	0.99306	0.99650	0.99468	0.99330	0.99181	0.99392	0.99556	0.99454	0.99449	0.99130	0.99480
σ	0.00154	0.00161	0.00152	0.00162	0.00157	0.00153	0.00155	0.00172	0.00165	0.00155	0.00166	0.00157

Table 6.7.2-3 LEU MCNP Validation Statistics (cont'd)

Case	16.23	16.24	16.25	16.26	16.27	16.28	16.29	16.30	16.31	16.32
Clusters	3	3	3	3	3	3	3	3	3	3
Enrichment (wt % ²³⁵ U)	2.35%	2.35%	2.35%	2.35%	2.35%	2.35%	2.35%	2.35%	2.35%	2.35%
Pitch(cm)	2.032	2.032	2.032	2.032	2.032	2.032	2.032	2.032	2.032	2.032
Fuel OD (cm)	1.118	1.118	1.118	1.118	1.118	1.118	1.118	1.118	1.118	1.118
Clad OD (cm)	1.270	1.270	1.270	1.270	1.270	1.270	1.270	1.270	1.270	1.270
Clad Material	Al	Al	Al	Al	Al	Al	Al	Al	Al	Al
H/U (fissile)	404	404	404	404	404	404	404	404	404	404
Soluble B (ppm)	--	--	--	--	--	--	--	--	--	--
Absorber Type	Cd	Cd	Cd	Cd	Cd	Al (no B)	Al (no B)	Al (no B)	Zircaloy-4	Zircaloy-4
Cluster Gap cm)	9.4	7.8	9.4	7.5	9.4	8.7	8.8	8.8	8.8	8.8
Reflector	H ₂ O	H ₂ O	H ₂ O	H ₂ O	H ₂ O	H ₂ O	H ₂ O	H ₂ O	H ₂ O	H ₂ O
Plate Loading (g ¹⁰ B/cm ²)	--	--	--	--	--	0.00000	0.00000	0.00000	--	--
EALCF (MeV)	1.010E-7	1.018E-7	1.006E-7	1.019E-7	9.948E-8	9.991E-8	9.843E-8	9.807E-8	9.964E-8	9.834E-8
Exp. σ	0.0031	0.0031	0.0031	0.0031	0.0031	0.0031	0.0031	0.0031	0.0031	0.0031
k _{eff}	0.99350	0.99400	0.99628	0.99262	0.99410	0.99647	0.99360	0.99702	0.99497	0.99195
σ	0.00184	0.00152	0.00169	0.00151	0.00168	0.00166	0.00157	0.00160	0.00163	0.00172

Table 6.7.2-3 LEU MCNP Validation Statistics (cont'd)

Case	35.01	35.02	40.01	40.02	40.03	40.04	40.05	40.06	40.07	40.08	40.09	40.10
Clusters	1	1	4	4	4	4	4	4	4	4	4	4
Enrichment (wt % ²³⁵ U)	2.60%	2.60%	4.74%	4.74%	4.74%	4.74%	4.74%	4.74%	4.74%	4.74%	4.74%	4.74%
Pitch (cm)	1.956	1.956	1.600	1.600	1.600	1.600	1.600	1.600	1.600	1.600	1.600	1.600
Fuel OD (cm)	1.250	1.250	0.790	0.790	0.790	0.790	0.790	0.790	0.790	0.790	0.790	0.790
Clad OD (cm)	1.417	1.417	0.940	0.940	0.940	0.940	0.940	0.940	0.940	0.940	0.940	0.940
Clad Material	Al	Al	Al alloy	Al alloy	Al alloy	Al alloy	Al alloy	Al alloy	Al alloy	Al alloy	Al alloy	Al alloy
H/U (fissile)	203	203	231	231	231	231	231	231	231	231	231	231
Soluble B (ppm)	70	148	--	--	--	--	--	--	--	--	--	--
Absorber Type	--	--	Z2 CN18/10 SS (1.10% B)	Z2 CN18/10 SS (1.10% B)	Z2 CN18/10 SS (1.10% B)	Z2 CN18/10 SS (1.10% B)	Boral	Boral	Boral	Boral	Boral	Boral
Cluster Gap (cm)	--	--	2.3	2.3	2.3	2.3	3.3	3.3	3.3	3.3	3.3	3.3
Reflector	H ₂ O	H ₂ O	H ₂ O	Lead	Lead	Lead	H ₂ O	Lead	Lead	Lead	Steel	Steel
Plate Loading (g ¹⁰ B/cm ²)	--	--	0.00252	0.00252	0.00252	0.00252	0.04608	0.04608	0.04608	0.04608	0.04608	0.04608
EALCF (MeV)	2.170E-7	2.202E-7	1.493E-7	1.717E-7	1.625E-7	1.576E-7	1.432E-7	1.515E-7	1.470E-7	1.459E-7	1.537E-7	1.469E-7
Exp. σ	0.0018	0.0019	0.0039	0.0041	0.0041	0.0041	0.0042	0.0044	0.0044	0.0044	0.0046	0.0046
k _{eff}	0.99341	0.99131	0.99586	0.99358	0.99539	0.99237	0.99144	0.99878	0.99418	0.99240	0.99693	0.99137
σ	0.00070	0.00078	0.00195	0.00192	0.00203	0.00194	0.00193	0.00196	0.00224	0.00216	0.00190	0.00208

Table 6.7.2-3 LEU MCNP Validation Statistics (cont'd)

Case	42.01	42.02	42.03	42.04	42.05	42.06	42.07
Clusters	3	3	3	3	3	3	3
Enrichment (wt % ²³⁵ U)	2.35%	2.35%	2.35%	2.35%	2.35%	2.35%	2.35%
Pitch (cm)	1.684	1.684	1.684	1.684	1.684	1.684	1.684
Fuel OD (cm)	1.118	1.118	1.118	1.118	1.118	1.118	1.118
Clad OD (cm)	1.270	1.270	1.270	1.270	1.270	1.270	1.270
Clad Material	Al	Al	Al	Al	Al	Al	Al
H/U (fissile)	221	221	221	221	221	221	221
Soluble B (ppm)	--	--	--	--	--	--	--
Absorber Type	304L SS (no B)	304L SS (1.05% B)	Boral B	Boroflex	Cd	Cu	Cu-Cd
Cluster Gap (cm)	8.3	4.8	2.7	3.0	3.9	7.8	5.4
Reflector	Steel	Steel	Steel	Steel	Steel	Steel	Steel
Plate Loading (g ¹⁰ B/cm ²)	0.00000	0.00455	0.03022	0.02361	--	--	--
EALCF (MeV)	1.813E-7	1.824E-7	1.915E-7	1.887E-7	1.857E-7	1.786E-7	1.833E-7
Exp. σ	0.0016	0.0016	0.0016	0.0017	0.0033	0.0016	0.0018
k_{eff}	0.99250	0.99514	0.99219	0.99476	0.99469	0.99434	0.99319
σ	0.00171	0.00183	0.00169	0.00169	0.00161	0.00191	0.00157

Table 6.7.2-3 LEU MCNP Validation Statistics (cont'd)

Case	50.03	50.03	50.03	50.03	50.03
Clusters	1	1	1	1	1
Enrichment (wt % ²³⁵ U)	4.74%	4.74%	4.74%	4.74%	4.74%
Pitch (cm)	1.300	1.300	1.300	1.300	1.300
Fuel OD (cm)	0.790	0.790	0.790	0.790	0.790
Clad OD (cm)	0.940	0.940	0.940	0.940	0.940
Clad Material	Al alloy	Al alloy	Al alloy	Al alloy	Al alloy
H/U (fissile)	124	124	124	124	124
Soluble B (ppm)	821	821	4986	4986	4986
Absorber Type	--	--	--	--	--
Cluster Gap (cm)	--	--	--	--	--
Reflector	Borated H ₂ O	Borated H ₂ O	Borated H ₂ O	Borated H ₂ O	Borated H ₂ O
Plate Loading (g ¹⁰ B/cm ²)	--	--	--	--	--
EALCF (MeV)	2.170E-7	2.083E-7	2.318E-7	2.252E-7	2.195E-7
Exp. σ	0.0010	0.0010	0.0010	0.0010	0.0010
k_{eff}	0.99330	0.99340	0.99489	0.99319	0.99306
σ	0.00080	0.00071	0.00075	0.00075	0.00080

Table 6.7.2-3 LEU MCNP Validation Statistics (cont'd)

Case	51.01	51.02	51.03	51.04	51.05	51.06	51.07	51.08	51.09
Clusters	9	9	9	9	9	9	9	9	9
Enrichment (wt % ²³⁵ U)	2.46%	2.46%	2.46%	2.46%	2.46%	2.46%	2.46%	2.46%	2.46%
Pitch (cm)	1.636	1.636	1.636	1.636	1.636	1.636	1.636	1.636	1.636
Fuel OD (cm)	1.030	1.030	1.030	1.030	1.030	1.030	1.030	1.030	1.030
Clad OD (cm)	1.206	1.206	1.206	1.206	1.206	1.206	1.206	1.206	1.206
Clad Material	Al	Al	Al	Al	Al	Al	Al	Al	Al
H/U (fissile)	219	219	219	219	219	219	219	219	219
Soluble B (ppm)	143	510	514	501	493	474	462	432	217
Absorber Type	none	SS	SS	SS	SS	SS	SS	SS	SS
Cluster Gap (cm)	4.9	1.6	1.6	1.6	1.6	1.6	1.6	1.6	3.3
Reflector	Borated H ₂ O	Borated H ₂ O	Borated H ₂ O	Borated H ₂ O	Borated H ₂ O	Borated H ₂ O	Borated H ₂ O	Borated H ₂ O	Borated H ₂ O
Plate Loading (g ¹⁰ B/cm ²)	0.00000	--	--	--	--	--	--	--	--
EALCF (MeV)	1.535E-7	2.045E-7	2.043E-7	2.067E-7	2.074E-7	2.083E-7	2.085E-7	2.098E-7	1.737E-7
Exp. σ	0.0020	0.0024	0.0024	0.0024	0.0024	0.0024	0.0024	0.0024	0.0019
k _{eff}	0.99133	0.99597	0.99555	0.99486	0.99504	0.99542	0.99530	0.99507	0.99368
σ	0.00033	0.00035	0.00033	0.00034	0.00034	0.00034	0.00034	0.00034	0.00033

Table 6.7.2-3 LEU MCNP Validation Statistics (cont'd)

Case	51.10	51.11	51.12	51.13	51.14	51.15	51.16	51.17	51.18	51.19
Clusters	9	9	9	9	9	9	9	9	9	9
Enrichment (wt % ²³⁵ U)	2.46%	2.46%	2.46%	2.46%	2.46%	2.46%	2.46%	2.46%	2.46%	2.46%
Pitch (cm)	1.636	1.636	1.636	1.636	1.636	1.636	1.636	1.636	1.636	1.636
Fuel OD (cm)	1.030	1.030	1.030	1.030	1.030	1.030	1.030	1.030	1.030	1.030
Clad OD (cm)	1.206	1.206	1.206	1.206	1.206	1.206	1.206	1.206	1.206	1.206
Clad Material	Al	Al	Al	Al	Al	Al	Al	Al	Al	Al
H/U (fissile)	219	219	219	219	219	219	219	219	219	219
Soluble B (ppm)	15	28	92	395	121	487	197	634	320	72
Absorber Type	B/Al Set 5	B/Al Set 5A	B/Al Set 4	B/Al Set 3	B/Al Set 3	B/Al Set 2	B/Al Set 2	B/Al Set 1	B/Al Set 1	B/Al Set 1
Cluster Gap (cm)	1.6	1.6	1.6	1.6	3.3	1.6	3.3	1.6	3.3	4.9
Reflector	Borated H ₂ O	Borated H ₂ O	Borated H ₂ O	Borated H ₂ O	Borated H ₂ O	Borated H ₂ O	Borated H ₂ O	Borated H ₂ O	Borated H ₂ O	Borated H ₂ O
Plate Loading (g ¹⁰ B/cm ²)	0.00517	0.00519	0.00403	0.00128	0.00128	0.00078	0.00078	0.00032	0.00032	0.00032
EALCF (MeV)	2.029E-7	2.015E-7	2.056E-7	2.112E-7	1.773E-7	2.106E-7	1.775E-7	2.119E-7	1.780E-7	1.587E-7
p. σ	0.0019	0.0019	0.0019	0.0022	0.0019	0.0024	0.0020	0.0027	0.0021	0.0019
k _{eff}	0.99210	0.99447	0.99073	0.98652	0.98634	0.99042	0.98974	0.99152	0.99029	0.98927
σ	0.00034	0.00034	0.00034	0.00034	0.00034	0.00034	0.00034	0.00034	0.00035	0.00035

Table 6.7.2-3 LEU MCNP Validation Statistics (cont'd)

Case	65.01	65.02	65.03	65.04	65.05	65.06	65.07	65.08
Clusters	2	2	2	2	2	2	2	2
Enrichment (wt % ²³⁵ U)	2.60%	2.60%	2.60%	2.60%	2.60%	2.60%	2.60%	2.60%
Pitch (cm)	1.956	1.956	1.956	1.956	1.956	1.956	1.956	1.956
Fuel OD (cm)	1.250	1.250	1.250	1.250	1.250	1.250	1.250	1.250
Clad OD (cm)	1.417	1.417	1.417	1.417	1.417	1.417	1.417	1.417
Clad Material	Al	Al	Al	Al	Al	Al	Al	Al
H/U (fissile)	203	203	203	203	203	203	203	203
Soluble B (ppm)	--	--	--	--	--	--	--	--
Absorber Type	none	304L SS (No B)	304L SS (0.67% B)	304L SS (0.98% B)	none	304L SS (No B)	304L SS (No B)	304L SS (No B)
Cluster Gap (cm)	5.9	5.9	5.9	5.9	7.8	7.8	7.8	7.8
Reflector	H ₂ O	H ₂ O	H ₂ O	H ₂ O	H ₂ O	H ₂ O	H ₂ O	H ₂ O
Plate Loading (g ¹⁰ B/cm ²)	--	0.00000	0.00599	0.00875	--	0.00000	0.00000	0.00000
EALCF [MeV]	2.045E-7	2.030E-7	2.054E-7	2.038E-7	2.049E-7	2.030E-7	2.055E-7	2.040E-7
Exp. σ	0.0014	0.0014	0.0015	0.0015	0.0014	0.0014	0.0014	0.0016
k _{eff}	0.99571	0.99618	0.99534	0.99547	0.99691	0.99614	0.99589	0.99624
σ	0.00023	0.00022	0.00023	0.00023	0.00023	0.00023	0.00023	0.00023

Table 6.7.2-3 LEU MCNP Validation Statistics (cont'd)

Case	65.09	65.10	65.11	65.12	65.13	65.14	65.15	65.16	65.17
Clusters	2	2	2	2	2	2	2	2	2
Enrichment (wt % ²³⁵ U)	2.60%	2.60%	2.60%	2.60%	2.60%	2.60%	2.60%	2.60%	2.60%
Pitch (cm)	1.956	1.956	1.956	1.956	1.956	1.956	1.956	1.956	1.956
Fuel OD (cm)	1.250	1.250	1.250	1.250	1.250	1.250	1.250	1.250	1.250
Clad OD (cm)	1.417	1.417	1.417	1.417	1.417	1.417	1.417	1.417	1.417
Clad Material	Al	Al	Al	Al	Al	Al	Al	Al	Al
H/U (fissile)	203	203	203	203	203	203	203	203	203
Soluble B (ppm)	--	--	--	--	--	--	--	--	--
Absorber Type	304L SS (No B)	304L SS (0.67% B)	304L SS (0.67% B)	304L SS (0.67% B)	304L SS (0.67% B)	304L SS (0.98% B)	304L SS (0.98% B)	304L SS (0.98% B)	304L SS (0.98% B)
Cluster Gap (cm)	7.8	7.8	7.8	7.8	7.8	7.8	7.8	7.8	7.8
Reflector	H ₂ O	H ₂ O	H ₂ O	H ₂ O	H ₂ O	H ₂ O	H ₂ O	H ₂ O	H ₂ O
Plate Loading (g ¹⁰ B/cm ²)	0.00000	0.00299	0.00299	0.00599	0.00599	0.00438	0.00438	0.00875	0.00875
EALCF [MeV]	1.993E-7	2.050E-7	2.069E-7	2.072E-7	1.977E-7	2.010E-7	2.004E-7	2.027E-7	2.017E-7
Exp. σ	0.0015	0.0016	0.0016	0.0017	0.0016	0.0016	0.0016	0.0017	0.0016
k_{eff}	0.99667	0.99676	0.99637	0.99643	0.99701	0.99650	0.99634	0.99658	0.99645
σ	0.00022	0.00022	0.00023	0.00023	0.00022	0.00023	0.00023	0.00022	0.00023

6.7.2.4 MOX (Plutonium Oxide/Uranium Oxide Mix) Results of Benchmark Calculations

The range of parameters included in the MOX benchmarks is shown in Table 6.7.2-4.

Experiments are chosen to reflect the fuel evaluated for shipment. This includes the use of arrays of MOX rods (<10 wt % Pu) with light water moderation. Trending in k_{eff} was evaluated for the following independent variables: isotope weight percent as a function of ^{238}U fraction, moderator to fuel volume ratio, and energy of the average neutron lethargy causing fission (EALCF). No statistically significant trends were found for any of the system parameters. USLs are, therefore, generated for each of the independent variables. A minimum USL covering the range of applicability of the benchmark set is determined.

To evaluate the relative importance of the trend analysis to the upper subcritical limits, correlation coefficients are required for all independent parameters. The linear correlation coefficient, R , is calculated by taking the square root of the R^2 value. In particular, the correlation coefficient, R , is a measure of the linear relationship between k_{eff} and a critical experiment parameter. If R is +1, a perfect linear relationship with a positive slope is indicated. If R is -1, a perfect linear relationship with a negative slope is indicated. When R is 0, no linear relationship is indicated.

Table 6.7.2-5 contains the correlation coefficient, R , for each linear fit of k_{eff} versus experimental parameter. Linear fits and correlation constants are based on the 59 data-point evaluation sets plotted in Section 6.7.2.5.

As there is no significant correlation to any of the independent variables, the USL for each independent variable is calculated and shown with its range of applicability in Table 6.7.2-2. A sample output for EALCF is shown in Figure 6.7.2-11. Uncertainties included in the USLSTATS evaluation are the Monte Carlo uncertainty associated with the reactivity calculation and experimental uncertainty that was provided in the literature for each of the cases.

The $^{242}\text{Pu}/^{238}\text{U}$ ratio had the strongest correlation and the water-to-fuel volume ratio produced the minimum USL for all the independent variables correlated. Upper subcritical limits (USLs) are generated based on minimum margins of subcriticality (MMS), also referred to as administrative margin of 5%. The resulting minimum USLSTATS derived USL is 0.9331.

Figure 6.7.2-11 PWR MOX USLSTATS Output for Water to Fuel Volume Ratio

uslstats: a utility to calculate upper subcritical
limits for criticality safety applications

Version 1.4, April 23, 2003
Oak Ridge National Laboratory

Input to statistical treatment from file:w2fvr5.in

Title: keff vs Water-to-Fuel Volume Ratio

Proportion of the population = .995
Confidence of fit = .950
Confidence on proportion = .950
Number of observations = 59
Minimum value of closed band = 0.00
Maximum value of closed band = 0.00
Administrative margin = 0.05

independent variable - x	dependent variable - y	deviation in y	independent variable - x	dependent variable - y	deviation in y
1.19000E+00	9.91550E-01	5.96000E-03	1.52000E+00	9.88170E-01	5.14000E-03
1.19000E+00	9.95580E-01	4.59000E-03	2.49000E+00	9.93450E-01	3.65000E-03
2.52000E+00	9.93540E-01	3.02000E-03	3.52000E+00	9.87870E-01	3.65000E-03
2.52000E+00	1.00039E+00	2.26000E-03	4.40000E+00	9.93650E-01	4.44000E-03
3.64000E+00	9.93960E-01	2.34000E-03	6.28000E+00	9.96480E-01	5.43000E-03
3.64000E+00	1.00264E+00	2.53000E-03	7.05000E+00	9.93170E-01	5.13000E-03
1.68000E+00	9.93170E-01	7.16000E-03	2.49000E+00	9.96100E-01	3.53000E-03
2.16000E+00	9.91940E-01	5.77000E-03	3.52000E+00	9.91630E-01	3.93000E-03
2.16000E+00	9.96120E-01	5.28000E-03	4.40000E+00	9.94460E-01	4.62000E-03
4.71000E+00	9.94700E-01	2.95000E-03	6.28000E+00	9.95150E-01	5.72000E-03
5.67000E+00	9.94430E-01	2.56000E-03	7.05000E+00	9.91400E-01	6.11000E-03
1.08000E+01	9.99990E-01	2.16000E-03	1.52000E+00	9.90720E-01	3.27000E-03
2.42000E+00	9.90540E-01	4.71000E-03	2.49000E+00	9.91190E-01	3.05000E-03
2.42000E+00	9.95620E-01	4.72000E-03	3.52000E+00	9.91770E-01	3.84000E-03
2.42000E+00	1.00016E+00	4.72000E-03	4.40000E+00	9.97310E-01	4.73000E-03
2.98000E+00	9.92510E-01	4.05000E-03	6.28000E+00	9.97440E-01	5.62000E-03
2.98000E+00	9.95970E-01	4.02000E-03	7.05000E+00	9.96110E-01	6.52000E-03
2.98000E+00	1.00453E+00	4.02000E-03	1.10000E+00	9.93110E-01	5.43000E-03
4.24000E+00	9.94610E-01	4.12000E-03	1.56000E+00	9.89370E-01	4.93000E-03
4.24000E+00	9.98940E-01	4.14000E-03	2.71000E+00	9.88960E-01	5.03000E-03
4.24000E+00	9.99980E-01	4.12000E-03	3.79000E+00	9.89000E-01	6.22000E-03
5.55000E+00	9.94400E-01	5.18000E-03	5.14000E+00	9.89770E-01	7.42000E-03
5.55000E+00	9.97870E-01	5.19000E-03	5.58000E+00	9.90580E-01	8.01000E-03
1.93000E+00	9.93380E-01	2.27000E-03	1.14000E+01	9.99200E-01	2.48000E-03
2.56000E+00	9.92740E-01	2.67000E-03	1.14000E+01	9.98350E-01	2.47000E-03
3.62000E+00	9.99510E-01	2.96000E-03	1.14000E+01	9.99230E-01	2.58000E-03
4.53000E+00	9.96420E-01	2.86000E-03	2.07000E+01	1.00066E+00	1.89000E-03
7.27000E+00	9.98140E-01	3.63000E-03	2.07000E+01	9.97920E-01	1.71000E-03
1.01000E+01	9.97360E-01	4.23000E-03	2.07000E+01	9.97870E-01	1.70000E-03
1.16000E+01	9.99430E-01	4.23000E-03			

chi = 1.2542 (upper bound = 9.49). The data tests normal.

Output from statistical treatment

keff vs Water-to-Fuel Volume Ratio

Number of data points (n) 59
Linear regression, k(X) 0.9932 + (3.5528E-04)*X
Confidence on fit (1-gamma) [input] 95.0%
Confidence on proportion (alpha) [input] 95.0%
Proportion of population falling above
lower tolerance interval (rho) [input] 99.5%
Minimum value of X 1.1000E+00
Maximum value of X 2.0700E+01
Average value of X 5.3212E+00
Average value of k 0.99509
Minimum value of k 0.98787
Variance of fit, s(k,X)^2 1.2095E-05
Within variance, s(w)^2 1.9626E-05
Pooled variance, s(p)^2 3.1721E-05
Pooled std. deviation, s(p) 5.6322E-03
C(alpha,rho)*s(p) 2.2969E-02
student-t @ (n-2,1-gamma) 1.67295E+00
Confidence band width, W 1.0388E-02

Figure 6.7.2-11 PWR MOX USLSTATS Output for Water to Fuel Volume Ratio

Minimum margin of subcriticality, C*s(p)-W 1.2582E-02

Upper subcritical limits: (1.1000 <= X <= 20.700)

USL Method 1 (Confidence Band with
Administrative Margin) USL1 = 0.9328 + (3.5528E-04)*X (X < 19.146)
= 0.9396 (X >= 19.146)

USL Method 2 (Single-Sided Uniform
Width Closed Interval Approach) USL2 = 0.9702 + (3.5528E-04)*X (X < 1.91462E+01)
= 0.9770 (X >= 1.91462E+01)

USLs Evaluated Over Range of Parameter X:

X:	1.10E+0	3.90E+0	6.70E+0	9.50E+0	1.23E+1	1.51E+1	1.79E+1	2.07E+1
USL-1:	0.9332	0.9342	0.9352	0.9362	0.9372	0.9382	0.9392	0.9396
USL-2:	0.9706	0.9716	0.9726	0.9736	0.9746	0.9756	0.9766	0.9770

Table 6.7.2-4 PWR MOX Range of Applicability for Complete Set of 59 Benchmark Experiments

Parameter	Minimum	Maximum
Energy of average neutron lethargy causing fission (eV)	8.10E-02	8.99E-01
Uranium-235/Uranium-238 Ratio	1.58E-03	1.51E+00
Plutonium-238/Uranium-238 Ratio	1.88E-06	1.54E-04
Plutonium-239/Uranium-238 Ratio	1.39E-02	7.77E-01
Plutonium-240/Uranium-238 Ratio	1.20E-03	8.48E-02
Plutonium-241/Uranium-238 Ratio	7.90E-05	7.59E-03
Plutonium-242/Uranium-238 Ratio	4.63E-06	6.38E-04
Water-to-fuel volume ratio	1.10E+00	2.07E+01

Table 6.7.2-5 PWR MOX Correlation Coefficients and USLs for Benchmark Experiments

Variable	R ²	R	Range of Applicability	USLSTATS Correlation	USL Low	USL High
Energy of average. neutron lethargy causing fission (eV)	0.0046	0.068	8.10E-02<=X<=8.99E-01	0.9372+-1.3542E-03X	0.9359	0.9370
U-235/U-238 Ratio	0.1148	0.339	1.58E-03<=X<=1.51E+00	0.9343+2.8147E-03X	0.9343	0.9385
Pu-238/U-238 Ratio	0.1030	0.321	1.88E-06<=X<=1.54E-04	0.9343+1.8044E+01X	0.9343	0.9370
Pu-239/U-238 Ratio	0.1202	0.347	1.39E-02<=X<=7.77E-01	0.9342+5.7481E-03X	0.9342	0.9386
Pu-240/U-238 Ratio	0.1409	0.375	1.20E-03<=X<=8.48E-02	0.9341+5.8088E-02X	0.9341	0.9390
Pu-241/U-238 Ratio	0.2160	0.465	7.90E-05<=X<=7.59E-03	0.9338+8.0681E-01X	0.9338	0.9399
Pu-242/U-238 Ratio	0.2440	0.494	4.63E-06<=X<=6.38E-04	0.9338+6.7569E+00X	0.9338	0.9381
Water-to-fuel volume ratio	0.1787	0.423	1.10E+00<=X<=2.07E+01	0.9328+3.5528E-04X	0.9331	0.9401

6.7.2.5 MOX (Plutonium Oxide/Uranium Oxide Mix) Critical Benchmarks

From the International Handbook of Evaluated Criticality Safety Benchmark Experiments, 59 experiments are selected as the basis of the MCNP benchmarking. Experiments were selected for compatibility with LWR MOX rods evaluated for shipment. Of particular interest are benchmarks with rectangular arrays of MOX rods with plutonium weight percent less than 10%.

MCNP benchmark cases represent a collection of files composed of inputs directly obtained from references (with cross-section sets adjusted to those used in the cask analysis), NAC modified input files representing unique geometries based on reference input files, and input files constructed from the experimental material and geometry information. All cases were reviewed on a "preparer/checker" principle for modeling consistency with the cask models and the choice of code options. Due to large variations in the benchmark complexities, not all options employed in the cask models are reflected in each of the benchmarks (e.g., UNIVERSE structure). A review of the criticality results did not indicate any result trend due to particular modeling choices (e.g., using the UNIVERSE structure versus a single universe, or employing KSRC versus SDEF sampling).

Identifiers for the experiment, uncertainty and calculated k_{eff} and σ for each experiment are shown in Table 6.7.2-6. Stochastic Monte Carlo error is kept within $\pm 0.2\%$ and each output is checked to assure that the MCNP built-in statistical checks on the results are passed and that all fissile material is sampled.

Scatter plots of k_{eff} versus system parameters for 59 data point sets (see Figure 6.7.2-12 through Figure 6.7.2-19). Included in these scatter plots are linear regression lines with a corresponding correlation coefficient (R^2) to statistically indicate any trend or lack thereof. Scatter plots are created for k_{eff} versus the following.

- Energy of average neutron lethargy causing fission
- $^{235}\text{U}/^{238}\text{U}$ ratio
- $^{238}\text{Pu}/^{238}\text{U}$ ratio
- $^{239}\text{Pu}/^{238}\text{U}$ ratio
- $^{240}\text{Pu}/^{238}\text{U}$ ratio
- $^{241}\text{Pu}/^{238}\text{U}$ ratio
- $^{242}\text{Pu}/^{238}\text{U}$ ratio
- Water-to-fuel volume ratio

Figure 6.7.2-12 Adjusted k_{eff} vs. Energy of Average Neutron Lethargy Causing Fission

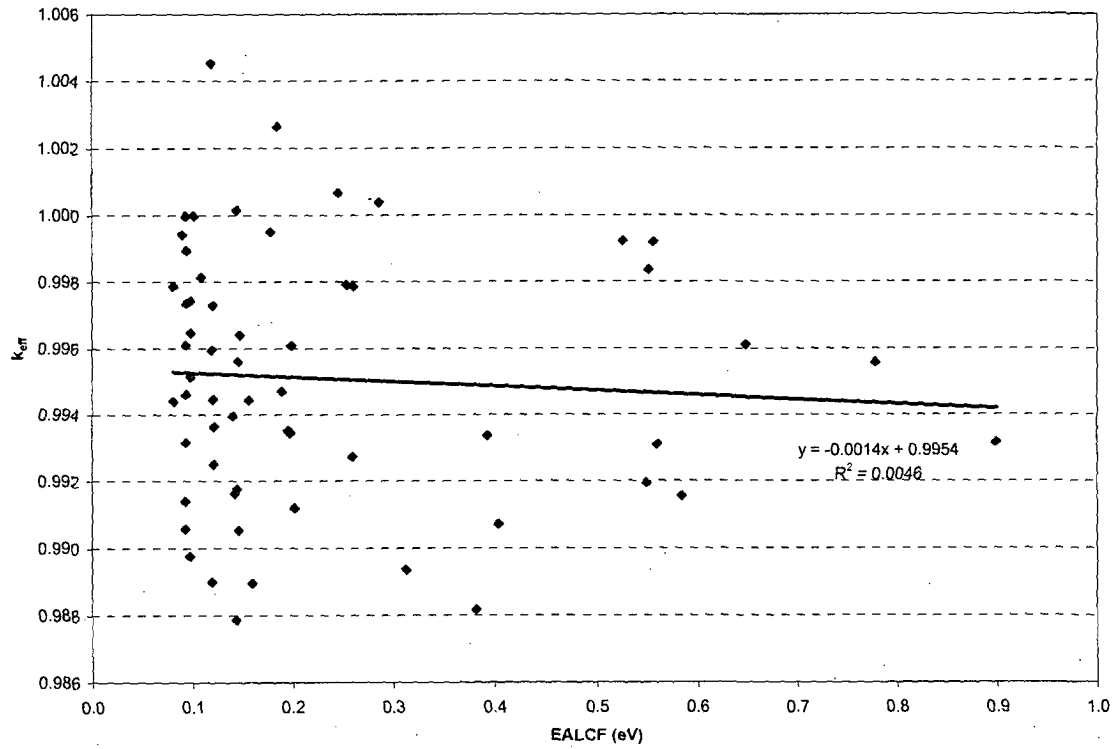


Figure 6.7.2-13 Adjusted k_{eff} vs. $^{235}\text{U}/^{238}\text{U}$ Ratio

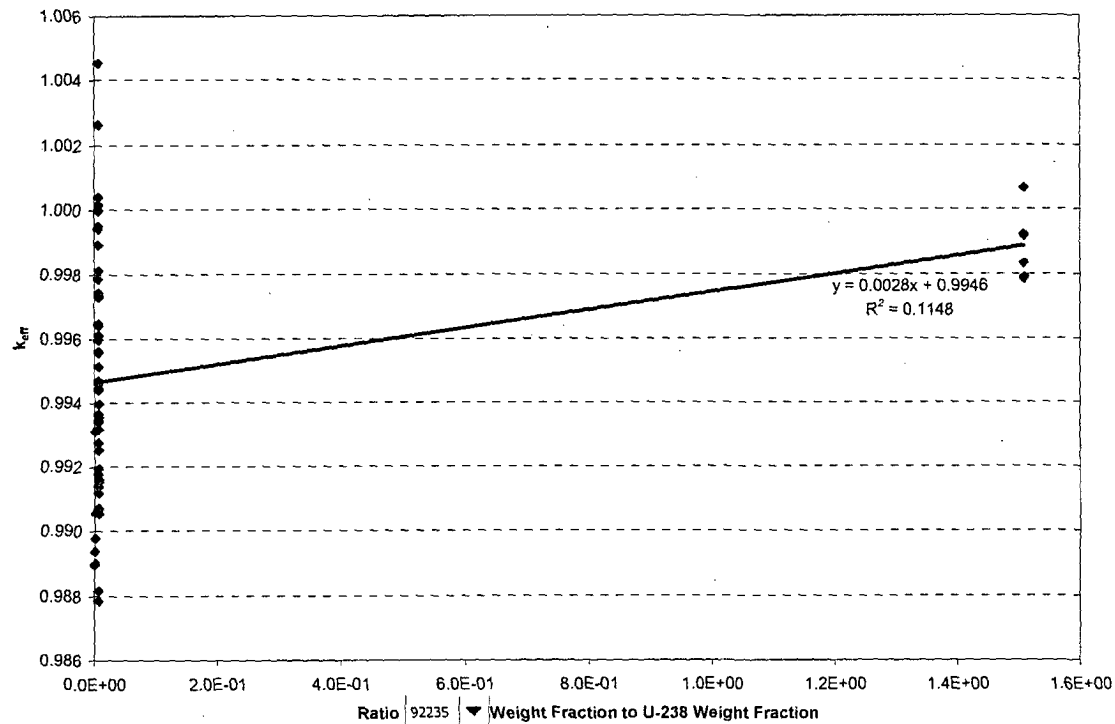


Figure 6.7.2-14 Adjusted k_{eff} vs. $^{238}\text{Pu}/^{238}\text{U}$ Ratio

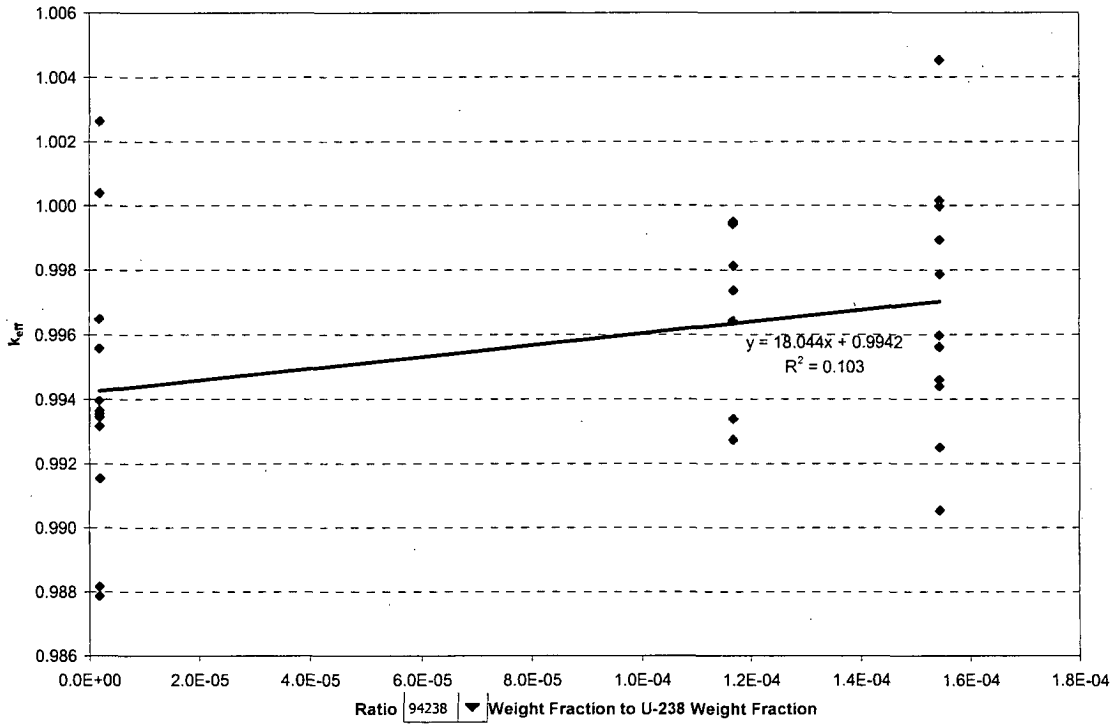


Figure 6.7.2-15 Adjusted k_{eff} vs. $^{239}\text{Pu}/^{238}\text{U}$ Ratio

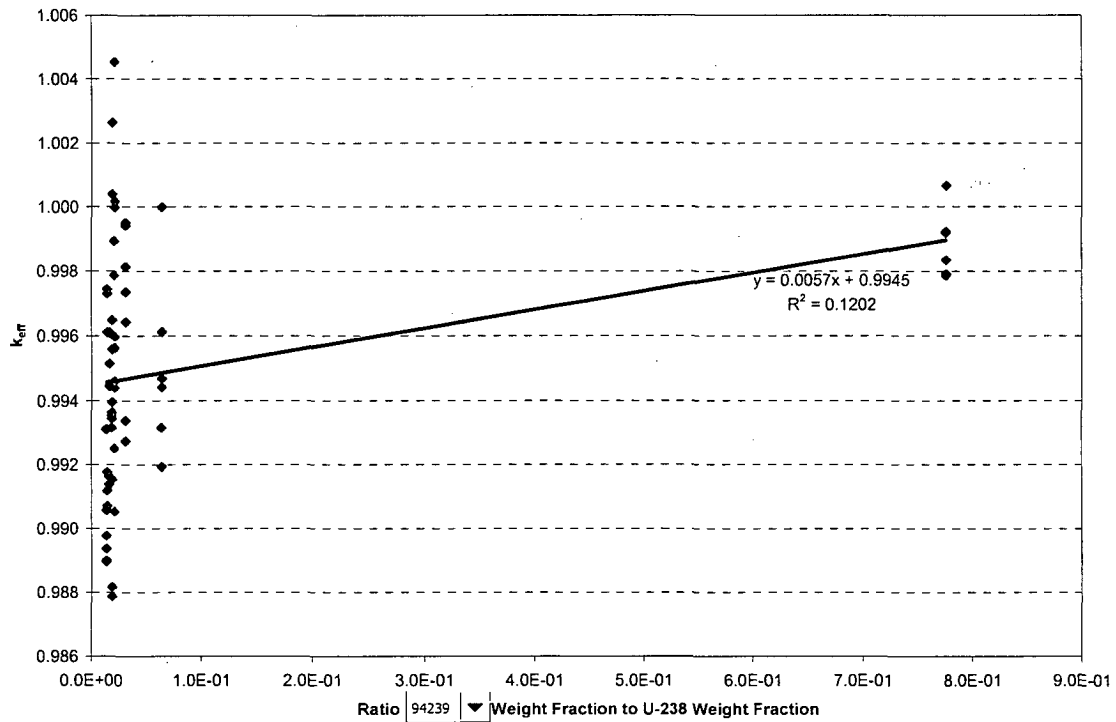


Figure 6.7.2-16 Adjusted k_{eff} vs. $^{240}\text{Pu}/^{238}\text{U}$ Ratio

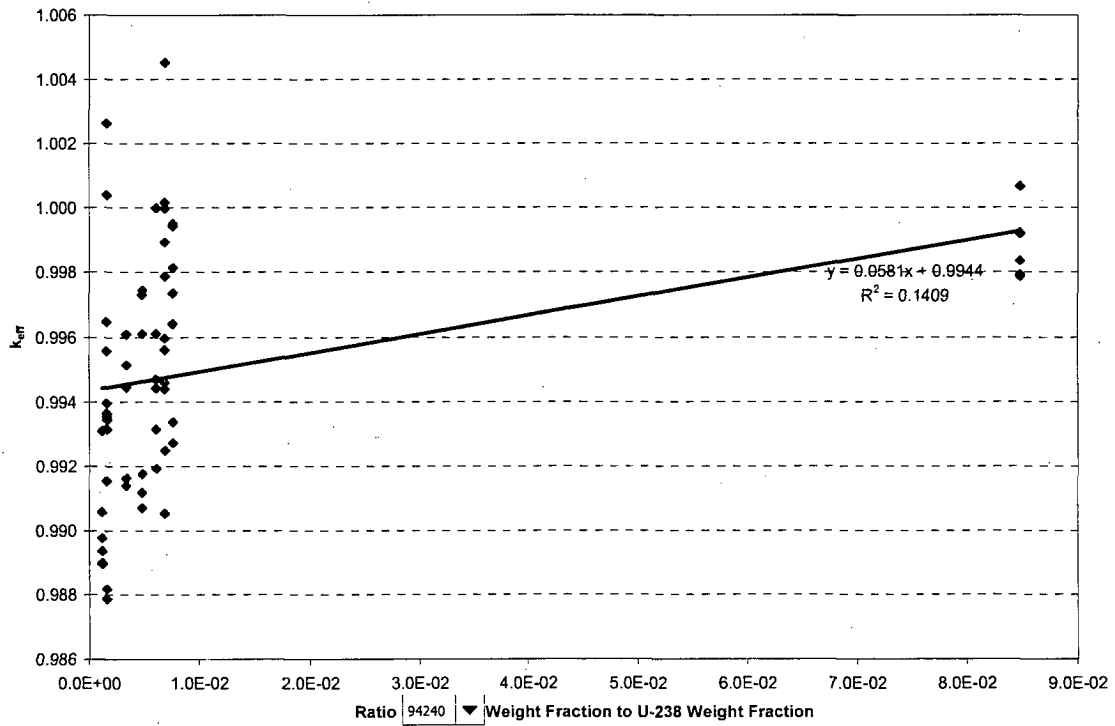


Figure 6.7.2-17 Adjusted k_{eff} vs. $^{241}\text{Pu}/^{238}\text{U}$ Ratio

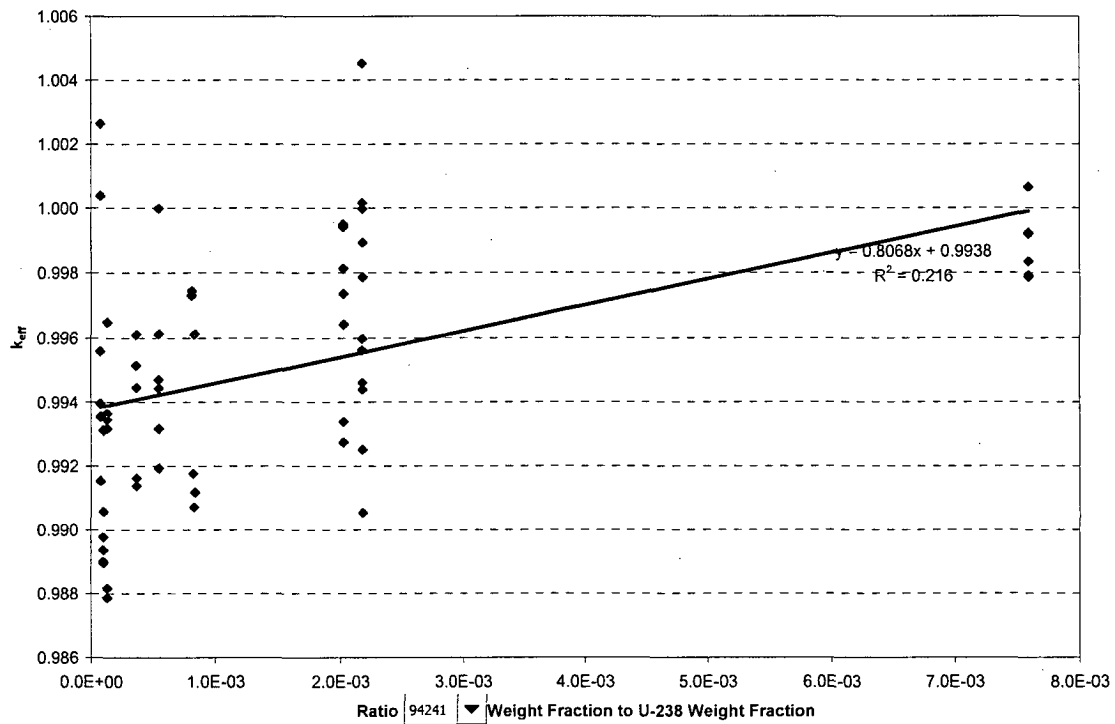


Figure 6.7.2-18 Adjusted k_{eff} vs. $^{242}\text{Pu}/^{238}\text{U}$ Ratio

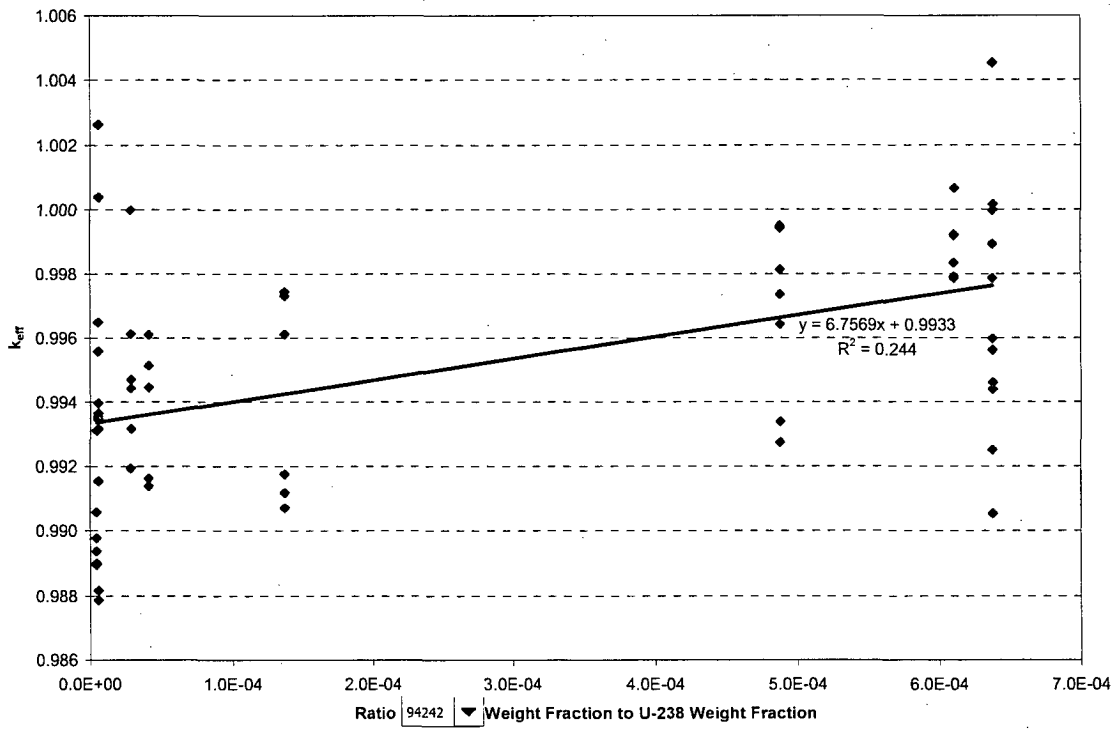


Figure 6.7.2-19 Adjusted k_{eff} vs. Water-to-Fuel Volume Ratio

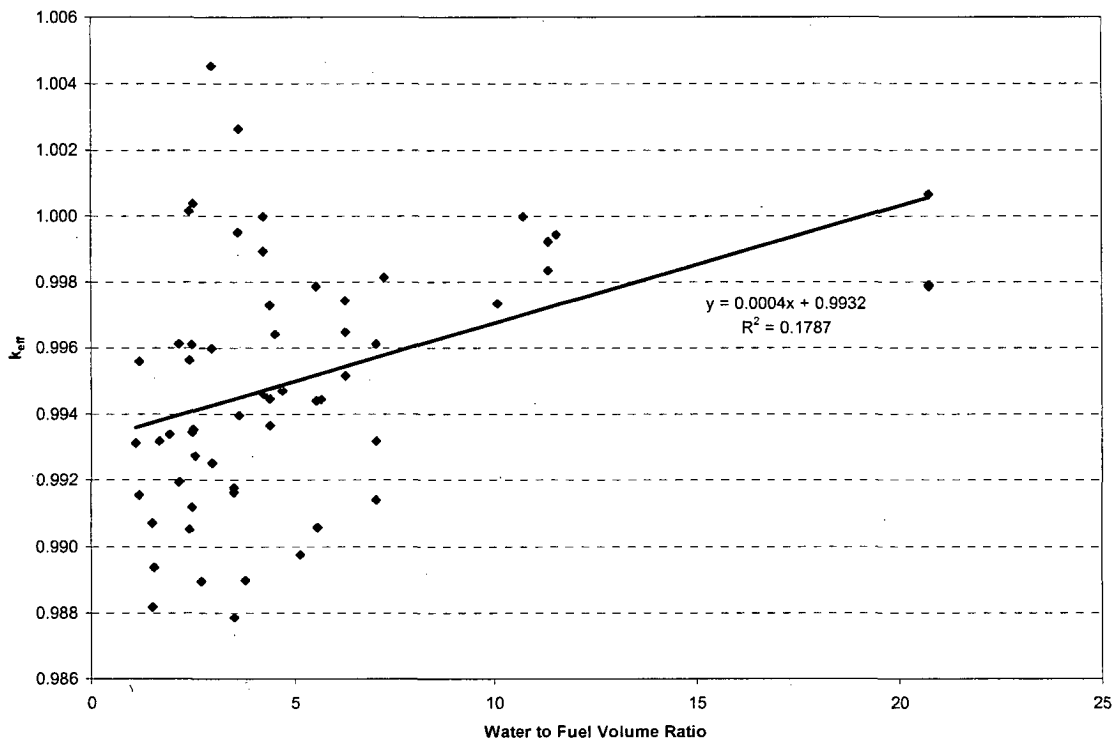


Table 6.7.2-6 MCNP Validation Statistics

Identification	Water-to-Fuel Ratio	Benchmark			MCNP5 v1.30			EALCF (eV)
		k_{eff}	σ	Δk	k_{eff}	σ	Adj. k_{eff}	
MIXCT-002-01	1.2	1.0010	0.0059	-0.0010	0.99255	0.00082	0.99155	0.58526
MIXCT-002-02	1.2	1.0009	0.0045	-0.0009	0.99648	0.00088	0.99558	0.77857
MIXCT-002-03	2.5	1.0024	0.0029	-0.0024	0.99594	0.00083	0.99354	0.19618
MIXCT-002-04	2.5	1.0024	0.0021	-0.0024	1.00279	0.00083	1.00039	0.28661
MIXCT-002-05	3.6	1.0038	0.0022	-0.0038	0.99776	0.00081	0.99396	0.14069
MIXCT-002-06	3.6	1.0029	0.0024	-0.0029	1.00554	0.00080	1.00264	0.18588
MIXCT-003-01	1.7	1.0000	0.0071	0.0000	0.99317	0.00092	0.99317	0.89937
MIXCT-003-02	2.2	1.0000	0.0057	0.0000	0.99194	0.00090	0.99194	0.54987
MIXCT-003-03	2.2	1.0000	0.0052	0.0000	0.99612	0.00093	0.99612	0.64918
MIXCT-003-04	4.7	1.0000	0.0028	0.0000	0.99470	0.00092	0.99470	0.18983
MIXCT-003-05	5.7	1.0000	0.0024	0.0000	0.99443	0.00088	0.99443	0.15707
MIXCT-003-06	10.8	1.0000	0.0020	0.0000	0.99999	0.00082	0.99999	0.10167
MIXCT-004-01	2.4	1.0000	0.0046	0.0000	0.99054	0.00099	0.99054	0.14647
MIXCT-004-02	2.4	1.0000	0.0046	0.0000	0.99562	0.00106	0.99562	0.14615
MIXCT-004-03	2.4	1.0000	0.0046	0.0000	1.00016	0.00107	1.00016	0.14470
MIXCT-004-04	3.0	1.0000	0.0039	0.0000	0.99251	0.00111	0.99251	0.12146
MIXCT-004-05	3.0	1.0000	0.0039	0.0000	0.99597	0.00098	0.99597	0.11971
MIXCT-004-06	3.0	1.0000	0.0039	0.0000	1.00453	0.00097	1.00453	0.11898
MIXCT-004-07	4.2	1.0000	0.0040	0.0000	0.99461	0.00100	0.99461	0.09396
MIXCT-004-08	4.2	1.0000	0.0040	0.0000	0.99894	0.00106	0.99894	0.09454
MIXCT-004-09	4.2	1.0000	0.0040	0.0000	0.99998	0.00097	0.99998	0.09350
MIXCT-004-10	5.6	1.0000	0.0051	0.0000	0.99440	0.00092	0.99440	0.08152
MIXCT-004-11	5.6	1.0000	0.0051	0.0000	0.99787	0.00094	0.99787	0.08098
MIXCT-005-01	1.9	1.0008	0.0022	-0.0008	0.99418	0.00057	0.99338	0.39380
MIXCT-005-02	2.6	1.0011	0.0026	-0.0011	0.99384	0.00059	0.99274	0.26049
MIXCT-005-03	3.6	1.0016	0.0029	-0.0016	1.00111	0.00058	0.99951	0.17856
MIXCT-005-04	4.5	1.0021	0.0028	-0.0021	0.99852	0.00057	0.99642	0.14820
MIXCT-005-05	7.3	1.0026	0.0036	-0.0026	1.00074	0.00049	0.99814	0.10925
MIXCT-005-06	10.1	1.0033	0.0042	-0.0033	1.00066	0.00048	0.99736	0.09455
MIXCT-005-07	11.6	1.0035	0.0042	-0.0035	1.00293	0.00046	0.99943	0.09019

Table 6.7.2-6 MCNP Validation Statistics (cont'd)

Identification	Water-to-Fuel Ratio	Benchmark			MCNP5 v1.30			EALCF (eV)
		k _{eff}	σ	Δk	k _{eff}	σ	Adj. k _{eff}	
MIXCT-006-01	1.5	1.0016	0.0051	-0.0016	0.98977	0.00060	0.98817	0.38252
MIXCT-006-02	2.5	1.0017	0.0036	-0.0017	0.99515	0.00061	0.99345	0.19894
MIXCT-006-03	3.5	1.0026	0.0036	-0.0026	0.99047	0.00059	0.98787	0.14393
MIXCT-006-04	4.4	1.0051	0.0044	-0.0051	0.99875	0.00058	0.99365	0.12231
MIXCT-006-05	6.3	1.0040	0.0054	-0.0040	1.00048	0.00055	0.99648	0.09904
MIXCT-006-06	7.1	1.0055	0.0051	-0.0055	0.99867	0.00052	0.99317	0.09438
MIXCT-007-01	2.5	1.0023	0.0035	-0.0023	0.99840	0.00049	0.99610	0.19918
MIXCT-007-02	3.5	1.0024	0.0039	-0.0024	0.99403	0.00050	0.99163	0.14313
MIXCT-007-03	4.4	1.0036	0.0046	-0.0036	0.99806	0.00048	0.99446	0.12122
MIXCT-007-04	6.3	1.0037	0.0057	-0.0037	0.99885	0.00043	0.99515	0.09818
MIXCT-007-05	7.1	1.0044	0.0061	-0.0044	0.99580	0.00042	0.99140	0.09330
MIXCT-008-01	1.5	0.9997	0.0032	0.0003	0.99042	0.00066	0.99072	0.40443
MIXCT-008-02	2.5	1.0008	0.0030	-0.0008	0.99199	0.00057	0.99119	0.20199
MIXCT-008-03	3.5	1.0023	0.0038	-0.0023	0.99407	0.00056	0.99177	0.14500
MIXCT-008-04	4.4	1.0015	0.0047	-0.0015	0.99881	0.00057	0.99731	0.12108
MIXCT-008-05	6.3	1.0022	0.0056	-0.0022	0.99964	0.00050	0.99744	0.09872
MIXCT-008-06	7.1	1.0028	0.0065	-0.0028	0.99891	0.00049	0.99611	0.09362
MIXCT-009-01	1.1	1.0003	0.0054	-0.0003	0.99341	0.00059	0.99311	0.56093
MIXCT-009-02	1.6	1.0020	0.0049	-0.0020	0.99137	0.00058	0.98937	0.31308
MIXCT-009-03	2.7	1.0035	0.0050	-0.0035	0.99246	0.00056	0.98896	0.16022
MIXCT-009-04	3.8	1.0046	0.0062	-0.0046	0.99360	0.00054	0.98900	0.11987
MIXCT-009-05	5.1	1.0059	0.0074	-0.0059	0.99567	0.00049	0.98977	0.09776
MIXCT-009-06	5.6	1.0067	0.0080	-0.0067	0.99728	0.00047	0.99058	0.09313
MIXCT-011-01	11.4	1.0000	0.0024	0.0000	0.99920	0.00063	0.99920	0.55670
MIXCT-011-02	11.4	1.0000	0.0024	0.0000	0.99835	0.00060	0.99835	0.55254
MIXCT-011-03	11.4	1.0000	0.0025	0.0000	0.99923	0.00062	0.99923	0.52644
MIXCT-011-04	20.7	1.0000	0.0018	0.0000	1.00066	0.00056	1.00066	0.24638
MIXCT-011-05	20.7	1.0000	0.0016	0.0000	0.99792	0.00059	0.99792	0.25390
MIXCT-011-06	20.7	1.0000	0.0016	0.0000	0.99787	0.00058	0.99787	0.26082

Table of Contents

6.6	Appendix.....	6.6-1
6.6.1	PWR Fuel Assemblies	6.6.1-1
6.6.2	BWR Fuel Assemblies	6.6.2-1
6.6.3	MTR Fuel Elements	6.6.3-1
6.6.4	Intact PWR and BWR Fuel Rods in a Rod Holder or Fuel Assembly Lattice.....	6.6.4-1
6.6.5	TRIGA Fuel Elements.....	6.6.5-1
6.6.6	TRIGA Fuel Cluster Rods.....	6.6.6-1
6.6.7	MTR Fuel Bounding Configuration.....	6.6.7-1
6.6.8	DIDO Fuel Assemblies	6.6.8-1
6.6.9	General Atomics Irradiated Fuel Material	6.6.9-1
6.6.10	Damaged Fuel Rods in a Rod Holder	6.6.10-1
6.6.11	PULSTAR Fuel Elements in the LWT Cask	6.6.11-1
6.6.12	Spiral Fuel Assemblies in the LWT Cask	6.6.12-1
6.6.13	MOATA Plate Bundles in the LWT Cask.....	6.6.13-1
6.6.14	High Fissile Mass LEU (32 g ²³⁵ U per Plate) MTR Fuel Elements	6.6.14-1
6.6.15	PWR MOX Fuel Rods.....	6.6.15-1

List of Figures

Figure 6.6.1-1 CSAS Input/Output for NAC-LWT with PWR Fuel – 3.7% Enrichment - Most Reactive Normal Condition Configuration..... 6.6.1-2

Figure 6.6.1-2 CSAS Input/Output for NAC-LWT with PWR Fuel – 3.7% Enrichment – Most Reactive Accident Condition Configuration..... 6.6.1-32

Figure 6.6.1-3 CSAS Input/Output for NAC-LWT with PWR Fuel – 3.5% Enrichment – Most Reactive Normal Condition Configuration 6.6.1-57

Figure 6.6.1-4 CSAS Input/Output for NAC-LWT with PWR Fuel – 3.5% Enrichment – Most Reactive Accident Condition Configuration..... 6.6.1-85

Figure 6.6.2-1 CSAS Input/Output for NAC-LWT with BWR Fuel Assemblies – Most Reactive Normal Condition Configuration..... 6.6.2-2

Figure 6.6.2-2 CSAS Input/Output for NAC-LWT with BWR Fuel Assemblies – Most Reactive Accident Condition Configuration..... 6.6.2-29

Figure 6.6.3-1 CSAS Input/Output for NAC-LWT with Design Basis MTR Fuel - Most Reactive Normal Condition Configuration..... 6.6.3-2

Figure 6.6.3-2 CSAS Input/Output for NAC-LWT with Design Basis MTR Fuel - Most Reactive Accident Condition Configuration – 94 w/o, 355 g ²³⁵U 6.6.3-37

Figure 6.6.4-1 CSAS Input/Output for NAC-LWT with 25 PWR Rods – Most Reactive Normal Condition Configuration..... 6.6.4-2

Figure 6.6.4-2 CSAS Input/Output for NAC-LWT with 25 PWR Rods – Most Reactive Accident Condition Configuration..... 6.6.4-21

Figure 6.6.4-3 CSAS Input/Output for NAC-LWT with 25 BWR Rods – Most Reactive Normal Condition Configuration..... 6.6.4-40

Figure 6.6.4-4 CSAS Input/Output for NAC-LWT with 25 BWR Rods – Most Reactive Accident Condition Configuration..... 6.6.4-59

Figure 6.6.5-1 Summary of CSAS Input/Output for NAC-LWT with TRIGA Fuel Elements - Most Reactive Nonpoisoned Basket Configuration..... 6.6.5-2

Figure 6.6.5-2 Summary of CSAS25 Input/Output for NAC-LWT with TRIGA Fuel Elements - Most Reactive Poisoned Basket Configuration 6.6.5-36

Figure 6.6.5-3 Summary of CSAS Input/Output for TRIGA Benchmark Core 132 6.6.5-73

Figure 6.6.6-1 TRIGA Fuel Cluster Rods – Most Reactive Nonpoisoned Basket Configuration 6.6.6-2

Figure 6.6.6-2 TRIGA Fuel Cluster Rods – Most Reactive Poisoned Basket Configuration 6.6.6-40

Figure 6.6.7-1 MTR Finite Cask Model 6.6.7-2

Figure 6.6.7-2 HEU MTR Finite Cask Model (460 g ²³⁵U) 6.6.7-49

Figure 6.6.8-1 Maximum Reactivity DIDO Configuration – Eight Cask Array 6.6.8-2

Figure 6.6.8-2 Maximum Reactivity DIDO Configuration – Infinite Array 6.6.8-93

Figure 6.6.9-1 Maximum Reactivity GA IFM Configuration 6.6.9-2

Figure 6.6.10-1 Damaged BWR Rods in a Rod Holder..... 6.6.10-2

Figure 6.6.11-1 Maximum Reactivity PULSTAR Configuration..... 6.6.11-2

Figure 6.6.12-1 Maximum Reactivity Spiral Fuel Assembly Configuration 6.6.12-2

Figure 6.6.13-1 Maximum Reactivity MOATA Plate Bundle Configuration 6.6.13-2

Figure 6.6.14-1 High Fissile Mass LEU MTR Sample Input 6.6.14-2

List of Figures (continued)

Figure 6.6.15-1	Maximum Reactivity MOX Rods – MOX Services Fuel Composition.....	6.6.15-2
Figure 6.6.15-2	Maximum Reactivity MOX Rods – ²⁴¹ Pu Fuel Composition	6.6.15-23

6.6.15 PWR MOX Fuel Rods

This section contains truncated sample output files from the evaluation of MOX fuel rods in the NAC-LWT cask. The output files are shown in Figure 6.6.15-1 (MOX Services fuel composition) and Figure 6.6.15-2 (^{241}Pu fuel composition).

Figure 6.6.15-1 Maximum Reactivity MOX Rods – MOX Services Fuel Composition

Thread Name & Version = MCNP5_RSICC, 1.30

MCNP5

This program was prepared by the Regents of the University of California at Los Alamos National Laboratory (the University) under contract number W-7405-ENG-36 with the U.S. Department of Energy (DoE). The University has certain rights in the program pursuant to the contract and the program should not be copied or distributed outside your organization. All rights in the program are reserved by the DoE and the University. Neither the U.S. Government nor the University makes any warranty, express or implied, or assumes any liability or responsibility for the use of this software.

```
lmcnp version 5 ld=06212004 10/25/07 21:05:56
*****
name=MS_Acc_NACCoC_c1.00_g0.00_e0.00_d0.01cm_HP_36mm.inp host=amdengl-it1458
probid = 10/25/07 21:05:56

1- NAC-LWT Cask - MOX Experiments - Accident Transport Conditions
2- C
3- C EXCEL File Version: v2.00
4- C Run Version: v2.00
5- C
6- C Fissile Material Type: MOX Services
7- C Rod Interior Void Moderator Density: 0.9982 g/cc
8- C Canister Interior Moderator Density: 0.9982 g/cc
9- C Canister to Cask Gap Moderator Density: 0.0001 g/cc
10- C Cask Exterior Moderator Density: 0.0001 g/cc
11- C Boundary Condition / Distance: Reflected / 0.01 cm
12- C
13- C Fuel Rod Pitch: 3.6 cm
14- C Fuel Rod Pitch Configuration: Hexagonal
15- C Number of Rods: 16
16- C
17- C Base Fuel Parameters: NACCoC
18- C
19- c Cells - Fuel Rod - NACCoC
20- 1 1 -10.555 -1 u=3 $ Fuel
21- 2 2 -0.9982 -2 +1 u=3 $ Plenum + Fuel to Clad Gap
22- 3 3 -6.56 -3 +2 u=3 $ Clad + End Plugs
23- 4 4 -0.9982 +3 u=3 $ Outside Fuel Rod
24- C 16 Rods - Hexagonal Pitch
25- 10 4 -0.9982 -10
26- *trcl=( 0.9000 -1.5588 0.0000 )
27- lat=2 u=2 fill=-7:6 -5:5 0:0
28- 2 2 2 2 2 2 2 2 2 2 2 2 2 2 2 2
29- 2 2 2 2 2 2 2 2 2 2 2 2 2 2 2 2
30- 2 2 2 2 2 2 2 2 2 2 2 2 2 2 2 2
31- 2 2 2 2 2 2 3 2 2 2 2 2 2 2 2 2
32- 2 2 2 2 2 3 3 3 2 2 2 2 2 2 2 2
33- 2 2 2 2 3 3 3 3 3 2 2 2 2 2 2 2
34- 2 2 2 2 3 3 3 3 2 2 2 2 2 2 2 2
35- 2 2 2 2 3 3 3 2 2 2 2 2 2 2 2 2
36- 2 2 2 2 2 2 2 2 2 2 2 2 2 2 2 2
37- 2 2 2 2 2 2 2 2 2 2 2 2 2 2 2 2
38- 2 2 2 2 2 2 2 2 2 2 2 2 2 2 2 2
39- C PWR Basket - Cells
40- 4 -0.9982 -20 fill=2 u=1 $ Rod Array Container
41- 21 5 -0.0001 +20 -21 u=1 $ Basket Cavity
42- 22 7 -2.7020 -22 +21 u=1 $ Basket Body
43- 23 5 -0.0001 +22 u=1 $ Outside
44- C Cells - LWT Cask Accident Conditions
45- 40 8 -11.344 -43 u=0 $ BotPb
46- 41 5 -0.0001 -42 fill=1 u=0 $ Cavity
47- 42 9 -7.9400 -41 +43 u=0 $ Bottom
48- 43 9 -7.9400 -40 +41 +45 +48 +42 u=0 $ OuterShell
49- 44 9 -7.9400 -44 +47 +42 u=0 $ InnerShellTaper
50- 45 9 -7.9400 -46 +42 u=0 $ InnerShell
51- 46 8 -11.344 -47 +46 u=0 $ Lead
52- 47 8 -11.344 -45 +44 +47 u=0 $ LeadTaper
53- 48 0 -48 +47 u=0 $ LeadGap
54- 49 6 -0.0001 -49 +40 u=0 $ Gap to Reflector
55- 50 0 +49 u=0 $ Boundary
56-
57- c Surfaces - Fuel Rod - NACCoC
58- 1 RCC 0.0000 0.0000 10.5207 0.0000 0.0000 389.8900 0.4781 $ Fuel pellet stack
59- 2 RCC 0.0000 0.0000 6.3990 0.0000 0.0000 409.4227 0.4876 $ Annulus + Plenum
60- 3 RCC 0.0000 0.0000 5.0800 0.0000 0.0000 411.8226 0.5588 $ Clad + End-Caps
61- c Surfaces - Pitch - NACCoC
62- 10 RHP 0.0000 0.0000 -1.0000 0.0000 0.0000 454.12 1.8000 0.0000 0.0000 $ Lattice
63- C PWR Basket - Surfaces
64- 20 1 RPP -7.4148 7.4148 -7.4148 7.4148 0.0000 452.1200 $ Array Container
65- 21 1 RPP -11.2713 11.2713 -11.2713 11.2713 0.0000 452.1200 $ Basket Opening
66- 22 RCC 0.0000 0.0000 0.0000 0.0000 0.0000 452.1200 16.83512 $ Basket Outer Body
67- C Surfaces - LWT Cask Accident Conditions
68- 40 RCC 0.0000 0.0000 -26.6700 0.0000 0.0000 507.3650 36.5189 $ Lwt Body
69- 41 RCC 0.0000 0.0000 -26.6700 0.0000 0.0000 26.6700 36.5189 $ Bottom
70- 42 RCC 0.0000 0.0000 0.0000 0.0000 0.0000 452.1200 16.9863 $ Cavity
```



```

71- 43 RCC 0.0000 0.0000 -17.7800 0.0000 0.0000 7.6200 26.3525 $ Bottom gamma shield
72- 44 RCC 0.0000 0.0000 0.0000 0.0000 0.0000 444.5000 20.1740 $ Lead id - taper
73- 45 RCC 0.0000 0.0000 0.0000 0.0000 0.0000 444.5000 31.5976 $ Lead od - taper
74- 46 RCC 0.0000 0.0000 13.8176 0.0000 0.0000 416.8648 18.9103 $ Lead id
75- 47 RCC 0.0000 0.0000 13.8176 0.0000 0.0000 416.8648 33.3271 $ Lead od
76- 48 RCC 0.0000 0.0000 13.8176 0.0000 0.0000 416.8648 33.4645 $ Lead gap
77- *49 RPP -36.5289 36.5289 -36.5289 36.5289 -26.6800 480.7050 $ Container
78-
79- c
80- c Materials List
81- c
82- C MOX Material Composition Fuel
83- m1 92235 -5.6994E-03
84- 92238 -8.0851E-01
85- 94238 -3.3724E-05
86- 94239 -6.4076E-02
87- 94240 -3.0352E-03
88- 94241 -2.6980E-04
89- 94242 -3.3724E-05
90- 8016 -1.1835E-01
91- C Rod Interior Void Material
92- m2 1001 2
93- 8016 1
94- mt2 lwtr.01
95- c Clad Material
96- m3 26054 -7.063E-05 24050 -4.179E-05 7014 -4.980E-04
97- 26056 -1.149E-03 24052 -8.370E-04 7015 -1.981E-06
98- 26057 -2.702E-05 24053 -9.673E-05
99- 26058 -3.631E-06 24054 -2.448E-05
100- 40000 -9.823E-01 50000 -1.500E-02
101- C Canister Interior Non-Fuel Space
102- m4 1001 2
103- 8016 1
104- mt4 lwtr.01
105- C Canister to Cask Gap Material
106- m5 1001 2
107- 8016 1
108- mt5 lwtr.01
109- C Cask Exterior Material
110- m6 1001 2
111- 8016 1
112- mt6 lwtr.01
113- c Aluminum
114- m7 13027 -1.000E+00
115- C Water/Glycol
116- m10 1001 -1.03651E-01
warning. material 10 is not used in the problem.
117- 8016 -6.75619E-01
118- 6000 -2.20730E-01
119- mt10 lwtr.01
warning. material 10 is not used in the problem.
120- c Lead
121- m8 82206 -2.534E-01
122- 82207 -2.207E-01
123- 82208 -5.259E-01
124- c SS304
125- m9 24050 -7.939E-03 26054 -3.927E-02 28058 -6.384E-02
126- 24052 -1.590E-01 26056 -6.387E-01 28060 -2.543E-02
127- 24053 -1.838E-02 26057 -1.502E-02 28061 -1.124E-03
128- 24054 -4.652E-03 26058 -2.019E-03 28062 -3.639E-03
129- 28064 -9.623E-04
130- 25055 -2.000E-02
131- C Aluminum Honeycomb Impact Limiter
132- m11 13027 -1.0
warning. material 11 is not used in the problem.
133- C Mode
134- mode n
135- C Cell Importances
136- imp:n 1 18r 0
137- C
138- C Criticality Controls
139- kcode 1000 0.80 30 530
140- C
141- C Starting Source Definition
142- sdef cell=41:20:10:1
143- erg=d1
144- pos=0 0 10.5207
145- rad=d2
146- axs=0 0 1
147- ext=d3
148- spl -3
149- si2 0.0000 0.4781
150- sp2 -21 1
151- si3 0.0000 389.8900
152- sp3 0 1
153- C Print Control
154- print
155- C Random Number Generator
156- rand gen=2 seed=19073486328125 stride=152917 hist=1
157- c
158- c Rotation Matrix
159- *TRI 0.0 0.0 0.0 -30 60 90 -120 -30 90 90 90 0 $ z-rotation -30 degrees

```

!source

print table 10

values of defaulted or explicitly defined source variables

```

sur      0.0000E+00
tme      0.0000E+00
dir      isotropic
pos      0.0000E+00  0.0000E+00  1.0521E+01
x        0.0000E+00
y        0.0000E+00
z        0.0000E+00
axs      0.0000E+00  0.0000E+00  1.0000E+00
vec      0.0000E+00  0.0000E+00  0.0000E+00
ccc      0.0000E+00
nrm      1.0000E+00
ara      0.0000E+00
wgt      1.0000E+00
eff      1.0000E-02
par      0.0000E+00
tr       0.0000E+00
    
```

probability distribution 1 for source variable erg
energy function 3: watt (fission) spectrum (endf law 10)

$$f(e) = c \cdot \exp(-e/a) \cdot \sinh(\sqrt{b \cdot e})$$

a = 9.6500E-01 b = 2.2900E+00 c = 4.5270E-01

the mean of source distribution 1 is 1.9806E+00

probability distribution 2 for source variable rad
power law 21: f(x) = c * abs(x)**k k = 1.0000E+00

probability distribution 3 for source variable ext
unbiased histogram distribution

source entry	source value	cumulative probability	probability of bin
1	0.00000E+00	0.000000E+00	0.000000E+00
2	3.89890E+02	1.000000E+00	1.000000E+00

the mean of source distribution 3 is 1.9494E+02

order of sampling source variables.
cel axs rad ext pos erg tme

comment. total fission nubar data are being used.
imaterial composition

print table 40

the sum of the fractions of material 2 was 3.000000E+00
the sum of the fractions of material 3 was 1.000050E+00
the sum of the fractions of material 4 was 3.000000E+00
the sum of the fractions of material 5 was 3.000000E+00
the sum of the fractions of material 6 was 3.000000E+00
the sum of the fractions of material 9 was 9.999753E-01

material number

material number	component nuclide, atom fraction			
1	92235, 2.18414E-03	92238, 3.05926E-01	94238, 1.27607E-05	94239, 2.41437E-02
	94240, 1.13889E-03	94241, 1.00815E-04	94242, 1.25493E-05	8016, 6.66481E-01
2	1001, 6.66667E-01	8016, 3.33333E-01		
	associated thermal s(a,b) data sets: lwtr.01t			
3	26054, 1.19346E-04	24050, 7.62600E-05	7014, 3.24139E-03	26056, 1.87224E-03
	24052, 1.46874E-03	7015, 1.20369E-05	26057, 4.32542E-05	24053, 1.66532E-04
	26058, 5.71247E-06	24054, 4.13652E-05	40000, 9.81436E-01	50000, 1.15166E-02
4	1001, 6.66667E-01	8016, 3.33333E-01		
	associated thermal s(a,b) data sets: lwtr.01t			
5	1001, 6.66667E-01	8016, 3.33333E-01		
	associated thermal s(a,b) data sets: lwtr.01t			
6	1001, 6.66667E-01	8016, 3.33333E-01		
	associated thermal s(a,b) data sets: lwtr.01t			
7	13027, 1.00000E+00			
	82206, 2.54963E-01	82207, 2.20987E-01	82208, 5.24050E-01	
9	24050, 8.79087E-03	26054, 4.02643E-02	28058, 6.09419E-02	24052, 1.69300E-01
	26056, 6.31511E-01	28060, 2.34673E-02	24053, 1.92010E-02	26057, 1.45900E-02
	28061, 1.02022E-03	24054, 4.76985E-03	26058, 1.92741E-03	28062, 3.24982E-03
	28064, 8.32505E-04	25055, 2.01337E-02		

print table 40

imaterial number

imaterial number	component nuclide, mass fraction			
1	92235, 5.69936E-03	92238, 8.08504E-01	94238, 3.37237E-05	94239, 6.40755E-02
	94240, 3.03518E-03	94241, 2.69798E-04	94242, 3.37237E-05	8016, 1.18349E-01
2	1001, 1.11915E-01	8016, 8.88085E-01		
	associated thermal s(a,b) data sets: lwtr.01t			
3	26054, 7.06265E-05	24050, 4.17879E-05	7014, 4.97975E-04	26056, 1.14894E-03
	24052, 8.36958E-04	7015, 1.98090E-06	26057, 2.70186E-05	24053, 9.67251E-05
	26058, 3.63082E-06	24054, 2.44788E-05	40000, 9.82251E-01	50000, 1.49992E-02
4	1001, 1.11915E-01	8016, 8.88085E-01		
	1001, 1.11915E-01	8016, 8.88085E-01		

6	1001, 1.11915E-01	8016, 8.88085E-01				
7	13027, 1.00000E+00					
8	82206, 2.53400E-01	82207, 2.20700E-01	82208, 5.25900E-01			
9	24050, 7.93920E-03	26054, 3.92710E-02	28058, 6.38416E-02	24052, 1.59004E-01		
	26056, 6.38716E-01	28060, 2.54306E-02	24053, 1.83805E-02	26057, 1.50204E-02		
	28061, 1.12403E-03	24054, 4.65211E-03	26058, 2.01905E-03	28062, 3.63909E-03		
	28064, 9.62324E-04	25055, 2.00005E-02				

warning. 6 materials had unnormalized fractions. print table 40.
lcell volumes and masses

print table 50

cell	atom density	gram density	input volume	calculated volume	mass	pieces	reason volume not calculated
1	1 7.05663E-02	1.05550E+01	0.00000E+00	2.79982E+02	2.95521E+03	1	
2	2 1.00128E-01	9.98200E-01	0.00000E+00	2.58267E+01	2.57802E+01	1	
3	3 4.33411E-02	6.56000E+00	0.00000E+00	9.81838E+01	6.44086E+02	1	
4	4 1.00128E-01	9.98200E-01	0.00000E+00	0.00000E+00	0.00000E+00	0	infinite
5	10 1.00128E-01	9.98200E-01	0.00000E+00	5.09690E+03	5.08773E+03	0	
6	20 1.00128E-01	9.98200E-01	0.00000E+00	9.94289E+04	9.92499E+04	0	
7	21 1.00309E-05	1.00000E-04	0.00000E+00	1.30324E+05	1.30324E+01	0	
8	22 6.03063E-02	2.70200E+00	0.00000E+00	0.00000E+00	0.00000E+00	0	asymmetric
9	23 1.00309E-05	1.00000E-04	0.00000E+00	0.00000E+00	0.00000E+00	0	infinite
10	40 3.29629E-02	1.13440E+01	0.00000E+00	1.66245E+04	1.88588E+05	1	
11	41 1.00309E-05	1.00000E-04	0.00000E+00	4.09828E+05	4.09828E+01	1	
12	42 8.64586E-02	7.94000E+00	0.00000E+00	9.51154E+04	7.55216E+05	1	
13	43 8.64586E-02	7.94000E+00	0.00000E+00	4.53784E+05	3.60304E+06	1	
14	44 8.64586E-02	7.94000E+00	0.00000E+00	1.02842E+04	8.16563E+04	2	
15	45 8.64586E-02	7.94000E+00	0.00000E+00	9.04489E+04	7.18165E+05	1	
16	46 3.29629E-02	1.13440E+01	0.00000E+00	9.86269E+05	1.11882E+07	1	
17	47 3.29629E-02	1.13440E+01	0.00000E+00	5.13461E+04	5.82470E+05	2	
18	48 0.00000E+00	0.00000E+00	0.00000E+00	1.20186E+04	0.00000E+00	1	
19	49 1.00309E-05	1.00000E-04	0.00000E+00	0.00000E+00	0.00000E+00	0	asymmetric
20	50 0.00000E+00	0.00000E+00	0.00000E+00	0.00000E+00	0.00000E+00	0	infinite

warning. 2 cells appear to consist of more than one piece.
lsurface areas

print table 50

surface	input area	calculated area	reason area not calculated
2	1.1 0.00000E+00	1.17123E+03	
3	1.2 0.00000E+00	7.18104E-01	
4	1.3 0.00000E+00	7.18104E-01	
6	2.1 0.00000E+00	1.25434E+03	
7	2.2 0.00000E+00	7.46925E-01	
8	2.3 0.00000E+00	7.46925E-01	
10	3.1 0.00000E+00	1.44593E+03	
11	3.2 0.00000E+00	9.80986E-01	
12	3.3 0.00000E+00	9.80986E-01	
14	10.1 0.00000E+00	0.00000E+00	not a boundary
15	10.2 0.00000E+00	0.00000E+00	not a boundary
16	10.3 0.00000E+00	0.00000E+00	not a boundary
17	10.4 0.00000E+00	0.00000E+00	not a boundary
18	10.5 0.00000E+00	0.00000E+00	not a boundary
19	10.6 0.00000E+00	0.00000E+00	not a boundary
20	10.7 0.00000E+00	1.12237E+01	
21	10.8 0.00000E+00	1.12237E+01	
23	20.1 0.00000E+00	6.70476E+03	
24	20.2 0.00000E+00	6.70476E+03	
25	20.3 0.00000E+00	6.70476E+03	
26	20.4 0.00000E+00	6.70476E+03	
27	20.5 0.00000E+00	0.00000E+00	asymmetric
28	20.6 0.00000E+00	0.00000E+00	asymmetric
30	21.1 0.00000E+00	1.01920E+04	
31	21.2 0.00000E+00	1.01920E+04	
32	21.3 0.00000E+00	1.01920E+04	
33	21.4 0.00000E+00	1.01920E+04	
37	22.1 0.00000E+00	4.78244E+04	
41	40.1 0.00000E+00	1.16417E+05	
42	40.2 0.00000E+00	4.18972E+03	
43	40.3 0.00000E+00	4.18972E+03	
49	42.1 0.00000E+00	4.82539E+04	
53	43.1 0.00000E+00	1.26170E+03	
54	43.2 0.00000E+00	2.18169E+03	
55	43.3 0.00000E+00	2.18169E+03	
57	44.1 0.00000E+00	3.50295E+03	
58	44.2 0.00000E+00	2.23013E+03	
61	45.1 0.00000E+00	5.48652E+03	
65	46.1 0.00000E+00	4.95306E+04	
66	46.2 0.00000E+00	2.61173E+03	
67	46.3 0.00000E+00	2.61173E+03	
69	47.1 0.00000E+00	8.72916E+04	
73	48.1 0.00000E+00	8.76515E+04	
77	49.1 0.00000E+00	3.70684E+04	
78	49.2 0.00000E+00	3.70684E+04	
79	49.3 0.00000E+00	3.70684E+04	
80	49.4 0.00000E+00	3.70684E+04	
81	49.5 0.00000E+00	5.33744E+03	
82	49.6 0.00000E+00	5.33744E+03	
84	10010.1 0.00000E+00	9.43871E+02	
85	10010.2 0.00000E+00	9.43871E+02	
86	10010.3 0.00000E+00	9.43871E+02	
87	10010.4 0.00000E+00	9.43871E+02	
88	10010.5 0.00000E+00	9.43871E+02	
89	10010.6 0.00000E+00	9.43871E+02	

lcells

print table 60

cell	mat	atom density	gram density	volume	mass	pieces	neutron importance
1	1	1 7.05663E-02	1.05550E+01	2.79982E+02	2.95521E+03	1	1.0000E+00
2	2	2s 1.00128E-01	9.98200E-01	2.58267E+01	2.57802E+01	1	1.0000E+00
3	3	3 4.33411E-02	6.56000E+00	9.81838E+01	6.44086E+02	1	1.0000E+00
4	4	4s 1.00128E-01	9.98200E-01	0.00000E+00	0.00000E+00	0	1.0000E+00
5	10	4s 1.00128E-01	9.98200E-01	5.09690E+03	5.08773E+03	0	1.0000E+00
6	20	4s 1.00128E-01	9.98200E-01	9.94289E+04	9.92499E+04	0	1.0000E+00
7	21	5s 1.00309E-05	1.00000E-04	1.30324E+05	1.30324E+01	0	1.0000E+00
8	22	7 6.03063E-02	2.70200E+00	0.00000E+00	0.00000E+00	0	1.0000E+00
9	23	5s 1.00309E-05	1.00000E-04	0.00000E+00	0.00000E+00	0	1.0000E+00
10	40	8 3.29629E-02	1.13440E+01	1.66245E+04	1.88588E+05	1	1.0000E+00
11	41	5s 1.00309E-05	1.00000E-04	4.09828E+05	4.09828E+01	1	1.0000E+00
12	42	9 8.64586E-02	7.94000E+00	9.51154E+04	7.55216E+05	1	1.0000E+00
13	43	9 8.64586E-02	7.94000E+00	4.53784E+05	3.60304E+06	1	1.0000E+00
14	44	9 8.64586E-02	7.94000E+00	1.02842E+04	8.16563E+04	2	1.0000E+00
15	45	9 8.64586E-02	7.94000E+00	9.04489E+04	7.18165E+05	1	1.0000E+00
16	46	8 3.29629E-02	1.13440E+01	9.86269E+05	1.11882E+07	1	1.0000E+00
17	47	8 3.29629E-02	1.13440E+01	5.13461E+04	5.82470E+05	2	1.0000E+00
18	48	0 0.00000E+00	0.00000E+00	1.20186E+04	0.00000E+00	1	1.0000E+00
19	49	6s 1.00309E-05	1.00000E-04	0.00000E+00	0.00000E+00	0	1.0000E+00
20	50	0 0.00000E+00	0.00000E+00	0.00000E+00	0.00000E+00	0	0.0000E+00

total
1surfaces 2.36097E+06 1.72254E+07

print table 70

surface	trans	type	surface coefficients
1	1	rcc	
2	1.1	cz	4.7810000E-01
3	1.2	pz	4.0041070E+02
4	1.3	p	0.0000000E+00
5	2	rcc	
6	2.1	cz	4.8760000E-01
7	2.2	pz	4.1582170E+02
8	2.3	p	0.0000000E+00
9	3	rcc	
10	3.1	cz	5.5880000E-01
11	3.2	pz	4.1690260E+02
12	3.3	p	0.0000000E+00
13	10	rhp	
14	10.1	px	1.8000000E+00
15	10.2	p	-1.0000000E+00
16	10.3	p	5.0000000E-01
17	10.4	p	-5.0000000E-01
18	10.5	p	-5.0000000E-01
19	10.6	p	5.0000000E-01
20	10.7	pz	4.5312000E+02
21	10.8	p	0.0000000E+00
22	20	rpp	
23	20.1	1 p	8.6602540E-01
24	20.2	1 p	-8.6602540E-01
25	20.3	1 p	-5.0000000E-01
26	20.4	1 p	5.0000000E-01
27	20.5	1 pz	4.5212000E+02
28	20.6	1 p	0.0000000E+00
29	21	rpp	
30	21.1	1 p	8.6602540E-01
31	21.2	1 p	-8.6602540E-01
32	21.3	1 p	-5.0000000E-01
33	21.4	1 p	5.0000000E-01
36	22	rcc	
37	22.1	cz	1.6835120E+01
40	40	rcc	
41	40.1	cz	3.6518900E+01
42	40.2	pz	4.8069500E+02
43	40.3	p	0.0000000E+00
44	41	rcc	
48	42	rcc	
49	42.1	cz	1.6986300E+01
52	43	rcc	
53	43.1	cz	2.6352500E+01
54	43.2	pz	-1.0160000E+01
55	43.3	p	0.0000000E+00
56	44	rcc	
57	44.1	cz	2.0174000E+01
58	44.2	pz	4.4450000E+02
60	45	rcc	
61	45.1	cz	3.1597600E+01
64	46	rcc	
65	46.1	cz	1.8910300E+01
66	46.2	pz	4.3068240E+02
67	46.3	p	0.0000000E+00
68	47	rcc	
69	47.1	cz	3.3327100E+01
72	48	rcc	
73	48.1	cz	3.3464500E+01
76	49	rpp	
77	49.1 refl.	px	3.6528900E+01
78	49.2 refl.	p	-1.0000000E+00
79	49.3 refl.	py	3.6528900E+01
80	49.4 refl.	p	0.0000000E+00
81	49.5 refl.	pz	4.8070500E+02
82	49.6 refl.	p	0.0000000E+00
83	10010	rhp	

84	10010.1	1001	px	2.7000000E+00					
85	10010.2	1001	p	-1.0000000E+00	0.0000000E+00	0.0000000E+00	9.0000000E-01		
86	10010.3	1001	p	5.0000000E-01	8.6602540E-01	0.0000000E+00	9.0003960E-01		
87	10010.4	1001	p	-5.0000000E-01	-8.6602540E-01	0.0000000E+00	2.6999604E+00		
88	10010.5	1001	p	-5.0000000E-01	8.6602540E-01	0.0000000E+00	3.9600581E-05		
89	10010.6	1001	p	5.0000000E-01	-8.6602540E-01	0.0000000E+00	3.5999604E+00		

1 identical surfaces

print table 70

master surface	identical surfaces						
10.7	10010.7						
10.8	10010.8						
20.5	21.5	22.2	42.2				
20.6	21.6	22.3	41.2	42.3	44.3	45.3	
40.1	41.1						
40.3	41.3						
44.2	45.2						
46.2	47.2	48.2					
46.3	47.3	48.3					

surface coefficients for identical surfaces not used.

surface	trans	type	surface coefficients				
90	10010.7	1001	pz	4.5312000E+02			
91	10010.8	1001	p	0.0000000E+00	0.0000000E+00	-1.0000000E+00	1.0000000E+00
34	21.5	1	pz	4.5212000E+02			
38	22.2		pz	4.5212000E+02			
50	42.2		pz	4.5212000E+02			
35	21.6	1	p	0.0000000E+00	0.0000000E+00	-1.0000000E+00	0.0000000E+00
39	22.3		p	0.0000000E+00	0.0000000E+00	-1.0000000E+00	0.0000000E+00
46	41.2		pz	0.0000000E+00			
51	42.3		p	0.0000000E+00	0.0000000E+00	-1.0000000E+00	0.0000000E+00
59	44.3		p	0.0000000E+00	0.0000000E+00	-1.0000000E+00	0.0000000E+00
63	45.3		p	0.0000000E+00	0.0000000E+00	-1.0000000E+00	0.0000000E+00
45	41.1		cz	3.6518900E+01			
47	41.3		p	0.0000000E+00	0.0000000E+00	-1.0000000E+00	2.6670000E+01
62	45.2		pz	4.4450000E+02			
70	47.2		pz	4.3068240E+02			
74	48.2		pz	4.3068240E+02			
71	47.3		p	0.0000000E+00	0.0000000E+00	-1.0000000E+00	-1.3817600E+01
75	48.3		p	0.0000000E+00	0.0000000E+00	-1.0000000E+00	-1.3817600E+01

1 cell temperatures in mev for the free-gas thermal neutron treatment.

print table 72

all non-zero importance cells with materials have a temperature for thermal neutrons of 2.5300E-08 mev.

```
*****
* Random Number Generator = 2 *
* Random Number Seed = 19073486328125 *
* Random Number Multiplier = 9219741426499971445 *
* Random Number Adder = 1 *
* Random Number Bits Used = 63 *
* Random Number Stride = 152917 *
*****
```

5 warning messages so far.
lphysical constants

print table 98

name	value	description
huge	1.0000000000000E+36	infinity
pie	3.1415926535898E+00	pi
euler	5.7721566490153E-01	euler constant
avogad	6.0220434469282E+23	avogadro number (molecules/mole)
aneut	1.0086649670000E+00	neutron mass (amu)
avgdn	5.9703109000000E-01	avogadro number/neutron mass (1.e-24*molecules/mole/amu)
slite	2.9979250000000E+02	speed of light (cm/shake)
planck	4.1357320000000E-13	planck constant (mev shake)
fscon	1.3703930000000E+02	inverse fine structure constant h*c/(2*pi*e**2)
gpt(1)	9.3958000000000E+02	neutron mass (mev)
gpt(3)	5.1100800000000E-01	electron mass (mev)

fission q-values:	nuclide	q(mev)	nuclide	q(mev)
	90232	171.91	91233	175.57
	92233	180.84	92234	179.45
	92235	180.88	92236	179.50
	92237	180.40	92238	181.31
	92239	180.40	92240	180.40
	93237	183.67	94238	186.65
	94239	189.44	94240	186.36
	94241	188.99	94242	185.98
	94243	187.48	95241	190.83
	95242	190.54	95243	190.25
	96242	190.49	96244	190.49
	other	180.00		

the following compilation options were used:

```
cheap
dec
plot
mcplot
```

xlib
default datapath: C:\Program Files\LANL\MCNPDATA
C:\Progra-1\LANL\MCNPDATA
cross-section tables print table 100

table	length				
tables from file actia					
1001.62c	5202	1-h-1 at 293.6K from endf-vi.8 njoy99.50	mat 125		12/05/01
7014.62c	67462	7-n-14 at 293.6K from endf-vi.8 njoy99.50	mat 725		12/05/01
8016.62c	170541	8-o-16 at 293.6K from endf-vi.8 njoy99.50	mat 825		12/05/01
13027.62c	75363	13-al-27 at 293.6K from endf-vi.8 njoy99.50	mat1325		12/17/01
24050.62c	194445	24-cr-50 at 293.6K from endf-vi.8 njoy99.50	mat2425		12/20/01
24052.62c	174773	24-cr-52 at 293.6K from endf-vi.8 njoy99.50	mat2431		12/20/01
24053.62c	147286	24-cr-53 at 293.6K from endf-vi.8 njoy99.50	mat2434		12/20/01
24054.62c	132737	24-cr-54 at 293.6K from endf-vi.8 njoy99.50	mat2437		12/20/01
25055.62c	134565	25-mn-55 at 293.6K from endf/b-vi.8 njoy99.50	mat2525		02/11/02
26054.62c	143370	26-fe-54 at 293.6K from endf-vi.8 njoy99.50	mat2625		12/20/01
26056.62c	230655	26-fe-56 at 293.6K from endf-vi.8 njoy99.50	mat2631		12/20/01
26057.62c	148842	26-fe-57 at 293.6K from endf-vi.8 njoy99.50	mat2634		12/20/01
26058.62c	87569	26-fe-58 at 293.6K from endf-vi.8 njoy99.50	mat2637		12/20/01
28058.62c	235403	28-ni-58 at 293.6K from endf-vi.8 njoy99.50	mat2825		12/20/01
28060.62c	158305	28-ni-60 at 293.6K from endf-vi.8 njoy99.50	mat2831		12/20/01
28061.62c	112032	28-ni-61 at 293.6K from endf-vi.8 njoy99.50	mat2834		12/20/01
28062.62c	104386	28-ni-62 at 293.6K from endf-vi.8 njoy99.50	mat2837		12/20/01
28064.62c	97689	28-ni-64 at 293.6K from endf-vi.8 njoy99.50	mat2843		12/20/01

tables from file endf66a					
7015.66c	19013	7-n-15 at 293.6K from endf-vi.0 njoy99.50	mat 728		07/13/01

tables from file endf66b					
40000.66c	98524	40-zr-0 at 293.6K from endf-vi.1 njoy99.50	mat4000		07/24/01

tables from file endl92
50000.42c 141628 ENDL library name: nd920609 LANL/XTM modified: 951222 911219
temperature = 2.5860E-08 adjusted to 2.5300E-08

tables from file endf66c					
82206.66c	219368	82-pb-206 at 293.6K from endf-vi.6 njoy99.50	mat8231		08/13/01
82207.66c	134389	82-pb-207 at 293.6K from endf-vi.6 njoy99.50	mat8234		08/13/01
82208.66c	135105	82-pb-208 at 293.6K from endf-vi.x njoy99.50	mat8237		03/16/02
94238.66c	53256	94-pu-238 at 293.6K from endf-vi.0 njoy99.50	mat9434		09/06/01
94240.66c	309518	94-pu-240 at 293.6K from endf-vi.2 njoy99.50	mat9440		09/06/01
94241.66c	126607	94-pu-241 at 293.6K from endf-vi.3 njoy99.50	mat9443		09/06/01
94242.66c	107114	94-pu-242 at 293.6K from endf-vi.0 njoy99.50	mat9446		09/06/01

tables from file t16_2003					
92235.69c	587997	92-u-235 at 293.6K from t16 u2351a9d njoy99.50	mat9228		07/02/03
92238.69c	713320	92-u-238 at 293.6K from t16 u2381a8h njoy99.50	mat9237		07/02/03
94239.69c	506320	94-pu-239 at 293.6K from t16 pu2391a7d njoy99.50	mat9437		07/02/03

tables from file tmccs					
lwtr.01t	10193	hydrogen in light water at 300 degrees kelvin	1001	0	010/22/85
total	5582977				

warning. neutron energy cutoff is below some cross-section tables.

comment. 1 cross sections modified by free gas thermal treatment.
assignment of s(a,b) data to nuclides. print table 102

mat	nuclide	s(a,b)
2	1001.62c	lwtr.01t
4	1001.62c	lwtr.01t
5	1001.62c	lwtr.01t
6	1001.62c	lwtr.01t

dump no. 1 on file MS_Acc_NACCoC_c1.00_g0.00_e0.00_d0.01cm_HP_36mm.inpr nps = 0 coll = 0
ctm = 0.00 nrn = 0

6 warning messages so far.
lestimated keff results by cycle print table 175

cycle	1	k(collison)	0.662630	prompt removal lifetime(abs)	8.1191E+03	source points generated	844
cycle	2	k(collison)	0.622585	prompt removal lifetime(abs)	8.6526E+03	source points generated	928
cycle	3	k(collison)	0.744636	prompt removal lifetime(abs)	8.5012E+03	source points generated	1189
cycle	4	k(collison)	0.686479	prompt removal lifetime(abs)	7.9407E+03	source points generated	916

cycle	5	k(collision)	0.671615	prompt removal lifetime(abs)	8.8591E+03	source points generated	972
cycle	6	k(collision)	0.675550	prompt removal lifetime(abs)	8.2834E+03	source points generated	999
cycle	7	k(collision)	0.693864	prompt removal lifetime(abs)	8.1740E+03	source points generated	1052
cycle	8	k(collision)	0.702859	prompt removal lifetime(abs)	8.6663E+03	source points generated	1006

estimator	cycle	526	ave of 496 cycles	combination	simple average	combined average	corr
k(collision)		0.741770	0.703646 0.0016	k(col/abs)	0.703392 0.0015	0.703372 0.0015	0.7953
k(absorption)		0.756647	0.703139 0.0016	k(abs/tk ln)	0.703262 0.0016	0.703196 0.0015	0.4218
k(trk length)		0.717143	0.703386 0.0022	k(tk ln/col)	0.703516 0.0017	0.703605 0.0016	0.5823
rem life(col)		8.4284E+03	8.4718E+03 0.0017	k(col/abs/tk ln)	0.703390 0.0015	0.703328 0.0015	
rem life(abs)		8.3911E+03	8.4726E+03 0.0016	life(col/abs/tl)	8.4742E+03 0.0015	8.4796E+03 0.0013	
source points generated 1046							

estimator	cycle	527	ave of 497 cycles	combination	simple average	combined average	corr
k(collision)		0.643842	0.703525 0.0016	k(col/abs)	0.703297 0.0015	0.703275 0.0015	0.7960
k(absorption)		0.668059	0.703068 0.0016	k(abs/tk ln)	0.703158 0.0016	0.703110 0.0015	0.4250
k(trk length)		0.634707	0.703247 0.0022	k(tk ln/col)	0.703386 0.0017	0.703482 0.0016	0.5863
rem life(col)		8.2199E+03	8.4713E+03 0.0017	k(col/abs/tk ln)	0.703280 0.0015	0.703227 0.0015	
rem life(abs)		8.1559E+03	8.4720E+03 0.0016	life(col/abs/tl)	8.4737E+03 0.0015	8.4793E+03 0.0013	
source points generated 869							

estimator	cycle	528	ave of 498 cycles	combination	simple average	combined average	corr
k(collision)		0.717239	0.703553 0.0016	k(col/abs)	0.703307 0.0015	0.703282 0.0015	0.7956
k(absorption)		0.699228	0.703060 0.0016	k(abs/tk ln)	0.703150 0.0016	0.703102 0.0015	0.4250
k(trk length)		0.699455	0.703240 0.0022	k(tk ln/col)	0.703396 0.0017	0.703504 0.0016	0.5860
rem life(col)		8.7750E+03	8.4719E+03 0.0017	k(col/abs/tk ln)	0.703284 0.0015	0.703229 0.0015	
rem life(abs)		8.6882E+03	8.4724E+03 0.0016	life(col/abs/tl)	8.4741E+03 0.0015	8.4795E+03 0.0013	
source points generated 1119							

estimator	cycle	529	ave of 499 cycles	combination	simple average	combined average	corr
k(collision)		0.699031	0.703544 0.0016	k(col/abs)	0.703286 0.0015	0.703261 0.0015	0.7954
k(absorption)		0.686971	0.703028 0.0016	k(abs/tk ln)	0.703156 0.0016	0.703088 0.0015	0.4238
k(trk length)		0.725578	0.703285 0.0022	k(tk ln/col)	0.703414 0.0017	0.703503 0.0016	0.5854
rem life(col)		8.4836E+03	8.4719E+03 0.0017	k(col/abs/tk ln)	0.703286 0.0015	0.703216 0.0015	
rem life(abs)		8.6100E+03	8.4727E+03 0.0016	life(col/abs/tl)	8.4744E+03 0.0015	8.4804E+03 0.0013	
source points generated 961							

estimator	cycle	530	ave of 500 cycles	combination	simple average	combined average	corr
k(collision)		0.702529	0.703542 0.0016	k(col/abs)	0.703276 0.0015	0.703251 0.0015	0.7954
k(absorption)		0.694516	0.703011 0.0015	k(abs/tk ln)	0.703094 0.0016	0.703049 0.0015	0.4238
k(trk length)		0.649825	0.703178 0.0022	k(tk ln/col)	0.703360 0.0017	0.703485 0.0016	0.5841
rem life(col)		8.2172E+03	8.4714E+03 0.0017	k(col/abs/tk ln)	0.703244 0.0015	0.703190 0.0015	
rem life(abs)		8.3284E+03	8.4724E+03 0.0016	life(col/abs/tl)	8.4741E+03 0.0015	8.4802E+03 0.0013	
source points generated 1018							

source distribution written to file MS_Acc_NACCoC_c1.00_g0.00_e0.00_d0.01cm_HP_36mm.inps cycle = 530
 problem summary (active cycles only) source particle weight for summary table normalization = 500000.00

run terminated when 530 kcode cycles were done.

+ NAC-LWT Cask - MOX Experiments - Accident Transport Conditions probid = 10/25/07 21:18:09
 0 10/25/07 21:05:56

neutron creation	tracks	weight (per source particle)	energy	neutron loss	tracks	weight (per source particle)	energy
source	500502	1.0000E+00	2.1043E+00	escape	0	0.	0.
				energy cutoff	0	0.	0.
				time cutoff	0	0.	0.
weight window	0	0.	0.	weight window	0	0.	0.
cell importance	0	0.	0.	cell importance	0	0.	0.
weight cutoff	0	1.0592E-01	4.8768E-06	weight cutoff	500977	1.0547E-01	4.3336E-06
e or t importance	0	0.	0.	e or t importance	0	0.	0.
dxtran	0	0.	0.	dxtran	0	0.	0.
forced collisions	0	0.	0.	forced collisions	0	0.	0.
exp. transform	0	0.	0.	exp. transform	0	0.	0.
upscattering	0	0.	2.2571E-07	downscattering	0	0.	2.0393E+00
photonuclear	0	0.	0.	capture	0	7.5486E-01	3.4580E-02
(n,xn)	949	1.6722E-03	1.5347E-03	loss to (n,xn)	474	8.3532E-04	8.0905E-03
prompt fission	0	0.	0.	loss to fission	0	2.4643E-01	2.3925E-02
delayed fission	0	0.	0.				
total	501451	1.1076E+00	2.1059E+00	total	501451	1.1076E+00	2.1059E+00

number of neutrons banked 501
 neutron tracks per source particle 1.0029E+00
 neutron collisions per source particle 1.5353E+02
 total neutron collisions 76766227
 net multiplication 1.0008E+00 0.0000

average time of (shakes)
 escape 0.0000E+00 cutoffs
 capture 9.4388E+03 tco 1.0000E+33
 capture or escape 9.4388E+03 eco 0.0000E+00
 any termination 9.7365E+03 wc1 -5.0000E-01
 wc2 -2.5000E-01

computer time so far in this run 12.12 minutes
 computer time in mcrun 11.96 minutes
 source particles per minute 4.4359E+04
 random numbers generated 776053288

maximum number ever in bank 2
 bank overflows to backup file 0
 most random numbers used was 12401 in history 255214

range of sampled source weights = 8.4104E-01 to 1.1848E+00

source efficiency = 1.0000 in cell 1
 source efficiency = 0.1042 in cell 10
 source efficiency = 1.0000 in cell 20

source efficiency = 1.0000 in cell 41
neutron activity in each cell

print table 126

cell	tracks entering	population	collisions	collisions * weight (per history)	number weighted energy	flux weighted energy	average track weight (relative)	average track mfp (cm)
1	1	1255010	500853	588249	9.5138E-01	1.2434E-03	1.1278E+00	2.6471E+00
2	2	1783820	500855	71781	1.0077E-01	4.1502E-04	8.2308E-01	8.3190E-01
3	3	1923591	500862	78833	1.3909E-01	5.6258E-04	8.8063E-01	8.8178E-01
4	4	4738894	500933	23063782	3.3926E+01	1.9840E-04	5.3541E-01	8.2904E-01
5	10	1421751	373841	6076166	8.6070E+00	1.3853E-04	3.5425E-01	7.9418E-01
6	20	0	0	0	0.0000E+00	0.0000E+00	0.0000E+00	0.0000E+00
7	21	1663380	374111	1888	2.7445E-03	4.9624E-04	4.1450E-01	8.2621E-01
8	22	2075969	374082	2123010	3.6862E+00	5.4141E-04	3.4564E-01	8.1935E-01
9	23	2178870	357717	98	1.4370E-04	5.9979E-04	3.0426E-01	8.1703E-01
10	40	26756	5352	105825	1.4813E-01	3.0621E-03	1.0020E-01	7.1747E-01
11	41	0	0	0	0.0000E+00	0.0000E+00	0.0000E+00	0.0000E+00
12	42	117397	15536	1374254	1.8224E+00	2.6104E-03	1.0374E-01	7.2074E-01
13	43	3367057	211757	13287925	1.9309E+01	3.4664E-03	1.7878E-01	7.8829E-01
14	44	42780	15974	147895	2.0621E-01	8.2779E-04	1.6867E-01	7.5443E-01
15	45	2192206	356597	5325642	8.0534E+00	9.0372E-04	3.0289E-01	8.1723E-01
16	46	2661735	296813	24149944	3.7756E+01	1.6531E-03	2.2215E-01	8.0496E-01
17	47	88453	20419	366868	5.3434E-01	1.7669E-03	1.3640E-01	7.4778E-01
18	48	3155968	210444	0	0.0000E+00	2.8143E-03	1.8703E-01	7.9827E-01
19	49	1754788	180075	4067	6.0877E-03	3.8995E-03	1.8293E-01	7.8977E-01
total		30448425	4796221	76766227	1.1525E+02			

print table 128 requires
neutron weight balance in each cell

1067 decimal words of dynamically allocated storage.

print table 130

cell index	1	2	3	4	5	6	7	8	9
cell number	1	2	3	4	10	20	21	22	23
external events:									
entering	1.2681E+00	3.1938E+00	3.4204E+00	7.9797E+00	2.3195E+00	0.0000E+00	2.7616E+00	3.4266E+00	3.5712E+00
source	1.0000E+00	0.0000E+00	0.0000E+00	0.0000E+00	0.0000E+00	0.0000E+00	0.0000E+00	0.0000E+00	0.0000E+00
energy cutoff	0.0000E+00	0.0000E+00	0.0000E+00	0.0000E+00	0.0000E+00	0.0000E+00	0.0000E+00	0.0000E+00	0.0000E+00
time cutoff	0.0000E+00	0.0000E+00	0.0000E+00	0.0000E+00	0.0000E+00	0.0000E+00	0.0000E+00	0.0000E+00	0.0000E+00
exiting	-1.8832E+00	-3.1934E+00	-3.4192E+00	-7.8425E+00	-2.2857E+00	0.0000E+00	-2.7616E+00	-3.3873E+00	-3.5712E+00
total	3.8488E-01	3.6018E-04	1.1827E-03	1.3724E-01	3.3874E-02	0.0000E+00	6.3609E-06	3.9247E-02	2.1550E-07
variance reduction events:									
weight window	0.0000E+00	0.0000E+00	0.0000E+00	0.0000E+00	0.0000E+00	0.0000E+00	0.0000E+00	0.0000E+00	0.0000E+00
cell importance	0.0000E+00	0.0000E+00	0.0000E+00	0.0000E+00	0.0000E+00	0.0000E+00	0.0000E+00	0.0000E+00	0.0000E+00
weight cutoff	2.8229E-05	2.7032E-06	-9.7040E-06	-1.9749E-05	-4.7973E-05	0.0000E+00	-9.9564E-07	5.7430E-05	0.0000E+00
e or t importance	0.0000E+00	0.0000E+00	0.0000E+00	0.0000E+00	0.0000E+00	0.0000E+00	0.0000E+00	0.0000E+00	0.0000E+00
dextran	0.0000E+00	0.0000E+00	0.0000E+00	0.0000E+00	0.0000E+00	0.0000E+00	0.0000E+00	0.0000E+00	0.0000E+00
forced collisions	0.0000E+00	0.0000E+00	0.0000E+00	0.0000E+00	0.0000E+00	0.0000E+00	0.0000E+00	0.0000E+00	0.0000E+00
exp. transform	0.0000E+00	0.0000E+00	0.0000E+00	0.0000E+00	0.0000E+00	0.0000E+00	0.0000E+00	0.0000E+00	0.0000E+00
total	2.8229E-05	2.7032E-06	-9.7040E-06	-1.9749E-05	-4.7973E-05	0.0000E+00	-9.9564E-07	5.7430E-05	0.0000E+00
physical events:									
capture (n, xn)	-1.3879E-01	-3.6289E-04	-1.1985E-03	-1.3722E-01	-3.3826E-02	0.0000E+00	-5.3652E-06	-3.9305E-02	-2.1550E-07
loss to (n, xn)	-3.1093E-04	0.0000E+00	-2.5430E-05	0.0000E+00	0.0000E+00	0.0000E+00	0.0000E+00	0.0000E+00	0.0000E+00
loss to fission	0.0000E+00	0.0000E+00	0.0000E+00	0.0000E+00	0.0000E+00	0.0000E+00	0.0000E+00	0.0000E+00	0.0000E+00
loss to fission photonuclear	-2.4643E-01	0.0000E+00	0.0000E+00	0.0000E+00	0.0000E+00	0.0000E+00	0.0000E+00	0.0000E+00	0.0000E+00
total	-3.8491E-01	-3.6289E-04	-1.1730E-03	-1.3722E-01	-3.3826E-02	0.0000E+00	-5.3652E-06	-3.9305E-02	-2.1550E-07
total	0.0000E+00	0.0000E+00	0.0000E+00	0.0000E+00	0.0000E+00	0.0000E+00	0.0000E+00	0.0000E+00	0.0000E+00
cell index 10 11 12 13 14 15 16 17 18									
cell number 40 41 42 43 44 45 46 47 48									
external events:									
entering	3.8410E-02	0.0000E+00	1.7109E-01	5.3543E+00	6.4450E-02	3.6004E+00	4.2962E+00	1.3246E-01	5.0388E+00
source	0.0000E+00	0.0000E+00	0.0000E+00	0.0000E+00	0.0000E+00	0.0000E+00	0.0000E+00	0.0000E+00	0.0000E+00
energy cutoff	0.0000E+00	0.0000E+00	0.0000E+00	0.0000E+00	0.0000E+00	0.0000E+00	0.0000E+00	0.0000E+00	0.0000E+00
time cutoff	0.0000E+00	0.0000E+00	0.0000E+00	0.0000E+00	0.0000E+00	0.0000E+00	0.0000E+00	0.0000E+00	0.0000E+00
exiting	-3.8338E-02	0.0000E+00	-1.5873E-01	-5.2124E+00	-6.0345E-02	-3.3858E+00	-4.2663E+00	-1.3214E-01	-5.0388E+00
total	7.1248E-05	0.0000E+00	1.2354E-02	1.4185E-01	4.1045E-03	2.1458E-01	2.9932E-02	3.1701E-04	0.0000E+00
variance reduction events:									
weight window	0.0000E+00	0.0000E+00	0.0000E+00	0.0000E+00	0.0000E+00	0.0000E+00	0.0000E+00	0.0000E+00	0.0000E+00
cell importance	0.0000E+00	0.0000E+00	0.0000E+00	0.0000E+00	0.0000E+00	0.0000E+00	0.0000E+00	0.0000E+00	0.0000E+00
weight cutoff	5.9575E-07	0.0000E+00	-3.9444E-05	1.7827E-04	8.9663E-06	2.2838E-04	5.6942E-05	7.6461E-06	0.0000E+00
e or t importance	0.0000E+00	0.0000E+00	0.0000E+00	0.0000E+00	0.0000E+00	0.0000E+00	0.0000E+00	0.0000E+00	0.0000E+00
dextran	0.0000E+00	0.0000E+00	0.0000E+00	0.0000E+00	0.0000E+00	0.0000E+00	0.0000E+00	0.0000E+00	0.0000E+00
forced collisions	0.0000E+00	0.0000E+00	0.0000E+00	0.0000E+00	0.0000E+00	0.0000E+00	0.0000E+00	0.0000E+00	0.0000E+00
exp. transform	0.0000E+00	0.0000E+00	0.0000E+00	0.0000E+00	0.0000E+00	0.0000E+00	0.0000E+00	0.0000E+00	0.0000E+00
total	5.9575E-07	0.0000E+00	-3.9444E-05	1.7827E-04	8.9663E-06	2.2838E-04	5.6942E-05	7.6461E-06	0.0000E+00
physical events:									
capture (n, xn)	-7.1844E-05	0.0000E+00	-1.2315E-02	-1.4204E-01	-4.1135E-03	-2.1481E-01	-3.0482E-02	-3.2465E-04	0.0000E+00
loss to (n, xn)	0.0000E+00	0.0000E+00	0.0000E+00	6.9717E-06	0.0000E+00	6.6859E-06	9.8428E-04	0.0000E+00	0.0000E+00
loss to (n, xn) photonuclear	0.0000E+00	0.0000E+00	0.0000E+00	-3.4859E-06	0.0000E+00	-3.3429E-06	-4.9214E-04	0.0000E+00	0.0000E+00

fission	0.0000E+00	0.0000E+00	0.0000E+00	0.0000E+00	0.0000E+00	0.0000E+00	0.0000E+00	0.0000E+00	0.0000E+00	0.0000E+00
loss to fission	0.0000E+00	0.0000E+00	0.0000E+00	0.0000E+00	0.0000E+00	0.0000E+00	0.0000E+00	0.0000E+00	0.0000E+00	0.0000E+00
photonuclear	0.0000E+00	0.0000E+00	0.0000E+00	0.0000E+00	0.0000E+00	0.0000E+00	0.0000E+00	0.0000E+00	0.0000E+00	0.0000E+00
total	-7.1844E-05	0.0000E+00	-1.2315E-02	-1.4203E-01	-4.1135E-03	-2.1481E-01	-2.9989E-02	-3.2465E-04	0.0000E+00	
total	0.0000E+00	0.0000E+00	0.0000E+00	0.0000E+00	0.0000E+00	0.0000E+00	0.0000E+00	0.0000E+00	0.0000E+00	

cell index 19
cell number 49 total

external events:

entering	2.7677E+00	4.9405E+01
source	0.0000E+00	1.0000E+00
energy cutoff	0.0000E+00	0.0000E+00
time cutoff	0.0000E+00	0.0000E+00
exiting	-2.7677E+00	-4.9405E+01
total	9.6082E-07	1.0000E+00

variance reduction events:

weight window	0.0000E+00	0.0000E+00
cell importance	0.0000E+00	0.0000E+00
weight cutoff	5.0063E-07	4.5179E-04
e or t importance	0.0000E+00	0.0000E+00
dxtran	0.0000E+00	0.0000E+00
forced collisions	0.0000E+00	0.0000E+00
exp. transform	0.0000E+00	0.0000E+00
total	5.0063E-07	4.5179E-04

physical events:

capture (n,xn)	-1.4614E-06	-7.5486E-01
loss to (n,xn) fission	0.0000E+00	1.6722E-03
loss to (n,xn) photonuclear	0.0000E+00	-8.3532E-04
total	-1.4614E-06	-1.0005E+00
total	0.0000E+00	0.0000E+00

neutron activity of each nuclide in each cell, per source particle

print table 140

cell index	cell name	nuclides	atom fraction	total collisions	collisions * weight	wgt. lost to capture	wgt. gain by fission	wgt. gain by (n,xn)	photons produced	photon produced	wgt avg photon energy
1	1	92235.69c	2.18E-03	13149	1.8238E-02	2.6523E-03	1.3545E-02	0.0000E+00	0	0.0000E+00	0.0000E+00
		92238.69c	3.06E-01	186994	3.3548E-01	2.5440E-02	5.4986E-03	3.0727E-04	0	0.0000E+00	0.0000E+00
		94238.66c	1.28E-05	67	9.7812E-05	7.8916E-05	4.0561E-06	0.0000E+00	0	0.0000E+00	0.0000E+00
		94239.66c	2.41E-02	247900	3.4650E-01	9.9448E-02	2.2599E-01	5.2057E-06	0	0.0000E+00	0.0000E+00
		94240.66c	1.14E-03	7457	1.1940E-02	1.0232E-02	1.0428E-04	0.0000E+00	0	0.0000E+00	0.0000E+00
		94241.66c	1.01E-04	1305	1.8084E-03	4.2713E-04	1.2840E-03	0.0000E+00	0	0.0000E+00	0.0000E+00
		94242.66c	1.25E-05	36	6.0894E-05	3.7138E-05	1.8504E-06	0.0000E+00	0	0.0000E+00	0.0000E+00
		8016.62c	6.66E-01	131341	2.3725E-01	4.7184E-04	0.0000E+00	0.0000E+00	0	0.0000E+00	0.0000E+00
		1001.62c	6.67E-01	66694	9.2467E-02	3.5248E-04	0.0000E+00	0.0000E+00	0	0.0000E+00	0.0000E+00
		8016.62c	3.33E-01	5087	8.3067E-03	1.0409E-05	0.0000E+00	0.0000E+00	0	0.0000E+00	0.0000E+00
3	3	26054.62c	1.19E-04	4	7.4446E-06	8.2238E-07	0.0000E+00	0.0000E+00	0	0.0000E+00	0.0000E+00
		24050.62c	7.63E-05	8	1.1117E-05	5.2938E-06	0.0000E+00	0.0000E+00	0	0.0000E+00	0.0000E+00
		7014.62c	3.24E-03	270	4.2214E-04	2.9134E-05	0.0000E+00	0.0000E+00	0	0.0000E+00	0.0000E+00
		26056.62c	1.87E-03	172	2.7365E-04	1.5704E-05	0.0000E+00	0.0000E+00	0	0.0000E+00	0.0000E+00
		24052.62c	1.47E-03	60	1.0627E-04	4.4084E-06	0.0000E+00	0.0000E+00	0	0.0000E+00	0.0000E+00
		7015.66c	1.20E-05	1	2.0715E-06	4.3673E-12	0.0000E+00	0.0000E+00	0	0.0000E+00	0.0000E+00
		26057.62c	4.33E-05	3	5.7570E-06	2.7967E-09	0.0000E+00	0.0000E+00	0	0.0000E+00	0.0000E+00
		24053.62c	1.67E-04	20	3.0965E-05	7.3217E-06	0.0000E+00	0.0000E+00	0	0.0000E+00	0.0000E+00
		26058.62c	5.71E-06	1	1.4554E-06	3.1973E-07	0.0000E+00	0.0000E+00	0	0.0000E+00	0.0000E+00
		24054.62c	4.14E-05	1	2.0725E-06	6.0645E-10	0.0000E+00	0.0000E+00	0	0.0000E+00	0.0000E+00
		40000.66c	9.81E-01	77568	1.3693E-01	1.0679E-03	0.0000E+00	2.5430E-05	0	0.0000E+00	0.0000E+00
50000.42c	1.15E-02	725	1.2911E-03	6.7541E-05	0.0000E+00	0.0000E+00	0	0.0000E+00	0.0000E+00		
4	4	1001.62c	6.67E-01	21628102	3.1581E+01	1.3528E-01	0.0000E+00	0.0000E+00	0	0.0000E+00	0.0000E+00
		8016.62c	3.33E-01	1435680	2.3453E+00	1.9355E-03	0.0000E+00	0.0000E+00	0	0.0000E+00	0.0000E+00
5	10	1001.62c	6.67E-01	5707107	8.0275E+00	3.3538E-02	0.0000E+00	0.0000E+00	0	0.0000E+00	0.0000E+00
		8016.62c	3.33E-01	369059	5.7955E-01	2.8754E-04	0.0000E+00	0.0000E+00	0	0.0000E+00	0.0000E+00
6	20	1001.62c	6.67E-01	0	0.0000E+00	0.0000E+00	0.0000E+00	0.0000E+00	0	0.0000E+00	0.0000E+00
		8016.62c	3.33E-01	0	0.0000E+00	0.0000E+00	0.0000E+00	0.0000E+00	0	0.0000E+00	0.0000E+00
7	21	1001.62c	6.67E-01	1732	2.5018E-03	5.3619E-06	0.0000E+00	0.0000E+00	0	0.0000E+00	0.0000E+00
		8016.62c	3.33E-01	156	2.4270E-04	3.2713E-09	0.0000E+00	0.0000E+00	0	0.0000E+00	0.0000E+00
8	22	13027.62c	1.00E+00	2123010	3.6862E+00	3.9305E-02	0.0000E+00	0.0000E+00	0	0.0000E+00	0.0000E+00
9	23	1001.62c	6.67E-01	88	1.2864E-04	2.1542E-07	0.0000E+00	0.0000E+00	0	0.0000E+00	0.0000E+00
		8016.62c	3.33E-01	10	1.5062E-05	8.2269E-11	0.0000E+00	0.0000E+00	0	0.0000E+00	0.0000E+00
10	40	82206.66c	2.55E-01	25173	3.4731E-02	2.7307E-05	0.0000E+00	0.0000E+00	0	0.0000E+00	0.0000E+00
		82207.66c	2.21E-01	23283	3.2961E-02	4.1971E-05	0.0000E+00	0.0000E+00	0	0.0000E+00	0.0000E+00
		82208.66c	5.24E-01	57369	8.0440E-02	2.5667E-06	0.0000E+00	0.0000E+00	0	0.0000E+00	0.0000E+00

11	41	1001.62c 6.67E-01	0	0.0000E+00	0.0000E+00	0.0000E+00	0.0000E+00	0	0.0000E+00	0.0000E+00
		8016.62c 3.33E-01	0	0.0000E+00	0.0000E+00	0.0000E+00	0.0000E+00	0	0.0000E+00	0.0000E+00
12	42	24050.62c 8.79E-03	22634	3.5886E-02	5.0283E-04	0.0000E+00	0.0000E+00	0	0.0000E+00	0.0000E+00
		26054.62c 4.03E-02	43963	7.0549E-02	4.1183E-04	0.0000E+00	0.0000E+00	0	0.0000E+00	0.0000E+00
		28058.62c 6.09E-02	185596	2.3990E-01	1.0944E-03	0.0000E+00	0.0000E+00	0	0.0000E+00	0.0000E+00
		24052.62c 1.69E-01	95848	1.4109E-01	7.2604E-04	0.0000E+00	0.0000E+00	0	0.0000E+00	0.0000E+00
		26056.62c 6.32E-01	808702	1.0013E+00	6.0096E-03	0.0000E+00	0.0000E+00	0	0.0000E+00	0.0000E+00
		28060.62c 2.35E-02	27885	4.6516E-02	2.8672E-04	0.0000E+00	0.0000E+00	0	0.0000E+00	0.0000E+00
		24053.62c 1.92E-02	65788	9.9650E-02	1.2037E-03	0.0000E+00	0.0000E+00	0	0.0000E+00	0.0000E+00
		26057.62c 1.46E-02	17938	2.8790E-02	2.1264E-04	0.0000E+00	0.0000E+00	0	0.0000E+00	0.0000E+00
		28061.62c 1.02E-03	1327	1.8701E-03	1.6196E-05	0.0000E+00	0.0000E+00	0	0.0000E+00	0.0000E+00
		24054.62c 4.77E-03	3571	5.5204E-03	1.2960E-05	0.0000E+00	0.0000E+00	0	0.0000E+00	0.0000E+00
		26058.62c 1.93E-03	1926	3.0589E-03	2.7125E-05	0.0000E+00	0.0000E+00	0	0.0000E+00	0.0000E+00
		28062.62c 3.25E-03	14955	2.2767E-02	1.4098E-04	0.0000E+00	0.0000E+00	0	0.0000E+00	0.0000E+00
		28064.62c 8.33E-04	1172	2.0355E-03	5.1368E-06	0.0000E+00	0.0000E+00	0	0.0000E+00	0.0000E+00
		25055.62c 2.01E-02	82949	1.2342E-01	1.6648E-03	0.0000E+00	0.0000E+00	0	0.0000E+00	0.0000E+00
13	43	24050.62c 8.79E-03	224394	3.7208E-01	5.8811E-03	0.0000E+00	0.0000E+00	0	0.0000E+00	0.0000E+00
		26054.62c 4.03E-02	457333	7.7117E-01	4.8990E-03	0.0000E+00	0.0000E+00	0	0.0000E+00	0.0000E+00
		28058.62c 6.09E-02	1729500	2.4409E+00	1.3150E-02	0.0000E+00	0.0000E+00	0	0.0000E+00	0.0000E+00
		24052.62c 1.69E-01	1032660	1.6563E+00	8.0696E-03	0.0000E+00	0.0000E+00	0	0.0000E+00	0.0000E+00
		26056.62c 6.32E-01	7735666	1.0652E+01	7.0255E-02	0.0000E+00	1.5751E-06	0	0.0000E+00	0.0000E+00
		28060.62c 2.35E-02	284768	4.9380E-01	3.3119E-03	0.0000E+00	0.0000E+00	0	0.0000E+00	0.0000E+00
		24053.62c 1.92E-02	635953	1.0153E+00	1.4020E-02	0.0000E+00	0.0000E+00	0	0.0000E+00	0.0000E+00
		26057.62c 1.46E-02	187135	3.1564E-01	2.2517E-03	0.0000E+00	1.9108E-06	0	0.0000E+00	0.0000E+00
		28061.62c 1.02E-03	13567	2.0961E-02	1.7693E-04	0.0000E+00	0.0000E+00	0	0.0000E+00	0.0000E+00
		24054.62c 4.77E-03	37002	6.1565E-02	1.1488E-04	0.0000E+00	0.0000E+00	0	0.0000E+00	0.0000E+00
		26058.62c 1.93E-03	19846	3.3234E-02	2.9139E-04	0.0000E+00	0.0000E+00	0	0.0000E+00	0.0000E+00
		28062.62c 3.25E-03	144771	2.3200E-01	1.7147E-03	0.0000E+00	0.0000E+00	0	0.0000E+00	0.0000E+00
		28064.62c 8.33E-04	12360	2.2167E-02	6.2663E-05	0.0000E+00	0.0000E+00	0	0.0000E+00	0.0000E+00
		25055.62c 2.01E-02	772970	1.2215E+00	1.7836E-02	0.0000E+00	0.0000E+00	0	0.0000E+00	0.0000E+00
14	44	24050.62c 8.79E-03	2257	3.6357E-03	1.7986E-04	0.0000E+00	0.0000E+00	0	0.0000E+00	0.0000E+00
		26054.62c 4.03E-02	4235	6.9394E-03	1.3937E-04	0.0000E+00	0.0000E+00	0	0.0000E+00	0.0000E+00
		28058.62c 6.09E-02	19754	2.6772E-02	3.8375E-04	0.0000E+00	0.0000E+00	0	0.0000E+00	0.0000E+00
		24052.62c 1.69E-01	10363	1.5850E-02	2.0913E-04	0.0000E+00	0.0000E+00	0	0.0000E+00	0.0000E+00
		26056.62c 6.32E-01	90447	1.1985E-01	2.1525E-03	0.0000E+00	0.0000E+00	0	0.0000E+00	0.0000E+00
		28060.62c 2.35E-02	2541	4.3191E-03	8.9712E-05	0.0000E+00	0.0000E+00	0	0.0000E+00	0.0000E+00
		24053.62c 1.92E-02	6508	1.0115E-02	4.1602E-04	0.0000E+00	0.0000E+00	0	0.0000E+00	0.0000E+00
		26057.62c 1.46E-02	1792	2.9469E-03	5.7133E-05	0.0000E+00	0.0000E+00	0	0.0000E+00	0.0000E+00
		28061.62c 1.02E-03	113	1.6337E-04	2.9738E-06	0.0000E+00	0.0000E+00	0	0.0000E+00	0.0000E+00
		24054.62c 4.77E-03	329	5.3342E-04	2.5471E-06	0.0000E+00	0.0000E+00	0	0.0000E+00	0.0000E+00
		26058.62c 1.93E-03	182	2.8460E-04	4.0371E-06	0.0000E+00	0.0000E+00	0	0.0000E+00	0.0000E+00
		28062.62c 3.25E-03	1520	2.4171E-03	5.6784E-05	0.0000E+00	0.0000E+00	0	0.0000E+00	0.0000E+00
		28064.62c 8.33E-04	111	1.9873E-04	2.0767E-07	0.0000E+00	0.0000E+00	0	0.0000E+00	0.0000E+00
		25055.62c 2.01E-02	7743	1.2184E-02	4.1947E-04	0.0000E+00	0.0000E+00	0	0.0000E+00	0.0000E+00
15	45	24050.62c 8.79E-03	81095	1.3624E-01	9.6184E-03	0.0000E+00	0.0000E+00	0	0.0000E+00	0.0000E+00
		26054.62c 4.03E-02	163277	2.8221E-01	6.7571E-03	0.0000E+00	0.0000E+00	0	0.0000E+00	0.0000E+00
		28058.62c 6.09E-02	685869	1.0095E+00	2.0192E-02	0.0000E+00	0.0000E+00	0	0.0000E+00	0.0000E+00
		24052.62c 1.69E-01	396986	6.5384E-01	9.5378E-03	0.0000E+00	0.0000E+00	0	0.0000E+00	0.0000E+00
		26056.62c 6.32E-01	3259168	4.7321E+00	1.1291E-01	0.0000E+00	3.3429E-06	0	0.0000E+00	0.0000E+00
		28060.62c 2.35E-02	92241	1.6289E-01	4.6046E-03	0.0000E+00	0.0000E+00	0	0.0000E+00	0.0000E+00
		24053.62c 1.92E-02	232819	3.7911E-01	2.3610E-02	0.0000E+00	0.0000E+00	0	0.0000E+00	0.0000E+00
		26057.62c 1.46E-02	66241	1.1455E-01	2.6634E-03	0.0000E+00	0.0000E+00	0	0.0000E+00	0.0000E+00
		28061.62c 1.02E-03	5093	8.0726E-03	1.8482E-04	0.0000E+00	0.0000E+00	0	0.0000E+00	0.0000E+00
		24054.62c 4.77E-03	12749	2.1779E-02	1.3347E-04	0.0000E+00	0.0000E+00	0	0.0000E+00	0.0000E+00
		26058.62c 1.93E-03	6698	1.1451E-02	2.0600E-04	0.0000E+00	0.0000E+00	0	0.0000E+00	0.0000E+00
		28062.62c 3.25E-03	51276	8.5061E-02	3.1530E-03	0.0000E+00	0.0000E+00	0	0.0000E+00	0.0000E+00
		28064.62c 8.33E-04	3626	6.6497E-03	8.9188E-05	0.0000E+00	0.0000E+00	0	0.0000E+00	0.0000E+00
		25055.62c 2.01E-02	268504	4.4997E-01	2.1151E-02	0.0000E+00	0.0000E+00	0	0.0000E+00	0.0000E+00
16	46	82206.66c 2.55E-01	5804104	8.9875E+00	6.8570E-03	0.0000E+00	6.0193E-05	0	0.0000E+00	0.0000E+00
		82207.66c 2.21E-01	5361381	8.4381E+00	2.2860E-02	0.0000E+00	1.4604E-04	0	0.0000E+00	0.0000E+00
		82208.66c 5.24E-01	12984459	2.0331E+01	7.6484E-04	0.0000E+00	2.8591E-04	0	0.0000E+00	0.0000E+00
17	47	82206.66c 2.55E-01	88291	1.2688E-01	7.9354E-05	0.0000E+00	0.0000E+00	0	0.0000E+00	0.0000E+00
		82207.66c 2.21E-01	80596	1.1838E-01	2.3687E-04	0.0000E+00	0.0000E+00	0	0.0000E+00	0.0000E+00
		82208.66c 5.24E-01	197981	2.8908E-01	8.4289E-06	0.0000E+00	0.0000E+00	0	0.0000E+00	0.0000E+00
19	49	1001.62c 6.67E-01	3648	5.4226E-03	1.4610E-06	0.0000E+00	0.0000E+00	0	0.0000E+00	0.0000E+00
		8016.62c 3.33E-01	419	6.6504E-04	3.9930E-10	0.0000E+00	0.0000E+00	0	0.0000E+00	0.0000E+00
total			76766227	1.1525E+02	7.5486E-01	2.4643E-01	8.3688E-04	0	0.0000E+00	0.0000E+00
total over all cells by nuclide			total collisions	collisions * weight	wgt. lost to capture	wgt. gain by fission	wgt. gain by (n,xn)	photons produced	photon wgt produced	avg photon energy
	1001.62c		27407371	3.9709E+01	1.6918E-01	0.0000E+00	0.0000E+00	0	0.0000E+00	0.0000E+00
	7014.62c		270	4.2214E-04	2.9134E-05	0.0000E+00	0.0000E+00	0	0.0000E+00	0.0000E+00
	7015.66c		1	2.0715E-06	4.3673E-12	0.0000E+00	0.0000E+00	0	0.0000E+00	0.0000E+00
	8016.62c		1941752	3.1714E+00	2.7053E-03	0.0000E+00	0.0000E+00	0	0.0000E+00	0.0000E+00
	13027.62c		2123010	3.6862E+00	3.9305E-02	0.0000E+00	0.0000E+00	0	0.0000E+00	0.0000E+00
	24050.62c		330388	5.4785E-01	1.6187E-02	0.0000E+00	0.0000E+00	0	0.0000E+00	0.0000E+00
	24052.62c		1535917	2.4672E+00	1.8547E-02	0.0000E+00	0.0000E+00	0	0.0000E+00	0.0000E+00
	24053.62c		941088	1.5042E+00	3.9257E-02	0.0000E+00	0.0000E+00	0	0.0000E+00	0.0000E+00
	24054.62c		53652	8.9400E-02	2.6385E-04	0.0000E+00	0.0000E+00	0	0.0000E+00	0.0000E+00
	25055.62c		1132166	1.8071E+00	4.1071E-02	0.0000E+00	0.0000E+00	0	0.0000E+00	0.0000E+00
	26054.62c		668812	1.1309E+00	1.2208E-02	0.0000E+00	0.0000E+00	0	0.0000E+00	0.0000E+00
	26056.62c		11894155	1.6506E+01	1.9134E-01	0.0000E+00	4.9180E-06	0	0.0	

28062.62c	212522	3.4224E-01	5.0655E-03	0.0000E+00	0.0000E+00	0	0.0000E+00	0.0000E+00
28064.62c	17269	3.1051E-02	1.5720E-04	0.0000E+00	0.0000E+00	0	0.0000E+00	0.0000E+00
40000.66c	77568	1.3693E-01	1.0679E-03	0.0000E+00	2.5430E-05	0	0.0000E+00	0.0000E+00
50000.42c	725	1.2911E-03	6.7541E-05	0.0000E+00	0.0000E+00	0	0.0000E+00	0.0000E+00
82206.66c	5917568	9.1491E+00	6.9637E-03	0.0000E+00	6.0193E-05	0	0.0000E+00	0.0000E+00
82207.66c	5465260	8.5894E+00	2.3138E-02	0.0000E+00	1.4604E-04	0	0.0000E+00	0.0000E+00
82208.66c	13239809	2.0700E+01	7.7584E-04	0.0000E+00	2.8591E-04	0	0.0000E+00	0.0000E+00
92235.69c	13149	1.8238E-02	2.6523E-03	1.3545E-02	0.0000E+00	0	0.0000E+00	0.0000E+00
92238.69c	186994	3.3548E-01	2.5440E-02	5.4986E-03	3.0727E-04	0	0.0000E+00	0.0000E+00
94238.66c	67	9.7812E-05	7.8916E-05	4.0561E-06	0.0000E+00	0	0.0000E+00	0.0000E+00
94239.69c	247900	3.4650E-01	9.9448E-02	2.2599E-01	5.2057E-06	0	0.0000E+00	0.0000E+00
94240.66c	7457	1.1940E-02	1.0232E-02	1.0428E-04	0.0000E+00	0	0.0000E+00	0.0000E+00
94241.66c	1305	1.8084E-03	4.2713E-04	1.2840E-03	0.0000E+00	0	0.0000E+00	0.0000E+00
94242.66c	36	6.0894E-05	3.7138E-05	1.8504E-06	0.0000E+00	0	0.0000E+00	0.0000E+00

1keff results for: NAC-LWT Cask - MOX Experiments - Accident Transport Conditions
21:05:56

probid = 10/25/07

the initial fission neutron source distribution was generated from a general sdef source description.
the criticality problem was scheduled to skip 30 cycles and run a total of 530 cycles with nominally 1000 neutrons per cycle.
this problem has run 30 inactive cycles with 29983 neutron histories and 500 active cycles with 500502 neutron histories.

this calculation has completed the requested number of keff cycles using a total of 530485 fission neutron source histories.
all cells with fissionable material were sampled and had fission neutron source points.

the results of the w test for normality applied to the individual collision, absorption, and track-length keff cycle values are:

the k (collision) cycle values appear normally distributed at the 95 percent confidence level
the k(absorption) cycle values appear normally distributed at the 95 percent confidence level
the k(trk length) cycle values appear normally distributed at the 95 percent confidence level

the final estimated combined collision/absorption/track-length keff = 0.70319 with an estimated standard deviation of 0.00102

the estimated 68, 95, & 99 percent keff confidence intervals are 0.70216 to 0.70422, 0.70115 to 0.70523, and 0.70048 to 0.70590

the final combined (col/abs/trk) prompt removal lifetime = 8.4802E-05 seconds with an estimated standard deviation of 1.0633E-07

the average neutron energy causing fission = 9.7087E-02 mev

the energy corresponding to the average neutron lethargy causing fission = 1.2505E-07 mev

the percentages of fissions caused by neutrons in the thermal, intermediate, and fast neutron ranges are:

(<0.625 ev): 91.72% (0.625 ev - 100 kev): 4.76% (>100 kev): 3.52%

the average fission neutrons produced per neutron absorbed (capture + fission) in all cells with fission = 1.8263E+00

the average fission neutrons produced per neutron absorbed (capture + fission) in all the geometry cells = 7.0264E-01

the average number of neutrons produced per fission = 2.855

the estimated average keffs, one standard deviations, and 68, 95, and 99 percent confidence intervals are:

corr	keff estimator	keff	standard deviation	68% confidence	95% confidence	99% confidence
	collision	0.70354	0.00111	0.70243 to 0.70465	0.70133 to 0.70575	0.70061 to 0.70648
	absorption	0.70301	0.00109	0.70192 to 0.70410	0.70084 to 0.70518	0.70013 to 0.70589
	track length	0.70318	0.00152	0.70165 to 0.70470	0.70014 to 0.70621	0.69915 to 0.70720
	col/absorp	0.70325	0.00104	0.70221 to 0.70430	0.70117 to 0.70533	0.70049 to 0.70601
0.7954	abs/trk len	0.70305	0.00104	0.70201 to 0.70409	0.70098 to 0.70512	0.70031 to 0.70579
0.4238	col/trk len	0.70349	0.00109	0.70239 to 0.70458	0.70130 to 0.70567	0.70059 to 0.70638
0.5841	col/abs/trk len	0.70319	0.00102	0.70216 to 0.70422	0.70115 to 0.70523	0.70048 to 0.70590

if the largest of each keff occurred on the next cycle, the keff results and 68, 95, and 99 percent confidence intervals would be:

keff estimator	keff	standard deviation	68% confidence	95% confidence	99% confidence
collision	0.70369	0.00112	0.70257 to 0.70481	0.70146 to 0.70592	0.70073 to 0.70664
absorption	0.70314	0.00110	0.70205 to 0.70424	0.70096 to 0.70532	0.70025 to 0.70604
track length	0.70339	0.00154	0.70186 to 0.70493	0.70034 to 0.70645	0.69934 to 0.70745
col/abs/trk len	0.70334	0.00103	0.70231 to 0.70437	0.70128 to 0.70540	0.70061 to 0.70607

the estimated average prompt removal lifetimes, one standard deviations, and 68, 95, and 99 percent confidence intervals are (sec):

estimator	lifetime	std. dev.	68% confidence	95% confidence	99% confidence
collision	8.47143E-05	1.42417E-07	8.4572E-05 to 8.4857E-05	8.4431E-05 to 8.4998E-05	8.4338E-05 to 8.5091E-05
absorption	8.47241E-05	1.37731E-07	8.4586E-05 to 8.4862E-05	8.4450E-05 to 8.4998E-05	8.4360E-05 to 8.5088E-05
track length	8.47846E-05	1.07925E-07	8.4677E-05 to 8.4893E-05	8.4570E-05 to 8.5000E-05	8.4499E-05 to 8.5070E-05
col/absorp	8.47240E-05	1.37879E-07	8.4586E-05 to 8.4862E-05	8.4449E-05 to 8.4999E-05	8.4360E-05 to 8.5088E-05
0.9665 abs/trk len	8.48024E-05	1.06263E-07	8.4696E-05 to 8.4909E-05	8.4591E-05 to 8.5014E-05	8.4522E-05 to 8.5083E-05
0.8746 col/trk len	8.47991E-05	1.06906E-07	8.4692E-05 to 8.4906E-05	8.4586E-05 to 8.5012E-05	8.4517E-05 to 8.5082E-05
0.8399 col/abs/trk len	8.48016E-05	1.06329E-07	8.4695E-05 to 8.4908E-05	8.4590E-05 to 8.5013E-05	8.4521E-05 to 8.5083E-05

absorption estimates of prompt lifetimes (sec):

	escape	capture	fission	removal
fraction	0.00000E+00	7.53886E-01	2.46114E-01	1.00000E+00
lifetime(abs)	0.00000E+00	1.12383E-04	3.44248E-04	8.47241E-05
lifetime(c/a/t)	0.00000E+00	1.12486E-04	3.44563E-04	8.48016E-05

laverage keff results summed over 10 cycles each to form 50 batch values of keff

print table 178

batch keff number dev	start cycle	end cycle	keff estimators by batch			average keff estimators and deviations						col/abs/tl	
			k(coll)	k(abs)	k(track)	k(coll)	st dev	k(abs)	st dev	k(track)	st dev	k(c/a/t) st	
1	31	40	0.69464	0.70858	0.69703								
2	41	50	0.69991	0.69995	0.71175	0.69728	0.00264	0.70427	0.00431	0.70439	0.00736		
3	51	60	0.69908	0.70175	0.71143	0.69788	0.00164	0.70343	0.00263	0.70674	0.00485		
4	61	70	0.70512	0.70586	0.70015	0.69969	0.00215	0.70404	0.00195	0.70509	0.00381	0.70399	
0.00052 5	71	80	0.70990	0.71146	0.70550	0.70173	0.00263	0.70552	0.00212	0.70517	0.00295	0.70603	
0.00173 6	81	90	0.70562	0.70888	0.70384	0.70238	0.00225	0.70608	0.00182	0.70495	0.00242	0.70627	
0.00132 7	91	100	0.69488	0.69474	0.70383	0.70131	0.00218	0.70446	0.00223	0.70479	0.00205	0.70515	
0.00189 8	101	110	0.70672	0.69958	0.71642	0.70198	0.00201	0.70385	0.00203	0.70624	0.00229	0.70565	
0.00159 9	111	120	0.70039	0.70157	0.69025	0.70181	0.00178	0.70360	0.00181	0.70447	0.00269	0.70369	
0.00169 10	121	130	0.70465	0.70223	0.69620	0.70209	0.00162	0.70346	0.00162	0.70364	0.00255	0.70323	
0.00141													
11	131	140	0.70238	0.70619	0.69735	0.70212	0.00146	0.70371	0.00149	0.70307	0.00237	0.70321	
0.00127 12	141	150	0.70607	0.70232	0.71159	0.70245	0.00137	0.70359	0.00136	0.70378	0.00228	0.70344	
0.00115 13	151	160	0.70037	0.70040	0.70984	0.70229	0.00127	0.70335	0.00128	0.70424	0.00215	0.70340	
0.00107 14	161	170	0.72037	0.71651	0.71747	0.70358	0.00175	0.70429	0.00151	0.70519	0.00220	0.70471	
0.00143 15	171	180	0.69433	0.69238	0.70387	0.70296	0.00174	0.70349	0.00162	0.70510	0.00205	0.70426	
0.00148 16	181	190	0.70269	0.70088	0.69643	0.70295	0.00163	0.70333	0.00152	0.70456	0.00199	0.70381	
0.00139 17	191	200	0.70976	0.70864	0.70773	0.70335	0.00158	0.70364	0.00146	0.70475	0.00188	0.70410	
0.00132 18	201	210	0.70393	0.71074	0.69819	0.70338	0.00149	0.70404	0.00143	0.70438	0.00181	0.70423	
0.00125 19	211	220	0.70859	0.70134	0.70737	0.70365	0.00144	0.70389	0.00136	0.70454	0.00172	0.70417	
0.00117 20	221	230	0.69003	0.68724	0.68572	0.70297	0.00152	0.70306	0.00154	0.70360	0.00188	0.70321	
0.00143													
21	231	240	0.69404	0.69697	0.70617	0.70255	0.00151	0.70277	0.00149	0.70372	0.00180	0.70307	
0.00138 22	241	250	0.70290	0.70303	0.70274	0.70256	0.00144	0.70278	0.00142	0.70368	0.00171	0.70307	
0.00131 23	251	260	0.69744	0.70080	0.69572	0.70234	0.00139	0.70270	0.00136	0.70333	0.00167	0.70288	
0.00127 24	261	270	0.68944	0.68842	0.69940	0.70180	0.00144	0.70210	0.00143	0.70317	0.00161	0.70253	
0.00130 25	271	280	0.71173	0.70875	0.69470	0.70220	0.00144	0.70237	0.00140	0.70283	0.00158	0.70256	
0.00123 26	281	290	0.69046	0.69795	0.68252	0.70175	0.00145	0.70220	0.00136	0.70205	0.00171	0.70218	
0.00125													

NAC-LWT Cask SAR
Revision LWT-08A

January 2008

0.00121	27	291	300	0.69890	0.70547	0.69782	0.70164	0.00140	0.70232	0.00131	0.70189	0.00165	0.70221
0.00131	28	301	310	0.72067	0.71493	0.72845	0.70232	0.00151	0.70277	0.00134	0.70284	0.00185	0.70287
0.00130	29	311	320	0.71248	0.71290	0.70837	0.70267	0.00150	0.70312	0.00134	0.70303	0.00180	0.70318
0.00126	30	321	330	0.70552	0.71034	0.68928	0.70277	0.00145	0.70336	0.00132	0.70257	0.00180	0.70322

0.00124	31	331	340	0.70673	0.70583	0.72029	0.70290	0.00141	0.70344	0.00128	0.70314	0.00183	0.70344
0.00119	32	341	350	0.71397	0.70181	0.72231	0.70324	0.00141	0.70339	0.00124	0.70374	0.00187	0.70352
0.00119	33	351	360	0.69317	0.69015	0.70837	0.70294	0.00140	0.70299	0.00126	0.70388	0.00182	0.70330
0.00116	34	361	370	0.70051	0.70177	0.69207	0.70287	0.00136	0.70295	0.00123	0.70353	0.00180	0.70316
0.00112	35	371	380	0.72093	0.70273	0.70370	0.70338	0.00142	0.70295	0.00119	0.70354	0.00174	0.70307
0.00114	36	381	390	0.70896	0.71222	0.71827	0.70354	0.00139	0.70320	0.00119	0.70395	0.00174	0.70338
0.00113	37	391	400	0.70283	0.69897	0.68309	0.70352	0.00135	0.70309	0.00116	0.70339	0.00179	0.70316
0.00114	38	401	410	0.71038	0.71680	0.71233	0.70370	0.00132	0.70345	0.00118	0.70362	0.00176	0.70351
0.00112	39	411	420	0.70453	0.69894	0.71991	0.70372	0.00129	0.70333	0.00116	0.70404	0.00176	0.70351
0.00111	40	421	430	0.71224	0.71442	0.70680	0.70393	0.00128	0.70361	0.00116	0.70411	0.00172	0.70375

0.00109	41	431	440	0.71180	0.70908	0.70762	0.70412	0.00126	0.70374	0.00114	0.70419	0.00168	0.70388
0.00107	42	441	450	0.69886	0.70084	0.70113	0.70400	0.00123	0.70368	0.00112	0.70412	0.00164	0.70380
0.00106	43	451	460	0.70033	0.69292	0.70745	0.70391	0.00121	0.70343	0.00112	0.70420	0.00160	0.70366
0.00103	44	461	470	0.70894	0.70544	0.69422	0.70403	0.00119	0.70347	0.00109	0.70397	0.00158	0.70365
0.00101	45	471	480	0.70260	0.70505	0.69236	0.70400	0.00116	0.70351	0.00107	0.70371	0.00157	0.70361
0.00099	46	481	490	0.69987	0.69934	0.69771	0.70391	0.00114	0.70342	0.00105	0.70358	0.00154	0.70351
0.00097	47	491	500	0.70292	0.70173	0.71993	0.70389	0.00111	0.70338	0.00103	0.70393	0.00154	0.70356
0.00099	48	501	510	0.69558	0.69375	0.68100	0.70371	0.00110	0.70318	0.00103	0.70345	0.00159	0.70332
0.00097	49	511	520	0.69737	0.69503	0.71016	0.70358	0.00109	0.70301	0.00102	0.70359	0.00156	0.70322
0.00096	50	521	530	0.70154	0.70293	0.68301	0.70354	0.00107	0.70301	0.00100	0.70318	0.00158	0.70313

average keff results summed over 20 cycles each to form 25 batch values of keff

keff number dev	batch cycle	start cycle	end cycle	keff estimators by batch			average keff estimators and deviations						col/abs/tl		
				k(coll)	k(abs)	k(track)	k(coll)	st dev	k(abs)	st dev	k(track)	st dev	k(c/a/t)..st		
	1	31	50	0.69728	0.70427	0.70439									
	2	51	70	0.70210	0.70381	0.70579	0.69969	0.00241	0.70404	0.00023	0.70509	0.00070			
	3	71	90	0.70776	0.71017	0.70467	0.70238	0.00303	0.70608	0.00205	0.70495	0.00043			
0.00037	4	91	110	0.70080	0.69716	0.71013	0.70198	0.00218	0.70385	0.00266	0.70624	0.00133	0.70631		
0.00204	5	111	130	0.70252	0.70190	0.69323	0.70209	0.00169	0.70346	0.00210	0.70364	0.00280	0.70281		
0.00154	6	131	150	0.70423	0.70425	0.70447	0.70245	0.00143	0.70359	0.00172	0.70378	0.00229	0.70309		
0.00181	7	151	170	0.71037	0.70846	0.71366	0.70358	0.00165	0.70429	0.00161	0.70519	0.00240	0.70431		
0.00178	8	171	190	0.69851	0.69663	0.70015	0.70295	0.00157	0.70333	0.00169	0.70456	0.00217	0.70344		
0.00158	9	191	210	0.70685	0.70969	0.70296	0.70338	0.00145	0.70404	0.00165	0.70438	0.00192	0.70383		
0.00148	10	211	230	0.69931	0.69429	0.69654	0.70297	0.00136	0.70306	0.00177	0.70360	0.00189	0.70311		

0.00138	11	231	250	0.69847	0.70000	0.70446	0.70256	0.00129	0.70278	0.00162	0.70368	0.00171	0.70287
0.00149	12	251	270	0.69344	0.69461	0.69756	0.70180	0.00140	0.70210	0.00163	0.70317	0.00164	0.70228
0.00137	13	271	290	0.70110	0.70335	0.68861	0.70175	0.00129	0.70220	0.00150	0.70205	0.00188	0.70186
0.00143	14	291	310	0.70978	0.71020	0.71314	0.70232	0.00133	0.70277	0.00150	0.70284	0.00191	0.70245
0.00138	15	311	330	0.70900	0.71162	0.69883	0.70277	0.00131	0.70336	0.00152	0.70257	0.00180	0.70275
0.00137	16	331	350	0.71035	0.70382	0.72130	0.70324	0.00132	0.70339	0.00142	0.70374	0.00205	0.70337
0.00135	17	351	370	0.69684	0.69596	0.70022	0.70287	0.00129	0.70295	0.00141	0.70353	0.00194	0.70300
0.00133	18	371	390	0.71494	0.70748	0.71099	0.70354	0.00139	0.70320	0.00135	0.70395	0.00187	0.70342

19 0.00126	391	410	0.70660	0.70788	0.69771	0.70370	0.00133	0.70345	0.00130	0.70362	0.00180	0.70352
20 0.00122	411	430	0.70839	0.70668	0.71336	0.70393	0.00128	0.70361	0.00124	0.70411	0.00178	0.70376

21 0.00116	431	450	0.70533	0.70496	0.70437	0.70400	0.00122	0.70368	0.00118	0.70412	0.00169	0.70381
22 0.00112	451	470	0.70464	0.69918	0.70084	0.70403	0.00116	0.70347	0.00115	0.70397	0.00162	0.70369
23 0.00108	471	490	0.70124	0.70219	0.69504	0.70391	0.00112	0.70342	0.00110	0.70358	0.00159	0.70355
24 0.00106	491	510	0.69925	0.69774	0.70046	0.70371	0.00109	0.70318	0.00108	0.70345	0.00153	0.70335
25 0.00103	511	530	0.69946	0.69898	0.69658	0.70354	0.00106	0.70301	0.00105	0.70318	0.00150	0.70317

average keff results summed over 25 cycles each to form 20 batch values of keff

batch keff number dev	start cycle	end cycle	keff estimators by batch			average keff estimators and deviations						col/abs/tl	
			k(coll)	k(abs)	k(track)	k(coll)	st dev	k(abs)	st dev	k(track)	st dev	k(c/a/t) st	
1	31	55	0.69657	0.70340	0.70573								
2	56	80	0.70689	0.70764	0.70461	0.70173	0.00516	0.70552	0.00212	0.70517	0.00056		
3	81	105	0.70330	0.70294	0.70696	0.70225	0.00303	0.70466	0.00150	0.70577	0.00068		
4	106	130	0.70161	0.69985	0.69725	0.70209	0.00215	0.70346	0.00160	0.70364	0.00218	0.70307	
5	131	155	0.70351	0.70440	0.70454	0.70238	0.00169	0.70365	0.00125	0.70382	0.00170	0.70330	
6	156	180	0.70590	0.70272	0.71151	0.70296	0.00150	0.70349	0.00104	0.70510	0.00189	0.70355	
7	181	205	0.70925	0.70930	0.70200	0.70386	0.00155	0.70432	0.00121	0.70466	0.00166	0.70439	
8	206	230	0.69675	0.69424	0.69617	0.70297	0.00161	0.70306	0.00164	0.70360	0.00178	0.70322	
9	231	255	0.69816	0.69762	0.70089	0.70244	0.00152	0.70246	0.00157	0.70330	0.00160	0.70281	
10	256	280	0.70007	0.70157	0.69860	0.70220	0.00138	0.70237	0.00140	0.70283	0.00151	0.70247	

11	281	305	0.69993	0.70605	0.69500	0.70199	0.00126	0.70270	0.00131	0.70212	0.00154	0.70230	
12	306	330	0.71128	0.71058	0.70758	0.70277	0.00139	0.70336	0.00137	0.70257	0.00148	0.70296	
13	331	355	0.70623	0.70055	0.71508	0.70303	0.00131	0.70314	0.00128	0.70353	0.00166	0.70325	
14	356	380	0.70789	0.70037	0.70362	0.70338	0.00126	0.70295	0.00120	0.70354	0.00154	0.70318	
15	381	405	0.70582	0.70761	0.70172	0.70354	0.00118	0.70326	0.00116	0.70342	0.00144	0.70335	
16	406	430	0.70975	0.70893	0.71445	0.70393	0.00117	0.70361	0.00114	0.70411	0.00151	0.70379	
17	431	455	0.70786	0.70519	0.71145	0.70416	0.00112	0.70370	0.00107	0.70454	0.00149	0.70397	
18	456	480	0.70116	0.70015	0.68966	0.70400	0.00107	0.70351	0.00103	0.70371	0.00163	0.70369	
19	481	505	0.70176	0.70044	0.70559	0.70388	0.00102	0.70334	0.00099	0.70381	0.00154	0.70357	
20	506	530	0.69715	0.69667	0.69113	0.70354	0.00103	0.70301	0.00100	0.70318	0.00159	0.70324	

average keff results summed over 50 cycles each to form 10 batch values of keff

batch keff number dev	start cycle	end cycle	keff estimators by batch			average keff estimators and deviations						col/abs/tl	
			k(coll)	k(abs)	k(track)	k(coll)	st dev	k(abs)	st dev	k(track)	st dev	k(c/a/t) st	
1	31	80	0.70173	0.70552	0.70517								
2	81	130	0.70245	0.70140	0.70211	0.70209	0.00036	0.70346	0.00206	0.70364	0.00153		
3	131	180	0.70471	0.70356	0.70803	0.70296	0.00090	0.70349	0.00119	0.70510	0.00171		
4	181	230	0.70300	0.70177	0.69909	0.70297	0.00063	0.70306	0.00095	0.70360	0.00193	0.70287	
5	231	280	0.69911	0.69960	0.69975	0.70220	0.00092	0.70237	0.00101	0.70283	0.00168	0.70213	
6	281	330	0.70561	0.70832	0.70129	0.70277	0.00094	0.70336	0.00129	0.70257	0.00140	0.70271	
7	331	380	0.70706	0.70046	0.70935	0.70338	0.00100	0.70295	0.00117	0.70354	0.00153	0.70322	
8	381	430	0.70779	0.70827	0.70808	0.70393	0.00103	0.70361	0.00121	0.70411	0.00144	0.70384	
9	431	480	0.70451	0.70267	0.70056	0.70400	0.00091	0.70351	0.00107	0.70371	0.00133	0.70380	
10	481	530	0.69946	0.69855	0.69836	0.70354	0.00093	0.70301	0.00108	0.70318	0.00130	0.70336	

average keff results summed over 100 cycles each to form 5 batch values of keff

batch keff number dev	start cycle	end cycle	keff estimators by batch			average keff estimators and deviations						col/abs/tl		
			k(coll)	k(abs)	k(track)	k(coll)	st dev	k(abs)	st dev	k(track)	st dev	k(c/a/t)	st	
1	31	130	0.70209	0.70346	0.70364									
2	131	230	0.70385	0.70266	0.70356	0.70297	0.00088	0.70306	0.00040	0.70360	0.00004			
3	231	330	0.70236	0.70396	0.70052	0.70277	0.00055	0.70336	0.00038	0.70257	0.00103			
4	331	430	0.70742	0.70436	0.70872	0.70393	0.00123	0.70361	0.00037	0.70411	0.00170			0.70359
0.00063														
5	431	530	0.70198	0.70061	0.69946	0.70354	0.00103	0.70301	0.00066	0.70318	0.00161			0.70330
0.00075														

average keff results summed over 125 cycles each to form 4 batch values of keff

batch keff number dev	start cycle	end cycle	keff estimators by batch			average keff estimators and deviations						col/abs/tl		
			k(coll)	k(abs)	k(track)	k(coll)	st dev	k(abs)	st dev	k(track)	st dev	k(c/a/t)	st	
1	31	155	0.70238	0.70365	0.70382									
2	156	280	0.70202	0.70109	0.70183	0.70220	0.00018	0.70237	0.00128	0.70283	0.00099			
3	281	405	0.70623	0.70503	0.70460	0.70354	0.00135	0.70326	0.00115	0.70342	0.00082			
4	406	530	0.70354	0.70227	0.70246	0.70354	0.00095	0.70301	0.00085	0.70318	0.00063			0.70379
0.00031														

average keff results summed over 250 cycles each to form 2 batch values of keff

batch number	start cycle	end cycle	keff estimators by batch			average keff estimators and deviations							
			k(coll)	k(abs)	k(track)	k(coll)	st dev	k(abs)	st dev	k(track)	st dev		
1	31	280	0.70220	0.70237	0.70283								
2	281	530	0.70488	0.70365	0.70353	0.70354	0.00134	0.70301	0.00064	0.70318	0.00035		

average individual and combined collision/absorption/track-length keff results for 10 different batch sizes

cycles per intervals keff batch confidence	number of k batches	average keff estimators and deviations						normality co/ab/trk	average k(c/a/t)		k(c/a/t) confidence	
		k(coll)	st dev	k(abs)	st dev	k(trk)	st dev		k(c/a/t)	st dev	95% confidence	99%
1	500	0.7035	0.0011	0.7030	0.0011	0.7032	0.0015	95/95/95	0.70319	0.00102	0.70115-0.70523	0.70048-
0.70590												
2	250	0.7035	0.0011	0.7030	0.0010	0.7032	0.0016	95/95/95	0.70319	0.00101	0.70119-0.70520	0.70054-
0.70585												
4	125	0.7035	0.0010	0.7030	0.0010	0.7032	0.0015	99/95/95	0.70316	0.00096	0.70125-0.70507	0.70063-
0.70570												
5	100	0.7035	0.0010	0.7030	0.0010	0.7032	0.0016	95/95/95	0.70315	0.00096	0.70125-0.70506	0.70063-
0.70568												
10	50	0.7035	0.0011	0.7030	0.0010	0.7032	0.0016	95/95/95	0.70313	0.00096	0.70121-0.70506	0.70057-
0.70570												
20	25	0.7035	0.0011	0.7030	0.0010	0.7032	0.0015	95/95/95	0.70317	0.00103	0.70102-0.70531	0.70025-
0.70608												
25	20	0.7035	0.0010	0.7030	0.0010	0.7032	0.0016	95/95/95	0.70324	0.00101	0.70110-0.70537	0.70031-
0.70616												
50	10	0.7035	0.0009	0.7030	0.0011	0.7032	0.0013	95/95/95	0.70336	0.00104	0.70091-0.70581	0.69973-
0.70699												
100	5	0.7035	0.0010	0.7030	0.0007	0.7032	0.0016	95/95/95	0.70330	0.00075	0.70010-0.70651	0.69591-
0.71070												
125	4	0.7035	0.0010	0.7030	0.0009	0.7032	0.0006	95/95/95	0.70379	0.00031	0.69989-0.70769	0.68426-
0.72332												

individual and average keff estimator results by cycle

keff cycle	neutron histories	keff estimators by cycle			average keff estimators and deviations				average k(c/a/t)		
		k(coll)	k(abs)	k(track)	k(coll)	st dev	k(abs)	st dev	k(track)	st dev	fom
1	1000	0.66263	0.67157	0.66002							
2	844	0.62259	0.63335	0.60633							
3	928	0.74464	0.73878	0.73698							
4	1189	0.68648	0.69320	0.71005							
5	916	0.67162	0.67449	0.66605							
6	972	0.67555	0.69125	0.65326							
7	999	0.69386	0.68906	0.66118							
8	1052	0.70286	0.67585	0.73216							
9	1006	0.69990	0.70969	0.76966							
10	1024	0.69455	0.70359	0.71872							
11	992	0.71945	0.72461	0.77486							
12	1044	0.74157	0.74571	0.71944							
13	1026	0.71667	0.70198	0.67162							
14	971	0.68381	0.69304	0.65735							
15	972	0.67127	0.68589	0.70914							
16	980	0.70348	0.68749	0.72402							
17	1075	0.67107	0.68658	0.63445							
18	942	0.69601	0.70231	0.71773							
19	1027	0.70549	0.71679	0.64485							
20	1045	0.77572	0.74148	0.75166							
21	1103	0.69297	0.68583	0.72338							
22	898	0.67206	0.66187	0.67595							

23	949	0.71079	0.69071	0.73845								
24	1052	0.68395	0.66337	0.74105								
25	970	0.68790	0.69966	0.67099								
26	1010	0.70855	0.69614	0.70095								
27	1009	0.67223	0.64488	0.68232								
28	973	0.73330	0.74610	0.69315								
29	1080	0.69622	0.71162	0.68492								
30	935	0.73041	0.69416	0.74775								

begin active keff cycles												

31	1047	0.71428	0.73079	0.71371								
32	971	0.69249	0.71990	0.70235	0.70338	0.01089	0.72534	0.00544	0.70803	0.00568		
33	981	0.69778	0.70563	0.66827	0.70151	0.00656	0.71877	0.00728	0.69478	0.01365		
34	994	0.68924	0.69195	0.69822	0.69845	0.00556	0.71207	0.00846	0.69564	0.00969	0.69375	0.01721
8655												
35	994	0.68162	0.70872	0.64083	0.69508	0.00547	0.71140	0.00658	0.68468	0.01329	0.69941	0.01388
10969												
36	977	0.71544	0.70426	0.72827	0.69847	0.00561	0.71021	0.00551	0.69194	0.01306	0.70431	0.00742
33097												
37	1037	0.73287	0.74246	0.72458	0.70339	0.00683	0.71481	0.00655	0.69660	0.01198	0.70980	0.01000
16163												
38	1015	0.69058	0.70612	0.77117	0.70179	0.00612	0.71373	0.00577	0.70593	0.01395	0.70945	0.00924
16573												
39	956	0.66418	0.66719	0.62670	0.69761	0.00683	0.70856	0.00726	0.69712	0.01513	0.70110	0.01044
10967												
40	956	0.66792	0.70877	0.69622	0.69464	0.00679	0.70858	0.00649	0.69703	0.01353	0.70301	0.00977
11412												

511	928	0.75910	0.74259	0.75416	0.70383	0.00113	0.70326	0.00111	0.70356	0.00154	0.70348	0.00104
20679												
512	1183	0.67984	0.69205	0.72746	0.70378	0.00113	0.70324	0.00111	0.70361	0.00154	0.70346	0.00104
20711												
513	882	0.68107	0.68076	0.70320	0.70373	0.00113	0.70319	0.00111	0.70361	0.00153	0.70342	0.00104
20724												
514	1007	0.69072	0.68108	0.70462	0.70370	0.00112	0.70315	0.00111	0.70361	0.00153	0.70339	0.00104
20741												
515	1027	0.64762	0.66328	0.62331	0.70359	0.00113	0.70306	0.00111	0.70344	0.00154	0.70328	0.00104
20556												
516	932	0.68972	0.68472	0.71744	0.70356	0.00113	0.70303	0.00111	0.70347	0.00153	0.70326	0.00104
20586												
517	1052	0.74062	0.71731	0.75135	0.70364	0.00113	0.70305	0.00111	0.70357	0.00153	0.70331	0.00104
20573												
518	1053	0.70672	0.69771	0.68843	0.70364	0.00112	0.70304	0.00110	0.70354	0.00153	0.70330	0.00104
20612												
519	938	0.67005	0.67215	0.67557	0.70357	0.00112	0.70298	0.00110	0.70348	0.00153	0.70323	0.00104
20571												
520	937	0.70825	0.71869	0.75603	0.70358	0.00112	0.70301	0.00110	0.70359	0.00153	0.70327	0.00104
20596												

521	1058	0.71063	0.71456	0.63479	0.70360	0.00112	0.70304	0.00110	0.70345	0.00153	0.70327	0.00103
20634												
522	1009	0.68556	0.69318	0.65900	0.70356	0.00112	0.70302	0.00110	0.70336	0.00153	0.70323	0.00103
20648												
523	969	0.67996	0.70849	0.66781	0.70351	0.00112	0.70303	0.00110	0.70329	0.00153	0.70321	0.00103
20690												
524	978	0.72088	0.70570	0.70327	0.70355	0.00111	0.70303	0.00109	0.70329	0.00153	0.70322	0.00103
20730												
525	1035	0.71400	0.70193	0.73850	0.70357	0.00111	0.70303	0.00109	0.70336	0.00153	0.70324	0.00103
20767												
526	1006	0.74177	0.75665	0.71714	0.70365	0.00111	0.70314	0.00110	0.70339	0.00152	0.70333	0.00103
20676												
527	1046	0.64384	0.66806	0.63471	0.70353	0.00112	0.70307	0.00110	0.70325	0.00153	0.70323	0.00103
20527												
528	869	0.71724	0.69923	0.69946	0.70355	0.00112	0.70306	0.00109	0.70324	0.00152	0.70323	0.00103
20572												
529	1119	0.69903	0.68697	0.72558	0.70354	0.00111	0.70303	0.00109	0.70328	0.00152	0.70322	0.00103
20601												
530	961	0.70253	0.69452	0.64982	0.70354	0.00111	0.70301	0.00109	0.70318	0.00152	0.70319	0.00102
20625												

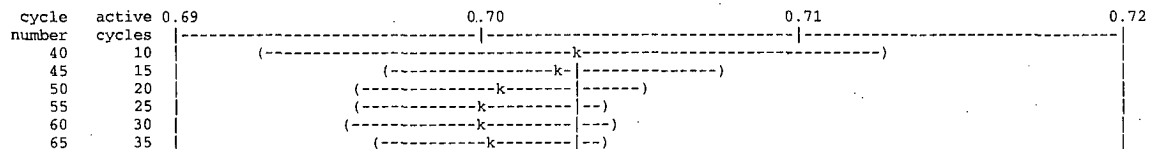
the largest active cycle keffs by estimator are:

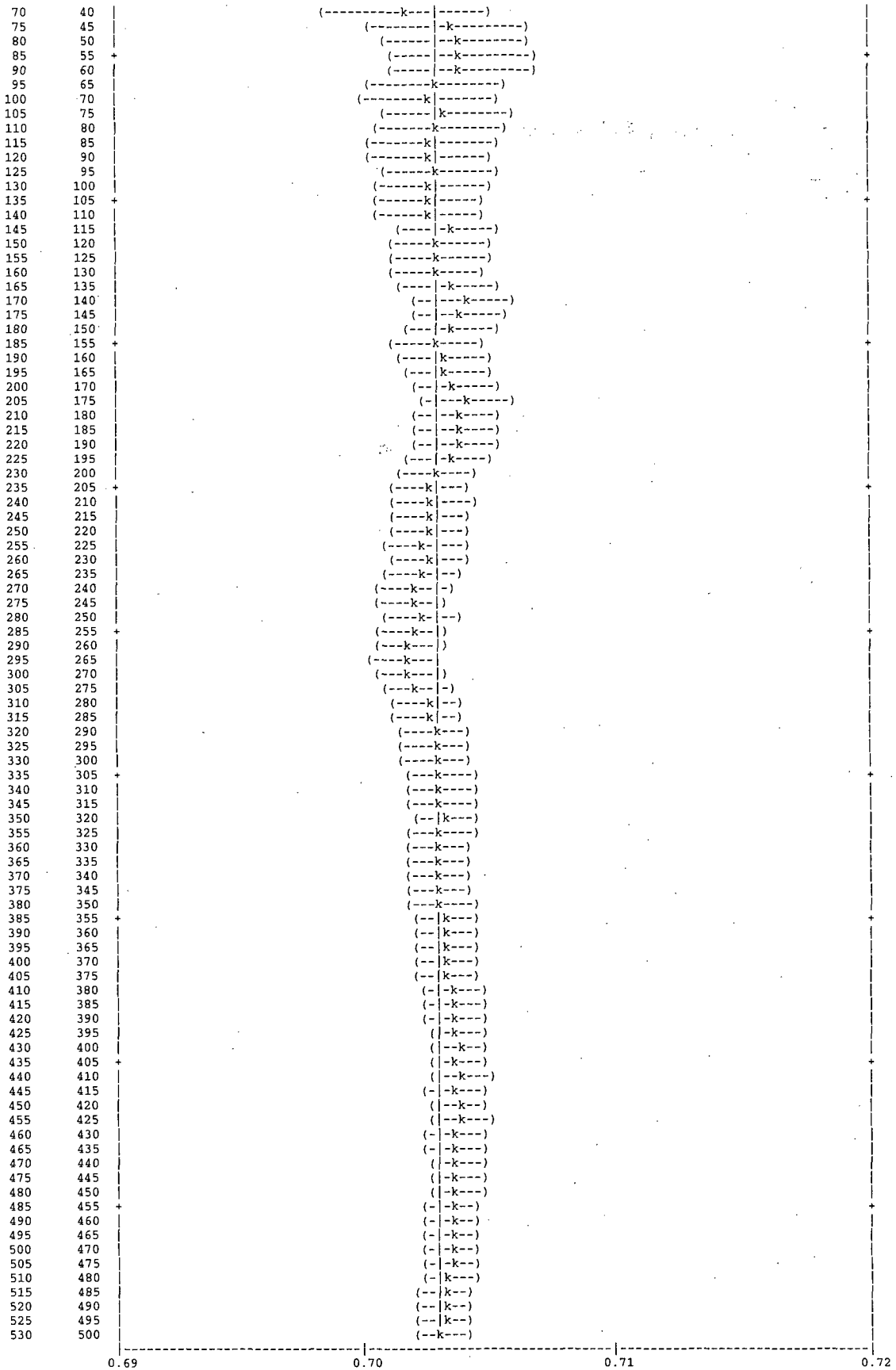
the smallest active cycle keffs by estimator

collision 0.77667 on cycle 250
absorption 0.76931 on cycle 201
track length 0.81127 on cycle 331

collision 0.63361 on cycle 397
absorption 0.63388 on cycle 510
track length 0.60593 on cycle 445

1plot of the estimated col/abs/track-length keff one standard deviation interval versus cycle number (| = final keff = 0.70319)





Individual and collision/absorption/track-length keffs for different numbers of inactive cycles skipped for fission source settling

skip intervals cycles confidence	active cycles	active neutrons	average keff estimators and deviations				normality co/ab/tl	average k(c/a/t)			k(c/a/t) confidence			
			k(col)	st dev	k(abs)	st dev		k(trk)	st dev	k(c/a/t)	st dev	95% confidence	99%	
0.70547	0	530	530485	0.7032	0.0011	0.7026	0.0011	0.7030	0.0015	95/95/95	0.70281	0.00101	0.70081-0.70482	0.70015-
0.70554	1	529	529485	0.7033	0.0011	0.7026	0.0011	0.7030	0.0015	95/95/95	0.70288	0.00101	0.70088-0.70488	0.70022-
0.70566	2	528	528641	0.7034	0.0011	0.7028	0.0011	0.7032	0.0015	95/95/95	0.70303	0.00100	0.70104-0.70502	0.70039-
0.70559	3	527	527713	0.7034	0.0011	0.7027	0.0011	0.7032	0.0015	95/95/95	0.70296	0.00100	0.70097-0.70495	0.70033-
0.70562	4	526	526524	0.7034	0.0011	0.7027	0.0011	0.7031	0.0015	95/95/95	0.70298	0.00100	0.70099-0.70497	0.70034-
0.70568	5	525	525608	0.7034	0.0011	0.7028	0.0011	0.7032	0.0015	95/95/95	0.70304	0.00100	0.70105-0.70503	0.70040-
0.70572	6	524	524636	0.7035	0.0011	0.7028	0.0011	0.7033	0.0015	95/95/95	0.70308	0.00100	0.70109-0.70507	0.70044-
0.70576	7	523	523637	0.7035	0.0011	0.7028	0.0011	0.7034	0.0015	95/95/95	0.70311	0.00100	0.70112-0.70511	0.70047-
0.70578	8	522	522585	0.7035	0.0011	0.7029	0.0011	0.7033	0.0015	95/95/95	0.70313	0.00100	0.70113-0.70513	0.70048-
0.70576	9	521	521579	0.7035	0.0011	0.7029	0.0011	0.7032	0.0015	95/95/95	0.70310	0.00100	0.70110-0.70510	0.70045-
0.70576	10	520	520555	0.7035	0.0011	0.7029	0.0011	0.7032	0.0015	95/95/95	0.70310	0.00101	0.70110-0.70511	0.70044-
0.70571	11	519	519563	0.7035	0.0011	0.7028	0.0011	0.7030	0.0015	95/95/95	0.70305	0.00101	0.70104-0.70505	0.70038-
0.70563	12	518	518519	0.7034	0.0011	0.7027	0.0011	0.7030	0.0015	95/95/95	0.70297	0.00101	0.70097-0.70498	0.70031-
0.70564	13	517	517493	0.7034	0.0011	0.7027	0.0011	0.7031	0.0015	95/95/95	0.70298	0.00101	0.70097-0.70499	0.70031-
0.70568	14	516	516522	0.7035	0.0011	0.7028	0.0011	0.7032	0.0015	95/95/95	0.70301	0.00101	0.70100-0.70502	0.70035-
0.70572	15	515	515550	0.7035	0.0011	0.7028	0.0011	0.7031	0.0015	95/95/95	0.70305	0.00101	0.70104-0.70506	0.70038-
0.70573	16	514	514570	0.7035	0.0011	0.7028	0.0011	0.7031	0.0015	95/95/95	0.70306	0.00101	0.70104-0.70508	0.70038-
0.70580	17	513	513495	0.7036	0.0011	0.7028	0.0011	0.7032	0.0015	95/95/95	0.70312	0.00101	0.70110-0.70514	0.70044-
0.70580	18	512	512553	0.7036	0.0011	0.7028	0.0011	0.7032	0.0015	95/95/95	0.70312	0.00102	0.70110-0.70514	0.70044-
0.70581	19	511	511526	0.7036	0.0011	0.7028	0.0011	0.7033	0.0015	95/95/95	0.70312	0.00102	0.70109-0.70515	0.70043-
0.70571	20	510	510481	0.7034	0.0011	0.7027	0.0011	0.7032	0.0015	95/95/95	0.70303	0.00101	0.70101-0.70505	0.70035-
0.70729	475	55	55110	0.6995	0.0033	0.6991	0.0032	0.6982	0.0046	95/95/95	0.69904	0.00308	0.69285-0.70523	0.69079-
0.70761	480	50	50070	0.6995	0.0034	0.6986	0.0034	0.6984	0.0049	95/95/95	0.69873	0.00330	0.69209-0.70538	0.68986-
0.70909	485	45	45025	0.6998	0.0038	0.6990	0.0037	0.6998	0.0053	95/95/95	0.69932	0.00362	0.69201-0.70663	0.68955-
0.70875	490	40	40100	0.6994	0.0039	0.6984	0.0038	0.6985	0.0056	95/95/95	0.69858	0.00374	0.69100-0.70617	0.68842-
0.70838	495	35	34999	0.6989	0.0043	0.6970	0.0041	0.6955	0.0062	95/95/95	0.69704	0.00414	0.68861-0.70547	0.68571-
0.70987	500	30	29990	0.6982	0.0049	0.6972	0.0046	0.6914	0.0068	95/95/95	0.69647	0.00484	0.68655-0.70640	0.68307-
0.71148	505	25	25031	0.6972	0.0057	0.6967	0.0053	0.6911	0.0079	95/95/95	0.69586	0.00554	0.68436-0.70735	0.68023-
0.71424	510	20	19989	0.6995	0.0066	0.6990	0.0052	0.6966	0.0092	95/95/95	0.69852	0.00542	0.68707-0.70996	0.68279-
0.71919	515	15	14962	0.7021	0.0066	0.7013	0.0055	0.6946	0.0104	95/95/95	0.70061	0.00608	0.68736-0.71386	0.68203-
0.73201	520	10	10050	0.7015	0.0085	0.7029	0.0072	0.6830	0.0122	95/95/95	0.69931	0.00934	0.67722-0.72141	0.66662-
0.92951	525	5	5001	0.7009	0.0161	0.7011	0.0149	0.6853	0.0182	95/95/95	0.69614	0.02351	0.59496-0.79732	0.46277-
	527	3	2949	0.7063	0.0056	0.6936	0.0036	0.6916	0.0222					
	528	2	2080	0.7008	0.0017	0.6907	0.0038	0.6877	0.0379					

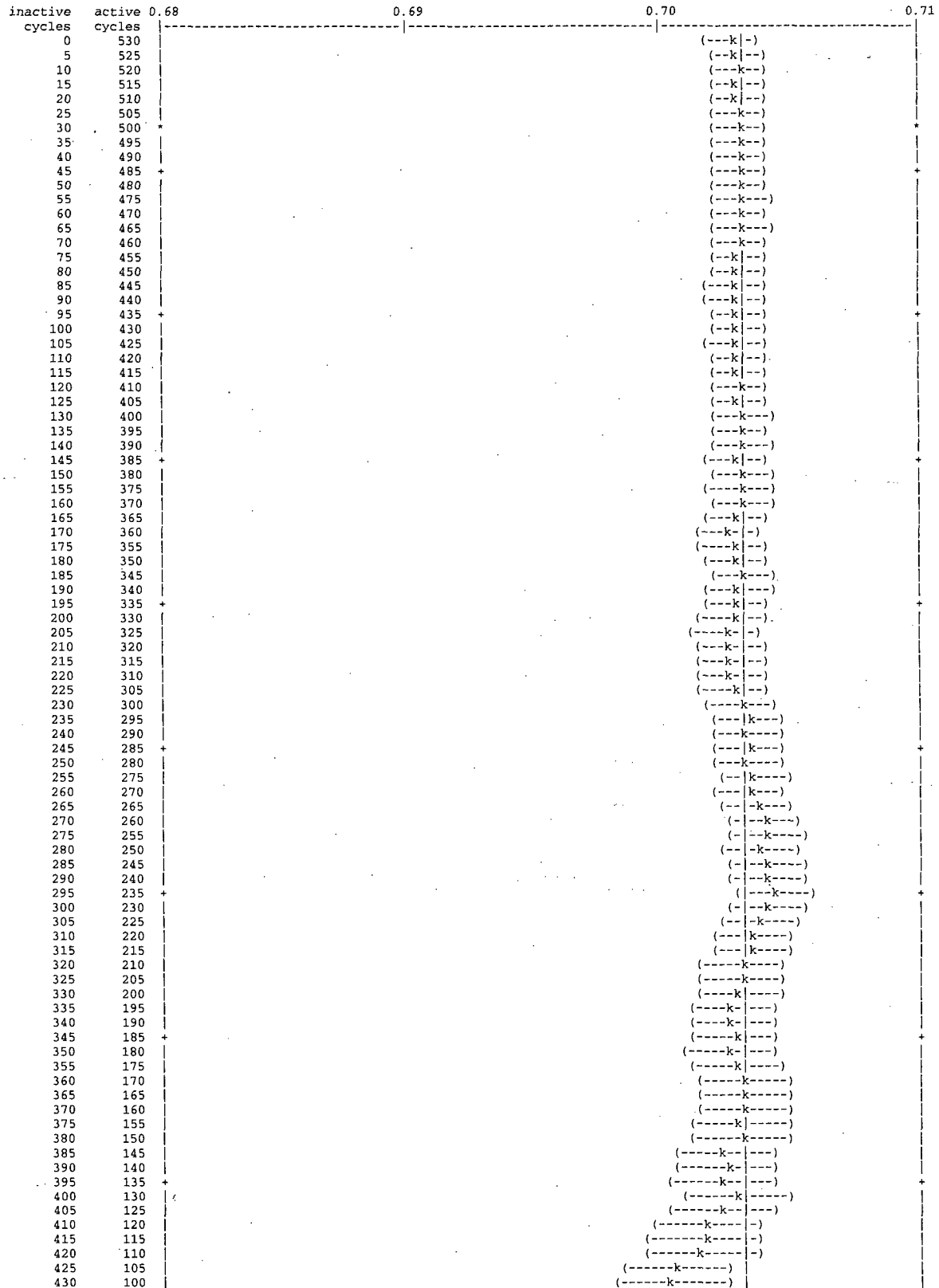
the minimum estimated standard deviation for the col/abs/tl keff estimator occurs with 3 inactive cycles and 527 active cycles.

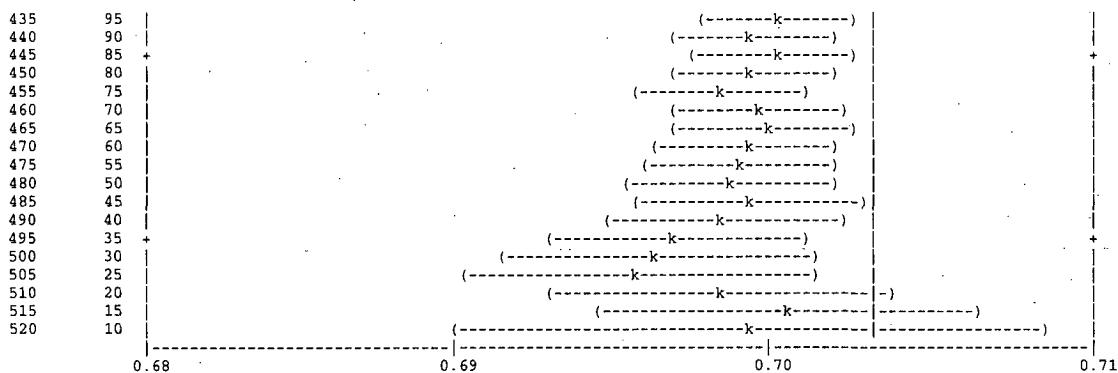
the first active half of the problem skips 30 cycles and uses 250 active cycles; the second half skips 280 and uses 250 cycles. the col/abs/trk-len keff, one standard deviation, and 68, 95, and 99 percent intervals for each active half of the problem are:

problem	keff	standard deviation	68% confidence	95% confidence	99% confidence
first half	0.70239	0.00143	0.70096 to 0.70381	0.69954 to 0.70523	0.69862 to 0.70616

second half	0.70385	0.00147	0.70238 to 0.70532	0.70092 to 0.70678	0.69997 to 0.70773
final result	0.70319	0.00102	0.70216 to 0.70422	0.70115 to 0.70523	0.70048 to 0.70590

the first and second half values of k(collision/absorption/track length) appear to be the same at the 68 percent confidence level.
 plot of the estimated col/abs/track-length keff one standard deviation interval by active cycle number (| = final keff = 0.70319)





dump no. 2 on file MS_Acc_NACCoC_c1.00_g0.00_e0.00_d0.01cm_HP_36mm.inpr nps = 530485 coll = 76766227
ctm = 11.96 nrn = 776053288

6 warning messages so far.

run terminated when 530 kcode cycles were done.

computer time = 12.12 minutes

mcnp version 5 06212004

10/25/07 21:18:09

probid = 10/25/07 21:05:56

Figure 6.6.15-2 Maximum Reactivity MOX Rods – ²⁴¹Pu Fuel Composition

Thread Name & Version = MCNP5_RSICC, 1.30

111 0 11 0 5

```
-----
This program was prepared by the Regents of the University of
California at Los Alamos National Laboratory (the University) under
contract number W-7405-ENG-36 with the U.S. Department of Energy
(DoE). The University has certain rights in the program pursuant to
the contract and the program should not be copied or distributed
outside your organization. All rights in the program are reserved
by the DoE and the University. Neither the U.S. Government nor the
University makes any warranty, express or implied, or assumes any
liability or responsibility for the use of this software.
-----
```

```
lmcnp version 5 ld=06212004 10/25/07 23:04:59
*****
name=P1_Acc_NACCoC_c1.00_g0.00_e0.00_d0.01cm_HP_36mm.inp host=amdeng2-it1459
probid = 10/25/07 23:04:59
```

```
1- NAC-LWT Cask - MOX Experiments - Accident Transport Conditions
2- C
3- C EXCEL File Version: v2.00
4- C Run Version: v2.00
5- C
6- C Fissile Material Type: All Pu-241
7- C Rod Interior Void Moderator Density: 0.9982 g/cc
8- C Canister Interior Moderator Density: 0.9982 g/cc
9- C Canister to Cask Gap Moderator Density: 0.0001 g/cc
10- C Cask Exterior Moderator Density: 0.0001 g/cc
11- C Boundary Condition / Distance: Reflected / 0.01 cm
12- C
13- C Fuel Rod Pitch: 3.6 cm
14- C Fuel Rod Pitch Configuration: Hexagonal
15- C Number of Rods: 16
16- C
17- C Base Fuel Parameters: NACCoC
18- C
19- c Cells - Fuel Rod - NACCoC
20- 1 1 -10.554 -1 u=3 $ Fuel
21- 2 2 -0.9982 -2 +1 u=3 $ Plenum + Fuel to Clad Gap
22- 3 3 -6.56 -3 +2 u=3 $ Clad + End Plugs
23- 4 4 -0.9982 +3 u=3 $ Outside Fuel Rod
24- C 16 Rods - Hexagonal Pitch
25- 10 4 -0.9982 -10
26- *trcl=( 0.9000 -1.5588 0.0000 )
27- lat=2 u=2 fill=-7:6 -5:5 0:0
28- 2 2 2 2 2 2 2 2 2 2 2 2 2 2 2 2
29- 2 2 2 2 2 2 2 2 2 2 2 2 2 2 2 2
30- 2 2 2 2 2 2 2 2 2 2 2 2 2 2 2 2
31- 2 2 2 2 2 2 2 3 2 2 2 2 2 2 2 2
32- 2 2 2 2 2 2 3 3 3 2 2 2 2 2 2 2
33- 2 2 2 2 2 3 3 3 3 2 2 2 2 2 2 2
34- 2 2 2 2 2 3 3 3 3 2 2 2 2 2 2 2
35- 2 2 2 2 2 3 3 3 2 2 2 2 2 2 2 2
36- 2 2 2 2 2 2 2 2 2 2 2 2 2 2 2 2
37- 2 2 2 2 2 2 2 2 2 2 2 2 2 2 2 2
38- 2 2 2 2 2 2 2 2 2 2 2 2 2 2 2 2
39- C PWR Basket - Cells
40- 20 4 -0.9982 -20 fill=2 u=1 $ Rod Array Container
41- 21 5 -0.0001 +20 -21 u=1 $ Basket Cavity
42- 22 7 -2.7020 -22 +21 u=1 $ Basket Body
43- 23 5 -0.0001 +22 u=1 $ Outside
44- C Cells - LWT Cask Accident Conditions
45- 40 8 -11.344 -43 u=0 $ BotPb
46- 41 5 -0.0001 -42 fill=1 u=0 $ Cavity
47- 42 9 -7.9400 -41 +43 u=0 $ Bottom
48- 43 9 -7.9400 -40 +41 +45 +48 +42 u=0 $ OuterShell
49- 44 9 -7.9400 -44 +47 +42 u=0 $ InnerShellTaper
50- 45 9 -7.9400 -46 +42 u=0 $ InnerShell
51- 46 8 -11.344 -47 +46 u=0 $ Lead
52- 47 8 -11.344 -45 +44 +47 u=0 $ LeadTaper
53- 48 0 -48 +47 u=0 $ LeadGap
54- 49 6 -0.0001 -49 +40 u=0 $ Gap to Reflector
55- 50 0 +49 u=0 $ Boundary
56-
57- c Surfaces - Fuel Rod - NACCoC
58- 1 RCC 0.0000 0.0000 10.5207 0.0000 0.0000 389.8900 0.4781 $ Fuel pellet stack
59- 2 RCC 0.0000 0.0000 6.3990 0.0000 0.0000 409.4227 0.4876 $ Annulus + Plenum
60- 3 RCC 0.0000 0.0000 5.0800 0.0000 0.0000 411.8226 0.5588 $ Clad + End-Caps
61- c Surfaces - Pitch - NACCoC
62- 10 RHP 0.0000 0.0000 -1.0000 0.0000 0.0000 454.12 1.8000 0.0000 0.0000 $ Lattice
63- C PWR Basket - Surfaces
64- 20 1 RPP -7.4148 7.4148 -7.4148 7.4148 0.0000 452.1200 $ Array Container
65- 21 1 RPP -11.2713 11.2713 -11.2713 11.2713 0.0000 452.1200 $ Basket Opening
66- 22 RCC 0.0000 0.0000 0.0000 0.0000 0.0000 452.1200 16.83512 $ Basket Outer Body
67- C Surfaces - LWT Cask Accident Conditions
68- 40 RCC 0.0000 0.0000 -26.6700 0.0000 0.0000 507.3650 36.5189 $ Lwt Body
69- 41 RCC 0.0000 0.0000 -26.6700 0.0000 0.0000 26.6700 36.5189 $ Bottom
```

```
70- 42 RCC 0.0000 0.0000 0.0000 0.0000 0.0000 452.1200 16.9863 $ Cavity
71- 43 RCC 0.0000 0.0000 -17.7800 0.0000 0.0000 7.6200 26.3525 $ Bottom gamma shield
72- 44 RCC 0.0000 0.0000 0.0000 0.0000 0.0000 444.5000 20.1740 $ Lead id - taper
73- 45 RCC 0.0000 0.0000 0.0000 0.0000 0.0000 444.5000 31.5976 $ Lead od - taper
74- 46 RCC 0.0000 0.0000 13.8176 0.0000 0.0000 416.8648 18.9103 $ Lead id
75- 47 RCC 0.0000 0.0000 13.8176 0.0000 0.0000 416.8648 33.3271 $ Lead od
76- 48 RCC 0.0000 0.0000 13.8176 0.0000 0.0000 416.8648 33.4645 $ Lead gap
77- *49 RPP -36.5289 36.5289 -36.5289 36.5289 -26.6800 480.7050 $ Container
78-
79- c
80- c Materials List
81- c
82- C MOX Material Composition Fuel
83- m1 92235 -5.7210E-03
84- 92238 -8.1157E-01
85- 94238 -6.4417E-10
86- 94239 -6.4417E-10
87- 94240 -6.4417E-10
88- 94241 -6.4417E-02
89- 94242 -6.4417E-10
90- 8016 -1.1829E-01
91- C Rod Interior Void Material
92- m2 1001 2
93- 8016 1
94- mt2 lwtr.01
95- c Clad Material
96- m3 26054 -7.063E-05 24050 -4.179E-05 7014 -4.980E-04
97- 26056 -1.149E-03 24052 -8.370E-04 7015 -1.981E-06
98- 26057 -2.702E-05 24053 -9.673E-05
99- 26058 -3.631E-06 24054 -2.448E-05
100- 40000 -9.823E-01 50000 -1.500E-02
101- C Canister Interior Non-Fuel Space
102- m4 1001 2
103- 8016 1
104- mt4 lwtr.01
105- C Canister to Cask Gap Material
106- m5 1001 2
107- 8016 1
108- mt5 lwtr.01
109- C Cask Exterior Material
110- m6 1001 2
111- 8016 1
112- mt6 lwtr.01
113- c Aluminum
114- m7 13027 -1.000E+00
115- C Water/Glycol
116- m10 1001 -1.03651E-01
warning. material 10 is not used in the problem.
117- 8016 -6.75619E-01
118- 6000 -2.20730E-01
119- mt10 lwtr.01
warning. material 10 is not used in the problem.
120- c Lead
121- m8 82206 -2.534E-01
122- 82207 -2.207E-01
123- 82208 -5.259E-01
124- c SS304
125- m9 24050 -7.939E-03 26054 -3.927E-02 28058 -6.384E-02
126- 24052 -1.590E-01 26056 -6.387E-01 28060 -2.543E-02
127- 24053 -1.838E-02 26057 -1.502E-02 28061 -1.124E-03
128- 24054 -4.652E-03 26058 -2.019E-03 28062 -3.639E-03
129- 28064 -9.623E-04
130- 25055 -2.000E-02
131- C Aluminum Honeycomb Impact Limiter
132- m11 13027 -1.0
warning. material 11 is not used in the problem.
133- C Mode
134- mode n
135- C Cell Importances
136- imp:n 1 18r 0
137- C
138- C Criticality Controls
139- kcode 1000 0.80 30 530
140- C
141- C Starting Source Definition
142- sdef cell=41:20:10:1
143- erg=d1
144- pos=0 0 10.5207
145- rad=d2
146- axs=0 0 1
147- ext=d3
148- sp1 -3
149- si2 0.0000 0.4781
150- sp2 -21 1
151- si3 0.0000 389.8900
152- sp3 0 1
153- C Print Control
154- print
155- C Random Number Generator
156- rand gen=2 seed=19073486328125 stride=152917 hist=1
157- c
158- C Rotation Matrix
159- *TR1 0.0 0.0 0.0 -30 60 90 -120 -30 90 90 90 0 $ z-rotation -30 degrees
```

!source

print table 10

values of defaulted or explicitly defined source variables

```

sur      0.0000E+00
tme      0.0000E+00
dir      isotropic
pos      0.0000E+00  0.0000E+00  1.0521E+01
x        0.0000E+00
y        0.0000E+00
z        0.0000E+00
axs      0.0000E+00  0.0000E+00  1.0000E+00
vec      0.0000E+00  0.0000E+00  0.0000E+00
ccc      0.0000E+00
nrm      1.0000E+00
ara      0.0000E+00
wgt      1.0000E+00
eff      1.0000E-02
par      0.0000E+00
tr       0.0000E+00
    
```

probability distribution 1 for source variable erg
energy function 3: watt (fission) spectrum (endf law 10)

$f(e)=c \cdot \exp(-e/a) \cdot \sinh(\sqrt{b \cdot e})$
a = 9.6500E-01 b = 2.2900E+00 c = 4.5270E-01

the mean of source distribution 1 is 1.9806E+00

probability distribution 2 for source variable rad
power law 21: $f(x)=c \cdot \text{abs}(x)^k$ k = 1.0000E+00

probability distribution 3 for source variable ext
unbiased histogram distribution

source entry	source value	cumulative probability	probability of bin
1	0.00000E+00	0.000000E+00	0.000000E+00
2	3.89890E+02	1.000000E+00	1.000000E+00

the mean of source distribution 3 is 1.9494E+02

order of sampling source variables.
cel axs rad ext pos erg tme

comment. total fission nuubar data are being used.
material composition

print table 40

the sum of the fractions of material 2 was 3.000000E+00
the sum of the fractions of material 3 was 1.000050E+00
the sum of the fractions of material 4 was 3.000000E+00
the sum of the fractions of material 5 was 3.000000E+00
the sum of the fractions of material 6 was 3.000000E+00
the sum of the fractions of material 9 was 9.999753E-01

material number

component nuclide, atom fraction

1	92235, 2.19354E-03	92238, 3.07241E-01	94238, 2.43869E-10	94239, 2.42846E-10
	94240, 2.41833E-10	94241, 2.40826E-02	94242, 2.39829E-10	8016, 6.66483E-01
2	1001, 6.66667E-01	8016, 3.33333E-01		
associated thermal s(a,b) data sets:	lwtr.01t			
3	26054, 1.19346E-04	24050, 7.62600E-05	7014, 3.24139E-03	26056, 1.87224E-03
	24052, 1.46874E-03	7015, 1.20369E-05	26057, 4.32542E-05	24053, 1.66532E-04
	26058, 5.71247E-06	24054, 4.13652E-05	40000, 9.81436E-01	50000, 1.15166E-02
4	1001, 6.66667E-01	8016, 3.33333E-01		
associated thermal s(a,b) data sets:	lwtr.01t			
5	1001, 6.66667E-01	8016, 3.33333E-01		
associated thermal s(a,b) data sets:	lwtr.01t			
6	1001, 6.66667E-01	8016, 3.33333E-01		
associated thermal s(a,b) data sets:	lwtr.01t			
7	13027, 1.00000E+00			
8	82206, 2.54963E-01	82207, 2.20987E-01	82208, 5.24050E-01	
9	24050, 8.79087E-03	26054, 4.02643E-02	28058, 6.09419E-02	24052, 1.69300E-01
	26056, 6.31511E-01	28060, 2.34673E-02	24053, 1.92010E-02	26057, 1.45900E-02
	28061, 1.02022E-03	24054, 4.76985E-03	26058, 1.92741E-03	28062, 3.24982E-03
	28064, 8.32505E-04	25055, 2.01337E-02		

print table 40

material number

component nuclide, mass fraction

1	92235, 5.72101E-03	92238, 8.11572E-01	94238, 6.44171E-10	94239, 6.44171E-10
	94240, 6.44171E-10	94241, 6.44171E-10	94242, 6.44171E-10	8016, 1.18290E-01
2	1001, 1.11915E-01	8016, 8.88085E-01		
3	26054, 7.06265E-05	24050, 4.17879E-05	7014, 4.97975E-04	26056, 1.14894E-03
	24052, 8.36958E-04	7015, 1.98090E-06	26057, 2.70186E-05	24053, 9.67251E-05
	26058, 3.63082E-06	24054, 2.44788E-05	40000, 9.82251E-01	50000, 1.49992E-02
4	1001, 1.11915E-01	8016, 8.88085E-01		

5	1001, 1.11915E-01	8016, 8.88085E-01			
6	1001, 1.11915E-01	8016, 8.88085E-01			
7	13027, 1.00000E+00				
8	82206, 2.53400E-01	82207, 2.20700E-01	82208, 5.25900E-01		
9	24050, 7.93920E-03	26054, 3.92710E-02	28058, 6.38416E-02	24052, 1.59004E-01	
	26056, 6.38716E-01	28060, 2.54306E-02	24053, 1.83805E-02	26057, 1.50204E-02	
	28061, 1.12403E-03	24054, 4.65211E-03	26058, 2.01905E-03	28062, 3.63909E-03	
	28064, 9.62324E-04	25055, 2.00005E-02			

warning. 6 materials had unnormalized fractions. print table 40.
lcell volumes and masses

print table 50

cell	atom density	gram density	input volume	calculated volume	mass	pieces	reason volume not calculated
1	1	7.05243E-02	1.05540E+01	0.00000E+00	2.79982E+02	2.95493E+03	1
2	2	1.00128E-01	9.98200E-01	0.00000E+00	2.58267E+01	2.57802E+01	1
3	3	4.33411E-02	6.56000E+00	0.00000E+00	9.81838E+01	6.44086E+02	1
4	4	1.00128E-01	9.98200E-01	0.00000E+00	0.00000E+00	0.00000E+00	infinite
5	10	1.00128E-01	9.98200E-01	0.00000E+00	5.09690E+03	5.08773E+03	0
6	20	1.00128E-01	9.98200E-01	0.00000E+00	9.94289E+04	9.92499E+04	0
7	21	1.00309E-05	1.00000E-04	0.00000E+00	1.30324E+05	1.30324E+01	0
8	22	6.03063E-02	2.70200E+00	0.00000E+00	0.00000E+00	0.00000E+00	asymmetric
9	23	1.00309E-05	1.00000E-04	0.00000E+00	0.00000E+00	0.00000E+00	infinite
10	40	3.29629E-02	1.13440E+01	0.00000E+00	1.66245E+04	1.88588E+05	1
11	41	1.00309E-05	1.00000E-04	0.00000E+00	4.09828E+05	4.09828E+01	1
12	42	8.64586E-02	7.94000E+00	0.00000E+00	9.51154E+04	7.55216E+05	1
13	43	8.64586E-02	7.94000E+00	0.00000E+00	4.53784E+05	3.60304E+06	1
14	44	8.64586E-02	7.94000E+00	0.00000E+00	1.02842E+04	8.16563E+04	2
15	45	8.64586E-02	7.94000E+00	0.00000E+00	9.04489E+04	7.18165E+05	1
16	46	3.29629E-02	1.13440E+01	0.00000E+00	9.86269E+05	1.11882E+07	1
17	47	3.29629E-02	1.13440E+01	0.00000E+00	5.13461E+04	5.82470E+05	2
18	48	0.00000E+00	0.00000E+00	0.00000E+00	1.20186E+04	0.00000E+00	1
19	49	1.00309E-05	1.00000E-04	0.00000E+00	0.00000E+00	0.00000E+00	asymmetric
20	50	0.00000E+00	0.00000E+00	0.00000E+00	0.00000E+00	0.00000E+00	infinite

warning. 2 cells appear to consist of more than one piece.

lsurface areas

print table 50

surface	input area	calculated area	reason area not calculated	
2	1.1	0.00000E+00	1.17123E+03	
3	1.2	0.00000E+00	7.18104E-01	
4	1.3	0.00000E+00	7.18104E-01	
6	2.1	0.00000E+00	1.25434E+03	
7	2.2	0.00000E+00	7.46925E-01	
8	2.3	0.00000E+00	7.46925E-01	
10	3.1	0.00000E+00	1.44593E+03	
11	3.2	0.00000E+00	9.80986E-01	
12	3.3	0.00000E+00	9.80986E-01	
14	10.1	0.00000E+00	0.00000E+00	not a boundary
15	10.2	0.00000E+00	0.00000E+00	not a boundary
16	10.3	0.00000E+00	0.00000E+00	not a boundary
17	10.4	0.00000E+00	0.00000E+00	not a boundary
18	10.5	0.00000E+00	0.00000E+00	not a boundary
19	10.6	0.00000E+00	0.00000E+00	not a boundary
20	10.7	0.00000E+00	1.12237E+01	
21	10.8	0.00000E+00	1.12237E+01	
23	20.1	0.00000E+00	6.70476E+03	
24	20.2	0.00000E+00	6.70476E+03	
25	20.3	0.00000E+00	6.70476E+03	
26	20.4	0.00000E+00	6.70476E+03	
27	20.5	0.00000E+00	0.00000E+00	asymmetric
28	20.6	0.00000E+00	0.00000E+00	asymmetric
30	21.1	0.00000E+00	1.01920E+04	
31	21.2	0.00000E+00	1.01920E+04	
32	21.3	0.00000E+00	1.01920E+04	
33	21.4	0.00000E+00	1.01920E+04	
37	22.1	0.00000E+00	4.78244E+04	
41	40.1	0.00000E+00	1.16417E+05	
42	40.2	0.00000E+00	4.18972E+03	
43	40.3	0.00000E+00	4.18972E+03	
49	42.1	0.00000E+00	4.82539E+04	
53	43.1	0.00000E+00	1.26170E+03	
54	43.2	0.00000E+00	2.18169E+03	
55	43.3	0.00000E+00	2.18169E+03	
57	44.1	0.00000E+00	3.50295E+03	
58	44.2	0.00000E+00	2.23013E+03	
61	45.1	0.00000E+00	5.48652E+03	
65	46.1	0.00000E+00	4.95306E+04	
66	46.2	0.00000E+00	2.61173E+03	
67	46.3	0.00000E+00	2.61173E+03	
69	47.1	0.00000E+00	8.72916E+04	
73	48.1	0.00000E+00	8.76515E+04	
77	49.1	0.00000E+00	3.70684E+04	
78	49.2	0.00000E+00	3.70684E+04	
79	49.3	0.00000E+00	3.70684E+04	
80	49.4	0.00000E+00	3.70684E+04	
81	49.5	0.00000E+00	5.33744E+03	
82	49.6	0.00000E+00	5.33744E+03	
84	10010.1	0.00000E+00	9.43871E+02	
85	10010.2	0.00000E+00	9.43871E+02	
86	10010.3	0.00000E+00	9.43871E+02	
87	10010.4	0.00000E+00	9.43871E+02	
88	10010.5	0.00000E+00	9.43871E+02	
89	10010.6	0.00000E+00	9.43871E+02	

lcells

print table 60

cell	mat	atom density	gram density	volume	mass	pieces	neutron importance
1	1	1	7.05243E-02	1.05540E+01	2.79982E+02	2.95493E+03	1 1.0000E+00
2	2	2s	1.00128E-01	9.98200E-01	2.58267E+01	2.57802E+01	1 1.0000E+00
3	3	3	4.33411E-02	6.56000E+00	9.81838E+01	6.44086E+02	1 1.0000E+00
4	4	4s	1.00128E-01	9.98200E-01	0.00000E+00	0.00000E+00	0 1.0000E+00
5	10	4s	1.00128E-01	9.98200E-01	5.09690E+03	5.08773E+03	0 1.0000E+00
6	20	4s	1.00128E-01	9.98200E-01	9.94289E+04	9.92499E+04	0 1.0000E+00
7	21	5s	1.00309E-05	1.00000E-04	1.30324E+05	1.30324E+01	0 1.0000E+00
8	22	7	6.03063E-02	2.70200E+00	0.00000E+00	0.00000E+00	0 1.0000E+00
9	23	5s	1.00309E-05	1.00000E-04	0.00000E+00	0.00000E+00	0 1.0000E+00
10	40	8	3.29629E-02	1.13440E+01	1.66245E+04	1.88588E+05	1 1.0000E+00
11	41	5s	1.00309E-05	1.00000E-04	4.09828E+05	4.09828E+01	1 1.0000E+00
12	42	9	8.64586E-02	7.94000E+00	9.51154E+04	7.55216E+05	1 1.0000E+00
13	43	9	8.64586E-02	7.94000E+00	4.53784E+05	3.60304E+06	1 1.0000E+00
14	44	9	8.64586E-02	7.94000E+00	1.02842E+04	8.16563E+04	2 1.0000E+00
15	45	9	8.64586E-02	7.94000E+00	9.04489E+04	7.18165E+05	1 1.0000E+00
16	46	8	3.29629E-02	1.13440E+01	9.86269E+05	1.11882E+07	1 1.0000E+00
17	47	8	3.29629E-02	1.13440E+01	5.13461E+04	5.82470E+05	2 1.0000E+00
18	48	0	0.00000E+00	0.00000E+00	1.20186E+04	0.00000E+00	1 1.0000E+00
19	49	6s	1.00309E-05	1.00000E-04	0.00000E+00	0.00000E+00	0 1.0000E+00
20	50	0	0.00000E+00	0.00000E+00	0.00000E+00	0.00000E+00	0 0.0000E+00

total
lsurfaces 2.36097E+06 1.72254E+07

print table 70

surface	trans	type	surface coefficients
1	1	rcc	
2	1.1	cz	4.7810000E-01
3	1.2	pz	4.0041070E+02
4	1.3	p	0.0000000E+00 0.0000000E+00 -1.0000000E+00 -1.0520700E+01
5	2	rcc	
6	2.1	cz	4.8760000E-01
7	2.2	pz	4.1582170E+02
8	2.3	p	0.0000000E+00 0.0000000E+00 -1.0000000E+00 -6.3990000E+00
9	3	rcc	
10	3.1	cz	5.5880000E-01
11	3.2	pz	4.1690260E+02
12	3.3	p	0.0000000E+00 0.0000000E+00 -1.0000000E+00 -5.0800000E+00
13	10	rhp	
14	10.1	px	1.8000000E+00
15	10.2	p	-1.0000000E+00 0.0000000E+00 0.0000000E+00 1.8000000E+00
16	10.3	p	5.0000000E-01 8.6602540E-01 0.0000000E+00 1.8000000E+00
17	10.4	p	-5.0000000E-01 -8.6602540E-01 0.0000000E+00 1.8000000E+00
18	10.5	p	-5.0000000E-01 8.6602540E-01 0.0000000E+00 1.8000000E+00
19	10.6	p	5.0000000E-01 -8.6602540E-01 0.0000000E+00 1.8000000E+00
20	10.7	pz	4.5312000E+02
21	10.8	p	0.0000000E+00 0.0000000E+00 -1.0000000E+00 1.0000000E+00
22	20	rpp	
23	20.1	p	8.6602540E-01 5.0000000E-01 0.0000000E+00 7.4148000E+00
24	20.2	p	-8.6602540E-01 -5.0000000E-01 0.0000000E+00 7.4148000E+00
25	20.3	p	-5.0000000E-01 8.6602540E-01 0.0000000E+00 7.4148000E+00
26	20.4	p	5.0000000E-01 -8.6602540E-01 0.0000000E+00 7.4148000E+00
27	20.5	pz	4.5212000E+02
28	20.6	p	0.0000000E+00 0.0000000E+00 -1.0000000E+00 0.0000000E+00
29	21	rpp	
30	21.1	p	8.6602540E-01 5.0000000E-01 0.0000000E+00 1.1271300E+01
31	21.2	p	-8.6602540E-01 -5.0000000E-01 0.0000000E+00 1.1271300E+01
32	21.3	p	-5.0000000E-01 8.6602540E-01 0.0000000E+00 1.1271300E+01
33	21.4	p	5.0000000E-01 -8.6602540E-01 0.0000000E+00 1.1271300E+01
36	22	rcc	
37	22.1	cz	1.6835120E+01
40	40	rcc	
41	40.1	cz	3.6518900E+01
42	40.2	pz	4.8069500E+02
43	40.3	p	0.0000000E+00 0.0000000E+00 -1.0000000E+00 2.6670000E+01
44	41	rcc	
48	42	rcc	
49	42.1	cz	1.6986300E+01
52	43	rcc	
53	43.1	cz	2.6352500E+01
54	43.2	pz	-1.0160000E+01
55	43.3	p	0.0000000E+00 0.0000000E+00 -1.0000000E+00 1.7780000E+01
56	44	rcc	
57	44.1	cz	2.0174000E+01
58	44.2	pz	4.4450000E+02
60	45	rcc	
61	45.1	cz	3.1597600E+01
64	46	rcc	
65	46.1	cz	1.8910300E+01
66	46.2	pz	4.3068240E+02
67	46.3	p	0.0000000E+00 0.0000000E+00 -1.0000000E+00 -1.3817600E+01
68	47	rcc	
69	47.1	cz	3.3327100E+01
72	48	rcc	
73	48.1	cz	3.3464500E+01
76	49	refl.	rpp
77	49.1	refl.	px
78	49.2	refl.	p
79	49.3	refl.	py
80	49.4	refl.	p
81	49.5	refl.	pz
82	49.6	refl.	p

83	10010		rhp						
84	10010.1	1001	px	2.7000000E+00					
85	10010.2	1001	p	-1.0000000E+00	0.0000000E+00	0.0000000E+00	9.0000000E-01		
86	10010.3	1001	p	5.0000000E-01	8.6602540E-01	0.0000000E+00	9.0003960E-01		
87	10010.4	1001	p	-5.0000000E-01	-8.6602540E-01	0.0000000E+00	2.6999604E+00		
88	10010.5	1001	p	-5.0000000E-01	8.6602540E-01	0.0000000E+00	3.9600581E-05		
89	10010.6	1001	p	5.0000000E-01	-8.6602540E-01	0.0000000E+00	3.5999604E+00		

1 identical surfaces

print table 70

master surface	identical surfaces						
10.7	10010.7						
10.8	10010.8						
20.5	21.5	22.2	42.2				
20.6	21.6	22.3	41.2	42.3	44.3	45.3	
40.1	41.1						
40.3	41.3						
44.2	45.2						
46.2	47.2	48.2					
46.3	47.3	48.3					

surface coefficients for identical surfaces not used.

surface	trans	type	surface coefficients				
90	10010.7	1001	pz	4.5312000E+02			
91	10010.8	1001	p	0.0000000E+00	0.0000000E+00	-1.0000000E+00	1.0000000E+00
34	21.5	1	pz	4.5212000E+02			
38	22.2		pz	4.5212000E+02			
50	42.2		pz	4.5212000E+02			
35	21.6	1	p	0.0000000E+00	0.0000000E+00	-1.0000000E+00	0.0000000E+00
39	22.3		p	0.0000000E+00	0.0000000E+00	-1.0000000E+00	0.0000000E+00
46	41.2		pz	0.0000000E+00			
51	42.3		p	0.0000000E+00	0.0000000E+00	-1.0000000E+00	0.0000000E+00
59	44.3		p	0.0000000E+00	0.0000000E+00	-1.0000000E+00	0.0000000E+00
63	45.3		p	0.0000000E+00	0.0000000E+00	-1.0000000E+00	0.0000000E+00
45	41.1		cz	3.6518900E+01			
47	41.3		p	0.0000000E+00	0.0000000E+00	-1.0000000E+00	2.6670000E+01
62	45.2		pz	4.4450000E+02			
70	47.2		pz	4.3068240E+02			
74	48.2		pz	4.3068240E+02			
71	47.3		p	0.0000000E+00	0.0000000E+00	-1.0000000E+00	-1.3817600E+01
75	48.3		p	0.0000000E+00	0.0000000E+00	-1.0000000E+00	-1.3817600E+01

1 cell temperatures in mev for the free-gas thermal neutron treatment.

print table 72

all non-zero importance cells with materials have a temperature for thermal neutrons of 2.5300E-08 mev.

```
*****
* Random Number Generator = 2 *
* Random Number Seed = 19073486328125 *
* Random Number Multiplier = 9219741426499971445 *
* Random Number Adder = 1 *
* Random Number Bits Used = 63 *
* Random Number Stride = 152917 *
*****
```

5 warning messages so far.
1physical constants

print table 98

name	value	description
huge	1.0000000000000E+36	infinity
pie	3.1415926535898E+00	pi
euler	5.7721566490153E-01	euler constant
avogad	6.0220434469282E+23	avogadro number (molecules/mole)
aneut	1.0086649670000E+00	neutron mass (amu)
avgdn	5.9703109000000E-01	avogadro number/neutron mass (1.e-24*molecules/mole/amu)
slite	2.9979250000000E+02	speed of light (cm/shake)
planck	4.1357320000000E-13	planck constant (mev shake)
fscon	1.3703930000000E+02	inverse fine structure constant h*c/(2*pi*e**2)
gpt(1)	9.3958000000000E+02	neutron mass (mev)
gpt(3)	5.1100800000000E-01	electron mass (mev)

fission q-values:	nuclide	q(mev)	nuclide	q(mev)
	90232	171.91	91233	175.57
	92233	180.84	92234	179.45
	92235	180.88	92236	179.50
	92237	180.40	92238	181.31
	92239	180.40	92240	180.40
	93237	183.67	94238	186.65
	94239	189.44	94240	186.36
	94241	188.99	94242	185.98
	94243	187.48	95241	190.83
	95242	190.54	95243	190.25
	96242	190.49	96244	190.49
	other	180.00		

the following compilation options were used:

```
cheap
dec
plot
```

mcplot
xlib
default datapath: C:\Program Files\LANL\MCNPDATA
C:\Progra-1\LANL\MCNPdata
1cross-section tables print table 100

table length

tables from file actia

1001.62c	5202	1-h-1 at 293.6K from endf-vi.8 njoy99.50	mat 125	12/05/01
7014.62c	67462	7-n-14 at 293.6K from endf-vi.8 njoy99.50	mat 725	12/05/01
8016.62c	170541	8-o-16 at 293.6K from endf-vi.8 njoy99.50	mat 825	12/05/01
13027.62c	75363	13-al-27 at 293.6K from endf-vi.8 njoy99.50	mat1325	12/17/01
24050.62c	194445	24-cr-50 at 293.6K from endf-vi.8 njoy99.50	mat2425	12/20/01
24052.62c	174773	24-cr-52 at 293.6K from endf-vi.8 njoy99.50	mat2431	12/20/01
24053.62c	147286	24-cr-53 at 293.6K from endf-vi.8 njoy99.50	mat2434	12/20/01
24054.62c	132737	24-cr-54 at 293.6K from endf-vi.8 njoy99.50	mat2437	12/20/01
25055.62c	134565	25-mn-55 at 293.6K from endf/b-vi.8 njoy99.50	mat2525	02/11/02
26054.62c	143370	26-fe-54 at 293.6K from endf-vi.8 njoy99.50	mat2625	12/20/01
26056.62c	230655	26-fe-56 at 293.6K from endf-vi.8 njoy99.50	mat2631	12/20/01
26057.62c	148842	26-fe-57 at 293.6K from endf-vi.8 njoy99.50	mat2634	12/20/01
26058.62c	87569	26-fe-58 at 293.6K from endf-vi.8 njoy99.50	mat2637	12/20/01
28058.62c	235403	28-ni-58 at 293.6K from endf-vi.8 njoy99.50	mat2825	12/20/01
28060.62c	158305	28-ni-60 at 293.6K from endf-vi.8 njoy99.50	mat2831	12/20/01
28061.62c	112032	28-ni-61 at 293.6K from endf-vi.8 njoy99.50	mat2834	12/20/01
28062.62c	104386	28-ni-62 at 293.6K from endf-vi.8 njoy99.50	mat2837	12/20/01
28064.62c	97689	28-ni-64 at 293.6K from endf-vi.8 njoy99.50	mat2843	12/20/01

tables from file endf66a

7015.66c	19013	7-n-15 at 293.6K from endf-vi.0 njoy99.50	mat 728	07/13/01
----------	-------	---	---------	----------

tables from file endf66b

40000.66c	98524	40-zr-0 at 293.6K from endf-vi.1 njoy99.50	mat4000	07/24/01
-----------	-------	--	---------	----------

tables from file endl92

50000.42c 141628 ENDL library name: nd920609 LANL/XTM modified: 951222 911219
temperature = 2.5860E-08 adjusted to 2.5300E-08

tables from file endf66c

82206.66c	219368	82-pb-206 at 293.6K from endf-vi.6 njoy99.50	mat8231	08/13/01
82207.66c	134389	82-pb-207 at 293.6K from endf-vi.6 njoy99.50	mat8234	08/13/01
82208.66c	135105	82-pb-208 at 293.6K from endf-vi.x njoy99.50	mat8237	03/16/02
94238.66c	53256	94-pu-238 at 293.6K from endf-vi.0 njoy99.50	mat9434	09/06/01
probability tables used from 2.0000E-04 to 1.0000E-02 mev.				
94240.66c	309518	94-pu-240 at 293.6K from endf-vi.2 njoy99.50	mat9440	09/06/01
probability tables used from 5.7000E-03 to 4.0000E-02 mev.				
94241.66c	126607	94-pu-241 at 293.6K from endf-vi.3 njoy99.50	mat9443	09/06/01
probability tables used from 3.0000E-04 to 4.0200E-02 mev.				
94242.66c	107114	94-pu-242 at 293.6K from endf-vi.0 njoy99.50	mat9446	09/06/01
probability tables used from 9.8600E-04 to 1.0000E-02 mev.				

tables from file t16_2003

92235.69c	587997	92-u-235 at 293.6K from t16 u2351a9d njoy99.50	mat9228	07/02/03
probability tables used from 2.2500E-03 to 2.5000E-02 mev.				
92238.69c	713320	92-u-238 at 293.6K from t16 u2381a8h njoy99.50	mat9237	07/02/03
probability tables used from 1.0000E-02 to 1.4903E-01 mev.				
94239.69c	506320	94-pu-239 at 293.6K from t16 pu2391a7d njoy99.50	mat9437	07/02/03
probability tables used from 2.5000E-03 to 3.0000E-02 mev.				

tables from file tmccs

lwtr.01t	10193	hydrogen in light water at 300 degrees kelvin	1001	0	010/22/85
total	5582977				

warning. neutron energy cutoff is below some cross-section tables.

comment. 1 cross sections modified by free gas thermal treatment.
lassignment of s(a,b) data to nuclides. print table 102

mat	nuclide	s(a,b)
2	1001.62c	lwtr.01t
4	1001.62c	lwtr.01t
5	1001.62c	lwtr.01t
6	1001.62c	lwtr.01t

lestimated keff results by cycle print table 175

cycle	k(collission)	prompt removal lifetime(abs)	source points generated
1	0.773576	7.9159E+03	986
2	0.761973	8.7479E+03	1002
3	0.792952	8.6388E+03	1019
4	0.798553	8.0609E+03	1013
5	0.846007	8.0978E+03	1058
6	0.778445	8.7756E+03	927

cycle 7 k(collision) 0.852315 prompt removal lifetime(abs) 8.2963E+03 source points generated 1086
cycle 8 k(collision) 0.776196 prompt removal lifetime(abs) 8.4369E+03 source points generated 916

estimator cycle 526 ave of 496 cycles combination simple average combined average corr
k(collision) 0.813156 0.812679 0.0016 k(col/abs) 0.811904 0.0015 0.811535 0.0015 0.8154
k(absorption) 0.811817 0.811128 0.0015 k(abs/tk ln) 0.811770 0.0015 0.811387 0.0014 0.4631
k(trk length) 0.745849 0.812412 0.0021 k(tk ln/col) 0.812546 0.0017 0.812633 0.0016 0.6279
rem life(col) 8.6684E+03 8.3853E+03 0.0016 k(col/abs/tk ln) 0.812073 0.0015 0.811477 0.0014
rem life(abs) 8.6270E+03 8.3849E+03 0.0016 life(col/abs/tl) 8.3888E+03 0.0014 8.3982E+03 0.0012
source points generated 1039

estimator cycle 527 ave of 497 cycles combination simple average combined average corr
k(collision) 0.809185 0.812672 0.0016 k(col/abs) 0.811898 0.0015 0.811530 0.0015 0.8154
k(absorption) 0.809090 0.811124 0.0015 k(abs/tk ln) 0.811777 0.0015 0.811387 0.0014 0.4630
k(trk length) 0.821169 0.812430 0.0021 k(tk ln/col) 0.812551 0.0017 0.812630 0.0016 0.6278
rem life(col) 8.0102E+03 8.3845E+03 0.0016 k(col/abs/tk ln) 0.812075 0.0015 0.811477 0.0014
rem life(abs) 8.0245E+03 8.3841E+03 0.0016 life(col/abs/tl) 8.3881E+03 0.0014 8.3977E+03 0.0012
source points generated 1005

estimator cycle 528 ave of 498 cycles combination simple average combined average corr
k(collision) 0.821391 0.812642 0.0016 k(col/abs) 0.811905 0.0015 0.811532 0.0015 0.8153
k(absorption) 0.809602 0.811121 0.0015 k(abs/tk ln) 0.811753 0.0015 0.811376 0.0014 0.4629
k(trk length) 0.790409 0.812386 0.0021 k(tk ln/col) 0.812538 0.0017 0.812636 0.0016 0.6272
rem life(col) 7.9693E+03 8.3837E+03 0.0016 k(col/abs/tk ln) 0.812066 0.0015 0.811468 0.0014
rem life(abs) 8.0772E+03 8.3835E+03 0.0016 life(col/abs/tl) 8.3875E+03 0.0014 8.3975E+03 0.0012
source points generated 1027

estimator cycle 529 ave of 499 cycles combination simple average combined average corr
k(collision) 0.788892 0.812642 0.0016 k(col/abs) 0.811869 0.0015 0.811499 0.0015 0.8154
k(absorption) 0.798522 0.811096 0.0015 k(abs/tk ln) 0.811733 0.0015 0.811352 0.0014 0.4630
k(trk length) 0.804736 0.812370 0.0021 k(tk ln/col) 0.812506 0.0017 0.812594 0.0016 0.6271
rem life(col) 8.4590E+03 8.3839E+03 0.0016 k(col/abs/tk ln) 0.812036 0.0015 0.811442 0.0014
rem life(abs) 8.4459E+03 8.3837E+03 0.0016 life(col/abs/tl) 8.3878E+03 0.0014 8.3979E+03 0.0012
source points generated 969

estimator cycle 530 ave of 500 cycles combination simple average combined average corr
k(collision) 0.864442 0.812746 0.0016 k(col/abs) 0.811973 0.0015 0.811603 0.0015 0.8166
k(absorption) 0.862854 0.811199 0.0015 k(abs/tk ln) 0.811816 0.0015 0.811450 0.0014 0.4642
k(trk length) 0.843483 0.812433 0.0021 k(tk ln/col) 0.812589 0.0017 0.812690 0.0016 0.6276
rem life(col) 8.0058E+03 8.3831E+03 0.0016 k(col/abs/tk ln) 0.812126 0.0015 0.811537 0.0014
rem life(abs) 8.0790E+03 8.3830E+03 0.0016 life(col/abs/tl) 8.3872E+03 0.0014 8.3977E+03 0.0012
source points generated 1088

source distribution written to file Pl_Acc_NACCoC_c1.00_g0.00_e0.00_d0.01cm_HP_36mm.inps cycle = 530
problem summary (active cycles only) source particle weight for summary table normalization = 500000.00

run terminated when 530 kcode cycles were done.
+ NAC-LWT Cask - MOX Experiments - Accident Transport Conditions 10/25/07 23:17:01
probid = 10/25/07 23:04:59

0
neutron creation tracks weight energy neutron loss tracks weight energy
(per source particle) (per source particle)
source 500798 1.0000E+00 2.0304E+00 escape 0 0. 0.
energy cutoff 0 0. 0.
time cutoff 0 0. 0.
weight window 0 0. 0. weight window 0 0. 0.
cell importance 0 0. 0. cell importance 0 0. 0.
weight cutoff 0 1.0507E-01 4.7424E-06 weight cutoff 501256 1.0507E-01 4.2477E-06
e or t importance 0 0. 0. e or t importance 0 0. 0.
dxtran 0 0. 0. dxtran 0 0. 0.
forced collisions 0 0. 0. forced collisions 0 0. 0.
exp. transform 0 0. 0. exp. transform 0 0. 0.
upscattering 0 0. 2.2358E-07 downscattering 0 0. 1.9694E+00
photonuclear 0 0. 0. capture 0 7.2325E-01 3.3293E-02
(n,xn) 914 1.5938E-03 1.3448E-03 loss to (n,xn) 456 7.9510E-04 7.6641E-03
prompt fission 0 0. 0. loss to fission 0 2.7755E-01 2.1466E-02
delayed fission 0 0. 0.
total 501712 1.1067E+00 2.0318E+00 total 501712 1.1067E+00 2.0318E+00
number of neutrons banked 487 average time of (shakes) cutoffs
neutron tracks per source particle 1.0034E+00 escape 0.0000E+00 tco 1.0000E+33
neutron collisions per source particle 1.5178E+02 capture 9.5720E+03 eco 0.0000E+00
total neutron collisions 75888898 capture or escape 9.5720E+03 wc1 -5.0000E-01
net multiplication 1.0008E+00 0.0000 any termination 9.6263E+03 wc2 -2.5000E-01
computer time so far in this run 11.91 minutes maximum number ever in bank 2
computer time in mcrun 11.75 minutes bank overflows to backup file 0
source particles per minute 4.5171E+04 most random numbers used was 12106 in history 314654
random numbers generated 769937194
range of sampled source weights = 8.5106E-01 to 1.1655E+00
source efficiency = 1.0000 in cell 1
source efficiency = 0.1042 in cell 10
source efficiency = 1.0000 in cell 20
source efficiency = 1.0000 in cell 41
1neutron activity in each cell

print table 126

cell	tracks entering	population	collisions	collisions * weight (per history)	number weighted energy	flux weighted energy	average track weight (relative)	average track mfp (cm)	
1	1	1241569	501146	586077	9.5153E-01	1.3646E-03	1.1014E+00	9.2286E-01	2.6348E+00
2	2	1753661	501152	72734	1.0239E-01	4.0488E-04	7.9744E-01	8.3249E-01	1.7794E+00
3	3	1892568	501155	78060	1.3835E-01	5.6811E-04	8.5842E-01	8.8595E-01	3.7904E+00
4	4	4675755	501209	22767197	3.3677E+01	1.9441E-04	5.2073E-01	8.3143E-01	1.3415E+00
5	10	1405445	371543	6018259	8.5610E+00	1.3456E-04	3.4232E-01	7.9570E-01	1.0857E+00
6	20	0	0	0	0.0000E+00	0.0000E+00	0.0000E+00	0.0000E+00	0.0000E+00
7	21	1643189	371205	1813	2.6501E-03	4.8443E-04	4.0398E-01	8.2611E-01	1.3004E+04
8	22	2050981	371181	2086136	3.6199E+00	5.2913E-04	3.3678E-01	8.1901E-01	9.7847E+00
9	23	2153778	354933	90	1.4430E-04	5.8421E-04	2.9581E-01	8.1614E-01	1.1843E+04
10	40	25792	5252	101677	1.4356E-01	3.2300E-03	1.0644E-01	7.2359E-01	3.2337E+00
11	41	0	0	0	0.0000E+00	0.0000E+00	0.0000E+00	0.0000E+00	0.0000E+00
12	42	115694	15185	1342637	1.7759E+00	2.6306E-03	1.0677E-01	7.2112E-01	2.5371E+00
13	43	3325425	208962	13169115	1.9143E+01	3.4252E-03	1.7553E-01	7.8816E-01	2.7485E+00
14	44	42149	15682	143930	2.0099E-01	8.1919E-04	1.6869E-01	7.5553E-01	2.3693E+00
15	45	2163315	353876	5282663	7.9853E+00	8.7776E-04	2.9482E-01	8.1629E-01	2.5676E+00
16	46	2626045	293982	23873147	3.7303E+01	1.6270E-03	2.1773E-01	8.0445E-01	3.5473E+00
17	47	87444	20018	361275	5.2806E-01	1.8325E-03	1.3891E-01	7.5094E-01	3.3232E+00
18	48	3117979	207568	0	0.0000E+00	2.7619E-03	1.8387E-01	7.9764E-01	0.0000E+00
19	49	1731775	177414	4088	6.0903E-03	3.8532E-03	1.7945E-01	7.8941E-01	1.0816E+04
total		30052564	4771463	7588898	1.1414E+02				

neutron weight balance in each cell

print table 130

cell index	1	2	3	4	5	6	7	8	9
cell number	1	2	3	4	10	20	21	22	23
external events:									
entering	1.2512E+00	3.1557E+00	3.3816E+00	7.8956E+00	2.2976E+00	0.0000E+00	2.7283E+00	3.3845E+00	3.5279E+00
source	1.0000E+00	0.0000E+00	0.0000E+00	0.0000E+00	0.0000E+00	0.0000E+00	0.0000E+00	0.0000E+00	0.0000E+00
energy cutoff	0.0000E+00	0.0000E+00	0.0000E+00	0.0000E+00	0.0000E+00	0.0000E+00	0.0000E+00	0.0000E+00	0.0000E+00
time cutoff	0.0000E+00	0.0000E+00	0.0000E+00	0.0000E+00	0.0000E+00	0.0000E+00	0.0000E+00	0.0000E+00	0.0000E+00
exiting	-1.8614E+00	-3.1553E+00	-3.3804E+00	-7.7598E+00	-2.2640E+00	0.0000E+00	-2.7283E+00	-3.3455E+00	-3.5279E+00
total	3.8978E-01	3.6619E-04	1.1670E-03	1.3572E-01	3.3608E-02	0.0000E+00	6.9143E-06	3.9023E-02	1.3065E-07
variance reduction events:									
weight window	0.0000E+00	0.0000E+00	0.0000E+00	0.0000E+00	0.0000E+00	0.0000E+00	0.0000E+00	0.0000E+00	0.0000E+00
cell importance	0.0000E+00	0.0000E+00	0.0000E+00	0.0000E+00	0.0000E+00	0.0000E+00	0.0000E+00	0.0000E+00	0.0000E+00
weight cutoff	1.1135E-04	3.7032E-06	1.9991E-06	4.5624E-05	-1.5941E-05	0.0000E+00	-1.4890E-06	-4.0693E-05	0.0000E+00
energy importance	0.0000E+00	0.0000E+00	0.0000E+00	0.0000E+00	0.0000E+00	0.0000E+00	0.0000E+00	0.0000E+00	0.0000E+00
dextran	0.0000E+00	0.0000E+00	0.0000E+00	0.0000E+00	0.0000E+00	0.0000E+00	0.0000E+00	0.0000E+00	0.0000E+00
forced collisions	0.0000E+00	0.0000E+00	0.0000E+00	0.0000E+00	0.0000E+00	0.0000E+00	0.0000E+00	0.0000E+00	0.0000E+00
exp. transform	0.0000E+00	0.0000E+00	0.0000E+00	0.0000E+00	0.0000E+00	0.0000E+00	0.0000E+00	0.0000E+00	0.0000E+00
total	1.1135E-04	3.7032E-06	1.9991E-06	4.5624E-05	-1.5941E-05	0.0000E+00	-1.4890E-06	-4.0693E-05	0.0000E+00
physical events:									
capture (n, xn)	-1.1266E-01	-3.6990E-04	-1.1822E-03	-1.3576E-01	-3.3593E-02	0.0000E+00	-5.4253E-06	-3.8983E-02	-1.3065E-07
loss to (n, xn)	-3.1285E-04	0.0000E+00	-1.3185E-05	0.0000E+00	0.0000E+00	0.0000E+00	0.0000E+00	0.0000E+00	0.0000E+00
fission	0.0000E+00	0.0000E+00	0.0000E+00	0.0000E+00	0.0000E+00	0.0000E+00	0.0000E+00	0.0000E+00	0.0000E+00
loss to fission	-2.7755E-01	0.0000E+00	0.0000E+00	0.0000E+00	0.0000E+00	0.0000E+00	0.0000E+00	0.0000E+00	0.0000E+00
photoneuclear	0.0000E+00	0.0000E+00	0.0000E+00	0.0000E+00	0.0000E+00	0.0000E+00	0.0000E+00	0.0000E+00	0.0000E+00
total	-3.8989E-01	-3.6990E-04	-1.1690E-03	-1.3576E-01	-3.3593E-02	0.0000E+00	-5.4253E-06	-3.8983E-02	-1.3065E-07
total	0.0000E+00	0.0000E+00	0.0000E+00	0.0000E+00	0.0000E+00	0.0000E+00	0.0000E+00	0.0000E+00	0.0000E+00
cell index									
cell number	10	11	12	13	14	15	16	17	18
	40	41	42	43	44	45	46	47	48
external events:									
entering	3.7341E-02	0.0000E+00	1.6904E-01	5.2877E+00	6.3487E-02	3.5504E+00	4.2362E+00	1.3150E-01	4.9768E+00
source	0.0000E+00	0.0000E+00	0.0000E+00	0.0000E+00	0.0000E+00	0.0000E+00	0.0000E+00	0.0000E+00	0.0000E+00
energy cutoff	0.0000E+00	0.0000E+00	0.0000E+00	0.0000E+00	0.0000E+00	0.0000E+00	0.0000E+00	0.0000E+00	0.0000E+00
time cutoff	0.0000E+00	0.0000E+00	0.0000E+00	0.0000E+00	0.0000E+00	0.0000E+00	0.0000E+00	0.0000E+00	0.0000E+00
exiting	-3.7270E-02	0.0000E+00	-1.5693E-01	-5.1469E+00	-5.9514E-02	-3.3370E+00	-4.2065E+00	-1.3116E-01	-4.9768E+00
total	7.0996E-05	0.0000E+00	1.2111E-02	1.4074E-01	3.9735E-03	2.1336E-01	2.9727E-02	3.4420E-04	0.0000E+00
variance reduction events:									
weight window	0.0000E+00	0.0000E+00	0.0000E+00	0.0000E+00	0.0000E+00	0.0000E+00	0.0000E+00	0.0000E+00	0.0000E+00
cell importance	0.0000E+00	0.0000E+00	0.0000E+00	0.0000E+00	0.0000E+00	0.0000E+00	0.0000E+00	0.0000E+00	0.0000E+00
weight cutoff	-2.4210E-06	0.0000E+00	9.0859E-05	-3.1358E-04	-1.0418E-05	1.3278E-04	2.2441E-05	-1.8057E-05	0.0000E+00
energy importance	0.0000E+00	0.0000E+00	0.0000E+00	0.0000E+00	0.0000E+00	0.0000E+00	0.0000E+00	0.0000E+00	0.0000E+00
dextran	0.0000E+00	0.0000E+00	0.0000E+00	0.0000E+00	0.0000E+00	0.0000E+00	0.0000E+00	0.0000E+00	0.0000E+00
forced collisions	0.0000E+00	0.0000E+00	0.0000E+00	0.0000E+00	0.0000E+00	0.0000E+00	0.0000E+00	0.0000E+00	0.0000E+00
exp. transform	0.0000E+00	0.0000E+00	0.0000E+00	0.0000E+00	0.0000E+00	0.0000E+00	0.0000E+00	0.0000E+00	0.0000E+00
total	-2.4210E-06	0.0000E+00	9.0859E-05	-3.1358E-04	-1.0418E-05	1.3278E-04	2.2441E-05	-1.8057E-05	0.0000E+00
physical events:									
capture (n, xn)	-6.8575E-05	0.0000E+00	-1.2202E-02	-1.4044E-01	-3.9631E-03	-2.1350E-01	-3.0195E-02	-3.2989E-04	0.0000E+00
loss to (n, xn)	0.0000E+00	0.0000E+00	0.0000E+00	1.4057E-05	0.0000E+00	2.9429E-05	8.8912E-04	7.4907E-06	0.0000E+00
fission	0.0000E+00	0.0000E+00	0.0000E+00	0.0000E+00	0.0000E+00	0.0000E+00	0.0000E+00	0.0000E+00	0.0000E+00
loss to fission	0.0000E+00	0.0000E+00	0.0000E+00	0.0000E+00	0.0000E+00	0.0000E+00	0.0000E+00	0.0000E+00	0.0000E+00
photoneuclear	0.0000E+00	0.0000E+00	0.0000E+00	0.0000E+00	0.0000E+00	0.0000E+00	0.0000E+00	0.0000E+00	0.0000E+00
total	-6.8575E-05	0.0000E+00	-1.2202E-02	-1.4043E-01	-3.9631E-03	-2.1349E-01	-2.9750E-02	-3.2614E-04	0.0000E+00

total 0.0000E+00 0.0000E+00 0.0000E+00 0.0000E+00 0.0000E+00 0.0000E+00 0.0000E+00 0.0000E+00 0.0000E+00

cell index 19
cell number 49 total

external events:-
entering 2.7311E+00 4.8806E+01
source 0.0000E+00 1.0000E+00
energy cutoff 0.0000E+00 0.0000E+00
time cutoff 0.0000E+00 0.0000E+00
exiting -2.7311E+00 -4.8806E+01
total 1.4036E-06 1.0000E+00

variance reduction events:
weight window 0.0000E+00 0.0000E+00
cell importance 0.0000E+00 0.0000E+00
weight cutoff 0.0000E+00 6.1524E-06
e or t importance 0.0000E+00 0.0000E+00
dxtran 0.0000E+00 0.0000E+00
forced collisions 0.0000E+00 0.0000E+00
exp. transform 0.0000E+00 0.0000E+00
total 0.0000E+00 6.1524E-06

physical events:
capture -1.4036E-06 -7.2325E-01
(n,xn) 0.0000E+00 1.5938E-03
loss to (n,xn) 0.0000E+00 -7.9510E-04
fission 0.0000E+00 0.0000E+00
loss to fission 0.0000E+00 -2.7755E-01
photonuclear 0.0000E+00 0.0000E+00
total -1.4036E-06 -1.0000E+00
total 0.0000E+00 0.0000E+00

neutron activity of each nuclide in each cell, per source particle

print table 140

cell index	cell name	nuclides	atom fraction	total collisions	collisions * weight	wgt. lost to capture	wgt. gain by fission	wgt. gain by (n,xn)	photons produced	photon produced	wgt produced	avg photon energy		
1	1	92235.69c	2.19E-03	11604	1.6516E-02	2.3773E-03	1.2018E-02	1.2382E-06	0	0.0000E+00	0.0000E+00			
		92238.69c	3.07E-01	182793	3.3056E-01	2.3571E-02	5.1778E-03	2.8296E-04	0	0.0000E+00	0.0000E+00			
		94238.66c	2.44E-10	0	0.0000E+00	0.0000E+00	0.0000E+00	0.0000E+00	0	0.0000E+00	0.0000E+00			
		94239.69c	3.24E-10	0	0.0000E+00	0.0000E+00	0.0000E+00	0.0000E+00	0	0.0000E+00	0.0000E+00			
		94240.66c	2.42E-10	0	0.0000E+00	0.0000E+00	0.0000E+00	0.0000E+00	0	0.0000E+00	0.0000E+00			
		94241.66c	2.41E-02	261894	3.6794E-01	8.6289E-02	2.6036E-01	3.0294E-05	0	0.0000E+00	0.0000E+00			
		94242.66c	2.40E-10	0	0.0000E+00	0.0000E+00	0.0000E+00	0.0000E+00	0	0.0000E+00	0.0000E+00			
		8016.62c	6.66E-01	129786	2.3652E-01	4.2088E-04	0.0000E+00	0.0000E+00	0	0.0000E+00	0.0000E+00			
		2	2	1001.62c	6.67E-01	67564	9.4009E-02	3.5973E-04	0.0000E+00	0.0000E+00	0	0.0000E+00	0.0000E+00	
				8016.62c	3.33E-01	5170	8.3772E-03	1.0168E-05	0.0000E+00	0.0000E+00	0	0.0000E+00	0.0000E+00	
3	3			26054.62c	1.19E-04	8	1.3417E-05	2.1703E-06	0.0000E+00	0.0000E+00	0	0.0000E+00	0.0000E+00	
				24050.62c	7.63E-05	8	1.5666E-05	3.9708E-06	0.0000E+00	0.0000E+00	0	0.0000E+00	0.0000E+00	
				7014.62c	3.24E-03	267	4.4474E-04	2.3671E-05	0.0000E+00	0.0000E+00	0	0.0000E+00	0.0000E+00	
				26056.62c	1.87E-03	192	3.0462E-04	2.1713E-05	0.0000E+00	0.0000E+00	0	0.0000E+00	0.0000E+00	
				24052.62c	1.47E-03	61	1.1116E-04	3.5581E-06	0.0000E+00	0.0000E+00	0	0.0000E+00	0.0000E+00	
				7015.66c	1.20E-05	1	2.0596E-06	1.1114E-12	0.0000E+00	0.0000E+00	0	0.0000E+00	0.0000E+00	
				26057.62c	4.33E-05	9	1.5459E-05	1.0398E-06	0.0000E+00	0.0000E+00	0	0.0000E+00	0.0000E+00	
				24053.62c	1.67E-04	32	4.9398E-05	9.4886E-06	0.0000E+00	0.0000E+00	0	0.0000E+00	0.0000E+00	
		26058.62c	5.71E-06	0	0.0000E+00	0.0000E+00	0.0000E+00	0.0000E+00	0	0.0000E+00	0.0000E+00			
		24054.62c	4.14E-05	2	4.1326E-06	3.8278E-08	0.0000E+00	0.0000E+00	0	0.0000E+00	0.0000E+00			
4	4	40000.66c	9.81E-01	76724	1.3605E-01	1.0591E-03	0.0000E+00	1.3185E-05	0	0.0000E+00	0.0000E+00			
		50000.42c	1.15E-02	756	1.3400E-03	5.7434E-05	0.0000E+00	0.0000E+00	0	0.0000E+00	0.0000E+00			
5	10	1001.62c	6.67E-01	21345331	3.1346E+01	1.3390E-01	0.0000E+00	0.0000E+00	0	0.0000E+00	0.0000E+00			
		8016.62c	3.33E-01	1421866	2.3311E+00	1.8663E-03	0.0000E+00	0.0000E+00	0	0.0000E+00	0.0000E+00			
6	20	1001.62c	6.67E-01	5653062	7.9858E+00	3.3326E-02	0.0000E+00	0.0000E+00	0	0.0000E+00	0.0000E+00			
		8016.62c	3.33E-01	365197	5.7522E-01	2.6681E-04	0.0000E+00	0.0000E+00	0	0.0000E+00	0.0000E+00			
7	21	1001.62c	6.67E-01	0	0.0000E+00	0.0000E+00	0.0000E+00	0.0000E+00	0	0.0000E+00	0.0000E+00			
		8016.62c	3.33E-01	0	0.0000E+00	0.0000E+00	0.0000E+00	0.0000E+00	0	0.0000E+00	0.0000E+00			
8	22	1001.62c	6.67E-01	1675	2.4240E-03	5.4231E-06	0.0000E+00	0.0000E+00	0	0.0000E+00	0.0000E+00			
		8016.62c	3.33E-01	138	2.2604E-04	2.2451E-09	0.0000E+00	0.0000E+00	0	0.0000E+00	0.0000E+00			
9	23	13027.62c	1.00E+00	2086136	3.6199E+00	3.8983E-02	0.0000E+00	0.0000E+00	0	0.0000E+00	0.0000E+00			
		1001.62c	6.67E-01	83	1.3264E-04	1.3062E-07	0.0000E+00	0.0000E+00	0	0.0000E+00	0.0000E+00			
10	40	8016.62c	3.33E-01	7	1.1663E-05	2.8285E-11	0.0000E+00	0.0000E+00	0	0.0000E+00	0.0000E+00			
		82206.66c	2.55E-01	24516	3.4087E-02	2.7874E-05	0.0000E+00	0.0000E+00	0	0.0000E+00	0.0000E+00			
11	41	82207.66c	2.21E-01	22486	3.2056E-02	3.8462E-05	0.0000E+00	0.0000E+00	0	0.0000E+00	0.0000E+00			
		82208.66c	5.24E-01	54675	7.7416E-02	2.2389E-06	0.0000E+00	0.0000E+00	0	0.0000E+00	0.0000E+00			
12	42	1001.62c	6.67E-01	0	0.0000E+00	0.0000E+00	0.0000E+00	0.0000E+00	0	0.0000E+00	0.0000E+00			
		8016.62c	3.33E-01	0	0.0000E+00	0.0000E+00	0.0000E+00	0.0000E+00	0	0.0000E+00	0.0000E+00			
		24050.62c	8.79E-03	21758	3.4511E-02	4.7860E-04	0.0000E+00	0.0000E+00	0	0.0000E+00	0.0000E+00			
		26054.62c	4.03E-02	42532	6.8094E-02	4.1345E-04	0.0000E+00	0.0000E+00	0	0.0000E+00	0.0000E+00			

		28058.62c	6.09E-02	181784	2.3443E-01	1.0840E-03	0.0000E+00	0.0000E+00	0	0.0000E+00	0.0000E+00
		24052.62c	1.69E-01	93120	1.3676E-01	6.9642E-04	0.0000E+00	0.0000E+00	0	0.0000E+00	0.0000E+00
		26056.62c	6.32E-01	791641	9.7764E-01	6.0022E-03	0.0000E+00	0.0000E+00	0	0.0000E+00	0.0000E+00
		28060.62c	2.35E-02	26722	4.4624E-02	2.8130E-04	0.0000E+00	0.0000E+00	0	0.0000E+00	0.0000E+00
		24053.62c	1.92E-02	64103	9.6929E-02	1.1944E-03	0.0000E+00	0.0000E+00	0	0.0000E+00	0.0000E+00
		26057.62c	1.46E-02	17618	2.8309E-02	2.0807E-04	0.0000E+00	0.0000E+00	0	0.0000E+00	0.0000E+00
		28061.62c	1.02E-03	1322	1.8890E-03	1.4576E-05	0.0000E+00	0.0000E+00	0	0.0000E+00	0.0000E+00
		24054.62c	4.77E-03	3470	5.4180E-03	9.0933E-06	0.0000E+00	0.0000E+00	0	0.0000E+00	0.0000E+00
		26058.62c	1.93E-03	1803	2.8359E-03	2.7057E-05	0.0000E+00	0.0000E+00	0	0.0000E+00	0.0000E+00
		28062.62c	3.25E-03	14741	2.2397E-02	1.4380E-04	0.0000E+00	0.0000E+00	0	0.0000E+00	0.0000E+00
		28064.62c	8.33E-04	1134	1.9718E-03	6.5208E-06	0.0000E+00	0.0000E+00	0	0.0000E+00	0.0000E+00
		25055.62c	2.01E-02	80889	1.2014E-01	1.6420E-03	0.0000E+00	0.0000E+00	0	0.0000E+00	0.0000E+00
13	43	24050.62c	8.79E-03	221175	3.6703E-01	5.7475E-03	0.0000E+00	0.0000E+00	0	0.0000E+00	0.0000E+00
		26054.62c	4.03E-02	451871	7.6283E-01	4.7802E-03	0.0000E+00	0.0000E+00	0	0.0000E+00	0.0000E+00
		28058.62c	6.09E-02	1715612	2.4243E+00	1.2971E-02	0.0000E+00	0.0000E+00	0	0.0000E+00	0.0000E+00
		24052.62c	1.69E-01	1019845	1.6356E+00	7.9758E-03	0.0000E+00	1.8340E-06	0	0.0000E+00	0.0000E+00
		26056.62c	6.32E-01	7666679	1.0557E+01	6.9499E-02	0.0000E+00	2.0166E-06	0	0.0000E+00	0.0000E+00
		28060.62c	2.35E-02	283261	4.9171E-01	3.2930E-03	0.0000E+00	0.0000E+00	0	0.0000E+00	0.0000E+00
		24053.62c	1.92E-02	630863	1.0081E+00	1.3984E-02	0.0000E+00	1.5387E-06	0	0.0000E+00	0.0000E+00
		26057.62c	1.46E-02	185000	3.1223E-01	2.2263E-03	0.0000E+00	1.6393E-06	0	0.0000E+00	0.0000E+00
		28061.62c	1.02E-03	13468	2.0832E-02	1.7934E-04	0.0000E+00	0.0000E+00	0	0.0000E+00	0.0000E+00
		24054.62c	4.77E-03	36356	6.0531E-02	1.2171E-04	0.0000E+00	0.0000E+00	0	0.0000E+00	0.0000E+00
		26058.62c	1.93E-03	19406	3.2608E-02	2.6030E-04	0.0000E+00	0.0000E+00	0	0.0000E+00	0.0000E+00
		28062.62c	3.25E-03	144976	2.3288E-01	1.6922E-03	0.0000E+00	0.0000E+00	0	0.0000E+00	0.0000E+00
		28064.62c	8.33E-04	12230	2.1954E-02	7.1773E-05	0.0000E+00	0.0000E+00	0	0.0000E+00	0.0000E+00
		25055.62c	2.01E-02	768373	1.2152E+00	1.7635E-02	0.0000E+00	0.0000E+00	0	0.0000E+00	0.0000E+00
14	44	24050.62c	8.79E-03	2269	3.6509E-03	1.8711E-04	0.0000E+00	0.0000E+00	0	0.0000E+00	0.0000E+00
		26054.62c	4.03E-02	4128	6.7625E-03	1.1885E-04	0.0000E+00	0.0000E+00	0	0.0000E+00	0.0000E+00
		28058.62c	6.09E-02	19305	2.6369E-02	3.6453E-04	0.0000E+00	0.0000E+00	0	0.0000E+00	0.0000E+00
		24052.62c	1.69E-01	9781	1.5040E-02	1.7043E-04	0.0000E+00	0.0000E+00	0	0.0000E+00	0.0000E+00
		26056.62c	6.32E-01	87969	1.1668E-01	2.1107E-03	0.0000E+00	0.0000E+00	0	0.0000E+00	0.0000E+00
		28060.62c	2.35E-02	2542	4.3148E-03	8.3706E-05	0.0000E+00	0.0000E+00	0	0.0000E+00	0.0000E+00
		24053.62c	1.92E-02	6286	9.7393E-03	4.0739E-04	0.0000E+00	0.0000E+00	0	0.0000E+00	0.0000E+00
		26057.62c	1.46E-02	1769	2.9096E-03	5.1876E-05	0.0000E+00	0.0000E+00	0	0.0000E+00	0.0000E+00
		28061.62c	1.02E-03	127	1.8882E-04	4.4798E-06	0.0000E+00	0.0000E+00	0	0.0000E+00	0.0000E+00
		24054.62c	4.77E-03	325	5.1374E-04	2.4205E-06	0.0000E+00	0.0000E+00	0	0.0000E+00	0.0000E+00
		26058.62c	1.93E-03	178	2.8855E-04	2.4763E-06	0.0000E+00	0.0000E+00	0	0.0000E+00	0.0000E+00
		28062.62c	3.25E-03	1408	2.2061E-03	5.8112E-05	0.0000E+00	0.0000E+00	0	0.0000E+00	0.0000E+00
		28064.62c	8.33E-04	92	1.6133E-04	2.3044E-06	0.0000E+00	0.0000E+00	0	0.0000E+00	0.0000E+00
		25055.62c	2.01E-02	7751	1.2164E-02	3.9874E-04	0.0000E+00	0.0000E+00	0	0.0000E+00	0.0000E+00
15	45	24050.62c	8.79E-03	80564	1.3531E-01	9.5234E-03	0.0000E+00	0.0000E+00	0	0.0000E+00	0.0000E+00
		26054.62c	4.03E-02	160789	2.7759E-01	6.8030E-03	0.0000E+00	0.0000E+00	0	0.0000E+00	0.0000E+00
		28058.62c	6.09E-02	681315	1.0027E+00	2.0061E-02	0.0000E+00	0.0000E+00	0	0.0000E+00	0.0000E+00
		24052.62c	1.69E-01	391001	6.4399E-01	9.4778E-03	0.0000E+00	1.6111E-06	0	0.0000E+00	0.0000E+00
		26056.62c	6.32E-01	3234714	4.6943E+00	1.1239E-01	0.0000E+00	8.7451E-06	0	0.0000E+00	0.0000E+00
		28060.62c	2.35E-02	91514	1.6155E-01	4.5728E-03	0.0000E+00	0.0000E+00	0	0.0000E+00	0.0000E+00
		24053.62c	1.92E-02	231983	3.7789E-01	2.3538E-02	0.0000E+00	0.0000E+00	0	0.0000E+00	0.0000E+00
		26057.62c	1.46E-02	64846	1.1199E-01	2.6033E-03	0.0000E+00	0.0000E+00	0	0.0000E+00	0.0000E+00
		28061.62c	1.02E-03	5128	8.0158E-03	2.0266E-04	0.0000E+00	0.0000E+00	0	0.0000E+00	0.0000E+00
		24054.62c	4.77E-03	12710	2.1748E-02	1.3227E-04	0.0000E+00	4.3583E-06	0	0.0000E+00	0.0000E+00
		26058.62c	1.93E-03	6657	1.1330E-02	1.9784E-04	0.0000E+00	0.0000E+00	0	0.0000E+00	0.0000E+00
		28062.62c	3.25E-03	51037	8.4785E-02	3.0676E-03	0.0000E+00	0.0000E+00	0	0.0000E+00	0.0000E+00
		28064.62c	8.33E-04	3627	6.6572E-03	7.6507E-05	0.0000E+00	0.0000E+00	0	0.0000E+00	0.0000E+00
		25055.62c	2.01E-02	266778	4.4741E-01	2.0862E-02	0.0000E+00	0.0000E+00	0	0.0000E+00	0.0000E+00
16	46	82206.66c	2.55E-01	5741763	8.8860E+00	6.7912E-03	0.0000E+00	6.4064E-05	0	0.0000E+00	0.0000E+00
		82207.66c	2.21E-01	5300449	8.3363E+00	2.2654E-02	0.0000E+00	1.2740E-04	0	0.0000E+00	0.0000E+00
		82208.66c	5.24E-01	12830935	2.0081E+01	7.5043E-04	0.0000E+00	2.5407E-04	0	0.0000E+00	0.0000E+00
17	47	82206.66c	2.55E-01	86445	1.2471E-01	8.9207E-05	0.0000E+00	1.9156E-06	0	0.0000E+00	0.0000E+00
		82207.66c	2.21E-01	79902	1.1779E-01	2.3046E-04	0.0000E+00	0.0000E+00	0	0.0000E+00	0.0000E+00
		82208.66c	5.24E-01	194928	2.8556E-01	1.0224E-05	0.0000E+00	1.8298E-06	0	0.0000E+00	0.0000E+00
19	49	1001.62c	6.67E-01	3653	5.3988E-03	1.4029E-06	0.0000E+00	0.0000E+00	0	0.0000E+00	0.0000E+00
		8016.62c	3.33E-01	435	6.9146E-04	6.3757E-10	0.0000E+00	0.0000E+00	0	0.0000E+00	0.0000E+00
total				75888898	1.1414E+02	7.2325E-01	2.7755E-01	7.9870E-04	0	0.0000E+00	0.0000E+00
total over all cells by nuclide											
				total collisions	collisions * weight	wgt. lost to capture	wgt. gain by fission	wgt. gain by (n,xn)	photons produced	photon wgt produced	avg photon energy
		1001.62c		27071368	3.9433E+01	1.6759E-01	0.0000E+00	0.0000E+00	0	0.0000E+00	0.0000E+00
		7014.62c		267	4.4474E-04	2.3671E-05	0.0000E+00	0.0000E+00	0	0.0000E+00	0.0000E+00
		7015.66c		1	2.0596E-06	1.1114E-12	0.0000E+00	0.0000E+00	0	0.0000E+00	0.0000E+00
		8016.62c		1922599	3.1521E+00	2.5641E-03	0.0000E+00	0.0000E+00	0	0.0000E+00	0.0000E+00
		13027.62c		2086136	3.6199E+00	3.8983E-02	0.0000E+00	0.0000E+00	0	0.0000E+00	0.0000E+00
		24050.62c		325774	5.4051E-01	1.5941E-02	0.0000E+00	0.0000E+00	0	0.0000E+00	0.0000E+00
		24052.62c		1513808	2.4315E+00	1.8324E-02	0.0000E+00	3.4452E-06	0	0.0000E+00	0.0000E+00
		24053.62c		933267	1.4927E+00	3.9133E-02	0.0000E+00	1.5387E-06	0	0.0000E+00	0.0000E+00
		24054.62c		52863	8.8215E-02	2.6554E-04	0.0000E+00	4.3583E-06	0	0.0000E+00	0.0000E+00
		25055.62c		1123791	1.7949E+00	4.0537E-02	0.0000E+00	0.0000E+00	0	0.0000E+00	0.0000E+00
		26054.62c		659328	1.1153E+00	1.2118E-02	0.0000E+00	0.0000E+00	0	0.0000E+00	0.0000E+00
		26056.62c		11781195	1.6346E+01	1.9002E-01	0.0000E+00	1.0762E-05	0	0.0000E+00	0.0000E+00
		26057.62c		269242	4.5546E-01	5.0906E-03	0.0000E+00	1.6393E-06	0	0.0000E+00	0.0000E+00
		26058.62c		28044							

82207.66c	5402837	8.4862E+00	2.2923E-02	0.0000E+00	1.2740E-04	0	0.0000E+00	0.0000E+00
82208.66c	13080538	2.0444E+01	7.6289E-04	0.0000E+00	2.5590E-04	0	0.0000E+00	0.0000E+00
92235.69c	11604	1.6516E-02	2.3773E-03	1.2018E-02	1.2382E-06	0	0.0000E+00	0.0000E+00
92238.69c	182793	3.3056E-01	2.3571E-02	5.1778E-03	2.8296E-04	0	0.0000E+00	0.0000E+00
94238.66c	0	0.0000E+00	0.0000E+00	0.0000E+00	0.0000E+00	0	0.0000E+00	0.0000E+00
94239.69c	0	0.0000E+00	0.0000E+00	0.0000E+00	0.0000E+00	0	0.0000E+00	0.0000E+00
94240.66c	0	0.0000E+00	0.0000E+00	0.0000E+00	0.0000E+00	0	0.0000E+00	0.0000E+00
94241.66c	261894	3.6794E-01	8.6289E-02	2.6036E-01	3.0294E-05	0	0.0000E+00	0.0000E+00
94242.66c	0	0.0000E+00	0.0000E+00	0.0000E+00	0.0000E+00	0	0.0000E+00	0.0000E+00

lkeff results for: NAC-LWT Cask - MOX Experiments - Accident Transport Conditions
23:04:59

the initial fission neutron source distribution was generated from a general sdef source description. the criticality problem was scheduled to skip 30 cycles and run a total of 530 cycles with nominally 1000 neutrons per cycle. this problem has run 30 inactive cycles with 30072 neutron histories and 500 active cycles with 500798 neutron histories.

this calculation has completed the requested number of keff cycles using a total of 530870 fission neutron source histories. all cells with fissionable material were sampled and had fission neutron source points.

the results of the w test for normality applied to the individual collision, absorption, and track-length keff cycle values are:

the k(collision) cycle values appear normally distributed at the 95 percent confidence level
the k(absorption) cycle values appear normally distributed at the 95 percent confidence level
the k(trk length) cycle values appear normally distributed at the 95 percent confidence level

the final estimated combined collision/absorption/track-length keff = 0.81154 with an estimated standard deviation of 0.00116

the estimated 68, 95, & 99 percent keff-confidence intervals are 0.81038 to 0.81269, 0.80923 to 0.81384, and 0.80848 to 0.81459

the final combined (col/abs/trk) prompt removal lifetime = 8.3977E-05 seconds with an estimated standard deviation of 1.0227E-07

the average neutron energy causing fission = 7.7342E-02 mev

the energy corresponding to the average neutron lethargy causing fission = 1.3304E-07 mev

the percentages of fissions caused by neutrons in the thermal, intermediate, and fast neutron ranges are:

(<0.625 ev): 89.17% (0.625 ev - 100 kev): 7.97% (>100 kev): 2.86%

the average fission neutrons produced per neutron absorbed (capture + fission) in all cells with fission = 2.0828E+00

the average fission neutrons produced per neutron absorbed (capture + fission) in all the geometry cells = 8.1209E-01

the average number of neutrons produced per fission = 2.928

the estimated average keffs, one standard deviations, and 68, 95, and 99 percent confidence intervals are:

corr	keff estimator	keff	standard deviation	68% confidence	95% confidence	99% confidence
	collision	0.81275	0.00130	0.81144 to 0.81405	0.81015 to 0.81534	0.80930 to 0.81619
	absorption	0.81120	0.00119	0.81001 to 0.81239	0.80883 to 0.81357	0.80805 to 0.81435
	track length	0.81243	0.00169	0.81074 to 0.81412	0.80907 to 0.81579	0.80797 to 0.81689
0.8166	col/absorp	0.81160	0.00118	0.81042 to 0.81279	0.80925 to 0.81396	0.80848 to 0.81472
	abs/trk len	0.81145	0.00115	0.81030 to 0.81260	0.80916 to 0.81374	0.80841 to 0.81449
0.4642	col/trk len	0.81269	0.00128	0.81141 to 0.81397	0.81013 to 0.81525	0.80930 to 0.81608
0.6276	col/abs/trk len	0.81154	0.00116	0.81038 to 0.81269	0.80923 to 0.81384	0.80848 to 0.81459

if the largest of each keff occurred on the next cycle, the keff results and 68, 95, and 99 percent confidence intervals would be:

keff estimator	keff	standard deviation	68% confidence	95% confidence	99% confidence
collision	0.81294	0.00132	0.81162 to 0.81426	0.81032 to 0.81556	0.80947 to 0.81642

absorption	0.81135	0.00120	0.81015 to 0.81255	0.80896 to 0.81374	0.80818 to 0.81452
track length	0.81269	0.00170	0.81098 to 0.81439	0.80929 to 0.81608	0.80819 to 0.81719
col/abs/trk len	0.81169	0.00117	0.81053 to 0.81286	0.80937 to 0.81402	0.80861 to 0.81478

the estimated average prompt removal lifetimes, one standard deviations, and 68, 95, and 99 percent confidence intervals are (sec):

estimator	lifetime	std. dev.	68% confidence	95% confidence	99% confidence
collision	8.38310E-05	1.35781E-07	8.3695E-05 to 8.3967E-05	8.3561E-05 to 8.4102E-05	8.3472E-05 to 8.4190E-05
absorption	8.38304E-05	1.31414E-07	8.3699E-05 to 8.3962E-05	8.3569E-05 to 8.4092E-05	8.3483E-05 to 8.4178E-05
track length	8.39544E-05	1.02540E-07	8.3852E-05 to 8.4057E-05	8.3750E-05 to 8.4159E-05	8.3684E-05 to 8.4225E-05
col/absorp	8.38305E-05	1.31533E-07	8.3699E-05 to 8.3962E-05	8.3568E-05 to 8.4092E-05	8.3483E-05 to 8.4178E-05
0.9641 abs/trk len	8.39766E-05	1.02177E-07	8.3874E-05 to 8.4079E-05	8.3773E-05 to 8.4180E-05	8.3707E-05 to 8.4247E-05
0.8463 col/trk len	8.39708E-05	1.02352E-07	8.3868E-05 to 8.4073E-05	8.3767E-05 to 8.4175E-05	8.3700E-05 to 8.4241E-05
0.8149 col/abs/trk len	8.39767E-05	1.02267E-07	8.3874E-05 to 8.4079E-05	8.3773E-05 to 8.4180E-05	8.3706E-05 to 8.4247E-05

absorption estimates of prompt lifetimes (sec):

	escape	capture	fission	removal
fraction	0.00000E+00	7.22671E-01	2.77329E-01	1.00000E+00
lifetime(abs)	0.00000E+00	1.16001E-04	3.02278E-04	8.38304E-05
lifetime(c/a/t)	0.00000E+00	1.16203E-04	3.02805E-04	8.39767E-05

laverage keff results summed over 10 cycles each to form 50 batch values of keff print table 178

batch keff number dev	start cycle	end cycle	keff estimators by batch			average keff estimators and deviations				col/abs/tl			
			k(coll)	k(abs)	k(track)	k(coll)	st dev	k(abs)	st dev	k(track)	st dev	k(c/a/t)	st
1	31	40	0.82966	0.83432	0.81935								
2	41	50	0.81388	0.81282	0.81550	0.82177	0.00789	0.82357	0.01075	0.81743	0.00193		
3	51	60	0.81591	0.81479	0.81007	0.81981	0.00496	0.82065	0.00686	0.81497	0.00269		
4	61	70	0.82413	0.82314	0.81926	0.82089	0.00367	0.82127	0.00489	0.81605	0.00218	0.81694	
0.00574													
5	71	80	0.82191	0.82228	0.81994	0.82110	0.00285	0.82147	0.00379	0.81683	0.00186	0.81825	
0.00362													
6	81	90	0.81341	0.81903	0.80153	0.81982	0.00265	0.82107	0.00312	0.81428	0.00297	0.81800	
0.00617													
7	91	100	0.81570	0.80876	0.80207	0.81923	0.00232	0.81931	0.00317	0.81253	0.00306	0.81900	
0.00447													
8	101	110	0.82256	0.81550	0.81347	0.81964	0.00205	0.81883	0.00279	0.81265	0.00265	0.81916	
0.00422													
9	111	120	0.82739	0.81588	0.82961	0.82050	0.00200	0.81850	0.00248	0.81453	0.00300	0.82101	
0.00377													
10	121	130	0.81189	0.80694	0.79886	0.81964	0.00199	0.81735	0.00250	0.81297	0.00311	0.82178	
0.00370													

11	131	140	0.81512	0.81798	0.81439	0.81923	0.00184	0.81741	0.00226	0.81310	0.00282	0.82030	
0.00312													
12	141	150	0.81892	0.80779	0.81619	0.81921	0.00168	0.81660	0.00222	0.81335	0.00258	0.82018	
0.00294													
13	151	160	0.81253	0.80385	0.81782	0.81869	0.00163	0.81562	0.00226	0.81370	0.00240	0.81873	
0.00276													
14	161	170	0.82293	0.81659	0.81584	0.81900	0.00154	0.81569	0.00210	0.81385	0.00223	0.81876	
0.00269													
15	171	180	0.81782	0.81307	0.81272	0.81892	0.00144	0.81552	0.00196	0.81378	0.00208	0.81870	
0.00256													
16	181	190	0.81490	0.80501	0.83582	0.81867	0.00137	0.81486	0.00195	0.81515	0.00238	0.81813	
0.00211													
17	191	200	0.80059	0.80287	0.80113	0.81760	0.00167	0.81416	0.00196	0.81433	0.00238	0.81579	
0.00232													
18	201	210	0.80941	0.79895	0.80353	0.81715	0.00164	0.81331	0.00203	0.81373	0.00233	0.81600	
0.00240													
19	211	220	0.81458	0.82191	0.81115	0.81701	0.00155	0.81376	0.00197	0.81359	0.00220	0.81590	
0.00210													
20	221	230	0.79879	0.80440	0.80211	0.81610	0.00173	0.81330	0.00193	0.81302	0.00217	0.81416	
0.00206													

21	231	240	0.82474	0.82558	0.81525	0.81651	0.00170	0.81388	0.00193	0.81312	0.00207	0.81450	
0.00204													
22	241	250	0.80621	0.81448	0.80174	0.81604	0.00169	0.81391	0.00184	0.81261	0.00204	0.81398	
0.00192													
23	251	260	0.80096	0.81176	0.80767	0.81539	0.00174	0.81381	0.00176	0.81239	0.00196	0.81344	
0.00172													
24	261	270	0.81023	0.80779	0.80387	0.81517	0.00168	0.81356	0.00170	0.81204	0.00191	0.81322	
0.00170													
25	271	280	0.82492	0.81865	0.82710	0.81556	0.00166	0.81377	0.00165	0.81264	0.00193	0.81362	
0.00168													
26	281	290	0.80925	0.81282	0.80933	0.81532	0.00161	0.81373	0.00158	0.81251	0.00186	0.81349	
0.00160													
27	291	300	0.81000	0.80975	0.80467	0.81512	0.00156	0.81358	0.00153	0.81222	0.00181	0.81331	
0.00156													
28	301	310	0.79874	0.79355	0.81099	0.81454	0.00162	0.81287	0.00164	0.81218	0.00174	0.81258	
0.00155													
29	311	320	0.81086	0.81598	0.80630	0.81441	0.00156	0.81298	0.00158	0.81197	0.00169	0.81254	
0.00149													

NAC-LWT Cask SAR
Revision LWT-08A

January 2008

30	321	330	0.80031	0.80718	0.80098	0.81394	0.00158	0.81278	0.00154	0.81161	0.00168	0.81215	
0.00145	-----												
31	331	340	0.80388	0.79876	0.81420	0.81362	0.00156	0.81233	0.00156	0.81169	0.00162	0.81188	
0.00140	32	341	350	0.81724	0.82617	0.81614	0.81373	0.00152	0.81276	0.00157	0.81183	0.00158	0.81229
0.00138	33	351	360	0.83520	0.81845	0.85451	0.81438	0.00161	0.81293	0.00153	0.81312	0.00200	0.81299
0.00149	34	361	370	0.80886	0.80069	0.80539	0.81422	0.00157	0.81257	0.00153	0.81290	0.00196	0.81279
0.00150	35	371	380	0.81531	0.81537	0.82615	0.81425	0.00152	0.81265	0.00149	0.81328	0.00194	0.81301
0.00145	36	381	390	0.81009	0.80545	0.81262	0.81413	0.00149	0.81245	0.00146	0.81326	0.00188	0.81287
0.00142	37	391	400	0.81143	0.80964	0.80847	0.81406	0.00145	0.81238	0.00142	0.81313	0.00184	0.81279
0.00138	38	401	410	0.82492	0.81788	0.80537	0.81435	0.00144	0.81252	0.00139	0.81292	0.00180	0.81280
0.00136	39	411	420	0.80586	0.80407	0.81463	0.81413	0.00142	0.81231	0.00137	0.81297	0.00175	0.81263
0.00133	40	421	430	0.80978	0.79689	0.81285	0.81402	0.00139	0.81192	0.00139	0.81296	0.00171	0.81250
0.00133	-----												
41	431	440	0.80815	0.81161	0.81895	0.81388	0.00136	0.81191	0.00136	0.81311	0.00167	0.81253	
0.00128	42	441	450	0.79458	0.80377	0.79193	0.81342	0.00140	0.81172	0.00134	0.81261	0.00171	0.81208
0.00128	43	451	460	0.81535	0.81672	0.81120	0.81346	0.00137	0.81184	0.00131	0.81257	0.00167	0.81215
0.00125	44	461	470	0.80700	0.81373	0.79954	0.81332	0.00135	0.81188	0.00128	0.81228	0.00166	0.81206
0.00122	45	471	480	0.79961	0.80600	0.81020	0.81301	0.00135	0.81175	0.00126	0.81223	0.00162	0.81191
0.00118	46	481	490	0.80546	0.79821	0.80770	0.81285	0.00133	0.81145	0.00127	0.81213	0.00159	0.81171
0.00119	47	491	500	0.82768	0.80894	0.82950	0.81316	0.00134	0.81140	0.00124	0.81250	0.00160	0.81175
0.00117	48	501	510	0.79942	0.80020	0.81243	0.81288	0.00134	0.81117	0.00124	0.81250	0.00156	0.81156
0.00115	49	511	520	0.81145	0.80954	0.81694	0.81285	0.00132	0.81113	0.00121	0.81259	0.00153	0.81157
0.00113	50	521	530	0.80779	0.81443	0.80466	0.81275	0.00129	0.81120	0.00119	0.81243	0.00151	0.81156
0.00110	-----												

average keff results summed over 20 cycles each to form 25 batch values of keff

batch keff number dev	start cycle	end cycle	keff estimators by batch			average keff estimators and deviations						col/abs/tl	
			k(coll)	k(abs)	k(track)	k(coll)	st dev	k(abs)	st dev	k(track)	st dev	k(c/a/t) st	
1	31	50	0.82177	0.82357	0.81743								
2	51	70	0.82002	0.81897	0.81466	0.82089	0.00088	0.82127	0.00230	0.81605	0.00138		
3	71	90	0.81766	0.82066	0.81074	0.81982	0.00119	0.82107	0.00135	0.81428	0.00194		
4	91	110	0.81913	0.81213	0.80777	0.81964	0.00086	0.81883	0.00243	0.81265	0.00213	0.82491	
0.00351	5	111	130	0.81964	0.81141	0.81424	0.81964	0.00067	0.81735	0.00240	0.81297	0.00168	0.82164
0.00234	6	131	150	0.81702	0.81289	0.81529	0.81921	0.00070	0.81660	0.00209	0.81335	0.00142	0.81897
0.00199	7	151	170	0.81773	0.81022	0.81683	0.81900	0.00063	0.81569	0.00199	0.81385	0.00130	0.81868
0.00149	8	171	190	0.81636	0.80904	0.82427	0.81867	0.00063	0.81486	0.00191	0.81515	0.00172	0.81847
0.00100	9	191	210	0.80500	0.80091	0.80233	0.81715	0.00162	0.81331	0.00229	0.81373	0.00208	0.81685
0.00310	10	211	230	0.80668	0.81316	0.80663	0.81610	0.00179	0.81330	0.00205	0.81302	0.00199	0.81400
0.00245	-----												
11	231	250	0.81547	0.82003	0.80849	0.81604	0.00162	0.81391	0.00195	0.81261	0.00185	0.81404	
0.00220	12	251	270	0.80559	0.80977	0.80577	0.81517	0.00171	0.81356	0.00181	0.81204	0.00178	0.81292
0.00199	13	271	290	0.81708	0.81574	0.81822	0.81532	0.00158	0.81373	0.00168	0.81251	0.00171	0.81341
0.00181	14	291	310	0.80437	0.80165	0.80783	0.81454	0.00166	0.81287	0.00178	0.81218	0.00162	0.81242
0.00178	15	311	330	0.80558	0.81158	0.80364	0.81394	0.00166	0.81278	0.00166	0.81161	0.00161	0.81191
0.00166	16	331	350	0.81056	0.81246	0.81517	0.81373	0.00157	0.81276	0.00155	0.81183	0.00152	0.81217
0.00147	17	351	370	0.82203	0.80957	0.82995	0.81422	0.00155	0.81257	0.00147	0.81290	0.00178	0.81256
0.00144	18	371	390	0.81270	0.81041	0.81938	0.81413	0.00146	0.81245	0.00139	0.81326	0.00172	0.81267
0.00133	19	391	410	0.81817	0.81376	0.80692	0.81435	0.00140	0.81252	0.00132	0.81292	0.00166	0.81265
0.00129	20	411	430	0.80782	0.80048	0.81374	0.81402	0.00137	0.81192	0.00139	0.81296	0.00157	0.81232
0.00130	-----												

0.00121	21	431	450	0.80137	0.80769	0.80544	0.81342	0.00143	0.81172	0.00133	0.81261	0.00154	0.81189
0.00114	22	451	470	0.81117	0.81523	0.80537	0.81332	0.00137	0.81188	0.00128	0.81228	0.00150	0.81185
0.00112	23	471	490	0.80253	0.80211	0.80895	0.81285	0.00139	0.81145	0.00130	0.81213	0.00145	0.81149
0.00108	24	491	510	0.81355	0.80457	0.82096	0.81288	0.00133	0.81117	0.00127	0.81250	0.00143	0.81149
0.00102	25	511	530	0.80962	0.81198	0.81080	0.81275	0.00128	0.81120	0.00122	0.81243	0.00137	0.81151

average keff results summed over 25 cycles each to form 20 batch values of keff

keff number dev	batch	start cycle	end cycle	keff estimators by batch			average keff estimators and deviations						col/abs/tl
				k(coll)	k(abs)	k(track)	k(coll)	st dev	k(abs)	st dev	k(track)	st dev	k(c/a/t) st
1	31	55	0.82053	0.82250	0.81285								
2	56	80	0.82167	0.82044	0.82080	0.82110	0.00057	0.82147	0.00103	0.81683	0.00397		
3	81	105	0.81838	0.81434	0.80979	0.82019	0.00096	0.81909	0.00245	0.81448	0.00328		
4	106	130	0.81800	0.81211	0.80842	0.81964	0.00087	0.81735	0.00246	0.81297	0.00277	0.82224	
5	131	155	0.81447	0.81041	0.81672	0.81861	0.00124	0.81596	0.00236	0.81372	0.00227	0.81922	
6	156	180	0.82046	0.81331	0.81407	0.81892	0.00106	0.81552	0.00198	0.81378	0.00186	0.81883	
7	181	205	0.80757	0.80137	0.81314	0.81730	0.00185	0.81350	0.00262	0.81368	0.00157	0.81729	
8	206	230	0.80773	0.81189	0.80835	0.81610	0.00200	0.81330	0.00228	0.81302	0.00152	0.81355	
9	231	255	0.81254	0.81725	0.80802	0.81571	0.00181	0.81374	0.00206	0.81246	0.00145	0.81295	
10	256	280	0.81428	0.81405	0.81423	0.81556	0.00162	0.81377	0.00184	0.81264	0.00131	0.81313	
11	281	305	0.80535	0.80546	0.80570	0.81463	0.00174	0.81301	0.00183	0.81201	0.00134	0.81211	
12	306	330	0.80631	0.81025	0.80721	0.81394	0.00173	0.81278	0.00168	0.81161	0.00129	0.81160	
13	331	355	0.81434	0.81294	0.82462	0.81397	0.00159	0.81279	0.00155	0.81261	0.00155	0.81274	
14	356	380	0.81786	0.81084	0.82194	0.81425	0.00150	0.81265	0.00144	0.81328	0.00158	0.81291	
15	381	405	0.81727	0.81240	0.81194	0.81445	0.00141	0.81264	0.00134	0.81319	0.00148	0.81288	
16	406	430	0.80757	0.80117	0.80963	0.81402	0.00139	0.81192	0.00145	0.81296	0.00140	0.81260	
17	431	455	0.80436	0.80922	0.80511	0.81345	0.00142	0.81176	0.00137	0.81250	0.00139	0.81203	
18	456	480	0.80551	0.81151	0.80762	0.81301	0.00141	0.81175	0.00129	0.81223	0.00134	0.81185	
19	481	505	0.81200	0.80345	0.81795	0.81296	0.00134	0.81131	0.00130	0.81253	0.00130	0.81180	
20	506	530	0.80872	0.80907	0.81054	0.81275	0.00129	0.81120	0.00123	0.81243	0.00124	0.81169	

average keff results summed over 50 cycles each to form 10 batch values of keff

keff number dev	batch	start cycle	end cycle	keff estimators by batch			average keff estimators and deviations						col/abs/tl
				k(coll)	k(abs)	k(track)	k(coll)	st dev	k(abs)	st dev	k(track)	st dev	k(c/a/t) st
1	31	80	0.82110	0.82147	0.81683								
2	81	130	0.81819	0.81322	0.80911	0.81964	0.00145	0.81735	0.00412	0.81297	0.00386		
3	131	180	0.81746	0.81186	0.81539	0.81892	0.00111	0.81552	0.00300	0.81378	0.00237		
4	181	230	0.80765	0.80663	0.81075	0.81610	0.00292	0.81330	0.00307	0.81302	0.00184	0.81410	
5	231	280	0.81341	0.81565	0.81112	0.81556	0.00233	0.81377	0.00243	0.81264	0.00147	0.81288	
6	281	330	0.80583	0.80786	0.80646	0.81394	0.00250	0.81278	0.00221	0.81161	0.00158	0.81120	
7	331	380	0.81610	0.81189	0.82328	0.81425	0.00213	0.81265	0.00187	0.81328	0.00214	0.81255	
8	381	430	0.81242	0.80678	0.81079	0.81402	0.00186	0.81192	0.00178	0.81296	0.00188	0.81238	
9	431	480	0.80494	0.81037	0.80636	0.81301	0.00193	0.81175	0.00158	0.81223	0.00181	0.81170	
10	481	530	0.81036	0.80626	0.81424	0.81275	0.00174	0.81120	0.00152	0.81243	0.00163	0.81151	

average keff results summed over 100 cycles each to form 5 batch values of keff

keff number dev	batch	start cycle	end cycle	keff estimators by batch			average keff estimators and deviations						col/abs/tl
				k(coll)	k(abs)	k(track)	k(coll)	st dev	k(abs)	st dev	k(track)	st dev	k(c/a/t) st
1	31	130	0.81964	0.81735	0.81297								

2	131	230	0.81256	0.80924	0.81307	0.81610	0.00354	0.81330	0.00405	0.81302	0.00005	
3	231	330	0.80962	0.81175	0.80879	0.81394	0.00297	0.81278	0.00240	0.81161	0.00141	
4	331	430	0.81426	0.80934	0.81703	0.81402	0.00210	0.81192	0.00190	0.81296	0.00168	0.81086
0.00109												
5	431	530	0.80765	0.80831	0.81030	0.81275	0.00207	0.81120	0.00164	0.81243	0.00141	0.81084
0.00058												

average keff results summed over 125 cycles each to form 4 batch values of keff

keff number	batch start cycle	end cycle	keff estimators by batch			average keff estimators and deviations						col/abs/tl k(c/a/t) st dev		
			k(coll)	k(abs)	k(track)	k(coll)	st dev	k(abs)	st dev	k(track)	st dev			
	1	31	155	0.81861	0.81596	0.81372								
	2	156	280	0.81252	0.81157	0.81156	0.81556	0.00305	0.81377	0.00219	0.81264	0.00108		
	3	281	405	0.81223	0.81038	0.81428	0.81445	0.00208	0.81264	0.00170	0.81319	0.00083		
	4	406	530	0.80763	0.80689	0.81017	0.81275	0.00225	0.81120	0.00187	0.81243	0.00095	0.80866	
0.00201														

average keff results summed over 250 cycles each to form 2 batch values of keff

batch number	start cycle	end cycle	keff estimators by batch			average keff estimators and deviations							
			k(coll)	k(abs)	k(track)	k(coll)	st dev	k(abs)	st dev	k(track)	st dev		
1	31	280	0.81556	0.81377	0.81264								
2	281	530	0.80993	0.80863	0.81223	0.81275	0.00282	0.81120	0.00257	0.81243	0.00021		

laverage individual and combined collision/absorption/track-length keff results for 10 different batch sizes

cycles per intervals keff confidence	batch number	number of batches	average keff estimators and deviations						normality co/ab/trk	average k(c/a/t) confidence			
			k(coll)	st dev	k(abs)	st dev	k(trk)	st dev		k(c/a/t)	st dev	95% confidence	99%
0.81459	1	500	0.8127	0.0013	0.8112	0.0012	0.8124	0.0017	[95/95/95]	0.81154	0.00116	0.80923-0.81384	0.80848-
0.81456	2	250	0.8127	0.0013	0.8112	0.0012	0.8124	0.0016	[95/95/95]	0.81152	0.00115	0.80924-0.81381	0.80849-
0.81424	4	125	0.8127	0.0012	0.8112	0.0011	0.8124	0.0016	[95/95/95]	0.81150	0.00104	0.80943-0.81356	0.80876-
0.81444	5	100	0.8127	0.0013	0.8112	0.0011	0.8124	0.0016	[95/95/95]	0.81156	0.00109	0.80939-0.81373	0.80868-
0.81452	10	50	0.8127	0.0013	0.8112	0.0012	0.8124	0.0015	[95/95/no]	0.81156	0.00110	0.80935-0.81378	0.80861-
0.81439	20	25	0.8127	0.0013	0.8112	0.0012	0.8124	0.0014	[95/95/95]	0.81151	0.00102	0.80939-0.81363	0.80863-
0.81475	25	20	0.8127	0.0013	0.8112	0.0012	0.8124	0.0012	[95/95/95]	0.81169	0.00105	0.80946-0.81391	0.80863-
0.81693	50	10	0.8127	0.0017	0.8112	0.0015	0.8124	0.0016	[95/95/95]	0.81151	0.00155	0.80785-0.81518	0.80610-
0.81658	100	5	0.8127	0.0021	0.8112	0.0016	0.8124	0.0014	[95/95/95]	0.81084	0.00058	0.80835-0.81333	0.80510-
0.93682	125	4	0.8127	0.0023	0.8112	0.0019	0.8124	0.0010	[95/95/95]	0.80866	0.00201	0.78307-0.83424	0.68049-

lindividual and average keff estimator results by cycle

keff cycle	neutron histories	keff estimators by cycle			average keff estimators and deviations						average k(c/a/t)		
		k(coll)	k(abs)	k(track)	k(coll)	st dev	k(abs)	st dev	k(track)	st dev	k(c/a/t)	st dev	from
1	1000	0.77358	0.79932	0.74740									
2	986	0.76197	0.79060	0.75265									
3	1002	0.79295	0.77210	0.82091									
4	1019	0.79855	0.80426	0.80619									
5	1013	0.84601	0.85820	0.82484									
6	1058	0.77844	0.75337	0.72031									
7	927	0.85231	0.84192	0.83283									
8	1086	0.77620	0.80320	0.77936									
9	916	0.79294	0.79449	0.78476									
10	1021	0.81179	0.81686	0.82052									

11	1034	0.77867	0.78231	0.75394									
12	960	0.81982	0.81026	0.73652									
13	1046	0.80821	0.82129	0.79494									
14	986	0.78548	0.78599	0.78331									
15	966	0.85796	0.85715	0.80780									
16	1101	0.79257	0.77507	0.78607									
17	912	0.82974	0.83238	0.82775									
18	1038	0.80387	0.79760	0.88017									
19	966	0.81923	0.79387	0.86437									
20	1014	0.82715	0.80886	0.80226									

21	1014	0.82259	0.85874	0.80640									
22	992	0.86693	0.86026	0.84444									
23	1050	0.84547	0.83464	0.84392									
24	963	0.76921	0.78385	0.77723									
25	914	0.86921	0.85248	0.88038									
26	1121	0.80505	0.83543	0.81121									
27	939	0.83546	0.81099	0.88213									
28	1027	0.80724	0.82815	0.77292									

29	976	0.83872	0.81914	0.85585							
30	1025	0.79872	0.80144	0.84044							
----- begin active keff cycles											
31	985	0.79769	0.81254	0.77994							
32	1003	0.78199	0.79373	0.78218	0.78984	0.00785	0.80313	0.00940	0.78106	0.00112	
33	999	0.82857	0.82168	0.80760	0.80275	0.01368	0.80931	0.00823	0.78991	0.00887	
34	1051	0.82903	0.85712	0.80382	0.80932	0.01170	0.82127	0.01329	0.79339	0.00717	0.78247 0.01718
14266											
35	1009	0.83682	0.82981	0.86441	0.81482	0.01060	0.82298	0.01044	0.80759	0.01525	0.81913 0.01641
14997											
36	1023	0.84764	0.83567	0.83147	0.82029	0.01024	0.82509	0.00878	0.81157	0.01307	0.82250 0.01228
22601											
37	1023	0.82213	0.82044	0.81896	0.82055	0.00866	0.82443	0.00745	0.81263	0.01110	0.82202 0.00976
30546											
38	974	0.83130	0.84804	0.85184	0.82190	0.00762	0.82738	0.00710	0.81753	0.01079	0.82559 0.00890
32910											
39	1015	0.82956	0.84174	0.80362	0.82275	0.00677	0.82897	0.00646	0.81598	0.00964	0.82631 0.00820
34663											
40	969	0.89183	0.88243	0.84970	0.82966	0.00919	0.83432	0.00787	0.81935	0.00926	0.82988 0.00961
23195											

511	1007	0.81678	0.82585	0.81586	0.81288	0.00132	0.81120	0.00120	0.81251	0.00170	0.81156 0.00116
30004											
512	1001	0.76297	0.75270	0.73827	0.81278	0.00132	0.81108	0.00121	0.81235	0.00171	0.81144 0.00117
29684											
513	943	0.80793	0.79311	0.77191	0.81277	0.00132	0.81104	0.00120	0.81227	0.00170	0.81140 0.00117
29688											
514	1074	0.84159	0.85901	0.82520	0.81283	0.00131	0.81114	0.00121	0.81230	0.00170	0.81149 0.00117
29623											
515	1059	0.79077	0.77557	0.83553	0.81278	0.00131	0.81106	0.00121	0.81234	0.00170	0.81145 0.00117
29618											
516	943	0.83794	0.82702	0.82522	0.81284	0.00131	0.81110	0.00120	0.81237	0.00170	0.81148 0.00116
29655											
517	1087	0.80995	0.82004	0.78851	0.81283	0.00131	0.81112	0.00120	0.81232	0.00169	0.81148 0.00116
29721											
518	968	0.89895	0.87356	0.93949	0.81301	0.00132	0.81124	0.00121	0.81258	0.00171	0.81162 0.00117
29252											
519	1102	0.78411	0.80850	0.85787	0.81295	0.00132	0.81124	0.00120	0.81268	0.00171	0.81163 0.00117
29329											
520	875	0.76352	0.75999	0.77152	0.81285	0.00132	0.81113	0.00121	0.81259	0.00171	0.81153 0.00117
29162											

521	989	0.80518	0.81700	0.80918	0.81283	0.00131	0.81115	0.00120	0.81258	0.00170	0.81154 0.00117
29234											
522	1062	0.82496	0.84155	0.83930	0.81286	0.00131	0.81121	0.00120	0.81264	0.00170	0.81160 0.00117
29242											
523	1036	0.82159	0.83155	0.85448	0.81287	0.00131	0.81125	0.00120	0.81272	0.00170	0.81165 0.00116
29266											
524	975	0.75715	0.77727	0.77199	0.81276	0.00131	0.81118	0.00120	0.81264	0.00170	0.81157 0.00116
29207											
525	920	0.77191	0.78500	0.76597	0.81268	0.00131	0.81113	0.00120	0.81255	0.00170	0.81150 0.00116
29183											
526	1036	0.81316	0.81182	0.74585	0.81268	0.00131	0.81113	0.00120	0.81241	0.00170	0.81148 0.00116
29223											
527	1039	0.80919	0.80909	0.82117	0.81267	0.00131	0.81112	0.00119	0.81243	0.00170	0.81148 0.00116
29277											
528	1005	0.82139	0.80960	0.79041	0.81269	0.00130	0.81112	0.00119	0.81239	0.00169	0.81147 0.00116
29327											
529	1027	0.78889	0.79852	0.80474	0.81264	0.00130	0.81110	0.00119	0.81237	0.00169	0.81144 0.00115
29371											
530	969	0.86444	0.86285	0.84348	0.81275	0.00130	0.81120	0.00119	0.81243	0.00169	0.81154 0.00116
29242											

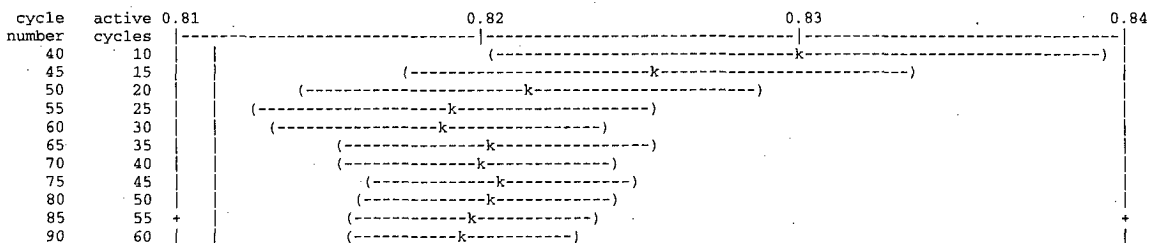
the largest active cycle keffs by estimator are:

the smallest active cycle keffs by estimator

collision 0.91061 on cycle 312
absorption 0.88814 on cycle 312
track length 0.93949 on cycle 518

collision 0.73198 on cycle 226
absorption 0.72474 on cycle 226
track length 0.71577 on cycle 390

1plot of the estimated col/abs/track-length keff one standard deviation interval versus cycle number (| = final keff = 0.81154)



95	65	(-----k-----)
100	70	(-----k-----)
105	75	(-----k-----)
110	80	(-----k-----)
115	85	(-----k-----)
120	90	(-----k-----)
125	95	(-----k-----)
130	100	(-----k-----)
135	105	(-----k-----)
140	110	(-----k-----)
145	115	(-----k-----)
150	120	(-----k-----)
155	125	(-----k-----)
160	130	(-----k-----)
165	135	(-----k-----)
170	140	(-----k-----)
175	145	(-----k-----)
180	150	(-----k-----)
185	155	(-----k-----)
190	160	(-----k-----)
195	165	(-----k-----)
200	170	(-----k-----)
205	175	(-----k-----)
210	180	(-----k-----)
215	185	(-----k-----)
220	190	(-----k-----)
225	195	(-----k-----)
230	200	(-----k-----)
235	205	(-----k-----)
240	210	(-----k-----)
245	215	(-----k-----)
250	220	(-----k-----)
255	225	(-----k-----)
260	230	(-----k-----)
265	235	(-----k-----)
270	240	(-----k-----)
275	245	(-----k-----)
280	250	(-----k-----)
285	255	(-----k-----)
290	260	(-----k-----)
295	265	(-----k-----)
300	270	(-----k-----)
305	275	(-----k-----)
310	280	(-----k-----)
315	285	(-----k-----)
320	290	(-----k-----)
325	295	(-----k-----)
330	300	(-----k-----)
335	305	(-----k-----)
340	310	(-----k-----)
345	315	(-----k-----)
350	320	(-----k-----)
355	325	(-----k-----)
360	330	(-----k-----)
365	335	(-----k-----)
370	340	(-----k-----)
375	345	(-----k-----)
380	350	(-----k-----)
385	355	(-----k-----)
390	360	(-----k-----)
395	365	(-----k-----)
400	370	(-----k-----)
405	375	(-----k-----)
410	380	(-----k-----)
415	385	(-----k-----)
420	390	(-----k-----)
425	395	(-----k-----)
430	400	(-----k-----)
435	405	(-----k-----)
440	410	(-----k-----)
445	415	(-----k-----)
450	420	(-----k-----)
455	425	(-----k-----)
460	430	(-----k-----)
465	435	(-----k-----)
470	440	(-----k-----)
475	445	(-----k-----)
480	450	(-----k-----)
485	455	(-----k-----)
490	460	(-----k-----)
495	465	(-----k-----)
500	470	(-----k-----)
505	475	(-----k-----)
510	480	(-----k-----)
515	485	(-----k-----)
520	490	(-----k-----)
525	495	(-----k-----)
530	500	(-----k-----)

individual and collision/absorption/track-length keffs for different numbers of inactive cycles skipped for fission source settling

skip intervals	active cycles	active neutrons	average k(col)	estimators st dev	and deviations k(abs)	normality k(trk)	average co/ab/tl	average k(c/a/t)	st dev	k(c/a/t)	confidence 95%	confidence 99%
----------------	---------------	-----------------	----------------	-------------------	-----------------------	------------------	------------------	------------------	--------	----------	----------------	----------------

0	530	530870	0.8127	0.0013	0.8113	0.0012	0.8122	0.0017	95/95/95	0.81157	0.00113	0.80932-0.81381	0.80859-
0.81454													
1	529	529870	0.8128	0.0013	0.8113	0.0012	0.8123	0.0017	95/95/95	0.81162	0.00113	0.80937-0.81386	0.80864-
0.81459													
2	528	528884	0.8129	0.0013	0.8114	0.0012	0.8124	0.0016	95/95/95	0.81168	0.00113	0.80943-0.81393	0.80870-
0.81466													
3	527	527882	0.8129	0.0013	0.8114	0.0012	0.8124	0.0017	95/95/95	0.81173	0.00113	0.80948-0.81398	0.80875-
0.81471													
4	526	526863	0.8130	0.0013	0.8114	0.0012	0.8124	0.0017	95/95/95	0.81175	0.00113	0.80949-0.81400	0.80876-
0.81473													
5	525	525850	0.8129	0.0013	0.8114	0.0012	0.8124	0.0017	95/95/95	0.81167	0.00113	0.80941-0.81392	0.80868-
0.81465													
6	524	524792	0.8130	0.0013	0.8115	0.0012	0.8126	0.0017	95/95/95	0.81177	0.00113	0.80952-0.81401	0.80879-
0.81474													
7	523	523865	0.8129	0.0013	0.8114	0.0012	0.8125	0.0017	95/95/95	0.81172	0.00113	0.80947-0.81396	0.80874-
0.81469													
8	522	522779	0.8129	0.0013	0.8114	0.0012	0.8126	0.0017	95/95/95	0.81175	0.00113	0.80950-0.81400	0.80877-
0.81473													
9	521	521863	0.8130	0.0013	0.8115	0.0012	0.8126	0.0017	95/95/95	0.81179	0.00113	0.80953-0.81404	0.80880-
0.81477													
10	520	520842	0.8130	0.0013	0.8114	0.0012	0.8126	0.0017	95/95/95	0.81177	0.00113	0.80952-0.81403	0.80878-
0.81477													

11	519	519808	0.8131	0.0013	0.8115	0.0012	0.8127	0.0017	95/95/95	0.81184	0.00113	0.80959-0.81410	0.80885-
0.81484													
12	518	518848	0.8130	0.0013	0.8115	0.0012	0.8129	0.0017	95/95/95	0.81187	0.00113	0.80961-0.81413	0.80887-
0.81487													
13	517	517802	0.8131	0.0013	0.8115	0.0012	0.8129	0.0017	95/95/95	0.81186	0.00114	0.80960-0.81413	0.80886-
0.81487													
14	516	516816	0.8131	0.0013	0.8115	0.0012	0.8130	0.0017	95/95/95	0.81191	0.00114	0.80965-0.81418	0.80891-
0.81492													
15	515	515850	0.8130	0.0013	0.8114	0.0012	0.8130	0.0017	95/95/95	0.81184	0.00114	0.80958-0.81411	0.80884-
0.81485													
16	514	514749	0.8131	0.0013	0.8115	0.0012	0.8130	0.0017	95/95/95	0.81190	0.00114	0.80964-0.81417	0.80890-
0.81491													
17	513	513837	0.8130	0.0013	0.8115	0.0012	0.8130	0.0017	95/95/95	0.81187	0.00114	0.80959-0.81414	0.80885-
0.81488													
18	512	512799	0.8130	0.0013	0.8115	0.0012	0.8129	0.0017	95/95/95	0.81186	0.00114	0.80959-0.81414	0.80885-
0.81488													
19	511	511833	0.8130	0.0013	0.8115	0.0012	0.8128	0.0017	95/95/95	0.81187	0.00114	0.80959-0.81415	0.80885-
0.81489													
20	510	510819	0.8130	0.0013	0.8115	0.0012	0.8128	0.0017	95/95/95	0.81187	0.00115	0.80959-0.81416	0.80885-
0.81490													

475	55	55160	0.8091	0.0040	0.8061	0.0037	0.8134	0.0053	95/95/95	0.80765	0.00368	0.80025-0.81504	0.79780-
0.81750													
480	50	50124	0.8104	0.0043	0.8063	0.0039	0.8142	0.0058	95/95/95	0.80785	0.00405	0.79971-0.81599	0.79698-
0.81871													
485	45	45138	0.8117	0.0047	0.8075	0.0042	0.8169	0.0058	95/95/95	0.80926	0.00443	0.80032-0.81820	0.79731-
0.82121													
490	40	40182	0.8116	0.0051	0.8083	0.0044	0.8159	0.0064	95/95/95	0.80894	0.00466	0.79949-0.81839	0.79628-
0.82160													
495	35	35116	0.8117	0.0056	0.8094	0.0049	0.8181	0.0071	95/95/95	0.81015	0.00517	0.79962-0.82067	0.79600-
0.82429													
500	30	30049	0.8062	0.0056	0.8081	0.0053	0.8113	0.0074	95/95/95	0.80779	0.00552	0.79646-0.81911	0.79250-
0.82308													
505	25	25133	0.8087	0.0064	0.8091	0.0061	0.8105	0.0086	95/95/95	0.80898	0.00634	0.79583-0.82214	0.79110-
0.82687													
510	20	20117	0.8096	0.0078	0.8120	0.0073	0.8108	0.0104	95/95/95	0.81175	0.00785	0.79518-0.82833	0.78898-
0.83452													
515	15	15033	0.8115	0.0097	0.8156	0.0077	0.8153	0.0125	95/95/95	0.81902	0.00788	0.80185-0.83620	0.79494-
0.84311													
520	10	10058	0.8078	0.0095	0.8144	0.0081	0.8047	0.0114	95/95/95	0.82210	0.01244	0.79269-0.85152	0.77857-
0.86564													

525	5	5076	0.8194	0.0125	0.8184	0.0114	0.8011	0.0164	95/99/95	0.81633	0.01852	0.73663-0.89603	0.63251-
1.00015													
527	3	3001	0.8249	0.0219	0.8237	0.0199	0.8129	0.0159					
528	2	1996	0.8267	0.0378	0.8307	0.0322	0.8241	0.0194					

the minimum estimated standard deviation for the col/abs/trk keff estimator occurs with 0 inactive cycles and 530 active cycles.

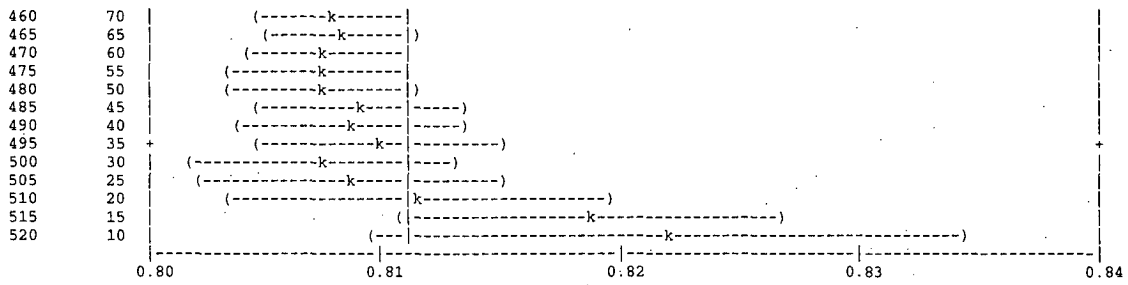
the first active half of the problem skips 30 cycles and uses 250 active cycles; the second half skips 280 and uses 250 cycles. the col/abs/trk-len keff, one standard deviation, and 68, 95, and 99 percent intervals for each active half of the problem are:

problem	keff	standard deviation	68% confidence	95% confidence	99% confidence
first half	0.81362	0.00164	0.81198 to 0.81526	0.81035 to 0.81688	0.80929 to 0.81794
second half	0.80936	0.00164	0.80771 to 0.81100	0.80608 to 0.81263	0.80501 to 0.81370
final result	0.81154	0.00116	0.81038 to 0.81269	0.80923 to 0.81384	0.80848 to 0.81459

the first and second half values of k(collision/absorption/track length) appear to be the same at the 95 percent confidence level.

lplot of the estimated col/abs/track-length keff one standard deviation interval by active cycle number (| = final keff = 0.81154)

inactive cycles	active cycles	0.80	0.81	0.82	0.83	0.84
0	530		(-k--)			
5	525		(- k--)			
10	520		(- k--)			
15	515		(- k--)			
20	510		(- k--)			
25	505		(- k--)			
30	500		(--k--)			
35	495		(--k--)			
40	490		(--k)			
45	485		(--k)			
50	480		(--k)			
55	475		(--k)			
60	470		(--k)			
65	465		(--k)			
70	460		(--k)			
75	455		(--k)			
80	450		(--k)			
85	445		(--k)			
90	440		(--k)			
95	435		(--k)			
100	430		(--k)			
105	425		(--k)			
110	420		(--k)			
115	415		(--k)			
120	410		(--k)			
125	405		(--k)			
130	400		(--k)			
135	395		(--k)			
140	390		(--k)			
145	385		(--k)			
150	380		(--k)			
155	375		(--k)			
160	370		(--k)			
165	365		(--k)			
170	360		(--k)			
175	355		(--k)			
180	350		(--k)			
185	345		(--k)			
190	340		(--k)			
195	335		(--k)			
200	330		(--k)			
205	325		(--k)			
210	320		(--k)			
215	315		(--k)			
220	310		(--k)			
225	305		(--k)			
230	300		(--k)			
235	295		(--k)			
240	290		(--k)			
245	285		(--k)			
250	280		(--k)			
255	275		(--k)			
260	270		(--k)			
265	265		(--k)			
270	260		(--k)			
275	255		(--k)			
280	250		(--k)			
285	245		(--k)			
290	240		(--k)			
295	235		(--k)			
300	230		(--k)			
305	225		(--k)			
310	220		(--k)			
315	215		(--k)			
320	210		(--k)			
325	205		(--k)			
330	200		(--k)			
335	195		(--k)			
340	190		(--k)			
345	185		(--k)			
350	180		(--k)			
355	175		(--k)			
360	170		(--k)			
365	165		(--k)			
370	160		(--k)			
375	155		(--k)			
380	150		(--k)			
385	145		(--k)			
390	140		(--k)			
395	135		(--k)			
400	130		(--k)			
405	125		(--k)			
410	120		(--k)			
415	115		(--k)			
420	110		(--k)			
425	105		(--k)			
430	100		(--k)			
435	95		(--k)			
440	90		(--k)			
445	85		(--k)			
450	80		(--k)			
455	75		(--k)			



dump no. 2 on file P1_Acc_NACCoC_c1.00_g0.00_e0.00_d0.01cm_HP_36mm.inpr nps = 530870 coll = 75888898
ctm = 11.75 nrn = 769937194

6 warning messages so far.

run terminated when 530 kcode cycles were done.

computer time = 11.91 minutes

mcnp version 5 06212004

10/25/07 23:17:01

probid = 10/25/07 23:04:59

Chapter 7

Table of Contents

7	OPERATING PROCEDURES	7.1-1
7.1	Procedures for Loading Packages	7.1-2
7.1.1	Procedures for Wet Loading of LWR Fuel Assemblies and Canistered LWR Fuel Rods	7.1-3
7.1.2	Procedures for Dry Loading of Metallic Fuel	7.1-7
7.1.3	Procedures for Loading Metallic Fuel and Filters Containing Severely Damaged Metallic Fuel into Damaged Fuel Canisters.....	7.1-10
7.1.4	Procedures for Dry Loading of DIDO, Spiral, MOATA and MTR Fuel Elements in Basket Modules into the NAC-LWT Cask	7.1-13
7.1.5	MTR General and Preferential Loading Procedures	7.1-18
7.1.6	Procedure for Dry Loading of TRIGA Fuel Basket Modules and GA IFM Modules into the NAC-LWT Cask	7.1-33
7.1.7	Procedure for Loading TRIGA Damaged Fuel or Fuel Debris into TRIGA Sealed Failed Fuel Cans	7.1-38
7.1.8	Procedure for Wet Loading of PWR/BWR Fuel Rods into the PWR/BWR Transport Canister.....	7.1-39
7.1.9	Procedure for Wet Loading of TPBAR Consolidation Canister into the NAC-LWT Cask	7.1-41
7.1.10	Procedure for the Dry Loading of PULSTAR Fuel Into the NAC-LWT Cask.....	7.1-44
7.1.11	Procedure for Dry Loading of TPBAR Waste Container.....	7.1-49
7.1.12	Procedure for Wet Loading PWR MOX Fuel Rods in a Transport Canister Into the NAC-LWT Cask	7.1-52
7.2	Procedures for Unloading Package	7.2-1
7.2.1	Procedures for Wet Unloading of LWR Fuel and PWR, PWR MOX and BWR Fuel Rods in Transport Canisters.....	7.2-1
7.2.2	Procedures for Wet Unloading of Metallic Fuel	7.2-3
7.2.3	Procedure for Wet Unloading of MTR, TRIGA, DIDO, ANSTO or PULSTAR Fuel Basket Contents.....	7.2-6
7.2.4	Procedure for Dry Unloading of MTR, TRIGA, DIDO, ANSTO or PULSTAR Fuel Contents.....	7.2-9
7.2.5	Procedure for Dry Unloading of TPBAR Contents	7.2-10
7.3	Procedures for Preparation of the Empty Package for Transport.....	7.3-1

List of Figures

Figure 7.1-1	MTR Fuel Basket Module Loading Pattern (Top View)	7.1-22
Figure 7.1-2	LEU MTR Fuel Basket Loading Guidelines for 30 W Uniform Loading	7.1-23
Figure 7.1-3	MEU MTR Fuel Basket Loading Guidelines for 30 W Uniform Loading	7.1-24
Figure 7.1-4	HEU MTR Fuel Basket Loading Guidelines for 30 W Uniform Loading – Maximum 380 grams ²³⁵ U	7.1-25
Figure 7.1-5	HEU MTR Fuel Basket Loading Guidelines for 30 W Uniform Loading – Maximum 460 grams ²³⁵ U	7.1-26
Figure 7.1-6	HEU MTR Fuel Basket Loading Guidelines for Preferential Loading – Maximum 380 grams ²³⁵ U	7.1-27
Figure 7.1-7	HEU MTR Fuel Basket Loading Guidelines for Preferential Loading – Maximum 460 grams ²³⁵ U	7.1-28
Figure 7.1-8	DIDO LEU Cooling Time vs. Fuel Burnup Basket Module Loading Guidelines for Uniform Loading.....	7.1-29
Figure 7.1-9	DIDO MEU Cooling Time vs. Fuel Burnup Basket Module Loading Guidelines for Uniform Loading.....	7.1-30
Figure 7.1-10	DIDO HEU Cooling Time vs. Fuel Burnup Basket Module Loading Guidelines for Uniform Loading.....	7.1-31
Figure 7.1-11	Bounding DIDO Element Minimum Cool Time vs. wt % ²³⁵ U Depletion.....	7.1-32

List of Tables

Table 7.3-1	Bolt and Torque Table	7.3-2
-------------	-----------------------------	-------

7 OPERATING PROCEDURES

This chapter describes the generic operating procedures for loading, unloading and preparing the NAC-LWT package for transport. These procedures shall be implemented to ensure the package is used in accordance with Certificate of Compliance (CoC) No. 9225 for the NAC-LWT packaging.

These procedures are based on generic site conditions and assume that the package arrives at the handling site with the appropriate internals installed in the cask. Additional operations and/or modifications (i.e., sequence of operations, use of parallel operations, etc.) to these procedures to address site-specific conditions may be required for each user's facility. These additional operations and/or modifications will be documented in site-specific procedures.

In addition, site-specific procedures may incorporate signoffs for activities or operational sequences as they are performed. Oversight organizations, such as Quality Assurance or Quality Control, may participate in certain package handling operations. The use of signoffs can assist the user in assuring that critical steps are not overlooked, that the package is handled in accordance with the CoC and Safety Analysis Report (SAR), and that appropriate records are retained as required by 10 CFR 71.91.

The NAC-LWT package is designed and certified to transport numerous fissile and radioactive contents, as described in the CoC, as a Type B(U)F-96 package. Certain radioactive material contents, such as PWR MOX fuel rods, require the NAC-LWT to be assembled in a leaktight containment configuration (i.e., closure lid with metallic seal, and vent and drain Alternate B port covers with metallic seals, each individually helium leak tested to leaktight criteria prior to transport).

The NAC-LWT is also certified for the transport of Tritium Producing Burnable Absorber Rod (TPBAR) contents, as described in the CoC, as a Type B(M)-96 package. NAC-LWT cask units designated for the transport of TPBAR contents shall be configured with Alternate B vent and drain port covers in accordance with the license drawings, and subjected to the additional hydrostatic test per the requirements of Section 8.1.2. TPBAR transports shall be performed with a leaktight containment boundary.

Loaded shipments received at U.S. Department of Energy (DOE) facilities shall be receipt surveyed and monitored in accordance with DOE regulations. As required, the shipper will be notified of any survey or shipping discrepancy and the shipper will ensure appropriate regulatory notifications are completed.

When the package is handled in accordance with the procedures provided herein, and is loaded within the conditions of the CoC and the SAR, the resulting occupational exposures will be maintained as low as reasonably achievable (ALARA), as required by 10 CFR 20.

7.1 Procedures for Loading Packages

For the shipment of loaded packages, the cavity shall be dry, the contents and nameplate package identification, corresponding to the contents, shall be verified as correct, and the other applicable conditions of the Certificate of Compliance (CoC) shall be verified as met. Site-specific procedures for dry handling and loading of fuel assemblies and other authorized contents will be prepared to incorporate the dry transfer system components required to safely and efficiently load the NAC-LWT at each loading facility. Dry loading and transfer procedures are not specifically described in the individual loading procedures due to these facility and required equipment variations. Content configurations may require spacers, baskets, basket inserts, canisters, etc., to support and/or control the content geometry during transport. The transport configurations identifying the specific contents and components required are specified in the license drawings. Solid, irradiated and contaminated hardware will generally be loaded wet utilizing the procedure guidance of Section 7.1.1. Alternatively, the solid, irradiated and contaminated hardware can be loaded dry utilizing dry loading procedures (i.e., per Section 7.1.2 or 7.1.1) modified to the requirements of the dry loading facilities.

Two port cover designs are available for use. The alternate port cover has an O-ring along the barrel and an O-ring on the inner end of the port cover. The alternate port cover was developed to facilitate ease of installation and removal in the field. The second port cover design is the Alternate B port cover that has two face seals on the inner end of the port cover. The Alternate B port cover was developed to provide a leaktight and high-pressure containment boundary seal per the requirements of ANSI N14.5-1997. The Alternate B port cover is required to be installed for the transport of TPBAR contents and other authorized contents requiring a leaktight containment capability (e.g., PWR MOX fuel rods). The two port cover designs can be used interchangeably for authorized contents not requiring a leaktight or high-pressure containment boundary capability.

The alternate port cover bolts are torqued to 100 ± 10 inch-pounds. The Alternate B port cover bolts are torqued to 285 ± 15 inch-pounds to ensure compression of the metallic containment O-ring seal.

As required for the specific contents, specific procedures will specify the use of the Alternate B port covers. In these loading procedures, the more restrictive Alternate B port cover helium leakage rate testing is described. For other content loading procedures, either port cover design

can be used. However, if the Alternate B port covers are used, the metallic O-ring seal will be replaced for each transport and the helium maintenance leakage rate test is required to be performed.

For cask loading operations performed under water or when water is introduced into the cask cavity, the cask cavity is required to be blown down to remove the cavity water, vacuum dried and verified as dry, and helium backfilled prior to final closure and leakage testing. The cavity is vacuum dried by attaching a vacuum pump to the vent and/or drain port and evacuating the cavity to a pressure of less than 10 torr (13 mbar), and continuing to vacuum pump for an additional 15 minutes. If the cavity pressure rise is less than 5 torr (6.7 mbar) during a 10-minute isolation and hold period, there is no free water in the cavity and the cask cavity is verified as dry. Final containment closure and leakage testing operations in preparation for transport can proceed. If the pressure rise is >5 torr (6.7 mbar), the vacuum drying will be continued until the dryness verification criteria are met. The successful performance of the dryness verification and backfilling the cavity with helium ensures that there is no free water in the cavity and oxidation of the cask's contents is precluded. When the cask is loaded in a dry cell or under other conditions where no water is introduced into the cask cavity, the procedure sequences for cavity blow down, vacuum drying and dryness verification can be eliminated and the loading sequence can proceed directly to final closure, containment boundary leakage testing and helium backfill operations.

7.1.1 Procedures for Wet Loading of LWR Fuel Assemblies and Canistered LWR Fuel Rods

The procedures for wet loading the NAC-LWT with LWR fuel are as follows:

1. Perform a receipt inspection of the empty cask and trailer/ISO container, inspecting for transport damage.
2. Position the trailer in the designated cask unloading area. Set the trailer brakes and chock the wheels to prevent unintended movement. If site-specific conditions exist that require the trailer to move to allow the cask to be uprighted on its rotation trunnions, release brakes and remove the chocks when required to complete uprighting operations. If an ISO container is used, it may be removed from the trailer and secured in the unloading area.
3. Remove the personnel barrier or the roof and roof cross-members from the ISO container.

Note: Verify that the package nameplate displays the correct package identification number in accordance with the CoC.

4. Perform a Health Physics survey of the cask and adjacent surfaces of the trailer.

Note: A receiving survey of the cask and transporter must be performed as soon as practicable after arrival at the site to assure compliance with 10 CFR 20, 10 CFR 71.87(i) and 10 CFR 71.47, and to assure timely reporting of any reportable noncompliance.

5. Remove the top and bottom impact limiters.
6. Remove the cask tie-down strap.
7. Using the lifting yoke with the guides removed, engage the lifting trunnions. Raise the cask to vertical by rotating the cask rotation sockets on the rear cask supports, moving the crane and/or trailer as required to keep the lift yoke engaged to the trunnions and the cask engaged in the rear supports. When the cask is fully vertical, lift the cask from the supports and remove it from the trailer/container.
8. Place the cask in the cask preparation area or other designated location. Disengage the lifting yoke. Clean cask surfaces of road dirt as required for entry into the spent fuel pool.
9. Visually inspect the neutron shield tank fill, drain and level inspection plugs for signs of neutron shield fluid leakage. If leakage is detected or suspected, verify shield tank fluid level and correct, as required.
10. Remove the vent and drain valve port covers. Prior to reinstallation of the port covers, carefully inspect the valve port cover O-ring seals and, if the O-rings show any damage, replace them with approved spares. Ensure that the replacement O-rings are properly installed and seated. Visually inspect the valved quick-disconnect nipples and replace them, if necessary.

Note: For Alternate B port covers, replace the metallic O-ring with an approved spare prior to reinstallation.

11. Remove closure lid bolts. Attach the lid lift slings to the closure lid. Remove the closure lid and set it on a support that is suitable for radiological control and for maintaining the cleanliness of the closure lid. Prior to reinstallation of the lid, carefully inspect the Teflon O-ring seal in the underside of the closure lid and, if it shows any damage, replace it. Remove the metallic O-ring and replace it with an approved spare. Ensure that the replacement O-rings are properly installed and seated. Inspect the lid bolts and replace any that are damaged.
12. Visually inspect the inner cavity for foreign material or damage. Install or verify the presence of the proper drain tube and basket assembly.
13. Fill the cask cavity with clean water.
14. Install lift yoke arm guides and remote actuation component on the cask lifting yoke.
15. Engage the cask lifting yoke with the cask lifting trunnions and pick up the cask. Carefully lower the cask to the bottom of the cask loading area. Rinse the cask surfaces with clean water to minimize cask surface contamination.
16. Disengage the lifting yoke from the cask and remove the yoke from the pool, if necessary, to provide fuel loading clearance.

17. Identify the fuel assembly(ies) or canistered LWR fuel rods to be loaded. Verify the identified materials comply with the content conditions and authorized quantities as specified in the CoC.
18. Pick up the fuel assembly or transport canister containing individual fuel rods, using the required grapple system.

Note: See Section 7.1.8 procedures for instructions for loading and preparing PWR or BWR rods in a transport canister.
19. Position the fuel contents over the cask and carefully lower them into the cask to avoid damage to the cask sealing surfaces. Confirm that the fuel assembly (or transport canister and insert, or material container) is fully seated, then release the grapple from the fuel assembly (or transport canister and insert) and raise the grapple to the full up position. Repeat this step as necessary to load multiple assemblies or containers (if required).
20. Position the cask lifting yoke over the cask closure lid. Attach the slings to the closure lid and cask lifting yoke. Lower the yoke over the cask.
21. Position the closure lid over the cask and slowly lower it into place using the cask and lid match marks as guides. Visually confirm that the closure lid is seated.
22. Lower the cask handling yoke to slack the closure lid cables. Engage the cask lifting trunnions with the yoke and begin lifting.

Note: Visually verify the yoke engagement before lifting the cask.
23. Raise the cask until the lid is slightly above the surface of the pool. At the option of the licensee/user, a number of closure lid bolts (i.e., 4 to 12) may be installed hand tight.
24. Raise the cask clear of the pool, rinsing the yoke and cask with clean water.
25. Transfer the cask to the decontamination pit or other work area. Remove the yoke and lid lift slings.
26. Install and tighten the 12 closure lid bolts to 260 ± 20 ft-lb in three passes, using the torque sequence stamped on the closure lid.
27. At the option of the licensee/user, a 25 to 50 gallon clean water flush of the cask cavity may be performed by connecting a valved, clean water line to the drain valve and a valved drain line to the vent valve. After the cavity flushing is completed, if performed, disconnect the water supply and drain lines.
28. Connect a gas supply line to the vent valve and the drain line to the drain valve.
29. Open the nitrogen or helium gas supply valve and pressurize the cask cavity (< 30 psig) to force any residual water out the drain line. Continue to supply pressurized gas to the cask for a minimum of five minutes after the last residual free water discharges from the drain. Remove the drain and gas supply lines and attach a vacuum drying system (VDS) to the vent.
30. Evacuate the cask cavity to less than or equal to 10 torr (13 mbar) and continue vacuum pumping for a minimum of 15 minutes.

31. At the end of the vacuum pumping period, isolate the cask cavity from the vacuum pump and stop the vacuum pump. Monitor the cask cavity pressure for a minimum of 10 minutes. If the pressure rise is less than 5 torr (6.7 mbar), the cavity is verified as dry of free water. If the pressure rise is >5 torr (6.7 mbar), repeat vacuum drying until the dryness verification results are satisfactory.
32. Backfill the cask cavity with helium to 0 psig (1 atmosphere, absolute), +1, -0 psi and disconnect the VDS from the vent valve.
33. Perform a helium leakage test of the closure lid containment O-ring using a Helium Mass Spectrometer Leak Detector (He MSLD) in accordance with the procedural requirements of Section 8.1.3.1, Steps 3 through 10.
34. Install the vent and drain alternate port covers and torque the bolts to 100 ± 10 inch-pounds.
35. If an alternate port cover containment O-ring seal was replaced, perform a helium leakage test on the affected port cover using a He MSLD in accordance with the requirements of Section 8.1.3.2.2.
36. If the alternate port cover containment seal was inspected and accepted for reuse, perform a gas pressure drop leakage test on the affected port cover as follows.
 - a. Install a pressure test fixture to the port cover test port, including a calibrated pressure gauge with a minimum sensitivity of 0.25 psi.
 - b. Pressurize the port cover seal annulus to 15 psig, +1, -0 psi.
 - c. Isolate the gas supply and observe the pressure gauge for a minimum of five minutes.
 - d. The acceptance criterion for the test is no measurable drop in pressure during the minimum test time. An acceptable test assures that the minimum assembly verification leakage test sensitivity is achieved.

Note: Alternate B port covers, if used, require the satisfactory completion of a helium maintenance leakage rate test to confirm a leaktight seal condition for each loaded transport. Install the Alternate B port cover, torque the high-strength bolts to 285 ± 15 inch-pounds, and perform the maintenance leakage rate test per the requirements of Section 8.1.3.3.
37. Decontaminate the cask surfaces. Survey the cask for surface contamination and radiation dose rates.

Note: Ensure compliance with 10 CFR 71.87(i) and 10 CFR 71.47.
38. Remove lift yoke arm guides. Engage the cask lifting yoke to the lifting trunnions.
39. Lift the cask and position the cask rotation sockets in the rear rotation trunnions of the rear support structure. Carefully lower the cask to the horizontal transport orientation resting on the front saddle by moving the crane and/or the trailer as required to maintain cask engagement to the rear supports.
40. Disengage the lifting yoke from the lifting trunnions and remove it from the area.

41. Install the cask tie-down strap. Install the top and bottom impact limiters.
42. Install tamper seal wire and number seal on the top attachment point on the top impact limiter.
43. Install ISO container bracing and lid or personnel barrier.
44. Complete radiation and contamination surveys of the external surfaces of the package and record the data. Ensure removable contamination and radiation dose rate survey results comply with the limits specified in 10 CFR 71.87(i) and (j).
45. Measure the dose rate in millirems per hour at one meter from the package surface to determine the Transport Index (TI). Indicate the TI on the Radioactive Material labels applied to the package in accordance with 49 CFR 172, Subpart E.
46. Determine the appropriate Criticality Safety Index (CSI) assigned to the package contents in accordance with the CoC, and indicate the correct CSI on the Fissile Material label applied to the package per 49 CFR 172, Subpart E.
47. Apply appropriate placards to the transport vehicle in accordance with 49 CFR 172, Subpart F.
48. Complete the shipping documents and provide the carrier with instructions regarding the requirements for maintaining an exclusive use shipment.

7.1.2 Procedures for Dry Loading of Metallic Fuel

The procedures for dry loading the package with metallic fuel are as follows:

1. Perform a receipt inspection of the empty cask and trailer/ISO container, inspecting for transport damage.
2. Position the trailer in the designated cask unloading area. Set the trailer brakes and chock the wheels to prevent unintended movement. If site-specific conditions exist that require the trailer to move to allow the cask to be uprighted on its rotation trunnions, release brakes and remove the chocks when required to complete uprighting operations. If an ISO container is used, it may be removed from the trailer and secured in the unloading area.
3. Remove the roof from the ISO container and open the front and rear ISO doors. Remove roof cross-members, if installed.
Note: Verify that the package nameplate displays the correct package identification number in accordance with the CoC.
4. Perform a Health Physics survey of the cask and adjacent surfaces of the container.
Note: A receiving survey of the cask and transporter must be performed as soon as practicable after arrival at the site to ensure compliance with 10 CFR 20, 10 CFR 71.87(i) and 10 CFR 71.47, and to ensure timely reporting of any reportable noncompliance.
5. Remove the top and bottom impact limiters.

6. Remove the cask tie-down strap.
7. Using the lifting yoke with the guides removed, engage the lifting trunnions. Raise the cask to vertical by rotating the cask rotation sockets on the rear cask supports, moving the crane and/or trailer as required to keep the lift yoke engaged to the trunnions and the cask engaged in the rear supports. When the cask is fully vertical, lift the cask from the supports and remove it from the trailer/container.
8. Place the cask in the dry loading stand. Disengage the lifting yoke.
9. Remove the vent and drain valve port covers. Prior to reinstallation of the port covers, carefully inspect the O-rings and, if the O-rings show any damage, replace them with approved spares. Ensure that the replacement O-rings are properly installed and seated. Visually inspect the valved quick-disconnect nipples and replace them, if necessary.

Note: For Alternate B port covers, replace the metallic O-ring with an approved spare prior to reinstallation.
10. Remove closure lid bolts. Attach the lid lift slings to the closure lid. Remove the closure lid and set it on a support that is suitable for radiological control and for maintaining the cleanliness of the closure lid. Prior to reinstallation of the lid, carefully inspect the Teflon O-ring seal in the underside of the closure lid and, if it shows any damage, replace it. Remove the metallic O-ring and replace it with an approved spare. Ensure that the replacement O-rings are properly installed and seated. Inspect the lid bolts and replace any that are damaged.
11. Visually inspect the inner cavity for foreign material or damage. Install, or verify the presence of the proper drain tube assembly and basket, as required.
12. Install the required dry transfer system components to the top of the cask.
13. Position the shielded transfer cask system components for fuel loading, as appropriate.
14. Identify the fuel to be loaded and verify that the fuel contents comply with the content conditions and authorized quantities as specified in the CoC. Up to five sound metallic fuel rods may be placed in an unsealed canister. Damaged rods may be placed in a sealed 2.75-inch or 4.0-inch failed fuel canister (FFC). Up to 10 filters containing oxide powder from severely damaged metallic fuel rods may be placed in one FFC. The FFC(s) containing filters may be loaded with up to two FFCs containing failed fuel rods to fill the three-element basket. The FFCs must be vacuum dried and sealed as described in Section 7.1.3.
15. Load the shielded transfer cask with the selected fuel contents.
16. Place the shielded transfer cask, containing a fuel canister, onto the dry transfer system components positioned on the top of the cask.
17. Lower the fuel canister from the transfer cask into the shipping cask.
18. Repeat the loading and transfer of fuel canisters until the approved cask loading plan is completed.

19. Install the closure lid onto the cask. Visually verify that the lid is properly seated.
20. Remove the dry transfer system components from the top of the cask.
21. Install and tighten the 12 closure lid bolts to 260 ± 20 ft-lb in three passes, using the torque sequence stamped on the closure lid.
22. This step applies only if the cask contains damaged metallic fuel or severely damaged metallic fuel.
 - a. Attach the vacuum pump to the cask vent valve.
 - b. Evacuate the cask cavity to ≤ 10 torr (13 mbar) and maintain for a minimum of 15 minutes.
 - c. Stop the vacuum pump and monitor pressure for a minimum of 10 minutes. If the pressure rise is less than 5 torr (6.5 mbar), the cask is adequately dried for shipment. If not, repeat vacuum drying and pressure rise verification.
 - d. Remove the vacuum pump and backfill the cask cavity with helium to 1 atmosphere (absolute) +1, -0 psi.
 - e. Remove the gas supply line.
23. Perform the helium mass spectrometer leakage rate test on the cask lid in accordance with the requirements of Section 8.1.3.1, Steps 3 through 10.
24. Install the vent and drain alternate port covers and torque the bolts to 100 ± 10 inch-pounds.
25. If an alternate port cover containment O-ring seal was replaced, perform a helium leakage test on the affected port cover using a He MSLD in accordance with the requirements of Section 8.1.3.2.2.
26. If the alternate port cover containment seal was inspected and accepted for reuse, perform a gas pressure drop leakage test on the affected port cover as follows.
 - a. Install a pressure test fixture to the port cover test port, including a calibrated pressure gauge with a minimum sensitivity of 0.25 psi.
 - b. Pressurize the port cover seal annulus to 15 psig, +1, -0 psi.
 - c. Isolate the gas supply and observe the pressure gauge for a minimum of five minutes.
 - d. The acceptance criterion for the test is no measurable drop in pressure during the minimum test time. An acceptable test assures that the minimum assembly verification leakage test sensitivity is achieved.

Note: Alternate B port covers, if used, require the satisfactory completion of a helium maintenance leakage rate test to confirm a leaktight seal condition for each loaded transport. Install the Alternate B port cover, torque the high-strength bolts to 285 ± 15 inch-pounds, and perform the maintenance leakage rate test per the requirements of Section 8.1.3.3.

27. Decontaminate the cask. Survey the cask for surface contamination and radiation dose rates.
Note: Ensure compliance with 10 CFR 71.87(i) and 10 CFR 71.47.
28. Remove lift yoke arm guides. Engage the cask lifting yoke to the lifting trunnions.
29. Lift the cask and position the cask rotation sockets in the rear rotation trunnions of the rear support structure. Carefully lower the cask to the horizontal transport orientation resting on the front saddle by moving the crane and/or the trailer as required to maintain cask engagement to the rear supports.
30. Disengage the lifting yoke from the lifting trunnions and remove it from the area.
31. Install the cask tie-down strap. Install the top and bottom impact limiters.
32. Install tamper seal wire and number seal on the top attachment point on the top impact limiter.
33. Install ISO container bracing and lid or personnel barrier.
34. Complete radiation and contamination surveys of the external surfaces of the package and record the data. Ensure removable contamination and radiation dose rate survey results comply with the limits specified in 10 CFR 71.87(i) and (j).
35. Measure the dose rate in millirems per hour at one meter from the package surface to determine the Transport Index (TI). Indicate the TI on the Radioactive Material labels applied to the package in accordance with 49 CFR 172, Subpart E.
36. Determine the appropriate Criticality Safety Index (CSI) assigned to the package contents in accordance with the CoC, and indicate the correct CSI on the Fissile Material label applied to the package per 49 CFR 172, Subpart E.
37. Apply appropriate placards to the transport vehicle in accordance with 49 CFR 172, Subpart F.
38. Complete the shipping documents and provide the carrier with instructions regarding the requirements for maintaining an exclusive use shipment.

7.1.3 Procedures for Loading Metallic Fuel and Filters Containing Severely Damaged Metallic Fuel into Damaged Fuel Canisters

7.1.3.1 Small Diameter Canisters (Damaged Metallic Fuel)

1. Examine the small diameter failed fuel canister (FFC) and check it for damage.
2. Place the FFC inside the containment barrier portion of the pool. Position the FFC in the failed rod loading station.

3. After verifying the accountability records, place the designated failed fuel rod into the FFC. If the rod is broken into two or more pieces, verify that the lid thread and seal area is not fouled during rod insertion.
4. When the can is loaded, install the lid using the FFC Lid Installation Tool.
5. Using the FFC handling tool, move the loaded FFC through the containment barrier door and place the FFC horizontally into the upender.
6. Operate the hand winch to move the FFC to the vertical position.
7. Torque the FFC lid to 100 ± 10 ft-lb for the small canister.
8. Connect the nitrogen supply line to the vent valve.
9. Open nitrogen supply valve and pressurize the FFC to force out the water. Blow gas through the FFC for at least 5 minutes after the first visible bubbles appear. Remove the gas supply line.
10. Invert the FFC in the upender and install the pipe plug.
11. Re-invert the FFC in the upender.
12. Attach the vacuum pump to the FFC vent valve. Evacuate the FFC to a pressure below 25 torr (33 mbar) for a minimum of 15 minutes. Remove the vacuum pump and backfill with nitrogen.
13. Remove the FFC from the upender and place it into temporary storage.

7.1.3.2 Large Diameter Canisters (Damaged Metallic Fuel)

1. Examine the large diameter FFC and check it for damage.
2. Place the FFC inside the containment barrier portion of the pool. Position the FFC in the failed rod loading station.
3. This step is to be used when loading up to three uncanned or canned fuel rods into the large diameter canister. After verifying the accountability records, remove the ceramic filter from the top of the original failed rod can. Position the can plug with aluminum screen onto the open can. Install the plug.
4. Verify the accountability records for the fuel to be loaded.
5. Place the designated fuel into the FFC. If the rod is broken into two or more pieces, verify that the lid thread and seal area is not fouled during rod or can insertion. If more than one failed rod is to be installed, repeat steps 3 through 5.
6. After the canister is loaded with fuel, install the lid using the FFC Lid Installation Tool.
7. Using the FFC handling tool, move the loaded FFC through the containment barrier door and place the FFC horizontally into the upender.
8. Operate the hand winch to move the FFC to the vertical position.

9. Torque the FFC lid to 130 ± 10 ft-lb for the large canister.
10. Connect the nitrogen supply line to the vent valve.
11. Open the nitrogen supply valve and pressurize the FFC to force out the water. Blow gas through the FFC for at least 5 minutes after the first visible traces of bubbles appear. Remove the gas supply line.
12. Invert the FFC in the upender and install the pipe plug.
13. Reinvert the FFC in the upender.
14. Attach the vacuum pump to the FFC vent valve. Evacuate the FFC to a pressure below 25 torr (33 mbar) for a minimum of 15 minutes. Remove the vacuum pump and backfill with nitrogen.
15. Remove the FFC from the upender and place it into temporary storage.

7.1.3.3 Large Diameter Canisters (Severely Damaged Metallic Fuel)

1. Examine the large diameter FFC and check it for damage.
2. Place the FFC inside the containment barrier portion of the pool. Position the FFC in the failed rod loading station.
3. Verify the accountability records for the fuel in the filter set (up to 10 filters) to be loaded into the FFC.
4. After verifying the accountability records, load the filter set into the FFC and place aluminum wool on top of the last filter.
5. Verify that the lid thread and seal area is not fouled during insertion of the filter set.
6. After the canister is loaded with fuel, insert the lid using the FFC Lid Installation Tool.
7. Using the FFC handling tool, move the loaded FFC through the containment barrier door and place the FFC horizontally into the upender.
8. Operate the hand winch to move the FFC to the vertical position.
9. Torque the FFC lid to 130 ± 10 ft-lb for the large canister.
10. Connect the nitrogen supply line to the vent valve.
11. Open the nitrogen supply valve and pressurize the FFC to force out the water. Continue to blow gas through the FFC for at least 5 minutes after the first visible traces of bubbles appear. Remove the gas supply line.
12. Invert the FFC in the upender and install the pipe plug.
13. Re-invert the FFC in the upender.
14. Attach the vacuum pump to the FFC vent valve. Evacuate the FFC to a pressure below 25 torr (33 mbar) for a minimum of 15 minutes. Remove the vacuum pump and backfill with nitrogen.

15. Remove the FFC from the upender and place it into temporary storage.

7.1.4 Procedures for Dry Loading of DIDO, Spiral, MOATA and MTR Fuel Elements in Basket Modules into the NAC-LWT Cask

This procedure presents the steps for dry loading of fuel basket modules into the NAC-LWT cask using a transfer cask, which can contain various types of reactor fuel elements such as MTR, DIDO, spiral and plate assemblies (i.e., MOATA elements). The design, materials, use and function of the various modular fuel basket assemblies such as MTR, DIDO and ANSTO are similar, and all can be loaded into the NAC-LWT utilizing these procedures.

The modular fuel basket assemblies all consist of three types of modules: a base module, intermediate modules, and a top module. Each basket module contains seven fuel element locations, consisting of a center cell and six peripheral cells. The top basket module interfaces with the cask lid to limit the axial movement of the basket assembly. The base module interfaces with the bottom of the cask cavity. The base and intermediate modules are provided with guide pins to provide for and maintain the proper alignment between basket modules. Each of the basket module types is provided with a guide bar assembly to provide for the proper interface of the basket assembly with the drain tube assembly.

Depending on the fuel type, the basket assembly may consist of 4, 5 or 6 modules, with a varying number of intermediate modules. For the DIDO, MOATA and spiral fuel types, the DIDO and ANSTO (the basket assembly identification for MOATA and spiral fuel types) basket assemblies consist of a top module, four intermediate modules and a base module. In the case of MTR fuel elements, the basket assembly can include 2, 3 or 4 intermediate modules, depending on the length and conditions of the fuel contents. Axial fuel spacers and plates may be used as dunnage to axially position the MTR fuel elements in the basket module to facilitate fuel unloading operations.

The fuel content condition (i.e., heat load, fissile mass, minimum cool time, etc.) limits for the various fuel types are discussed or referenced in the following paragraphs.

MTR fuel elements shall be selected and loaded in accordance with the MTR General and Preferential Loading Procedures in Section 7.1.5. The MTR plate canister, if required, shall be loaded in accordance with Section 7.1.4.1.

DIDO fuel elements shall meet the following loading conditions:

- The maximum decay heat per DIDO fuel element shall not exceed 25 W.
- The maximum decay heat load for a loaded DIDO fuel basket assembly shall not exceed 1.05 kW.

- The heat load for each DIDO fuel element shall be verified by use of cool time versus burnup (MWd/MTU) curves in Figure 7.1-8 (LEU fuel), Figure 7.1-9 (MEU fuel), and Figure 7.1-10 (HEU fuel), or by use of minimum cool time versus ^{235}U depletion curves in Figure 7.1-11 (generic for LEU, MEU and HEU fuels). Note that significantly lower uranium content for a loaded assembly compared to the design basis assembly may result in a loaded assembly calculated burnup higher than that included in Figure 7.1-8 through Figure 7.1-10. Use of Figure 7.1-11 ^{235}U depletion curves is required for fuel assemblies in this category.
- An additional requirement for fuel element loading of the top module limits the heat load to 18 W per element, unless there is a spacer bolted to the underside of the closure lid, or there is sufficient fuel element hardware to ensure that axial movement of the fuel element is limited, to ensure that the active fuel region is radially shielded by the gamma shield lead layer. A lid spacer, if required, shall be as shown on NAC Drawing No. 315-40-113.

Spiral and MOATA fuel elements shall meet the content conditions specified in the Certificate of Compliance for loading into the ANSTO fuel basket assembly. Full spiral fuel loads or mixed spiral and MOATA fuel loads are authorized with separate basket modules containing the two fuel types.

The procedures for loading the NAC-LWT cask with MTR, DIDO or ANSTO fuel baskets in a dry configuration or using a dry transfer system are as follows:

1. Perform a receipt inspection of the empty cask and trailer/ISO container, inspecting for transport damage.
2. Position the trailer in the designated cask unloading area. Set the trailer brakes and chock the wheels to prevent unintended movement. If site-specific conditions exist that require the trailer to move to allow the cask to be uprighted on its rotation trunnions, release brakes and remove the chocks when required to complete uprighting operations. If an ISO container is used, it may be removed from the trailer and secured in the unloading area.
3. Remove the personnel barrier or the roof and roof cross-members from the ISO container.

Note: Verify that the package nameplate displays the correct package identification number in accordance with the CoC.

4. Perform a Health Physics survey of the cask and adjacent surfaces of the trailer.

Note: A receiving survey of the cask and transporter must be performed as soon as practicable after arrival at the site to assure compliance with 10 CFR 20, 10 CFR 71.87(i) and 10 CFR 71.47, and to assure timely reporting of any reportable noncompliance.

5. Remove the top and bottom impact limiters.
6. Remove the cask tie-down strap.

7. Using the lifting yoke with the guides removed, engage the lifting trunnions. Raise the cask to vertical by rotating the cask rotation sockets on the rear cask supports, moving the crane and/or trailer as required to keep the lift yoke engaged to the trunnions and the cask engaged in the rear supports. When the cask is fully vertical, lift the cask from the supports and remove it from the trailer/container.
8. Place the cask onto the dry loading station/stand. Disengage the lifting yoke and move clear.
9. Visually inspect the neutron shield tank fill, drain and level inspection plugs for signs of neutron shield fluid leakage. If leakage is detected or suspected, verify shield tank fluid level and correct, as required.
10. Remove the vent and drain valve port covers. Prior to reinstallation of the port covers, carefully inspect the O-ring seals and, if the O-rings show any damage, replace them with approved spares. Ensure that the replacement O-rings are properly installed and seated. Visually inspect the valved quick-disconnect nipples and replace them, if necessary.

Note: For Alternate B port covers, replace the metallic O-ring with an approved spare prior to reinstallation.
11. Remove closure lid bolts. Attach the lid lift slings to the closure lid. Remove the closure lid and set it on a support that is suitable for radiological control and for maintaining the cleanliness of the closure lid. Prior to reinstallation of the lid, carefully inspect the Teflon O-ring seal in the underside of the closure lid and, if it shows any damage, replace it. Remove the metallic O-ring and replace it with an approved spare. Ensure that the replacement O-rings are properly installed and seated. Inspect the lid bolts and replace any that are damaged.
12. Visually inspect the inner cavity for foreign material or damage. Install or verify presence of a proper drain tube including drain tube alignment ring, as required.
13. Install the required dry transfer system components on the top of the cask.
14. Position the shielded transfer cask system components for fuel loading, as appropriate.
15. Identify the fuel to be loaded into each fuel basket module. Fuel elements loaded into each basket and/or module shall comply with the approved content conditions specified in Condition 5.(b)(1) and 5.(b)(2) of CoC No. 9225. Specific guidance on fuel selection, use of loading diagrams and preferential loading procedures is provided in Section 7.1.5. Perform an independent verification of the loading diagrams and fuel loading operations per Section 7.1.5.3.

Note: If a basket module is to be loaded with a LEU MTR fuel element having ^{235}U content >470 g (>22 g ^{235}U per plate), cell black spacers, as shown on Drawing 315-40-085, shall be installed in basket module cell positions 1, 2 and 3 to prevent inadvertent loading of more than four LEU MTR fuel elements.

Note: For the loading of HEU MTR fuel elements having ^{235}U content >380 g, a minimum of 2.0 cm of nonfuel hardware and /or spacer plates shall be provided at both ends of the fuel element to meet criticality control analysis requirements.

16. Load the shielded transfer cask and basket module with the selected fuel contents.
17. Place the shielded transfer cask containing a loaded fuel basket module onto the dry transfer system components positioned on the top of the cask.
18. Lower the loaded basket module from the transfer cask into the shipping cask.
19. Repeat the loading and transfer of loaded basket modules until the approved cask loading plan is completed.
20. Install the closure lid onto the cask using the dry transfer system. Visually verify that the lid is properly seated.
21. Remove the dry transfer system components from the top of the cask.
22. Install and tighten the 12 closure bolts to 260 ± 20 ft-lb in three passes, using the sequence stamped on the lid.
23. Connect a gas supply line to the vent valve and the drain line to the drain valve.
24. Open the air, nitrogen or helium gas supply valve and pressurize the cask cavity (< 30 psig) to force any residual water out the drain line. Continue to supply pressurized gas to the cask for a minimum of five minutes after the last residual free water discharges from the drain. Remove the drain and gas supply lines and attach a vacuum drying system (VDS) to the vent.
25. Evacuate the cask cavity to less than or equal to 10 torr (13 mbar) and continue vacuum pumping for a minimum of 15 minutes.
26. At the end of the vacuum pumping period, isolate the cask cavity from the vacuum pump and stop the vacuum pump. Monitor the cask cavity pressure for a minimum of 10 minutes. If the pressure rise is less than 5 torr (6.7 mbar), the cavity is verified as dry of free water. If pressure rise is >5 torr (6.7 mbar), repeat vacuum drying until the dryness verification results are satisfactory.
27. Backfill the cask cavity with helium to 0 psig (1 atmosphere, absolute), +1, -0 psi and disconnect the VDS from the vent valve.
28. Perform a helium leakage test of the closure lid containment O-ring using a Helium Mass Spectrometer Leak Detector (He MSLD) in accordance with the procedural requirements of Section 8.1.3.1, Steps 3 through 10.
29. Install the vent and drain alternate port covers and torque the bolts to 100 ± 10 inch-pounds.
30. If an alternate port cover containment O-ring seal was replaced, perform a helium leakage test on the affected port cover using a He MSLD in accordance with the requirements of 8.1.3.2.2.
31. If the alternate port cover containment seal was inspected and accepted for reuse, perform a gas pressure drop leakage test on the affected port cover as follows.
 - a. Install a pressure test fixture to the port cover test port including a calibrated pressure gauge with a minimum sensitivity of 0.25 psi.

- b. Pressurize the port cover seal annulus to 15 psig, +1, -0 psi.
- c. Isolate the gas supply and observe the pressure gauge for a minimum of five minutes.
- d. The acceptance criterion for the test is no measurable drop in pressure during the minimum test time. An acceptable test assures that the minimum assembly verification leakage test sensitivity is achieved.

Note: Alternate B port covers, if used, require the satisfactory completion of a helium maintenance leakage rate test to confirm a leaktight seal condition for each loaded transport. Install the Alternate B port cover, torque the high-strength bolts to 285 ± 15 inch-pounds, and perform the maintenance leakage rate test per the requirements of Section 8.1.3.3.

32. Decontaminate the cask surfaces. Survey the cask for surface contamination and radiation dose rates.

Note: Ensure compliance with 10 CFR 71.87(i) and 10 CFR 71.47

33. Remove lift yoke arm guides. Engage the cask lifting yoke to the lifting trunnions.
34. Lift the cask and position the cask rotation sockets in the rear rotation trunnions of the rear support structure. Carefully lower the cask to the horizontal transport orientation resting on the front saddle by moving the crane and/or the trailer as required to maintain cask engagement to the rear supports.
35. Disengage the lifting yoke from the lifting trunnions and remove it from the area.
36. Install the cask tie-down strap. Install the top and bottom impact limiters.
37. Install tamper seal wire and number seal on the top attachment point on the top impact limiter.
38. Install ISO container bracing and lid, or personnel barrier.
39. Complete radiation and contamination surveys of the external surfaces of the package and record the data. Ensure removable contamination and radiation dose rate survey results comply with the limits specified in 10 CFR 71.87(i) and (j).
40. Measure the dose rate in millirems per hour at one meter from the package surface to determine the Transport Index (TI). Indicate the TI on the Radioactive Material labels applied to the package in accordance with 49 CFR 172, Subpart E.
41. Determine the appropriate Criticality Safety Index (CSI) assigned to the package contents in accordance with the CoC, and indicate the correct CSI on the Fissile Material label applied to the package per 49 CFR 172, Subpart E.
42. Apply appropriate placards to the transport vehicle in accordance with 49 CFR 172, Subpart F.
43. Complete the shipping documents and provide the carrier with instructions regarding the requirements for maintaining an exclusive use shipment.

7.1.4.1 Procedure for Loading MTR Fuel Plates into MTR Plate Canister

1. Examine the MTR plate canister and inspect for damage. Visually verify that one end of the canister is installed, the six associated bolts are installed and the other end is removed.
2. Place the can in the loading fixture.
3. Load the fuel plates into the canister. Verify that the number of fuel plates in the canister is no more than the maximum number of plates in an intact MTR fuel element of its type.
4. Install the lid and lid bolts.

7.1.5 MTR General and Preferential Loading Procedures

Up to 42 LEU, MEU, and HEU MTR fuel elements may be loaded into the NAC-LWT MTR Fuel Basket, i.e., 7 fuel elements per basket module \times 6 basket modules per fuel basket, except for LEU MTR fuel elements with greater than 470 g ^{235}U , which are limited to 4 elements per basket module as detailed in the following paragraphs. Each MTR basket module has 7 fuel element positions. The MTR basket module loading diagram presented in Figure 7.1-1 has a center position (Position 1), two exterior positions (Positions 2 and 3) that are in line with the center position, and four exterior positions (Positions 4, 5, 6, and 7) that are adjacent to the center row positions. The basket module's fuel element locations are specifically identified to ensure loading of each location with the appropriate fuel element. Ensuring MTR fuel loadings are performed in strict accordance with the procedures presented herein will ensure that the MTR fuel content conditions of the Certificate of Compliance (CoC) are met and that the analyses presented in this SAR are bounded.

MTR fuel elements are selected for loading into specific fuel element locations based on the decay heat of each individual fuel element at the time of loading. Figure 7.1-2 through Figure 7.1-5 are provided to assist in determining the acceptability of a MTR fuel element for loading in a 30 W uniform loading pattern depending on enrichment (i.e., LEU, MEU or HEU) or ^{235}U content (i.e. 380 or 460 grams). For determining the acceptability of higher heat load HEU fuel elements, Figure 7.1-6 and Figure 7.1-7 are provided for 380 and 460 grams of ^{235}U , respectively. The use of the fuel element cool time versus fuel burnup figures are described in Section 7.1.5.4. LEU MTR fuel elements with a ^{235}U content greater than 470 grams, but not exceeding 640 grams, are restricted to baskets containing a maximum of four fuel elements (or an equivalent number of fuel plates per opening). The four element per basket module is in effect even if only one LEU MTR assembly exceeds 470 g per element. Specific basket locations and restrictions for the high load LEU elements are described in Section 7.1.5.1.

The procedural steps and sequence to ensure the MTR fuel loading and content condition limits are met are: 1) determine ^{235}U content weight per element; 2) determine fuel element decay heat load per Section 7.1.5.4; 3) determine basket module loading position for each element and overall basket loading pattern; and 4) individual basket module loading and assembly of the fuel basket in the NAC-LWT. Each of these steps is independently verified.

Attention to the overall cask loading pattern allows the decay heat load of the cask to be maintained as uniform, as is practical and within CoC total heat load limits. Loading diagrams for each individual module and the complete cask assembly shall be developed and used during the basket module and cask loading operations. After the decay heat load of each of the MTR fuel elements to be loaded and transported is calculated or determined and verified, the loading and content considerations of Sections 7.1.5.1 through 7.1.5.3 shall be met or complied with to establish the final acceptable loading pattern and sequence.

7.1.5.1 General Loading Requirements

1. The maximum decay heat load per MTR fuel basket module shall not exceed 210 W and the maximum decay heat load per cask (package) shall not exceed 1.26 kW. A MTR fuel element with a decay heat greater than 120 W shall not be loaded.
2. LEU, MEU and HEU MTR fuel elements with decay heat not exceeding 30 W per element may be loaded in any basket module fuel element location in any combination.
3. HEU MTR fuel elements with decay heats exceeding 30 W shall be preferentially loaded in a basket module in decreasing decay heat order according to the loading diagram in Figure 7.1-1, with the highest heat load element loaded in fuel location one. Fuel elements with heat loads of up to 120 W shall only be loaded in the center fuel element location of any MTR fuel basket module. The decay heat of the fuel element in either of the two fuel element locations (i.e., number 2 or 3), in line with the center fuel element location of a MTR fuel basket module, shall not exceed 70 W.
4. LEU MTR fuel elements (or canistered fuel plates) with a ^{235}U content greater than 470 g, and not exceeding 640 g, shall only be loaded into basket positions 4, 5, 6 and 7 shown in Figure 7.1-1. In order to ensure that baskets containing the high fissile mass LEU MTR elements ($>470\text{ g }^{235}\text{U}$) will not be loaded with fuel elements (or fuel plates) in basket opening positions 1, 2 and 3, a cell block spacer shall be installed in each of these three basket openings. The cell block spacer, as shown on Drawing 315-40-085, is of sufficient height and diameter to ensure that LEU MTR fuel elements are prevented from being placed in these openings. The capacity limitation of a maximum of four MTR fuel elements per module is in effect even if a single LEU MTR fuel elements (or canistered fuel plates) having $>470\text{ g }^{235}\text{U}$ is to be loaded.
5. An MTR plate canister may be loaded into any fuel basket module fuel element location. The contents of each plate canister shall be limited to the number of fuel plates, dimensions and masses of an equivalent intact MTR fuel element.

6. MTR fuel elements with corrosion and/or mechanically damaged cladding may be loaded, provided that the total surface area of through-clad corrosion and/or mechanical damage does not exceed 2,775 cm² per package.

7.1.5.2 Determination of Basket Module Loading Pattern

1. Perform an evaluation of the full inventory of fuel elements to be loaded into the NAC-LWT cask(s) and develop an overall loading plan that minimizes overall dose rates to minimize general population dose and operator dose. The loading of LEU MTR fuel elements with greater than 470 g ²³⁵U shall be governed by the loading restrictions in item 4 of Section 7.1.5.1, and cell block spacers shall be placed in basket loading positions 1, 2 and 3 to prevent inadvertent loading of more than four high fissile mass LEU MTR elements.
2. Select up to seven MTR fuel elements to be loaded in a basket module meeting the general loading requirements of Section 7.1.5.1. Identify if spacers or spacer plates are required to properly position the MTR elements axially in the basket module.
3. Rank the fuel elements in order of decreasing decay heat load from 1 to 7. (i.e., the assembly with the highest decay heat is designated number 1.)
4. Generate loading diagrams for each basket module based on Figure 7.1-1, by placing the numbered assemblies in the matching numbered basket module positions, except that fuel elements ranked 4,5,6 or 7 may be loaded in any of the outer (i.e., 4-7) basket module positions.
5. Repeat steps 1 through 4 for all of the basket modules to be loaded.
6. Independently verify the basket module loading diagrams.
7. The loading diagrams shall be used to direct the loading of the basket modules per Section 7.1.5.3.

Once the basket module loading charts are complete, they are used to direct the loading of the basket modules.

7.1.5.3 Basket Loading Procedure

1. Locate the MTR fuel element to be loaded into the basket module per the loading diagram prepared for that module type (i.e., base, intermediate or top).
2. Independently verify the element identification.
3. Load the element into the predetermined fuel basket module fuel element location using the loading diagram. Ensure spacers are installed in positions 1, 2 and 3 of any basket module containing a high fissile mass LEU MTR element.
4. Independently verify that the fuel element and spacer loading in the basket module complies with the loading diagram.
5. Repeat steps 1 through 4 until all identified fuel elements have been loaded into basket modules in compliance with the loading diagrams.

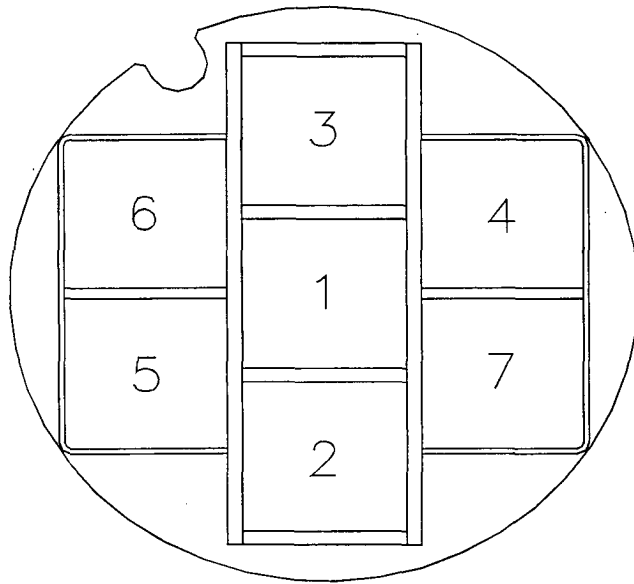
7.1.5.4 Estimating Assembly Decay Heat

When the decay heat of a fuel element is not known, the assembly burnup (MWd/MTU) and cooling time (years) can be used to define the allowable basket module positions using Figure 7.1-2 through Figure 7.1-7, depending on fuel enrichment (i.e., LEU, MEU or HEU) or ^{235}U content.

HEU MTR fuel elements may be loaded with heat loads greater than 30 W. HEU elements exceeding 30 W shall be preferentially loaded, and Figure 7.1-6 and Figure 7.1-7 identify the appropriate cooling times and burnup limits for 120 W, 70 W and 20 W HEU elements, having a ^{235}U mass of up to 380 grams and a ^{235}U mass of up to 460 grams, respectively. The following steps are used to develop the appropriate loading patterns.

1. Locate the point on Figure 7.1-6 or Figure 7.1-7 for the fuel element burnup and cooling time, and ^{235}U content.
2. If the located point is above the 20 W line, there are no restrictions on fuel element placement in the basket module.
3. If the located point is between the 20 W and 70 W lines, the element is loaded as a 70 W element.
4. If the located point is between the 70 W and 120 W lines, the element is loaded as a 120 W element.
5. If the located point is below the 120 W line, the element shall not be loaded in the NAC-LWT cask.
6. The maximum total decay heat load for a preferentially loaded basket module shall not exceed 210 W and 1.26 kW for a loaded NAC-LWT cask.
7. Each shipper shall ensure that the Certificate of Compliance maximum decay heat load limits of 210 W per basket module and 1.26 kW per cask are not exceeded.

Figure 7.1-1 MTR Fuel Basket Module Loading Pattern (Top View)



Loading Diagram

Figure 7.1-2 LEU MTR Fuel Basket Loading Guidelines for 30 W Uniform Loading

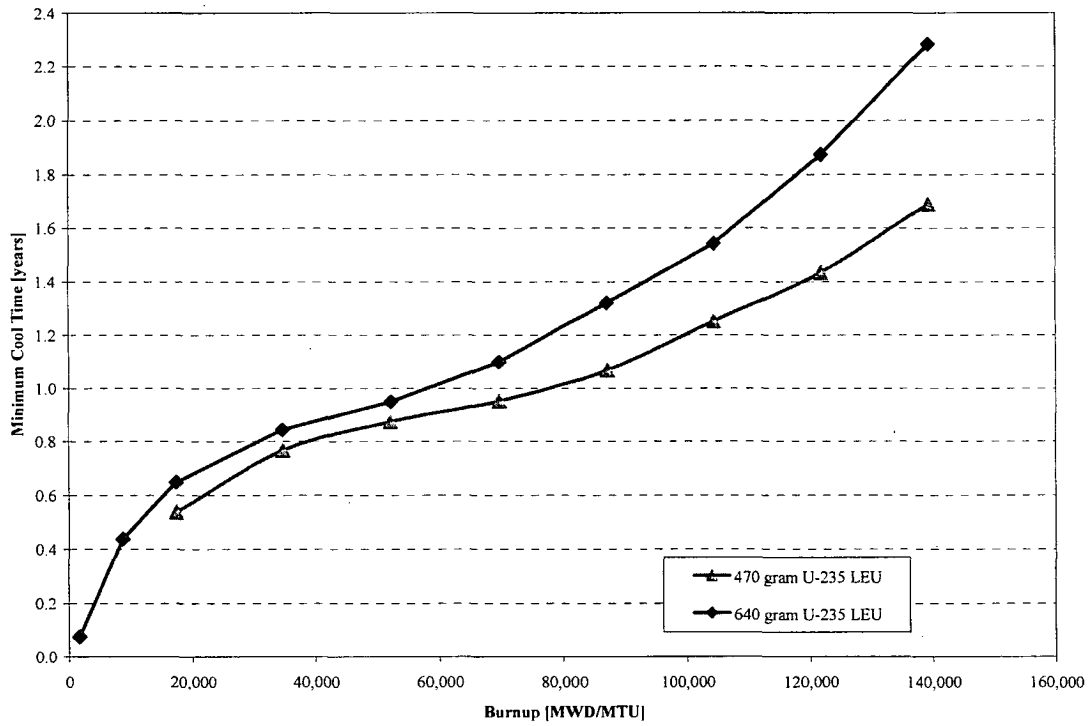


Figure 7.1-3 MEU MTR Fuel Basket Loading Guidelines for 30 W Uniform Loading

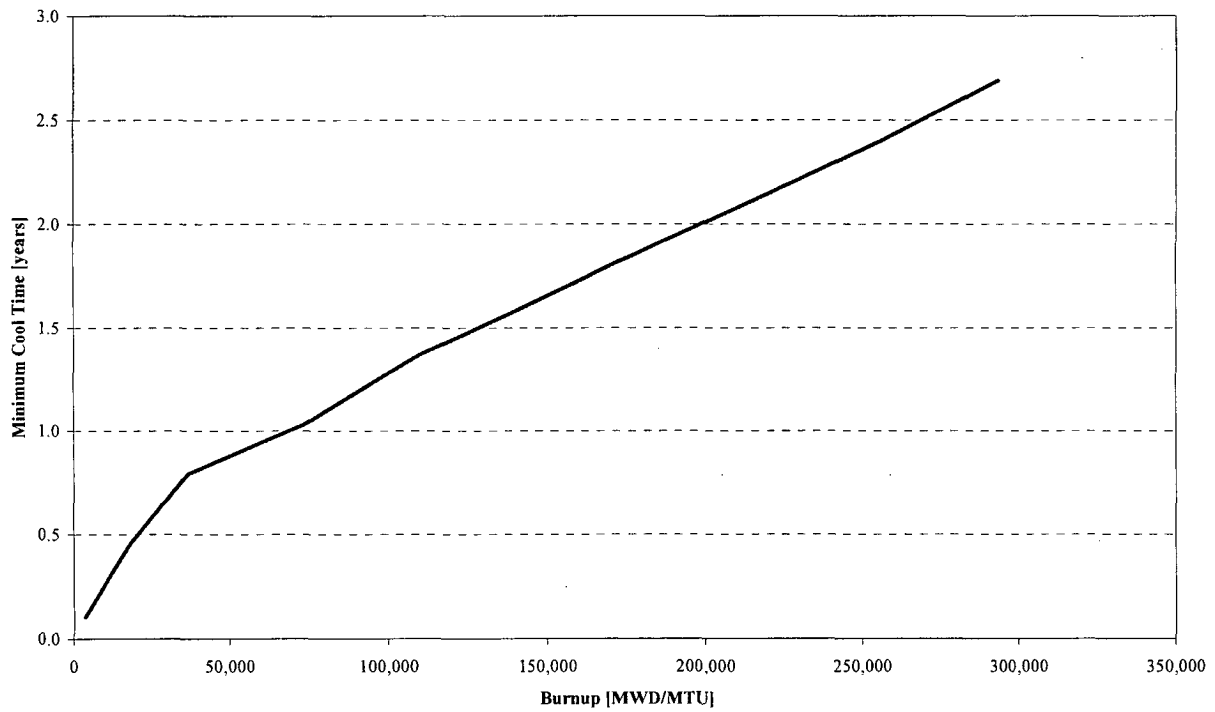


Figure 7.1-4 HEU MTR Fuel Basket Loading Guidelines for 30 W Uniform Loading –
Maximum 380 grams ²³⁵U

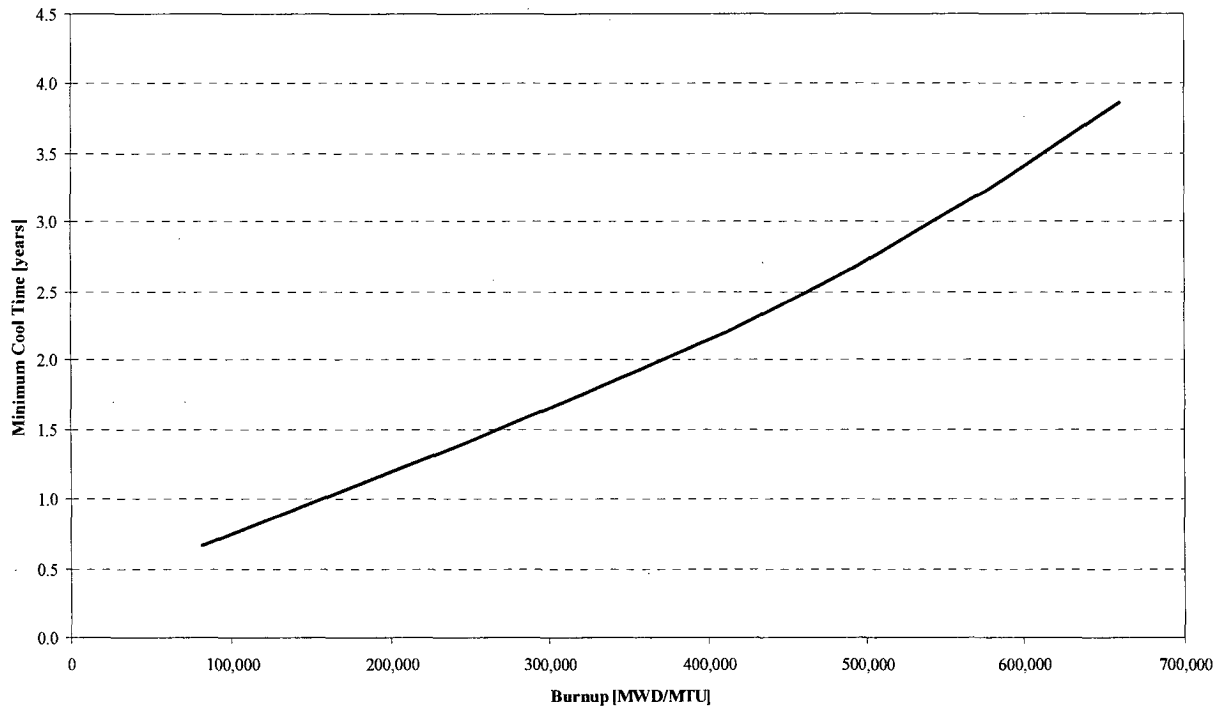


Figure 7.1-5 HEU MTR Fuel Basket Loading Guidelines for 30 W Uniform Loading –
Maximum 460 grams ²³⁵U

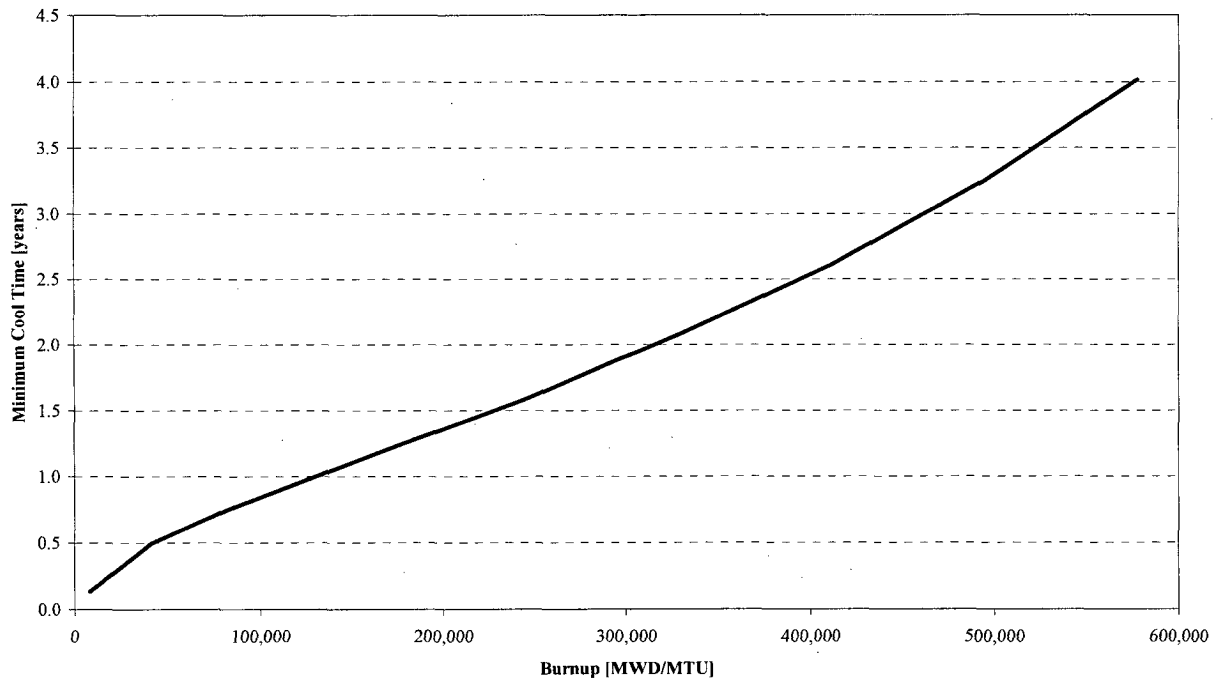


Figure 7.1-6 HEU MTR Fuel Basket Loading Guidelines for Preferential Loading – Maximum 380 grams ²³⁵U

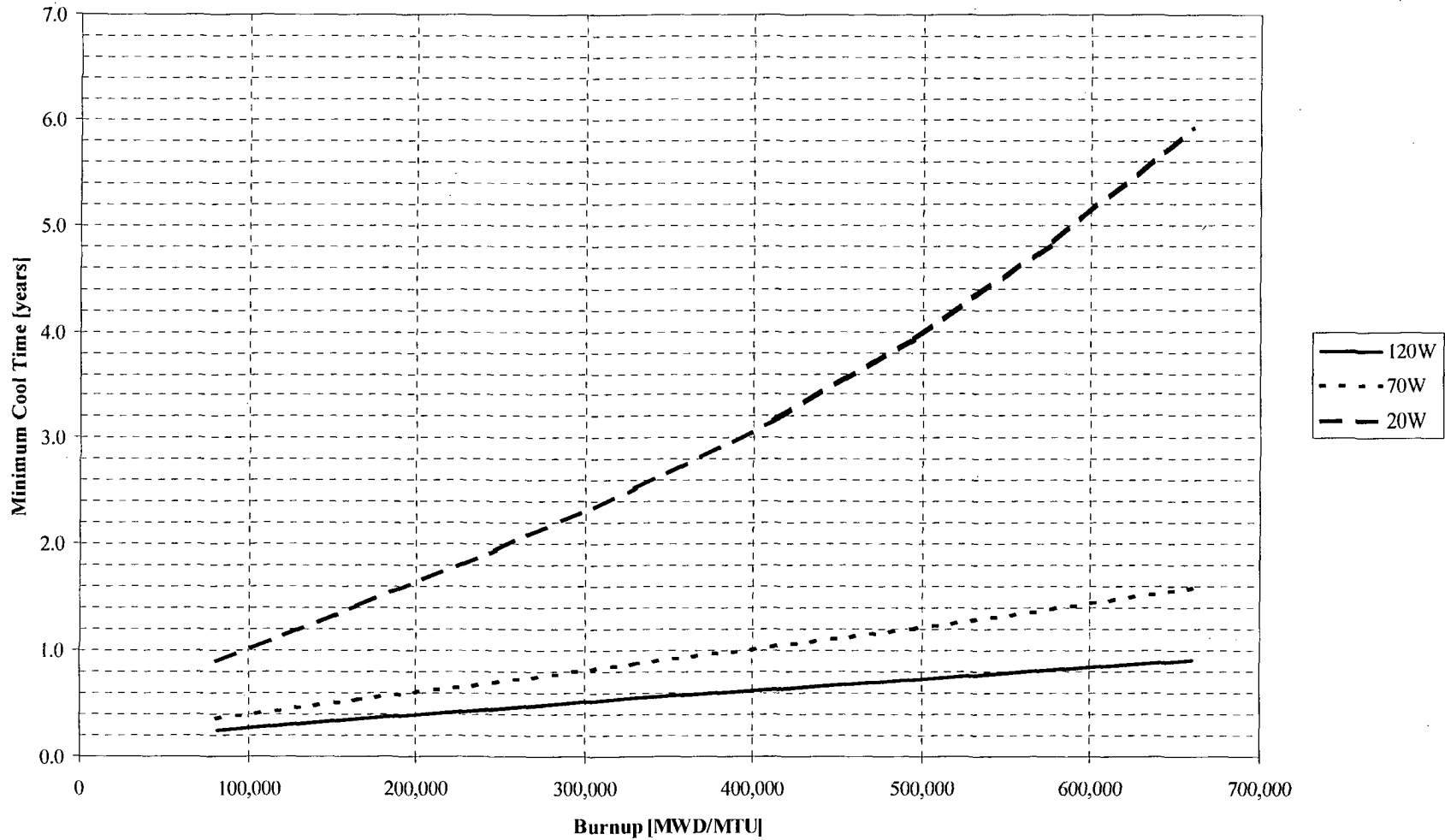


Figure 7.1-7 HEU MTR Fuel Basket Loading Guidelines for Preferential Loading – Maximum 460 grams ²³⁵U

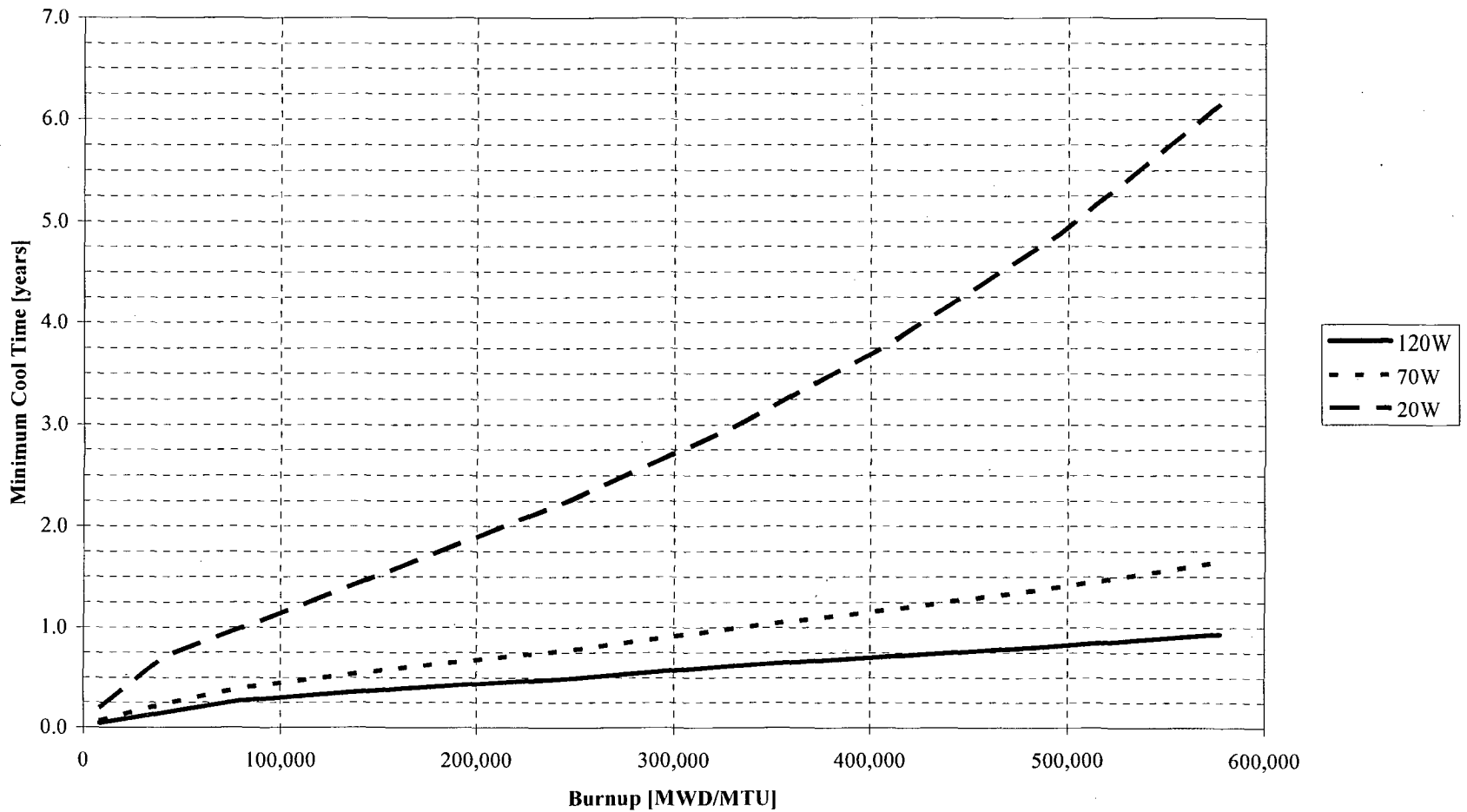


Figure 7.1-8 DIDO LEU Cooling Time vs. Fuel Burnup Basket Module Loading Guidelines for Uniform Loading

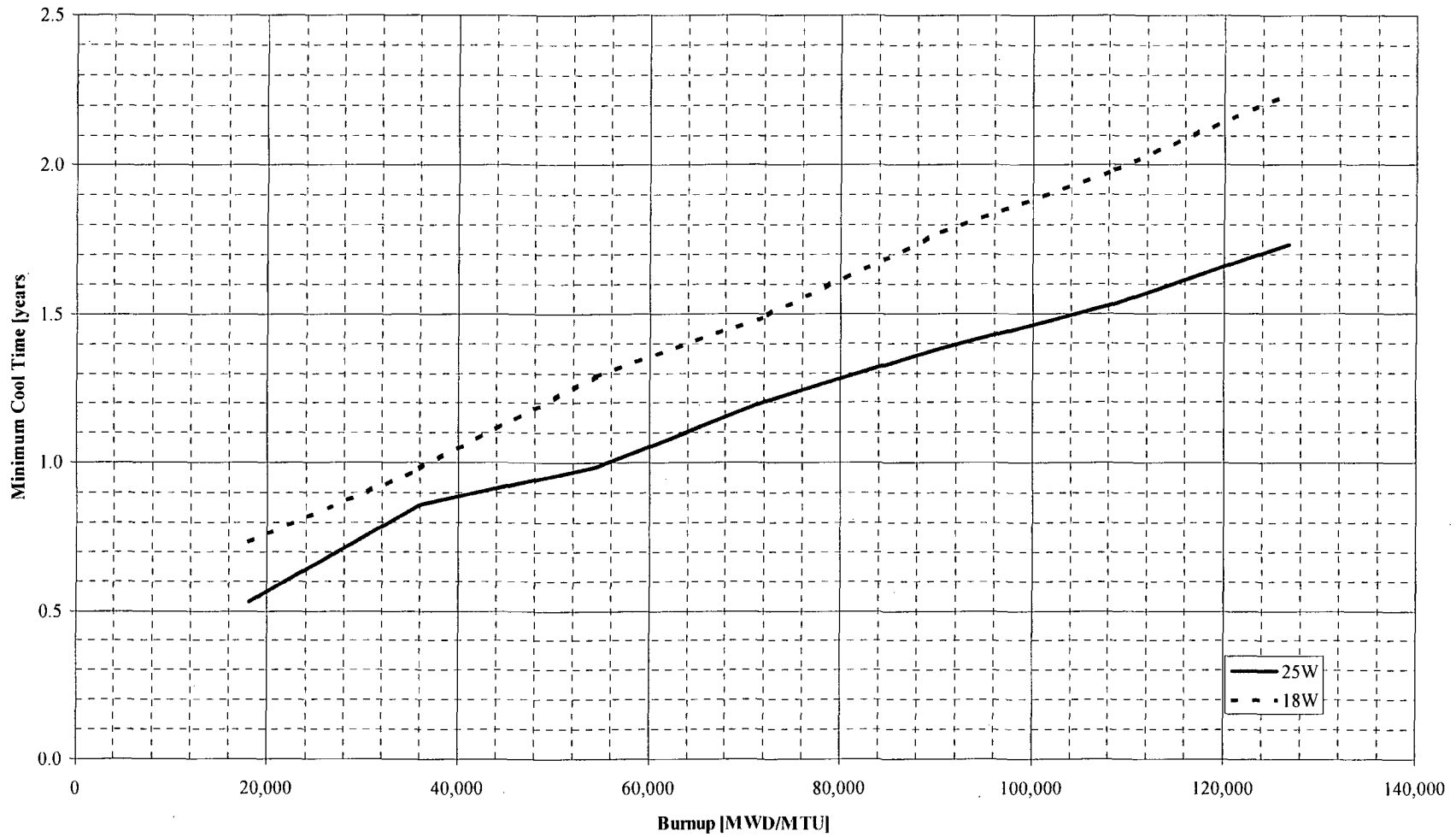


Figure 7.1-9 DIDO MEU Cooling Time vs. Fuel Burnup Basket Module Loading Guidelines for Uniform Loading

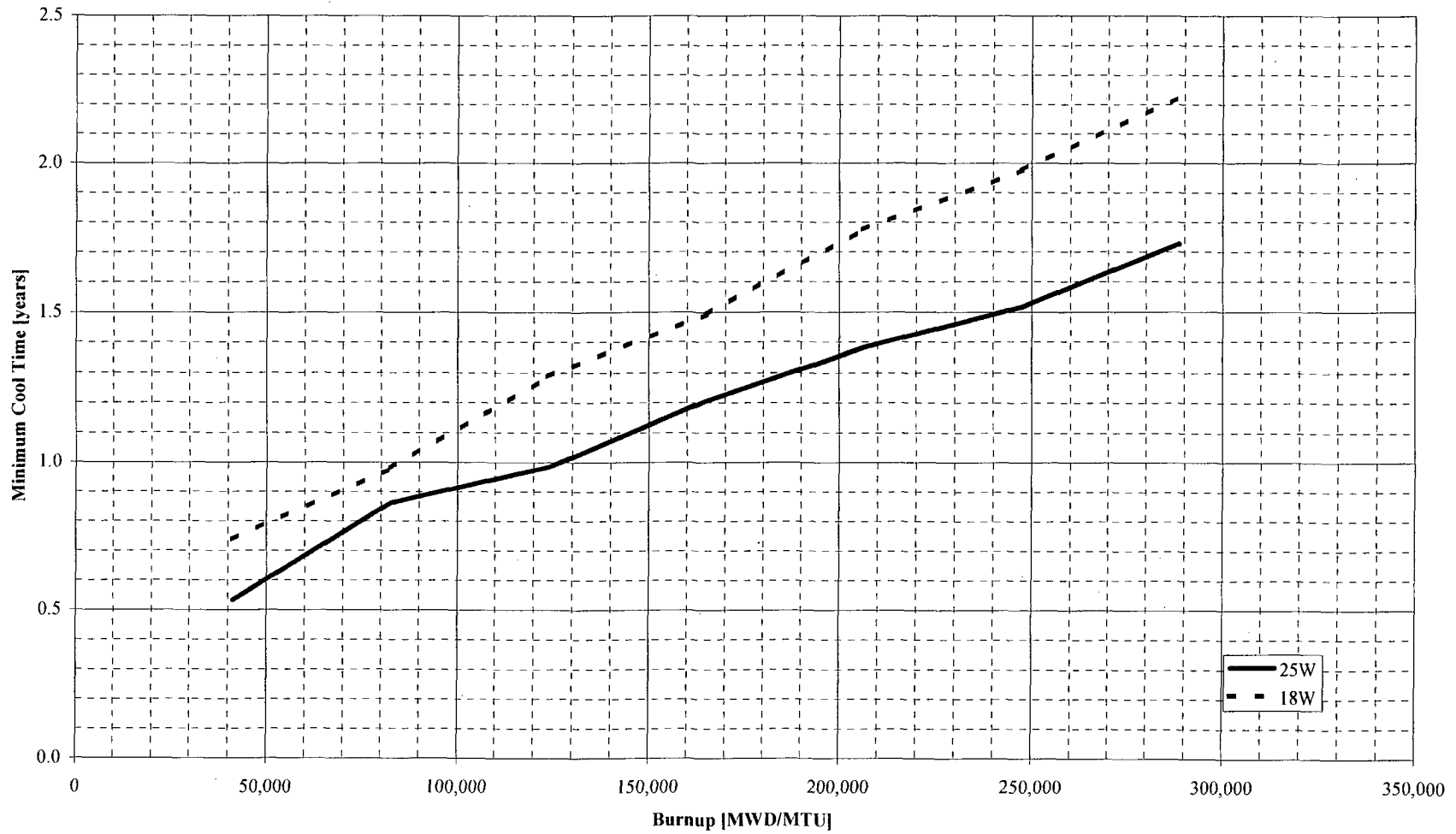


Figure 7.1-10 DIDO HEU Cooling Time vs. Fuel Burnup Basket Module Loading Guidelines for Uniform Loading

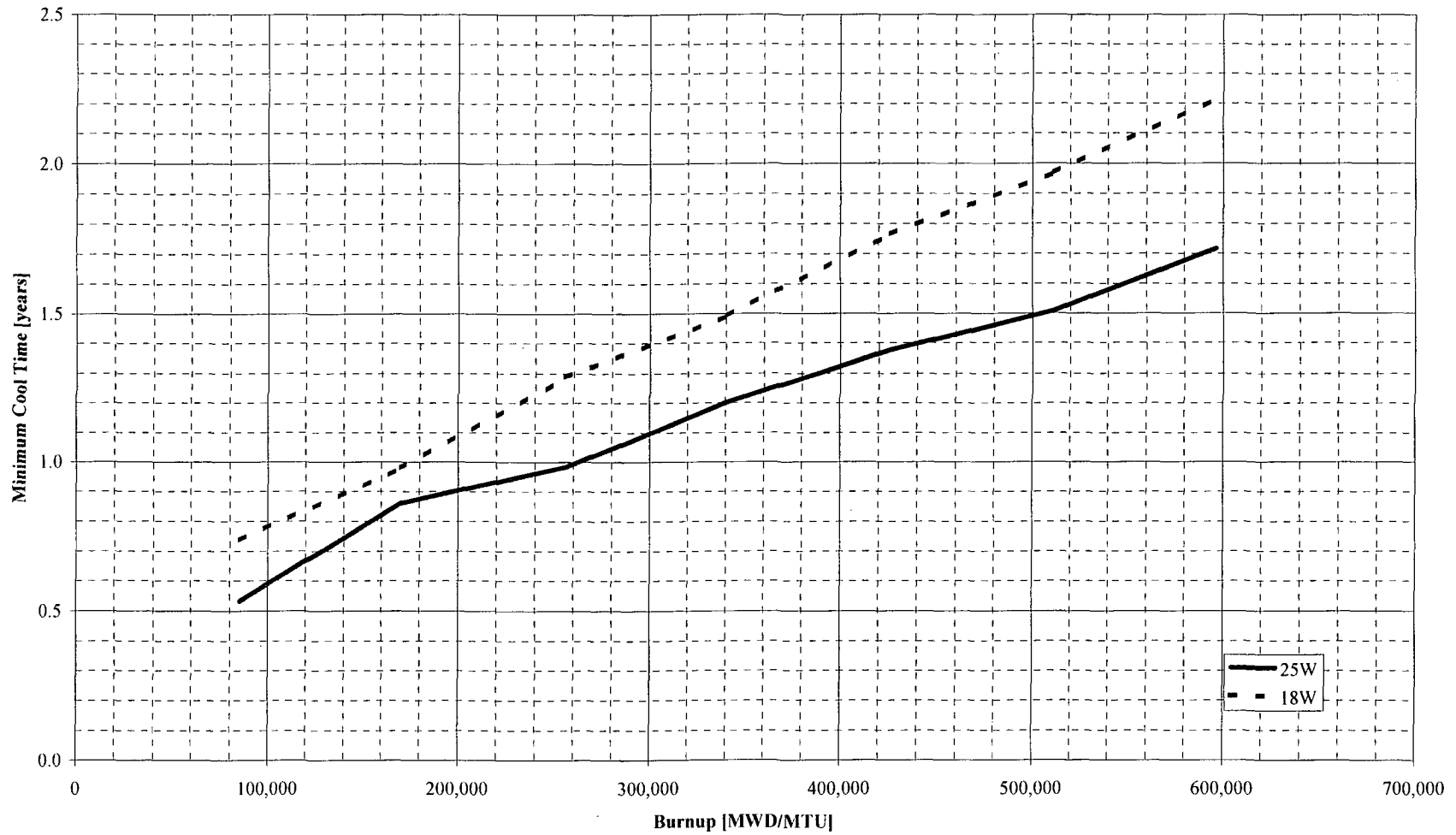
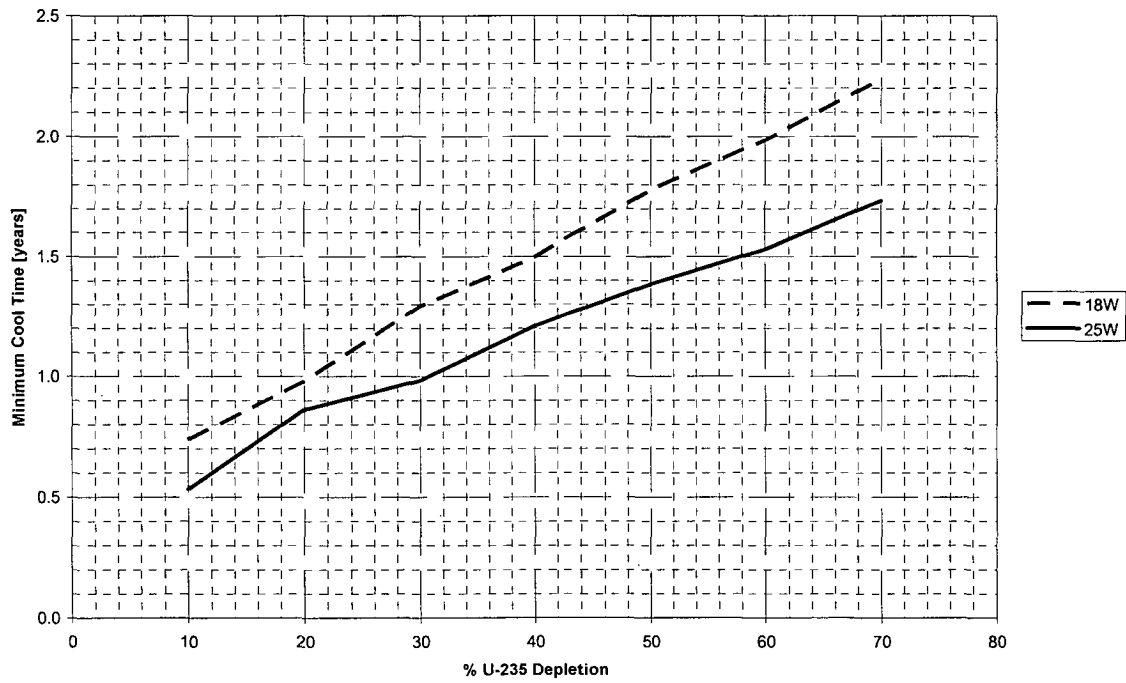


Figure 7.1-11 Bounding DIDO Element Minimum Cool Time vs. wt % ^{235}U Depletion



7.1.6 Procedure for Dry Loading of TRIGA Fuel Basket Modules and GA IFM Modules into the NAC-LWT Cask

This procedure presents the steps for dry loading, using a transfer cask, of the non-poisoned or poisoned TRIGA fuel basket modules into the NAC-LWT. For transport, five TRIGA fuel basket modules, consisting of a top module, a base module, and three intermediate modules must be loaded into the NAC-LWT. An alternative loading option is available for the poisoned TRIGA basket modules. This configuration, Configuration 2, consists of 1 base module and 4 intermediate modules. A spacer attached to the underside of the NAC-LWT lid is used with Configuration 2. Each basket module consists of seven cells, a center cell, and six peripheral cells. The center cell of the nonpoisoned basket design is blocked and cannot be loaded. Each unblocked cell may contain up to four TRIGA fuel elements, or up to 16 TRIGA fuel cluster rods within a fuel rod insert placed into the cell prior to loading. Each nonpoisoned basket module may contain up to 24 TRIGA fuel elements, for a total of 120 elements, or up to 96 TRIGA fuel cluster rods, for a total of 480 rods. Each poisoned basket module may contain up to 28 TRIGA fuel elements, for a total of 140 elements, or up to 112 TRIGA fuel cluster rods, for a total of 560 rods. The maximum decay heat load of any TRIGA fuel element is 7.5 watts, while the maximum decay heat load of a TRIGA fuel cluster rod is 1.875 watts. An alternative loading option is available for the General Atomics (GA) Irradiated Fuel Material (IFM) Fuel Handling Units (FHU). This configuration consists of one GA IFM top module and one GA IFM spacer. The GA IFM top module, based on the TRIGA basket design, has two canister storage tubes that hold the GA IFM FHU.

TRIGA fuel elements may be transported directly in the basket module cell, in a screened failed fuel can, or in a sealed failed fuel can. TRIGA fuel cluster rods may be transported within the fuel rod insert in a basket cell, or in a sealed failed fuel can. The screened and sealed failed fuel cans fit in a module cell. The screened failed fuel can holds up to four damaged TRIGA fuel elements or two TRIGA fuel elements as fuel debris. The sealed failed fuel can holds up to two damaged TRIGA fuel elements, two equivalent TRIGA elements as fuel debris, or up to six damaged TRIGA fuel cluster rods.

When loading TRIGA fuel elements directly into the basket cells of a TRIGA basket module, the fuel elements may be loaded with either 4 elements per cell, or one element per cell, without shoring. If a basket cell is loaded with 2 or 3 intact elements, dummy rods will be inserted as necessary to fill the remaining space in the cell.

Screened failed fuel cans are provided in two lengths. The short can is intended for TRIGA fuel elements having a nominal length of about 30 inches, which includes all of the TRIGA fuel

elements except fuel follower control rod elements. The long can accommodates the fuel follower control elements, which have a nominal length of 45 inches. The short can may be used in the top or base basket module. The long can may only be installed in the top module. The cans have a screened bottom that permits water draining but retains gross particulate material. TRIGA fuel cluster rods may not be loaded into screened failed fuel cans.

TRIGA fuel debris or damaged fuel cluster rods are required to be loaded into sealed failed fuel cans. The cans are provided in two lengths. The short can may be used in the base or top basket modules. The long can may only be used in the top module. The sealed cans are vacuum dried prior to loading into a TRIGA fuel basket.

There are two separate GA IFM FHU designs. One FHU is designed to hold research reactor fuel and the other is designed to hold High-Temperature Gas-Cooled Reactor fuel pellets. Each FHU consists of a sealed inner canister within a sealed outer canister. Each FHU contains irradiated fuel materials as described in Chapter 1. When loading the GA IFM FHUs, each individual sealed FHU will be loaded separately into a single GA IFM basket. This single basket containing two GA IFM FHUs and a spacer will comprise the entire cask load. Loading of the GA IFM basket into the NAC-LWT cask will utilize the TRIGA dry configuration loading procedure that is described in the following paragraphs.

TRIGA fuel elements that can be loaded into the cask are limited to a maximum decay heat of 7.5 watts per element, as discussed in Section 1.2.3. The decay heat load of the element must be calculated, and verified to be equal to or less than 7.5 watts per element prior to loading. TRIGA fuel cluster rods that can be loaded into the cask are limited to a maximum decay heat of 1.875 watts per element, as discussed in Section 1.2.3 (by reference to Table 5.1.1). The decay heat load of the fuel cluster rod must be calculated, and verified to be equal to or less than 1.875 watts per element prior to loading.

The procedure for loading the package with TRIGA fuel in a dry configuration is as follows:

1. Perform a receipt inspection of the empty cask and trailer/ISO container, inspecting for transport damage.
2. Position the trailer in the designated cask unloading area. Set the trailer brakes and chock the wheels to prevent unintended movement. If site-specific conditions exist that require the trailer to move to allow the cask to be uprighted on its rotation trunnions, release brakes and remove the chocks when required to complete uprighting operations. If an ISO container is used, it may be removed from the trailer and secured in the unloading area.
3. Remove the personnel barrier or the roof and roof cross-members from the ISO container.

Note: Verify that the package nameplate displays the correct package identification number in accordance with the CoC.

4. Perform a Health Physics survey of the cask and adjacent surfaces of the trailer.

Note: A receiving survey of the cask and transporter must be performed as soon as practicable after arrival at the site to assure compliance with 10 CFR 20, 10 CFR 71.87(i) and 10 CFR 71.47, and to assure timely reporting of any reportable noncompliance.

5. Remove the top and bottom impact limiters.
6. Remove the cask tie-down strap.
7. Using the lifting yoke with the guides removed, engage the lifting trunnions. Raise the cask to vertical by rotating the cask rotation sockets on the rear cask supports, moving the crane and/or trailer as required to keep the lift yoke engaged to the trunnions and the cask engaged in the rear supports. When the cask is fully vertical, lift the cask from the supports and remove it from the trailer/container.
8. Place the cask onto the dry loading station. Disengage the lifting yoke and move clear.
9. Visually inspect the neutron shield tank fill, drain and level inspection plugs for signs of neutron shield fluid leakage. If leakage is detected or suspected, verify shield tank fluid level and correct, as required.
10. Remove the vent and drain valve port covers. Prior to reinstallation of the port covers, carefully inspect the O-rings and, if the O-rings show any damage, replace them with approved spares. Ensure that the replacement O-rings are properly installed and seated. Visually inspect the valve quick-disconnect nipples and replace them, if necessary.

Note: For Alternate B port covers, replace the metallic O-ring with an approved spare prior to reinstallation.

11. Remove closure lid bolts. Attach the lid lift slings to the closure lid. Remove the closure lid and set it on a support that is suitable for radiological control and for maintaining the cleanliness of the closure lid. Prior to reinstallation of the lid, carefully inspect the Teflon O-ring seal in the underside of the closure lid and, if it shows any damage, replace it. Remove the metallic O-ring and replace it with an approved spare. Ensure that the replacement O-rings are properly installed and seated. Inspect the lid bolts and replace any that are damaged.
12. Visually inspect the inner cavity for foreign material or damage. Install, or verify the presence of the proper drain tube and drain alignment ring.
13. Install the required dry transfer system components on the top of the cask.
14. Position the shielded transfer cask system components for fuel loading, as appropriate.

15. Identify the TRIGA fuel basket modules to be loaded. Modular baskets consisting of one base unit, three intermediate units, and one top unit, may be loaded into the cask cavity. The base unit must be the first unit loaded and the top unit must be the last unit loaded. The intermediate modules may be loaded in any of the other loading operations. If the poisoned basket Configuration 2 is used, ensure that the TRIGA fuel spacer is attached to the NAC-LWT lid. To install the fuel spacer, orient the bolt in the hole positioned immediately below the center arc shaped clearance on the edge of the spacer and place the bolt in the hole marked "top of cask" adjacent to the hole. Install the remaining three bolts and torque bolts to 40 foot-pounds. If TRIGA fuel cluster rods are to be transported, ensure that fuel rod inserts are placed into each cell location that will contain fuel cluster rods. For the GA IFM basket load, install the GA IFM spacer, shown on NAC drawing 315-40-123, prior to inserting the loaded GA IFM top module.

- Notes:
- a. When utilizing nonpoisoned TRIGA baskets, visually verify that the center blocking plate is welded in place on each basket module.
 - b. When utilizing poisoned TRIGA baskets, visually inspect each cell of each basket module for foreign material or damage and verify the presence of the neutron poison material (borated stainless steel plates) as shown on NAC Drawings 315-40-080, -081, and -082.
 - c. When utilizing the GA IFM top module, follow the TRIGA loading procedure below, noting that this is a single basket load.

16. Identify the TRIGA fuel contents to be loaded and verify that the fuel contents comply with the content, heat load and quantity conditions as specified in the CoC.
17. Load a TRIGA fuel basket module into the shielded transfer cask.
18. Place the shielded transfer cask containing the loaded basket module onto the dry transfer system components positioned on the top of the cask.
19. Lower the fuel basket from the shielded transfer cask into the shipping cask.
20. Repeat the loading and transfer of loaded basket modules until the approved cask loading plan is completed.
21. Install the closure lid onto the cask. Visually verify that the lid is properly seated.
22. Remove the dry transfer system components from the top of the cask.
23. Install and tighten the 12 closure bolts to 260 ± 20 ft-lbs in three passes, using the torque sequence stamped on the closure lid.
24. Connect a gas supply line to the vent valve and the drain line to the drain valve.
25. Open the air, nitrogen or helium gas supply valve and pressurize the cask cavity (< 30 psig) to force any residual water out the drain line. Continue to supply pressurized gas to the cask for a minimum of five minutes after the last residual free water discharges from the drain. Remove the drain and gas supply lines and attach a vacuum drying system (VDS) to the vent.

26. Evacuate the cask cavity to less than or equal to 10 torr (13 mbar) and continue vacuum pumping for a minimum of 15 minutes.
 27. At the end of the vacuum pumping period, isolate the cask cavity from the vacuum pump and stop the vacuum pump. Monitor the cask cavity pressure for a minimum of ten minutes. If the pressure rise is less than 5 torr (6.7 mbar), the cavity is verified as dry of free water. If pressure rise is >5 torr (6.7 mbar), repeat vacuum drying until the dryness verification results are satisfactory.
 28. Backfill the cask cavity with helium to 0 psig (1 atmosphere, absolute), +1, -0 psi and disconnect the VDS from the vent valve.
 29. Perform a helium leakage test of the closure lid containment O-ring using a Helium Mass Spectrometer Leak Detector (He MSLD) in accordance with the procedural requirements of Section 8.1.3.1, Steps 3 through 10.
 30. Install the vent and drain alternate port covers and torque the bolts to 100 ±10 inch-pounds.
 31. If an alternate port cover containment O-ring seal was replaced, perform a helium leakage test on the affected port cover using a He MSLD in accordance with the requirements of 8.1.3.2.2.
 32. If the alternate port cover containment seal was inspected and accepted for reuse, perform a gas pressure drop leakage test on the affected port cover as follows.
 - a. Install a pressure test fixture to the port cover test port including a calibrated pressure gauge with a minimum sensitivity of 0.25 psi.
 - b. Pressurize the port cover seal annulus to 15 psig, +1, -0 psi.
 - c. Isolate the gas supply and observe the pressure gauge for a minimum of five minutes.
 - d. The acceptance criterion for the test is no measurable drop in pressure during the minimum test time. An acceptable test assures that the minimum assembly verification leakage test sensitivity is achieved.
- Note: Alternate B port covers, if used, require the satisfactory completion of a helium maintenance leakage rate test to confirm a leaktight seal condition for each loaded transport. Install the Alternate B port cover, torque the high-strength bolts to 285 ± 15 inch-pounds, and perform the maintenance leakage rate test per the requirements of Section 8.1.3.3.
33. Decontaminate the cask surfaces. Survey the cask for surface contamination and radiation dose rates.

Note: Ensure compliance with 10 CFR 71.87(i) and 10 CFR 71.47.
 34. Engage the cask lifting yoke to the lifting trunnions.
 35. Lift the cask and position the cask rotation sockets in the rear rotation trunnions of the rear support structure. Carefully lower the cask to the horizontal transport orientation

- resting on the front saddle by moving the crane and/or the trailer as required to maintain cask engagement to the rear supports.
36. Disengage the lifting yoke from the lifting trunnions and remove it from the area. Install the cask tie-down strap. Install the top and bottom impact limiters. Install tamper seal wire and number seal on the top attachment point on the top impact limiter.
 37. Install ISO container bracing and lid, or personnel barrier.
 38. Complete radiation and contamination surveys of the external surfaces of the package and record the data. Ensure removable contamination and radiation dose rate survey results comply with the limits specified in 10 CFR 71.87(i) and (j).
 39. Measure the dose rate in millirems per hour at one meter from the package surface to determine the Transport Index (TI). Indicate the TI on the Radioactive Material labels applied to the package in accordance with 49 CFR 172, Subpart E.
 40. Determine the appropriate Criticality Safety Index (CSI) assigned to the package contents in accordance with the CoC, and indicate the correct CSI on the Fissile Material label applied to the package per 49 CFR 172, Subpart E.
 41. Apply appropriate placards to the transport vehicle in accordance with 49 CFR 172, Subpart F.
 42. Complete the shipping documents and provide the carrier with instructions regarding the requirements for maintaining an exclusive use shipment.

7.1.7 Procedure for Loading TRIGA Damaged Fuel or Fuel Debris into TRIGA Sealed Failed Fuel Cans

1. Examine the sealed failed fuel can (can) body and inspect for damage. Verify that the lid sealing surface is clean and free of defects. Visually verify that the drain plug seal is installed and the drain plug is partially threaded into the drain plug adapter to allow for draining.
2. Lower the can into the pool and position it for fuel loading.
3. Load the damaged TRIGA fuel or fuel debris into the can. Verify that no more than the equivalent of 2 fuel elements or 6 fuel cluster rods are loaded into the can. Visually verify that there is no debris in the lid sealing surface and thread areas.
4. Examine the can lid and inspect for damage. Visually verify that the sealing surface is clean and free of defects. Lubricate the lid bolts, install the lid seal and verify that the lid valve is in the open position and the valve lock set screw is retracted.
5. Attach the testing hose to the lid test connection and ensure that the fitting is properly seated.
6. Install the lid and torque the lid bolts to 150 ± 10 inch-pound.

- Note: Torque any two diametrically opposed bolts first, then torque the remaining two bolts. Complete the torque sequence by verifying the torque of all four bolts in a clockwise direction.
7. Pressurize the can with air or helium to remove the water. Continue the purge for at least 5 minutes after bubbles appear from the base of the can.
 8. Access and torque the drain plug to 50 ± 10 inch-pound.
 9. Evacuate the can to a pressure below 10 torr (13 mbar) and continue vacuum pumping for 10 minutes.
 10. Stop and isolate the vacuum pump and monitor the cask cavity vacuum pressure for a minimum of 10 minutes. If the pressure rise is less than 5 torr (6.7 mbar), the cavity is verified as dry of free water. If the pressure rise is >5 torr (6.7 mbar), repeat vacuum drying until the dryness verification results are satisfactory.
 11. Backfill the can with helium to a pressure of 1 atmosphere (0 psig), +1, -0 psi.
 12. Shut and lock the lid valve.
 13. Disconnect the testing hose from the lid test connection.
 14. The sealed failed fuel can is now ready for loading into a TRIGA basket module.

7.1.8 Procedure for Wet Loading of PWR/BWR Fuel Rods into the PWR/BWR Transport Canister

The PWR/BWR transport canister has three configurations: sealed canister, screened canister, and free-flow canister. All three canister configurations may be used to contain either intact or damaged fuel rods, or a combination of both damaged and intact fuel rods. The loaded transport canisters are loaded into the NAC-LWT cask containing a LWT PWR basket assembly with an appropriate bottom weldment spacer. For transport canisters containing any damaged fuel rod contents, a can and an insert spacer are required to be installed and bolted to the underside of the closure lid to limit the axial movement of the canister. The use of the can and insert spacer requires the use of the PWR basket assembly fitted with the Alternate B spacer. Transport canisters containing intact rods may be placed in any of the three types of PWR basket assemblies. Upon completion of loading the transport canister, the canister and the insert spacer are loaded, either together or individually, into the basket assembly in a manner similar to loading a PWR assembly.

1. If the transport canister is to be shipped in a sealed configuration, verify the five drain plugs are installed and torqued to 50 ± 2 foot-pound. If the transport canister is to be shipped in the free flow configuration, verify the five drain plugs are not installed. If the transport canister is to be shipped in the screened configuration, verify the screened plugs are installed and torqued to 50 ± 2 foot-pound in the bottom of the canister.

2. Lower the transport canister (and insert) into the fuel pool for loading.
3. Load the spent fuel rods into the transport canister in accordance with site-specific procedures. Separate failed fuel rod capsules may be used to contain either intact or damaged fuel rods within the canister. The capsules are intended to limit dispersal of radioactive material to the canister internals. Visually upon completion of loading, verify that there is no debris on the lid sealing surface and threaded areas.
4. Using the appropriate lid (sealed, screened or free-flow), examine and inspect for damage. Visually verify that the sealing surface is clean and free of defects. Lubricate the lid bolts.
5. Install the lid and torque the lid bolts to 35 ± 5 inch-pound.

Note: Torque any two diametrically opposed bolts first, then torque the remaining six bolts. Complete the torque sequence by verifying the torque of all eight bolts in a clockwise direction.

6. If the transport canister is being shipped in either the screened or free-flow configuration, it is now ready for shipment and shall be loaded into the NAC-LWT cask in accordance with Section 7.1.1, Procedures for Wet Loading of LWR Fuel. If the transport canister is being shipped in the sealed configuration, complete steps 7-13 of this section.
7. Connect vent and drain lines to the respective quick-disconnect fittings on the sealed transport canister lid. The drain hose discharge should be directed to the plant drain system for radiological wastewater or another appropriate collection point.
8. Pressurize and purge the transport canister using helium. (Caution do not exceed 25 psig. while dewatering the transport canister.) Secure the purge once no fluid is observed exiting the discharge for at least 10 minutes.
9. Connect the vent line to a suitable vacuum pump. Maintain connection of drain line to the can, but isolate the line to allow vacuum drying of the sealed failed fuel can.
10. Evacuate the can to a pressure below 10 torr (13 mbar) and continue vacuum pumping for 10 minutes.
11. Stop and isolate the vacuum pump and monitor the cask cavity vacuum pressure for a minimum of 10 minutes. If the pressure rise is less than 5 torr (6.7 mbar), the cavity is verified as dry of free water. If the pressure rise is >5 torr (6.7 mbar), repeat vacuum drying until the dryness verification results are satisfactory.
12. Backfill the transport canister cavity with helium to 1 atmosphere (absolute), +1, -0 psi.
13. Disconnect the vent and drain lines from the transport canister.
14. The sealed transport canister is now ready for shipment and may be loaded into the NAC-LWT cask in accordance with Section 7.1.1.

7.1.9 Procedure for Wet Loading of TPBAR Consolidation Canister into the NAC-LWT Cask

This section describes the procedures for loading the NAC-LWT with a TPBAR consolidation canister. The consolidation canister can contain up to 300 TPBARs, two of which may be prefailed. Dunnage (i.e., spacer grids, stainless steel tubes, etc.) may be used in consolidation canisters containing fewer than 300 TPBARs. The total weight and volume of the contents (i.e., dunnage and reduced number of TPBARs) must be less than, or equal to, the weight and volume of the full load of 300 TPBARs.

Appropriate radiological controls and procedures addressing tritium shall be utilized by the licensee, including appropriate personnel monitoring for tritium exposure.

NAC-LWT casks to be used for the transport TPBARs shall be configured as shown on Drawing No. 315-40-128, including Alternate B port covers.

1. Perform a receiving survey of the empty cask and inspect for damage. Verify, by cask serial number, that the cask is approved for TPBAR shipment.
2. Position a trailer in the designated cask unloading area. Set the trailer brakes and chock the wheels to prevent unintended movement. If site-specific conditions exist that require the trailer to move to allow the cask to be uprighted on its rotation trunnions, release brakes and remove the chocks when required to complete uprighting operations. If an ISO is used, it may be removed from the trailer and secured in the unloading area.
3. Remove the roof from the ISO container and open the front and rear ISO doors. Remove roof cross-members, if installed.

Note: Verify that the package nameplate displays the package identification number, USA/9225/B(M)-96, as required by the CoC for TPBAR contents.

4. Perform a Health Physics survey of the cask and adjacent surfaces of the trailer.

Note: A receiving survey of the cask and transporter must be performed as soon as practical after arrival at the site to assure compliance with 10 CFR 71.87(i) and 10 CFR 71.47, and to assure timely reporting of any reportable noncompliance.

5. Remove the top and bottom impact limiters.
6. Remove the cask tie-down strap.
7. Using the lifting yoke with the guides removed, engage the lifting trunnions. Raise the cask to vertical by rotating the cask rotation sockets on the rear cask supports, moving the crane and/or trailer as required to keep the lift yoke engaged to the trunnions and the cask engaged in the rear supports. When the cask is fully vertical, lift the cask from the supports and remove it from the trailer/container.

8. Place the cask in the decontamination pit or other designated area. Disengage the lifting yoke. Clean cask surfaces of road dirt as required for entry into the spent fuel pool.
9. Visually inspect the neutron shield tank fill, drain and level inspection plugs for signs of neutron shield fluid leakage. If leakage is detected, verify shield tank fluid level and correct, as required.
10. Remove the Alternate B vent and drain valve port covers. Prior to reinstallation of the port covers, replace the metallic O-ring seal with an approved spare and inspect the Viton® O-ring seal for each port cover. If the Viton® O-ring shows any damage, replace it. Ensure that the replacement O-rings are properly installed and seated. Store the port covers to protect the seal surfaces. Visually inspect the valved quick-disconnect nipples and replace them, if necessary.
11. Remove closure lid bolts. Attach the lid lift slings to the closure lid. Remove the closure lid and set it on a support that is suitable for radiological control and for maintaining the cleanliness of the closure lid. Prior to reinstallation of the lid, carefully inspect the Teflon O-ring seal in the underside of the closure lid. If the O-ring shows any damage, replace it. Remove the metallic O-ring and replace it with an approved spare. Ensure that the replacement O-rings are properly installed and seated. Inspect the lid bolts and replace any that are damaged. Ensure that the TPBAR spacer is installed on the bottom of the cask lid and not damaged when the lid is set down.
12. Visually inspect the inner cavity for foreign material or damage. Install or verify the presence of the standard drain tube and the TPBAR basket assembly.
13. Fill the cask cavity with clean water. Install lift yoke arm guides and remote actuation components on the cask lifting yoke.
14. Engage the cask lifting yoke with the cask lifting trunnions and pick up the cask. Carefully lower the cask to the bottom of the cask loading area while spraying the cask down with clean water.
15. Disengage the lifting yoke from the cask and remove the yoke from the pool.
16. Identify the TPBAR consolidation canister to be loaded.
17. Pick up the consolidation canister using the required grapple system.
18. Position the container over the cask and then carefully lower it into the cask to avoid damage to the cask sealing surfaces. Orient the canister bail so that it is aligned with the drain tube location. Confirm that the container is fully seated, then release and raise the grapple to the full up position.
19. Position the cask lifting yoke over the cask closure lid. Attach the slings to the closure lid and cask lifting yoke. Lower the yoke over the cask.
20. Position the closure lid over the cask and slowly lower it into place allowing the consolidation canister bail to engage with the TPBAR spacer on the bottom of the lid.

- Use the cask and lid match marks as guides to properly align the lid. Visually confirm that the closure lid is seated.
21. Lower the cask handling yoke to slack the closure lid cables. Engage the lift yoke to the lifting trunnions and begin lifting.
Note: Visually verify the yoke engagement before lifting the cask.
 22. Raise the cask until the lid is slightly above the surface of the pool. At the option of the licensee/user, a number of closure lid bolts (4 to 12) may be installed hand tight.
 23. Raise the cask clear of the pool, rinsing the yoke and cask with clean water.
 24. Transfer the cask to the decontamination pit or other work area. Remove the yoke and lid lift slings.
 25. Install and tighten the 12 closure lid bolts to 260 ± 20 ft-lb in three passes, using the torque sequence stamped on the closure lid.
 26. At the option of the licensee/user, a 25 to 50 gallon clean water flush of the cask cavity may be performed by connecting a valved clean water line to the drain valve and a valved drain line to the vent valve. After the cavity flushing is completed, if performed, disconnect the water supply and drain lines.
 27. Connect a gas supply line to the vent valve and the drain line to the drain valve.
 28. Open the air, nitrogen or helium gas supply valve and pressurize the cask cavity (<30 psig) to force out the water. Continue to supply pressurized gas to the cask for a minimum of five minutes after the last residual free water discharges from the drain line. Remove the drain and gas supply lines and attach a vacuum drying system (VDS) to the cask vent valve.
 29. Evacuate the cask cavity to a vacuum pressure of less than 10 torr (13 mbar) and continue vacuum pumping for a minimum of 15 minutes.
 30. At the end of the vacuum pumping period, isolate the cask cavity from the vacuum pump and stop the pump. Monitor the cask cavity pressure for a minimum of ten (10) minutes. If the pressure rise is less than 5 torr (6.7 mbar), the cavity is verified as dry of free water. If the pressure rise >5 torr (6.7 mbar), repeat vacuum drying until the dryness verification results are satisfactory.
 31. Backfill the cask cavity with helium to 0 psig (1 atmosphere, absolute), +1, -0 psi. Disconnect the VDS.
 32. Perform the helium leakage test of the closure lid containment O-ring using a Helium Mass Spectrometer Leak Detector (He MSLD) in accordance with the requirements of Section 8.1.3.1, Steps 3 through 10.
 33. Install, torque the high-strength bolts to 285 ± 15 inch-pounds, and helium leakage test the Alternate B vent and drain port covers to leaktight criteria in accordance with Section 8.1.3.3.
 34. Decontaminate the cask. Survey the cask for surface contamination and radiation dose rates.

- Note: Ensure compliance with 10 CFR 71.87(i) and 10 CFR 71.47.
35. Remove lift yoke arm guides. Engage the cask lifting yoke to the lifting trunnions.
 36. Lift the cask and position the cask rotation sockets in the rear rotation trunnions of the rear support structure. Carefully lower the cask to the horizontal transport orientation resting on the front saddle by moving the crane and/or trailer, as required, to maintain cask engagement to the rear supports.
 37. Disengage the cask lifting yoke from the cask lifting trunnions and remove it from the area.
 38. Install the cask tie-down strap. Install the top and bottom impact limiters.
 39. Install tamper seal wire and number seal on the top attachment point of the top impact limiter.
 40. Install roof cross-members, close ISO container doors, and replace ISO container roof.
 41. Complete radiation and contamination surveys of the external surfaces of the package and record the data. Ensure removable contamination and radiation dose rate survey results comply with the limits specified in 10 CFR 71.87(i) and (j).
 42. Measure the dose rate in millirems per hour at one meter from the package surface to determine the Transport Index (TI). Indicate the TI on the Radioactive Material labels applied to the package in accordance with 49 CFR 172, Subpart E.
 43. Determine the appropriate Criticality Safety Index (CSI) assigned to the package contents in accordance with the CoC, and indicate the correct CSI on the Fissile Material label applied to the package per 49 CFR 172, Subpart E.
 44. Apply appropriate placards to the transport vehicle in accordance with 49 CFR 172, Subpart F.
 45. Complete the shipping documents and provide the carrier with instructions regarding the requirements for maintaining an exclusive use shipment.

7.1.10 Procedure for the Dry Loading of PULSTAR Fuel Into the NAC-LWT Cask

This section describes the procedures for loading the NAC-LWT cask with intact PULSTAR fuel assemblies, intact PULSTAR fuel rods in fuel rod inserts, and intact or damaged PULSTAR fuel assemblies, fuel rods, fuel debris, and nonfuel components of PULSTAR fuel assemblies in either sealed or screened PULSTAR cans. Up to 28 PULSTAR fuel assemblies, rod inserts, and sealed or screened cans can be loaded in the 28 MTR (four module × seven cells/module) basket assembly. The 28 MTR basket assembly consists of a base module, two intermediate modules, and a top module.

Damaged PULSTAR fuel assemblies, damaged fuel rods, fuel debris, and nonfuel components of fuel assemblies are required to be loaded in either a sealed failed fuel or screened PULSTAR can. Intact PULSTAR fuel rods may be loaded into either one of the cans at the option of the licensee. The PULSTAR cans are limited to being loaded in any cell in either the top or the base module. The top and base basket modules can also contain intact PULSTAR fuel assemblies and fuel rod inserts containing intact PULSTAR fuel rods.

The NAC-LWT cask will be loaded dry, utilizing a transfer cask for loading each of the four basket modules. The basket modules will be preloaded with the PULSTAR fuel contents. The damaged fuel cans will be preloaded, closed, drained and dried, if applicable, prior to loading in either the top or base basket module. The PULSTAR cans shall be loaded and prepared for transport in accordance with the applicable steps of Section 7.1.7.

The NAC-LWT dry PULSTAR fuel loading and preparation for transport procedures are as follows.

1. Perform a receipt inspection of the empty cask and trailer/ISO container, inspecting for transport damage.
2. Position the trailer in the designated cask unloading area. Set the trailer brakes and chock the wheels to prevent unintended movement. If site-specific conditions exist that require the trailer to move to allow the cask to be uprighted on its rotation trunnions, release brakes and remove the chocks when required to complete uprighting operations. If an ISO container is used, it may be removed from the trailer and secured in the unloading area.
3. Remove the lid/top of the ISO container and remove any bracing.
Note: Verify that the package nameplate displays the correct package identification number in accordance with the CoC.
4. Perform a Health Physics survey of the cask and adjacent surfaces of the trailer.
Note: A receiving survey of the cask and transporter must be performed as soon as practical after arrival at the site to assure compliance with 10 CFR 71.87(i) and 10 CFR 71.47, and to assure timely reporting of any reportable noncompliance.
5. Remove the top and bottom impact limiters.
6. Remove the cask tie-down strap.
7. Using the lifting yoke with the guides removed, engage the lifting trunnions. Raise the cask to vertical by rotating the cask rotation sockets on the rear cask supports, moving the crane and/or trailer as required to keep the lift yoke engaged to the trunnions and the cask engaged in the rear supports. When the cask is fully vertical, lift the cask from the supports and remove it from the trailer/container.
8. Place the cask into the dry loading station.

9. Disengage the lift yoke.
10. Visually inspect the neutron shield tank fill, drain and level inspection plugs for signs of neutron shield fluid leakage. If leakage is detected or suspected, verify shield tank fluid level and correct, as required.
11. Remove the vent and drain port covers. Prior to reinstallation of the port covers, carefully inspect the port cover O-ring seals and, if the O-rings show any damage, replace them with approved spares. Ensure that the replacement O-rings are properly installed and seated. Visually inspect the vent and drain quick-disconnect nipples and replace them, if necessary.

Note: For Alternate B port covers, replace the metallic O-ring with an approved spare prior to reinstallation.
12. Remove closure lid bolts. Attach the lid lift slings to the closure lid. Remove the closure lid and set it on a support that is suitable for radiological control and for maintaining the cleanliness of the closure lid. Prior to reinstallation of the lid, carefully inspect the Teflon O-ring seal in the underside of the closure lid. If the O-ring shows any damage, replace it. Remove the metallic O-ring and replace it with an approved spare. Ensure that the replacement O-rings are properly installed and seated. Inspect the lid bolts and replace any that are damaged.
13. Visually inspect the cask cavity for foreign material or damage. Clean as necessary. Install or verify the presence of a correct drain tube assembly including alignment ring.
14. Install the required dry transfer system components to the top of the cask.
15. Position the shielded transfer cask components for basket module loading, as appropriate.
16. Identify the PULSTAR fuel assemblies, fuel rod holders, and fuel cans to be loaded, and verify that the PULSTAR fuel contents comply with the authorized content, heat load and quantity conditions of the CoC. Four basket modules (e.g., one base module, two intermediate modules, and a top module) constitute the 28 MTR basket assembly. Spacers will be used as provided to position the PULSTAR fuel contents, as required.
17. Each module is capable of containing up to seven intact fuel assemblies, fuel rod inserts or a PULSTAR fuel can. Fuel cans are restricted to being loaded into the top and base modules, where the cans may be loaded with intact fuel assemblies or fuel rod holders without loading preference. There are no limitations on loading location for intact fuel assemblies or fuel rod holders in any of the four basket modules.

The base module is loaded into the cask first, followed by the two intermediate modules and the top module is loaded last.
18. Load the shielded transfer cask with the loaded base basket module.
19. Place the shielded transfer cask containing the base module unit onto the dry transfer system components positioned on the top of the cask.
20. Lower the fuel basket from the transfer cask into the NAC-LWT cask cavity.

21. Repeat the loading and transfer of loaded basket modules until the approved cask loading plan is completed.
22. Install the closure lid onto the cask using the dry transfer system. Visually verify that the lid is properly seated.
23. Remove the dry transfer cask system components from the top of the cask.
24. Install and torque the 12 closure lid bolts to 260 ± 20 ft-lb in three passes using the torquing sequence stamped on the lid.
25. Connect a gas supply line to the vent valve and a drain line to the drain valve.
26. Open the nitrogen or helium gas supply valve and pressurize the cask cavity (< 30 psig) to force any residual water out the drain line. Continue to supply pressurized gas to the cask for a minimum of five minutes after the last residual free water discharges from the drain. Remove the drain and gas supply lines and attach a vacuum drying system (VDS) to the vent.
27. Evacuate the cask cavity to less than or equal to 10 torr (13 mbar) and continue vacuum pumping for a minimum of 15 minutes.
28. At the end of the vacuum pumping period, isolate the cask cavity from the vacuum pump and stop the vacuum pump, and monitor the cask cavity pressure for a minimum of 10 minutes. If the pressure rise is less than 5 torr (6.7 torr), the cavity is verified dry of free water. If the pressure rise is >5 torr (6.7 mbar), continue vacuum drying until the dryness verification is completed satisfactorily.
29. Backfill the cask cavity with helium to 0 psig (1 atmosphere, absolute), $+1, -0$ psi. Disconnect the VDS from the vent valve.
30. Perform the helium leakage test of the closure lid containment O-ring using a Helium Mass Spectrometer Leak Detector (He MSLD) in accordance with the requirements of Section 8.1.3.1, Steps 3 through 10.
31. Install the vent and drain alternate port covers and torque the bolts to 100 ± 10 inch-pounds.
32. If an alternate port cover containment O-ring seal was replaced, perform a helium leakage test on the affected port cover using a He MSLD in accordance with the requirements of Section 8.1.3.2.2.
33. If the alternate port cover containment seal was inspected and accepted for reuse, perform an air pressure drop leakage test on the affected port cover as follows.
 - a. Install a pressure test fixture to the port cover test port, including a calibrated pressure gauge with a minimum sensitivity of 0.25 psi.
 - b. Pressurize the port cover seal annulus to 15 psig, $+1, -0$ psi.
 - c. Isolate the gas supply and observe the pressure gauge for a minimum of five minutes.

- d. The acceptance criterion for the test is no measurable drop in pressure during the minimum test time. An acceptable test assures that the minimum assembly verification leakage test sensitivity is achieved.

Note: Alternate B port covers, if used, require the satisfactory completion of a helium maintenance leakage rate test to confirm the leaktight seal condition for each loaded transport. Install the Alternate B port cover, torque the high-strength bolts to 285 ± 15 inch-pounds, and perform the maintenance leakage rate test per the requirements of 8.1.3.3.

34. Decontaminate the cask. Survey the cask for surface contamination and radiation dose rates.
- Note: Ensure compliance with 10 CFR 71.87(i) and 10 CFR 71.47.
35. Engage the cask lifting yoke to the lifting trunnions.
36. Lift the cask and position the cask rotation sockets in the rear rotation trunnions of the rear support structure. Carefully lower the cask to the horizontal transport orientation resting on the front saddle by moving the crane and/or the trailer as required to maintain cask engagement to the rear supports.
37. Disengage the lifting yoke from the lifting trunnions and remove it from the area.
38. Install the cask tie-down strap. Install the top and bottom impact limiters.
39. Install tamper seal wire and number seal on the top attachment point on the top impact limiter.
40. Install ISO container bracing and lid.
41. Complete radiation and contamination surveys of the external surfaces of the package and record the data. Ensure removable contamination and radiation dose rate survey results comply with the limits specified in 10 CFR 71.87(i) and (j).
42. Measure the dose rate in millirems per hour at one meter from the package surface to determine the Transport Index (TI). Indicate the TI on the Radioactive Material labels applied to the package in accordance with 49 CFR 172, Subpart E.
43. Determine the appropriate Criticality Safety Index (CSI) assigned to the package contents in accordance with the Certificate of Compliance, and indicate the correct CSI on the Fissile Material label applied to the package per 49 CFR 172, Subpart E.
44. Apply appropriate placards to the transport vehicle in accordance with 49 CFR 172, Subpart F.
45. Complete the shipping documents and provide the carrier with instructions regarding the requirements for maintaining an exclusive use shipment.

7.1.11 Procedure for Dry Loading of TPBAR Waste Container

This section describes the procedure for the loading of a TPBAR Waste Container into a NAC-LWT cask in a dry loading facility. Appropriate radiological controls and procedures addressing tritium shall be utilized by the licensee, including appropriate monitoring for tritium exposure.

NAC-LWT casks to be used for the transport of TPBARs shall be configured as shown on Drawing No. 315-40-128, including Alternate B port covers.

1. Perform a receiving survey of the ISO and trailer, and inspect for damage.
2. Position the trailer in the designated cask unloading area. Set the trailer brakes and chock the wheels to prevent unintended movement. If site-specific conditions exist that require the trailer to move to allow the cask to be uprighted on its rotation trunnions, release the brakes and remove the chocks when required to complete the uprighting operations. If necessary, the ISO container may be removed from the trailer and secured in the unloading area.
3. Licensees shall receive and survey the package for radiation and removable contamination (for both gross beta-gamma and tritium) per 10 CFR 20 and 49 CFR 173. Record the survey results. If radiation or contamination levels exceed the limits of 49 CFR 173.441 or 173.443, respectively, the licensee shall notify the shipper and ensure the appropriate notifications are completed.
4. Remove the roof from the ISO container and open the front and rear ISO doors. Remove the ISO roof cross members, if installed.
5. Remove the top and bottom impact limiters.
6. Remove the cask tie-down strap. Complete the radiation and contamination surveys of the package as additional surfaces become accessible. Clean the cask surfaces as required for entry into the dry loading facility.
7. Using the cask lifting yoke with lift yoke arm guides removed, engage the lifting trunnions of the front end of the cask. Raise the cask to a vertical position on the rear cask supports, moving the crane and/or trailer, as required, to keep the cask engaged in the rear cask supports and the crane cable vertical. When the cask is vertical, block the trailer wheels and lift the cask from the container.
8. Place the cask in a transfer cart or a loading fixture. Disengage the lifting yoke.
9. Remove the Alternate B vent and drain valve port covers. Replace the metallic seal with an approved spare and inspect the Viton[®] O-ring seal on each cover. If the Viton[®] O-ring shows any damage, replace it. Ensure the replacement O-rings are properly installed and seated. Store the port cover to protect the seal surfaces. Visually inspect the vent and drain valved quick-disconnect nipples and replace, if necessary.
10. Loosen and remove all closure lid bolts.
11. Attach the lid removal fixture to the closure lid.

12. Use a transfer cart or loading fixture and move the cask into the loading position.
13. Remove the closure lid and set it on a support that is suitable for radiological control and for maintaining the cleanliness of the closure lid. Carefully inspect the Teflon O-ring seal in the underside of the closure lid. If the O-ring shows any damage, replace it. Remove the metallic O-ring and replace it with an approved spare. Ensure the replacement O-rings are properly installed and seated. Inspect the lid bolts and replace any that are damaged. Verify that the TPBAR spacer is installed on the bottom of the cask lid and not damaged when the lid is set down.
14. Install the seal surface protector in the lid cavity, if required.
15. Load the TPBAR Waste Container into the TPBAR basket positioned in the cask cavity using the required grapple or handling system. Verify the contents of the Waste Container comply with the CoC content conditions.
16. Remove the cask seal surface protector, if used, and install the cask closure lid.
17. Use the transfer cart or loading fixture and remove the cask from the loading area.
18. Inspect, install and tighten all 12 closure lid bolts to 260 ± 20 ft-lbs in three passes using the torque sequence indicated on the closure lid.
19. Connect a vacuum pump to the cask vent valve.
20. Install the drain port cover, if drain valve is not required for operations, and torque the port cover bolts to 285 ± 15 in-lbs.
21. Perform the helium mass spectrometer maintenance leakage rate test on the cask lid to leaktight criteria in accordance with the requirements of Section 8.1.3.1, Steps 3 through 10.
22. Following successful completion of the helium backfill and helium leak testing of the lid seal, monitor the cavity volume for tritium and record the results.

Note: Tritium monitoring system shall have a minimum sensitivity of 5×10^{-3} micro curies/cc.

23. Install Alternate B port covers on the vent and drain openings and torque each port cover bolt to 285 ± 15 in-lbs. Perform a helium leakage rate test on each port cover to leaktight criteria in accordance with Section 8.1.3.3.
24. Decontaminate the cask. Survey the cask surface for gross beta-gamma and tritium removable contamination levels, and radiation dose rates.

Note: Removable contamination levels and radiation levels shall comply with 49 CFR 173.443 and 173.441, respectively.

25. Using the cask lifting yoke with the guide arms removed, lift and position the cask in the rear cask supports on the ISO/trailer. Engage the trunnion pockets in the bottom end of the cask with the rotation trunnions. Lower the cask to rest on the front tiedown

- saddle, moving the crane, and/or trailer, as required, to keep the crane cables vertical. Disengage the cask lifting yoke from the cask lifting trunnions and set it aside.
26. Install and attach the cask tiedown strap. Install the cask top and bottom impact limiters.
 27. Install a tamper-indicating seal to one of the top impact limiter ball lock pins.
 28. Install roof cross members, close ISO container doors, and replace ISO container roof.
 29. Complete a Health Physics survey on the external surface of the package and record the results. Complete dose rate measurements at the cask surface, at 1 meter from the cask surface, and at 2 meters from the vertical plane of the side of the transport vehicle. The maximum dose rate at 1 meter from the cask is the transport index (TI). Ensure compliance with 10 CFR 71.87(i) and observe the following criteria.
 - If the dose rate is less than 2 mSv/h (200 mrem/hr) at all accessible points on the external surface of the cask, and the TI is less than 10, the package must meet the requirements of 10 CFR 71.47 (a).
 - If the dose rate is greater than 2 mSv/h (200 mrem/hr), but is less than 10 mSv/h (1000 mrem/hr) at any point on the external surface of the package, or the TI is greater than 10, the package must be shipped as “exclusive use” and meet the requirements of 10 CFR 71.47 (b), (c) and (d). If the dose rate and shipping requirements of 10 CFR 71.47 (b), (1), (2), (3) and (4) cannot be met, the package cannot be shipped.
- Note: 10 CFR 71.47 (c) and (d) require the shipper to provide the carrier with written instructions for maintenance of the exclusive use shipment. The instructions must be included with the shipping paper information. The instructions must be sufficient so that, when followed, they cause the carrier to avoid actions that unnecessarily delay delivery or unnecessarily result in increased radiation levels or radiation exposures to transport workers or members of the general public.
- If the dose rate is > 10 mSv/h (1000 mrem/hr) at any point on the external surface of the cask, the cask exceeds the limits of 10 CFR 71.47 and cannot be shipped.
30. Complete the shipping document, carrier instructions (if required), and apply appropriate placards and labels.

7.1.12 Procedure for Wet Loading PWR MOX Fuel Rods in a Transport Canister Into the NAC-LWT Cask

PWR MOX fuel rods (or combinations of PWR MOX and UO₂ PWR fuel rods) are required to be loaded into a screened or free flow PWR/BWR Rod Transport Canister prior to loading into the NAC-LWT cask for transport. Although a maximum quantity of 16 MOX fuel rods may be shipped, it is required that the 5 × 5 rod insert be used to position the rods in the transport canister (i.e., the 4 × 4 insert is not authorized for use for the transport of MOX fuel rods).

In order to satisfy the increased potential for release of significant quantities of radioactive materials, and as recommended by NUREG-1617, Supplement 1, the NAC-LWT cask assembly specified for the transport of PWR MOX fuel rods contained in a transport canister provides a leaktight containment boundary (e.g., Alternate B port covers with metallic seals are utilized in combination with the closure lid and its metallic seal). All cask penetrations are individually helium leakage tested to meet the leaktight containment testing requirements of ANSI N14.5-1997.

The screened or free flow transport canister with a 5 × 5 rod insert will be loaded with up to 16 PWR MOX fuel rods (or a combination of up to 16 PWR MOX and UO₂ PWR fuel rods). In addition to the 16 PWR MOX fuel rods, up to 9 zirconium alloy-based burnable poison rods (BPRs) may be loaded into the unused insert openings.

NAC-LWT casks to be used for the transport of MOX fuel rods shall be configured as shown on Drawing No. 315-40-104, Assembly 97, including Alternate B port covers.

1. Perform a receiving survey of the empty cask and inspect for damage.
2. Position a trailer in the designated cask unloading area. Set the trailer brakes and chock the wheels to prevent unintended movement. If site-specific conditions exist that require the trailer to move to allow the cask to be uprighted on its rotation trunnions, release brakes and remove the chocks when required to complete uprighting operations. If an ISO is used, it may be removed from the trailer and secured in the unloading area.
3. Remove the roof from the ISO container and open the front and rear ISO doors. Remove roof cross-members, if installed.

Note: Verify that the package nameplate displays the package identification number, USA/9225/B(U)F-96, as required by the CoC for PWR MOX fuel rods.

4. Perform a Health Physics survey of the cask and adjacent surfaces of the trailer.

Note: A receiving survey of the cask and transporter must be performed as soon as practical after arrival at the site to assure compliance with 10 CFR 71.87(i) and 10 CFR 71.47, and to assure timely reporting of any reportable noncompliance.

5. Remove the top and bottom impact limiters.
6. Remove the cask tie-down strap.
7. Using the lifting yoke with the guides removed, engage the lifting trunnions. Raise the cask to vertical by rotating the cask rotation sockets on the rear cask supports, moving the crane and/or trailer as required to maintain the lift yoke engaged to the trunnions and the cask engaged in the rear supports. When the cask is fully vertical, lift the cask from the supports and remove it from the trailer/container.
8. Place the cask in the decontamination pit or other designated area. Disengage the lifting yoke. Clean cask surfaces of road dirt, as required, for entry into the spent fuel pool.
9. Visually inspect the neutron shield tank fill, drain and level inspection plugs for signs of neutron shield fluid leakage. If leakage is detected, verify shield tank fluid level and correct, as required.
10. Remove the Alternate B vent and drain valve port covers. Prior to reinstallation of the port covers, replace the metallic O-ring seal with an approved spare and inspect the Viton[®] O-ring seal for each port cover. If the Viton[®] O-ring shows any damage, replace it. Ensure that the replacement O-rings are properly installed and seated. Store the port covers to protect the seal surfaces. Visually inspect the valved quick-disconnect nipples and replace them, if necessary.
11. Remove closure lid bolts. Attach the lid lift slings to the closure lid. Remove the closure lid and set it on a support that is suitable for radiological control and for maintaining the cleanliness of the closure lid. Prior to reinstallation of the lid, carefully inspect the Teflon O-ring seal in the underside of the closure lid. If the O-ring shows any damage, replace it. Remove the metallic O-ring and replace it with an approved spare. Ensure that the replacement O-ring(s) is properly installed and seated. Inspect the lid bolts and replace any that are damaged. Ensure that the Rod Transport Canister spacer is not damaged when the lid is set down.
12. Visually inspect the inner cavity for foreign material or damage. Install or verify the presence of the drain tube and the PWR basket assembly.
13. Fill the cask cavity with clean water. Install lift yoke arm guides and remote actuation components on the cask lifting yoke.
14. Engage the cask lifting yoke with the cask lifting trunnions and pick up the cask. Carefully lower the cask to the bottom of the cask loading area while spraying the cask down with clean water.
15. Disengage the lifting yoke from the cask and remove the yoke from the pool.
16. Identify the PWR/BWR Rod Transport Canister to be loaded and verify that a 5 × 5 rod insert is located in the canister.
17. Identify the PWR MOX fuel rods (and standard PWR rods and BPRs, as applicable) to be loaded into the PWR/BWR Rod Transport Canister. Verify that the fuel rods and BPRs comply with the content type, form and quantity conditions of the NAC-

- LWT CoC. Load the screened or free flow PWR/BWR transport canister with up to 16 PWR MOX fuel rods, a combination of MOX and standard PWR rods, and up to 9 BPRs in the open tube locations in the 5 × 5 insert. Perform an independent verification of the fuel rod selection and loading process.
18. Install the transport canister lid and torque the lid bolts to 35 ± 5 inch-pounds.
 19. Position the loaded PWR/BWR Rod Transport Canister over the cask and then carefully lower it into the cask to avoid damage to the cask sealing surfaces. Note that the transport canister may be loaded into the cask with the PWR basket insert.
 20. Position the cask lifting yoke over the cask closure lid. Attach the slings to the closure lid and cask lifting yoke. Lower the yoke over the cask.
 21. Position the closure lid over the cask and verify that the appropriate lid spacer is installed per the approved PWR MOX fuel rod transport arrangement in Drawing 315-40-104, Section 1.4. Lower the closure lid into the lid recess using the lid match marks as guides to align the lid. Visually confirm that the closure lid is flush with the top of the cask and properly seated.
 22. Lower the cask handling yoke to slack the closure lid cables. Engage the lift yoke to the lifting trunnions and begin lifting the cask.

Note: Visually verify the yoke engagement before lifting the cask.
 23. Raise the cask until the lid is slightly above the surface of the pool. At the option of the licensee/user, a number of closure lid bolts (4 to 12) may be installed hand tight.
 24. Raise the cask clear of the pool, rinsing the yoke and cask with clean water and transfer the cask to the decontamination pit or other work area. Remove the yoke and lid lift slings.
 25. Install and tighten the 12 closure lid bolts to 260 ± 20 ft-lb in three passes, using the torque sequence stamped on the closure lid.
 26. At the option of the licensee/user, a 25 to 50 gallon clean water flush of the cask cavity may be performed by connecting a valved clean water line to the drain valve and a valved drain line to the vent valve. After the cavity flushing is completed, if performed, disconnect the water supply and drain lines.
 27. Connect a nitrogen or helium gas supply line to the vent valve and the drain line to the drain valve.
 28. Open the nitrogen or helium gas supply valve and pressurize the cask cavity (<30 psig) to force out the water. Continue to supply pressurized helium to the cask for a minimum of five minutes after the last residual free water discharges from the drain line. Remove the drain and gas supply lines and attach a vacuum drying system (VDS) to the cask vent valve.
 29. Evacuate the cask cavity to a vacuum pressure of less than 10 torr (13 mbar) and continue vacuum pumping for a minimum of 15 minutes.

30. At the end of the vacuum pumping period, isolate the cask cavity from the vacuum pump and stop the pump. Monitor the cask cavity pressure for a minimum of 10 minutes. If the pressure rise is less than 5 torr (6.7 mbar), the cavity is verified as dry of free water. If the pressure rise is greater than 5 torr (6.7 mbar), repeat vacuum drying until the dryness verification results are satisfactory.
31. Backfill the cask cavity with helium to 0 psig (1 atmosphere, absolute), +2, -0 psi. Disconnect the VDS.
32. Perform the helium leakage test of the closure lid containment O-ring using a Helium Mass Spectrometer Leak Detector (He MSLD) in accordance with the requirements of Section 8.1.3.1, Steps 6 through 10, with leakage rate acceptance criteria per 8.1.3.1, Step 9(b).
33. Install, torque the high-strength bolts to 285 ± 15 inch-pounds, and helium leakage test the Alternate B vent and drain port covers to leaktight criteria in accordance with Section 8.1.3.3.2, Steps 1-10.
34. Decontaminate the cask. Survey the cask for surface contamination and radiation dose rates.

Note: Ensure compliance with 10 CFR 71.87(i) and 10 CFR 71.47.
35. Remove lift yoke arm guides. Engage the cask lifting yoke to the lifting trunnions.
36. Lift the cask and position the cask rotation sockets in the rear rotation trunnions of the rear support structure. Carefully lower the cask to the horizontal transport orientation resting on the front saddle by moving the crane and/or trailer, as required, to maintain cask engagement to the rear supports.
37. Disengage the cask lifting yoke from the cask lifting trunnions and remove it from the area.
38. Install the cask tie-down strap. Install the top and bottom impact limiters.
39. Install tamper seal wire and number seal on the top attachment point of the top impact limiter.
40. Install roof cross-members, close ISO container doors, and replace ISO container roof.
41. Complete radiation and contamination surveys of the external surfaces of the package and record the data. Ensure removable contamination and radiation dose rate survey results comply with the limits specified in 10 CFR 71.87(i) and (j).
42. Measure the dose rate in millirems per hour at one meter from the package surface to determine the Transport Index (TI). Indicate the TI on the Radioactive Material labels applied to the package in accordance with 49 CFR 172, Subpart E.
43. Determine the appropriate Criticality Safety Index (CSI) assigned to the package contents in accordance with the CoC, and indicate the correct CSI on the Fissile Material label applied to the package per 49 CFR 172, Subpart E.

44. Apply appropriate placards to the transport vehicle in accordance with 49 CFR 172, Subpart F.
45. Complete the shipping documents and provide the carrier with instructions regarding the requirements for maintaining an exclusive use shipment.

7.2 Procedures for Unloading Package

In general, the procedure for unloading the package is the reverse of that presented for loading the package (Section 7.1). Specific generic procedures are provided in this section for the wet and dry unloading of various authorized contents from the NAC-LWT cask. As required to accommodate specific facilities and equipment, site-specific procedures shall be prepared and utilized for the unloading operations as appropriate to the contents.

7.2.1 Procedures for Wet Unloading of LWR Fuel and PWR, PWR MOX and BWR Fuel Rods in Transport Canisters

The procedures for unloading the package are as follows:

1. Perform a receipt inspection of the cask and trailer/ISO container, inspecting for transport damage.
2. Position the trailer in the designated cask unloading area. Set the trailer brakes and chock the wheels to prevent unintended movement. If site-specific conditions exist that require the trailer to move to allow the cask to be uprighted on its rotation trunnions, release brakes and remove the chocks when required to complete uprighting operations. If an ISO container is used, it may be removed from the trailer and secured in the unloading area.
3. Remove the lid/top of the ISO container and remove any bracing, or the personnel barrier.

Note: Verify that the package nameplate displays the correct package identification number in accordance with the CoC.

4. Licensees shall monitor the package for radioactive contamination and radiation levels in accordance with 10 CFR 20.1906. If contamination levels exceed 10 CFR 71.87(i) or radiation levels exceed the limits of 10 CFR 71.47, the licensee shall notify the NRC Operations Center.
5. Inspect the security seal and wire on the top impact limiter and confirm the seal number is correct per the shipper's documentation.
6. Remove the top and bottom impact limiters.
7. Remove the cask tie-down strap.
8. Using the lifting yoke with the guides removed, engage the lifting trunnions. Raise the cask to vertical by rotating the cask rotation sockets on the rear cask supports, moving the crane and/or trailer as required to keep the lift yoke engaged to the trunnions and the cask engaged in the rear supports. When the cask is fully vertical, lift the cask from the supports and remove it from the trailer/container.

9. Place the cask in the decontamination pit or other designated area. Disengage the lifting yoke. Clean cask surfaces of road dirt as required for entry into the spent fuel pool.
10. Remove the vent and fill/drain valve port covers. Connect a pressure gauge and isolation valve assembly to the cask vent valve.
11. Connect vent and clean water fill lines to the vent and drain valves.
12. Open the water supply valve to allow water to slowly enter the cask cavity.

Note: The hot gases exiting from the vent valve could be highly radioactive. The exhaust gases must, therefore, be routed to an off-gas process system. The cask cavity does not contain a relief valve; therefore, any system for cooling down the package must be provided with a pressure relief device set so that the maximum pressure in the cask cavity does not exceed 100 psig. Coolant flow rates should be controlled to avoid thermal shock to the cask internals.
13. Continue the filling procedure until the cask cavity is filled with water. Remove fill and vent lines.
14. Loosen and remove the closure lid bolts. At the option of licensee/user, some bolts (i.e., 4-12) may be left installed hand tight for the cask movement to the spent fuel pool.
15. Engage the cask lifting yoke (with slings, yoke arm guides and remote actuation system components attached) with the cask lifting trunnions and connect the closure lid to the lifting yoke slings.
16. Position the cask over the spent fuel pool and lower the cask until the top of the cask is at an elevation that permits access to the closure lid bolts.
17. Remove any remaining closure lid bolts.
18. Carefully lower the cask to rest on the bottom of the cask unloading area while spraying the cask's exterior surfaces with clean water to minimize contamination.
19. Disengage the lifting yoke from the cask and slowly raise the yoke until the closure lid is raised clear of the cask. Remove the yoke from the vicinity of the cask to provide clearance for unloading the cask.
20. Unload the contents of the cask cavity (i.e., fuel assemblies or Rod Transport Canisters) using the required grapple system. Verify that the unloaded contents conform to the contents described in the cask loading report. Place the fuel assemblies or transport canisters into storage or prepare them for further processing.
21. Position the cask lifting yoke with the cask closure lid over the cask cavity and slowly lower it into place using the cask and closure lid match marks as guides. Visually confirm that the closure lid is seated.
22. Engage the cask lifting yoke with the cask trunnions and raise the cask.

Note: Verify yoke engagement before lifting the cask.

23. Raise the cask until the lid is slightly above the surface of the pool. At the option of the licensee/user, several of the closure lid bolts (i.e., 4-12) may be installed hand tight.
24. Raise the cask clear of the pool, rinsing the yoke and cask with clean water.
25. Transfer the cask to the decontamination pit or other work area. Remove the yoke and lid lift slings.
26. Install and tighten all 12 closure lid bolts to 260 ± 20 ft-lb in three passes, using the torque sequence stamped on the closure lid.
27. At the option of the licensee/user, a 25 to 50 gallon clean water flush of the cask cavity may be performed by connecting a valved, clean water line to the drain valve and a valved drain line to the vent valve. After the cavity flushing is completed, if performed, disconnect the water supply and drain lines.
28. Connect a gas (air, nitrogen or helium) supply line to the vent valve and the drain line to the drain valve.
29. Open the gas supply valve and pressurize the cask cavity (<30 psig) to force out the water. Continue to supply gas to the cask cavity for a minimum of five minutes after the last residual free water discharges from the drain line.
30. Remove the gas supply and drain lines.
31. Install the alternate port covers over the vent and drain valves and tighten the port cover bolts to 100 ± 10 inch-pounds. For Alternate B port covers, install and torque the high-strength bolts to 285 ± 15 inch-pounds.

Note: It is not necessary to inspect or replace the port cover seals. Seal inspection and replacement, if required, will be performed prior to the next loaded transport.

7.2.2 Procedures for Wet Unloading of Metallic Fuel

The procedure for unloading the metallic fuel from the package in a spent fuel pool is as follows.

1. Perform a receipt inspection of the cask and trailer/ISO container, inspecting for transport damage.
2. Position the trailer in the designated cask unloading area. Set the trailer brakes and chock the wheels to prevent unintended movement. If site-specific conditions exist that require the trailer to move to allow the cask to be uprighted on its rotation trunnions, release brakes and remove the chocks when required to complete uprighting operations. If an ISO container is used, it may be removed from the trailer and secured in the unloading area.
3. Remove the lid/top of the ISO container and remove any bracing, or the personnel barrier.

Note: Verify that the package nameplate displays the correct package identification number in accordance with the CoC.

4. Licensees shall monitor the package for radioactive contamination and radiation levels in accordance with 10 CFR 20.1906. If contamination levels exceed 10 CFR 71.87(i) or radiation levels exceed the limits of 10 CFR 71.47, the licensee shall notify the NRC Operations Center.
5. Inspect the security seal and wire on the top impact limiter and confirm the seal number is correct per the shipper's documentation.
6. Remove the top and bottom impact limiters.
7. Remove the cask tie-down strap.
8. Using the lifting yoke with the guides removed, engage the lifting trunnions. Raise the cask to vertical by rotating the cask rotation sockets on the rear cask supports, moving the crane and/or trailer as required to keep the lift yoke engaged to the trunnions and the cask engaged in the rear supports. When the cask is fully vertical, lift the cask from the supports and remove it from the trailer/container.
9. Place the cask in the decontamination pit or other designated area. Disengage the lifting yoke. Clean cask surfaces of road dirt as required for entry into the spent fuel pool.
10. Remove the vent valve and drain valve port covers. Connect a pressure gauge and isolation valve assembly to the cask vent valve. Open the isolation valve and record the internal pressure reading (if any). Using a suitable air line and the gauge/valve assembly, vent the cask cavity to an off-gas handling unit.
11. Connect vent and clean water fill lines to the vent and drain valves.
12. Open the water supply valve to allow water to slowly enter the cask cavity.

Note: The hot gases exiting from the vent valve could be highly radioactive. The exhaust gases must, therefore, be routed to an off-gas process system. The cask cavity does not contain a relief valve; therefore, any system for cooling down the package must be provided with a pressure relief device set so that the maximum pressure in the cask cavity does not exceed 100 psig. Coolant flow rates should be controlled to avoid thermal shock to the cask internals.
13. Continue the filling procedure until the cask cavity is filled with water. Remove fill and vent lines.
14. Loosen and remove the 12 closure lid bolts. At the option of licensee/user, some bolts (i.e., 4-12) may be left installed hand tight for the cask movement to the spent fuel pool.
15. Engage the cask lifting yoke (with slings, lift yoke arm guides and remote actuation system components attached) with the cask lifting trunnions and connect the closure lid to the lifting yoke slings.
16. Position the cask over the spent fuel pool and lower the cask until the top of the cask is at an elevation, which permits access to the closure lid bolts.
17. Remove any remaining closure lid bolts, inspect and store.

18. Carefully lower the cask to rest on the bottom of the cask unloading area while spraying the exterior surfaces of the cask with clean water to minimize contamination. Disengage the lifting yoke from the cask and slowly raise the yoke until the closure lid is raised clear of the cask. Remove the yoke from the vicinity of the cask to provide clearance for unloading the cask.

Note: Closure lid may be brought out of the pool and later assembled to the empty cask.

19. Unload the contents of the cask cavity using the required grapple system.
20. Position the cask lifting yoke with the cask closure lid over the cask cavity and slowly lower it into place using the cask and closure lid match marks as guides. Visually confirm that the closure lid is seated.
21. Engage the cask lifting yoke with the cask trunnions and raise the cask.
22. Raise the cask until the lid is slightly above the surface of the pool. At the option of the licensee/user, several of the closure lid bolts (i.e., 4-12) may be installed hand tight.
23. Raise the cask clear of the pool, rinsing the yoke and cask with clean water.
24. Transfer the cask to the decontamination pit or other work area. Remove the yoke and lid lift slings.
25. Install and tighten the 12 closure lid bolts to 260 ± 20 ft-lb in three passes, using the torque sequence stamped on the closure lid.
26. At the option of the licensee/user, a 25 to 50 gallon clean water flush of the cask cavity may be performed by connecting a valved, clean water line to the drain valve and a valved drain line to the vent valve. After the cavity flushing is completed, if performed, disconnect the water supply and drain lines.
27. Connect a gas (air, nitrogen or helium) supply line to the vent valve and the drain line to the drain valve.
28. Open the gas supply valve and pressurize the cask cavity (<30 psig) to force out the water. Continue to supply gas to the cask cavity for a minimum of five minutes after the last residual free water discharges from the drain line.
29. Remove the gas supply and drain lines.
30. Install the alternate port covers over the vent and drain valves and tighten the port cover bolts to 100 ± 10 in-lb. For Alternate B port covers, install and torque the high-strength bolts to 285 ± 15 inch-pound.

Note: It is not necessary to inspect or replace the port cover seals. Seal inspection and replacement, if required, will be performed prior to the next loaded transport.

7.2.3 Procedure for Wet Unloading of MTR, TRIGA, DIDO, ANSTO or PULSTAR Fuel Basket Contents

The procedure for the unloading of MTR, TRIGA, DIDO, ANSTO or PULSTAR fuel basket contents from the package in a spent fuel pool is as follows:

1. Perform a receiving survey of the cask and inspect for transport damage.
2. Position the trailer in the designated cask unloading area. Set the trailer brakes and chock the wheels to prevent unintended movement. If site-specific conditions exist that require the trailer to move to allow the cask to be uprighted on its rotation trunnions, release the brakes and remove the chocks when required to complete the uprighting operations. If an ISO container is used, it may be removed from the trailer and secured in the loading area.
3. Remove the roof from the ISO container, and open the front and rear ISO doors. Remove roof cross-members, if installed.

Note: Verify that the package nameplate displays the correct package identification number in accordance with the CoC.
4. Licensees shall monitor the package for radioactive contamination and radiation levels in accordance with 10 CFR 20.1906. If contamination levels exceed 10 CFR 71.87(i) or radiation levels exceed the limits of 10 CFR 71.47, the licensee shall notify the NRC Operations Center.
5. Inspect the security seal and wire on the top impact limiter and confirm the seal number is correct per the shipper's documentation.
6. Remove the top and bottom impact limiters.
7. Remove the cask tie-down strap.
8. Using the cask lifting yoke with left yoke arm guides removed, engage the lifting trunnions of the front end of the cask. Raise the cask to a vertical position on the rear cask support, moving the crane as necessary to keep the cask engaged in the rear rotation supports and the crane cable vertical. When the cask is vertical, lift the cask from the container supports.
9. Place the cask in the decontamination pit or other site designated area. Disengage the lifting yoke. Clean cask surfaces of road dirt as required for entry into the spent fuel pool.
10. Remove the vent valve and drain valve port covers. Connect a pressure gauge and isolation valve assembly to the cask vent valve. Open the isolation valve and record the internal pressure reading (if any). Using a suitable air line and the gauge/valve assembly, vent the cask cavity to an off-gas handling unit.
11. Connect vent and clean water fill lines to the vent and drain valves.
12. Open the water supply valve to allow water to slowly enter the cask cavity.

- Note: Gases or steam exiting the vent may be radioactive. The vent line should be routed to an off-gas process system or a HEPA filter. The system for cooling down the package shall contain a pressure relief device set to ensure that the cask internal pressure is maintained below 100 psig. Coolant flow rates are to be controlled to avoid thermal shock to the fuel contents.
13. Continue the filling procedure until the cask cavity is filled with water. Remove fill and vent lines.
 14. Loosen and remove the 12 closure lid bolts. At the option of licensee/user, some bolts (i.e., 4-12) may be left installed hand tight for the cask movement to the spent fuel pool.
 15. Engage the cask lifting yoke (with slings, yoke arm guides and remote actuation system components attached) with the cask lifting trunnions and connect the closure lid to the lifting yoke slings.
 16. Position the cask over the spent fuel storage pool and lower the cask until the top of the cask is at an elevation which allows access for the removal of the closure lid bolts.
 17. Remove any remaining closure lid bolts, inspect and store.
 18. Carefully lower the cask to rest on the bottom of the cask unloading area while spraying the exterior surfaces of the cask with clean water to minimize contamination. Disengage the lifting yoke from the lifting trunnions and slowly raise the yoke until the closure lid is raised clear of the cask. Remove the yoke from the vicinity of the cask to provide for clearance for unloading the cask.

Note: The closure lid may be brought out of the pool and later assembled to the empty cask.
 19. Unload the MTR, TRIGA, DIDO, spiral, MOATA plate or PULSTAR fuel assemblies or fuel cans from the top basket module using the appropriate grapple or handling system. As required, remove empty basket modules from the cask cavity to allow access to the next basket module. Continue fuel unloading operations until all fuel assemblies, fuel cans, and empty basket modules are removed from the cavity. Alternatively, each basket module containing fuel assemblies or damaged fuel cans may be unloaded from the cask cavity and stored in the spent fuel pool. Continue unloading until all basket modules have been removed.
 20. Position the cask lifting yoke with guide arms and remote actuation components installed over the cask closure lid. Attach the slings to the cask closure lid and cask lifting yoke.

21. Position the cask lifting yoke and closure lid over the cask cavity and slowly lower it into place using the cask and closure lid match marks as guides. Visually confirm that the closure lid is seated.
Note: The closure lid may be installed separately after the empty cask is removed from the spent fuel pool.
22. Engage the cask lifting yoke with the cask trunnions and raise the cask.
23. Raise the cask until the lid is slightly above the surface of the pool. At the option of the licensee/user, several of the closure lid bolts (i.e., 4-12) may be installed hand tight.
24. Raise the cask clear of the pool, rinsing the yoke and cask with clean water.
25. Transfer the cask to the decontamination pit or other work area. Remove the yoke and lid lift slings.
26. Install and tighten four closure lid bolts to 100 ± 10 ft-lb using the torque sequence stamped on the closure lid.
27. At the option of the licensee/user, a 25 to 50 gallon clean water flush of the cask cavity may be performed by connecting a valved, clean water line to the drain valve and a valved drain line to the vent valve. After the cavity flushing is completed, if performed, disconnect the water supply and drain lines.
28. Connect a gas (air, nitrogen or helium) supply line to the vent valve and the drain line to the drain valve.
29. Open the gas supply valve and pressurize the cask cavity (<30 psig) to force out the water. Continue to supply gas to the cask cavity for a minimum of five minutes after the last residual free water discharges from the drain line.
30. Remove the gas supply and water drain lines.
31. Remove the four closure lid bolts and lift the lid clear of the cask.
Note: It is not necessary to inspect or replace the closure lid metallic seal. A new metallic seal will be installed and tested prior to the next loaded transport.
32. Remove the drain tube assembly and drain tube alignment ring from the cask cavity.
33. Reinstall the closure lid and install the 12 closure lid bolts. Torque the bolts to 260 ± 20 ft-lbs in three passes using the torque sequence indicated in the closure lid.
34. Install the alternate port covers over the vent and drain valves and tighten the port cover bolts to 100 ± 10 in-lb. For Alternate B port covers, install and torque the high-strength bolts to 285 ± 15 inch-pound.

Note: It is not necessary to inspect or replace the port cover seals. Seal inspection and replacement, if required, will be performed prior to the next loaded transport.

7.2.4 Procedure for Dry Unloading of MTR, TRIGA, DIDO, ANSTO or PULSTAR Fuel Contents

This section describes the procedure for unloading of MTR, TRIGA, DIDO, ANSTO or PULSTAR fuel basket contents from the NAC-LWT in a cell or a dry unloading fixture.

1. Perform a receiving survey of the cask and inspect for transport damage.
2. Position the trailer in the designated cask unloading area. Set the trailer brakes and chock the wheels to prevent unintended movement. If site-specific conditions exist that require the trailer to move to allow the cask to be uprighted on its rotation trunnions, release the brakes and remove the chocks when required to complete the uprighting operations. If an ISO container is used, the ISO container may be removed from the trailer and secured in the unloading area.
3. Remove the roof from the ISO container and open the front and rear ISO doors. Remove roof cross members, if installed.

Note: Verify that the package nameplate displays the correct package identification number in accordance with the CoC.

4. Licensees shall monitor the package for radioactive contamination and radiation levels in accordance with 10 CFR 20.1906. If contamination levels exceed 10 CFR 71.87(i) or radiation levels exceed the limits of 10 CFR 71.47, the licensee shall notify the NRC Operations Center.
5. Inspect the security seal and wire on the top impact limiter and confirm the seal number is correct per the shipper's documentation.
6. Remove the top and bottom impact limiters.
7. Remove the cask tie-down strap. Clean the cask surfaces as required for entry into the hot cell.
8. Using the cask lifting yoke with lift yoke arm guides removed, engage the lifting trunnions of the front end of the cask. Raise the cask to a vertical position on the rear cask support, moving the crane and/or trailer, as required, to keep the cask engaged in the rear rotation supports and the crane cable vertical. When the cask is vertical, block the trailer wheels and lift the cask from the container.
9. Place the cask in the cell transfer cart or unloading fixture. Disengage the lifting yoke.
10. Remove the vent valve port cover.
11. Connect vent line to the vent valve.

Note: The hot gases exiting from the vent may be highly radioactive and the exhaust gas should be routed to an off-gas process system or to a HEPA filter.

12. Allow the cask to vent. Remove vent line.
13. Loosen and remove the 12 closure lid bolts. Visually inspect and store the bolts.
14. Attach the lid removal fixture.
15. Using the hot cell transfer cart or unloading fixture, move the cask into the unloading position.
16. Remove the cask lid.

Note: It is not necessary to inspect or replace the closure lid metallic seal. A new metallic seal will be installed and tested prior to the next loaded shipment.

17. Install the seal surface protector in the lid cavity, if required.
18. Unload the MTR, TRIGA, DIDO, ANSTO or PULSTAR fuel basket modules or TPBAR consolidation canister from the cask cavity using the required grapple or handling system.
19. Remove the cask seal surface protector, if installed, and replace the cask lid.
20. Using the cell transfer cart or unloading fixture, remove the cask.
21. Remove the lid from the cask and remove the drain tube and drain tube alignment ring (not required for TPBAR configuration).
22. Replace the cask lid and remove the lid removal fixture.
23. Install and tighten all 12 closure lid bolts to 260 ± 20 ft-lbs in three passes using the torque sequence indicated on the closure lid.
24. Install the port covers over the vent and drain valves and tighten the port cover bolts to 100 ± 10 inch-pounds. For Alternate B port covers, install and torque the high-strength bolts to 285 ± 10 inch-pounds.

Note: It is not necessary to inspect or replace the port cover seals. Seal inspection replacement and leak testing will be performed prior to the next loaded transport.

7.2.5 Procedure for Dry Unloading of TPBAR Contents

This section describes the procedure for the unloading of a TPBAR Consolidation Canister or Waste Container from the NAC-LWT in a dry unloading facility.

1. Perform a receiving survey of the ISO container and trailer, and inspect for damage.
2. Position the trailer in the designated cask unloading area. Set the trailer brakes and chock the wheels to prevent unintended movement. If site-specific conditions exist that require the trailer to move to allow the cask to be uprighted on its rotation trunnions, release the

brakes and remove the chocks when required to complete the uprighting operations. If necessary, the ISO container may be removed from the trailer and secured in the unloading area.

3. Licensees shall receive and survey the package for radiation and removable contamination (for both gross beta-gamma and tritium) per 10 CFR 20 and 49 CFR 173. Record the survey results. If radiation or contamination levels exceed the limits of 49 CFR 173.441 or 173.443, respectively, the licensee shall notify the shipper and ensure the appropriate notifications are completed.
4. Remove the roof from the ISO container and open the front and rear ISO doors. Remove the ISO roof cross members, if installed.
5. Remove the top and bottom impact limiters.
6. Remove the cask tie-down strap. Complete the radiation and contamination surveys of the package as additional surfaces become accessible. Clean the cask surfaces as required for entry into the dry unloading facility.
7. Using the cask lifting yoke with lift yoke arm guides removed; engage the lifting trunnions of the front end of the cask. Raise the cask to a vertical position on the rear cask support, moving the crane and/or trailer, as required, to keep the cask engaged in the rear rotation supports and the crane cable vertical. When the cask is vertical, block the trailer wheels and lift the cask from the container.
8. Place the cask in a transfer cart or an unloading fixture. Disengage the lifting yoke.
9. Remove the vent valve port cover.
10. Remove the drain valve port cover
11. Connect a tritium monitoring system to the vent and drain quick-disconnect valves, and operate the device in accordance with the manufacturer's instructions. The tritium monitoring system shall have a minimum sensitivity of 5×10^{-3} micro curie/cc.
12. Monitor the cavity gas for tritium. If the gas sample measurement indicates a tritium gas concentration greater than 1×10^{-2} micro curie/cc, the cask internals must be decontaminated after unloading is completed and prior to subsequent use in transporting non-TPBAR contents.

Note: The gases exiting from the cavity may be radioactive and contaminated with tritium, and at an elevated temperature. Cavity gases should be controlled per the site requirements.

13. Vent the cask cavity. Remove the gas lines and monitoring system from the vent and drain valves.
14. Loosen and remove all closure lid bolts.
15. Attach the lid removal fixture.
16. Use a transfer cart or unloading fixture and move the cask into the unloading position.

17. Remove the cask lid.

Note: Replacement of the closure lid metallic seal is not required. A new metallic seal will be installed and leak tested prior to the next loaded shipment.

18. Install the seal surface protector in the lid cavity, if required.
19. Unload the TPBAR contents from the cask cavity using the required grapple or handling system.
20. Using the transfer cart or unloading fixture, remove the cask from the unloading area.
21. Collect an ambient air sample near the cask cavity opening. If the measured tritium gas concentration exceeds 1×10^{-2} micro curie/cc, the cask cavity must be decontaminated after unloading and prior to subsequent use in transporting non-TPBAR contents.
22. Survey the accessible inside surfaces of the cask cavity and internal components (i.e., upper 2 feet) for tritium contamination. If measured tritium removable contamination is greater than $2.2 \times 10^{+4}$ dpm/100 cm², the cask must be decontaminated after unloading is completed and prior to subsequent use in transporting non-TPBAR contents.

Note: If significantly higher tritium contamination levels and the need for repeated decontamination become indicative of residual tritium contamination in the crystalline structure of the cask interior with potential for weeping, NAC will notify NRC of the condition and its action.

23. Remove the cask seal surface protector, if used, and install the cask lid.
24. Inspect, install and tighten all 12 closure lid bolts to 260 ± 20 ft-lbs in three passes using the torque sequence indicated on the closure lid.

Note: Replacement of the vent and drain port cover metallic seals is not required. New metallic seals will be installed and leak tested prior to the next loaded shipment.

25. Install the port covers on the vent and drain ports and torque the port cover bolts to 285 ± 15 inch-pounds.

7.2.6 Procedure for Dry Unloading of PWR/BWR/MOX Fuel Rod Contents

This section describes the procedure for the unloading of a PWR/BWR Rod Transport Canister from the NAC-LWT cask in a dry unloading facility.

1. Perform a receiving survey of the ISO container and trailer, and inspect for damage.
2. Position the trailer in the designated cask unloading area. Set the trailer brakes and chock the wheels to prevent unintended movement. If site-specific conditions exist that require the trailer to move to allow the cask to be uprighted on its rotation trunnions, release the brakes and remove the chocks when required to complete the uprighting operations. If

necessary, the ISO container may be removed from the trailer and secured in the unloading area.

3. Licensees shall receive and survey the package for radiation and removable contamination per 10 CFR 20 and 49 CFR 173. Record the survey results. If radiation or contamination levels exceed the limits of 49 CFR 173.441 or 173.443, respectively, the licensee shall notify the shipper and ensure the appropriate notifications are completed.
4. Remove the roof from the ISO container and open the front and rear ISO doors. Remove the ISO roof cross members, if installed.
5. Verify the TID identification number on the top impact limiter to confirm tampering of the package did not occur.
6. Remove the top and bottom impact limiters.
7. Remove the cask tie-down straps. Complete the radiation and contamination surveys of the package as additional surfaces become accessible. Clean the cask surfaces as required for entry into the dry unloading facility.
8. Using the cask lifting yoke with lift yoke arm guides removed, engage the lifting trunnions of the front end of the cask. Raise the cask to a vertical position on the rear cask support, moving the crane and/or trailer, as required, to keep the cask engaged in the rear rotation supports and the crane cable vertical. When the cask is vertical, block the trailer wheels and lift the cask from the container.
9. Place the cask in a transfer cart or an unloading fixture. Disengage the lifting yoke.
10. Remove the vent valve port cover.
11. Remove the drain valve port cover
12. Connect the vent line with pressure gauge and isolation valve to the vent port quick disconnect coupling.

Note: At the discretion of the receiving facility, a gas sample may be taken prior to cavity venting to determine if leakage from the fuel rods occurred during transport.

Note: The gases exiting from the cavity may be radioactive and at an elevated temperature and pressure. Cavity gases should be controlled and vented to radioactive gas treatment systems per site requirements.

13. Vent the cask cavity. Remove the vent line from the vent valves.
14. Attach the lid removal fixture.
15. Loosen and remove all closure lid bolts.
16. Use the transfer cart or unloading fixture and move the cask into the unloading position.
17. Remove the cask lid.

Note: Replacement of the closure lid metallic seal is not required. A new metallic seal will be installed and leak tested prior to the next loaded shipment.

18. Install the seal surface protector in the lid cavity, if required.
19. Unload the PWR/BWR Rod Transport Canister and/or its contents using the appropriate grapple or handling system.
20. Using the transfer cart or unloading fixture, remove the cask from the unloading area.
21. Remove the cask seal surface protector, if used, and install the cask lid.
22. Inspect, install and tighten all 12 closure lid bolts to 260 ± 20 ft-lbs in three passes using the torque sequence indicated on the closure lid.

Note: Replacement of the vent and drain port cover metallic seals is not required. New metallic seals will be installed and leak tested prior to the next loaded shipment.

23. Install the port covers on the vent and drain ports and torque the port cover bolts to 285 ± 15 inch-pounds.

Chapter 8

Table of Contents

8	ACCEPTANCE TESTS AND MAINTENANCE PROGRAM.....	8.1-1
8.1	Acceptance Tests.....	8.1-1
8.1.1	Visual Inspection	8.1-1
8.1.2	Structural and Pressure Tests	8.1-2
8.1.3	Leak Tests	8.1-3
8.1.4	Component Tests	8.1-7
8.1.5	Tests for Shielding Integrity	8.1-9
8.1.6	Thermal Acceptance Tests	8.1-9
8.1.7	Neutron Absorber Tests	8.1-10
8.2	Maintenance Program	8.2-1
8.3	Appendix.....	8.3-1
8.3.1	General Description	8.3-1
8.3.2	Preparation	8.3-1
8.3.3	Pouring Procedure.....	8.3-2
8.3.4	Cooling Process	8.3-2

List of Figures

Figure 8.3-1	Lead Pour Configuration.....	8.3-3
Figure 8.3-2	Allowable Height Difference.....	8.3-4

List of Tables

Table 8.2-1	Maintenance Program Schedule.....	8.2-3
-------------	-----------------------------------	-------

8 **ACCEPTANCE TESTS AND MAINTENANCE PROGRAM**

This chapter discusses the acceptance test and maintenance program to be used for the NAC-LWT cask, in compliance with 10 CFR 71, Subpart G.

Where required, specific procedures for testing will be developed in conjunction with the cask fabrication, in accordance with an approved Quality Assurance program.

8.1 **Acceptance Tests**

This section discusses the tests to be performed prior to first use of the cask.

Two port cover designs are available for use. The alternate port cover has a face seal containment boundary Viton® O-ring and a secondary test boundary O-ring seal along the barrel of the port cover. The alternate port cover was developed to facilitate ease in installation and removal in the field. The Alternate B port cover has two face seals on the inner end of the port cover, one metallic containment boundary seal and one Viton® test boundary seal. The Alternate B port cover was developed to provide a leaktight configuration for content conditions requiring a leaktight and/or high pressure containment boundary. The Alternate B port covers utilize higher strength bolts and a higher installed torque value.

To simplify the testing procedures below, when “port cover” or “port cover O-ring” is mentioned, it is intended to mean the port cover which has been chosen for that specific fabrication or cask configuration, either the alternate or the Alternate B and their respective O-rings. The different testing procedures are described in the applicable sections.

8.1.1 **Visual Inspection**

All components making up the cask lid, body, and baskets are to be visually inspected. This inspection verifies that all items are properly cleaned, free of nicks, gouges and damage, and are assembled in accordance with the license drawings. Each item is compared to the appropriate drawing to verify that it is in the correct orientation, position, and location.

All dirt, oil residue, metal chips or other forms of debris are removed by appropriate cleaning methods. Any entrapped water is removed. Any component found to deviate from its drawing is re-installed, replaced, or otherwise reworked as necessary in order to bring it into conformance.

Acceptance criteria require complete cask cleanliness, that foreign objects are removed, and that nicks or gouges that might preclude sealing or cask closure are not permitted. Valve and system components are visually inspected for leaks during pressure checks. Leaks are not permitted. Any case of noncompliance shall be corrected prior to final acceptance. All welds are visually inspected in accordance with the methods of Article 9, Section V of the “ASME Boiler and

Pressure Vessel Code.” The acceptance criteria are in accordance with part NB-4424, Section III, and parts UW-35 or UW-36, Section VIII, of the “ASME Boiler and Pressure Vessel Code.”

8.1.2 Structural and Pressure Tests

Following completion of fabrication, a hydrostatic test is performed on the cask cavity in accordance with the “ASME Boiler and Pressure Vessel Code,” Section III, Subsection NB, Article NB-6000, to 209 (+5/-0) psig. This test is performed in accordance with a procedure prepared by the fabricator and approved by NAC International (NAC). For casks intended for transport of TPBARs, an additional post-fabrication hydrostatic test is performed to 450 +15/-0 psig ($1.5 \times$ MNOP of 289 psig = 434 psig). Alternate B port covers are installed for the 450 +15/-0 psig test. The test requirements and acceptance criteria for both tests are described below.

The cask cavity is hydrostatically tested using demineralized water. The test is conducted with the closure lid and valve port covers installed in accordance with the cask handling procedure for loaded casks, but with the quick-disconnect valves removed. During these two 30-minute pressure tests (conducted alternately with one port cover installed and the other removed for access to the cavity), an inspection is made to detect any visual or other evidence of leakage. Any evidence of leakage, including drop of gauge pressure, is cause for rejection.

Following the hydrostatic test, the cask cavity, lid, and port covers are dried and made ready for visual and dye penetrant testing (PT) inspections.

The cask cavity (containment boundary including lid and port covers) is visually inspected. All accessible welds within the cask cavity are examined by PT in accordance with ASME Code, Section V, Article 6, with acceptance criteria in accordance with ASME Code, Section III, Subsection NB, Article NB-5350. Any evidence of cracking, permanent deformation, or exceeding of material yield strength is cause for rejection.

Following completion of the fabrication pressure test or the postfabrication TPBAR-required pressure test, the cask containment boundary is leakage tested in accordance with the requirements of Section 8.1.3.

The neutron shield tank and the expansion tank are hydrostatically tested simultaneously, since they are joined by a siphon tube. The test is in accordance with the “ASME Boiler and Pressure Vessel Code,” Section VIII, Division 1, to 248 (+5/-0) psig (165 psig maximum hypothetical accident pressure \times 1.5). The neutron shield relief valve is replaced by a plug during the test. All tank seams and joints are inspected for evidence of leakage. The pressure is monitored by use of a pressure gauge. Any evidence of leakage or drop in pressure is cause for rejection. All accessible welds on the neutron shield structure are PT examined following the hydrostatic test.

Each of the two pairs of the cask lift trunnions is load tested. The load test is performed for one pair and, then, repeated for the other pair.

The test consists of applying a vertical load of 159,375 lbs + 3,000 lbs, -0 lbs (300 % of the maximum service load), to each trunnion pair. The load is applied in a vertical direction and equally distributed between the two trunnions.

This test may be carried out by the use of calibrated hydraulic rams combined with a beam, or the cask lifting yoke, and appropriate dead weight attached to the trunnion pair. The load is held for a minimum of 10 minutes.

Following the load test, all welds and material are visually inspected for plastic deformation and cracking and liquid penetrant inspected in accordance with the "ASME Boiler and Pressure Vessel Code," Section V, Article 6, and Section III, Division I, Subsection NF, Article NF-5350, as called for in ANSI N14.6-1993.

Any evidence of permanent deformation or any evidence of cracking, galling, or exceeding of yield strength is cause for rejection of that item.

The rotation sockets at the lower end of the cask are not load tested, being monolithic steel block with a suitably machined opening. Prior to first use, each socket is visually inspected for cleanliness and signs of deformation or other unsuitability. Accessible welds are inspected in accordance with the standards for the cask trunnions.

8.1.3 Leak Tests

The cask containment boundary is subjected to a fabrication leakage rate test, as described in the sections below, to verify containment following fabrication. The test is performed using helium inside the cask cavity and a helium mass spectrometer connected to the test port of the lid or one of the port covers. The mass spectrometer has a minimum sensitivity such that it is capable of detecting a leak rate of at least 1×10^{-9} ref cm^3/sec and is calibrated before and after the test with a standard having a known leak rate between 4×10^{-7} and 1×10^{-9} ref cm^3/sec . The procedure is performed between 40°F and 125°F and is temperature corrected. New O-rings are to be used. The basic procedures for the cask lid and for the vent and drain port covers are provided in the following sections.

A required maintenance leakage rate test adheres to the criteria listed above and follows the replacement of any containment component or seal. Containment components having single-use metallic containment seals (i.e., closure lid and Alternate B port covers) require a maintenance leakage rate test prior to each loaded transport. All containment components shall be subjected to a periodic leakage rate test annually while the cask is in service, or prior to returning the cask

to service if the period since the last leakage rate test exceeds 12 months. The acceptance criteria for the fabrication, maintenance, and periodic leakage rate tests appear in the following sections.

8.1.3.1 Closure Lid Leakage Rate Test

The following procedure shall be used to perform the fabrication, maintenance, periodic and pre-shipment leakage rate tests on the closure lid. Steps 1 and 2 are not performed for the pre-shipment leakage rate test performed during cask loading operations as described in Chapter 7.

1. Remove the vent and drain port covers and install the closure lid fitted with a new metallic seal on the cask body.
2. Install the 12 lid bolts and torque them to 260 ± 20 ft-lb in three passes, using the torque sequence stamped on the lid.
3. Connect the vacuum pump to the vent valve and evacuate the cask cavity to a pressure ≤ 100 torr (130 mbar).
4. Backfill the cask cavity with 99.9% (minimum) pure helium to atmospheric pressure.
5. Repeat Steps 3 and 4 to ensure that the cask cavity helium concentration is approximately 98%.
6. Remove the test port plug from the lid.
7. Connect a helium mass spectrometer leak detector (MSLD) to the cask lid test port. Start the helium MSLD.

Note: The specific test procedure depends on the helium MSLD used. The test commences when a vacuum is pulled on the test port by the MSLD and the MSLD is placed in the "test" mode.

8. Monitor the test leakage rate until the leakage rate is stable or a minimum of 30 seconds.
9. The acceptance criteria for the helium leakage test for the various NAC-LWT contents are as follows:
 - a. For contents not requiring a leaktight containment boundary, the measured leakage rate shall be $\leq 5.5 \times 10^{-7}$ cm³/s, helium.
 - b. For contents requiring a leaktight containment boundary (e.g., TPBAR contents, MOX fuel rods), the measured leakage rate shall be $\leq 2 \times 10^{-7}$ cm³/s, helium (i.e., leaktight per ANSI N14.5-1997 under the test conditions).
10. Remove helium MSLD from test port plug and reinstall port plug and torque to 60 ± 5 inch-pounds.

8.1.3.2 Alternate Port Cover Leakage Rate Tests

8.1.3.2.1 Fabrication and Periodic Leakage Rate Tests

The following procedure shall be used to perform the fabrication and periodic leakage rate tests on the alternate port covers.

1. If the port cover leakage rate tests are not performed immediately following the closure lid leakage rate test of Section 8.1.3.1, evacuate the cask cavity to ≤ 100 torr (130 mbar) and backfill to atmospheric pressure with 99.9% (minimum) pure helium. Reevacuate to ≤ 100 torr (130 mbar) and perform the final helium backfill to atmospheric pressure.
2. Install new O-rings on the port cover.
3. Remove the port valve (either vent or drain valve) and install the port cover.
4. Install and torque the port cover bolts to 100 ± 10 inch-pounds.
5. Remove the test port plug from the port cover.
6. Connect a helium MSLD to the test port. Start the helium MSLD.
7. Monitor the test leakage rate until the leakage rate is stable or for a minimum of 30 seconds.
8. The acceptance criteria for the helium leakage rate test shall be $\leq 5.5 \times 10^{-7}$ cm³/s, helium.
9. Remove helium MSLD from the test port and reinstall port plug and torque to 60 ± 5 inch-pounds.
10. Repeat Steps 1 through 9 for the second port cover.

8.1.3.2.2 Maintenance Leakage Rate Test

The following procedure shall be used to perform the maintenance leakage rate test on the alternate port covers following the field replacement of a port cover containment face seal during cask loading operations.

1. Replace the affected seal(s).
2. Insert port cover in a plastic test bag and seal the bag to the cask body around the port opening using suitable tape.
3. Evacuate test bag and backfill with 99.9% (minimum) pure helium to one atmosphere absolute.
4. Reevacuate test bag and perform final helium backfill to one atmosphere absolute.
5. Without breaking the seal of the plastic bag to the cask body, insert the port cover into the port opening and hand tighten the bolts.
6. Torque the bolts to 100 ± 10 inch-pounds. Remove the plastic bag.
7. Remove the test port plug from the port plug.

8. Attach helium MSLD to the port cover test port and evacuate the volume between the seals.
9. Monitor the test leakage rate until stable or for a minimum of 30 seconds.
10. The test is acceptable if the measured leakage rate is $\leq 5.5 \times 10^{-7} \text{ cm}^3/\text{s}$, helium.
11. Remove helium MSLD from test port and reinstall the test port plug and torque to 60 ± 5 inch-pounds.

8.1.3.3 Alternate B Port Cover Leakage Rate Tests

8.1.3.3.1 Fabrication and Periodic Leakage Rate Tests

The following test procedure shall be used to perform the fabrication and periodic leakage rate tests for the Alternate B port cover. For NAC-LWT casks to be used to transport TPBARs, the fabrication leakage rate test shall be performed immediately following the post-fabrication hydrostatic test to 450 +15/-0 psig required for transport of TPBAR contents. The Alternate B port covers shall be installed for the 450 +15/-0 psig hydrostatic test. The periodic leakage rate test will be performed as part of a cask's annual maintenance and certification program.

1. If the Alternate B port cover leakage rate tests are not performed immediately after the closure lid leakage rate test in Section 8.1.3.1, evacuate the cask cavity to ≤ 100 torr (130 mbar) and perform the final helium backfill to atmospheric pressure with 99.9% (minimum) pure helium. Reevacuate to ≤ 100 torr (130 mbar) and perform final helium backfill to atmospheric pressure.
2. Install the new metallic O-ring on the Alternate B port cover.
3. Remove the port nipple (either vent or drain valve) and install the Alternate B port cover.
4. Install and torque the port cover bolts to 285 ± 15 inch-pounds.
5. Remove the test port plug from the port cover.
6. Connect a helium MSLD to the test port. Start the helium MSLD.
7. Monitor the test leakage rate until the leakage rate is stable or for a minimum of 30 seconds.
8. The acceptance criteria for the Alternate B port cover is that the measured leakage rate shall be $\leq 2 \times 10^{-7} \text{ cm}^3/\text{s}$, helium, i.e., leaktight per ANSI N14.5-1997.
9. Remove helium MSLD from the test port and reinstall the test port plug and torque to 60 ± 5 inch-pounds.
10. Repeat Steps 1 through 9 for the second Alternate B port cover.

8.1.3.3.2 Maintenance and Preshipment Leakage Rate Tests

The following maintenance leakage rate test procedure for the Alternate B port cover is used after metallic O-ring replacement during each cask loading operation, or if another containment component of an Alternate B port cover is replaced, for contents requiring leaktight containment per ANSI N14.5-1997, such as TPBARs and MOX fuel rods.

1. Replace metallic seal.
2. Insert Alternate B port cover in plastic test bag and seal to cask body around port opening with suitable tape.
3. Evacuate test bag and backfill with 99.9% (minimum) pure helium to one atmosphere absolute.
4. Reevacuate test bag and perform final helium backfill to one atmosphere absolute.
5. Without breaking seal of plastic bag to the cask body, insert the Alternate B port cover into the port opening and tighten bolts hand tight.
6. Remove plastic bag and torque bolts to 285 ± 15 inch-pounds.
7. Remove test port plug from the Alternate B port cover.
8. Attach helium mass spectrometer to the Alternate B port cover test port and evacuate the volume between the seals.
9. Monitor the leakage rate test until stable or a minimum of 30 seconds.
10. The test is acceptable if the indicated leakage rate is $\leq 2 \times 10^{-7}$ cm³/s (helium), i.e., leaktight per ANSI N14.5-1997.
11. Repeat Steps 1 through 10 for the second Alternate B port cover.

8.1.4 Component Tests

Tests performed on individual components are designed to ensure that the components meet the design requirements for correct operation of the cask system.

Acceptance criteria are functions of the purpose of the component being tested.

8.1.4.1 Valves, Pressure Relief Device, and Fluid Transport Devices

Overpressurization protection is afforded the neutron shield tank in the form of a relief valve that is designed to open at 165 psig (plus or minus 10 percent), and reseal. The relief valve is removed from the cask and hydraulically pressure tested using a calibrated system to verify relief valve opening and closing pressures. Failure to operate within tolerance is cause for rejection. Rejected valves are rebuilt or replaced and retested prior to use.

The cask cavity does not contain overpressurization protection because the maximum pressures developed in the worst case (fuel or TPBAR rupture) are well below the structural capability of the cask structure, lid, port covers, and seals.

The cask ports for vent/drain operations (two ports) contain valved quick disconnect fittings. These valves do not require testing to verify valved operation, because no credit is taken for these valves in the cask analyses. The valves provide a convenient method of attaching lines and fixtures, but serve no safety-related function.

The NAC-LWT cask package does not use rupture disks.

A siphon tube is used to connect the neutron shield tank to the neutron shield expansion tank. The tube is a passive device and allows expanding fluid to enter the expansion tank and returns the fluid as the liquid cools. It contains no moving parts and cannot be inspected after installation. The tube will be inspected for cleanliness and to verify that its passage is free of debris and clear prior to installation.

8.1.4.2 Gaskets

Cask closure lid and port cover O-rings will be hydrostatically pressure tested to verify suitability for use and for operation in the Maximum Normal Operating Pressure (MNOP) condition. The O-rings are arranged in pairs with an annulus between them. The annulus is connected by a drilled passageway to a test port. In the acceptance test, each of the three O-ring sets (one closure lid set, one vent port cover set, and one drain port cover set) is pressurized to 209 (+5/-0) psig for 30 minutes. Casks having TPBARs as approved contents are subjected to additional hydrostatic tests at 450 +15/-0 psig (one with the vent cover installed and one with the drain port cover installed). Loss of pressure or any other sign of leakage is cause for rejection.

A seal is installed at the outer edge of the lid, between the lid and the top cask forging, during transport. This seal is a weather seal and is not a pressure boundary. It is not pressure tested.

8.1.4.3 Sealed Canisters

Prior to underwater application of sealed canisters, each design shall be qualified by testing to demonstrate the ability of the canister to be vacuum dried and to stay sealed during subsequent underwater handling and storage. The qualification tests performed will simulate underwater vacuum drying and subsequent handling/storage. Acceptance criteria include no residual water in, or water ingress to, the sealed canister.

8.1.4.4 Miscellaneous

The cask impact limiter structures contain a two-part, aluminum honeycomb that is fabricated to have dynamic crush strengths of 3,500 psi. (plus 5 percent, minus 10 percent) and 250 psi (plus 10 percent, minus 10 percent), respectively. Sample lots of honeycomb material are subjected to dynamic crush testing to verify the crush strength of the impact limiter material. A dynamic crush strength of a sample outside of the allowable variation is cause for rejection of the batch lot of honeycomb material.

8.1.5 Tests for Shielding Integrity

A gamma scan inspection of all steel and lead shielding is conducted in order to verify shielding integrity. This inspection is performed on the cask body, including the cask bottom.

The test is conducted by continuous scanning or probing over 100 percent of all accessible surfaces, using a 3-inch detector and a ^{60}Co source of sufficient strength to produce a count rate that equals or exceeds three times the background count rate.

Scan path spacing is 2.5 inches. Scan speed is 4.5 feet-per-minute or less. All probing is on a 2-inch grid pattern (when using a 3-inch detector) and the count time is a minimum of one minute.

Acceptance is based on a lead and steel mock-up, where the material thicknesses are equivalent to the minimum thicknesses specified by the drawings. The lead and steel mock-up is produced using the same pouring technique as that approved for the cask.

Any area that produces a count rate over that established by the mock-up is considered rejected and must be corrected and retested prior to use.

Test equipment is checked before and after each use to ensure that shield test results are accurate.

8.1.6 Thermal Acceptance Tests

8.1.6.1 Thermal Test

A heat transfer acceptance test is conducted to test the integrity of the lead/stainless steel interface and to establish the heat rejection capability of the cask. The test is conducted with the neutron shield tank full¹ and the pressurized water reactor (PWR) basket located in the dry cask cavity.

¹ The neutron shield tank is filled with a liquid consisting of 58 weight percent ethylene glycol, 39 weight percent demineralized water and 3 weight percent potassium tetraborate ($\text{K}_2\text{B}_4\text{O}_7$).

The cask is internally heated at a rate of 8,500 BTU per hour ($\pm 1,000$ BTU per hour). A minimum of 12 internal and 12 external temperatures on the cask are measured with thermocouples. A test closure lid is used to allow penetrations for electric heaters and thermocouples. The steady state heat rate, transient cask temperatures, and ambient temperature are recorded. The test is conducted with the cask 3 feet (approximately) above the ground, horizontal and in still air.

8.1.6.2 Retest

If any equipment should fail during the test, such that the test must be aborted, the test is repeated.

8.1.6.3 Heat Source

The heat source for the thermal test is an electrical heater (cal-rod type) with an active length of 144 to 150 inches and is capable of generating at least 2.5 kilowatts.

8.1.7 Neutron Absorber Tests

8.1.7.1 General

Neutron absorber material in the form of borated stainless steel sheets is used in the TRIGA poison basket modules. After manufacturing, test samples from each batch of neutron absorber (poison) sheets shall be tested using neutron absorption techniques to verify the presence, proper distribution, and minimum weight percent of enriched boron. The tests shall be performed in accordance with approved written procedures.

8.1.7.2 Preparation of Samples for Spectroscopic Examination

Detailed written procedures to perform neutron absorption tests of each batch of neutron absorber sheets shall be established by the manufacturer and approved by NAC. For each batch of neutron absorber sheets, a sample shall be taken from each sheet. The samples shall be indelibly marked and recorded for identification.

At least 2 percent of the sheets in a batch shall be tested using a grid pattern of locations covering the entire surface of the sheet. Each of the remaining sheets in a batch shall be tested at one random location to ensure the presence of boron.

8.1.7.3 Neutron Absorption Test Performance

An approved facility with a neutron source and neutron detection capability shall be selected to perform the described tests. The tests will assure that the neutron absorption capacity of the material tested is equal to, or higher than, the given reference value and will verify the uniformity of boron distribution of a batch of neutron absorber sheets. The principle of measurement of neutron absorption is that the presence of boron results in a slowing down of neutron flux between the neutron sources, the reflector, and the neutron detector – depending on the material thickness and boron content.

Typical test equipment will consist of a neutron source/neutron detector, a reflector, and a counting instrument. The test equipment is calibrated using approved reference sheet(s), whose ^{10}B content has been checked and verified by an independent method such as chemical analysis. The highest permissible counting rate is determined from the neutron counting rates of the reference sheet(s), which should be ground to the minimum allowable plate thickness. This calibration process shall be repeated daily (at least once every 24 hours) while tests are being performed.

8.1.7.4 Acceptance Criteria

The neutron absorption test shall be considered acceptable if the neutron count determined for each test specimen is less than or equal to the highest permissible neutron count rate determined from the reference sheet(s). The poison sheets shall have a minimum of 1.04 weight-percent enriched boron content, with ^{10}B being a minimum of 93.88 atom percent. Any specimen not meeting the acceptance criteria for maximum neutron count shall be rejected and all of the sheets from that lot shall be similarly rejected.

8.2 Maintenance Program

Each NAC-LWT cask is subjected to a series of tests and inspections prior to each loaded shipment and annually, as shown in the Maintenance Program Schedule (Table 8.2-1).

Prior to each loaded transport, the metallic O-rings of the closure lid and Alternate B port covers, if used, are replaced. The O-ring seals of the alternate port covers are inspected and replaced as necessary. The cask cavity, trunnions, and all removable components (i.e., closure lid, port covers, attachment bolts, impact limiters, etc.) are visually inspected for damage. Following loading, the closure lid and port covers are installed and the bolting torqued. Leakage rate tests are performed on the closure lid and port covers as detailed in the cask loading procedures of Chapter 7.1. Depending on the port cover design and content conditions, helium leakage rate tests and air pressure drop tests verify the pre-shipment integrity of the containment boundary.

The completion of the annual maintenance and test program is required for each NAC-LWT cask while it is in service. The completion of the annual maintenance is documented on an annual inspection certification document. Each NAC-LWT cask must have a current annual certification before it can be used. The required annual cask maintenance test program is performed during or before the calendar month in which the annual program is due, but it is required to be performed no later than 30 days following the due date. During periods when the cask is not in use, the annual maintenance program may be deferred provided that the annual maintenance is completed and documented prior to the cask's next use.

For NAC-LWT casks to be used to transport TPBAR contents, a one-time post-fabrication hydrostatic test of the cask containment boundary shall be performed to a pressure of 450 +15/-0 psig.

For NAC-LWT casks to be used to transport radioactive contents requiring a leaktight containment boundary (e.g., TPBARs and MOX fuel rods), helium leakage rate testing to the leaktight criteria of ANSI N14.5-1997 is performed on the closure lid and Alternate B port cover containment seals. The annual maintenance program certification documentation shall specifically identify that a NAC-LWT packaging has been qualified by testing for TPBAR contents and/or for a leaktight containment condition.

Engineering approval is required prior to making any repairs of damaged areas or areas that need refurbishing as a result of normal wear and tear. All such repairs shall be fully documented in accordance with NAC's approved Quality Assurance program. The replacement of valves, fittings, seals, thread fasteners, or use of calibrated pressure gauges are considered normal maintenance and do not require engineering approval.

Testing of the cask shielding and heat rejection capabilities is conducted during original packaging acceptance testing. The structures that provide shielding and heat rejection are passive and do not require verification during routine use of the package. Consequently, the efficiency of these systems is not tested during the annual maintenance program. Radiation surveys conducted at the time of cask loading provide verification of continued shielding effectiveness.

Testing of the neutron absorber material utilized in TRIGA poisoned basket modules are conducted prior to fabrication of the basket modules. The neutron absorber material is in the form of borated stainless steel sheets that are visually inspected for wear or damage prior to each use, and do not require routine maintenance.

Table 8.2-1 Maintenance Program Schedule

Cask Cavity (Including Port Cover and Lid Seals Annulus)

Annually	Visual Inspection Lid and Port Cover Seal Replacement Helium Leak Tests (per Section 8.1.3)
----------	---

Valve Port Covers

Each Loaded Shipment	Visual Inspection Air Pressure Drop Test at 15 +1/-0 psig (Alternate port covers) Helium Leakage Testing (Alternate B port covers) Seal Replacement as Necessary ¹
----------------------	--

Drain Line Gasket

Each Shipment	Seal Replacement as Necessary
Annually	Seal Replacement

Water Jacket and Expansion Tank

Annually	Visual Inspection Check Fluid Level, Specific Gravity, and Boron Concentration ²
Each Shipment	Visually Inspect Fill, Drain and Inspection Port Plugs for Leakage

Cask Lid Bolts

Each Shipment	Visually Inspect for Damage and Replace, as required.
Long Term Maintenance	Bolt replacement upon reaching 20-year life or 550 operational cycles.

¹ Helium leak testing (per Section 8.1.3.2.2) is required following replacement of alternate port cover seals. For Alternate B port covers, seal replacement and leak testing are required for each shipment per the requirements specified in the Operating Procedures in Chapter 7 and Section 8.1.3.3.2.

² The neutron shield fluid must be verified to contain greater than 1.0 wt % boron and the specific gravity must be such that the solution does not freeze at temperatures above -40°F.

Table 8.2-1 Maintenance Program Schedule (continued)

Water Jacket Relief Valve	
Annually	Replace With New Pre-set Valve, or Verify Opening and Reseating Pressure (Allowable variation is ± 10 psig of Nominal Valve Opening Pressure, 165 psig)
Fasteners, Valved Nipples, Washers, Reusable O-rings, and Helicoils	
Each Shipment	Inspect and Replace as necessary
Lid and Alternate B Port Cover Metallic O-rings	
Each Loaded Shipment	Replace and perform helium leakage rate testing to the criteria specified in Section 8.1.3, as applicable.

Chapter 9

Table of Contents

9.0 REFERENCES..... 9-1

9 REFERENCES

“AISC Manual of Steel Construction,” 8th Edition, The American Institute of Steel Construction, Inc., 1990.

Alcoa Aluminum Handbook, Pittsburgh, PA, Aluminum Company of America, 1959.

“Aluminum Construction Manual,” 2nd Edition, Section 3, The Aluminum Association, Washington, D.C., 1972.

“Annual Book of ASTM Standards,” Section 3, Volume 03.01, American Society for Testing and Materials, 1986.

“ANSYS’ Computer Code for Large-Scale General Purpose Engineering Analysis,” Swanson Analysis Systems, Inc., Houston, PA.

“ASME Boiler and Pressure Vessel Code,” Section III, Subsection NG – Core Support Structures and Subsection NH – Class 1 – Components in Elevated Temperature Service, The American Society of Mechanical Engineers, 1995 with Addenda through 1997.

Baker, E.H., L. Kovalevsky, and F.L. Rish, Structural Analysis of Shells, New York, McGraw-Hill Book Co., December 1966.

Bates, O.K., “Thermal Conductivities of Aqueous Ethylene Glycol Solutions,” St. Lawrence University, Canton, NY.

Baumeister, T. and L.S. Marks, Standard Handbook for Mechanical Engineers, 7th Edition, New York, McGraw-Hill Book Co., December 1966.

BAW-246, “NULIF – A Neutron Spectrum Generator, Few-Group Constant Calculator, and Depletion Code,” Babcock & Wilcox, August 1976.

Bevington, P.R., Data Reduction and Error Analysis for the Physical Sciences, New York, McGraw-Hill Book Company.

Biggs, J.M., Introduction to Structural Dynamics, New York, McGraw-Hill Book Co., 1964.

Blake, A., “Charts Simplify Calculations for Moments and Deflections of Circular Arches,” Machine Design, Cleveland, Penton Publishing Co., December 25, 1958.

Blodgett, O.W., Design of Welded Structures, Cleveland, James F. Lincoln Arc Welding Foundation, 1972.

Book of Standards, Part 7, American Society for Testing and Materials, 1970.

Bruhn, E.F., Analysis and Design of Flight Vehicle Structures, 1st Edition, Cincinnati, Tri-State Offset, Co., 1965.

Bucholz, J.A., "Scoping Design Analyses for Optimized Shipping Casks Containing 1-, 2-, 3-, 5-, 7-, or 10-year old PWR Spent Fuel," Oak Ridge National Laboratory, ORNL/CSD/TM-149, January 1983.

Bucholz, J.A., "XSDOSE: A Module for Calculating Fluxes and Dose Rates at Points Outside A Shield," Vol. 2, Sect. F4 of SCALE-4, August 1981.

Bucholz, J.A., et. Al., "SAS1: A One-Dimensional Shielding Analysis Module."

Cain, V.R. and R.E. Malenfant, "QAD-CG, The Combinatorial Geometry Version of the QAD-P5A Point Kernam Shielding Code," Bechtel Power Corporation, July 1977.

CCC-545, "SCALE-4, A Modular Code System for Performing Standardized Computer Analysis of Licensing Evaluation," ORNL, June 1990.

Chun, R., M. Witte, and M. Schwartz, "Dynamic Impact Effects on Spent Fuel Assemblies," UCID-21246, Lawrence Livermore National Laboratory, October 1987.

"Coefficient of Cubical Expansion for Glycol, Water, and Glycol-Water Solutions," E.I. du Pont de Nemours & Co., Inc., Wilmington, DE, 1963.

Cook, I. And R.S. Peckover, "Effective Thermal Conductivity of Debris Beds," Post Accident Debris Cooling, Proceedings of the Fifth Post Accident Heat Removal Information Exchange Meeting, 40-45, 1982.

Cragoe, C.S., "Properties of Ethylene Glycol and Its Aqueous Solutions," National Bureau of Standards.

DOE/ET/34014-10, "Extended Fuel Burnup Demonstration Program," U.S. Department of Energy, September 1983.

Gallagher, C., "NL Industries Internal Test Report on Tensile Properties of Chemical Lead at Elevated Temperatures," Central Research Laboratory, Highstown, NJ, February 1976.

Gerard, G. and H. Becker, "Handbook of Structural Stability," Part III, TN3783, National Advisory Committee for Aeronautics, 1957.

Greene, N.M., J.L. Lucius, L.M. Petrie, W.E. Ford III, J.E. White, and R.Q. Wright, "AMPX – A Modular Code System for Generating Multigroup Neutron-Gamma Libraries from ENDF/B," ORNL/TM-3706, Oak Ridge National Laboratory, March 1976.

Greene, N.M. and L.M. Petrie, "XSDRNPM-S: A One-Dimensional Discrete Ordinates Code for Transport Analysis," Vol. 2, Sect. F3 of SCALE-4, January 1983.

Handbook of Chemistry and Physics, 49th Edition, Cleveland, OH, The Chemical Rubber Company, 1968.

Hermann, O.W. and R.M. Westfall, "ORIGEN-S: SCALE System Module to Calculate Fuel Depletion, Actinide Transmutation, Fission Product Buildup and Decay and Associated Radiation Source Terms," Vol. 2, Sect. F7 of SCALE-4, February 1989.

Hermann, O.W., "SAS2(H): A Coupled One-Dimensional Depletion and Shielding Analysis Code," Vol. 1, Sect. S2 of SCALE-4, June 1990.

IAEA Transportation Safety Standards (TS-R-1), "Regulations for the Safe Transport of Radioactive Material," June 2000.

Johnson, E.B. and R.K. Reedy, "Critical Experiments with SPERT-D Fuel Elements," ORNL-TM-1207, July 14, 1965.

Jordan, W.C., N.F. Landers, and L.M. Petrie, "Validation of KENO-Va Comparison with Critical Experiments," ORNL/CSD/TM-238, December 1986.

Juvinall, R.C., Stress, Strain, and Strength, New York, McGraw-Hill Book Co., 1967.

Kinsey, R., "Data Formats and Procedures for the Evaluated Nuclear Data File, ENDF," ENDF-102, Second Edition, Brookhaven National Laboratory, 1979.

Kreith, F., Principles of Heat Transfer, 2nd Edition, Scranton, PA, International Textbook Company, 1965.

Manual of Steel Construction, 8th Edition, New York, American Institute of Steel Construction, Inc., 1990.

Mark's Standard Handbook for Mechanical Engineers, 9th Edition, McGraw-Hill Book Company, New York.

Merritt, F.S., Standard Handbook for Civil Engineers, McGraw-Hill Book Company, New York, 1968.

Metals Handbook, 9th Edition, American Society of Metals.

MIL-HDBK-5A, "Metallic Materials and Elements for Aerospace Vehicle Structures," Department of Defense, February 1966.

MIL-HDBK-5C, "Metallic Materials and Elements for Aerospace Vehicle Structures," Department of Defense, December 1978.

MIL-HDBK-5E, "Metallic Materials and Elements for Aerospace Vehicle Structures," Department of Defense, May 1989.

Nelms, H.A., "Effects of Jacket Physical Properties and Curvature on Puncture Resistance," Structural Analysis of Shipping Casks, Volume 3, ORNL/TM-1312, Oak Ridge National Laboratory, June 1968.

"Nuclear Systems Materials Handbook," Volume 1, Revision 1, Hanford Engineering Development Laboratories, Richland, WA, March 10, 1976.

NUREG-0612, "Control of Heavy Loads at Nuclear Power Plants," U.S. Nuclear Regulatory Commission, July 1980.

NUREG-1617, Supplement 1, "Standard Review Plan for Transportation Packages for MOX Spent Nuclear Fuel," U.S. Nuclear Regulatory Commission, September 2005.

NUREG/CR-0733, "Critical Separation Between Sub-Critical Clusters of 4.29 w/o U²³⁵ Enriched UO₂ Rods in Water with Fixed Neutron Poisons," S.R. Bierman, B.M. Durst, E.D. Clayton, Battelle Pacific Northwest Laboratories, May 1978.

NUREG/CR-0200, Volume 2, Section F2, "SCALE-2 NITAWL-S, Resonance Self-Shielding by the Nordheim Method," N. M. Green and L. M. Petrie, Oak Ridge National Laboratory, October 1981.

NUREG/CR-6361, "Criticality Benchmark Guide for Light-Water-Reactor Fuel in Transportation and Storage Packages," U.S. Nuclear Regulatory Commission, March 1997.

NUREG/CR-6487, Anderson, B.L., Carlson, R.W., and Fisher, L.E., "Containment Analysis for Type B Packages Used to Transport Various Contents," Lawrence Livermore Laboratory, 1996.

NUREG/CR-0200, Volume 2, Section F3, "SCALE-2 XSDRNMP-S, A One Dimensional Discrete Ordinates Program for Transport Analysis," R.M. Westfall, L.M. Petrie, N.M. Greene, J.L. Lucius, Oak Ridge National Laboratory, June 1983.

NUREG/CR-0481, "An Assessment of Stress-Strain Data Suitable for Finite-Element Elastic-Plastic Analysis of Shipping Containers," H.J. Rack and G.A. Knorovsky, Sandia Laboratories, SAND77-1872, September 1978.

NUREG/CR-0796 PNL-2827, "Criticality Experiments with Sub-Critical Clusters of 2.35 and 4.29 w/o U²³⁵ Enriched UO₂ Rods in Water with Uranium or Lead Reflecting Walls," S.R. Bierman, B.M. Durst, E.D. Clayton, Battelle Pacific Northwest Laboratories, April 1979.

Paxton, H.C., Critical Dimensions of Systems Containing U²³⁵, Pu²³⁹, and U²³³," TID-7028, June 1964.

Peery, D.J., Aircraft Structures, New York, McGraw-Hill Book Company, 1950.

Petrie, L.M. and N.F. Cross, "KENO-IV: An Improved Monte Carlo Criticality Program," ORNL-4938, Oak Ridge National Laboratory, November 1975.

PNL-2438, "Critical Separation Between Sub-Critical Clusters of 2.35 w/o U²³⁵ Enriched UO₂ Rods in Water with Fixed Neutron Poisons," S.R. Bierman, E.D. Clayton, B.M. Durst, Battelle Pacific Northwest Laboratories, October 1977.

Radiological Health Handbook, U.S. Department of Health, Education and Welfare, Rockville, MD, January 1970.

"Regulations for the Safe Transport of Radioactive Materials," Safety Series No. 6, Revised Edition, International Atomic Energy Agency, 1973.

"Research and Advanced Development Applied Mechanics," Volume 1, Engineering Data Sheets, Avco Corporation, 1962.

Resnick, R. and D. Halliday, Physics, 3rd Edition, Part 1, New York, John Wiley & Sons, 1977.

Roark, R.J., Formulas for Stress and Strain, 4th Edition, New York, McGraw-Hill, Inc., 1965.

Roark, R.J., and W.C. Young, Formulas for Stress and Strain, 5th Edition, New York, McGraw-Hill, Inc., 1975; 6th Edition, 1989.

Roddy, J.W., H.C. Claiborne, R.C. Ashline, P.J. Johnson, B.T. Rhyne, "Physical and Decay Characteristics of Commercial LWR Spent Fuel," ORNL/TM-9591/VI-R1, Oak Ridge National Laboratory, January 1986.

"Safety Analysis Report for the NLI-1/2 Spent Fuel Shipping Cask," Nuclear Assurance Corporation, USA/9010/B()F, December 12, 1985.

Schaeffer, N.M., Reactor Engineering for Nuclear Engineers, Springfield, VA, 1984.

"Screw-Thread Standards for Federal Services," U.S. Department of Commerce, 1957.

Shamban TFE O-Ring Seals, Spec. 22-53, Part No. S11214-460, W.S. Shamban & Co., Fort Wayne, IN, 1966.

Shappert, L.B., "Cask Designer's Guide: A Guide for the Design, Fabrication, and Operation of Shipping Casks for Nuclear Applications," ORNL-NSIC-68, Oak Ridge National Laboratories, February 1970.

Shappert, L.B., and W.D. Box, "The Drop Test Facility at the Oak Ridge National Laboratory: A Facility Available to Private Industry," Oak Ridge National Laboratory, Oak Ridge, TN.

Shigley, J.E., Mechanical Engineering Design, 3rd Edition, New York, McGraw-Hill, Inc., 1977.

Shigley, J.E., and C.R. Mischke, Standard Handbook of Machine Design, New York, 1986.

Singer, F.L., Strength of Materials, New York, Harper & Brothers, 1951.

"Table Speeds Calculation of Strength of Threads," Product Engineering, November 27, 1961.

Tang, J.S. "SAS4: A Monte Carlo Cask Shielding Analysis Module Using An Automated Biasing Procedure," March 1989.

"Test Plan: LWT Quarter-Scale Model Drop Tests," Document No. 315-P-01. Nuclear Assurance Corporation, May 31, 1988.

Tietz, T.E., "Determination of the Mechanical Properties of High Purity Lead and a 0.058% Copper-Lead Alloy," Stanford Research Institute, Menlo Park, CA, WADC Technical Report 57-695, ASTIA Document No. 151165, April 1958.

Timoshenko, S., Strength of Materials, 3rd Edition, New York, R. E. Krieger Publishing Co., 1976.

Timoshenko, S., Theory of Plates and Shells, 1st Edition, New York, McGraw-Hill Book Co., 1940.

Timoshenko and Gere, Theory of Elastic Stability, 2nd Edition, New York, McGraw-Hill, Inc., 1961.

Timoshenko, S. and Young, Theory of Structures, New York, McGraw-Hill Book Co., 1965.

Turner, W.D., D.C. Elrod, and I.I. Simon-Tov, "HEATING 5 - An IBM 360 Heat Conduction Program," Oak Ridge National Laboratory, ORNL/CSD/TM-15, March 1977.

Williamson, R.A. and R.R. Alvy, "Impact Effect of Fragments Striking Structural Elements," Holmes and Harver, Inc., 1973.

Childs, K.W., HEATING 7.2 User's Manual, Oak Ridge National Laboratory, ORNL/NUREG/CSD-2/V2/R5, September 1995.

Avallone, E. and T. Baumeister, Marks' Standard Handbook for Mechanical Engineers, 9th Edition, New York, McGraw-Hill Book Company, 1987.

"SCALE 4.3 Modular Code System for Performing Standardized Computer Analyses for Licensing Evaluation for Workstations and Personal Computers," CCC-545, September 1995.

Herman, O.W., "SAS2H: A Coupled One-Dimensional Depletion and Shielding Analysis Module," and C.V. Parks, ORNL/NUREG/CSD-2/V1/R5, Volume 1, Section S2, September 1995.

Tang, S., "SAS4: A Monte Carlo Cask Shielding Analysis Module Using an Automated Biasing Procedure," ORNL/NUREG/CSD-2/V1/R5, Volume 1, Section S4, September, 1995.

Bucholz, J.A., Landers, N.F., and Petrie, L.M., ORNL/NUREG/CSD-2/V3/R5, Section M7, "The Material Information Processor For Scale," September 1995.

Greene, M., Westfall, R.M., and L.M. Petrie, ORNL/NUREG/CSD-2/V2/R5, "NITAWL-II: Scale System Module For Performing Resonance Shielding And Working Library Production" September 1995.

Jordan, W.C., ORNL/NUREG/CSD-2/V3/R5, Section M4, "Scale Cross-Section Libraries," September 1995.

Landers, N. F., and Petrie L.M, ORNL/NUREG/CSD-2/V1/R5, Section C4, "CSAS: Control Module For Enhanced Criticality Safety Analysis Sequences," September 1995.

Mele, Ravink and Trkov, "TRIGA Mark II Benchmark Experiment, Part I Steady State Operation," Jozef Stefan Institute, Nuclear Technology, Vol. 105, January 1994.

Petrie L.M., and Landers, N.F., ORNL/NUREG/CSD-2/V2/R5, Section F11, "KENO-Va: An Improved Monte Carlo Criticality Program with Supergrouping," September 1995.

Tomsio, M., "Characterization of Triga Fuel," ORNL/Sub/86-22047/3, GA-C18542, Oak Ridge National Laboratory, Oak Ridge, Tennessee, October 1986.

Krieth, F., and Bohn, M.S., "Principals of Heat Transfer," 5th Edition, West Publishing Company, 1993.

Incropera, F.P., and DeWitt, D.P., "Fundamentals of Heat and Mass Transfer," 4th Edition, John Wiley and Sons, 1996.

Owen, D.B., "Factors for One-Sided Tolerance Limits and for Variables Sampling Plans," SCR-607, 1963.

ANSI N14.5-1987, "American National Standard for Radioactive Materials - Leakage Tests on Packages for Shipment," American National Standards Institute, 1987.

ANSI/ANS - 8.1-1983, "Nuclear Criticality Safety in Operations with Fissionable Materials Outside Reactors."

ANSI/ANS - 8.17-1984, "Criticality Safety Criteria for the Handling, Storage, and Transportation of LWR Fuel Outside Reactors."

Bierman, S.R., Clayton, E.D., "Criticality Experiments with Subcritical Clusters of 2.35 w/o and 4.31 w/o ²³⁵U Enriched UO₂ Rods in Water at a Water-to-Fuel Volume Ratio of 1.6," NUREG/CR-1547, July 1980.

Baldwin, N.M., Hoovler, G.S., Eng, R.L., and Welfare, F.G., "Critical Experiments Supporting Close Proximity Water Storage of Power Reactor Fuel," B&W-1484-7, July 1979.

Bierman, S.R., and E.D. Clayton, "Criticality Experiments with Subcritical Clusters of 2.35 w/o and 4.31 w/o ^{235}U Enriched UO_2 Rods in Water with Steel Reflecting Walls," Nuclear Technology, Volume 54, pp. 131-144, August 1981.

Bierman, S.R., Durst, B.M., and Clayton, E.D., "Criticality Experiments with Subcritical Clusters of 2.35 and 4.31 w/o ^{235}U Enriched UO_2 Rods in Water with Uranium or Lead Reflecting Walls," NUREG/CR-0796, April 1979.

Bierman, S.R., "Criticality Experiments to Provide Benchmark Data on Neutron Flux Traps," PNL-6205/UC-714, June 1988.

Manaranche, J.C. et al, "Dissolution and Storage Experiment with 4.75 w/o ^{235}U Enriched UO_2 Rods," Nuclear Technology, Volume 50, September 1980.

Machinery's Handbook, 25th Edition, Industrial Press, Inc., New York, NY, 1996.

BISCO Products Data, "FPC Fireblock Silicone Foam," BISCO Products, Inc., Park Ridge, IL, February 1988.

Letter from Rogers Corporation, Bisco Materials Unit, dated February 2, 1999, from Daniel J. Kubrick.

Interim Staff Guidance-11 (ISG-11), Revision 1, "Transportation and Storage of Spent Fuel Having Burnups in Excess of 45 GWd/MTU," Nuclear Regulatory Commission, May 2000.

Holometrix Micromet test report NCN-2, dated May 2000.

Ugural, A.C. and Fenster, S.K., "Advanced Strength and Applied Elasticity," Second Edition, Elsevier Science Publishing Company, New York, New York, 1987.

NAC Specification 315-S-09, "O-Ring Temperature Testing for the LWT Alternate Port Cover," Revision 0, February 2000.

"HTGR/RERTR Fuel Materials Characterization and Packaging Report," PC-00384/1, General Atomics, San Diego, CA, April 2002.

UNIFRAX Product Specifications, Fiberfrax[®] Ceramic Fiber Paper, C-1423, Unifrax Corporation, Niagara Falls, NY, June 1996.

LLNL Report UCRL-53441, "Review of Hydrogen Isotope Permeability Through Materials" RSIC Computer Code Collection, *ORIGEN2.1; Isotope Generation and Depletion Code – Matrix Exponential Method*, CCC-371, Oak Ridge National Laboratory, Oak Ridge TN, 1996.

Y.K. Sakamoto and M. Sugisaki, "Fusion Science and Technology," Vol. 41, pp 912-914, May 2002.

"Aluminum Standards and Data," Table 2.2, The Aluminum Association, Washington, DC, 1997.

Blake, Alexander, "Practical Stress Analysis in Engineering Design," 2nd Edition, Marcel Dekker Inc., New York, 1990.